



# Performance of Skewed Reinforcing in Inverted-T Bridge Caps

---

Final Report

University of Houston

Y.L Mo  
Bhagirath Joshi  
Nagesh Ramaswamy  
Priyanka Shrestha  
Jiaji Wang  
Xiaonan Shan  
Thomas T.C. Hsu

1. Report No. FHWA/TX-24/0-6905-01-R1		2. Government Accession No.		3. Recipient's Catalog No.	
4. Title and Subtitle Performance of Skew Reinforcing in Inverted-T Bridge Caps of Donigan Road Bridge, Katy, Texas.			5. Report Date August 2023		
			6. Performing Organization Code		
7. Author(s) Bhagirath Joshi, Nagesh Ramaswamy, Priyanka Shrestha, Jiayi Wang, Xiaonan Shan, Y.L. Mo and Thomas T.C. Hsu			8. Performing Organization Report No. 0-6905-01-R1		
9. Performing Organization Name and Address University of Houston 4800 Calhoun Road Houston, TX 77204			10. Work Unit No. (TRAIS)		
			11. Contract or Grant No. 0-6905-01		
12. Sponsoring Agency Name and Address Texas Department of Transportation Research and Technology Implementation Office P.O. Box 5080 Austin, TX 78763-5080			13. Type of Report and Period Covered Technical Report September 2021– August 2023		
			14. Sponsoring Agency Code		
15. Supplementary Notes Project performed in cooperation with the Texas Department of Transportation and the Federal Highway Administration.					
16. Abstract Reinforced concrete inverted-T bridge caps (ITBCs) have been widely used in Texas and the United States bridges. They are aesthetically pleasing, offer a practical means to increase vertical clearance, and have practical applications to address landscaping requirements. The ITBCs in Texas are designed using the traditional empirical procedures outlined in the TxDOT Bridge Design Manual (TxDOT BDM) LRFD that conform to the AASHTO (American Association of State Highway and Transportation Officials) LRFD (2014) Bridge Design Specifications. The traditional method of flaring the transverse reinforcement out in skew ITBCs brings in significant design and construction complexity. In addition, the detailing of the transverse reinforcement has a profound influence on the overall shear capacity of the bent cap as well as the performance of the support ledge. Therefore, improper detailing can cause poor placement of concrete and cracks within the concrete structure, reducing the load-carrying capacity and increasing future maintenance costs. Faster and easier construction can be obtained if the skew transverse reinforcing throughout ITBCs is utilized, with significantly reduced design complexities. TxDOT Project 0-6905-01 focuses on implementing skew reinforcing on ITBCs and performs the load tests on the Donigan Road Bridge over I-10. Bent Cap 2 (skew angle 43°) and Bent Cap 7 (skew angle 33°) were examined in the preliminary finite element (FE) analysis in 15 loading cases. Further, two critical cases of each bent cap were critically examined in five positions. Each bent cap was examined in two cases: Static Test 1, Static Test 2, Dynamic Test 1, and one case of Dynamic Test 2. The FE models of ITBCs are calibrated with the load test results to perform the parametric study. The influence of the skew angle of ITBC, the performance of skew transverse reinforcement, displacements of the end face of ITBC, the influence of the location of exterior loading pads, and critical loading cases are examined. The research project presents the following findings: (1) the skew angle of an ITBC is the most influential parameter that governs the tensile strains on the transverse rebars, torsional effect on the bent caps, end face displacement, compressive stress on exterior loading pads and tensile strain on the concrete (stem/ledge interface); (2) the location of exterior loading pads influences the compressive stresses on it; (3) the inclusion of diagonal G bars has dual beneficial effects - (i) delay the appearance of cracks at the stem/ledge interface, and (ii) reduce tensile strains on S and M bars.					
17. Key Words ITBC, inverted-T bridge cap, load test			18. Distribution Statement No restrictions. This document is available to the public through the National Technical Information Service, Springfield, Virginia 22161; www.ntis.gov.		
19. Security Classif. (of report) Unclassified		20. Security Classif. (of this page) Unclassified		21. No. of pages TBD	
22. Price					

**TxDOT Project 0-6905-01**

**PERFORMANCE OF SKEWED REINFORCING  
IN INVERTED-T BRIDGE CAPS**

Bhagirath Joshi, Nagesh Ramaswamy, Priyanka Shrestha, Jiaji Wang,  
Xiaonan Shan, Y.L. Mo, Thomas T.C. Hsu

Department of Civil and Environmental Engineering  
University of Houston

**Research Report 0-6905-01-R1**

## **DISCLAIMERS**

**Author's Disclaimer:** The contents of this report reflect the views of the authors, who are responsible for the facts and the accuracy of the data presented herein., The contents do not necessarily reflect the official view or policies of the Federal Highway Administration or the Texas Department of Transportation (TxDOT). This report does not constitute a standard, specification, or regulation.

**Patent Disclaimer:** There was no invention or discovery conceived or first actually reduced to practice in the course of or under this contract, including any art, method, process, machine manufacture, design, or composition of matter, or any new useful improvement thereof, or any variety of plant, which is or may be patentable under the patent laws of the United States of America or any foreign country.

**Research Supervisor: Y.L. Mo**

**Professional Engineer License State and Number: Texas No. 110677 P.E.**

## **ACKNOWLEDGMENTS**

The authors would like to express their gratitude to the Texas Department of Transportation (TxDOT) for their financial support and collaborative efforts for this project. This research is supported by TxDOT for Grant 0-6905-01. The authors would like to specifically thank the contributions of the project supervisory committee, which consists of Jade Adediwura, RTI (Research and Technology Implementation Office); Michael Carlson, HOU; Bobby Bari, HOU; Walter “Ray” Fisher, DAL; Courtney Holle, BRG; Aaron Garza, BRG; Hector Garcia, DOT and Andrew Smyth, DOT.

Finally, the authors appreciate CONSOR Engineers, Williams Brothers, the rest of the support staff at the Thomas T.C. Hsu Structural Lab at UH (University of Houston), and the many other researchers who helped with instrumentation, testing, and analysis of results.

## ABSTRACT

Reinforced concrete inverted-T bridge caps (ITBCs) have been widely used in Texas and the United States bridges. They are aesthetically pleasing, offer a practical means to increase vertical clearance, and have practical applications to address landscaping requirements. Many of the ITBCs are skew when two roads are not aligned perpendicularly and exceed the angle of 45 degrees based on the construction requirements. The ITBCs in Texas are designed using the traditional empirical procedures outlined in the TxDOT Bridge Design Manual (TxDOT BDM) LRFD that conform to the AASHTO (American Association of State Highway and Transportation Officials) LRFD (2014) Bridge Design Specifications. No precise calculation methods or guidelines are given in the AASHTO LRFD (2014) or TxDOT BDM-LRFD (2015) to design skew ITBCs. For a skew ITBC, the TxDOT Manual states that hanger and ledge reinforcement should be placed perpendicular to the centerline of the skew bent, and the detailing of the skew ends of the bent should be done with a section of skewed stirrups and ledge reinforcements. Typically, the transition of perpendicular bars to the skew bars is carried out over column support, where the transverse reinforcement spacing is less critical. The designer of ITBC flares the bars out to match the skew angle while trying to maintain a minimum and maximum spacing based on the outcome of the design calculations. Such detailing of transverse reinforcements creates unequal spacing on both sides of the web, producing congestion of reinforcements on one side. The traditional method of flaring the transverse reinforcement out in skew ITBCs brings in significant design and construction complexity. In addition, the detailing of the transverse reinforcement has a profound influence on the overall shear capacity of the bent cap as well as the performance of the support ledge. Therefore, improper detailing can cause poor placement of concrete and cracks within the concrete structure, reducing the load-carrying capacity and increasing future maintenance costs. Faster and easier construction can be obtained if the skew transverse reinforcing throughout ITBCs is utilized, and it can provide an alternative approach that will significantly reduce the design complexities and construction period. According to the results of lab tests (TxDOT Project 0-6905, *Initial Investigation of Performance of Skewed Reinforcing in Inverted-T Bridge Caps*), using skewed transverse reinforcement throughout ITBCs will have the same load capacity as the traditional design. In addition, it is found that using skewed transverse reinforcement throughout ITBCs will have less number of cracks and smaller crack widths compared to the traditional design.

The TxDOT Bridge Detailing Guide (2022) updated the transverse reinforcement detailing practices based on TxDOT Research Project 0-6905. As per the bridge detailing guide, the transverse bar in the stem (double S bars) should be placed throughout the bent cap, where the spacing of S bars can be increased at the location of the column support to 12 inches maximum. As per the TxDOT Bridge Design Guide (2022), the cap hanger and ledge reinforcement may be aligned to match the cap skew when simpler detailing can be achieved.

The ITBCs in the Donigan Road Bridge have adopted skew transverse reinforcing because of the advantages presented in TxDOT Project 0-6905. TxDOT Project 0-6905-01 focuses on implementing skew reinforcing on ITBCs and performs the load tests on the Donigan Road bridge over I-10. The research team selected Bent Cap 2 (skew angle  $43^\circ$ ) and Bent Cap 7 (skew angle  $33^\circ$ ) for the load tests. The significant bent caps were examined in the preliminary finite element (FE) analysis in 15 loading cases for each bent cap in the research project. Further, two critical cases of each bent cap were critically examined in five positions. The rebar cages of both bent caps are instrumented with sensors (strain gauges, carbon nanofiber aggregates, and thermocouples). Each bent cap was examined in two cases: Static Test 1, Static Test 2, Dynamic Test 1, and one case of Dynamic Test 2. The preliminary FE models of Bent Cap 2 and Bent Cap 7 are calibrated with the load test results to perform the parametric study. The influence of the skew angle of ITBC, the performance of skew transverse reinforcement, displacements of the end face of ITBC, the influence of the location of exterior loading pads, and critical loading cases are examined. From the load tests and finite element analyses, the research findings are as follows: (1) the skew angle of an ITBC is the most influential parameter that governs the tensile strains on the transverse rebars, torsional effect on the bent caps, end face displacement, compressive stress on exterior loading pads and tensile strain on the concrete (stem/ledge interface); (2) the location of exterior loading pads influences the compressive stresses on it; (3) the inclusion of diagonal G bars has dual beneficial effects - (i) delay the appearance of cracks at the stem/ledge interface, and (ii) reduce tensile strains on S and M bars.

# TABLE OF CONTENTS

1. INTRODUCTION .....	1
1.1 PROJECT OVERVIEW.....	1
1.2 PROJECT OBJECTIVES .....	8
1.3 VALUE OF RESEARCH .....	8
1.4 ORGANIZATION .....	9
2. PRELIMINARY FINITE ELEMENT SIMULATIONS OF THE SIGNIFICANT ITBCs .....	10
2.1 OVERVIEW.....	10
2.2 THREE-DIMENSIONAL FINITE ELEMENT ANALYSES.....	10
2.2.1 Modeling Scheme .....	10
2.2.2 Materials Models .....	14
2.3 BENT CAP 2.....	16
2.3.1 Static Test-1 Finite Element Simulation.....	16
2.3.2 Static Test-2 Simulation at Five Positions .....	39
2.4 BENT CAP 7.....	57
2.4.1 Static Test-1 Finite Element Simulation.....	57
2.4.2 Static Test-2 Simulation at Five Positions .....	79
3. CALIBRATION AND INSTALLATION OF SENSORS .....	98
3.1 OVERVIEW.....	98
3.2 CALIBRATION OF CNFAs .....	98
3.3 INSTRUMENTATION OF SENSOR .....	99
3.3.1 Bent Cap 2.....	100
3.3.2 Bent Cap 7.....	106
4. EXPERIMENTAL PROGRAMS.....	112
4.1 OVERVIEW.....	112

4.2	LOAD TEST .....	113
4.3	EXPERIMENTAL RESULTS .....	115
4.3.1	Bent Cap 2.....	115
4.3.2	Bent Cap 7.....	136
4.4	DISCUSSION OF TEST RESULTS .....	157
4.4.1	Performance of Transverse Rebars .....	158
4.4.2	Displacement of West Face of Bent Cap 2 and Bent Cap 7 .....	162
4.4.3	Compressive Stress on Exterior Loading Pad.....	164
4.4.4	Comparison of Static and Dynamic Tests.....	165
4.4.5	Influence of Skew Angle .....	171
4.5	SUMMARY .....	173
5.	FINITE ELEMENT ANALYSES .....	176
5.1	OVERVIEW.....	176
5.2	FINITE ELEMENT ANALYSIS OF BENT CAP 2 AND BENT CAP 7 .....	176
5.2.1	Finite Element Modeling .....	176
5.2.2	Concrete Material Property.....	179
5.3	CALIBRATION OF FE MODELS OF BENT CAP 2 WITH LOAD TEST DATA ..	181
5.3.1	Static Test-1 .....	181
5.3.2	Static Test-2 .....	186
5.3.3	Dynamic Test-1.....	198
5.4	CALIBRATION OF FE MODELS OF BENT CAP 7 WITH LOAD TEST DATA ..	203
5.4.1	Static Test-1 .....	203
5.4.2	Static Test-2 .....	208
5.4.3	Dynamic Test-1.....	220
5.5	PARAMETRIC STUDY .....	225

5.5.1	West Face Deformation of Bent Cap 2 and Bent Cap 7 .....	225
5.5.2	Tensile Strains of Transverse Rebars.....	227
5.5.3	Maximum Tensile Concrete Strain .....	235
5.5.4	Compressive Stresses Under Exterior Loading Pads.....	237
5.5.5	Influence of Skew Angle .....	240
5.6	SUMMARY .....	240
6.	DESIGN RECOMMENDATIONS .....	242
6.1	OVERVIEW.....	242
6.2	DESIGN RECOMMENDATIONS .....	244
6.3	DISCUSSION ON DESIGN EXAMPLES.....	245
7.	CONCLUSIONS.....	247
7.1	SUMMARY OF THE RESEARCH WORKS.....	247
7.2	CONCLUSIONS.....	248
7.3	FUTURE STUDY .....	250
	REFERENCES .....	252
	APPENDIX-1 .....	255
	APPENDIX-2 .....	264
	APPENDIX-3 .....	273
	APPENDIX-4 .....	296
	APPENDIX-5 .....	308
	APPENDIX-6 .....	320
	APPENDIX-7 .....	370

## LIST OF FIGURES

Figure 1.1. Component of ITBC .....	1
Figure 1.2. Traditional Method of Transverse Reinforcing in a Skew ITBC (Top View) .....	3
Figure 1.3. Skew Transverse Reinforcing in a Skew ITBC (Top View) .....	4
Figure 1.4 Layout of Bent Cap 2 .....	6
Figure 1.5 Layout of Bent Cap 7 .....	7
Figure 2.1. 3D Finite Element Model of Bent Cap 2, including Columns, Girders, and Deck ....	11
Figure 2.2. 3D Finite Element Model of Bent Cap 7, including Columns, Girders, and Deck ....	12
Figure 2.3. 3D Finite Element Mesh of Simulated Model for Bent Cap 2 .....	13
Figure 2.4. 3D Finite Element Mesh of Simulated Model for Bent Cap 7 .....	13
Figure 2.5. Element Type of Bent Cap 2 .....	14
Figure 2.6. Element Type of Bent Cap 7 .....	14
Figure 2.7. Stress-Strain Curves of Concrete in Tension and Compression.....	15
Figure 2.8. Stress-Strain Curve of Mild Steel.....	16
Figure 2.9. Four-Truck Locations for Cases 1 to 15 of Bent Cap 2 .....	24
Figure 2.10. Tensile Strain Distribution in Concrete for Cases 1 to 15 of Bent Cap 2 .....	31
Figure 2.11. Displacement Profile for Cases 1 to 15 of Bent Cap 2.....	33
Figure 2.12. Stress Distribution in Rebar Cage for Cases 1 to 15 of Bent Cap 2.....	38
Figure 2.13. Four-Truck Loading at Five Positions for Case 3 of Bent Cap 2.....	42

Figure 2.14. Tensile Strain Distribution of Concrete for Case 3 of Bent Cap 2 under Four-Truck Loading at Five Positions.....	44
Figure 2.15. Displacement Profile for Case 3 of Bent Cap 2 under Four-Truck Loading at Five Positions.....	46
Figure 2.16. Stress Distribution in Rebar Cage for Case 3 of Bent Cap 2 under Four-Truck Loading at Five Positions.....	47
Figure 2.17. Five Positions of Four-Truck Loading for Case 9 of Bent Cap-2.....	51
Figure 2.18. Tensile Strain Distribution of Concrete for Case 9 of Bent Cap 2 under Four-Truck Loading at Five Positions.....	53
Figure 2.19. Displacement Profile for Case 9 of Bent Cap 2 under Four-Truck Loading at Five Positions.....	54
Figure 2.20. Stress Distribution in Rebar Cage for Case 9 of Bent Cap 2 under Four-Truck Loading at Five Positions.....	56
Figure 2.21. Four Trucks Locations for Cases 1 to 15 of Bent Cap 7.....	64
Figure 2.22. Tensile Strain Distribution in Concrete for Cases 1 to 15.....	71
Figure 2.23. Displacement Profile for Cases 1 to 15 of Bent Cap 7.....	73
Figure 2.24. Stress Distribution in Rebar Cage for Cases 1 to 15 of Bent Cap 7.....	78
Figure 2.25. Four-Truck Loading at Five Positions for Case 9 of Bent Cap 7.....	82
Figure 2.26. Tensile Strain Distribution of Concrete for Case 9 of Bent Cap 7 under Four-Truck Loading at Five Positions.....	84
Figure 2.27. Displacement Profile for Case 9 of Bent Cap 7 under Four-Truck Loading at Five Positions.....	86

Figure 2.28. Stress Distribution in Rebar Cage for Case 9 of Bent Cap 7 under Four-Truck Loading at Five Positions .....	87
Figure 2.29. Four-Truck Loading at Five Positions for Case 14 of Bent Cap 7 .....	91
Figure 2.30. Tensile Strain Distribution of Concrete for Case 14 of Bent Cap 7 under Four-Truck Loading at Five Positions.....	93
Figure 2.31. Displacement Profile for Case 14 of Bent Cap 7 under Four-Truck Loading at Five Positions.....	94
Figure 2.32. Stress Distribution in Rebar Cage for Case 14 of Bent Cap 7 under Four-Truck Loading at Five Positions.....	96
Figure 3.1. A Typical Stress-Strain Curve of a CNFA .....	99
Figure 3.2. Sensors Installation on Rebars of Bent Cap 2 .....	104
Figure 3.3. Sensors Installed in Bent Cap 2.....	105
Figure 3.4. Sensors Installation on Rebars of Bent Cap 7 .....	109
Figure 3.5. Sensors Installed in Bent Cap 7.....	111
Figure 4.1. Load Tests on Bent Cap 2 .....	112
Figure 4.2. Load Tests on Bent Cap 7 .....	113
Figure 4.3. Schematic Profile of Four Trucks.....	114
Figure 4.4. Schematic of Load Test on Bent Cap 2 .....	115
Figure 4.5. Schematic of Load Test on Bent Cap 7 .....	115
Figure 4.6. Static Test-1 on Bent Cap 2.....	116
Figure 4.7. Rebar Strains in Static Test-1, Case 1 on Bent Cap 2 .....	117

Figure 4.8. West Face Displacement of Bent Cap 2 in Static Test-1, Case 1 .....	117
Figure 4.9. Average Compressive Stresses on Concrete in Static Test-1, Case 1 on Bent Cap 2 .....	118
Figure 4.10. Rebar Strains in Static Test-1, Case 14 on Bent Cap 2 .....	119
Figure 4.11. West Face Displacement of Bent Cap 2 in Static Test-1, Case 14.....	119
Figure 4.12. Average Compressive Stresses on Concrete in Static Test-1, Case 14 on Bent Cap 2 .....	120
Figure 4.13. Static Test-2 on Bent Cap 2.....	122
Figure 4.14. Rebar Strains in Static Test-2, Case 3 on Bent Cap 2 .....	124
Figure 4.15. West Face Displacements of Bent Cap 2 in Static Test-2, Case 3 .....	124
Figure 4.16. Average Compressive Stresses on Concrete in Static Test-2, Case 3 at Position 3 on Bent Cap 2.....	125
Figure 4.17. Average Compressive Stresses on Concrete in Static Test-2, Case 3 at Position 4 on Bent Cap 2.....	126
Figure 4.18. Rebar Strains in Static Test-2, Case 9 on Bent Cap 2 .....	127
Figure 4.19. West Face Displacements of Bent Cap 2 in Static Test-2, Case 9 .....	128
Figure 4.20. Average Compressive Stresses on Concrete in Static Test-2, Case 9 at Position 3 on Bent Cap 2.....	129
Figure 4.21. Average Compressive Stresses on Concrete in Static Test-2, Case 9 at Position 4 on Bent Cap 2.....	129
Figure 4.22 Dynamic Test-1 on Bent Cap 2 .....	130
Figure 4.23. Rebar Strains in Dynamic Test-1, Case 9 on Bent Cap 2.....	131

Figure 4.24. West Face Displacement of Bent Cap 2 in Dynamic Test-1, Case 9 .....	131
Figure 4.25. Rebar Strains in Dynamic Test-1, Case 14 on Bent Cap 2.....	132
Figure 4.26. West Face Displacement of Bent Cap 2 in Dynamic Test-1, Case 14 .....	133
Figure 4.27. Dynamic Test-2, Case 9 on Bent Cap 2 .....	134
Figure 4.28. Rebar Strains in Dynamic Test-2, Case 9 on Bent Cap 2.....	135
Figure 4.29. West Face Displacements of Bent Cap 2 in Dynamic Test-2, Case 9.....	136
Figure 4.30. Static Test-1 on Bent Cap 7 .....	137
Figure 4.31. Rebar Strains in Static Test-1, Case 1 on Bent Cap 7 .....	138
Figure 4.32. West Face Displacement of Bent Cap 2 in Static Test-1, Case 7.....	138
Figure 4.33. Average Compressive Stresses on Concrete in Static Test-1, Case 1 on Bent Cap 7 .....	139
Figure 4.34. Rebar Strain in Static Test-1, Case 11 on Bent Cap 7.....	140
Figure 4.35. West Face Displacement of Bent Cap 7 in Static Test-1, Case 11.....	140
Figure 4.36. Average Compressive Stresses on Concrete in Static Test-1, Case 11 on Bent Cap 7 .....	141
Figure 4.37. Static Test-2 on Bent Cap 7 .....	143
Figure 4.38. Rebar Strains in Static Test-2, Case 9 on Bent Cap 7 .....	145
Figure 4.49. West Face Displacements of Bent Cap 7 in Static Test-2, Case 9 .....	145
Figure 4.50. Average Compressive Stresses on Concrete in Static Test-2, Case 9 at Position 3 on Bent Cap 7.....	146

Figure 4.51. Average Compressive Stresses on Concrete in Static Test-2, Case 9 at Position 4 on Bent Cap 7.....	147
Figure 4.52. Rebar Strains in Static Test-2, Case 14 on Bent Cap 7 .....	148
Figure 4.53. West Face Displacements of Bent Cap 7 in Static Test-2, Case 14 .....	149
Figure 4.54. Average Compressive Stresses on Concrete in Static Test-2, Case 14 at Position 3 on Bent Cap 7.....	150
Figure 4.55. Average Compressive Stresses on Concrete in Static Test-2, Case 14 at Position 4 on Bent Cap 7.....	150
Figure 4.56. Dynamic Test-1 on Bent Cap 7 .....	151
Figure 4.57. Rebar Strains in Dynamic Test-1, Case 9 on Bent Cap 7.....	152
Figure 4.58. West Face Displacement of Bent Cap 7 in Dynamic Test-1, Case 9 .....	152
Figure 4.59. Rebar Strains in Dynamic Test-1, Case 14 on Bent Cap 7.....	153
Figure 4.60. West Face Displacement of Bent Cap 7 in Dynamic Test-1, Case 14 .....	154
Figure 4.61. Dynamic Test-2, Case 9 on Bent Cap 7 .....	155
Figure 4.62. Rebar Strains in Dynamic Test-2, Case 9 on Bent Cap 7.....	157
Figure 4.63. Transverse Rebar Strains in Static Test on Bent Cap 2.....	160
Figure 4.64. Transverse Rebar Strains in Static Test on Bent Cap 7.....	161
Figure 4.65. West Face Displacement of Bent Cap 2 in Static Test.....	162
Figure 4.66. West Face Displacement of Bent Cap 7 in Static Test.....	163
Figure 4.67. Rebar Strain Comparison in Case 9 (Static Test Vs. Dynamic Test).....	166

Figure 4.68. West Face Displacements Comparison of Bent Cap 2 in Case 9 (Static Test Vs. Dynamic Test).....	166
Figure 4.69. Rebar Strains Comparison in Case 14, Bent Cap 2 (Static Test Vs. Dynamic Test) .....	167
Figure 4.70. West Face Displacements Comparison of Bent Cap 2 in Case 14 (Static Test Vs. Dynamic Test).....	168
Figure 4.71. Rebar Strains Comparison in Case 9, Bent Cap 7 (Static Test Vs. Dynamic Test) .....	169
Figure 4.72. West Face Displacements Comparison of Bent Cap 2 in Case 9 (Static Test Vs. Dynamic Test).....	169
Figure 4.73. Rebar Strains Comparison in Case 14, Bent Cap 7 (Static Test Vs. Dynamic Test) .....	170
Figure 4.74. West Face Displacements Comparison of Bent Cap 7 in Case 14 (Static Test Vs. Dynamic Test).....	170
Figure 5.1. 3D Finite Element Model of Bent Cap 2, including Columns, Girders, and Deck .	178
Figure 5.2. 3D Finite Element Model of Bent Cap 7, including Columns, Girders, and Deck .	179
Figure 5.3. Locations of Trucks in Static Test-1, Case 1 on Bent Cap 2.....	181
Figure 5.4. Locations of Trucks in Static Test-1, Case 14 on Bent Cap 2.....	182
Figure 5.5. Rebar Strains Comparison of Static Test-1, Bent Cap 2 for Case 1.....	183
Figure 5.6. West Face Displacements Comparison of Static Test-1, Bent Cap 2 for Case 1 .....	183
Figure 5.7. Comparison of Average Compressive Stresses on Concrete of Static Test-1, Bent Cap 2 for Case 1 .....	184
Figure 5.8. Rebar Strains Comparison of Static Test-1, Bent Cap 2 for Case 14.....	185

Figure 5.9. West Face Displacements Comparison of Static Test-1, Bent Cap 2 for Case 14 ..	185
Figure 5.10. Comparison of Average Compressive Stresses on Concrete of Static Test-1, Bent Cap 2 for Case 14.....	186
Figure 5.11. Locations of Trucks in Static Test-2, Case 3 on Bent Cap 2.....	187
Figure 5.12. Locations of Trucks in Static Test-2, Case 9 on Bent Cap 2.....	188
Figure 5.13. Rebar Strains Comparison of Static Test-2, Case 3 at Position 3 on Bent Cap 2 .	189
Figure 5.14. Rebar Strains Comparison of Static Test-2, Case 3 at Position 4 on Bent Cap 2 .	190
Figure 5.15. West Face Displacements Comparison of Static Test-2, Case 3 at Position 3 on Bent Cap 2 .....	190
Figure 5.16. West Face Displacements Comparison of Static Test-2, Case 3 at Position 4 on Bent Cap 2 .....	191
Figure 5.17. Comparison of Average Compressive Stresses on Concrete of Static Test-2, Bent Cap 2 for Case 3 at Position 3 .....	192
Figure 5.18. Comparison of Average Compressive Stresses on Concrete of Static Test-2, Bent Cap 2 for Case 3 at Position 4 .....	192
Figure 5.19. Rebar Strains Comparison of Static Test-2, Case 9 at Position 3 on Bent Cap 2 .	193
Figure 5.20. Rebar Strains Comparison of Static Test-2, Case 9 at Position 4 on Bent Cap 2 .	194
Figure 5.21. West Face Displacements Comparison of Static Test-2, Case 3 at Position 3 on Bent Cap 2 .....	194
Figure 5.22. West Face Displacements Comparison of Static Test-2, Case 3 at Position 4 on Bent Cap 2 .....	195
Figure 5.23. Comparison of Average Compressive Stresses on Concrete of Static Test-2, Bent Cap 2 for Case 9 at Position 3 .....	196

Figure 5.24. Comparison of Average Compressive Stresses on Concrete of Static Test-2, Bent Cap 2 for Case 9 at Position 4 .....	196
Figure 5.26. Performance of CNFAs in Tension Zone of Bent Cap 2.....	198
Figure 5.27 Locations of Trucks in Dynamic Test-1, Case 9 on Bent Cap 2 .....	199
Figure 5.28. Locations of Trucks in Dynamic Test-1, Case 14 on Bent Cap 2 .....	199
Figure 5.29. Rebar Strains Comparison of Dynamic Test-1, Bent Cap 2 for Case 9 .....	200
Figure 5.30. West Face Displacements Comparison of Dynamic Test-1, Bent Cap 2 for Case 9 .....	201
Figure 5.31. Rebar Strains Comparison of Dynamic Test-1, Bent Cap 2 for Case 14 .....	202
Figure 5.32. West Face Displacements Comparison of Dynamic Test-1, Bent Cap 2 for Case 14 .....	202
Figure 5.33. Locations of Trucks in Static Test-1, Case 1 on Bent Cap 7.....	203
Figure 5.34. Locations of Trucks in Static Test-1, Case 11 on Bent Cap 7.....	204
Figure 5.35. Rebar Strains Comparison of Static Test-1, Bent Cap 7 for Case 1.....	205
Figure 5.36. West Face Displacements Comparison of Static Test-1, Bent Cap 7 for Case 1 ..	205
Figure 5.37. Comparison of Average Compressive Stresses on Concrete of Static Test-1, Bent Cap 7 for Case 1.....	206
Figure 5.38. Rebar Strains Comparison of Static Test-1, Bent Cap 7 for Case 11.....	207
Figure 5.39. West Face Displacements Comparison of Static Test-1, Bent Cap 7 for Case 11	207
Figure 5.40. Comparison of Average Compressive Stresses on Concrete of Static Test-1, Bent Cap 7 for Case 11.....	208
Figure 5.41. Locations of Trucks in Static Test-2, Case 9 on Bent Cap 7.....	209

Figure 5.42. Locations of Trucks in Static Test-2, Case 14 on Bent Cap 7.....	210
Figure 5.43. Rebar Strains Comparison of Static Test-2, Case 9 at Position 3 on Bent Cap 7 .	211
Figure 5.44. Rebar Strains Comparison of Static Test-2, Case 9 at Position 4 on Bent Cap 7 .	212
Figure 5.45. West Face Displacements Comparison of Static Test-2, Case 3 at Position 3 on Bent Cap 7 .....	212
Figure 5.46. West Face Displacements Comparison of Static Test-2, Case 3 at Position 4 on Bent Cap 7 .....	213
Figure 5.47. Comparison of Average Compressive Stresses on Concrete of Static Test-2, Bent Cap 7 for Case 9 at Position 3.....	214
Figure 5.48. Comparison of Average Compressive Stresses on Concrete of Static Test-2, Bent Cap 7 for Case 9 at Position 4.....	214
Figure 5.49. Rebar Strains Comparison of Static Test-2, Case 14 at Position 3 on Bent Cap 7	215
Figure 5.50. Rebar Strains Comparison of Static Test-2, Case 14 at Position 4 on Bent Cap 7	216
Figure 5.51. West Face Displacements Comparison of Static Test-2, Case 14 at Position 3 on Bent Cap 7 .....	216
Figure 5.52. West Face Displacements Comparison of Static Test-2, Case 14 at Position 4 on Bent Cap 7 .....	217
Figure 5.53. Comparison of Average Compressive Stresses on Concrete of Static Test-2, Bent Cap 7 for Case 14 at Position 3.....	218
Figure 5.54. Comparison of Average Compressive Stresses on Concrete of Static Test-2, Bent Cap 7 for Case 14 at Position 4.....	218
Figure 5.55. Performance of CNFAs in Tension Zone of Bent Cap 7.....	220
Figure 5.56. Locations of Trucks in Dynamic Test-1, Case 9 on Bent Cap 7 .....	221

Figure 5.57. Locations of Trucks in Dynamic Test-1, Case 14 on Bent Cap 7 .....	221
Figure 5.58. Rebar Strain Comparison of Dynamic Test-1, Bent Cap 7 for Case 9.....	222
Figure 5.59. West Face Displacements Comparison of Dynamic Test-1, Bent Cap 7 for Case 9 .....	223
Figure 5.60. Rebar Strains Comparison of Dynamic Test-1, Bent Cap 7 for Case 14 .....	224
Figure 5.61. West Face Displacements Comparison of Dynamic Test-1, Bent Cap 7 for Case 14 .....	224
Figure 5.62. West Face Displacements of Bent Cap 2 and Bent Cap 7.....	226
Figure 5.63. Stresses on Rebars of Bent Cap 2 Calibrated Model for Static Tests .....	230
Figure 5.64. Stresses on Rebars of Bent Cap 7 Calibrated Model for Static Tests .....	232
Figure 5.65. Tensile Stresses on 5th Transverse Rebars of Bent Cap 2 and Bent Cap 7.....	235
Figure 5.66. Concrete Tensile Strain of Bent Cap 2 and Bent Cap 7 .....	237
Figure 5.67. Average Compressive Stresses on the Exterior Loading Pads of Bent Cap 2.....	238
Figure 5.68. Average Compressive Stresses on the Exterior Loading Pads of Bent Cap 7.....	238
Figure 5.69. Average Compressive Stresses on the South Side Exterior Loading Pads .....	239
Figure 5.70. Average Compressive Stresses on the North Side Loading Pads .....	239
Figure 7.2. Rebar Congestion (S-bars), Bent Cap 2 .....	251
Figure A3.1. Stress-Strain-EZV Curves of CNFA ‘A’ at 21°C, 30°C, and 40°C .....	273
Figure A3.2. Stress-Strain-EZV Curves of CNFA ‘B’ at 21°C, 30°C, and 40°C.....	274
Figure A3.3. Stress-Strain-EZV Curves of CNFA ‘C’ at 21°C, 30°C, and 40°C.....	275
Figure A3.4. Stress-Strain-EZV Curves of CNFA ‘E’ at 21°C, 30°C, and 40°C.....	276

Figure A3.5. Stress-Strain-EZV Curves of CNFA ‘F’ at 21°C, 30°C, and 40°C.....	277
Figure A3.6. Stress-Strain-EZV Curves of CNFA ‘H’ at 21°C, 30°C, and 40°C .....	278
Figure A3.7. Stress-Strain-EZV Curves of CNFA ‘J’ at 21°C, 30°C, and 40°C.....	279
Figure A3.8. Stress-Strain-EZV Curves of CNFA ‘K’ at 21°C, 30°C, and 40°C .....	280
Figure A3.9. Stress-Strain-EZV Curves of CNFA ‘L’ at 21°C, 30°C, and 40°C.....	281
Figure A3.10. Stress-Strain-EZV Curves of CNFA ‘M’ at 21°C, 30°C, and 40°C.....	282
Figure A3.11. Stress-Strain-EZV Curves of CNFA ‘N’ at 21°C, 30°C, and 40°C .....	283
Figure A3.12. Stress-Strain-EZV Curves of CNFA ‘O’ at 21°C, 30°C, and 40°C .....	284
Figure A3.13. Stress-Strain-EZV Curves of CNFA ‘P’ at 21°C, 30°C, and 40°C.....	285
Figure A3.14. S-E-T Models of CNFAs Embedded in Bent Cap 2 and Bent Cap 7 .....	292
Figure A6.1 Sensor Box Installed on Bent Cap 2.....	321
Figure A6.2. Strain Gauges and CNFA Instrumented on Bent Cap 2 .....	327
Figure A6.3. 3D Visualization of Instrumented Sensors on Rebar Cage of Bent Cap 2 .....	331
Figure A6.4. Sensor Box Installed on Bent Cap 7 .....	332
Figure A6.5. Strain Gauges and CNFA instrumented on Bent Cap 7 .....	337
Figure A6.6. 3D Visualization of Instrumented Sensors on Rebar Cage of Bent Cap 7 .....	341

## LIST OF TABLES

Table 1.1. Details of Bent Cap for Instrumentation.....	5
Table 2.1. Material Parameters for the Concrete Damaged Plasticity Model .....	16
Table 2.2. Identified Locations of Strain Gauges in Bent Cap 2 .....	25
Table 2.3. Identified Location of CNFAs in Bent Cap 2 .....	27
Table 2.4. Identified Locations of Strain Gauges in Bent Cap 7 .....	65
Table 2.5. Identified Location of CNFAs in Bent Cap 7 .....	67
Table 3.1 Compressive strength of 28-day Cured CNFA Samples .....	98
Table 3.2. Locations of Strain Gauges Installed in Bent Cap 2.....	100
Table 3.3. Locations of CNFAs Installed in Bent Cap 2 .....	102
Table 3.4. Location of Strain Gauges Installed in Bent Cap 7 .....	106
Table 3.5. Location of CNFAs Installed in Bent Cap 7 .....	108
Table 4.1. Trucks Position in Dynamic Test-2 (Case 9) on Bent Cap 2.....	134
Table 4.2. Trucks Position in Dynamic Test-2 (Case 9) on Bent Cap 7.....	156
Table 4.3. West Face Displacement of Bent Cap 7 for Case 9 from Dynamic Test-2 .....	157
Table 4.4. Compressive Stress on Exterior Loading Pad of Bent Cap 2 in Static Tests.....	164
Table 4.5. Compressive Stress on Exterior Loading Pad of Bent Cap 7 in Static Tests.....	164
Table 4.6. Compressive Stress on North side Exterior Loading Pad of Bent Cap 2 and Bent Cap 7 in Static Tests .....	165
Table 4.7. Performance Comparison of Bent Cap 2 and Bent Cap 7 in Static Tests.....	172

Table 5.1. Compressive Strength of Bent Cap 2 and Bent Cap 7 .....	176
Table 5.2. Material Parameters of the Concrete Damaged Plasticity Model of Bent Cap 2 and Bent Cap 7 .....	180
Table 5.3. Performance of CNFAs in Tension Zone (Location-3) of Bent Cap 2.....	197
Table 5.4. Performance of SSCNFAs in Tension Zone (Location-3) of Bent Cap 7 .....	219
Table 5.5. Tensile Strains on G bars of Bent Cap 2 and Bent Cap 7 .....	227
Table A1.1. Strain Values in Cases 1 to 15 of Bent Cap 2 for 31 Locations.....	255
Table A1.2. Maximum Concrete Strain in Tension and Compression and Displacement at West Face of ITBC 2 in Cases 1 to 15 .....	258
Table A1.3. CNFA Stress Values of Loading Cases 1 to 15 of Bent Cap 2.....	259
Table A1.4. Strain Values at Five Positions for Case 3 of Bent Cap 2 under Static Test-2 .....	260
Table A1.5. Maximum Concrete Strains in Tension and Compression and Displacement of Five Positions of Four-Trucks Load in Case 3 at West Face of ITBC .....	261
Table A1.6. CNFA Stress Values of Five Positions of Four-Trucks Load in Case 3.....	261
Table A1.7. Strain Values at Five Positions for Case 9 of Bent Cap 2 under Four-Truck Loading .....	262
Table A1.8. Maximum Concrete Strains in Tension and Compression and Displacement of Five Positions of Four-Trucks Load in Case 9 at West Face of ITBC .....	263
Table A1.9. CNFA Stress Values of Five Positions of Four-Trucks Load in Case 9.....	263
Table A2.1. Strain Values in Cases 1 to 15 of Bent Cap 7 for 30 Locations.....	264
Table A2.2. Maximum Concrete Strain in Tension and Compression and Displacement at West Face of ITBC 7 in Cases 1 to 15 .....	267

Table A2.3. CNFA Stress Values of Loading Cases 1 to 15 of Bent Cap 7.....	268
Table A2.4. Strain Values for Case 9 of Bent Cap 7 under Four-Truck Loading at Five Positions .....	269
Table A2.5. Maximum Tensile and Compressive Concrete Strains and Displacements for Case 9 of Bent Cap 7 under Four-Truck Loading at Five Positions.....	270
Table A2.6. CNFA Stress Values for Case 9 of Bent Cap 7 under Four-Truck Loading at Five Positions.....	270
Table A2.7. Strain Values for Case 14 of Bent Cap 7 under Four-Truck Loading at Five Positions .....	271
Table A2.8. Maximum Tensile and Compressive Concrete Strains and Displacements for Case 14 of Bent Cap 7 under Four-Truck Loading at Five Positions.....	272
Table A2.9. CNFA Stress Values for Case 14 of Bent Cap 7 under Four-Truck Loading at Five Positions.....	272
Table A3.1. Constants of S-E-T Models of CNFAs Embedded in Bent Cap 2.....	293
Table A3.2. Constants of S-E-T Models of CNFAs Embedded in Bent Cap 7.....	293
Table A3.3. Temperature Recorded During Static Load Tests on Bent Cap 2.....	294
Table A3.4. Temperature Recorded During Static Load Tests on Bent Cap 7.....	295
Table A4.1. Rebar Strains from Load Test and FE Simulation from Static Test-1, Case 1 on Bent Cap 2.....	296
Table A4.2. West Face Displacements of Bent Cap 2 from Static Test-1 for Case 1 .....	297
Table A4.3. Average Compressive Stresses on Concrete from Load Tests and FE Simulation of Static Test-1, Case 1 of Bent Cap 2 .....	297

Table A4.4. Rebar Strains from Load Test and FE Simulation from Static Test-1, Case 14 on Bent Cap 2 .....	298
Table A4.5. West Face Displacements of Bent Cap 2 from Static Test-1 for Case 14 .....	299
Table A4.6. Average Compressive Stresses on Concrete from Load Tests and FE Simulation of Static Test-1, Case 14 of Bent Cap 2 .....	299
Table A4.7. Rebar Strains from Load Test and FE Simulation from Static Test-2, Case 3 at Position 3 and Position 4 on Bent Cap 2.....	300
Table A4.8. West Face Displacements of Bent Cap 2 from Static Test-2 for Case 3 .....	301
Table A4.9. Average Compressive Stresses on Concrete from Load Tests and FE Simulation of Static Test-2, Case 3 of Bent Cap 2 .....	301
Table A4.10. Rebar Strains from Load Test and FE Simulation from Static Test-2, Case 9 at Position 3 and Position 4 on Bent Cap 2.....	302
Table A4.11. West Face Displacements of Bent Cap 2 from Static Test-2 for Case 9 .....	303
Table A4.12. Average Compressive Stresses on Concrete from Load Tests and FE Simulation of Static Test-2, Case 9 of Bent Cap 2 .....	303
Table A4.13. Rebar Strains from Load Test and FE Simulation of Dynamic Test-1, Case 9 of Bent Cap 2 .....	304
Table A4.14. West Face Displacements of Bent Cap 2 from Dynamic Test-1, Case 9 .....	305
Table A4.15. Rebar Strains from Load Test and FE Simulation of Dynamic Test-1, Case 14 of Bent Cap 2.....	306
Table A4.16. West Face Displacements of Bent Cap 2 from Dynamic Test-1, Case 14 .....	307
Table A5.1. Rebar Strains from Load Test and FE Simulation from Static Test-1, Case 1 on Bent Cap 7 .....	308

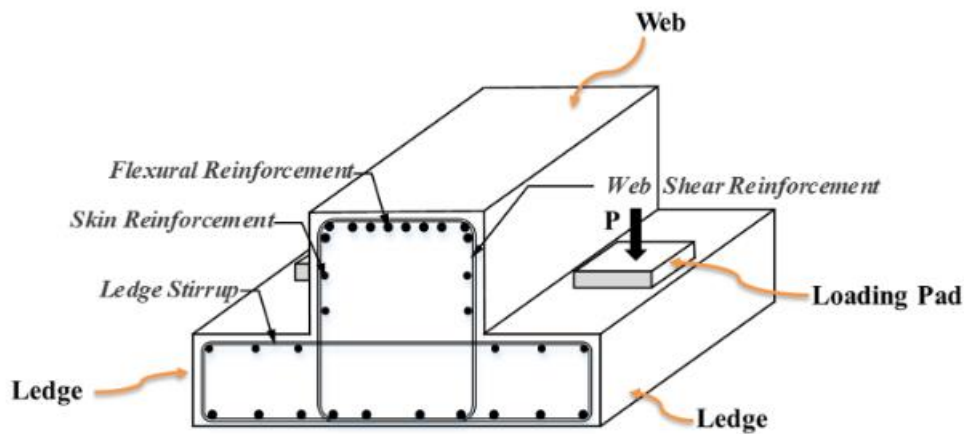
Table A5.2. West Face Displacements of Bent Cap 7 from Load Test and FE Simulation of Static Test-1 for Case 1 .....	309
Table A5.3. Average Compressive Stresses on Concrete from Load Tests and FE Simulation of Static Test-1, Case 1 of Bent Cap 7 .....	309
Table A5.4. Rebar Strains from Load Test and FE Simulation from Static Test-1, Case 11 on Bent Cap 7 .....	310
Table A5.5. West Face Displacements of Bent Cap 7 from Load Test and FE Simulation of Static Test-1 for Case 11 .....	311
Table A5.6. Average Compressive Stresses on Concrete from Load Tests and FE Simulation of Static Test-1, Case 1 of Bent Cap 7 .....	311
Table A5.7. Rebar Strains from Load Test and FE Simulation from Static Test-2, Case 9 at Position 3, and Position 4 on Bent Cap 7.....	312
Table A5.8. West Face Displacements of Bent Cap 7 in Static Test-2 for Case 9.....	313
Table A5.9. Average Compressive Stresses on Concrete from Load Tests and FE Simulation of Static Test-2, Case 9 of Bent Cap 7 .....	313
Table A5.10. Rebar Strains from Load Test and FE Simulation from Static Test-2, Case 14 at Position 3, and Position 4 on Bent Cap 7.....	314
Table A5.11. West Face Displacements of Bent Cap 7 in Static Test-2 for Case 14.....	315
Table A5.12. Average Compressive Stresses on Concrete from Load Tests and FE Simulation of Static Test-2, Case 14 of Bent Cap 7 .....	315
Table A5.13. Rebar Strains from Load Test and FE Simulation of Dynamic Test-1, Case 9 of Bent Cap 7 .....	316
Table A5.14. West Face Displacements of Bent Cap 7 from Dynamic Test-1, Case 9 .....	317

Table A5.15. Rebar Strains from Load Test and FE Simulation of Dynamic Test-1, Case 14 of Bent Cap 7.....	318
Table A5.16. West Face Displacements of Bent Cap 7 from Dynamic Test-1, Case 14 .....	319
Table A6.1. Locations of Strain Gauges Installed in Bent Cap 2 - South Side .....	322
Table A6.2. Locations of CNFAs Installed in Bent Cap 2- South Side .....	324
Table A6.3. Locations of Strain Gauges Installed in Bent Cap 2 - North Side .....	325
Table A6.4. Locations of CNFAs Installed in Bent Cap 2 - North Side .....	326
Table A6.5. Locations of Strain Gauges Installed in Bent Cap 7 .....	333
Table A6.6. Locations of CNFAs Installed in Bent Cap 7 .....	335

# 1 INTRODUCTION

## 1.1 PROJECT OVERVIEW

A highway bridge system is comprised of superstructure, substructure, and foundation. A bent cap provides the intermediary function of transferring vertical loads and lateral loads from the superstructure to the foundation through the column. The ITBC is constructed in the form of an inverted T (Figure 1.1), which has a ledge on both sides of the stem that supports the girders. The cross-section of ITBC consists of a web and ledge. The web transfers the shear forces, and the ledge serves in transferring the girder load to the web. Such ITBC reduces the elevation of bridges and improves the clearance beneath the girders (Gomez, 2012).



**Figure 1.1. Component of ITBC** (Sapath Roy et al., 2021)

Inverted-T Bridge Cap (ITBC) is a widely accepted structural element in bridge structures over conventional rectangular bent caps (Roy, 2019). As elaborated in TxDOT Project 0-6905 (Wang et al., 2020), unlike the traditional top-loaded beam structures, the force transfer mechanism of the skewed ITBC is as follows: (1) the loads are transferred from the ledge to the web in the transverse direction through the vertical hanger reinforcements; (2) the loads are transferred into the web section and reach the supports in the longitudinal direction (Zhou et al., 2020). The ITBC is aesthetically pleasing and provides vertical clearance to the bridge. In addition, the ITBC provides the option of skewed geometry for practical applications to address the landscaping requirements, such as in road systems, railways, and waterways that are not perpendicular to each other at the intersection. Another significant advantage of the ITBC system is its usage of precast

beams, which can be quickly assembled on-site without any extra formwork (Snyder, 2010). The skew inverted-T bent caps are commonly adopted in the state of Texas for increased bridge clearance, reduced elevation of bridges, lower abutments, larger spans with increased clearance, and aesthetics. Despite the benefits, the structural performance of the ITBC requires special attention during the design, construction, and service period. The unequal loading position on the cantilevered skewed ledge induces a three-dimensional flexural-shear-torsional combined load and complex cracking problem (Wang et al., 2020). Several experimental studies were conducted on ITBC specimens. Mirza et al. defined six modes of failures of the ITBC. The six modes are flexure failure, shear failure, torsion failure, punching shear failure, shear friction failure, and hanger failure (Mirza & Furlong, 1983, 1985). Zhu and Hsu investigated the crack control of ITBCs and predicted the diagonal crack widths observed in tests based on a two-dimensional analytical model (Hsu & Zhu, 2005). Ambare and Peterman performed finite element (FE) simulations of inverted-T bridge systems to check the effects of live load distribution on the behavior of the inverted-T bridge system (Ambare & Peterman, 2006). The results were compared to AASHTO LRFD (AASHTO LRFD Bridge Design Specifications., 2014) and AASHTO Standard Specifications (AASHTO Standard Specifications for Highway Bridges, 2002). It was observed that the loading pattern directly affected the bridge system, and the code method was more conservative than the FE method.

The TxDOT Bridge Design Manual allows the design of a bent cap up to 60 degrees skew angle (Texas Department of Transportation, 2020). The skew angle greater than 45 degrees creates additional torsion due to the unsymmetrical location of the loading pads on the ledge. When the live load approaches the ITBC, the reaction from the girder causes torsion toward the approaching loads. As the live load passes the ITBC, the direction of the twist reverses that reaction on the opposite ledge. Further, the torsional moments cause uneven deflection at the end face of a skew ITBC (Roy, 2019).

As per the TxDOT Bridge Design Manual, the hanger and ledge reinforcement should be perpendicular to the centerline of the skew bent (Texas Department of Transportation, 2020). The transverse reinforcement should be placed parallel to the skew angle from the end face of the ITBC to the location of the column. The transition of skew placement of the rebars to straight bars is carried out over the column where the transverse reinforcement is less critical. Figure 1.2 shows the top view of the reinforcement layout of an ITBC with the traditional method. The traditional

method of transverse reinforcing has complexities associated with design and construction that compromises the structural performance of an ITBC. The uneven spacing of transverse rebars (that violates the requirement of maximum and minimum reinforcement spacing), difficulties in the concrete pour, reduction in shear capacity, and early crack appearance are disadvantages of the traditional method.

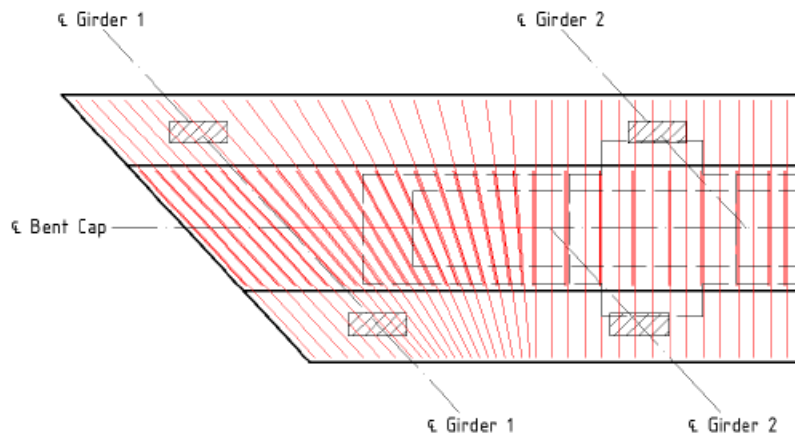


**Figure 1.2. Traditional Method of Transverse Reinforcing in a Skew ITBC (Top View)**  
(Oz, 2020)

Roy et al. investigated an alternative method of skew reinforcing in scaled ITBC specimens with different skew angles ( $0^\circ$ ,  $30^\circ$ ,  $45^\circ$ , and  $60^\circ$ ) (Sapath Roy et al., 2021). Figure 1.3 shows the top view of the skew-reinforcing layout of an ITBC. A total of 13 specimens were experimented on comparing the performance of skew reinforcing of transverse reinforcements with the traditional method. Further, the parametric study of the calibrated models was performed to understand the structural behavior of skew reinforcing in an ITBC (Zhou et al., 2020).

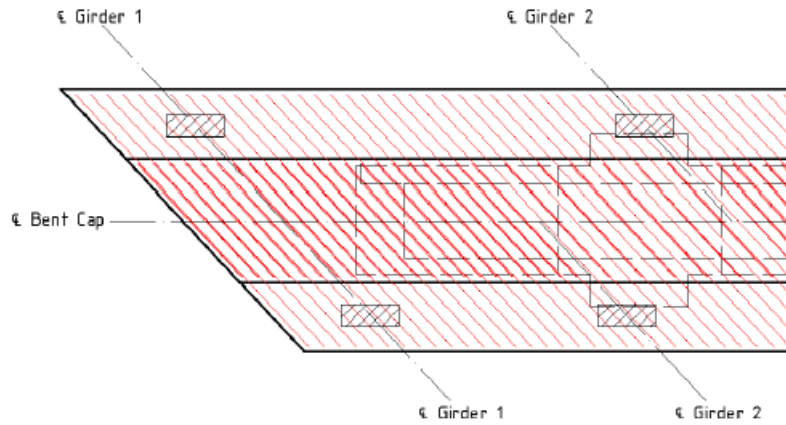


**Figure 1.3. Skew Transverse Reinforcing in a Skew ITBC (Top View) (Oz, 2020)**

Roy et al. concluded that the skew arrangement plan is better than the traditional arrangement of practical applications as the peak load carrying capacity is not compromised, and labor costs are reduced (Roy, 2019). Moreover, the skew-reinforced ITBCs had fewer cracks, smaller crack widths. In addition, design and construction complexities were significantly reduced, and a faster and easier construction process was achieved. Based on these findings, the implementation of the skewed transverse reinforcing in ITBC was suggested to implement the full-scale skewed ITBC. A seven-span bridge on Donigan Road over I-10 near Brookshire in Waller County was selected.

Oz et al. and Wang et al. performed a parametric study on Bent Cap 2, Bent Cap 6, and Bent Cap 7 of the Donigan Road Bridge over I-10 (Oz et al., 2022; Wang et al., 2020). The parametric study investigated the skew angle, the detailing method of the transverse reinforcements (traditional method and skew-reinforcing), the amount of end reinforcements, and the compressive strength of concrete. The parametric study concluded that the skew transverse reinforcements are safe under service and ultimate state loading, achieve better structural performance with notably reduced cost, improve the ultimate capacity of skew ITBC, and lower the design and construction time.

The TxDOT Bridge Detailing Guide updated the transverse reinforcement detailing practices based on TxDOT Research Project 0-6905 (Texas Department of Transportation, 2022a). As per the guideline, transverse reinforcement should be placed along the skew for inverted-T bent caps with skewed ends. The transverse bar in the stem (double S bars) should be used throughout

the bent cap. The spacing of S bars can be increased at the location of the column support to 12 inches maximum. As per the TxDOT Bridge Design Guide, the cap hanger and ledge reinforcement may be aligned to match the cap skew when simpler detailing can be achieved (Texas Department of Transportation, 2022b).

TxDOT Project 0-6905 completed eight tasks to understand the structural behavior of skewed ITBCs. Following the final report submission, the project was extended in February 2019 for the field implementation of skew-reinforcing of transverse rebars. Due to environmental issues, it was decided to place Project 0-6905 on pause at the end of October 2020. The project was resumed in August 2021 as TxDOT Project 0-6905-01 for the controlled load tests to investigate the performance of the skew ITBCs with skew reinforcing.

Bent Cap 2 and Bent Cap 7 are selected for the investigation of skew reinforcing. The details of the bent caps for the instrumentation are presented in Table 1.1.

**Table 1.1. Details of Bent Cap for Instrumentation**

<b>Description</b>	<b>Bent Cap 2</b>	<b>Bent Cap 7</b>
Skew angle	43°	33°
Loading condition	Unsymmetrical dead loading	Unsymmetrical dead loading
Elevation from ground level	18 ft	19 ft
Span length	100 ft (back station)	135 ft (back station)
	135 ft (forward station)	115 ft (forward station)
No. of girders	9 (back station)	15 (back station)
	15 (forward station)	9 (forward station)

Figures 1.4 and 1.5 present the plan view for the layout of Bent Cap 2 and Bent Cap 7 (adopted from the structural design drawings presented by TxDOT).

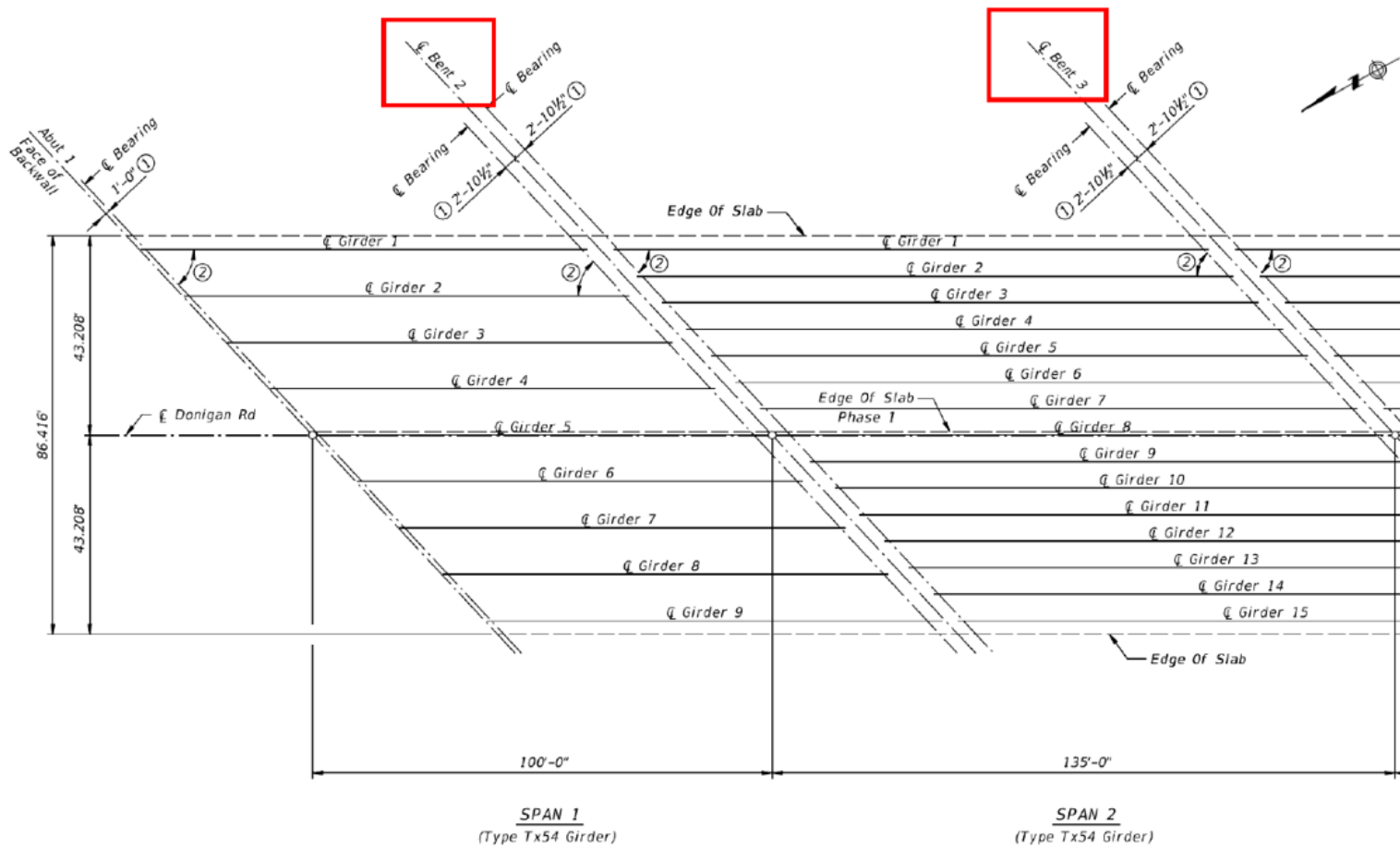


**Figure 1.4 Layout of Bent Cap 2**



## **1.2 PROJECT OBJECTIVES**

The project objectives can be summarized as follows:

1. To understand the overall structural behavior of skewed reinforcements in actual large-scale ITBCs and to determine critical loading patterns during the load tests and crucial sensor locations.
2. To investigate the critical factors that affect the structural performance of the ITBC. The critical factors are skew angle, skew reinforcing of transverse rebars, location of exterior loading pads, and loading cases.
3. To conduct the load test on Donigan Road Bridge to examine the structural integrity and performance of the ITBC.
4. The ITBC test specimens will be modeled in 3D Finite Element software (ABAQUS), and all the test results will be calibrated. Additional parameters that were not considered in the proposed test matrix will be investigated in detail to establish enough databases.
5. The general design recommendations to design skewed ITBC reinforcements in the ITBC will be proposed.
6. Secure the sensor and establish the sensor box for structural health monitoring of the ITBC.

## **1.3 VALUE OF RESEARCH**

The value of research is presented in APPENDIX-7. TxDOT Project 0-6905-01 will provide the following benefits to the TxDOT and other stakeholders:

1. Implementation of skew reinforcing for the transverse rebars could ensure an easier and faster method of construction, which could optimize the construction cost. According to the cost-benefit analysis results, when the skew transverse reinforcement method is preferred over the traditional method, the estimated cost of skewed ITBCs reduces by 11% - 16%, depending on the other design parameters (Wang et al., 2020).
2. Skewed reinforcement would reduce the congestion in the skew region of the bent cap. As a result, proper placement of concrete could be achieved. It would reduce the complexity of detailing the skew region of the bent cap by providing uniform spacing and the same size reinforcing bars. Therefore, fewer working hours and laborers would be required for the fabrication/construction of the ITBC with skewed reinforcement.

3. The peak load-carrying capacity of the ITBC with the skewed transverse reinforcement remains the same, with fewer number of cracks that have a smaller crack width than the traditional method. Hence, the ITBC with skewed transverse reinforcing is resilient with a prolonged service life that will require less maintenance effort when compared to the traditional reinforcing.
4. No research has been undertaken to study the performance of skew transverse reinforcement in the ITBC. A lack of experimental research has thwarted the use of skew reinforcing. Therefore, there are no specific design guidelines for the design of skew reinforcements in inverted-T bent caps, which makes the design unreliable with increased risks of failure. By providing proper design guidelines for different skew angles, high levels of lifetime uncertainties and risks of failure could be prevented. The skew reinforcement approach could reduce the repair and replacement cost and increase reliability, thereby benefiting the TxDOT and other stakeholders financially.
5. Implementation of skew reinforcement in the full-scale ITBC in an actual bridge helped to achieve a higher technology readiness level (TRL 9).
6. Three sensor boxes are installed on the ITBCs to preserve the installed sensors. These sensors can be utilized to monitor the structural performance of ITBCs regularly.

#### **1.4 ORGANIZATION**

This report is divided into seven chapters. Chapter 1 introduces an overview and the objectives of the research in addition to an outline of the report. Chapter 2 focuses on the preliminary finite element simulations of the selected ITBC 2 and ITBC 7 to identify the sensor locations. Chapter 3 presents the calibration of carbon nanofiber aggregates (CNFAs) and the installation of sensors on the rebar cage of bent caps. Chapter 4 presents the load tests on the Donigan Road Bridge, experimental results, and the analysis of the load tests. Chapter 5 focuses on calibrating the finite element models of significant ITBCs and parametric studies to examine the bent caps critically. The general design recommendations based on the experimental findings and parametric study are listed in Chapter 6. All the findings and conclusions of the research program are summarized in Chapter 7.

## **2 PRELIMINARY FINITE ELEMENT SIMULATIONS OF THE SIGNIFICANT ITBCs**

### **2.1 OVERVIEW**

The experimental and analytical studies of Inverted-T Bent Cap (ITBC) in TxDOT Project 0-6905 found that the peak load-carrying capacity of the ITBCs with the skewed reinforcement is the same as the traditional one with fewer cracks that have smaller crack widths. TxDOT Project 0-6905-01 focuses on implementing skewed reinforcement on the Donigan Road Bridge over I-10 near Brookshire in Waller Country. Bent Cap 2 and Bent Cap 7 with skew angles  $43^\circ$  and  $33^\circ$ , respectively, are selected to investigate the performance of skewed reinforcement in the full-scale bridge.

The project team (PT) guided that the point of fixity between the bent cap and columns should be based on actual column and foundation behavior but not on an arbitrary point of fixity in the finite element (FE) models. The FE model includes the deck, girders, ITBC, and four columns. The geometry of the FE model is based on the design drawing provided by the PT. The FE models are analyzed to identify the critical locations of sensors, which are also helpful for structural health monitoring. Further, 15 cases of four-truck loading in Static Test 1 on both bent caps are performed to identify the loading case that produces higher strains on the traverse rebars and greater displacements of the extended region of the bent cap. Moreover, two cases are examined in Static Test 2 at five positions of four-truck loading along the backward and forward span of Bent Cap 2 and Bent Cap 7. Bent Cap 2 and Bent Cap 7 are instrumented with strain gauges and carbon nanofiber aggregates (CNFAs) at critical locations.

### **2.2 THREE-DIMENSIONAL FINITE ELEMENT ANALYSES**

#### **2.2.1 Modeling Scheme**

Three-dimensional (3D) finite element (FE) models of Inverted-T Bent Cap 2 (ITBC 2) and Inverted-T Bent Cap 7 (ITBC 7) were developed using ABAQUS (2020). The point of fixity between the bent cap and columns should be based on actual column and foundation behavior but not on an arbitrary point of fixity. Based on this concept, global FE models with the deck, girders, ITBC, and four supporting columns were developed. The global FE models for ITBC 2 and ITBC 7 are shown in Figures 2.1(a-c) and 2.2(a-c), respectively. The geometry of the FE models is based on the design drawing of the Donigan Bridge provided by TxDOT. The boundary conditions of

columns for both models are provided with fixed support, and girders on ITBCS are assumed to be simply supported.

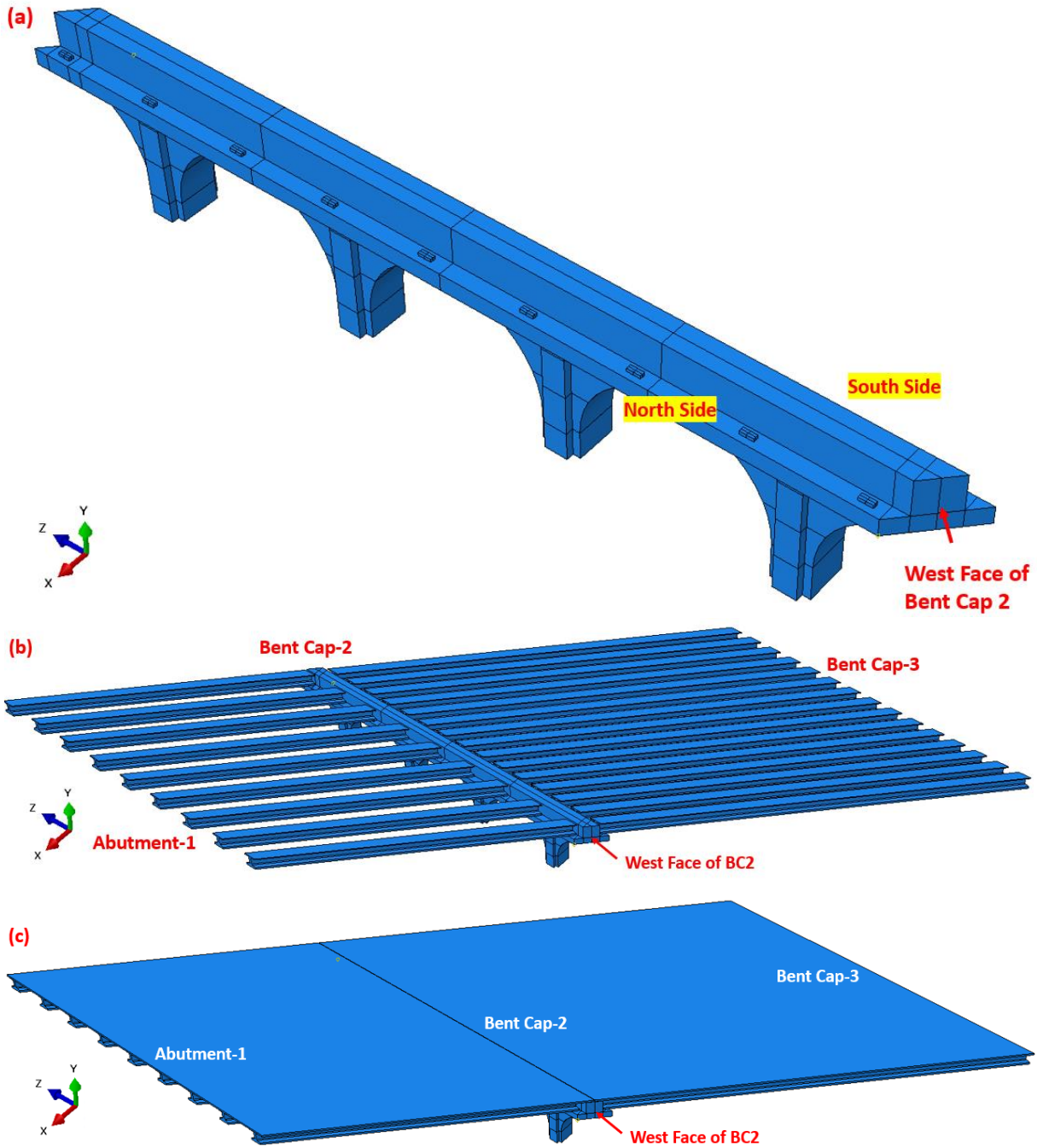


**Figure 2.1. 3D Finite Element Model of Bent Cap 2, including Columns, Girders, and Deck**

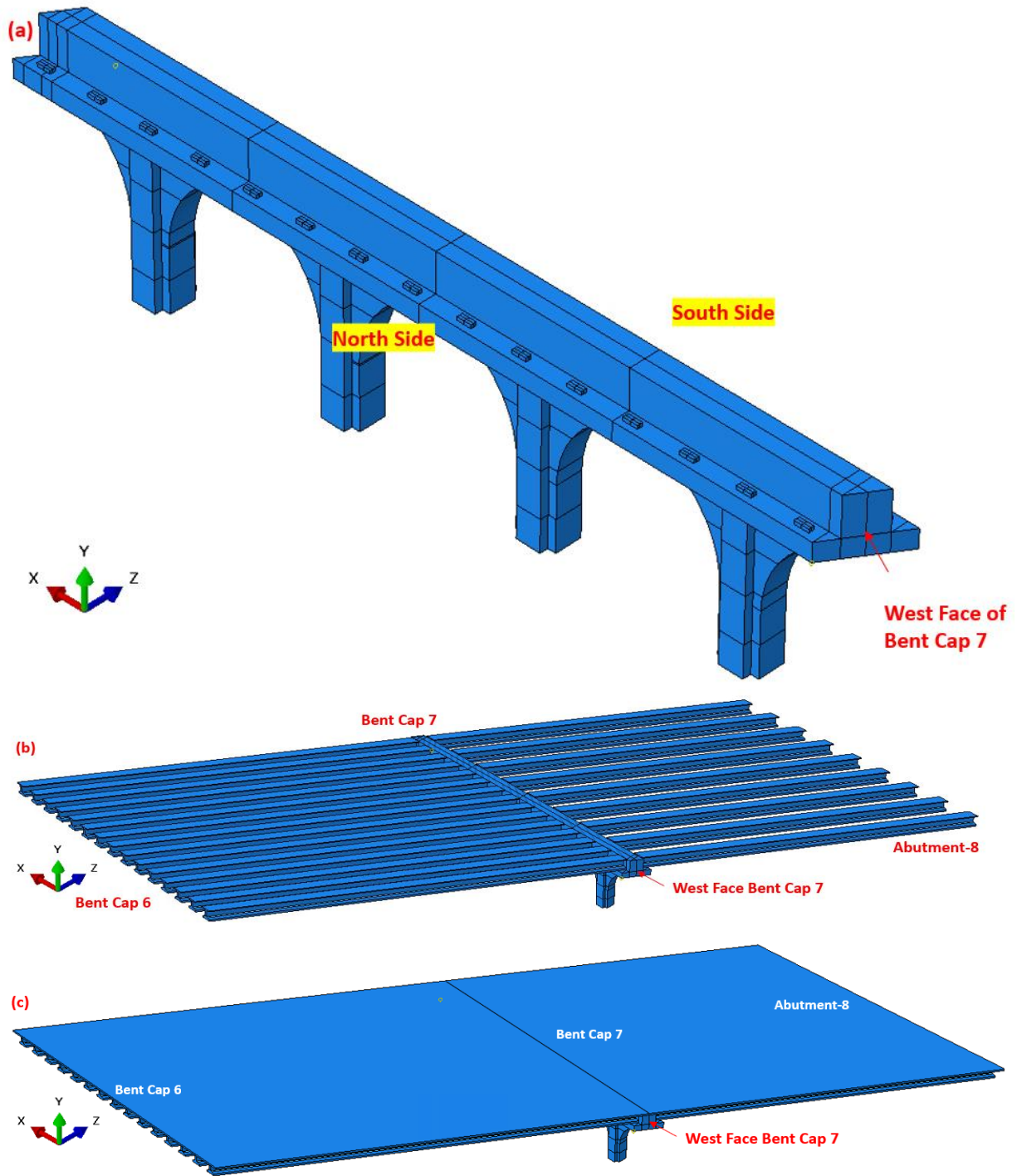
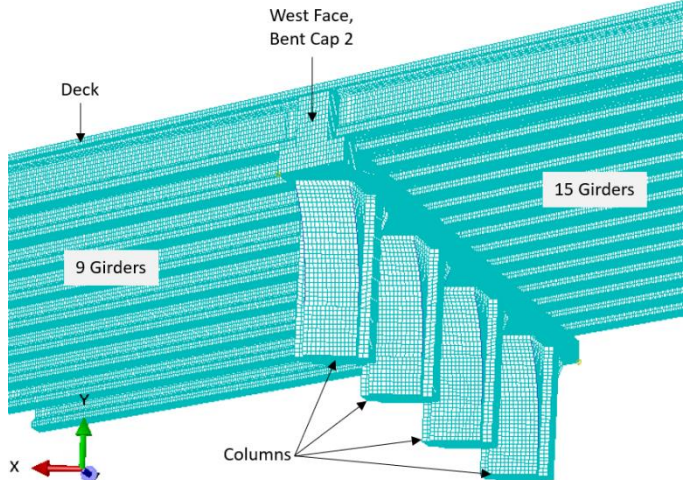
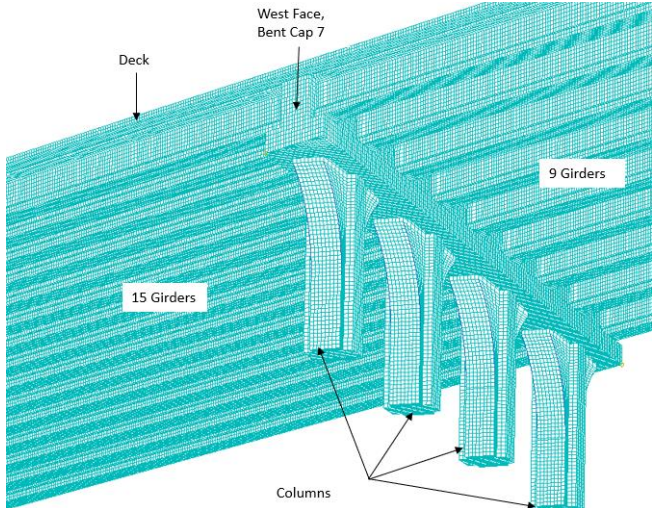


Figure 2.2. 3D Finite Element Model of Bent Cap 7, including Columns, Girders, and Deck

The FE mesh of the simulated models for Bent Cap 2 and Bent Cap 7 are shown in Figures 2.3 and 2.4. The concrete of the structure for both bent caps was meshed using the eight-node, reduced integration, hourglass control solid elements (C3D8R), as shown in Figures 2.5 and 2.6. The two-node linear three-dimensional (3D) truss elements (T3D2) were used to model the reinforcement since it is only subjected to axial force. There are a total of 24 bearing pads and 24 girders on both bent caps, which are supported by 4 columns.



**Figure 2.3. 3D Finite Element Mesh of Simulated Model for Bent Cap 2**



**Figure 2.4. 3D Finite Element Mesh of Simulated Model for Bent Cap 7**

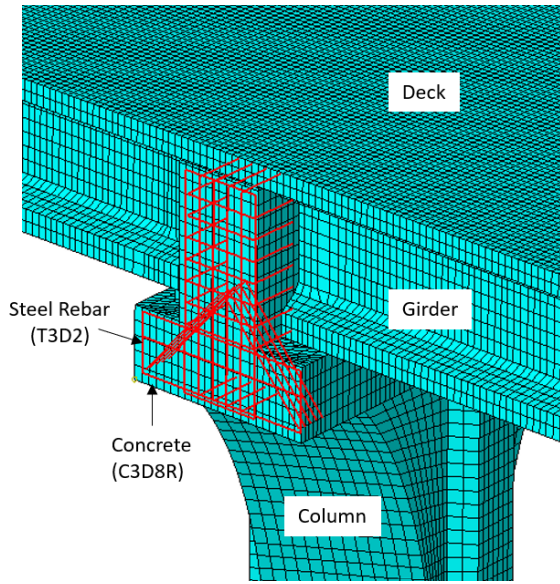


**Figure 2.5. Element Type of Bent Cap 2**

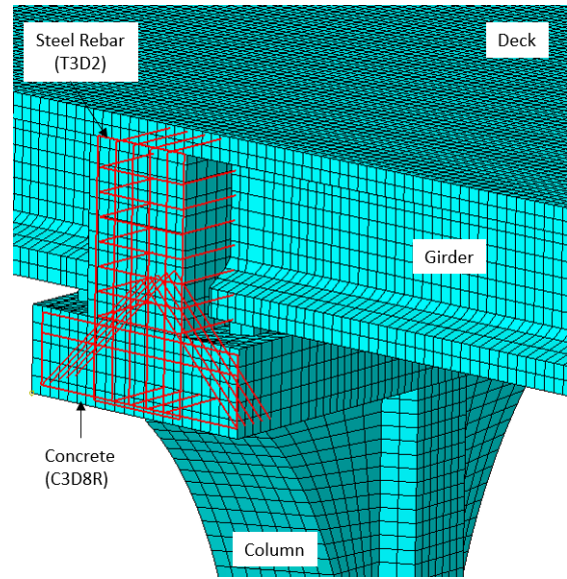


**Figure 2.6. Element Type of Bent Cap 7**

**(C3D8R Solid Element for Concrete and T3D2 Truss Element for Reinforcements)**

### 2.2.2 Materials Models

The Concrete Damaged Plasticity (CDP) model was used as the constitutive model of concrete in the FE model (Lee & Fenves, 1998). The CDP model requires the definition of uniaxial behavior in compression and tension. The stress-strain curves of concrete considered in the constitutive model were adopted from the book “Unified Theory of Concrete Structures” by Thomas T. C. Hsu and Y. L. Mo (Hsu & Mo, 2010).

The uniaxial compression stress-strain behavior of concrete can be defined using the parabolic stress-strain model, as shown in Figure 2.7. Equation 1 is used to develop the compression stress-strain curve.

$$\sigma_c = f'_c \left[ \frac{2\varepsilon_c}{\varepsilon_0} - \left( \frac{\varepsilon_c}{\varepsilon_0} \right)^2 \right] \quad (1)$$

In ABAQUS, the model of concrete (Lubliner et al., 1989) requires the definitions of initial elastic modulus  $E_c$  and Poisson ratio  $\nu$ . The initial elastic modulus  $E_c$  can be calculated using the AASHTO empirical equation (AASHTO LRFD Bridge Design Specifications., 2014):

$$E_c = 57000 \sqrt{f'_c} \text{ (psi)} \quad (2)$$

The Poisson ratio of concrete under uniaxial compressive stress ranges from about 0.15 to 0.22, with a representative value of 0.19 or 0.2 (*AASHTO LRFD Bridge Design Specifications.*, 2014). In this report, the Poisson ratio of concrete is assumed to be  $\nu = 0.2$ .

Equations 3 and 4 are used to develop the tensile stress-strain curve (Figure 2.8).

Ascending branch:

$$\sigma_c = E_c \epsilon_c \quad \text{if } \epsilon_c \leq \epsilon_{cr} \quad (3)$$

Descending branch:

$$\sigma_c = f_{cr} \left( \frac{\epsilon_{cr}}{\epsilon_c} \right)^{0.4} \quad \text{if } \epsilon_c > \epsilon_{cr} \quad (4)$$

where  $E_c$  is the elastic modulus of concrete,  $\epsilon_{cr}$  is the cracking strain of concrete taken as 0.00008, and  $f_{cr}$  is the cracking stress of concrete taken as  $0.00008E_c$ .

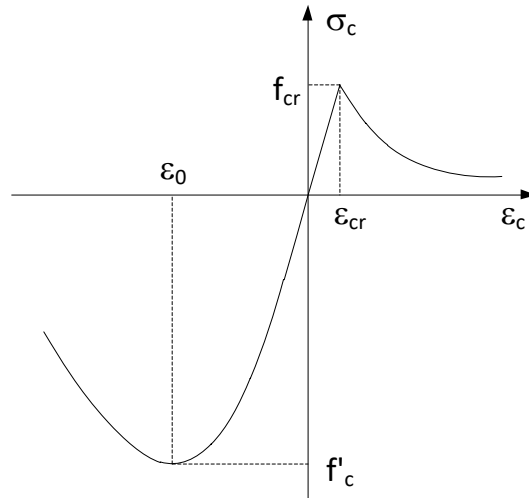


**Figure 2.7. Stress-Strain Curves of Concrete in Tension and Compression**

The stress-strain curve of the reinforcing bars is assumed to be perfect elasto-plastic as shown in Figure 2.8. In the ABAQUS program, the bond-slip effect between concrete and steel is neglected and perfect bonding is assumed. In order to properly model the steel bars, the cross-section area, position, and orientation of each steel bar within the concrete element need to be specified.

Elastic branch:

$$f_s = E_s \epsilon_s \quad \epsilon_s \leq \epsilon_y \quad (5)$$

Plastic branch:

$$f_s = f_y \epsilon_s > \epsilon_y \quad (6)$$

where  $E_s$  is the elastic modulus of steel taken as 29000 ksi and  $\epsilon_y$  is the yielding strain of steel.

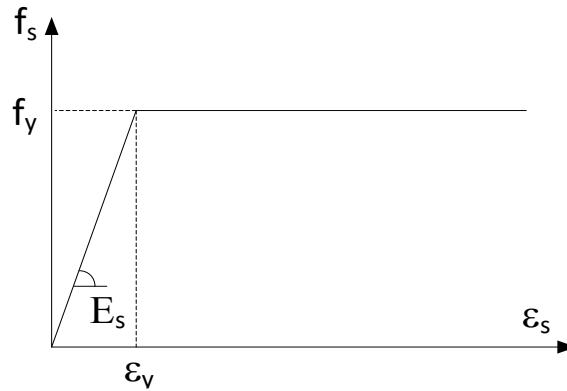


**Figure 2.8. Stress-Strain Curve of Mild Steel**

The details of the material parameters of the concrete damaged plasticity model for full-scale bent caps are listed in Table 2.1.

**Table 2.1. Material Parameters for the Concrete Damaged Plasticity Model**

Concrete grade	Young's modulus (ksi)	Poisson's ratio	Tensile strength (ksi)	Density (lb/ft <sup>3</sup> )	Dilation angle (°)	Flow potential eccentricity	K
5 ksi	4031	0.2	0.325	150	31	0.1	0.6667

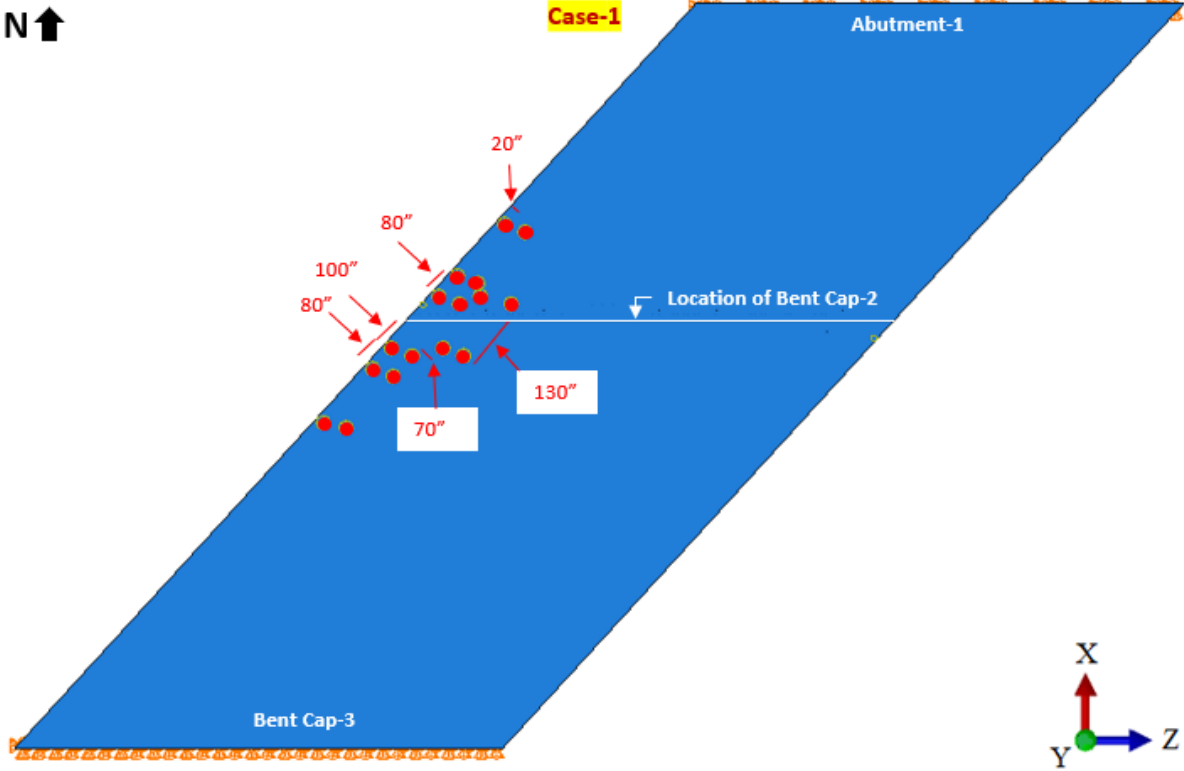
### 2.3 BENT CAP 2

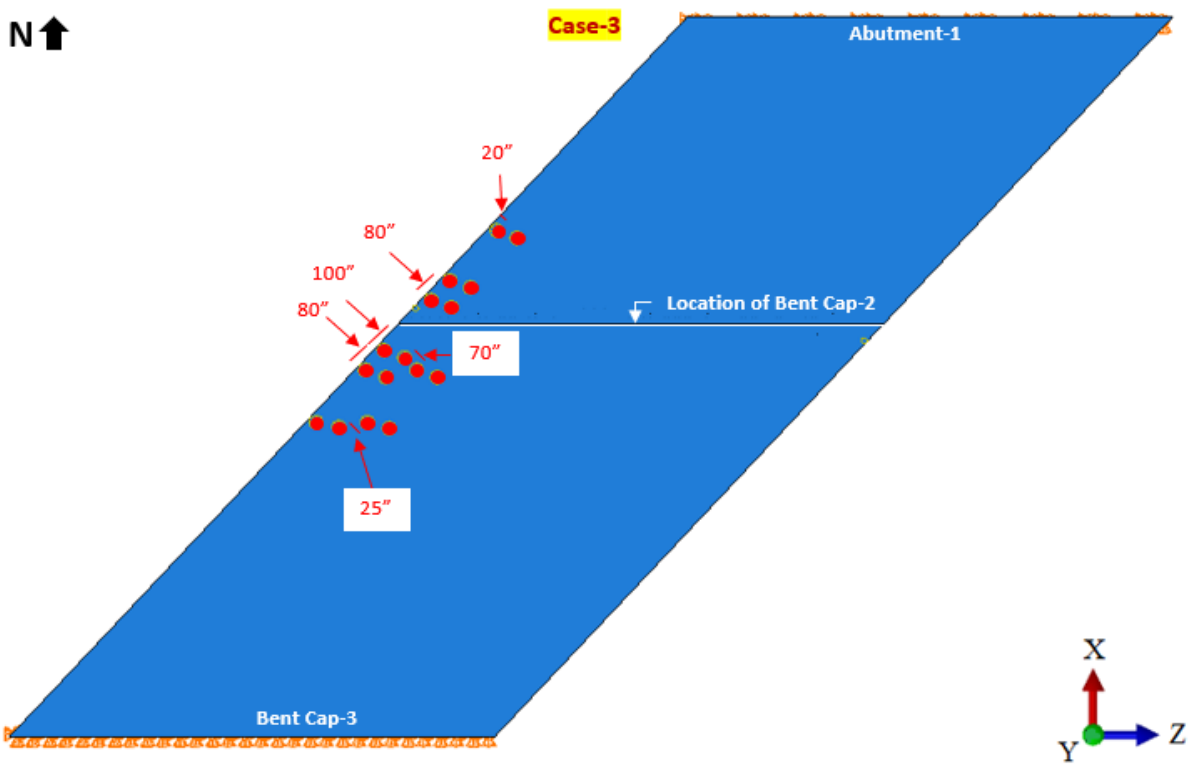
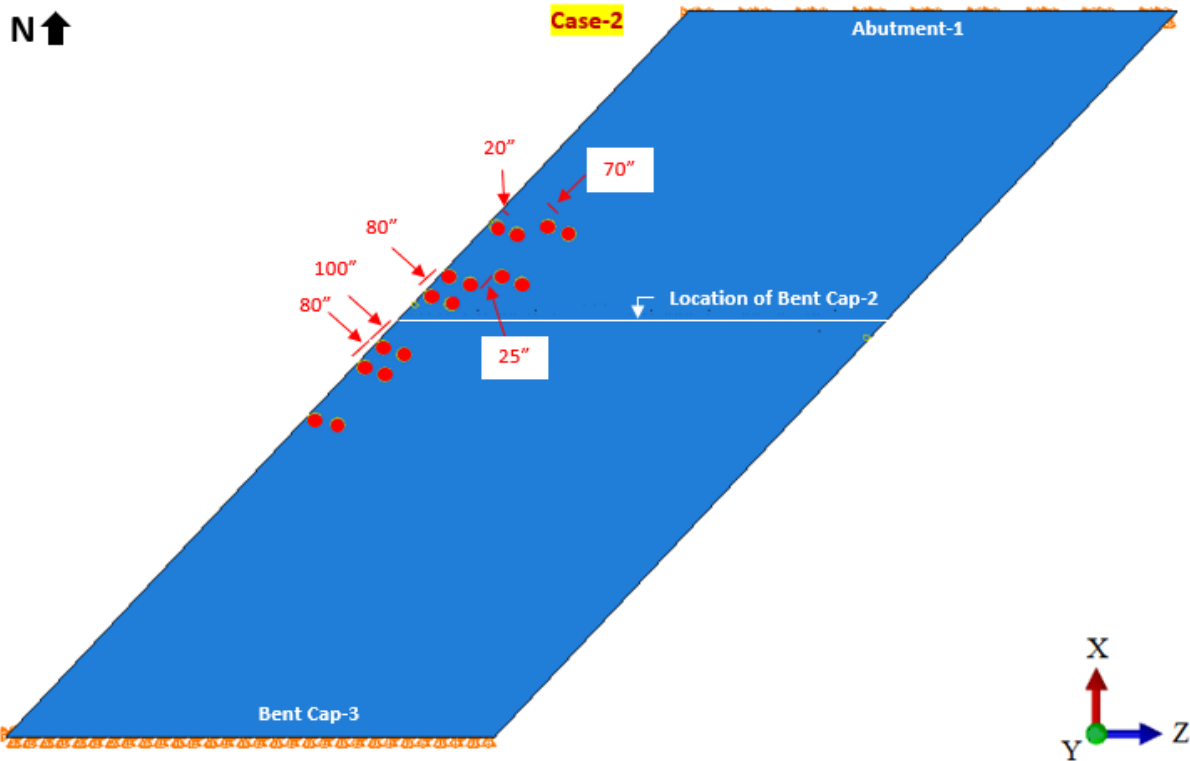
The finite element simulation of Bent Cap 2 is based on the four trucks loading. The vertical loads from four trucks with 43.2 kips each are applied on top of the bridge deck. Point loads for front tires and rear tires are 11.0 kips and 32.2 kips, respectively.

#### 2.3.1 Static Test-1 Finite Element Simulation

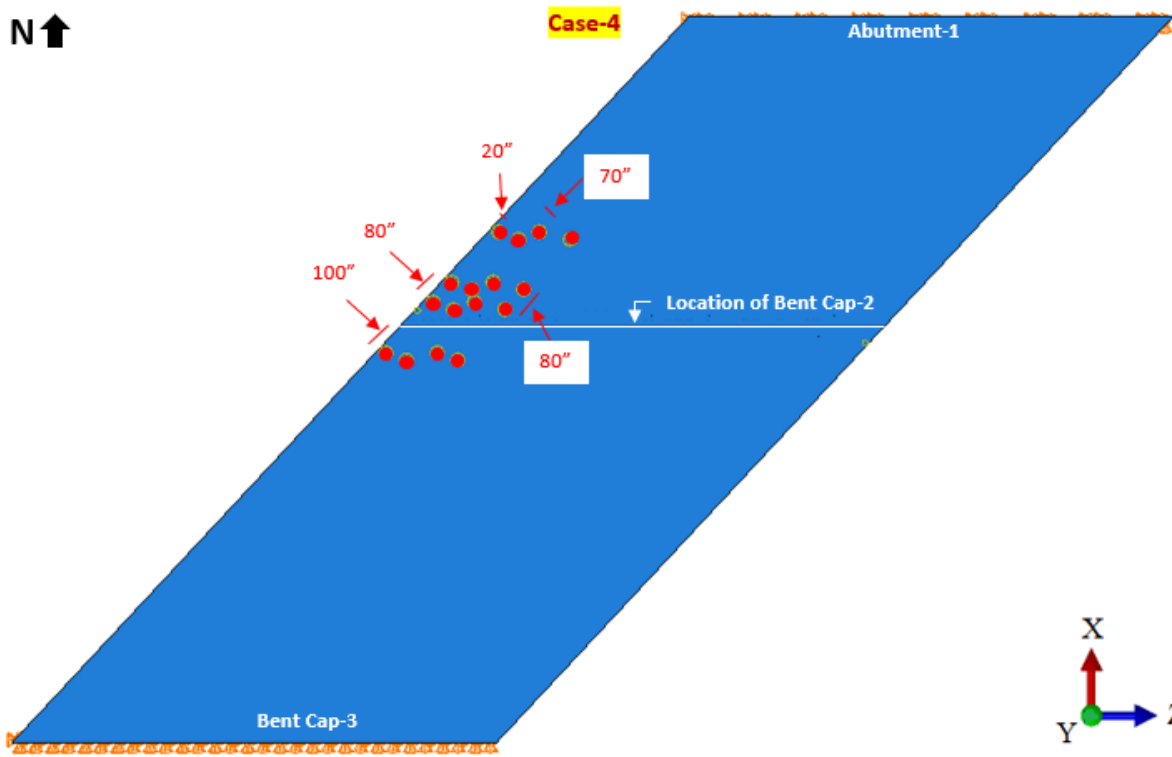
There are 15 cases of four-truck loading simulated on the global finite element model for Bent Cap 2. The extended region and interface between the ledge and stem of the skewed ITBC are critical regions in the ITBC (Sapath Roy et al., 2021; Sapath et al., 2019; Zhou et al., 2020).

These 15 simulations are focused on observing the strain on the extended regions. The location of the front tires and rear tires of the loading trucks are shown in Figure 2.9.

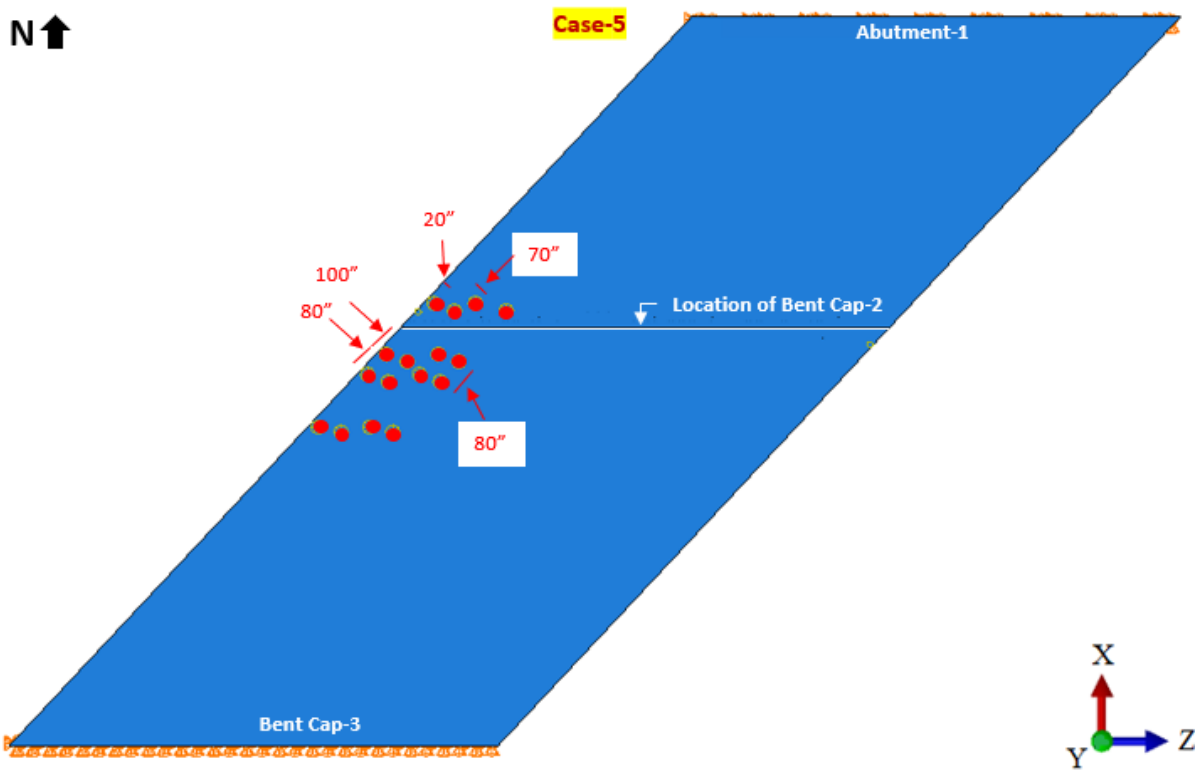


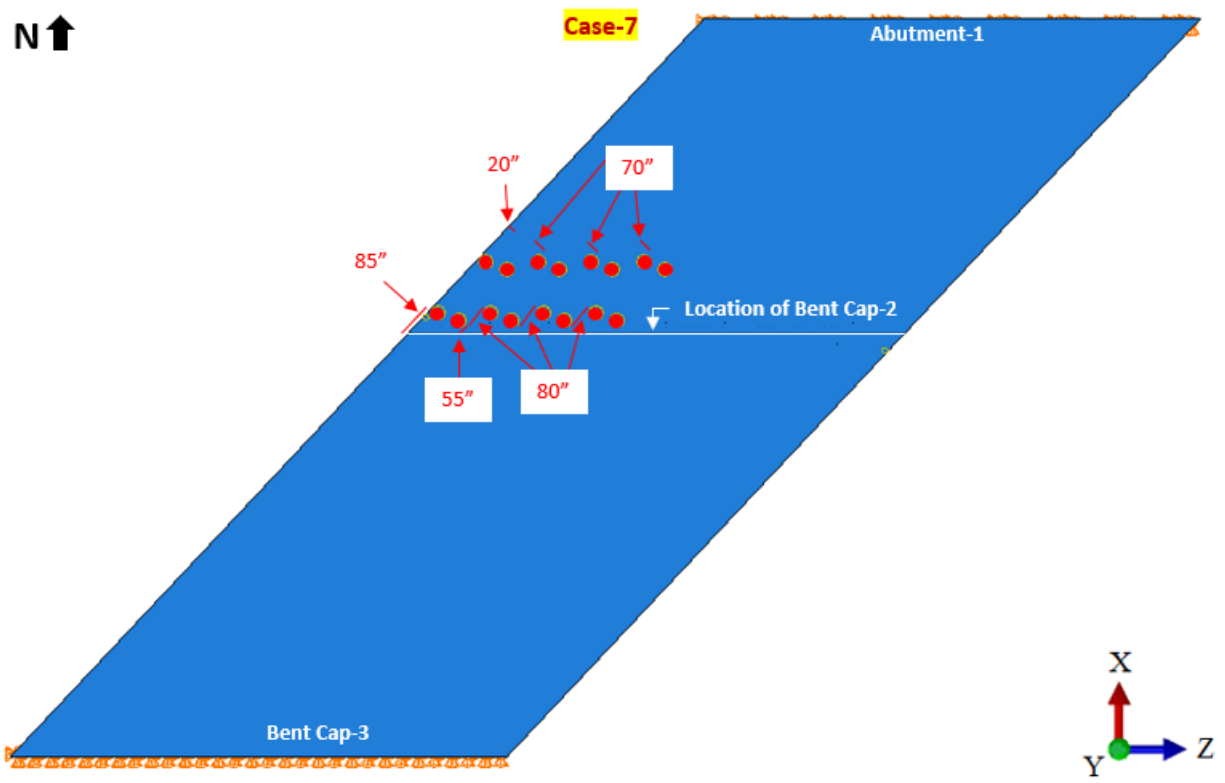
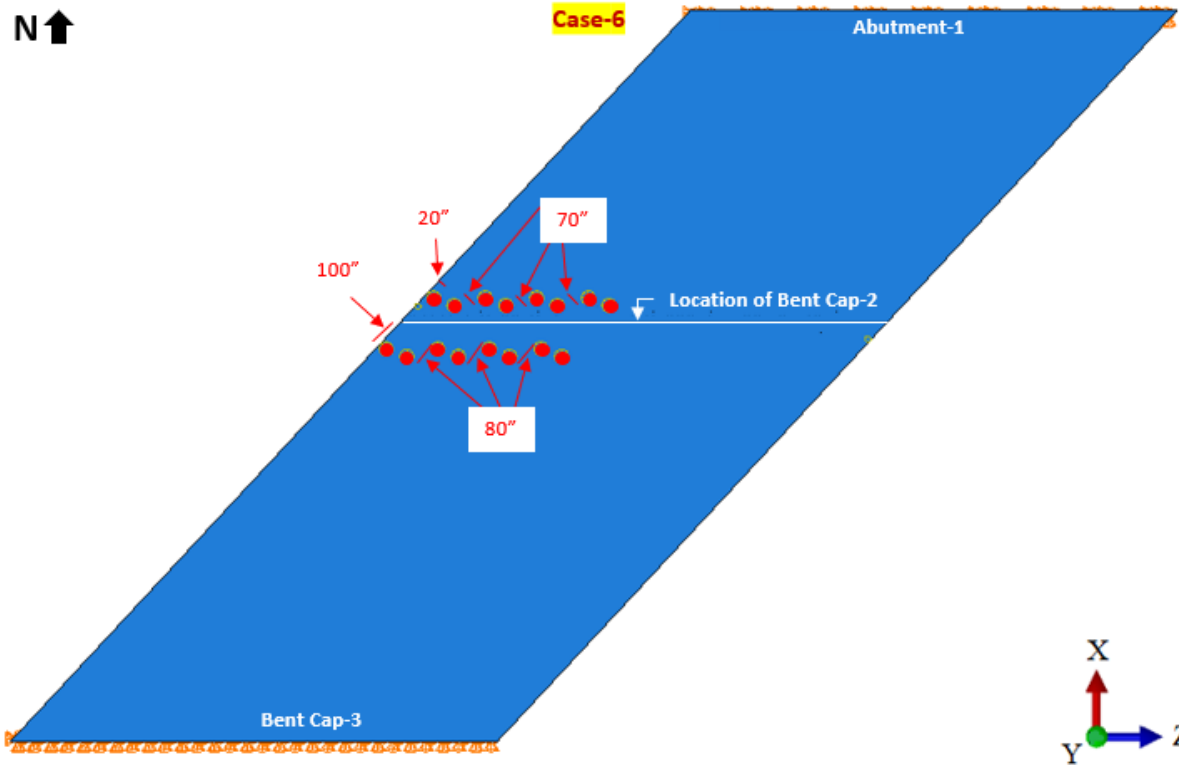


N ↑

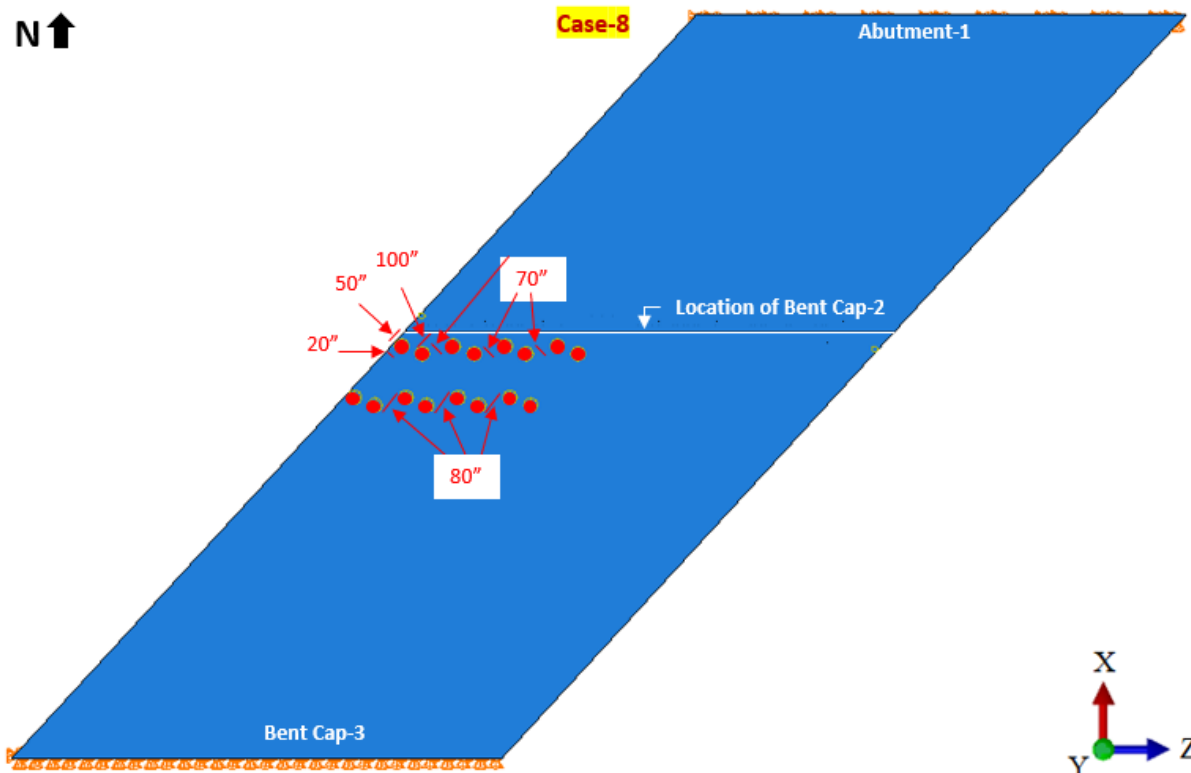


N ↑

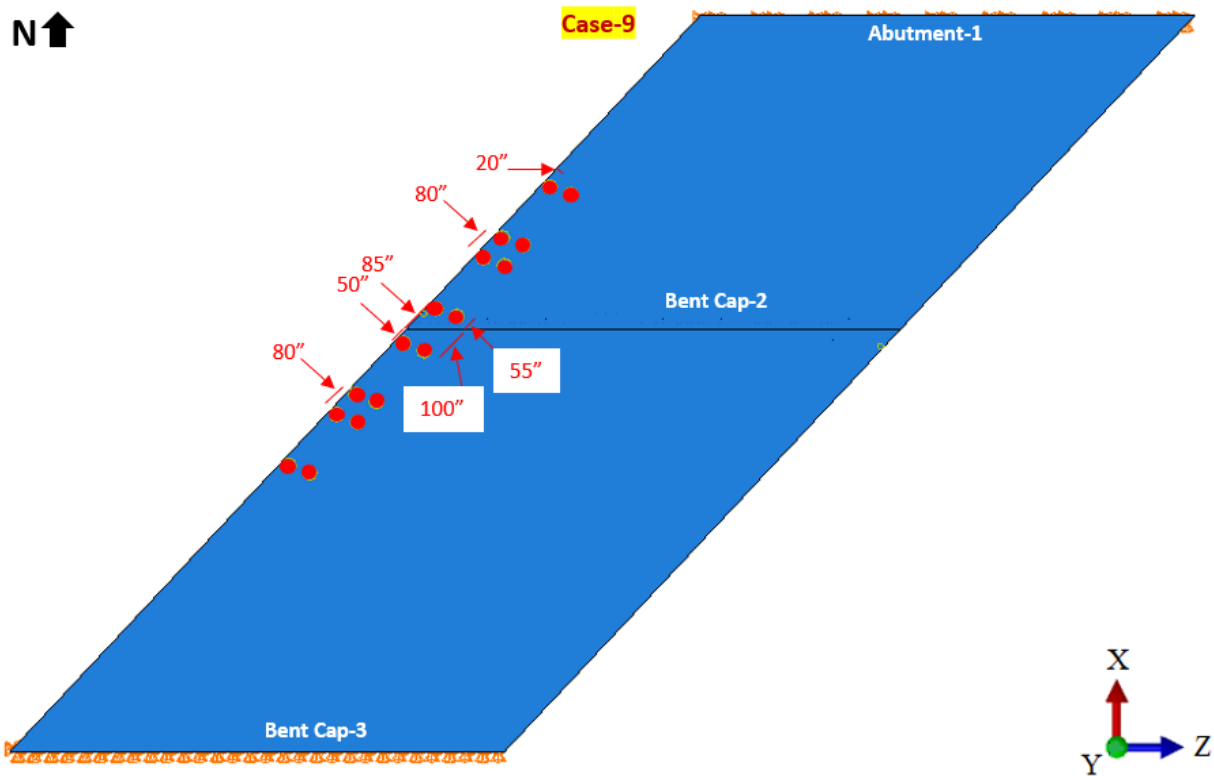




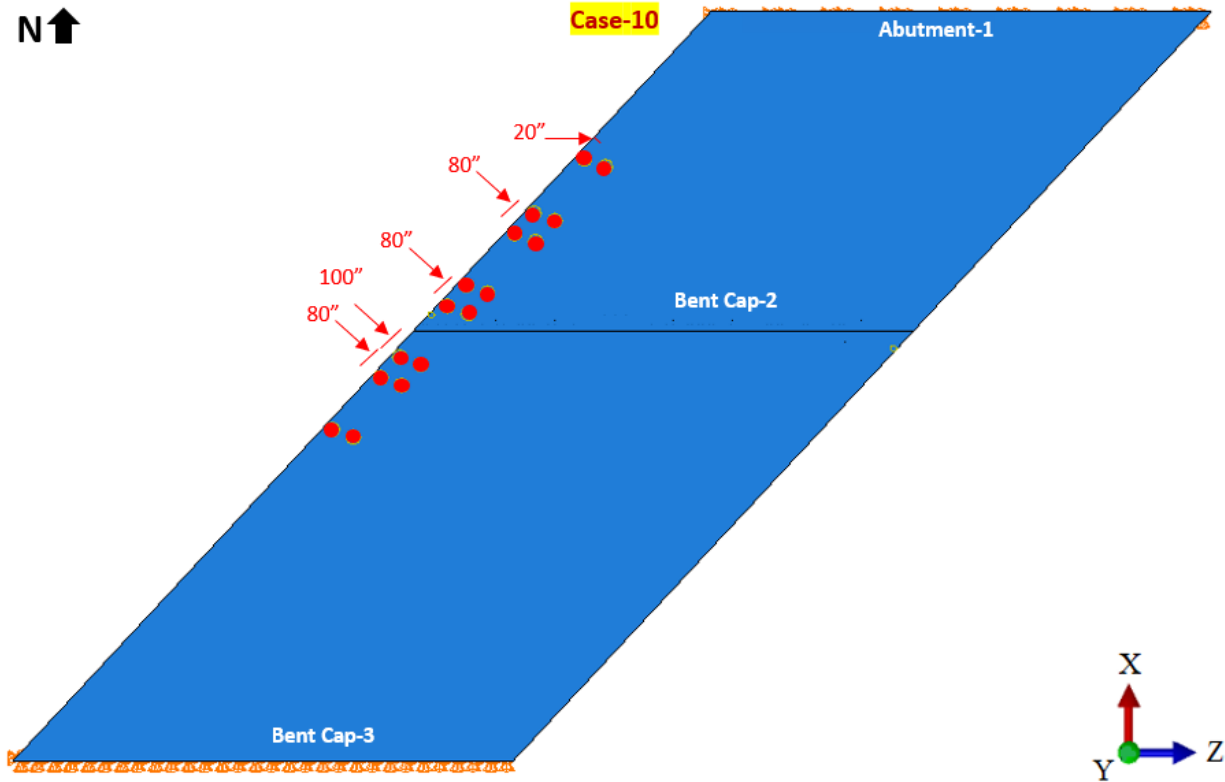
N ↑



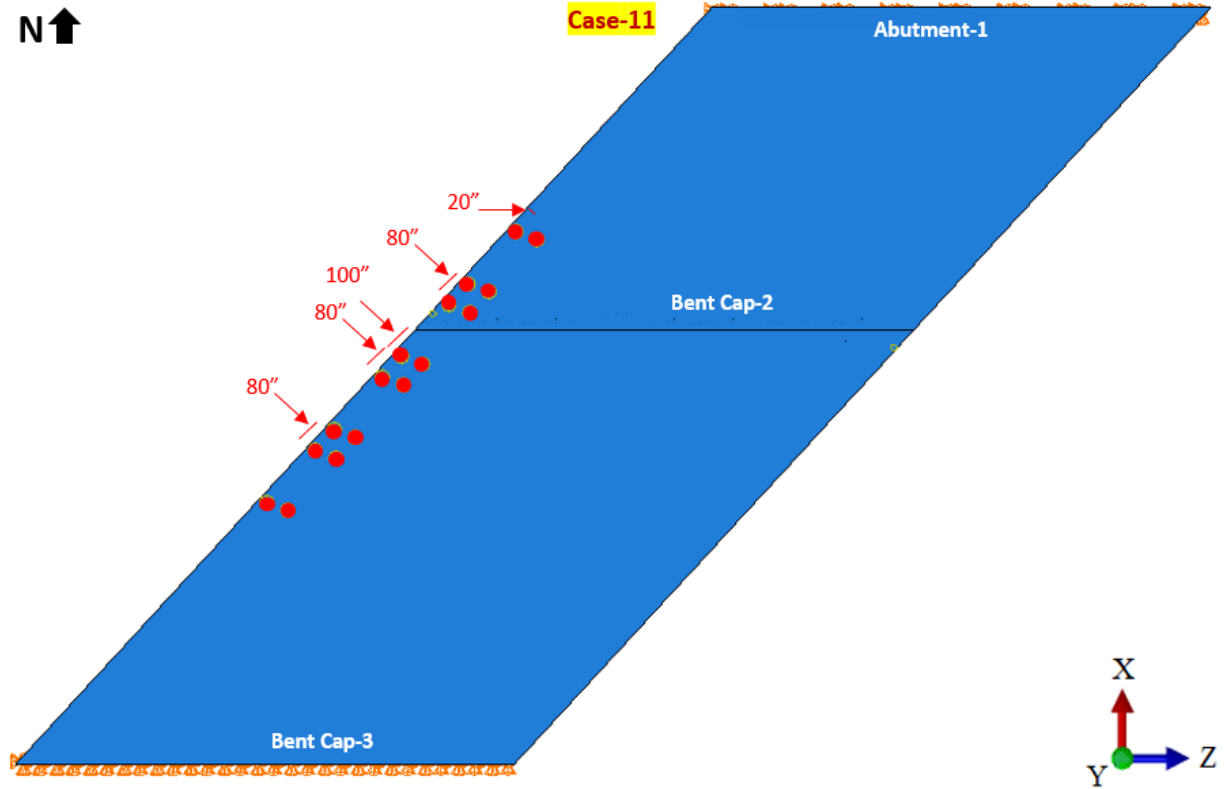
N ↑



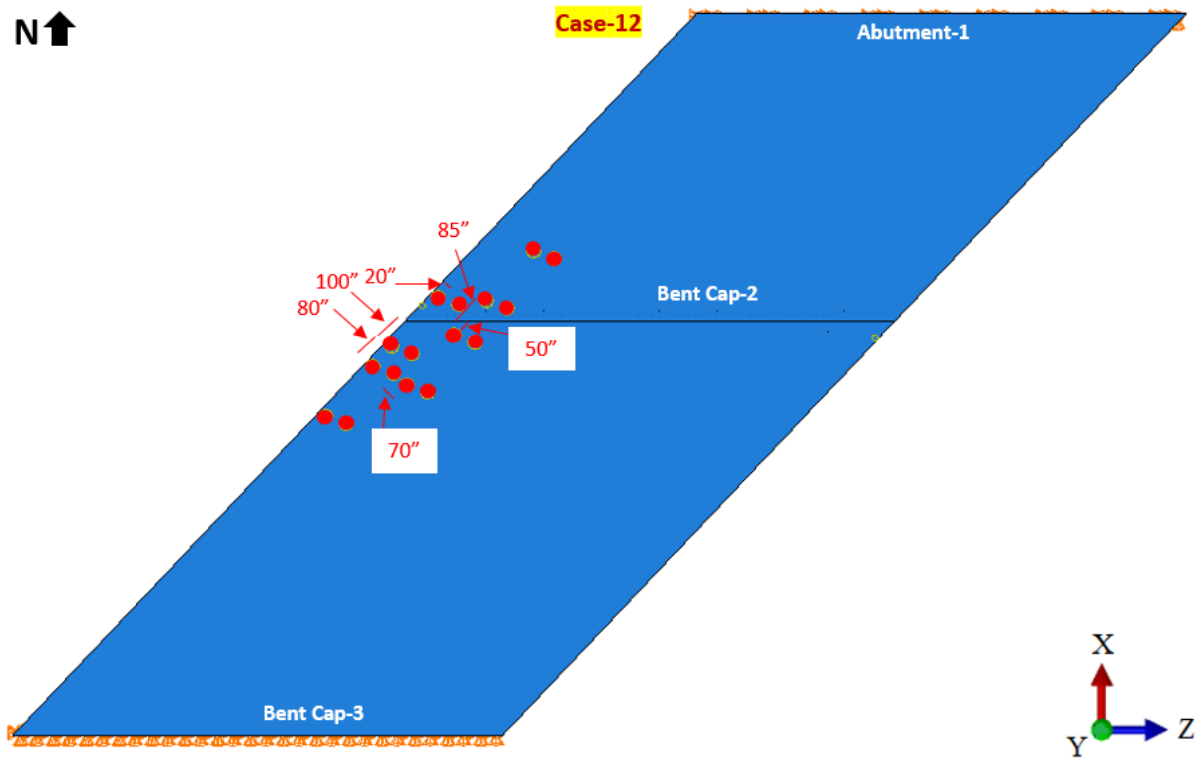
N ↑



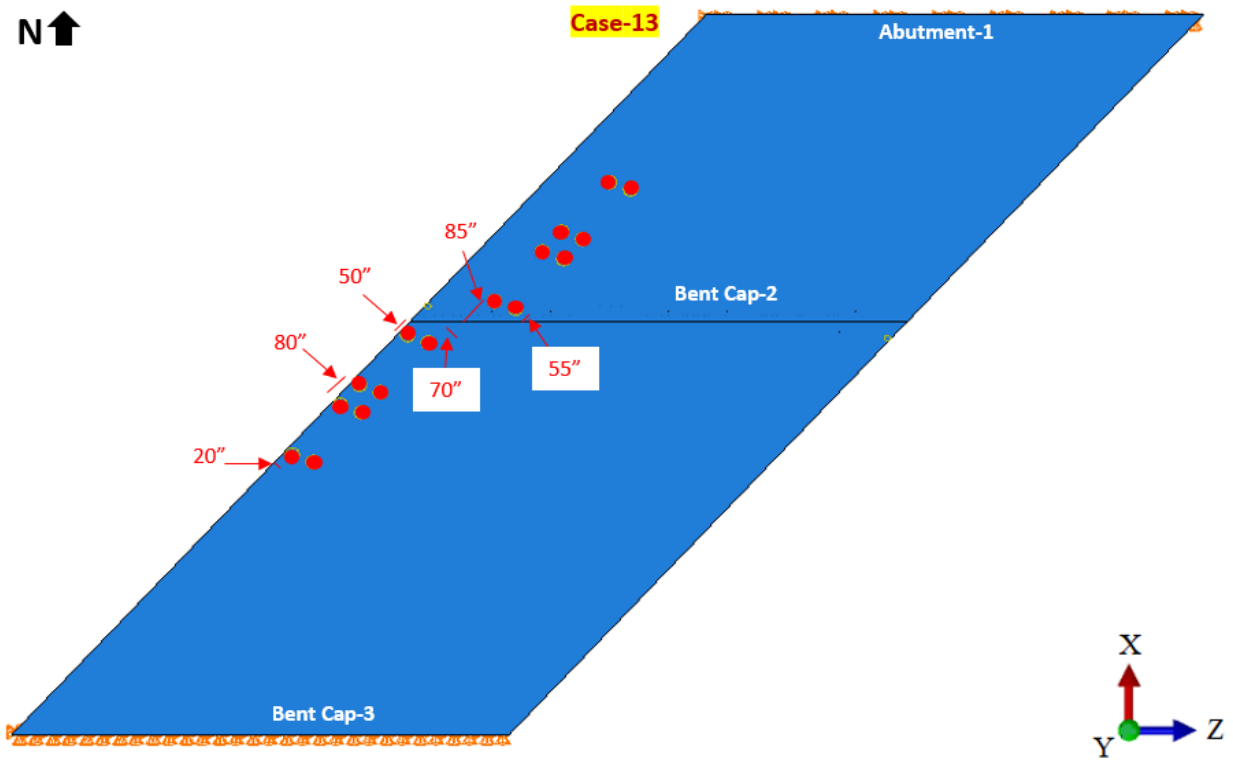
N ↑



N ↑



N ↑



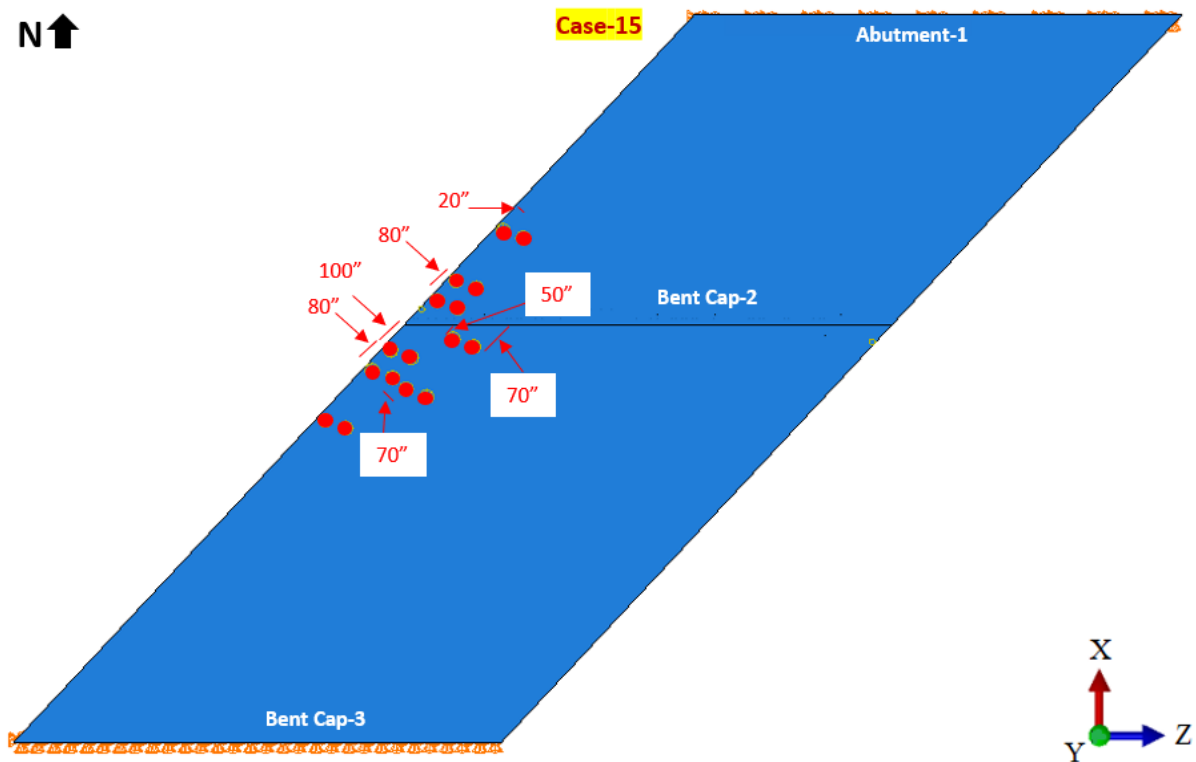
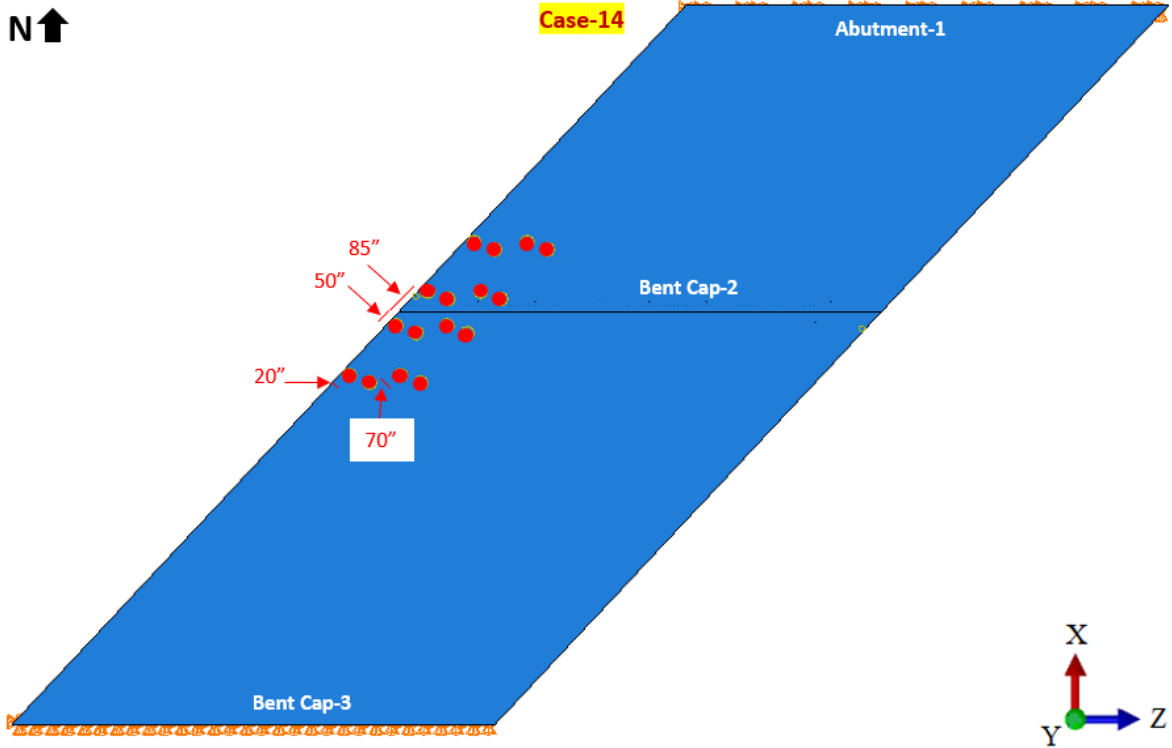


Figure 2.9. Four-Truck Locations for Cases 1 to 15 of Bent Cap 2

Based on FE simulations of 15 cases of four trucks loading, the locations for strain gauges, carbon nanofiber aggregates (CNFAs), and laser sensors are identified for Bent Cap 2. Carbon nanofiber aggregates are robust cement-based sensors (Gautam et al., 2019; Joshi et al., 2023; Joshi, Li, Oz, Wang, et al., 2021; Joshi, Shan, Wang, Oz, et al., 2021; Joshi, Shan, Wang, Yang, et al., 2021; Mo et al., 2020). Table 2.2 shows the details of the locations for the strain gauge installation. Table 2.3 shows Carbon NanoFiber Aggregate (CNFAs) installation locations. The finite element simulated strains for the 15 cases at 31 locations, the maximum concrete strains in tension and compression and the displacements at the West face of ITBC, the stress values of the 15 cases for the 9 Carbon Nanofiber Aggregates (CNFAs) locations on Bent Cap 2 are presented in APPENDIX-1. Figures 2.10(a) – 2.10(o) show the tensile strain distribution on concrete for Cases 1 to 15, respectively. Figures 2.11(a) – 2.11(o) show the displacements of the West face of Bent Cap 2 for Cases 1 to 15, respectively. Figures 2.12(a) – 2.12(o) show the stress distribution on the rebar cage of Bent Cap 2 for Cases 1 to 15, respectively.

**Table 2.2. Identified Locations of Strain Gauges in Bent Cap 2**

No.	Label	Explanation	X (in)	Y (in)	Z (in)	Bar Group
			Coordinates shown in Figure 2.12			
1	B2-SS1s1	Bent Cap 2 - Southside, 1st S Bar from the east face, 1st SG located on the Side of the bar	-19.1	-20.5	35	S Bars
2	B2-SS1s2	Bent Cap 2 - Southside, 1st S Bar from the east face, 2nd SG located on the Side of the bar	-19.1	-20.5	30	
3	B2-SS2s1	Bent Cap 2 - Southside, 2nd S Bar from the east face, 1st SG located on the Side of the bar	-13.3	-20.5	35	
4	B2-SS2s2	Bent Cap 2 - Southside, 2nd S Bar from the east face, 2nd SG located on the Side of the bar	-13.3	-20.5	30	
5	B2-SS3s1	Bent Cap 2 - Southside, 3rd S Bar from the east face, 1st SG located on the Side of the bar	-7.4	-20.5	35	
6	B2-SS3s2	Bent Cap 2 - Southside, 3rd S Bar from the east face, 2nd SG located on the Side of the bar	-7.4	-20.5	30	
7	B2-SS4s1	Bent Cap 2 - Southside, 4th S Bar from the east face, 2nd	-1.56	-20.5	35	

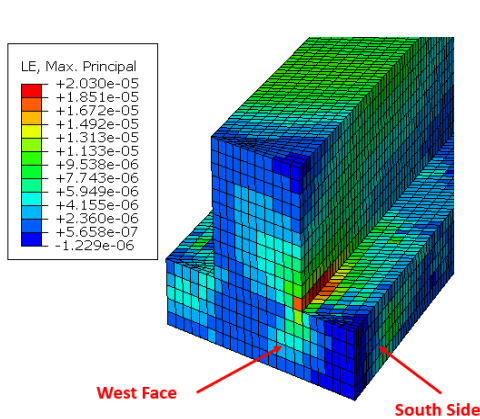
		SG located on the Side of the bar					
<b>8</b>	<b>B2-SS4s2</b>	Bent Cap 2 - Southside, 4th S Bar from the east face, 2nd SG located on the Side of the bar	-1.56	-20.5	30		
<b>9</b>	<b>B2-NS5s1</b>	Bent Cap 2 - Northside, 6th S Bar from the east face, 1st SG located on the Side of the bar	49.21	20.5	35		
<b>10</b>	<b>B2-NS5s2</b>	Bent Cap 2 - Northside, 6th S Bar from the east face, 2nd SG located on the Side of the bar	49.21	20.5	30		
<b>11</b>	<b>B2-NS6s1</b>	Bent Cap 2 - Northside, 7th S Bar from the east face, 1st SG located on the Side of the bar	55.07	20.5	35	<b>S Bars</b>	
<b>12</b>	<b>B2-NS6s2</b>	Bent Cap 2 - Northside, 7th S Bar from the east face, 2nd SG located on the Side of the bar	55.07	20.5	30		
<b>13</b>	<b>B2-NS7s1</b>	Bent Cap 2 - Northside, 8th S Bar from the east face, 1st SG located on the Side of the bar	60.93	20.5	35		
<b>14</b>	<b>B2-NS7s2</b>	Bent Cap 2 - Northside, 8th S Bar from the east face, 2nd SG located on the Side of the bar	60.93	20.5	30		
<b>15</b>	<b>B2-SS8s1</b>	Bent Cap 2 - Northside, 9th S Bar from the east face, 1st SG located on the Side of the bar	66.77	20.5	35		
<b>16</b>	<b>B2-SS8s2</b>	Bent Cap 2 - Northside, 9th S Bar from the east face, 2nd SG located on the Side of the bar	66.77	20.5	30		
<b>17</b>	<b>B2-SM5t</b>	Bent Cap 2 - Southside, 6th M Bar from the east face, SG located on the top of the bar	7.8	-24	23		<b>M Bars</b>
<b>18</b>	<b>B2-SM6t</b>	Bent Cap 2 - Southside, 7th M Bar from the east face, SG located on the top of the bar	13.6	-24	23		
<b>19</b>	<b>B2-SM7t</b>	Bent Cap 2 - Southside, 8th M Bar from the east face, SG located on the top of the bar	19.4	-24	23		
<b>20</b>	<b>B2-M8t</b>	Bent Cap 2 - Southside, 9th M Bar from the east face, SG located on the top of the bar	25.3	-24	23		

21	B2-SM16b	Bent Cap 2 - Southside, 16th M Bar from the east face, SG located on the bottom of the bar	73.2	-16.7	0	
22	B2-SM17b	Bent Cap 2 - Southside, 17th M Bar from the east face, SG located on the bottom of the bar	79	-16.7	0	M Bars
23	B2-A7	Bent Cap 2 – 7th A Bar from the south side	86.8	9.9	78.2	A Bars
24	B2-A8	Bent Cap 2 – 8th A Bar from the south side	91.4	14.8	78.2	
25	B2-A9	Bent Cap 2 – 9th A Bar from the south side	96	19.8	78.2	
26	B2-U1-1	Bent Cap 2 - 1st U1 Bar from the west face	-10.84	-12.07	14.71	U1 Bar
27	B2-SG1	Bent Cap 2 - Southside, 4th G Bar from the west face	-1.59	-22.03	23.27	G Bar
28	B2-SG2	Bent Cap 2 - Southside, 5th G Bar from the east face	4.25	-22.03	23.27	
29	B2-B10	Bent Cap 2 - 10th B Bar from the west face	70.4	8.5	1.1	B Bar
30	B2-T7-N	Bent Cap 2- Northside, 7th T bar from the East face under the bearing pad	62.3	37.5	24	T Bar
31	B2-T3-S	Bent Cap 2- Southside, 3rd T bar from the East face under the bearing pad	5.36	36.8	24	T Bar

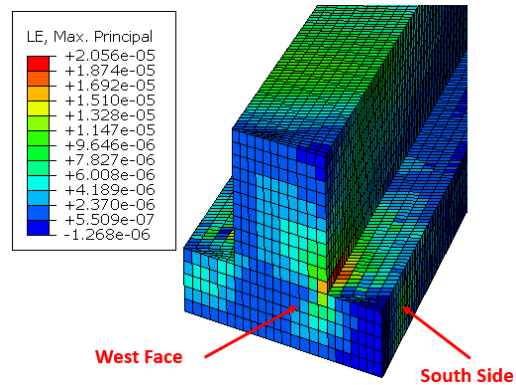
**Table 2.3. Identified Location of CNFAs in Bent Cap 2**

No.	Label	Explanation	X (in)	Y (in)	Z (in)	Group
1	B2-CNFA1zz1	Bent Cap 2 - 10th B Bar from the west face, First CNFA location in Z-Z direction	77.3	8.5	1.1	Location 1
2	B2-CNFA2zz1	Bent Cap 2 - T Bar, First CNFA at Location 2 on Z-Z direction (Bearing Pad-North face)	57.3	37.5	24	Location 2
3	B2-CNFA2zz2	Bent Cap 2 - T Bar, Second CNFA at Location 2 on Z-Z direction (Bearing Pad-North face)	62.3	37.5	24	
4	B2-CNFA2zz3	Bent Cap 2 - T Bar, Third CNFA at Location 2 on Z-Z direction (Bearing Pad-North face)	67.3	37.5	24	

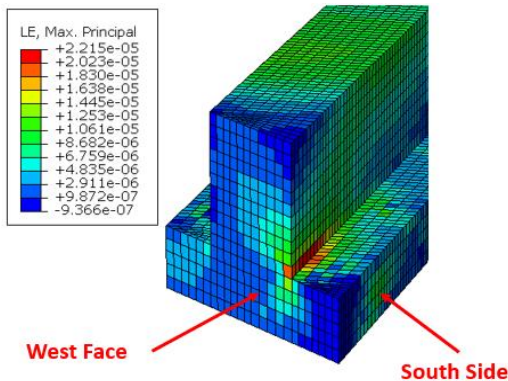
5	<b>B2- CNFA3zz1</b>	Bent Cap 2 - 1st S Bar, First CNFA at Location 3 on Z-Z direction (First S-bar-South face)	-19.1	-20.5	30	Location 3
6	<b>B2- CNFA3zz2</b>	Bent Cap 2 – 2nd S Bar, Second CNFA at Location 3 on Z-Z direction (Second S-bar-South face)	-13.3	-20.5	30	
7	<b>B2- CNFA3zz3</b>	Bent Cap 2 – 3rd S Bar, Third CNFA at Location 3 on Z-Z direction (Third S-bar-South face)	-7.4	-20.5	30	
8	<b>B2- CNFA4zz1</b>	Bent Cap 2 - T Bar, First CNFA at Location 4 on Z-Z direction (Bearing Pad-South face)	5.36	-20.5	32	Location 4
9	<b>B2- CNFA4zz2</b>	Bent Cap 2 - T Bar, Second CNFA at Location 4 on Z-Z direction (Bearing Pad-South face)	5.36	-20.5	32	



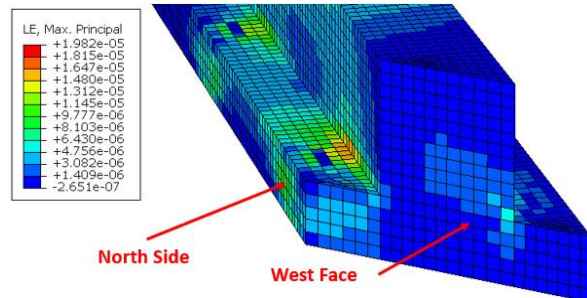
(a) Concrete Tensile Strain for Case 1



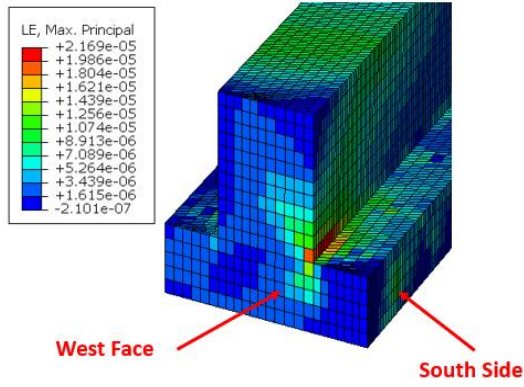
(b) Concrete Tensile Strain for Case 2



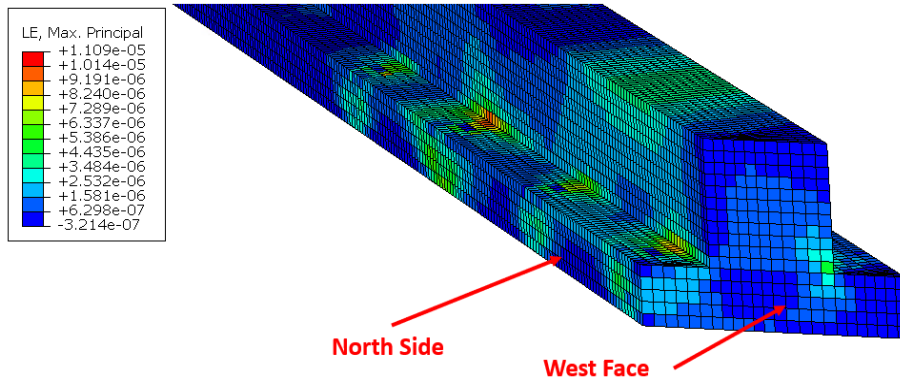
(c) Concrete Tensile Strain for Case 3



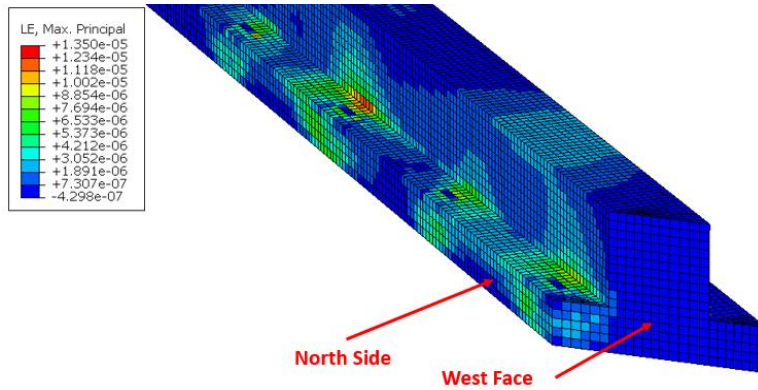
(d) Concrete Tensile Strain for Case 4



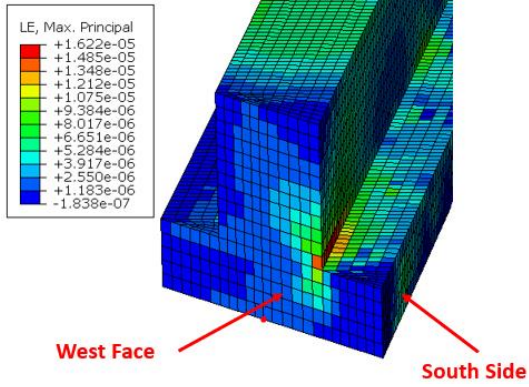
(e) Concrete Tensile Strain for Case 5



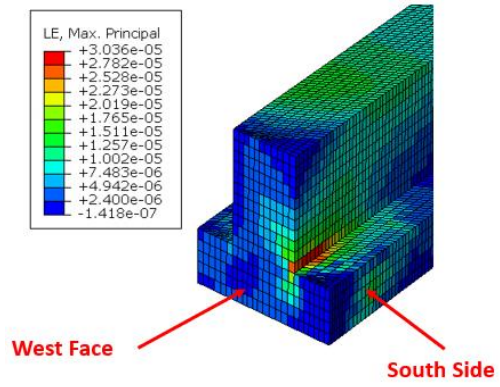
(f) Concrete Tensile Strain for Case 6



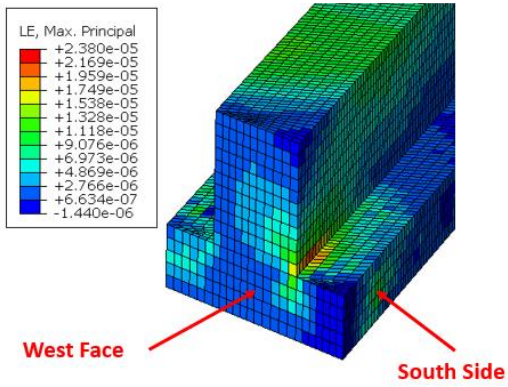
(g) Concrete Tensile Strain for Case 7



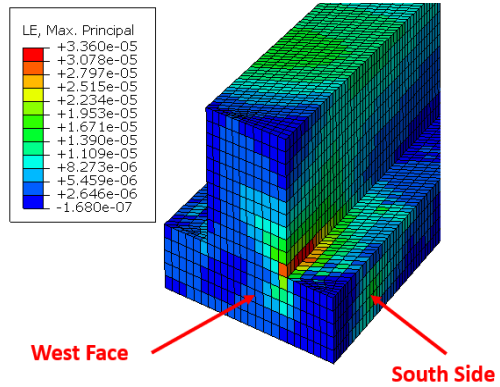
(h) Concrete Tensile Strain for Case 8



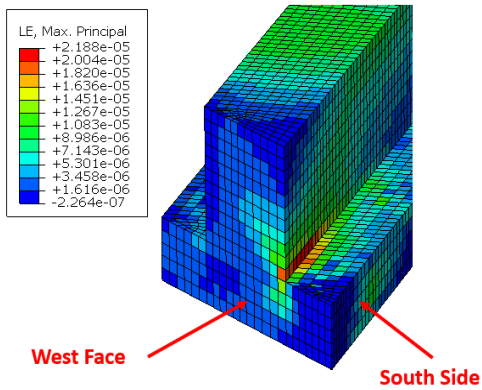
(i) Concrete Tensile Strain for Case 9



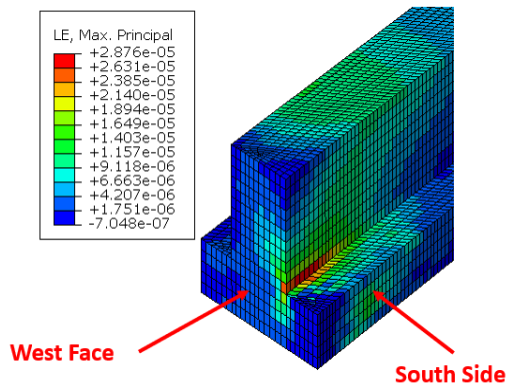
(j) Concrete Tensile Strain for Case 10



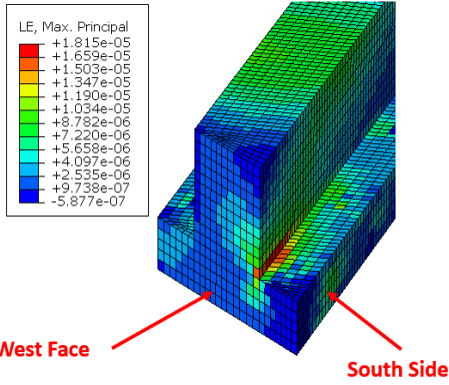
(k) Concrete Tensile Strain for Case 11



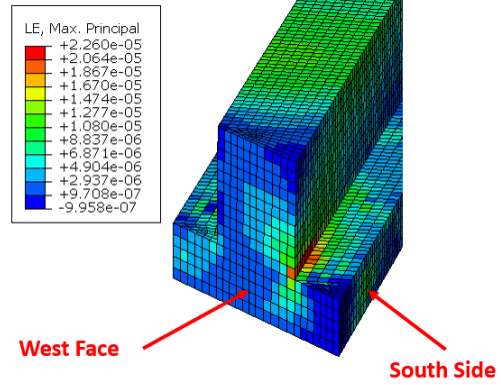
(l) Concrete Tensile Strain for Case 12



(m) Concrete Tensile Strain for Case 13

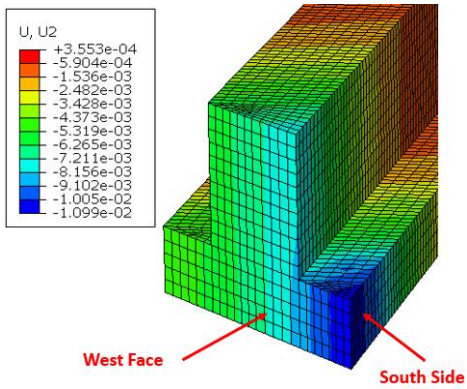


(n) Concrete Tensile Strain for Case 14

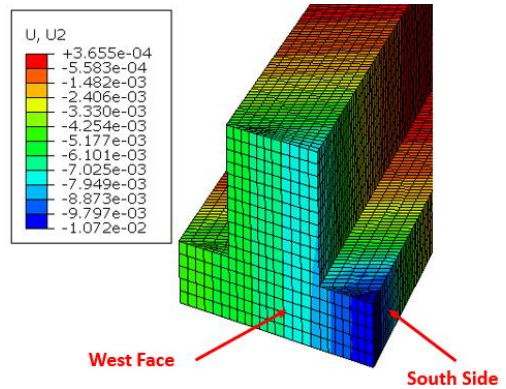


(o) Concrete Tensile Strain for Case 15

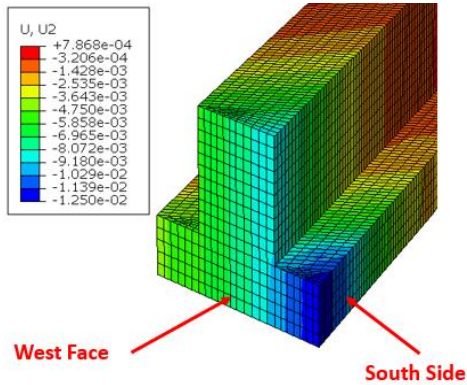
**Figure 2.10. Tensile Strain Distribution in Concrete for Cases 1 to 15 of Bent Cap 2**



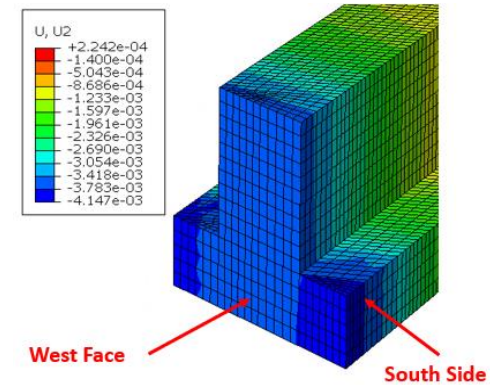
(a) West Face Displacement for Case 1



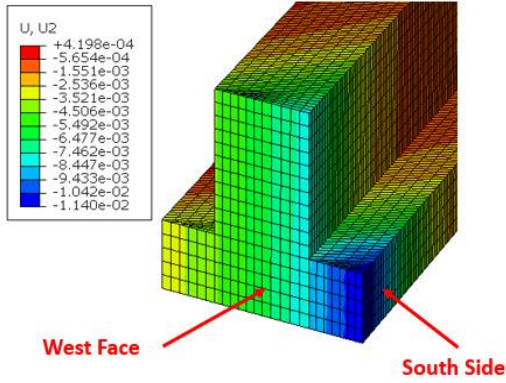
(b) West Face Displacement for Case 2



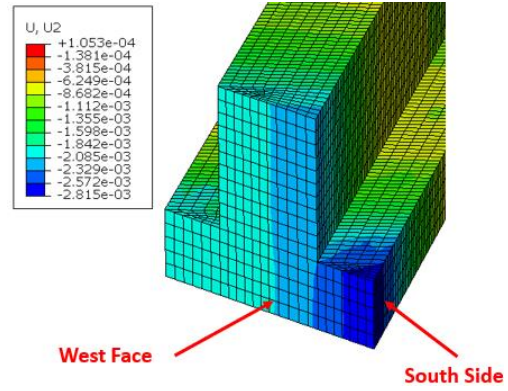
(c) West Face Displacement for Case 3



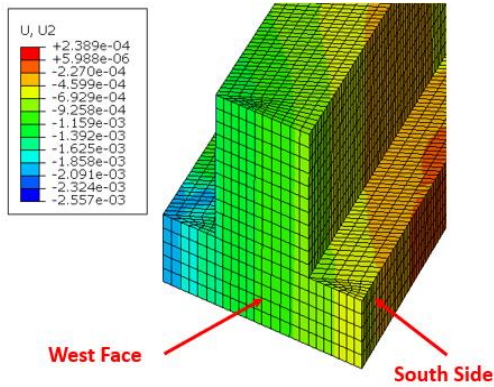
(d) West Face Displacement for Case 4



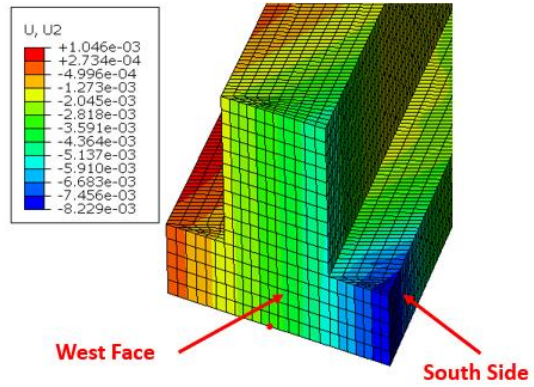
(e) West Face Displacement for Case 5



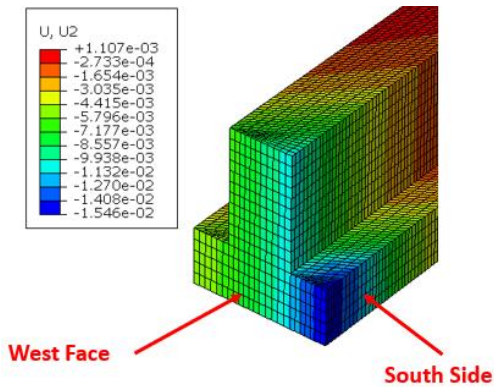
(f) West Face Displacement for Case 6



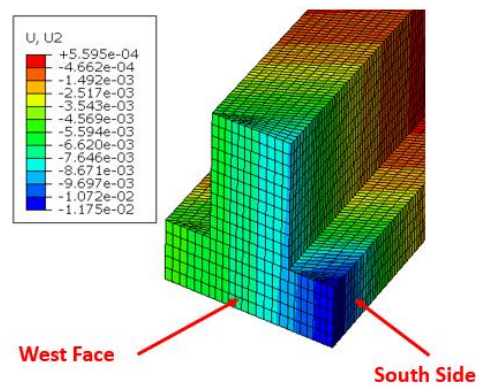
(g) West Face Displacement for Case 7



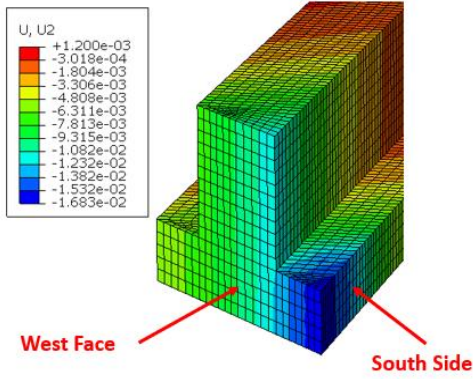
(h) West Face Displacement for Case 8



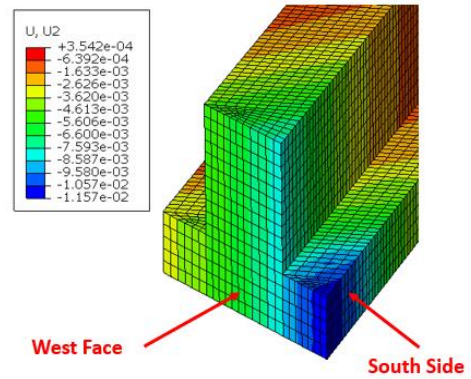
(i) West Face Displacement for Case 9



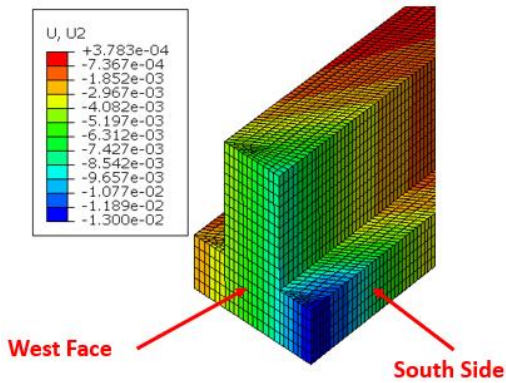
(j) West Face Displacement for Case 10



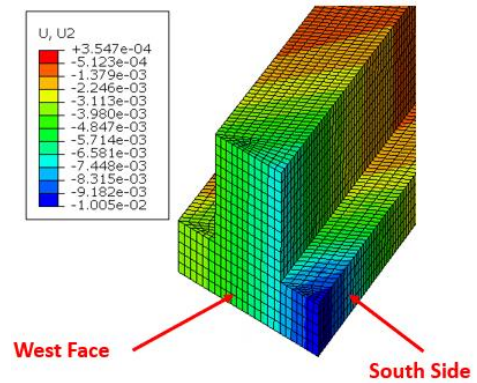
(k) West Face Displacement for Case 11



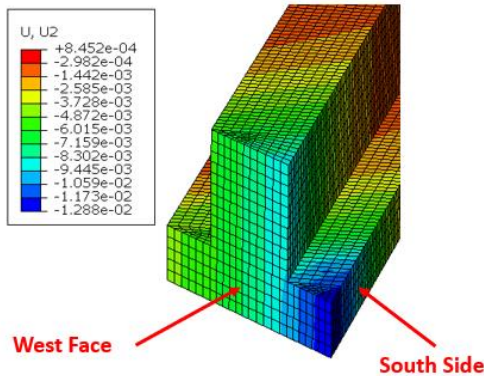
(l) West Face Displacement for Case 12



(m) West Face Displacement for Case 13

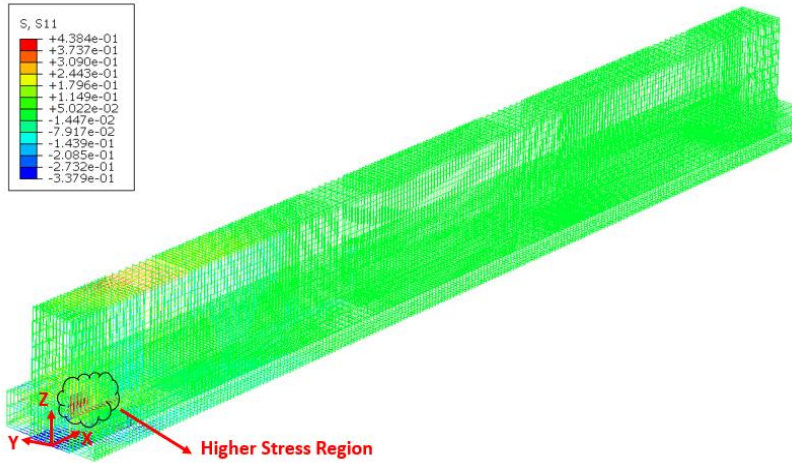


(n) West Face Displacement for Case 14

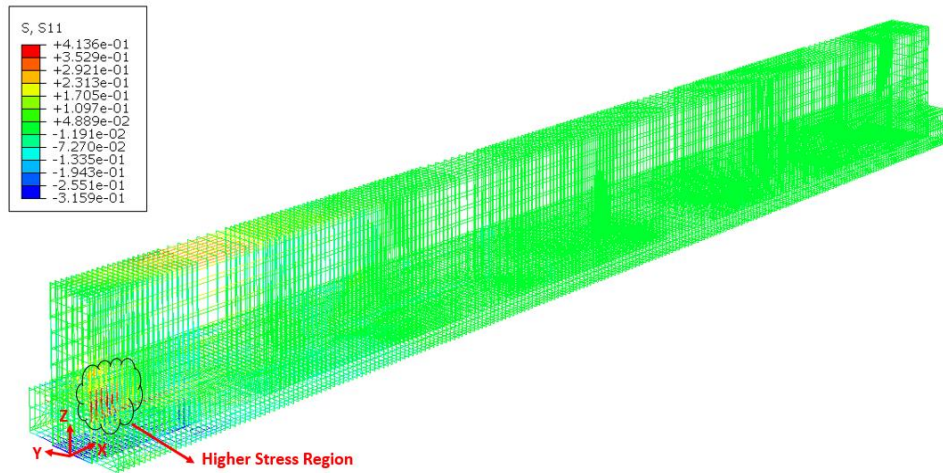


(o) West Face Displacement for Case 15

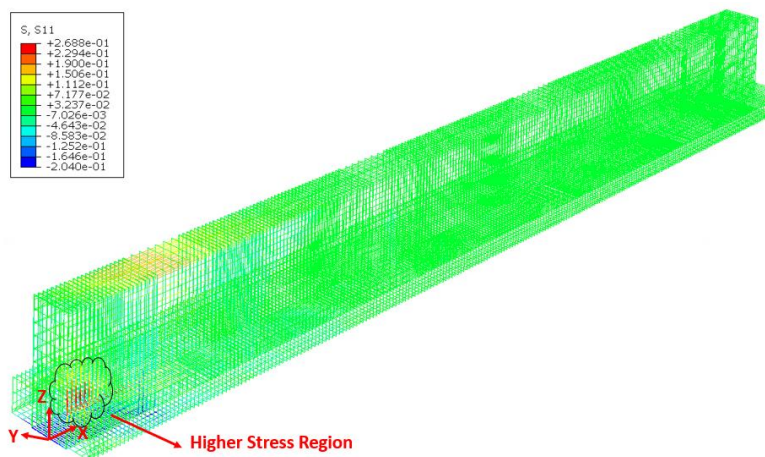
**Figure 2.11. Displacement Profile for Cases 1 to 15 of Bent Cap 2**



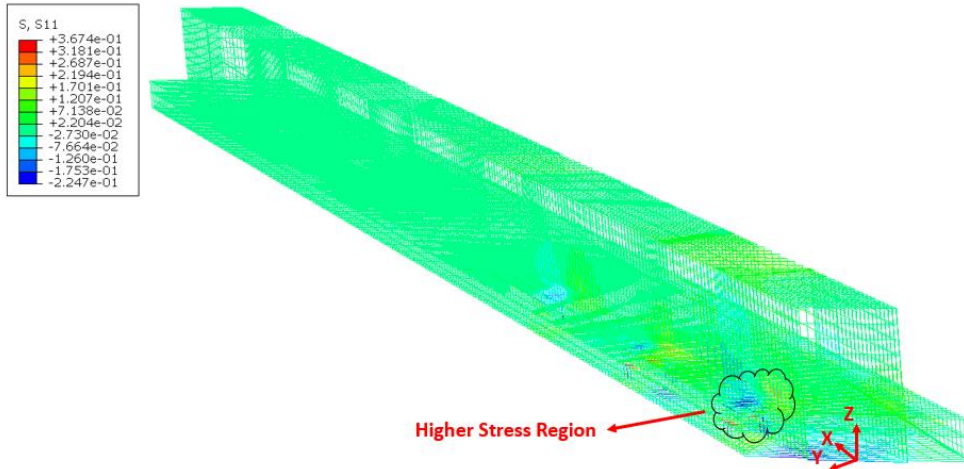
(a) Stresses on Rebar Cage for Case 1 (units in ksi)



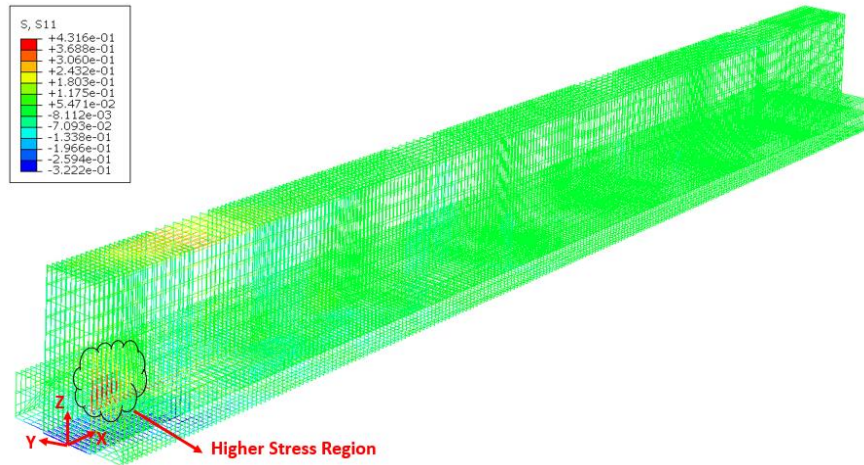
(b) Stresses on Rebar Cage for Case 2 (units in ksi)



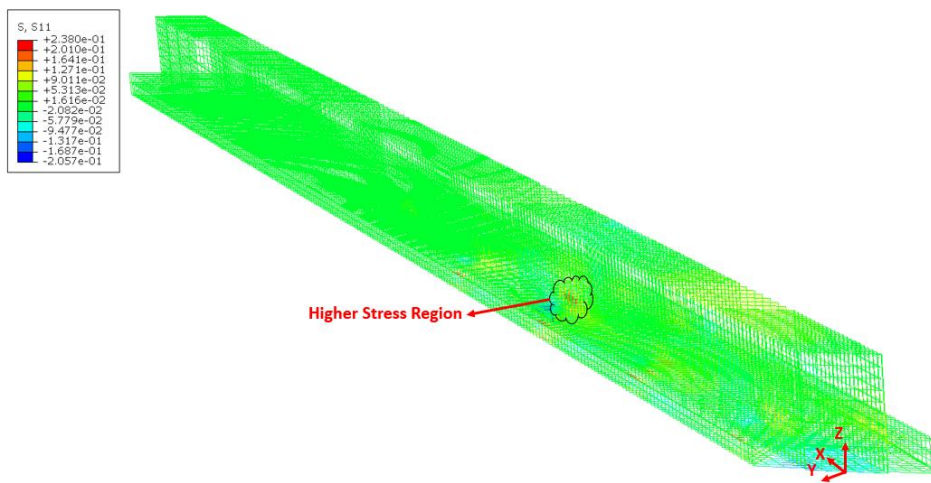
(c) Stresses on Rebar Cage for Case 3 (units in ksi)



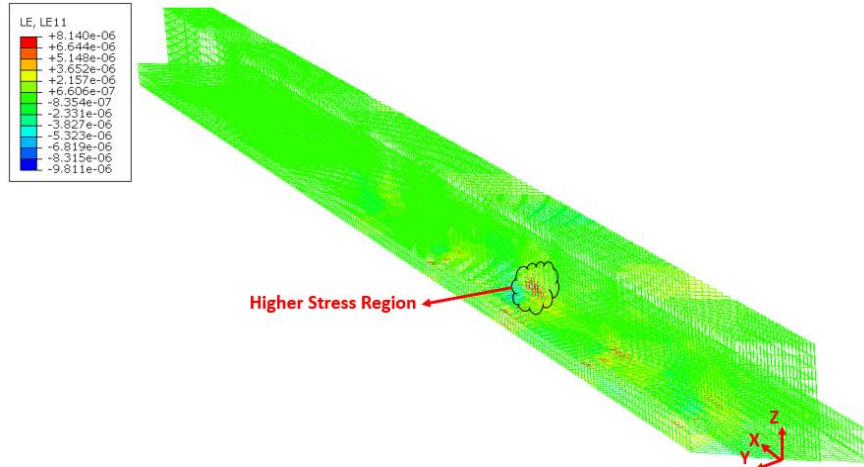
(d) Stresses on Rebar Cage for Case 4 (units in ksi)



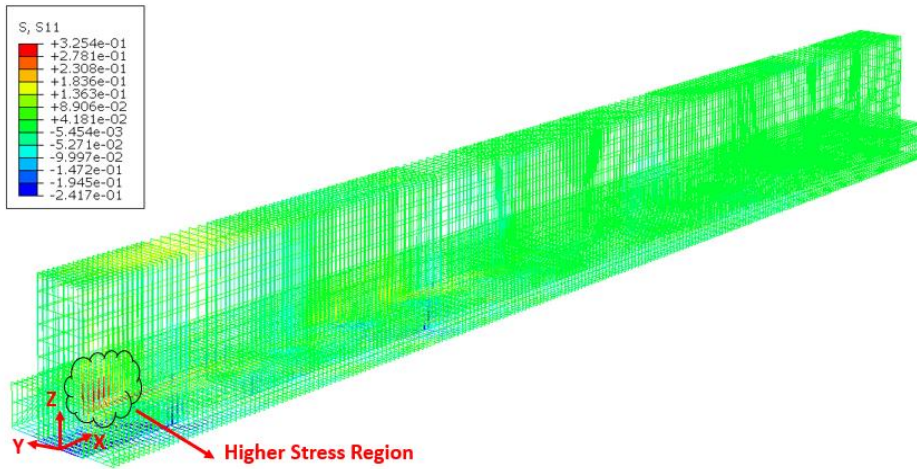
(e) Stresses on Rebar Cage for Case 5 (units in ksi)



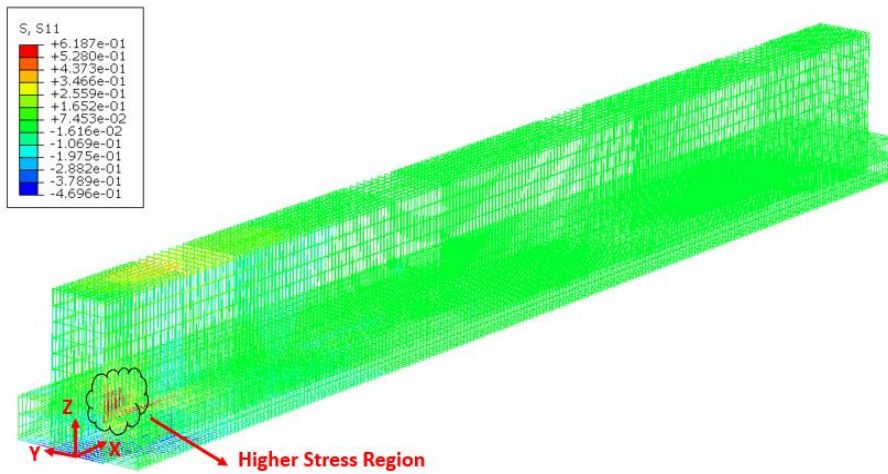
(f) Stresses on Rebar Cage for Case 6 (units in ksi)



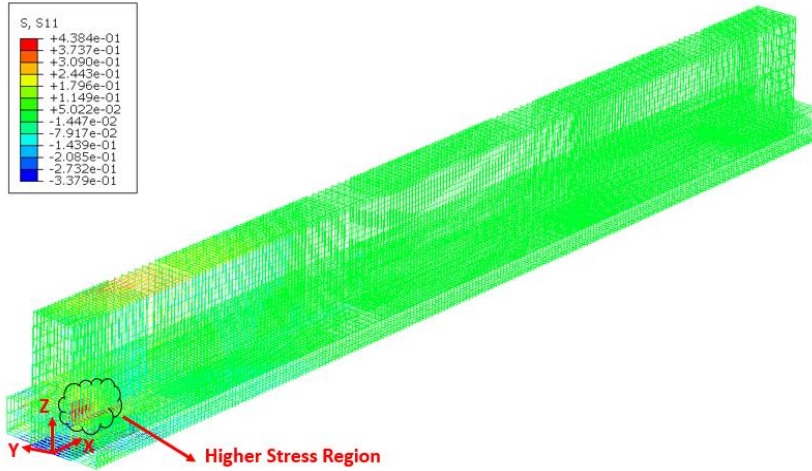
(g) Stresses on Rebar Cage for Case 7 (units in ksi)



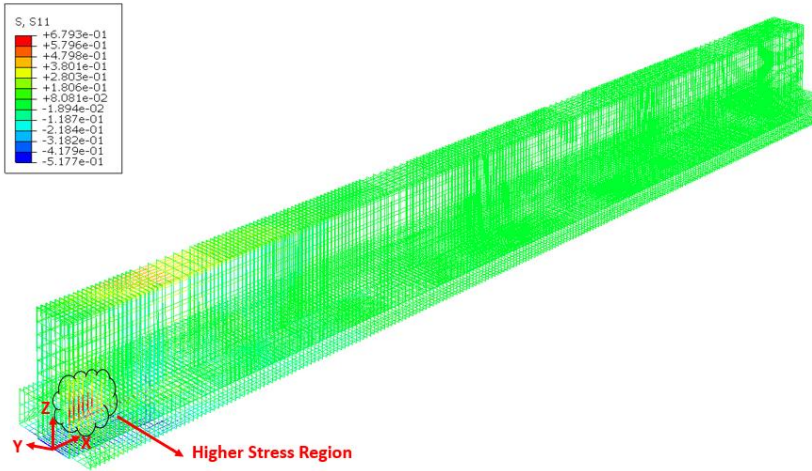
(h) Stresses on Rebar Cage for Case 8 (units in ksi)



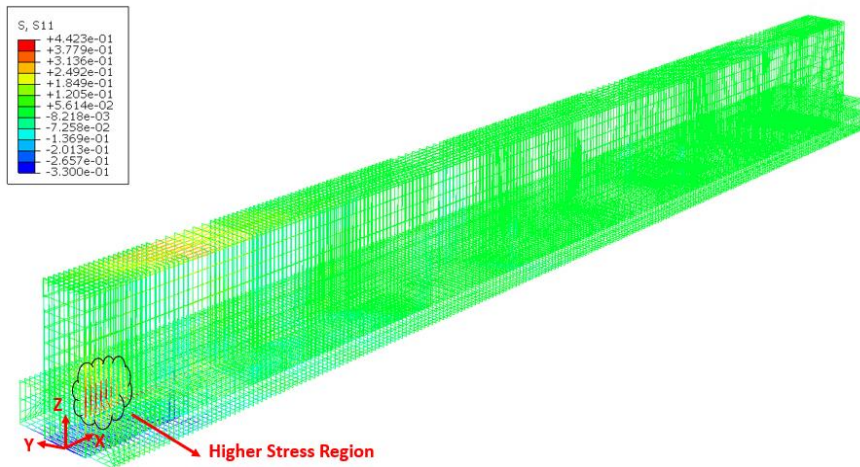
(i) Stresses on Rebar Cage for Case 9 (units in ksi)



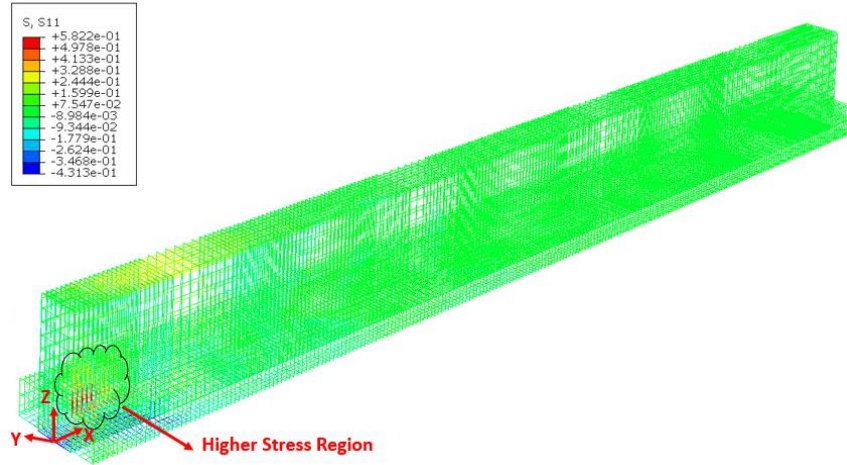
(j) Stresses on Rebar Cage for Case 10 (units in ksi)



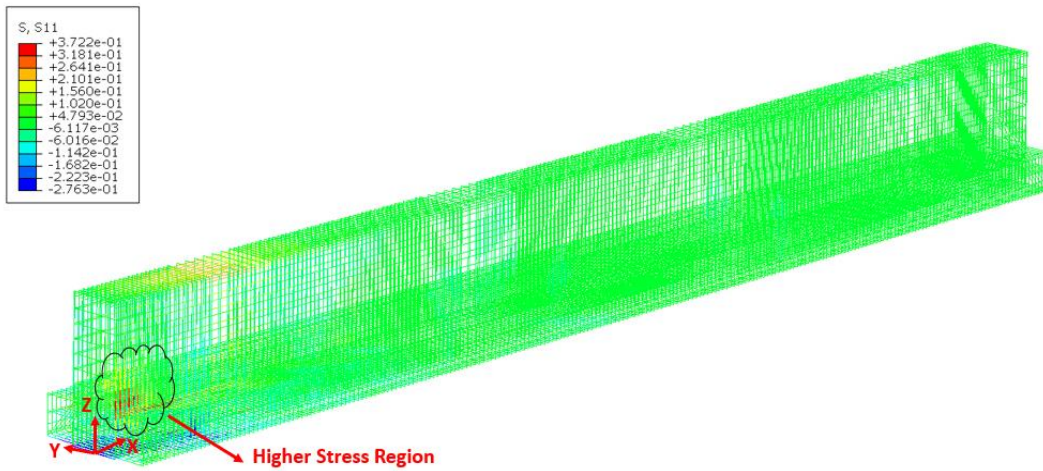
(k) Stresses on Rebar Cage for Case 11 (units in ksi)



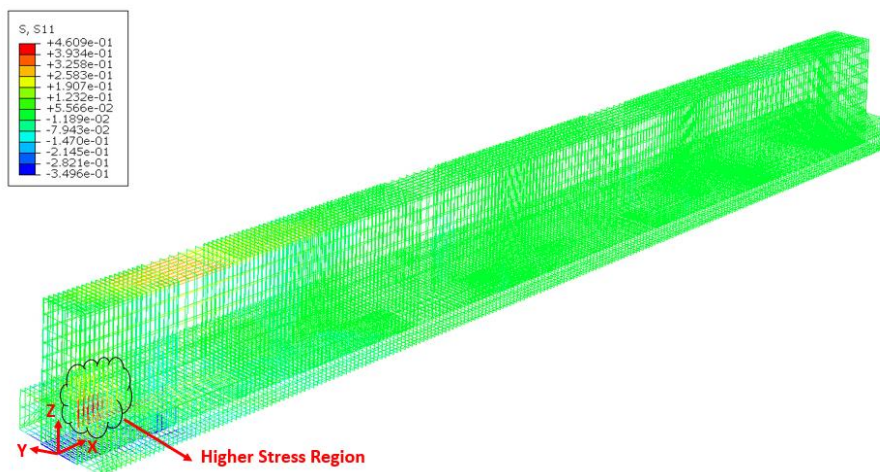
(l) Stresses on Rebar Cage for Case 12 (units in ksi)



(m) Stresses on Rebar Cage for Case 13 (units in ksi)



(n) Stresses on Rebar Cage for Case 14 (units in ksi)



(o) Stresses on Rebar Cage for Case 15 (units in ksi)

**Figure 2.12. Stress Distribution in Rebar Cage for Cases 1 to 15 of Bent Cap 2**

The concrete tensile strain at the extended region and ledge/stem interface for Cases 1 to 15 are 20.30  $\mu\epsilon$ , 20.56  $\mu\epsilon$ , 22.15  $\mu\epsilon$ , 19.82  $\mu\epsilon$ , 21.69  $\mu\epsilon$ , 11.09  $\mu\epsilon$ , 13.50  $\mu\epsilon$ , 16.22  $\mu\epsilon$ , 30.36  $\mu\epsilon$ , 23.80  $\mu\epsilon$ , 33.60  $\mu\epsilon$ , 21.88  $\mu\epsilon$ , 28.76  $\mu\epsilon$ , 18.15  $\mu\epsilon$ , and 22.60  $\mu\epsilon$ , respectively. The displacement observed on the extended region of the West face of ITBC-2 for Cases 1 to 15 are -0.01099-inch, -0.01072-inch, -0.01250-inch, -0.00413-inch, -0.01140-inch, -0.00282-inch, -0.00054-inch, -0.00823-inch, -0.01546-inch, -0.01175-inch, -0.01683-inch, -0.01157-inch, -0.01300-inch, -0.01005-inch, and -0.01288-inch, respectively. The maximum displacement is -0.01683-inch observed in Case 11. Figures 2.10(a) – 2.10(o) shows higher concrete tensile strain at the stem and ledge interface. As shown in Figures 2.11(a) – 2.11(o), the maximum displacement at the West face of ITBC is observed in the extended region. Based on the simulation results from 15 cases, the higher tensile stress is observed on transverse rebars of the stem, as shown in Figures 2.12(a)-2.12(o).

Case 9 is the most critical load case because it results in higher strains and stresses in the ledge/stem interface and the rebars. In addition, Case 1, 3, 10, 11 and 14 are selected for candidate Static Test-1 as it results in higher strains and stresses. The loading cases (Cases 6, 7, and 8) with load distribution on four lanes did not yield higher stress/strain on transverse rebars.

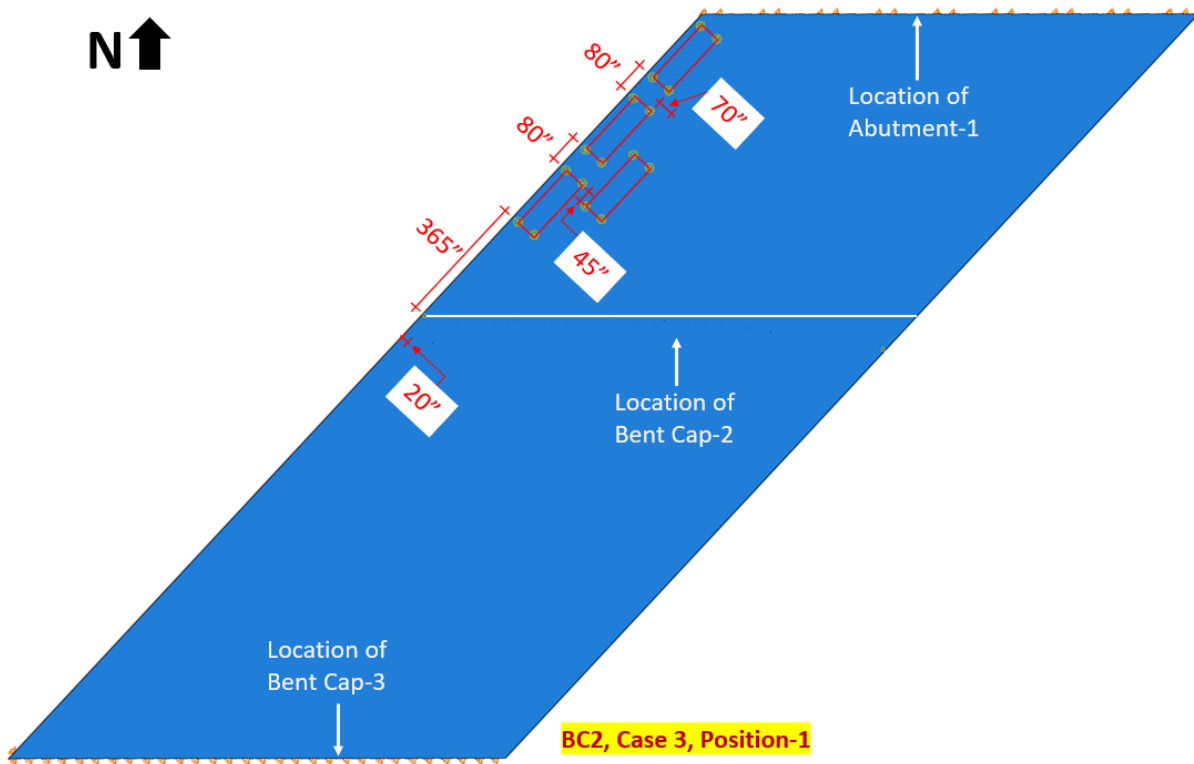
### **2.3.2 Static Test-2 Simulation at Five Positions**

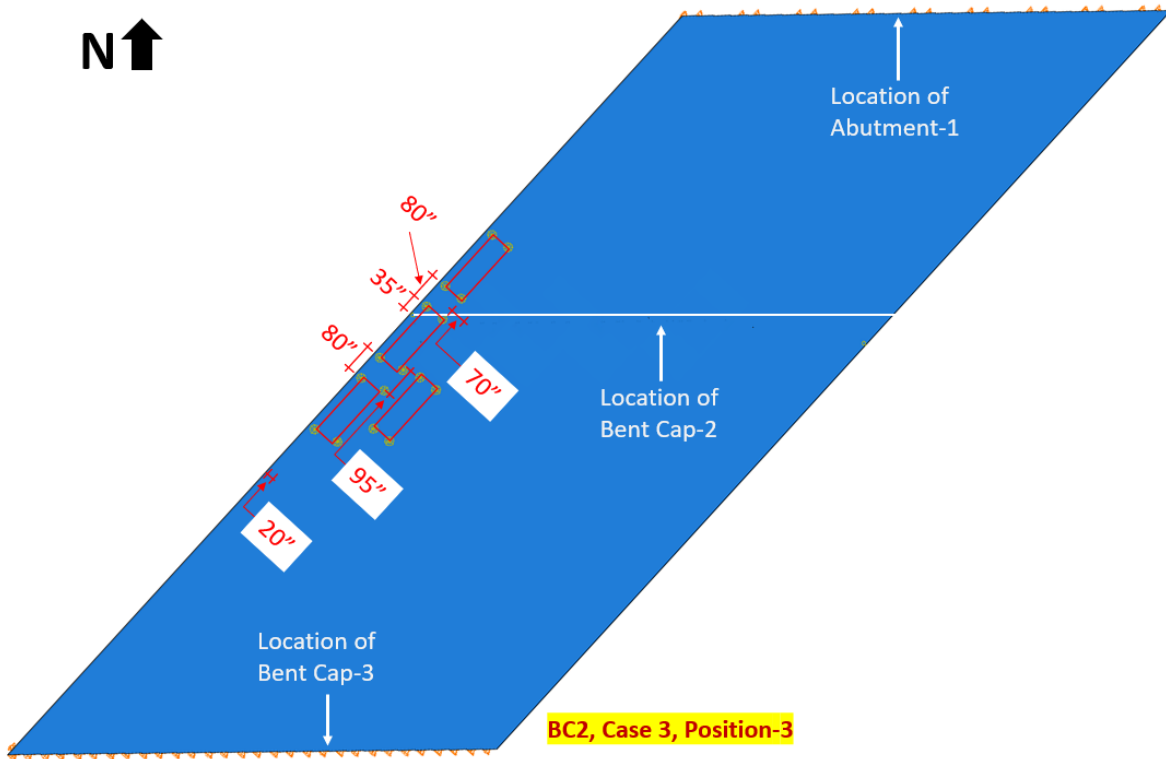
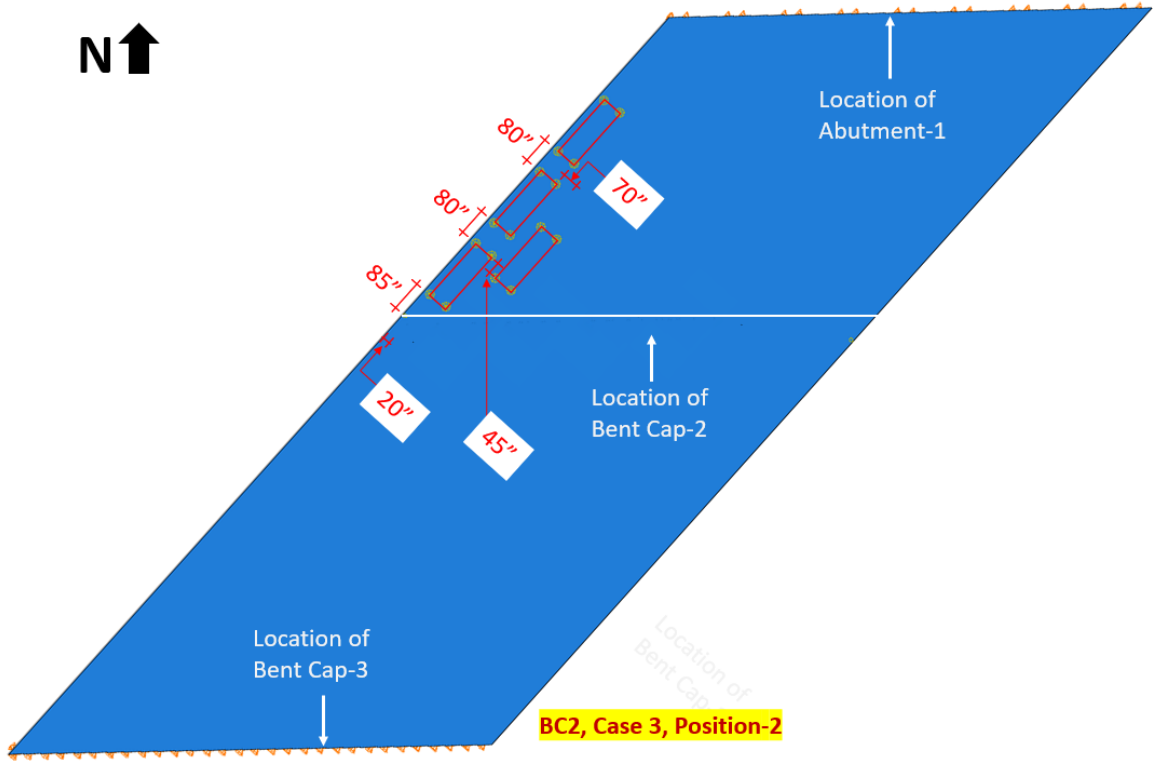
Based on 15 cases of FE simulation of Bent Cap 2 with Static Test-1, Cases 1, 3, 9, 10, 11, and 14 are identified as candidates for load tests. Among six cases, Case 3 and Case 9 are selected for Static Test-2 with four-track load at five positions. Case 3 has four trucks arranged in two lanes: three trucks are aligned to the edge of the deck, and the last truck is located next to them. Case 9 has all four trucks aligned next to the edge of the deck. The selection of Cases 3 and 9 for Static Test-2 at five positions provides:

- Varieties in load distribution (on one lane and two lanes) along the forward and backward span of Bent Cap 2,
- Examination of higher stress/strain distribution on transverse rebars at multiple positions of four-truck load, the higher concrete tensile strain on the ledge interface and stem, and higher displacement of the extended region of skewed ITBCs.

Case 3 of Bent Cap 2 is one of the critical loading cases with four-truck load. Case 3 is critically examined with four-truck load at five positions, as shown in Figure 2.13. The finite

element simulated strains for Case 3 of Bent Cap 2 under four-truck loading at five positions, maximum tensile and compressive concrete strains and the displacements for Case 3 of Bent Cap 2 under four-truck loading at five positions, and Carbon Nanofiber Aggregates (CNFAs) stress values for Case 3 of Bent Cap 2 under four-truck loading at five positions are presented in APPENDIX-1. Figures 2.14(a) – 2.14(e) show the tensile strain distribution of concrete for Case 3 of Bent Cap 2, respectively. Figures 2.15(a) – 2.15(e) show the displacements of the West face for Case 3 of Bent Cap 2, respectively. Figures 2.16(a) – 2.16(e) show the stress distribution in the rebar cage for Case 3 of Bent Cap 2, respectively.





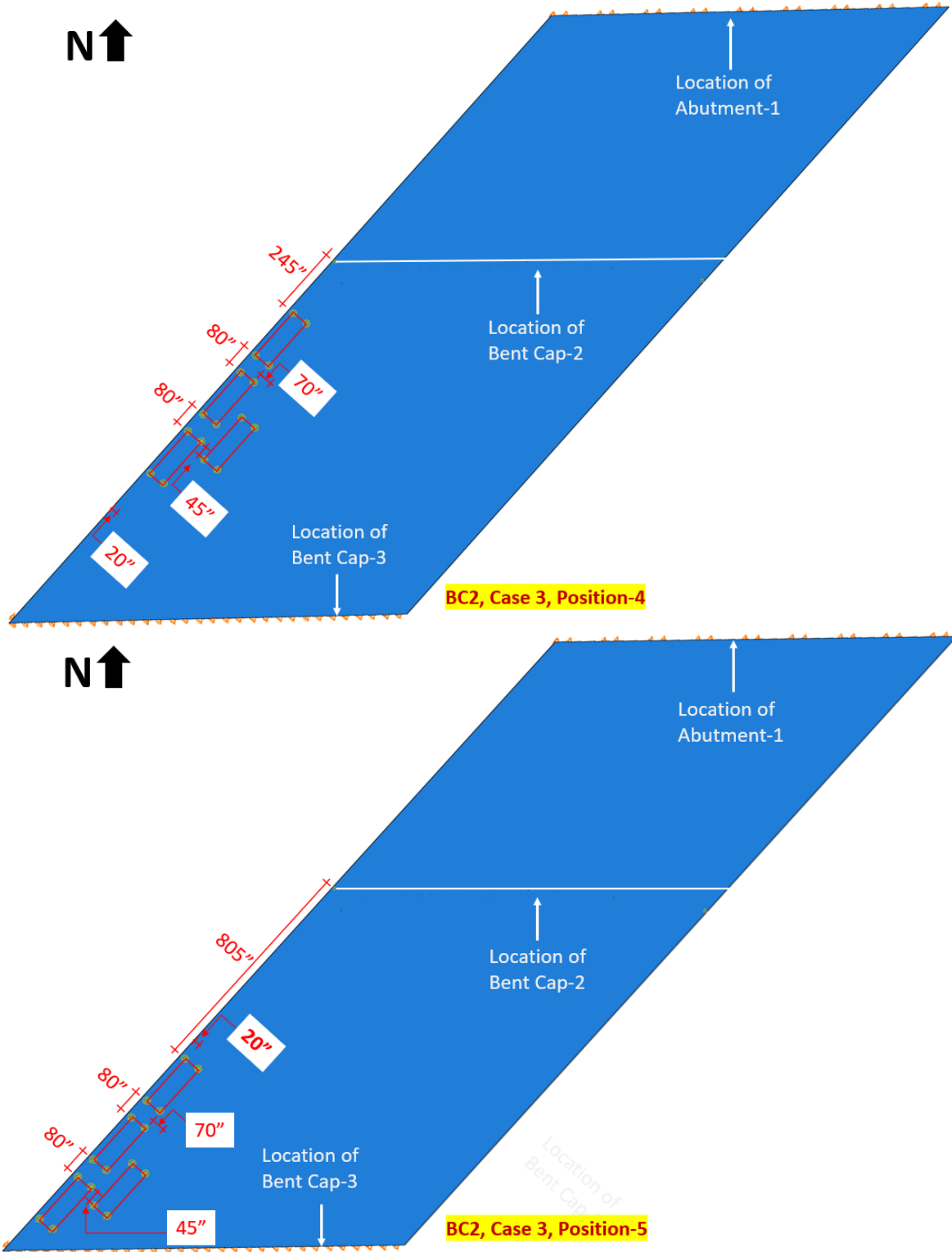
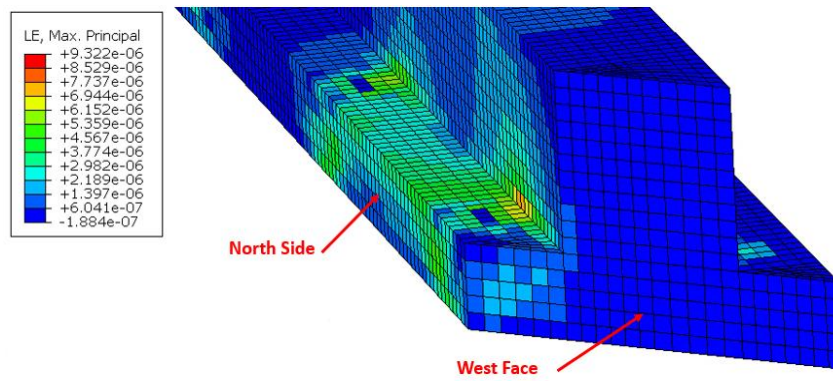
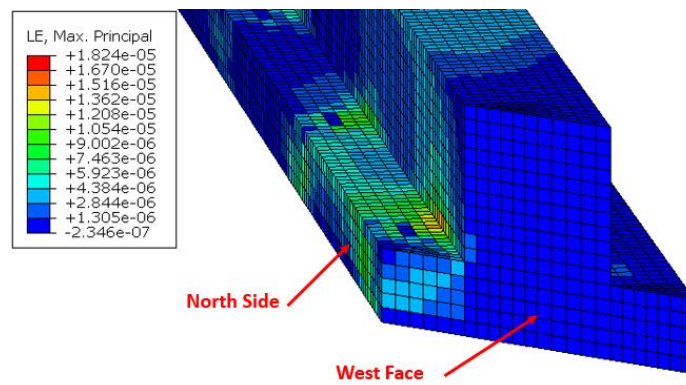


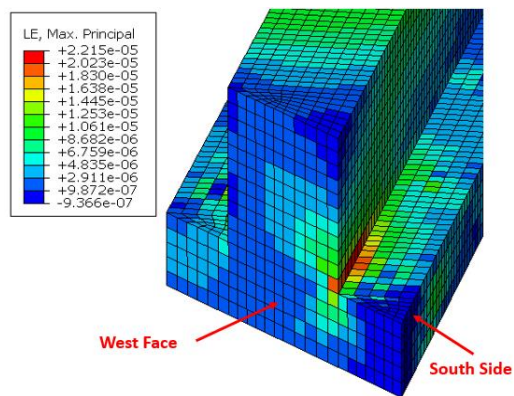
Figure 2.13. Four-Truck Loading at Five Positions for Case 3 of Bent Cap 2



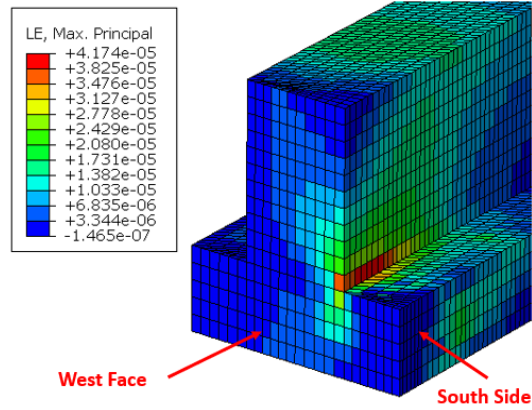
(a) Concrete Tensile Strain for Case 3 of Bent Cap 2 at Position 1



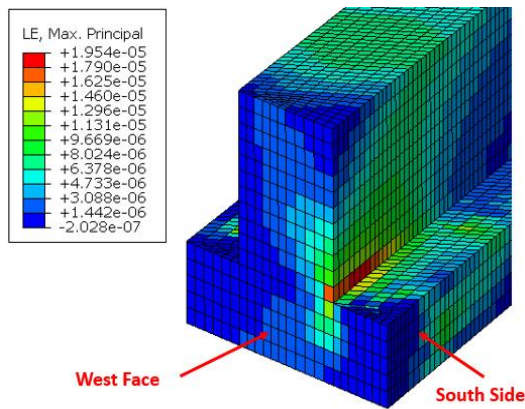
(b) Concrete Tensile Strain for Case 3 of Bent Cap 2 at Position 2



(c) Concrete Tensile Strain for Case 3 of Bent Cap 2 at Position 3

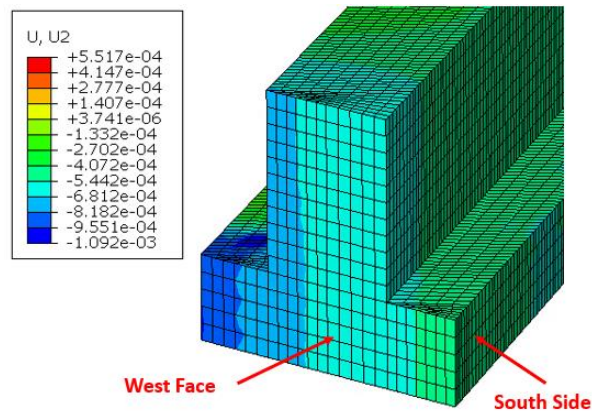


(d) Concrete Tensile Strain for Case 3 of Bent Cap 2 at Position 4

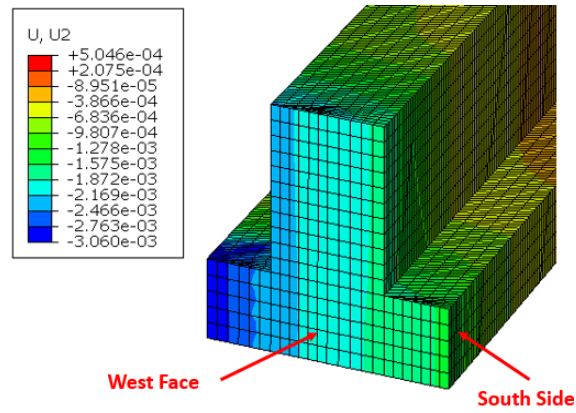


(e) Concrete Tensile Strain for Case 3 of Bent Cap 2 at Position 5

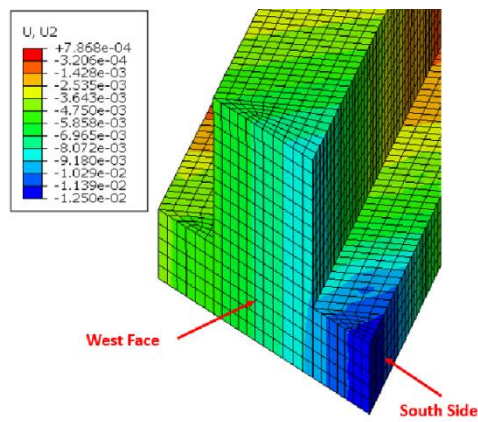
**Figure 2.14. Tensile Strain Distribution of Concrete for Case 3 of Bent Cap 2 under Four-Truck Loading at Five Positions**



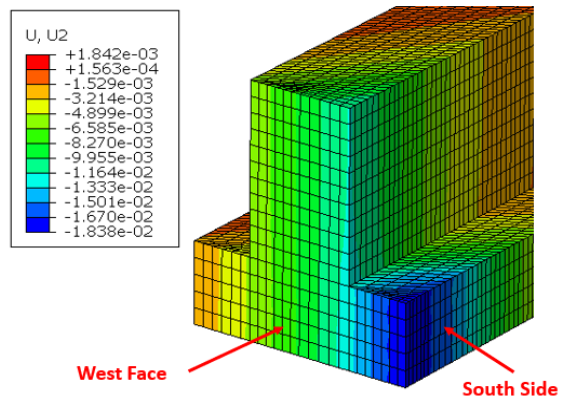
(a) West Face Displacement for Case 3 of Bent Cap 2 at Position 1 (units in inches)



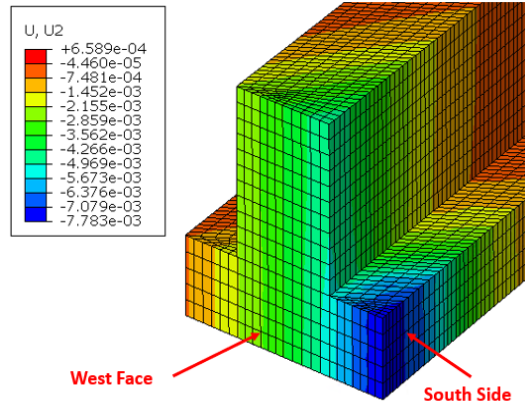
(b) West Face Displacement for Case 3 of Bent Cap 2 at Position 2 (units in inches)



(c) West Face Displacement for Case 3 of Bent Cap 2 at Position 3 (units in inches)

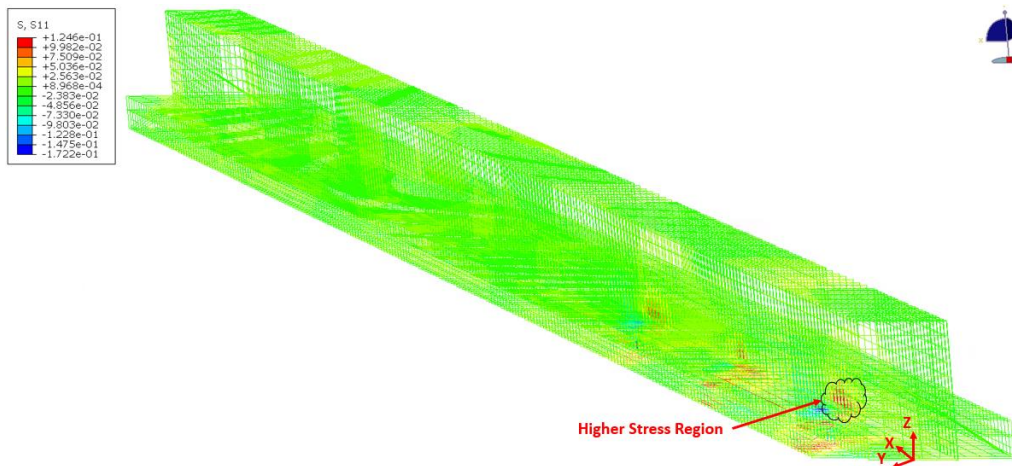


(d) West Face Displacement for Case 3 of Bent Cap 2 at Position 4 (units in inches)

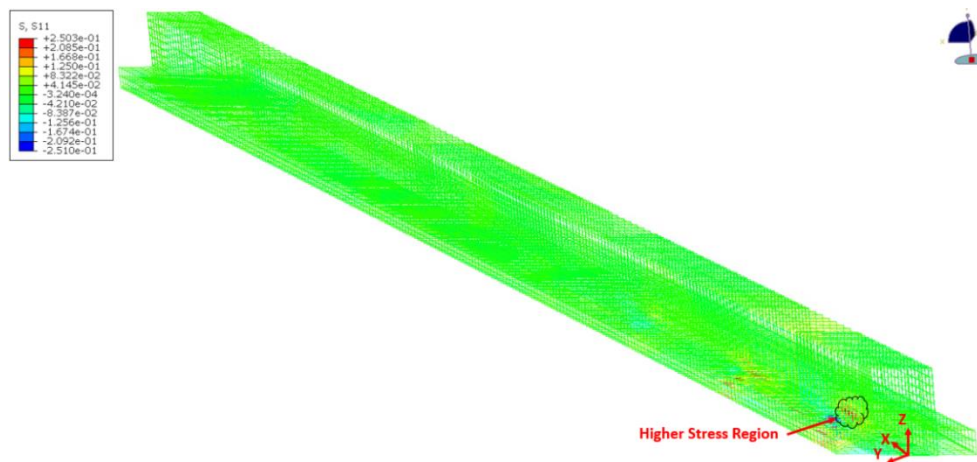


(e) West Face Displacement for Case 3 of Bent Cap 2 at Position 5 (units in inches)

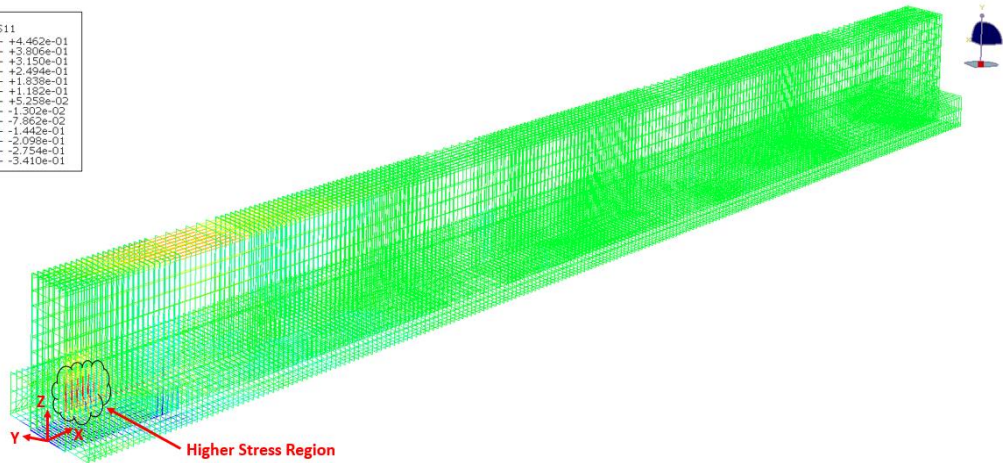
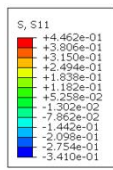
**Figure 2.15. Displacement Profile for Case 3 of Bent Cap 2 under Four-Truck Loading at Five Positions**



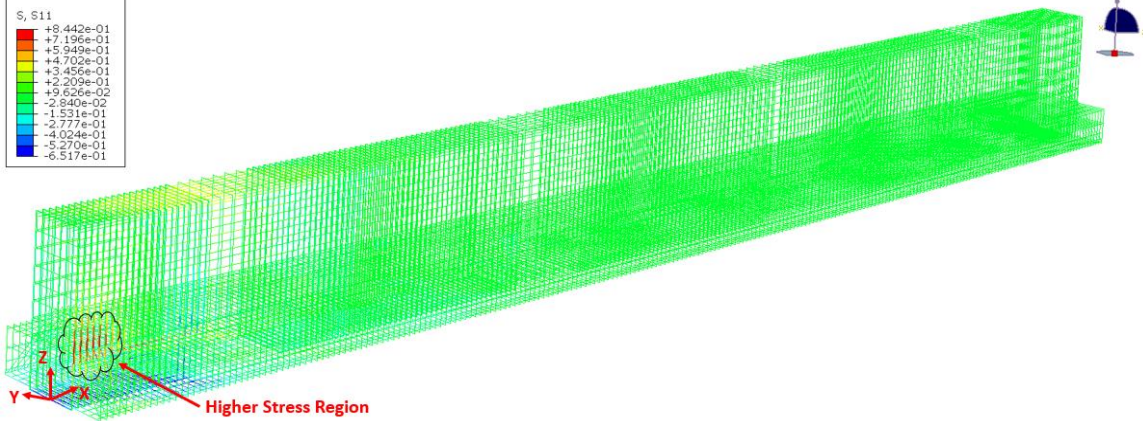
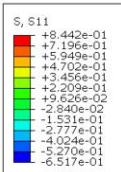
(a) Stresses in Rebar Cage for Case 3 of Bent Cap 2 at Position 1 (units in ksi)



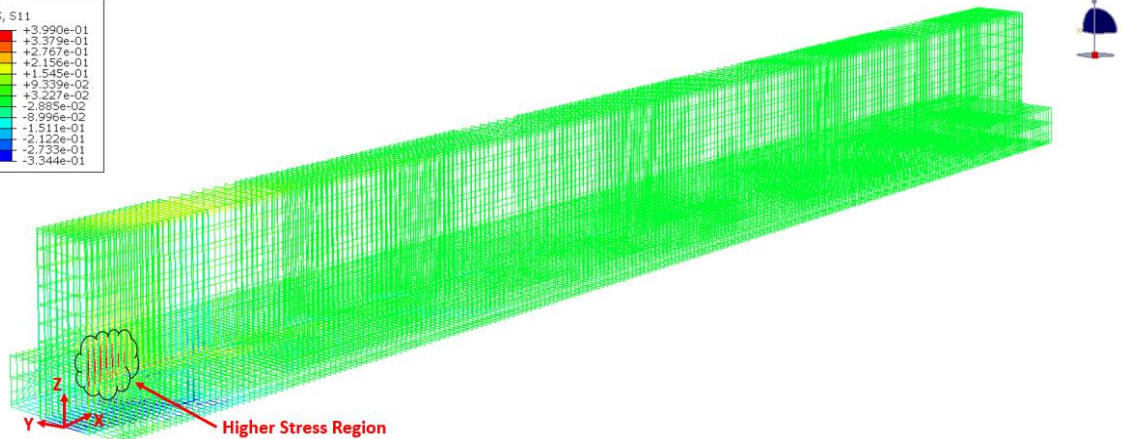
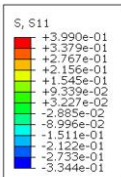
(b) Stresses in Rebar Cage for Case 3 of Bent Cap 2 at Position 2 (units in ksi)



(c) Stress in Rebar Cage for Case 3 of Bent Cap 2 at Position 3 (units in ksi)



(d) Stresses in Rebar Cage for Case 3 of Bent Cap 2 at Position 4 (units in ksi)

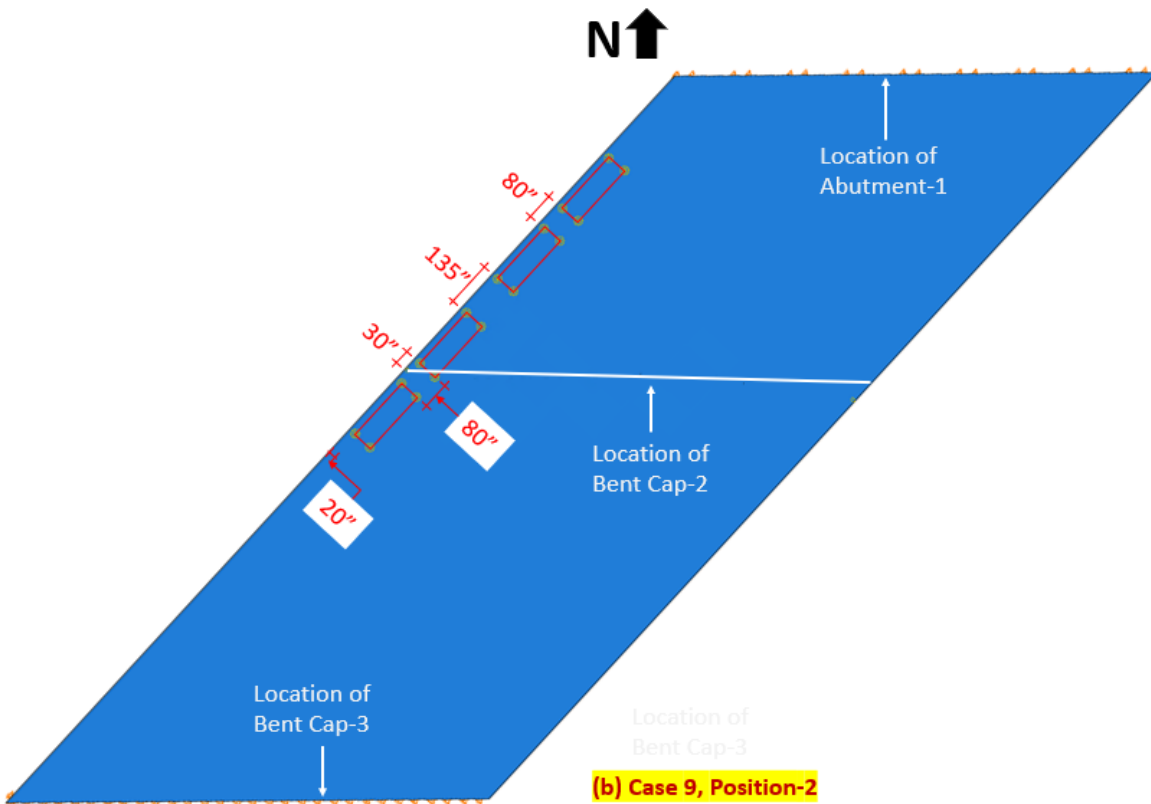
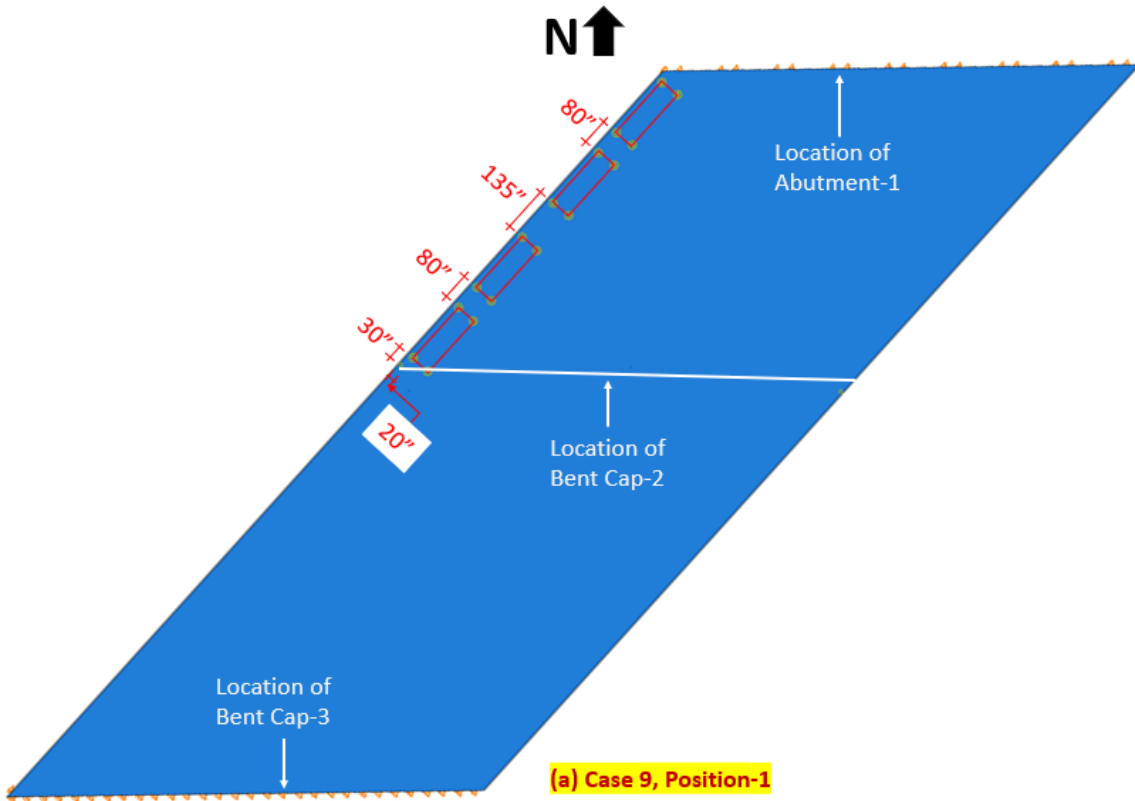


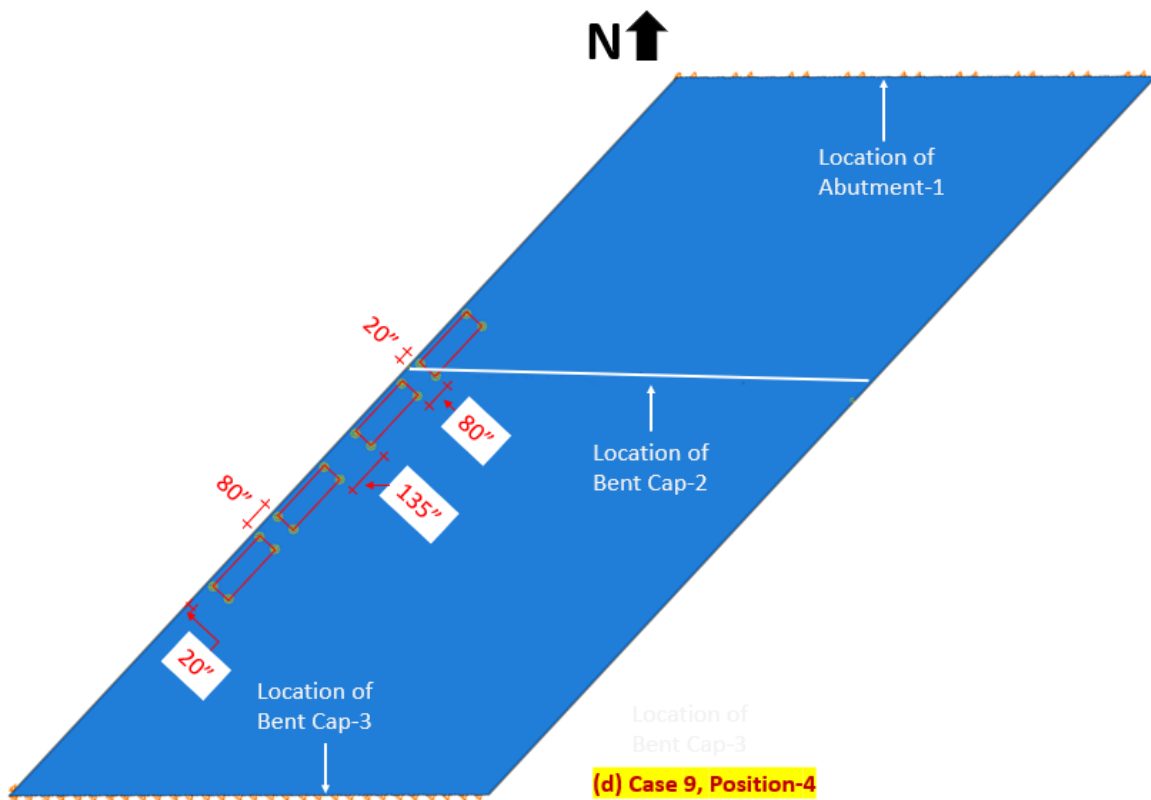
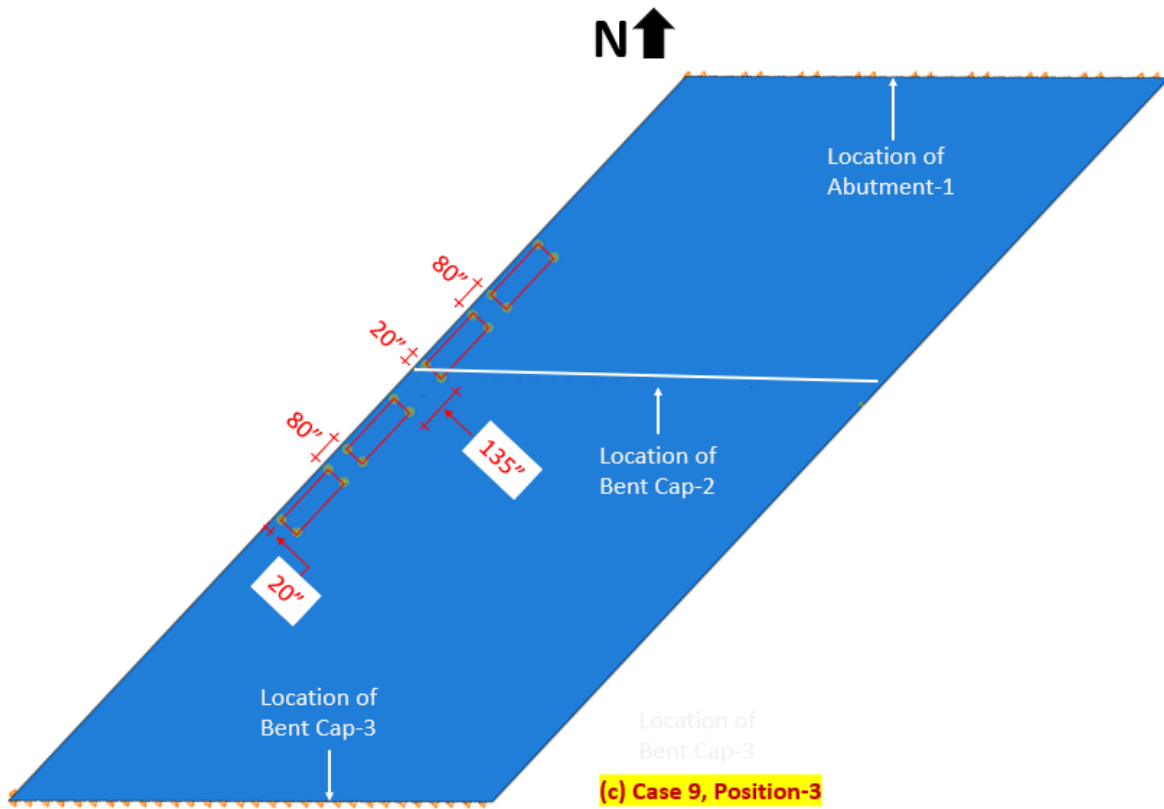
(e) Stresses in Rebar Cage for Case 3 of Bent Cap 2 at Position 5 (units in ksi)

**Figure 2.16. Stress Distribution in Rebar Cage for Case 3 of Bent Cap 2 under Four-Truck Loading at Five Positions**

At Position 1, four-truck loading is placed in the backward span of Bent Cap 2. The 3D FE simulation results show that the higher tensile strain is distributed on the North side of Bent Cap 2. Similarly, a higher displacement of Bent Cap 2 is observed at the end of the North side of Bent Cap 2. The stresses on the rebar cage are concentrated on the S-bars of the North side. The concrete tensile strain, displacement of the west face, and stresses in the S-bars at Position 2 are higher than those at Position 1. Four trucks loaded at Positions 3 to 5 are concentrated on the forward span of the Bent Cap 2. Positions 3 to 5 show that the concrete tensile strain, displacement of the west face, and stresses in the S-bars are higher in the extended region of the South side. The concrete tensile strains at the intersection of the ledge and stem under four-truck loading at five positions are  $9.32 \mu\epsilon$ ,  $18.24 \mu\epsilon$ ,  $22.05 \mu\epsilon$ ,  $41.74 \mu\epsilon$ , and  $19.51 \mu\epsilon$ , respectively. The peak displacements of the West face under four-truck loading at Positions 1 to 5 are -0.000962-inch, -0.00301-inch, -0.0125-inch, -0.01838-inch, and -0.007783-inch, respectively. The highest stresses in the S-bar under four-truck loading at Position 1 to 5 are 0.125 ksi, 0.25 ksi, 0.446 ksi, 0.844 ksi, and 0.4 ksi, respectively. Based on these simulation results, Position 3 and Position 4 of Case 3 of Bent Cap 2 yielded higher transverse rebar stresses, concrete strain, and greater displacement.

Case 9 is also critically examined with four-truck load at 5 positions, as shown in Figure 2.17. The finite element simulated strains for Case 9 of Bent Cap 2 under four-truck loading at 5 positions, the maximum tensile and compressive concrete strains and the displacements for Case 9 of Bent Cap 2 under four-truck loading at 5 positions, Carbon Nanofiber Aggregates (CNFAs) stress values for Case 9 of Bent Cap 2 under four-truck loading at 5 positions are presented in APPENDIX-1. Figures 2.18(a) – 2.18(e) show the tensile strain distribution of concrete for Case 9 of Bent Cap 2, respectively. Figures 2.19(a) – 2.19(e) show the displacements of the West face for Case 9 of Bent Cap 2, respectively. Figures 2.20(a) – 2.20(e) show the stress distribution in the rebar cage for Case 9 of Bent Cap 2, respectively.





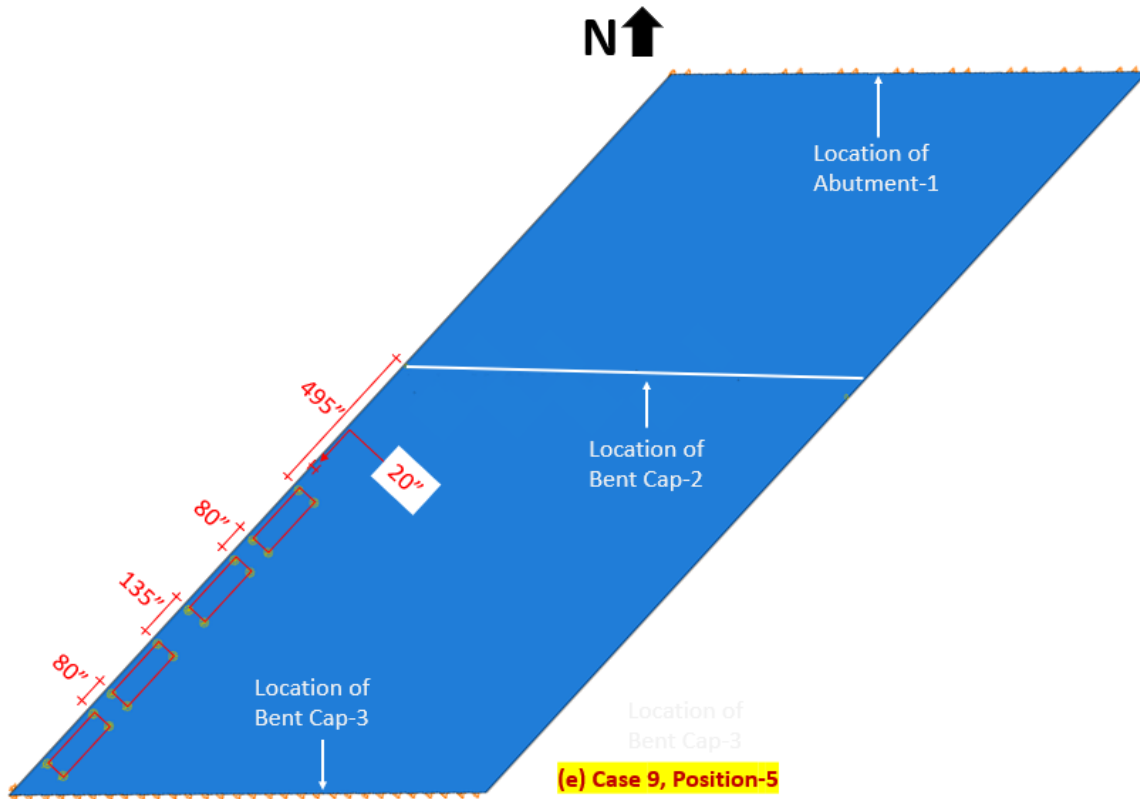
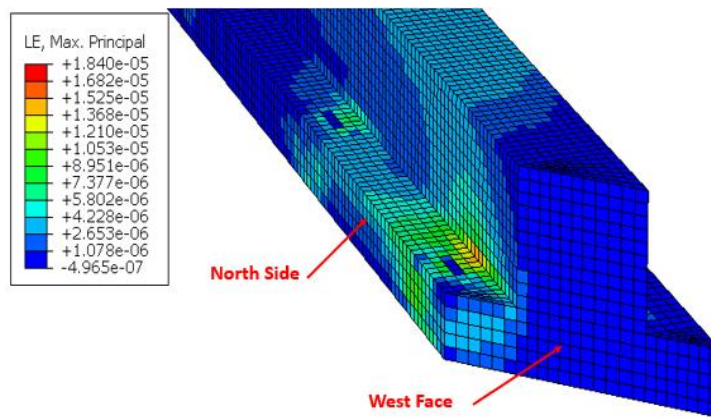
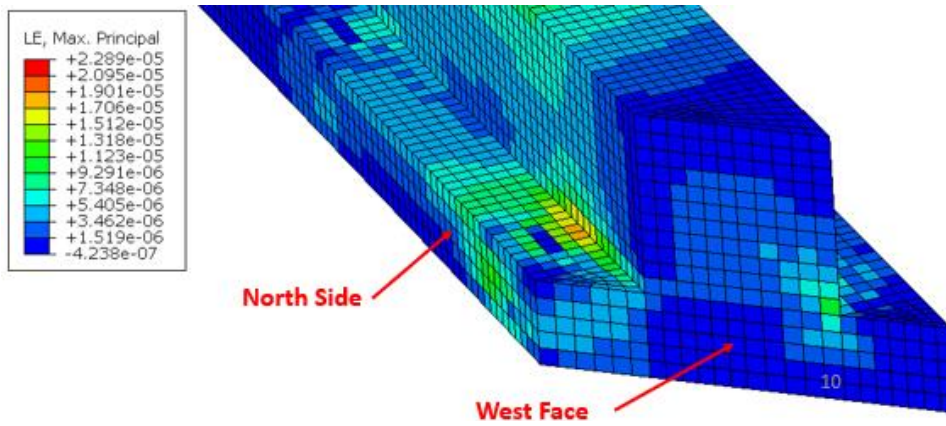


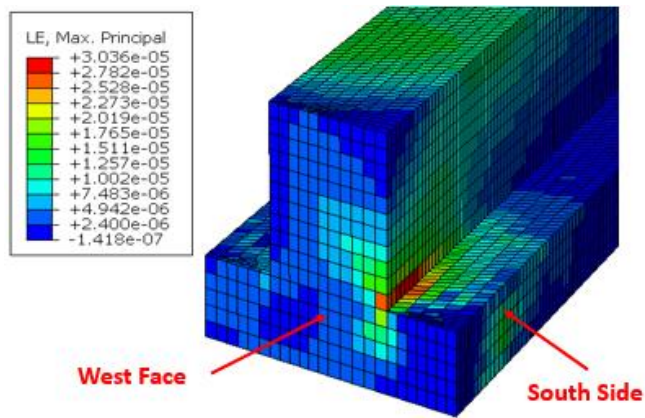
**Figure 2.17. Five Positions of Four-Truck Loading for Case 9 of Bent Cap-2**



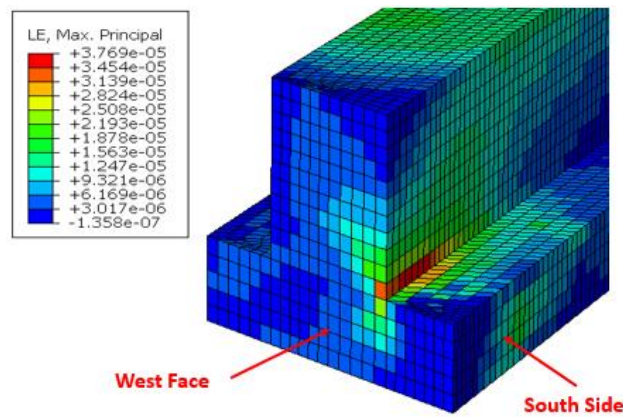
**(a) Concrete Tensile Strain for Case 9 in Position-1**



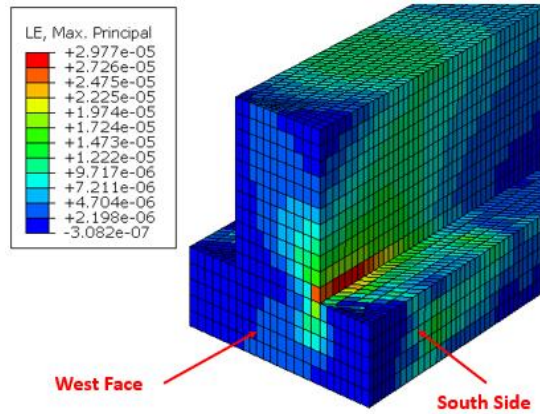
(b) Concrete Tensile Strain for Case 9 in Position-2



(c) Concrete Tensile Strain for Case 9 in Position-3

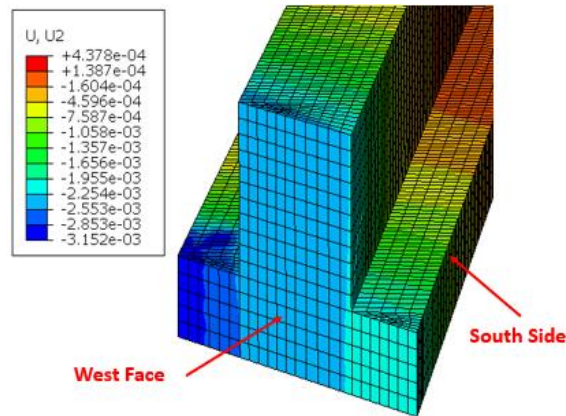


(d) Concrete Tensile Strain for Case 9 in Position-4

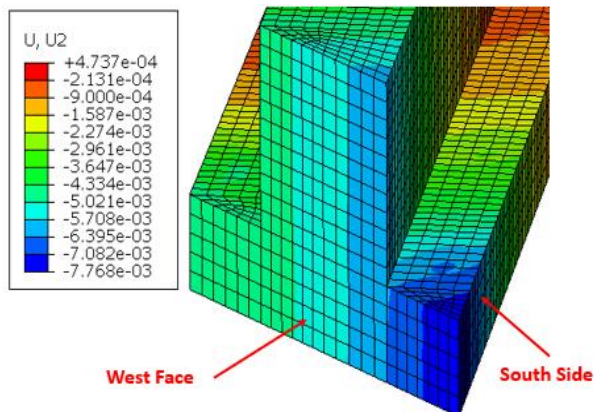


(e) Concrete Tensile Strain for Case 9 in Position-5

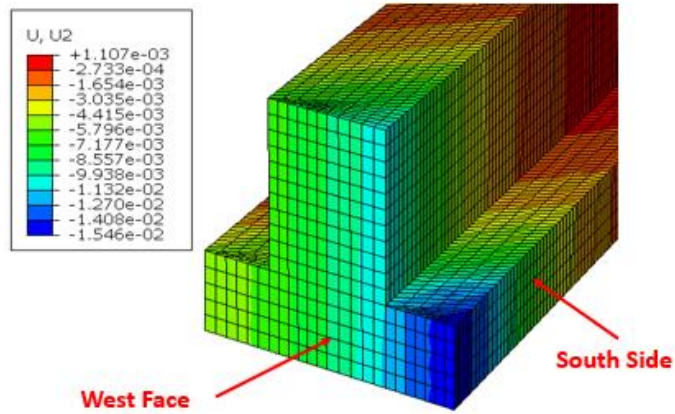
**Figure 2.18. Tensile Strain Distribution of Concrete for Case 9 of Bent Cap 2 under Four-Truck Loading at Five Positions**



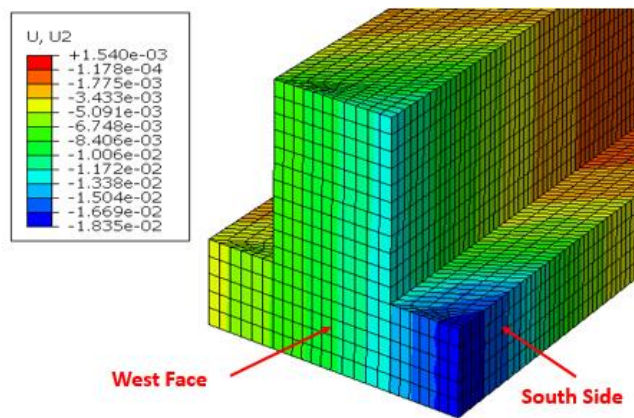
(a) West Face Displacement for Case 9 in Position-1 (units in inches)



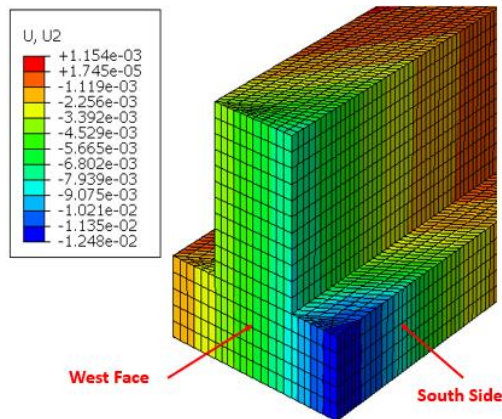
(b) West Face Displacement for Case 9 in Position-2 (units in inches)



(c) West Face Displacement for Case 9 in Position-3 (units in inches)

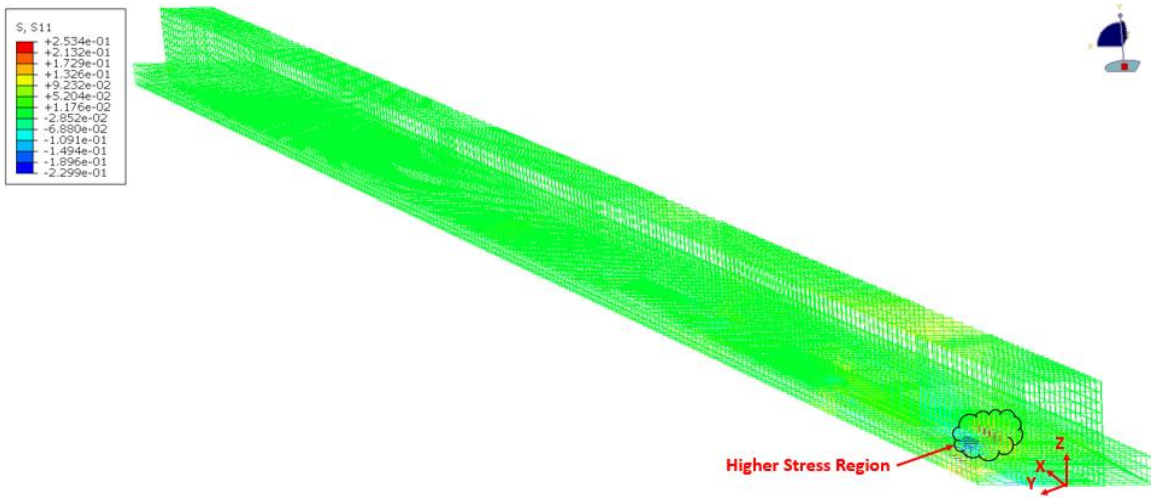


(d) West Face Displacement for Case 9 in Position-4 (units in inches)

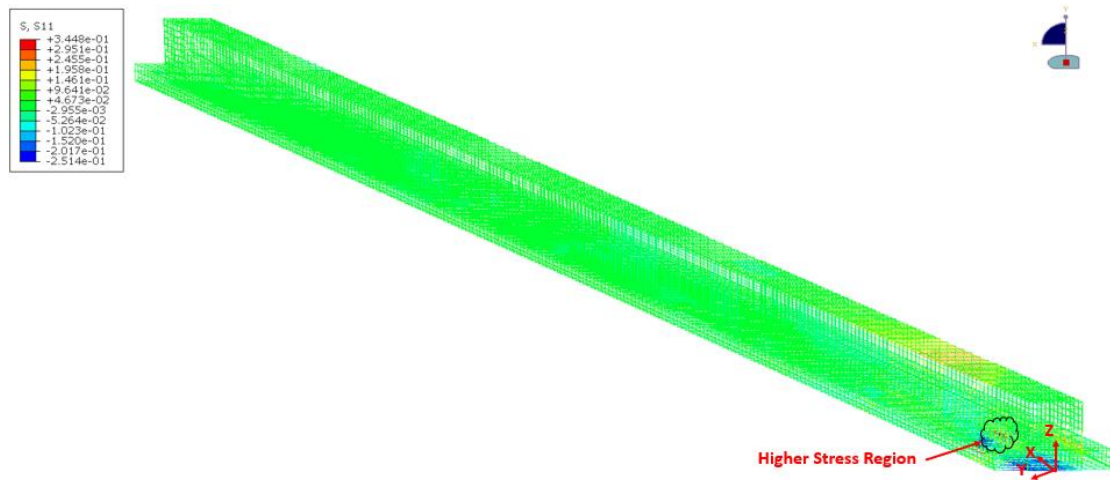


(e) West Face Displacement for Case 9 in Position-5 (units in inches)

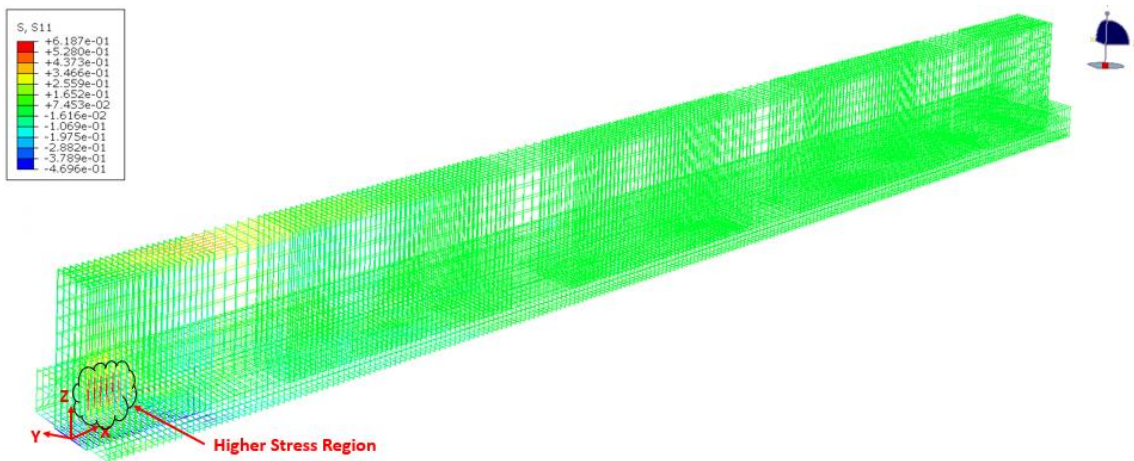
**Figure 2.19. Displacement Profile for Case 9 of Bent Cap 2 under Four-Truck Loading at Five Positions**



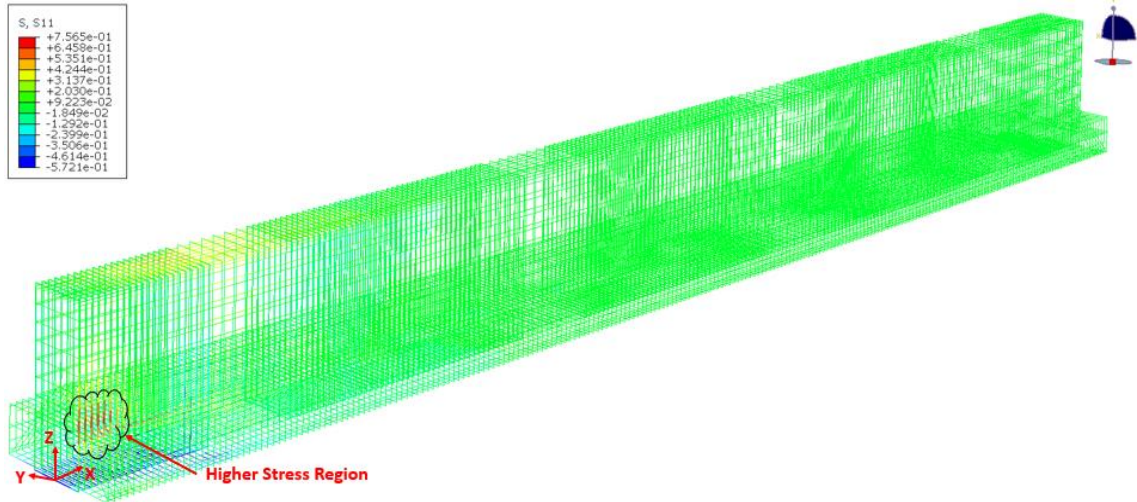
(a) Stresses in Rebar Cage for Case 9 in Position-1 (units in ksi)



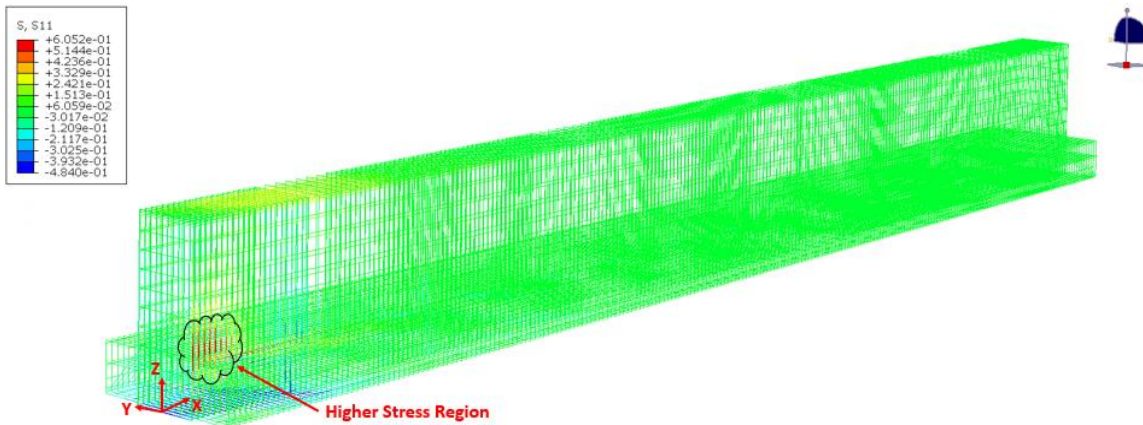
(b) Stresses in Rebar Cage for Case 9 in Position-2 (units in ksi)



(c) Stress in Rebar Cage for Case 9 in Position-3 (units in ksi)



(d) Stresses in Rebar Cage for Case 9 in Position-4 (units in ksi)



(e) Stresses in Rebar Cage for Case 9 in Position-5 (units in ksi)

**Figure 2.20. Stress Distribution in Rebar Cage for Case 9 of Bent Cap 2 under Four-Truck Loading at Five Positions**

In Position-1, four-truck loading is placed in the backward span of Bent Cap-2. The 3D FE simulation results show that the higher tensile strain is distributed on the North side of Bent Cap-2. Similarly, higher displacement of Bent Cap-2 is observed on the left end (North side) of Bent Cap-2. The stresses on the rebar cage are concentrated on the S-bars of the North side. The concrete tensile strain, displacement of the west face, and stresses in the S-bars are higher on the North side in Position-2 than in Position-1. Four trucks loaded in Positions 3 to 5 are concentrated on the forward span of the Bent Cap-2. Positions 3 to 5 show that the concrete tensile strain, displacement of the west face, and stresses in the S-bars are higher in the extended region of the South side. The concrete tensile strains of the five positions at the intersection of ledge and stem are  $18.4 \mu\epsilon$ ,  $22.89$

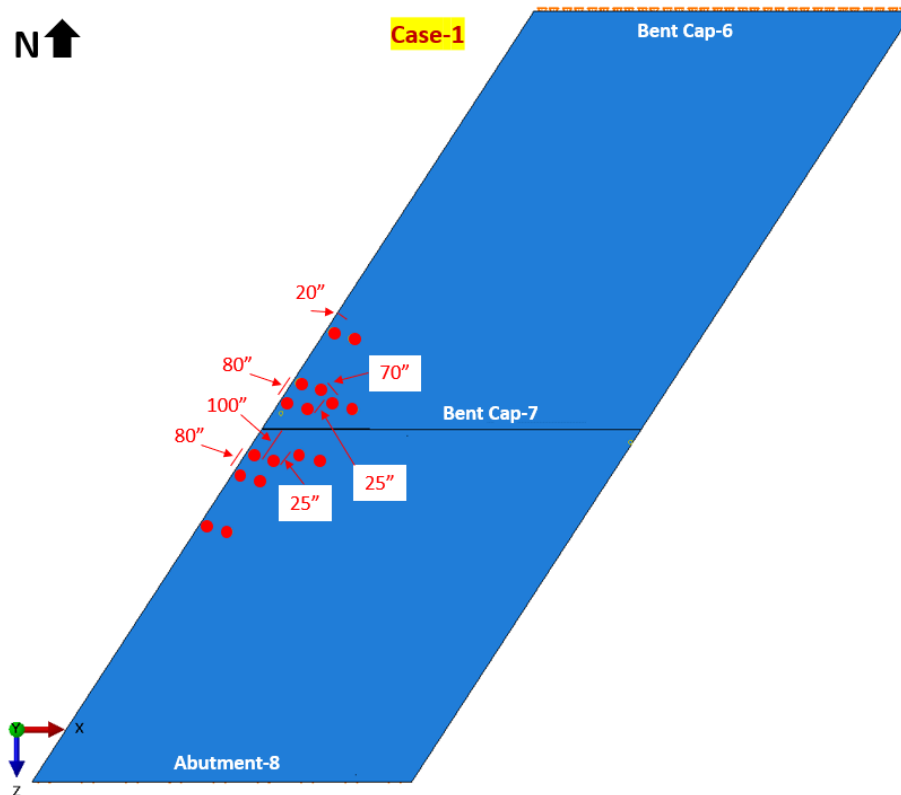
$\mu\epsilon$ ,  $30.36 \mu\epsilon$ ,  $37.69 \mu\epsilon$ , and  $29.77 \mu\epsilon$  respectively. The peak displacements of the West face in Positions 1 to 5 are -0.003152-inch, -0.007768-inch, -0.01546-inch, -0.01835-inch, and -0.01248-inch, respectively. The highest stresses in the S-bar in Position 1 to 5 are 0.25 ksi, 0.34 ksi, 0.62 ksi, 0.76 ksi, and 0.61 ksi, respectively. Based on these simulation results, Position-3 and Position-4 of Case 9 yielded

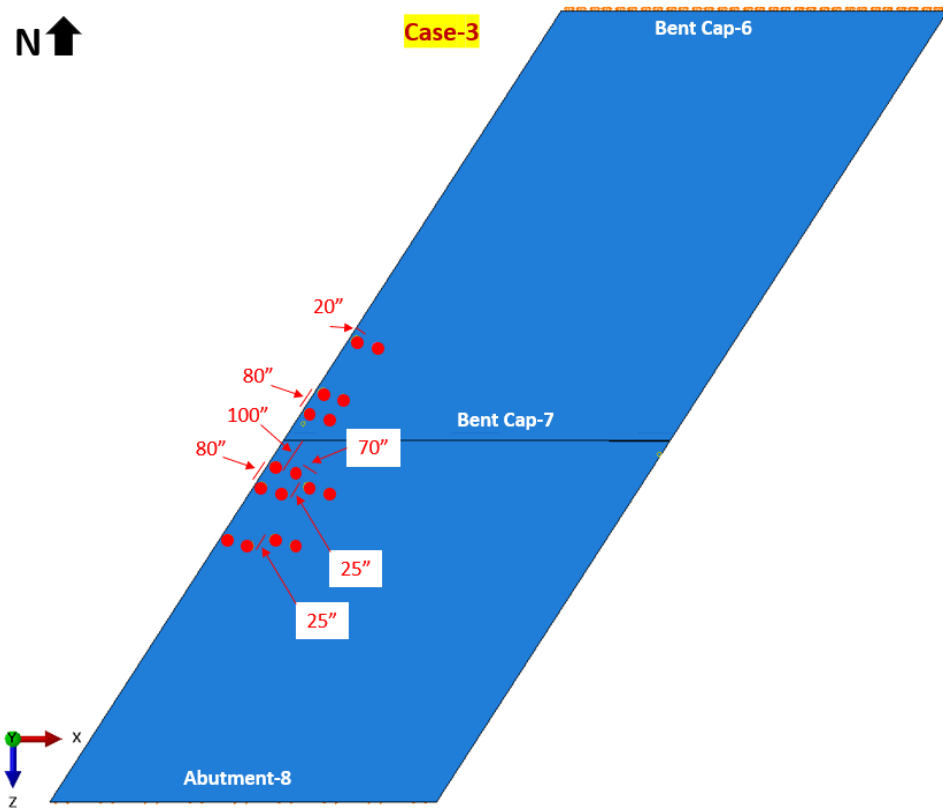
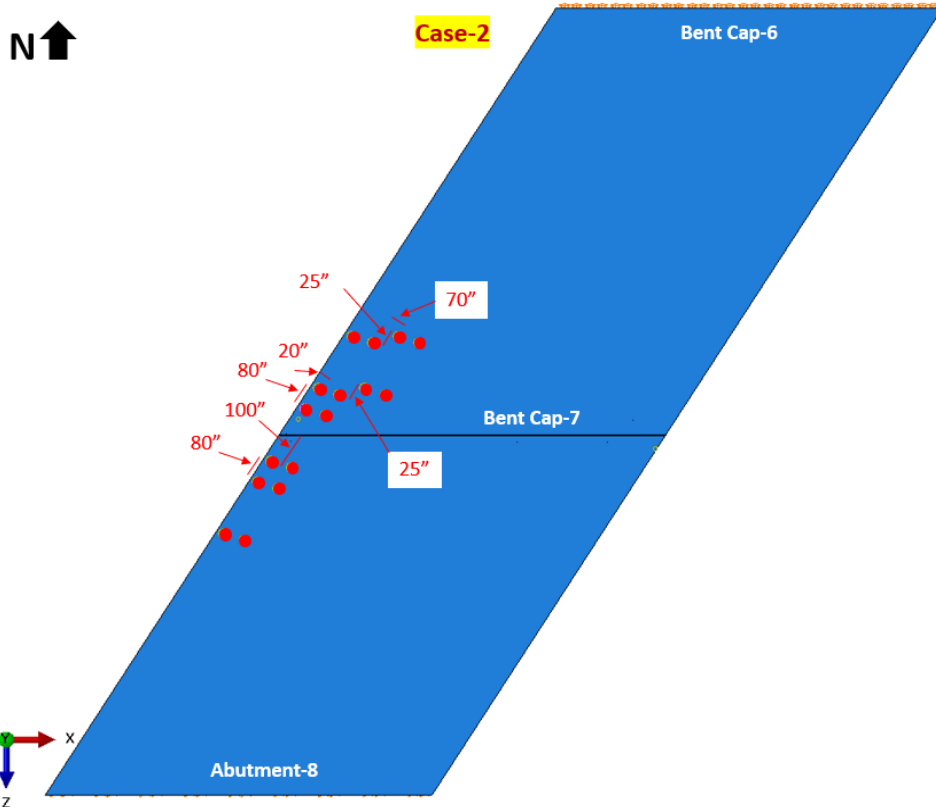
## 2.4 BENT CAP 7

The finite element simulation of Bent Cap 7 is based on the four trucks loading. The vertical loads from four trucks with 43.2 kips each are applied on top of the bridge deck. Point loads for front tires and rear tires are 11.0 kips and 32.2 kips, respectively.

### 2.4.1 Static Test-1 Finite Element Simulation

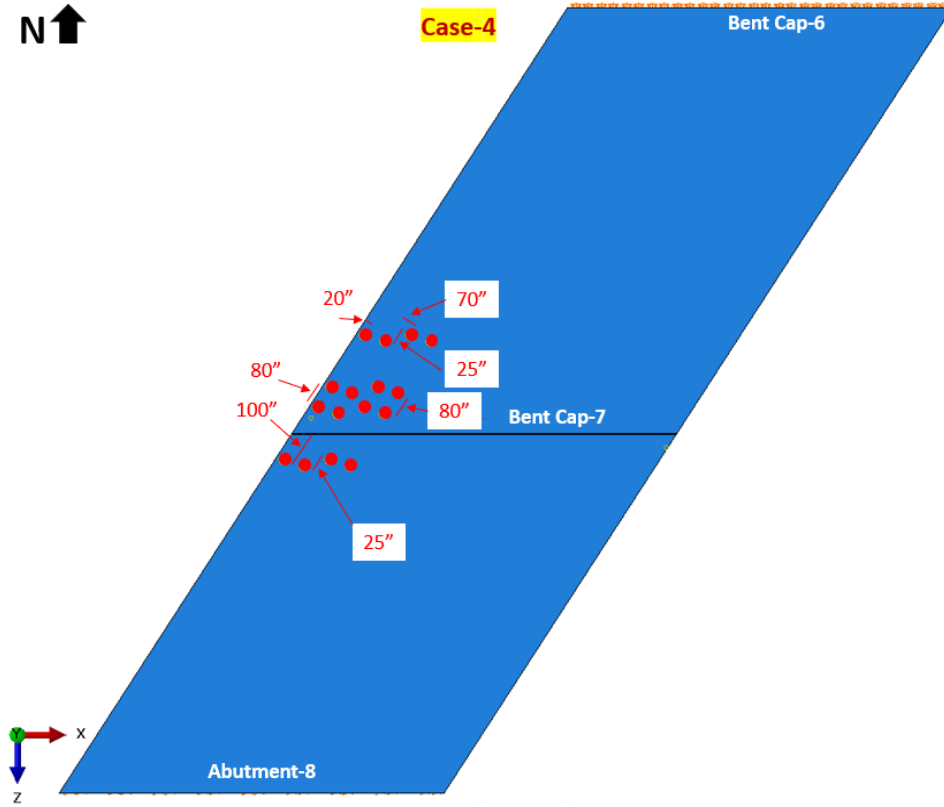
There are 15 cases of four-truck loading simulated on the global finite element model for Bent Cap 2. The extended region and interface between the ledge and stem of the skewed ITBC are critical regions in the ITBC (Sapath Roy et al., 2021; Sapath et al., 2019; Zhou et al., 2020). These 15 simulations are focused on observing the strain on the extended regions. The location of the front tires and rear tires of the loading trucks are shown in Figure 2.21.



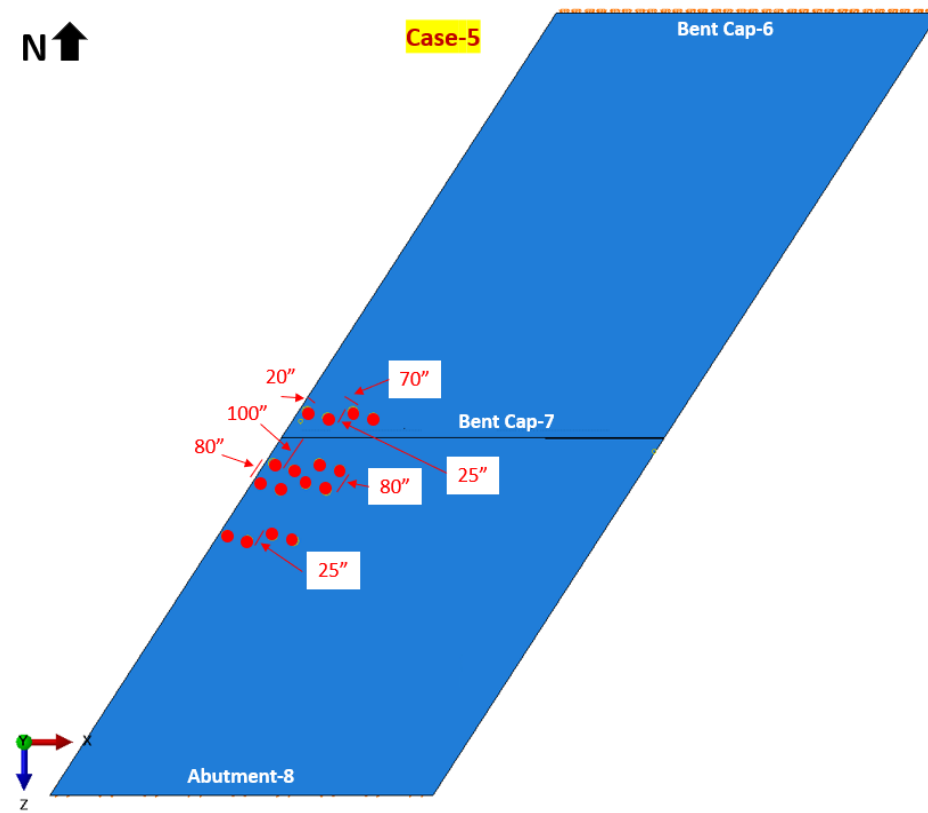




Case-4

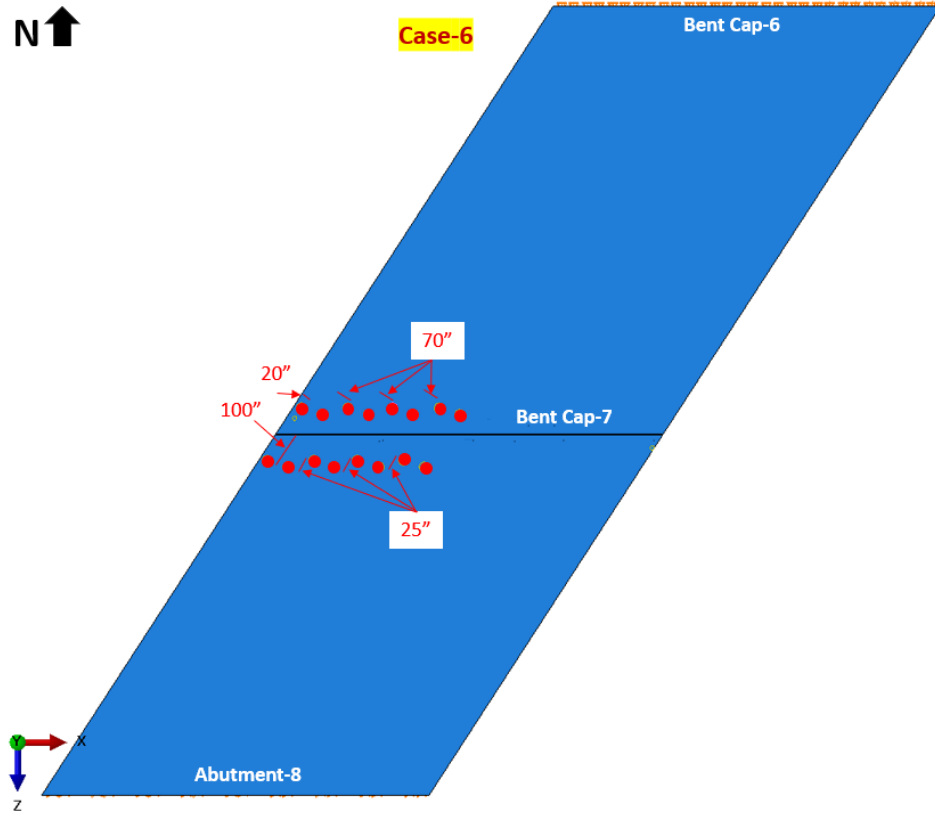


Case-5

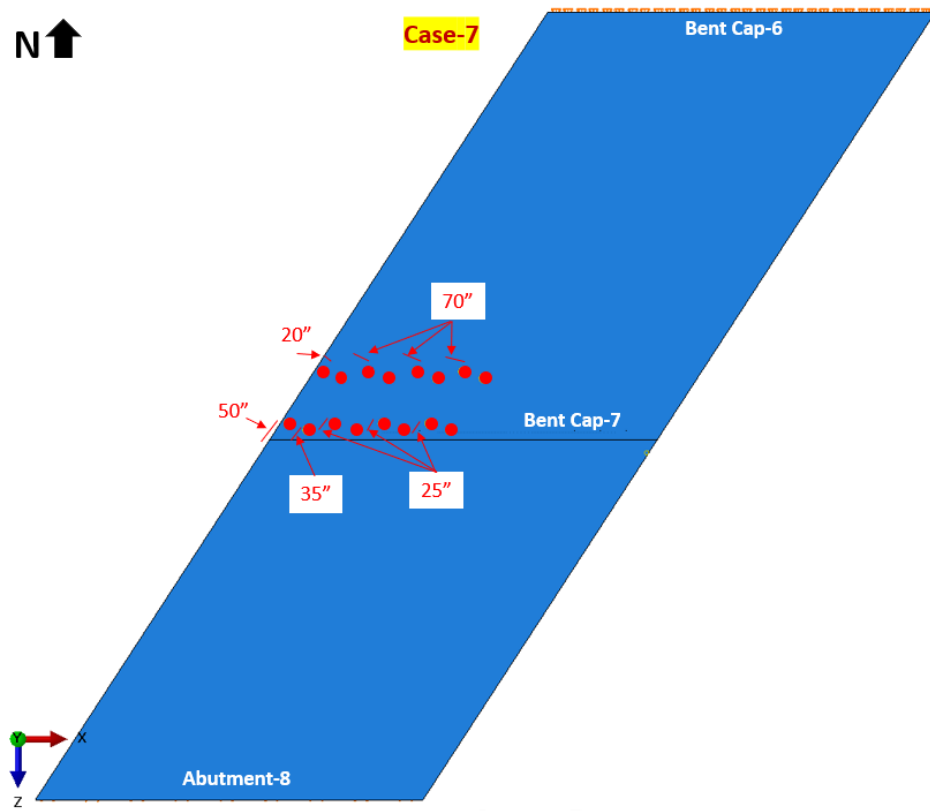




**Case-6**

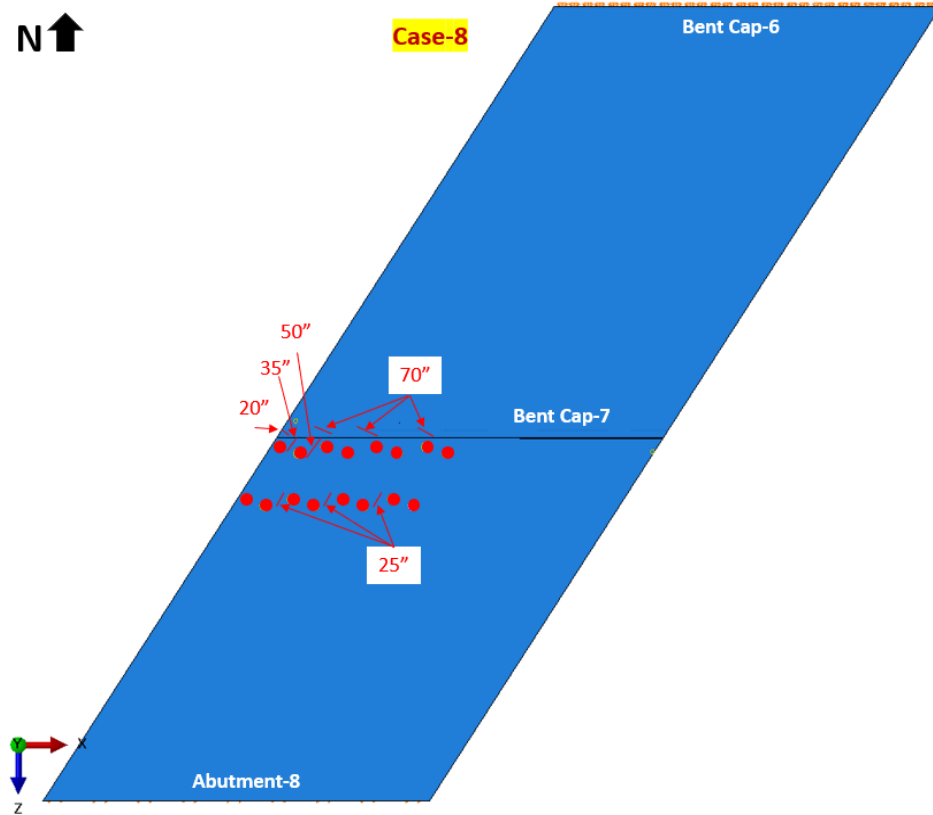


**Case-7**

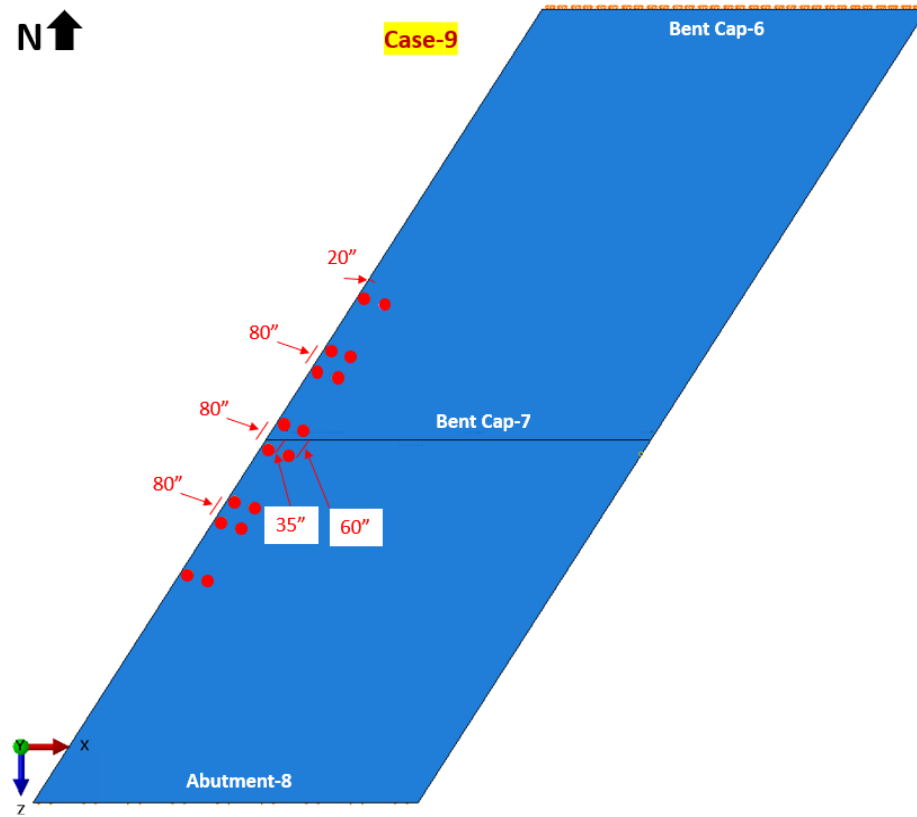


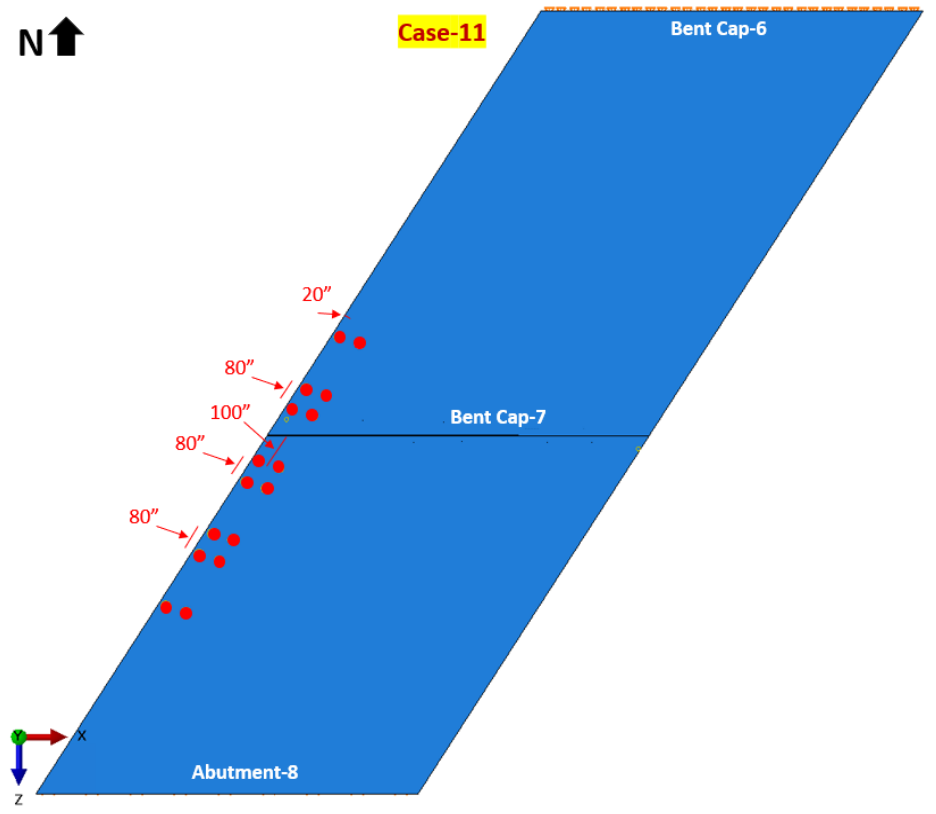
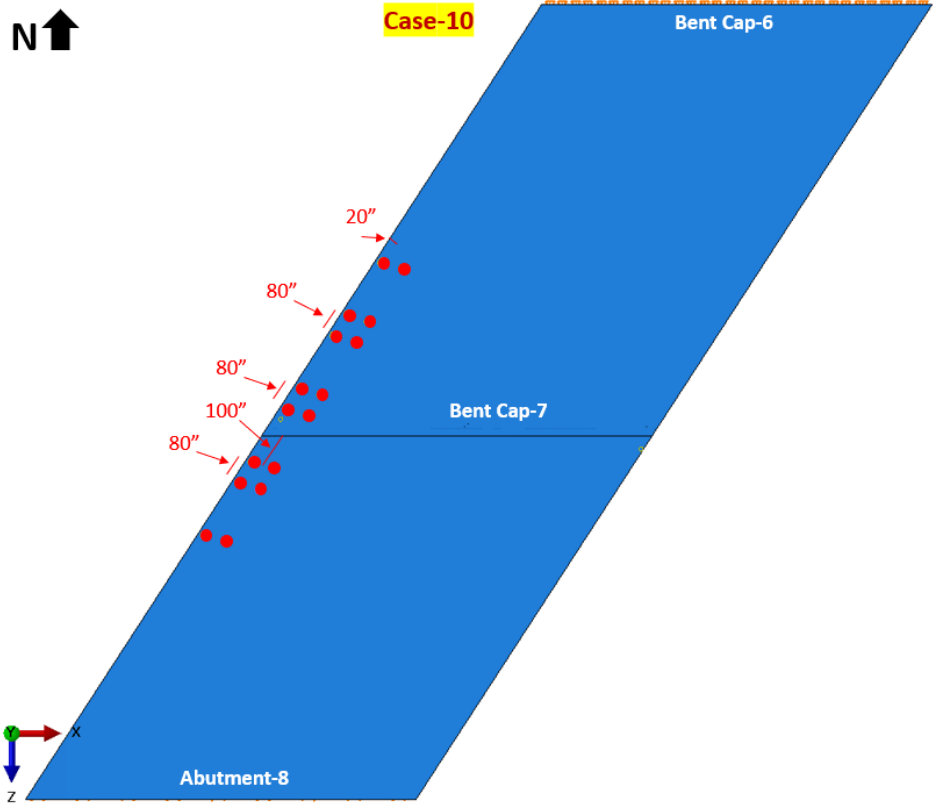


Case-8



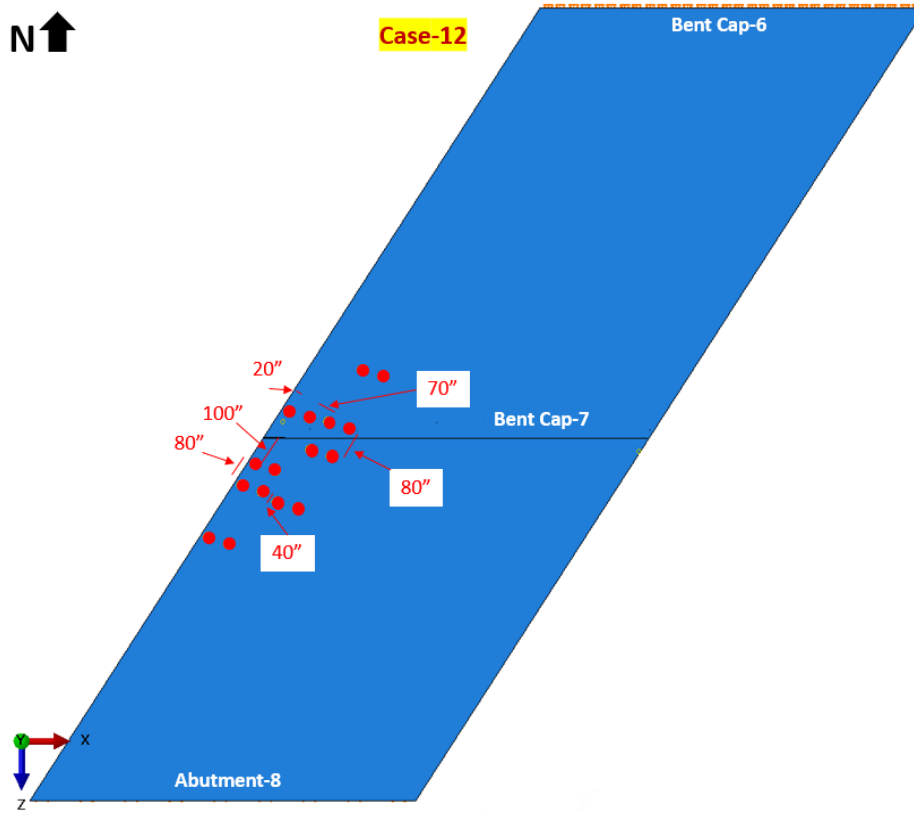
Case-9



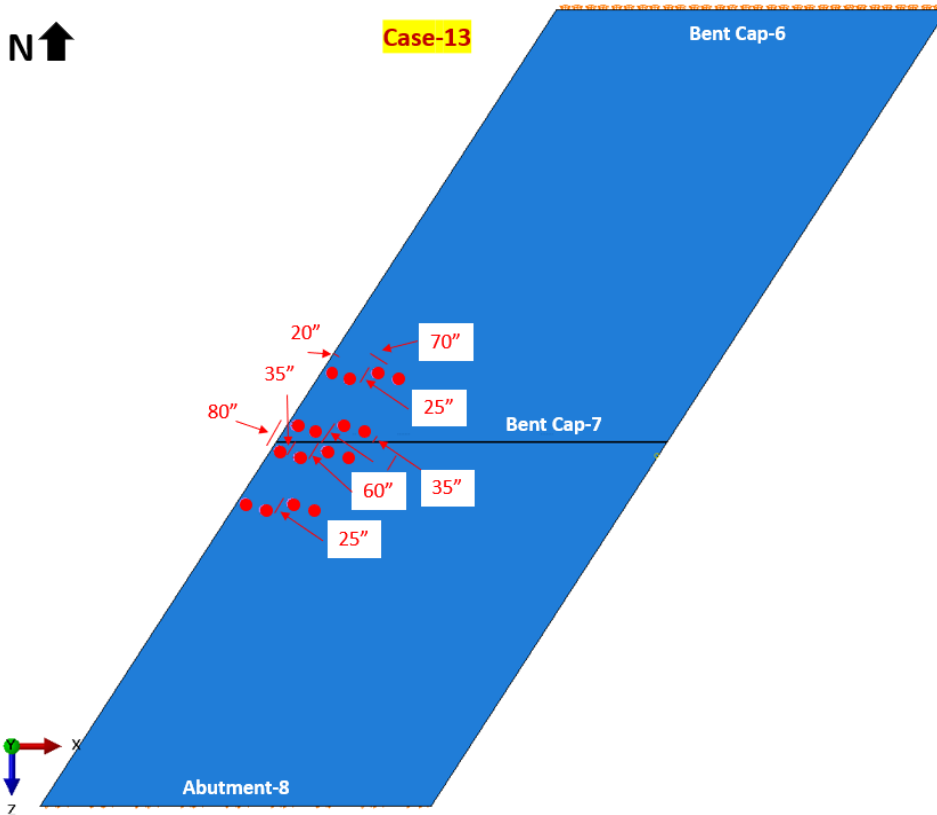




Case-12



Case-13



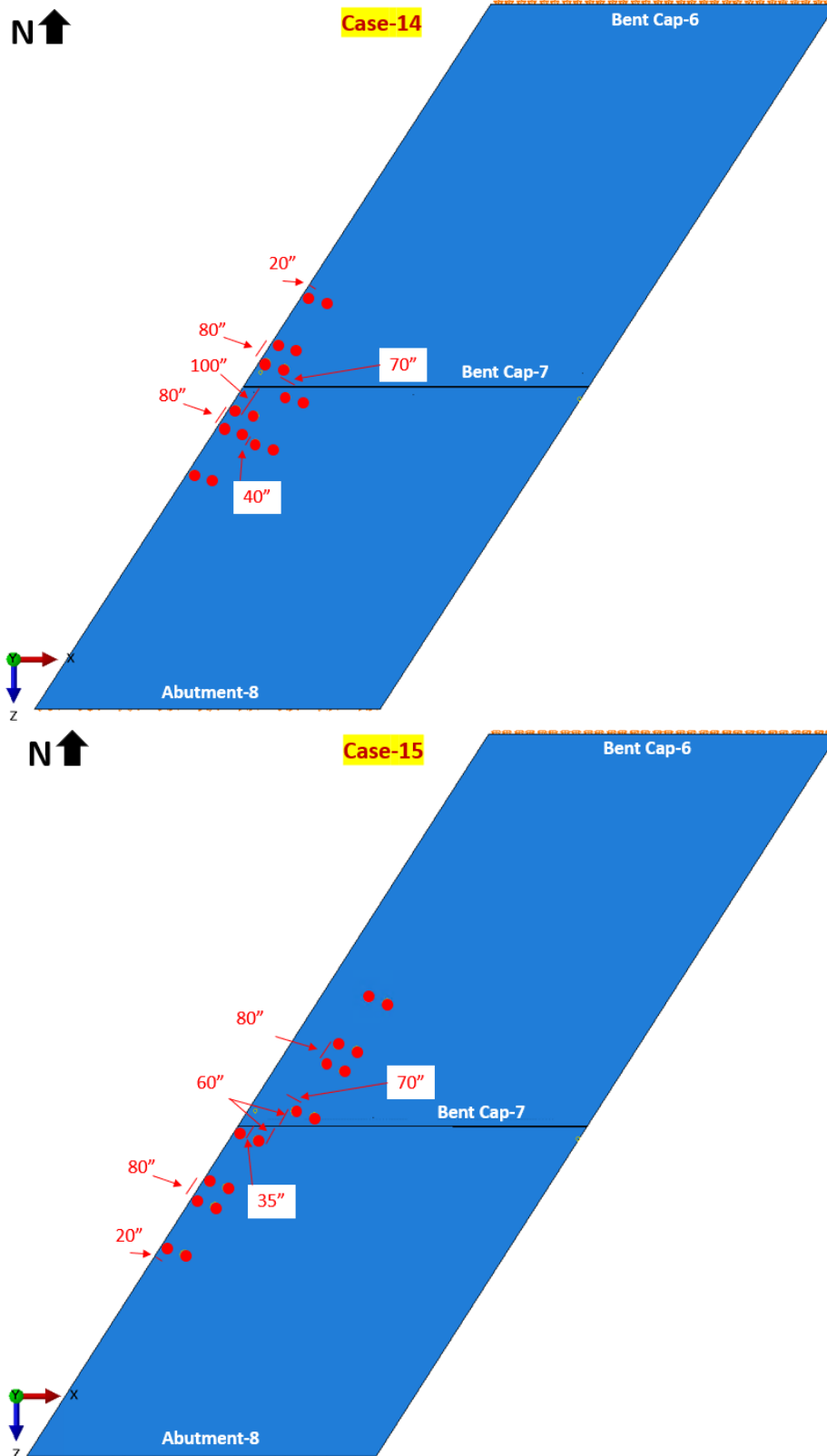


Figure 2.21. Four Trucks Locations for Cases 1 to 15 of Bent Cap 7

Based on FE simulations of 15 cases of four trucks loading, the locations for strain gauges, carbon nanofiber aggregates (CNFAs), and laser sensors are identified for Bent Cap 7. Table 2.4 shows the details of the locations for the strain gauge installation. Table 2.5 shows Carbon Nanofiber Aggregate (CNFAs) installation locations. The finite element simulated strains for the 15 cases at 30 locations, the maximum concrete strains in tension and compression and the displacements at the West face of ITBC, the stress values of the 15 cases for the 9 Carbon Nanofiber Aggregates (CNFAs) locations on Bent Cap 7 are presented in APPENDIX-2. Figures 2.22(a) – 2.22(o) show the tensile strain distribution on concrete for Cases 1 to 15, respectively. Figures 2.23(a) – 2.23(o) show the displacements of the West face of Bent Cap 7 for Cases 1 to 15, respectively. Figures 2.24(a) – 2.24(o) show the stress distribution on the rebar cage of Bent Cap 7 for Cases 1 to 15, respectively.

**Table 2.4. Identified Locations of Strain Gauges in Bent Cap 7**

No.	Label	Explanation	X (in)	Y (in)	Z (in)	Bar Group
			Coordinates shown in Figure 2.24			
1	<b>B7-SS1s1</b>	Bent Cap 7 - South side, 1st S Bar from the West face, 1st SG located on the Side of the bar	-13.3	-20.5	30	S Bars
2	<b>B7-SS1s2</b>	Bent Cap 7 - South side, 1st S Bar from the West face, 2nd SG located on the Side of the bar	-13.3	-20.5	35	
3	<b>B7-SS2s1</b>	Bent Cap 7 - South side, 2nd S Bar from the West face, 1st SG located on the Side of the bar	-7.5	-20.5	30	
4	<b>B7-SS2s2</b>	Bent Cap 7 - South side, 2nd S Bar from the West face, 2nd SG located on the Side of the bar	-7.5	-20.5	35	
5	<b>B7-SS3s1</b>	Bent Cap 7 - South side, 3rd S Bar from the West face, 1st SG located on the Side of the bar	-1.6	-20.5	30	
6	<b>B7-SS3s2</b>	Bent Cap 7 - South side, 3rd S Bar from the West face, 2nd SG located on the Side of the bar	-1.6	-20.5	35	
7	<b>B7-SS4s1</b>	Bent Cap 7 - South side, 4th S Bar from the West face, 1st SG located on the Side of the bar	4.72	-20.5	30	

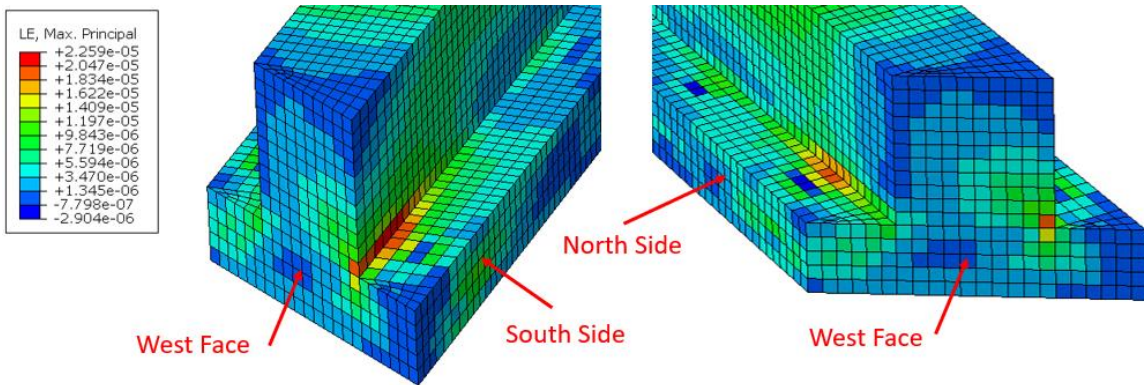
8	<b>B7-SS4s2</b>	Bent Cap 7 - South side, 4th S Bar from the West face, 2nd SG located on the Side of the bar	4.72	-20.5	35		
9	<b>B7-NS5s1</b>	Bent Cap 7 - North side, 5th S Bar from the West face, 1st SG located on the Side of the bar	43.9	20.5	30		
10	<b>B7-NS5s2</b>	Bent Cap 7 - North side, 5th S Bar from the West face, 2nd SG located on the Side of the bar	43.9	20.5	35		
11	<b>B7-NS6s1</b>	Bent Cap 7 - North side, 6th S Bar from the West face, 1st SG located on the Side of the bar	49.9	20.5	30		
12	<b>B7-NS6s2</b>	Bent Cap 7 - North side, 6th S Bar from the West face, 2nd SG located on the Side of the bar	49.9	20.5	35		
13	<b>B7-NS7s1</b>	Bent Cap 7 - North side, 7th S Bar from the West face, 1st SG located on the Side of the bar	55.7	20.5	30		
14	<b>B7-NS7s2</b>	Bent Cap 7 - North side, 7th S Bar from the West face, 2nd SG located on the Side of the bar	55.7	20.5	35		
15	<b>B7-NS8s1</b>	Bent Cap 7 - North side, 8th S Bar from the West face, 1st SG located on the Side of the bar	61.57	20.5	30		
16	<b>B7-NS8s2</b>	Bent Cap 7 - North side, 8th S Bar from the West face, 2nd SG located on the Side of the bar	61.57	20.5	35		
17	<b>B7-SM5t</b>	Bent Cap 7 - South side, 5th M Bar from the West face, SG located on the Top of the bar	10.8	-20.8	23		M Bars
18	<b>B7-SM6t</b>	Bent Cap 7 - South side, 6th M Bar from the West face, SG located on the Top of the bar	16.6	-20.8	23		
19	<b>B7-SM7t</b>	Bent Cap 7 - South side, 7th M Bar from the West face, SG located on the Top of the bar	22.4	-20.8	23		
20	<b>B7-SM8t</b>	Bent Cap 7 - South side, 8th M Bar from the West face, SG located on the Top of the bar	28.2	-20.8	23		

21	<b>B7-SM15b</b>	Bent Cap 7 - South side, 15th M Bar from the West face, SG located on the Bottom of the bar	71.6	-17	0	
22	<b>B7-SM17b</b>	Bent Cap 7 - South side, 17th M Bar from the West face, SG located on the Bottom of the bar	83	-17	0	
23	<b>B7-A7</b>	Bent Cap 7 - 7th A Bar of 1st alignment from the West face	99	9.9	78.2	A Bars
24	<b>B7-A8</b>	Bent Cap 7 - 8th A Bar of 1st alignment from the West face	107	14.8	78.2	
25	<b>B7-A9</b>	Bent Cap 7 - 9th A Bar of 1st alignment from the West face	109	19.8	78.2	
26	<b>B7-U1-1</b>	Bent Cap 7 - 1st U1 Bar from the West face	-7.24	12.05	39.25	U1 Bar
27	<b>B7-SG1</b>	Bent Cap 7 - South side, 1st G Bar from the West face	-1.59	-21	25.5	G Bar
28	<b>B7-SG2</b>	Bent Cap 7 - South side, 2nd G Bar from the West face	4.25	-21	25.5	
29	<b>B7-B10</b>	Bent Cap 7 - 10th B Bar from the West face	76	18	1.1	B Bar
30	<b>B7-T7</b>	Bent Cap 7 - North side, 7th T bar from the West face under the bearing pad	51.2	39.5	24	T Bar

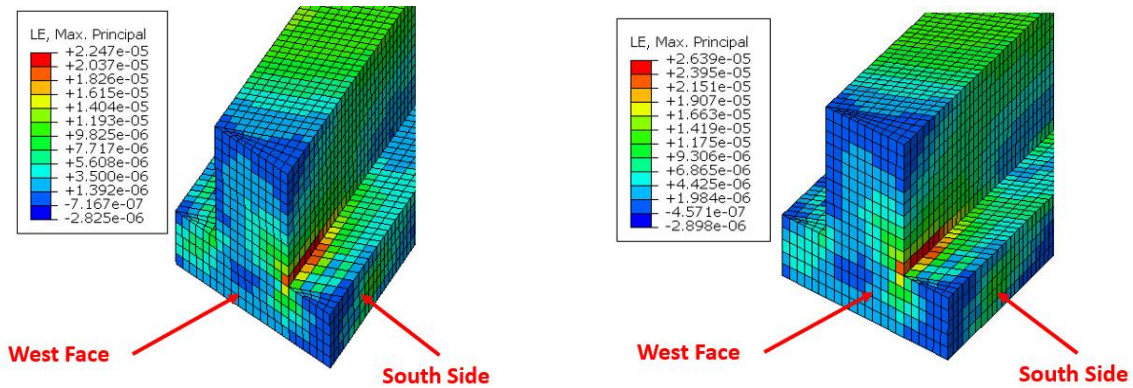
**Table 2.5. Identified Location of CNFAs in Bent Cap 7**

No.	Label	Explanation	X (in)	Y (in)	Z (in)	Group
1	<b>B7-CNFA1z1</b>	Bent Cap 7 - 10th B Bar from the West face, CNFA1 located in Z-direction	68.7	8.5	1.1	Location 1
2	<b>B7-CNFA1z2</b>	Bent Cap 7 - 13th M Bar from the West face, CNFA2 located in Z-direction	77	8.5	1.1	
3	<b>B7-CNFA2z1</b>	Bent Cap 7 - T Bar, First CNFA at Location 2 in Z-direction (North face)	43.7	37.5	24	Location 2
4	<b>B7-CNFA2z2</b>	Bent Cap 7 - T Bar, Second CNFA at Location 2 in Z-direction (North face)	46.2	37.5	24	
5	<b>B7-CNFA2z3</b>	Bent Cap 7 - T Bar, Third CNFA at Location 2 in Z-direction (North face)	48.7	37.5	24	

6	<b>B7-CNFA2z4</b>	Bent Cap 7 - T Bar, Fourth CNFA at Location 2 in Z-direction (North face)	51.2	37.5	24	
7	<b>B7-CNFA3z1</b>	Bent Cap 7 - 1st S Bar, First CNFA at Location 3 in Z-direction	-13.3	-20.5	30	Location 3
8	<b>B7-CNFA3z2</b>	Bent Cap 7 - 2nd S Bar, Second CNFA at Location 3 in Z-direction	-7.5	-20.5	35	
9	<b>B7-CNFA3z3</b>	Bent Cap 7 - 3rd S Bar, Third CNFA at Location 3 in Z-direction	-1.6	-20.5	35	

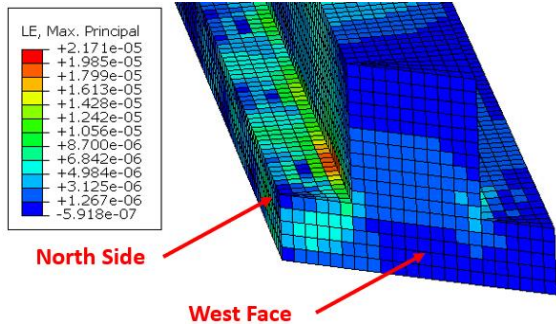


(a) Concrete Tensile Strain for Case 1

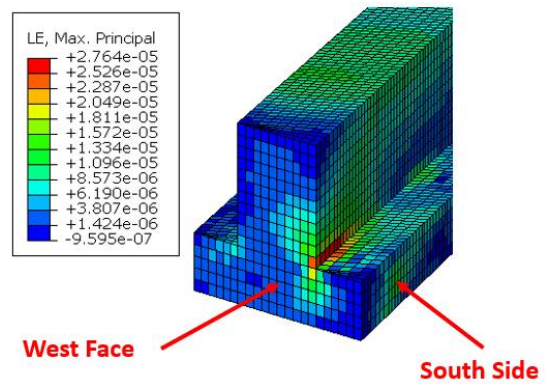


(b) Concrete Tensile Strain for Case 2

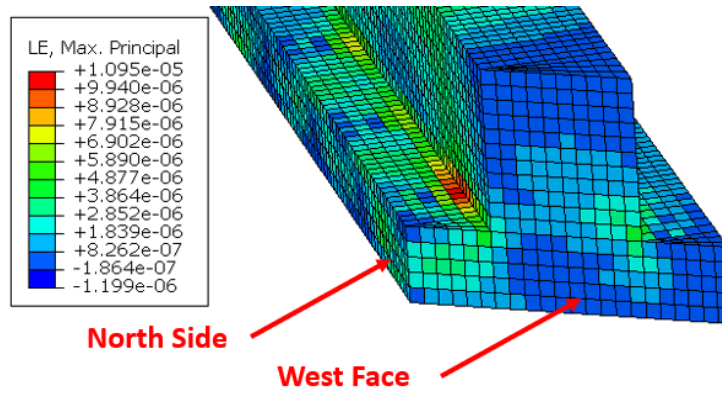
(c) Concrete Tensile Strain for Case 3



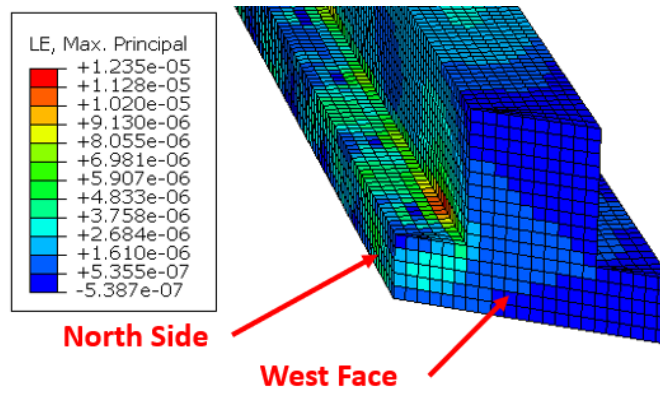
(d) Concrete Tensile Strain for Case 4



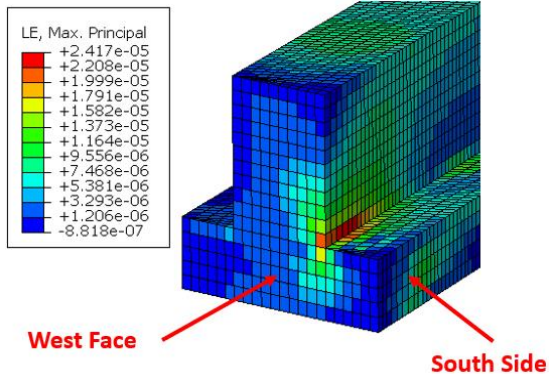
(e) Concrete Tensile Strain for Case 5



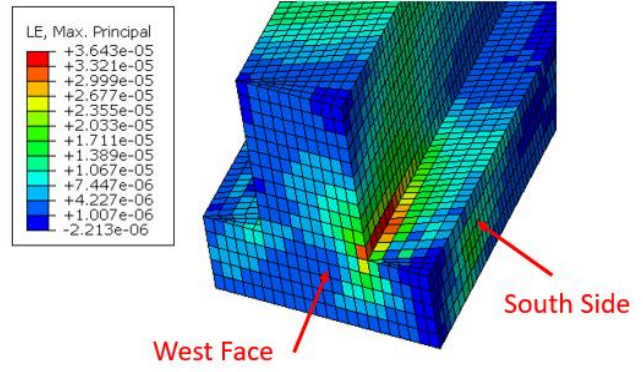
(f) Concrete Tensile Strain for Case 6



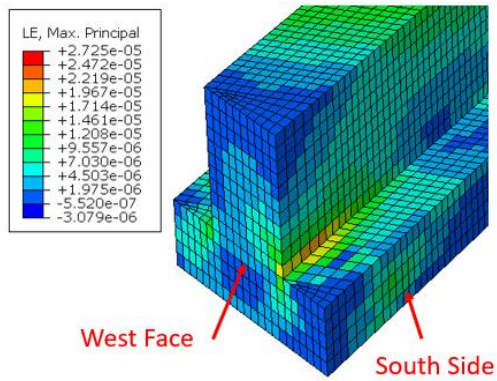
(g) Concrete Tensile Strain for Case 7



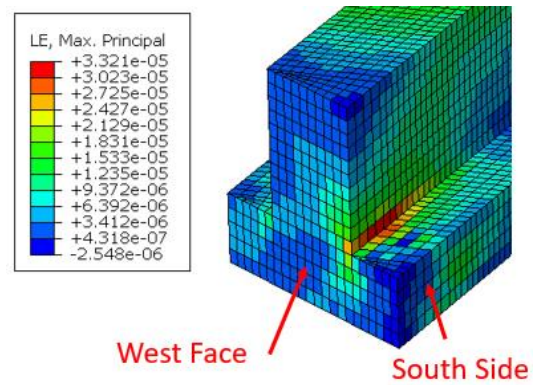
(h) Concrete Tensile Strain for Case 8



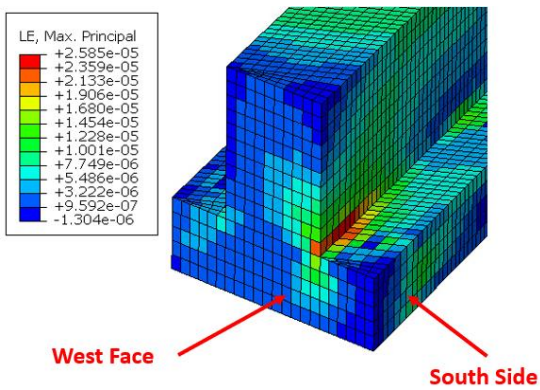
(i) Concrete Tensile Strain for Case 9



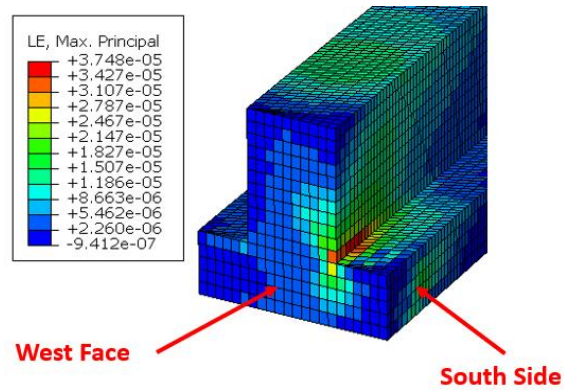
(j) Concrete Tensile Strain for Case 10



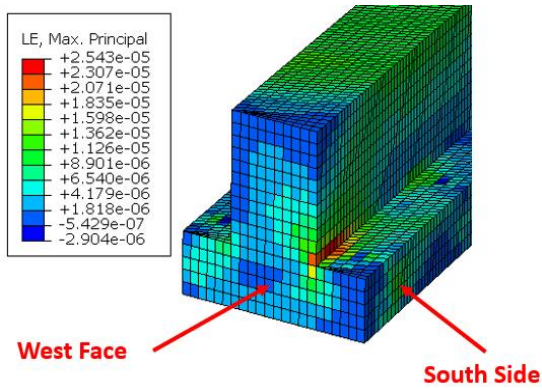
(k) Concrete Tensile Strain for Case 11



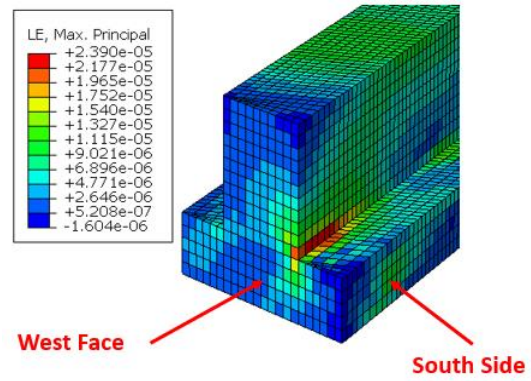
(l) Concrete Tensile Strain for Case 12



(m) Concrete Tensile Strain for Case 13

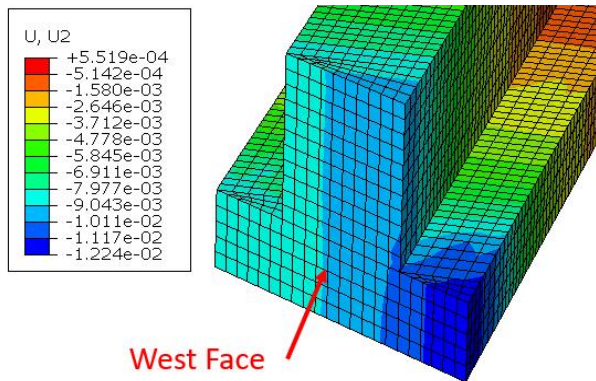


(n) Concrete Tensile Strain for Case 14

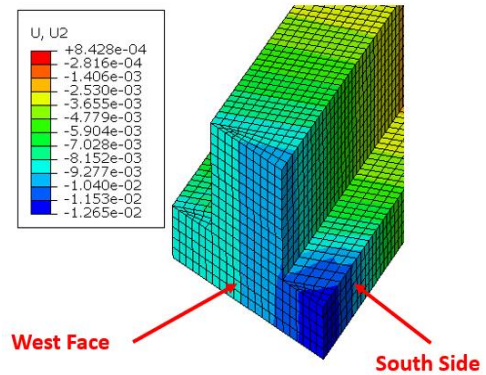


(o) Concrete Tensile Strain for Case 15

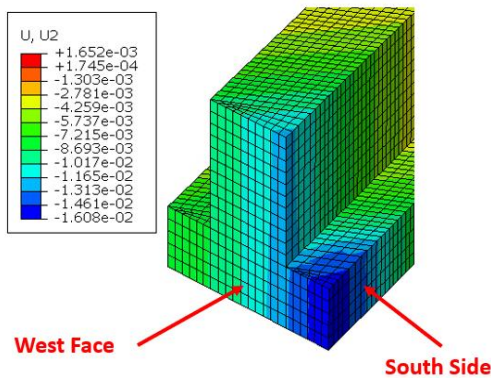
**Figure 2.22. Tensile Strain Distribution in Concrete for Cases 1 to 15**



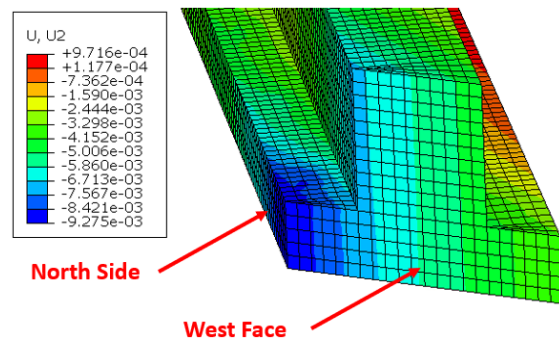
(a) West Face Displacement for Case 1



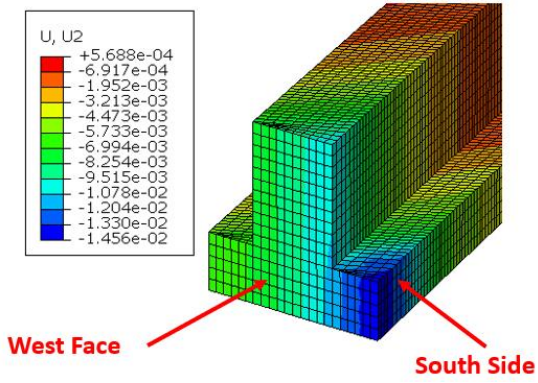
(b) West Face Displacement for Case 2



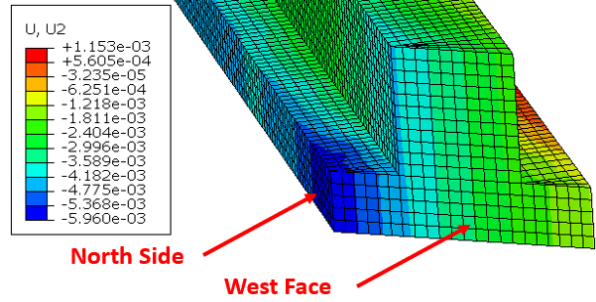
(c) West Face Displacement for Case 3



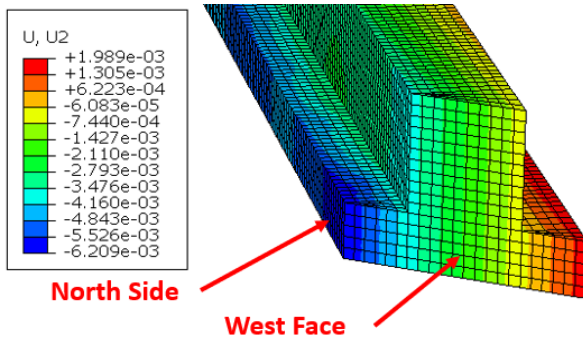
(d) West Face Displacement for Case 4



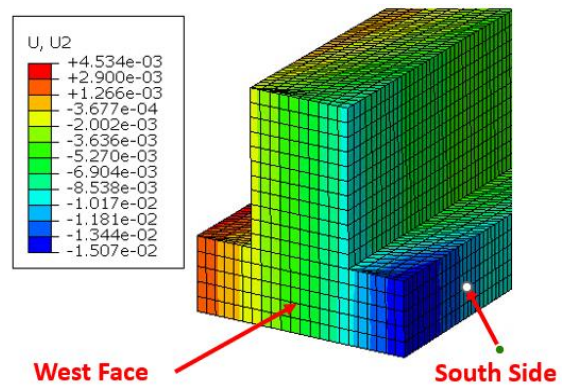
(e) West Face Displacement for Case 5



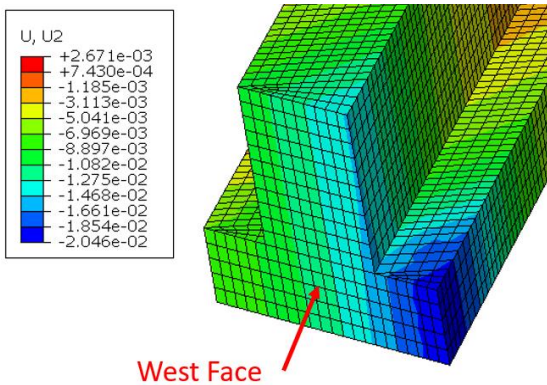
(f) West Face Displacement for Case 6



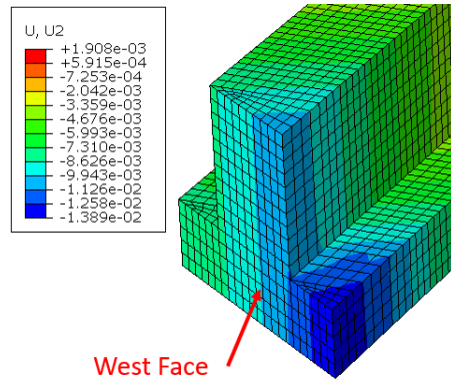
(g) West Face Displacement for Case 7



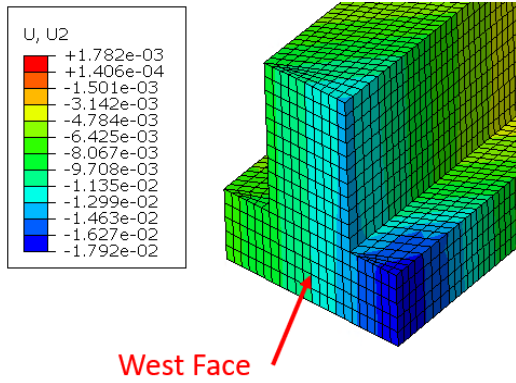
(h) West Face Displacement for Case 8



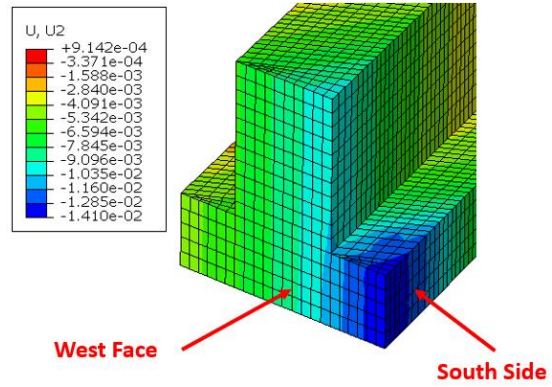
(i) West Face Displacement for Case 9



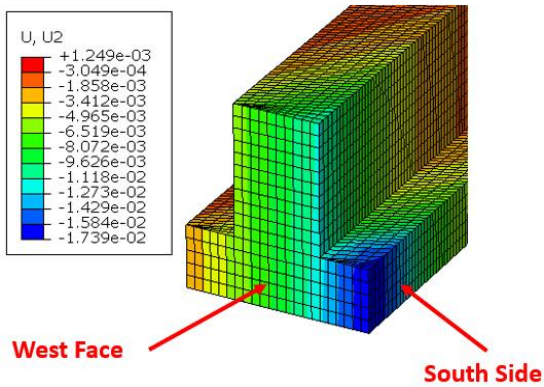
(j) West Face Displacement for Case 10



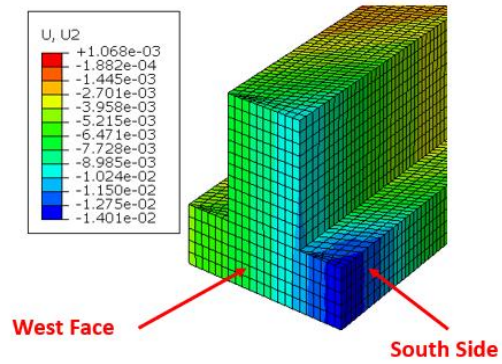
(k) West Face Displacement for Case 11



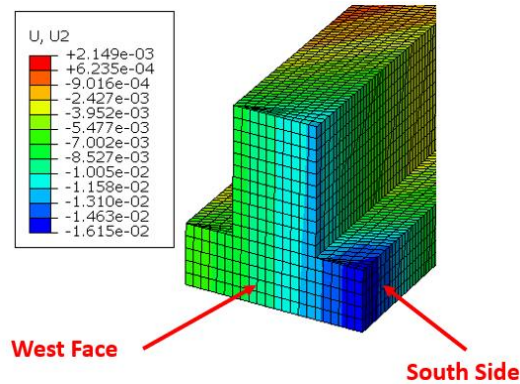
(l) West Face Displacement for Case 12



(m) West Face Displacement for Case 13

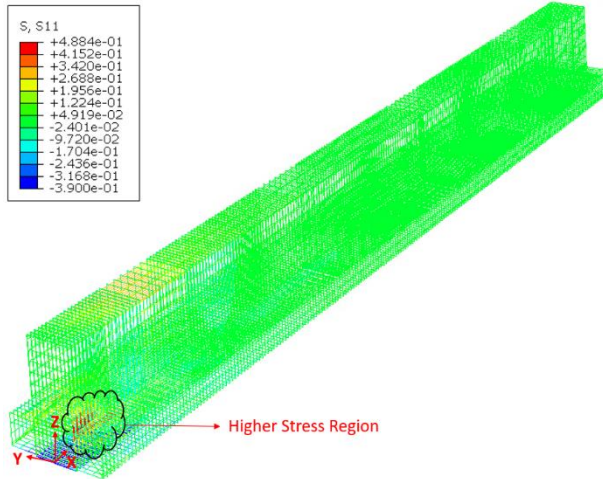


(n) West Face Displacement for Case 14

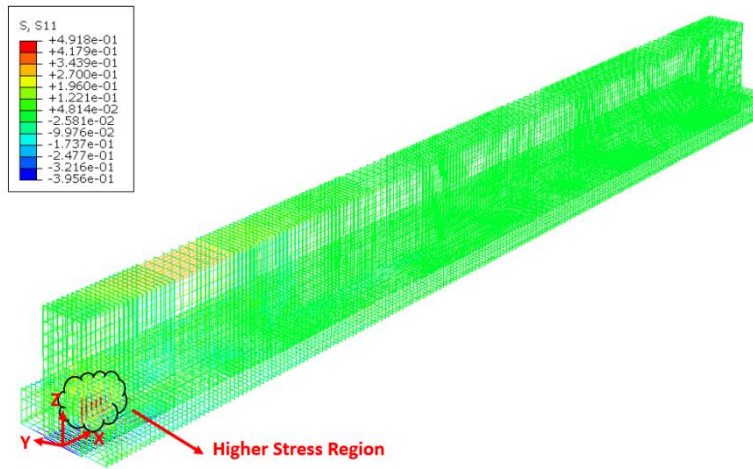


(o) West Face Displacement for Case 15

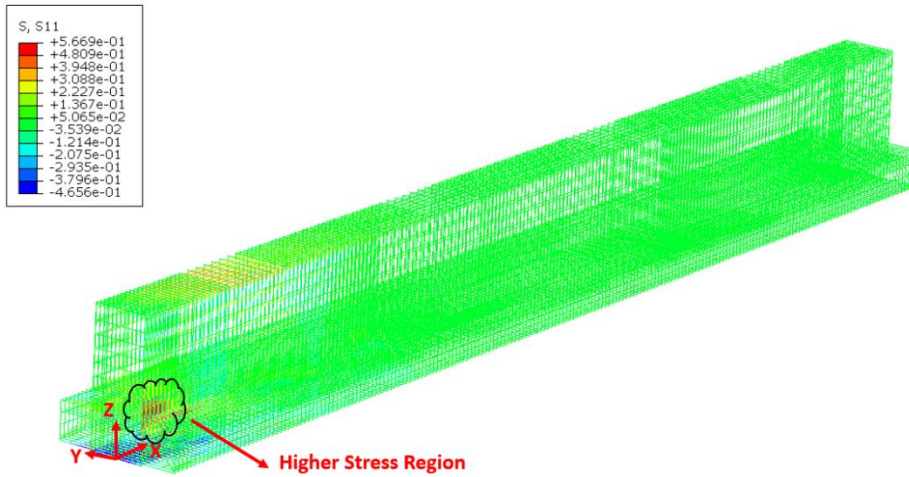
**Figure 2.23. Displacement Profile for Cases 1 to 15 of Bent Cap 7 (units in inches)**



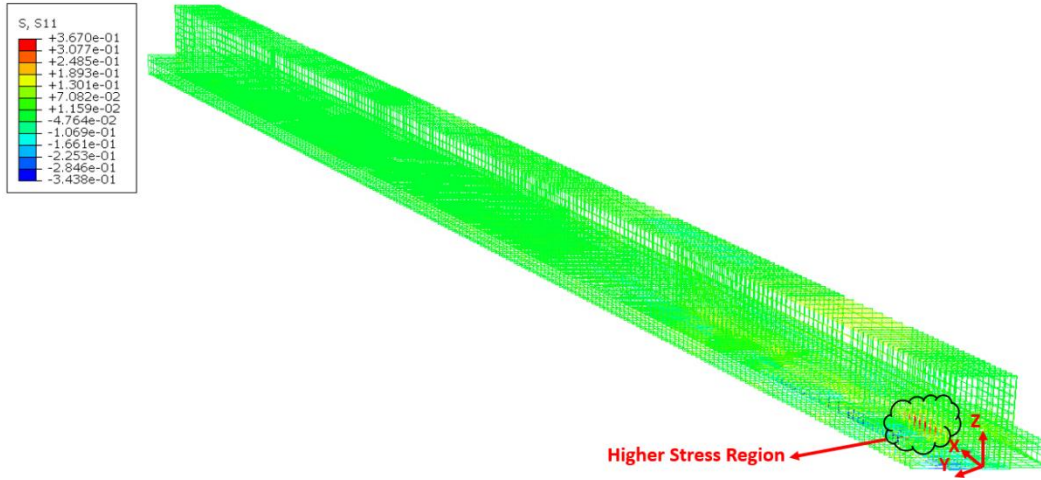
(a) Stresses on Rebar Cage for Case 1



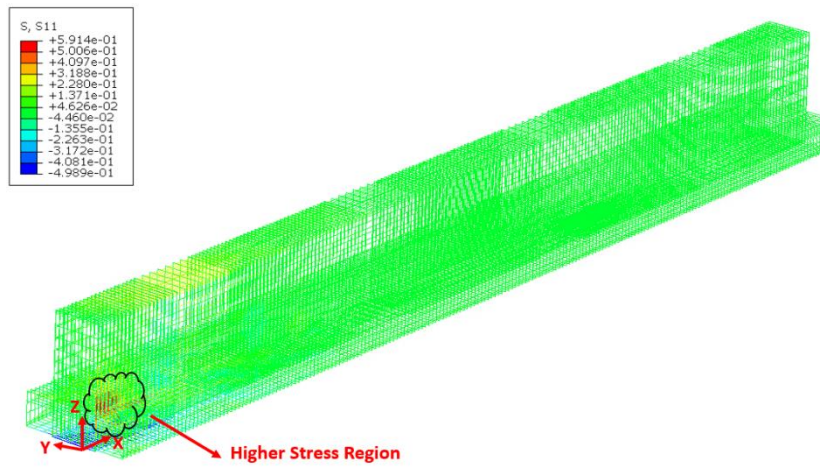
(b) Stresses on Rebar Cage for Case 2



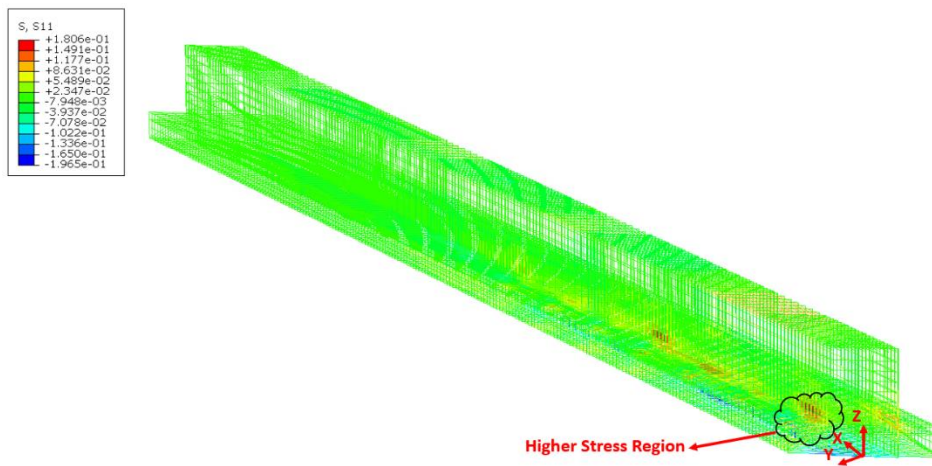
(c) Stresses on Rebar Cage for Case 3



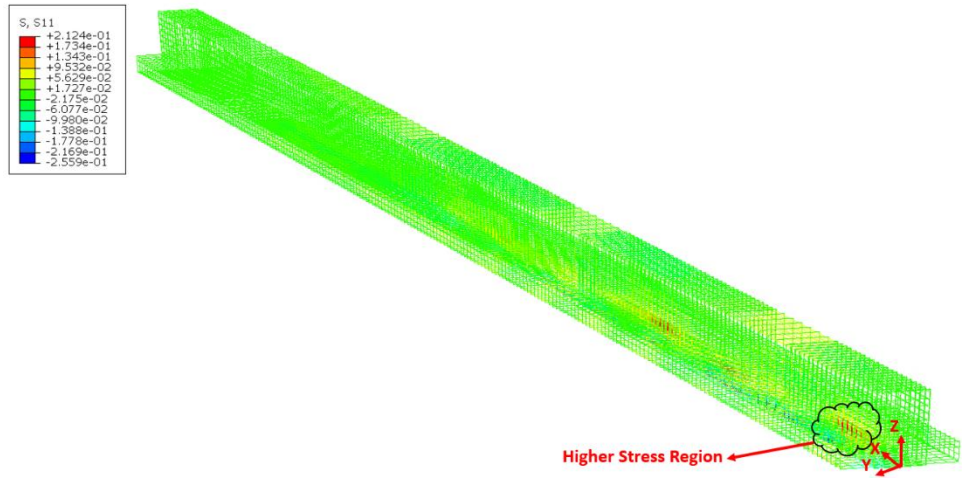
(d) Stresses on Rebar Cage for Case 4



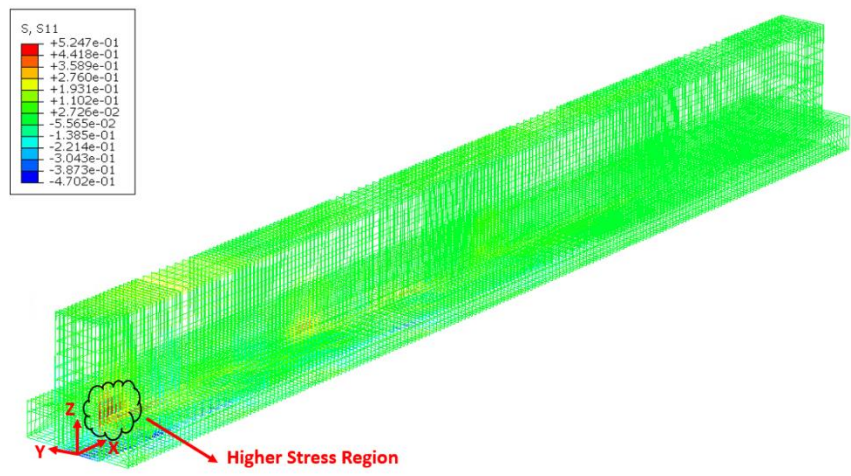
(e) Stresses on Rebar Cage for Case 5



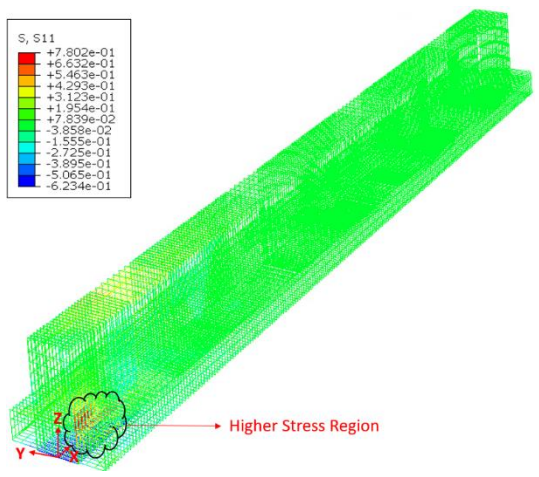
(f) Stresses on Rebar Cage for Case 6



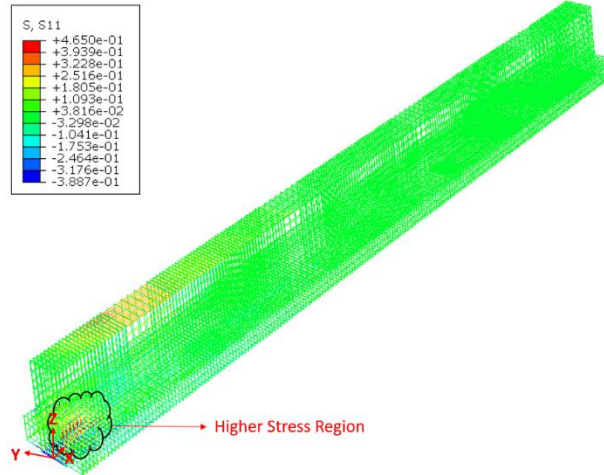
(g) Stresses on Rebar Cage for Case 7



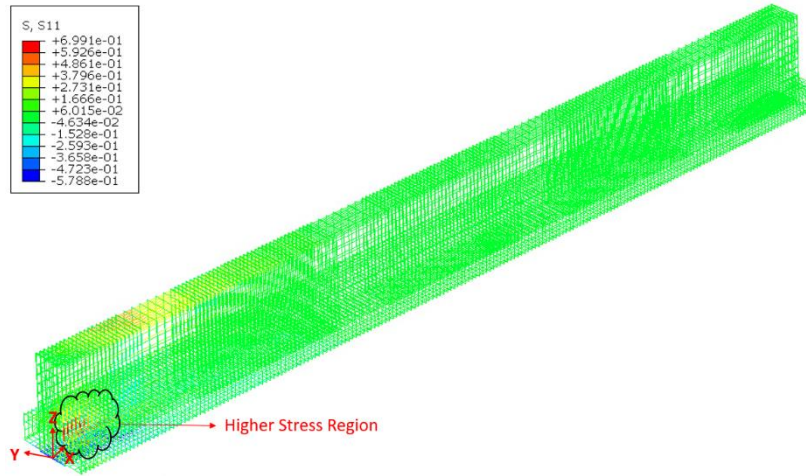
(h) Stresses on Rebar Cage for Case 8



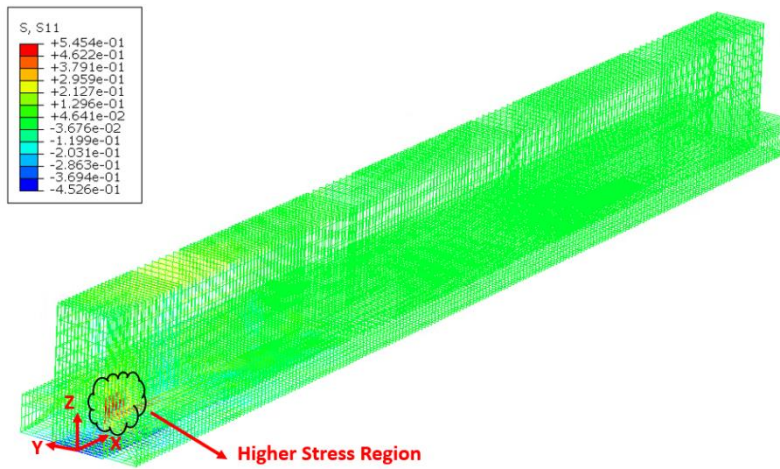
(i) Stresses on Rebar Cage for Case 9



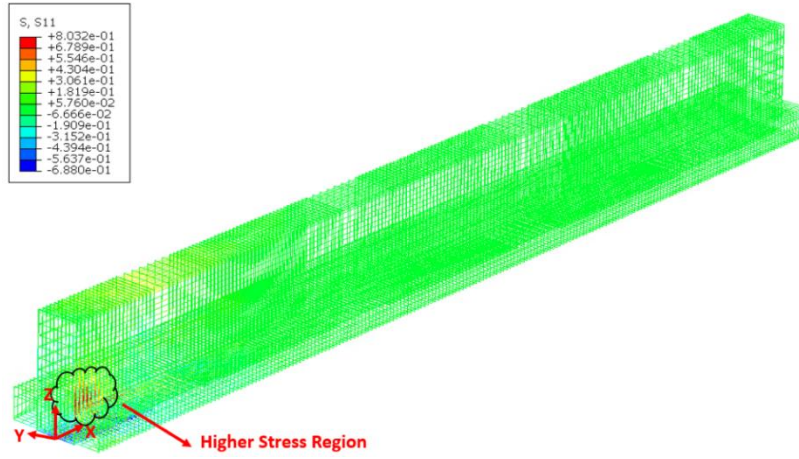
(j) Stresses on Rebar Cage for Case 10



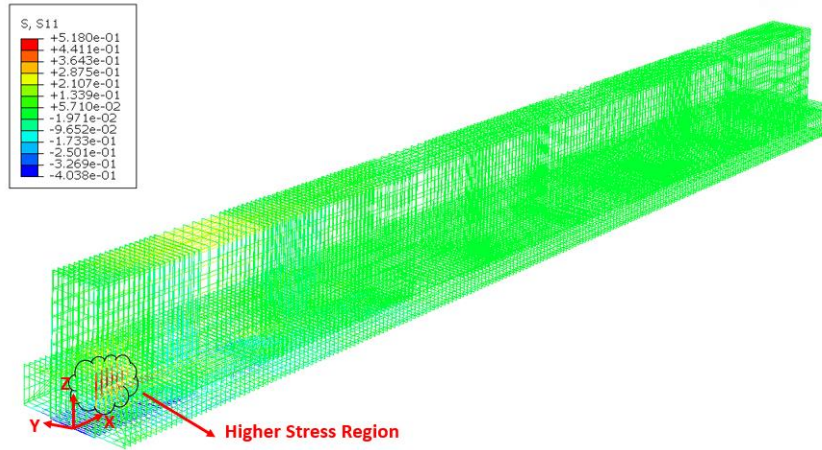
(k) Stresses on Rebar Cage for Case 11



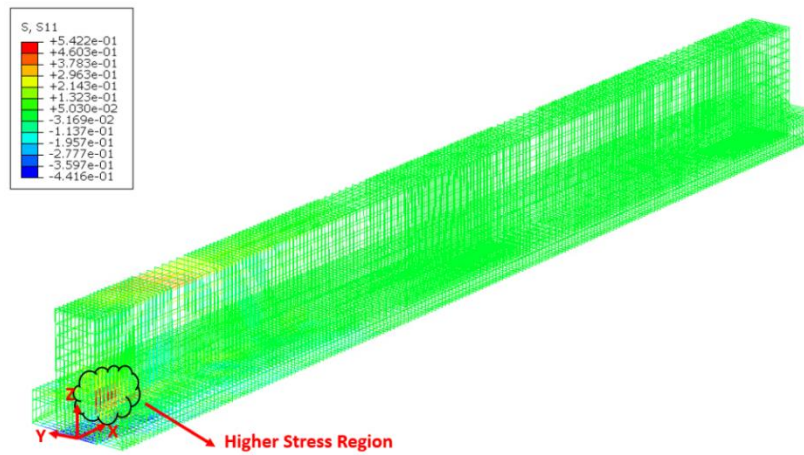
(l) Stresses on Rebar Cage for Case 12



(m) Stresses on Rebar Cage for Case 13



(n) Stresses on Rebar Cage for Case 14



(o) Stresses on Rebar Cage for Case 15

**Figure 2.24. Stress Distribution in Rebar Cage for Cases 1 to 15 of Bent Cap 7**

The concrete tensile strain at the extended region and ledge/stem interface for Cases 1 to 15 are 22.59  $\mu\epsilon$ , 22.47  $\mu\epsilon$ , 26.39  $\mu\epsilon$ , 21.71  $\mu\epsilon$ , 27.64  $\mu\epsilon$ , 10.95  $\mu\epsilon$ , 12.35  $\mu\epsilon$ , 24.17  $\mu\epsilon$ , 36.43  $\mu\epsilon$ , 27.25  $\mu\epsilon$ , 33.21  $\mu\epsilon$ , 25.85  $\mu\epsilon$ , 37.48  $\mu\epsilon$ , 25.43  $\mu\epsilon$ , and 23.90  $\mu\epsilon$ , respectively. The displacement observed on the extended region of the West face of ITBC-2 for Cases 1 to 15 are -0.01224-inch, -0.01265-inch, -0.01055-inch, -0.00337-inch, -0.01456-inch, -0.00120-inch, -0.00171-inch, -0.01507-inch, -0.02046-inch, -0.01389-inch, -0.01792-inch, -0.01410-inch, -0.01401-inch, -0.01615-inch, and -0.01739-inch, respectively. The maximum displacement is -0.02046-inch observed in Case 9. Figures 2.22(a) – 2.22(o) shows higher concrete tensile strain at the stem and ledge interface. As shown in Figures 2.23(a) – 2.23(o), the maximum displacement at the West face of ITBC is observed in the extended region. Based on the simulation results from the 15 cases, the higher tensile stress is observed on transverse rebars of the stem, as shown in Figures 2.24(a)-2.24(o).

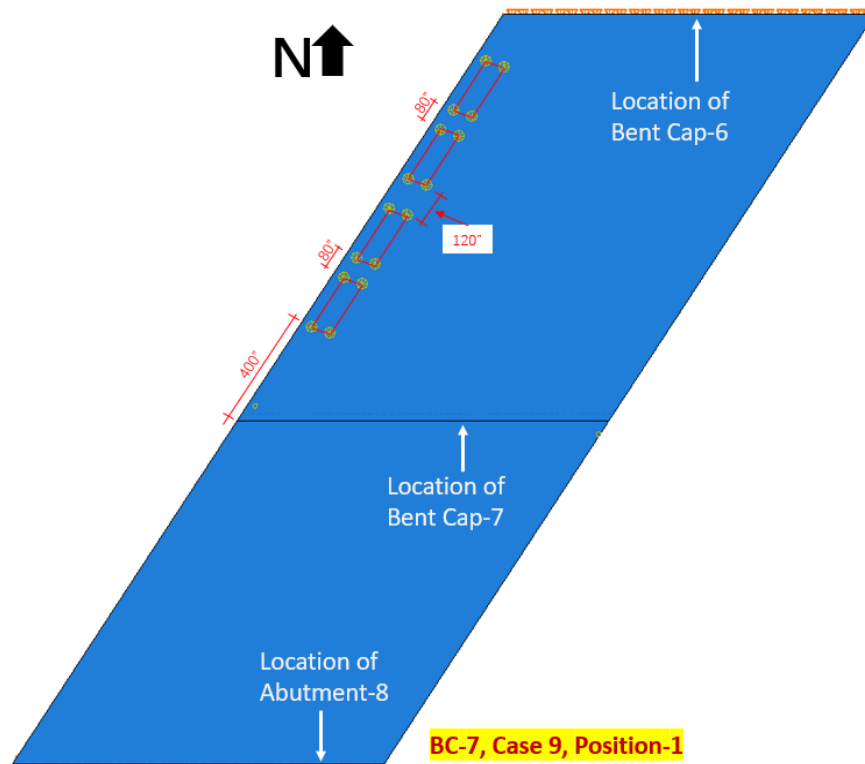
Case 9 is the most critical load case because it results in higher strains and stresses in the ledge/stem interface and the rebars, as presented in Table 3. In addition, Cases 1, 9, 10, 11, and 14 are selected for candidate Static Test-1 as it results in higher strains and stresses. The loading cases (Cases 6, 7, and 8) with load distribution on four lanes did not yield higher stress/strain on transverse rebars.

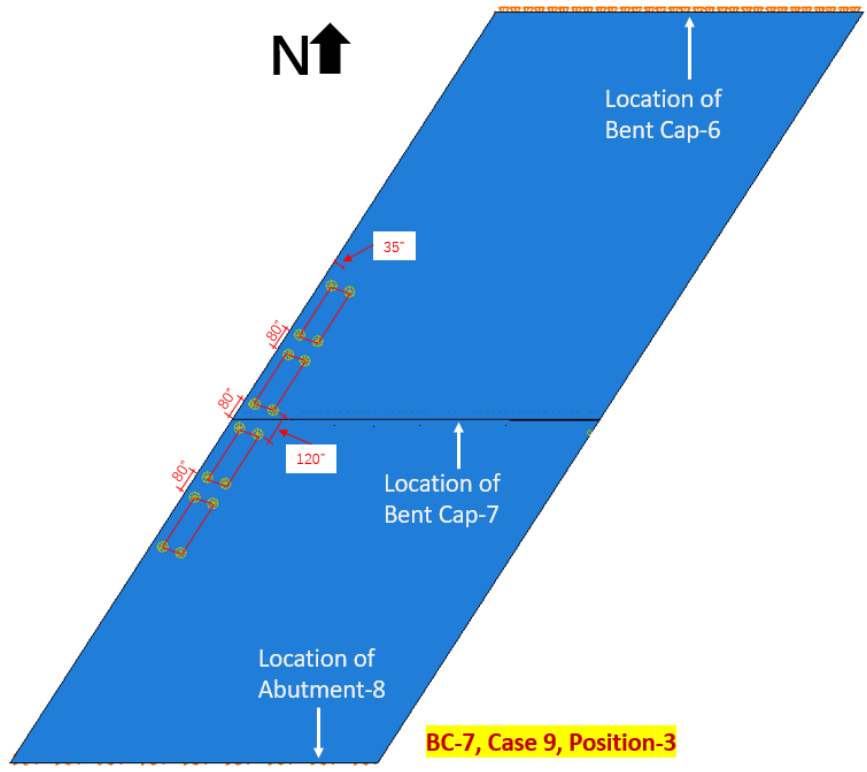
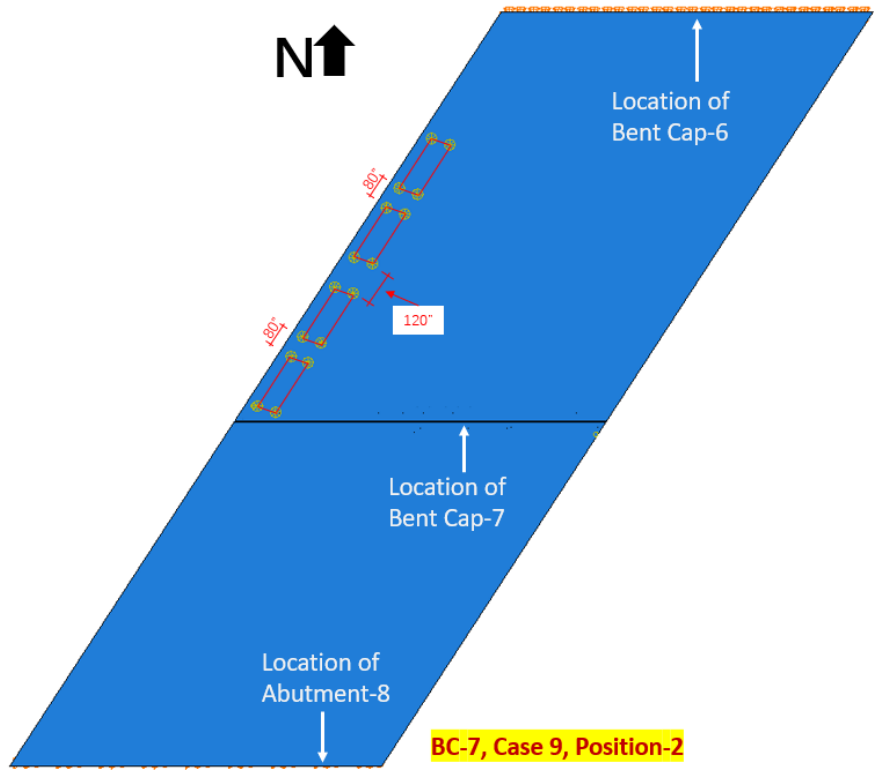
#### **2.4.2 Static Test-2 Simulation at Five Positions**

Based on 15 cases of FE simulation of Bent Cap 2 with Static Test-1, Cases 1, 9, 10, 11, and 14 are identified as candidates for load tests. Among six cases, Case 9 and Case 14 are selected for Static Test-2 with four-track load at five positions. Case 9 has all four trucks aligned next to the edge of the deck. Case 14 has four trucks arranged in two lanes: two trucks are aligned to the edge of the deck, and the last two trucks are located next to them. The selection of Cases 9 and 14 for Static Test-2 at five positions provides:

- Varieties in load distribution (on one lane and two lanes) along the forward and backward span at multiple positions of Bent Cap 7,
- Examination of higher stress/strain distribution on transverse rebars at multiple positions of four-truck load, the higher concrete tensile strain on the ledge interface and stem, and higher displacement of the extended region of skewed ITBCs.

Case 9 of Bent Cap 7 is the critical loading case with a four-truck load. Case 9 of Bent Cap 7 yields higher strains and stresses in the stem/ledge interface and the rebars. Case 9 of Bent Cap 7 is critically examined with a four-truck load at five positions, as shown in Figure 2.25. The finite element simulated strains for Case 9 of Bent Cap 7 under four-truck loading at five positions, the maximum tensile and compressive concrete strains and the displacements for Case 9 of Bent Cap 7 under four-truck loading at five positions, Carbon Nanofiber Aggregates (CNFAs) stress values for Case 9 of Bent Cap 7 under four-truck loading at five positions are shown in APPENDIX-2. Figures 2.26(a) – 2.26(e) show the tensile strain distribution of concrete for Case 9 of Bent Cap 7, respectively. Figures 2.27(a) – 2.27(e) show the displacements of the West face for Case 9 of Bent Cap 7, respectively. Figures 2.28(a) – 2.28(e) show the stress distribution in the rebar cage for Case 9 of Bent Cap 7, respectively.





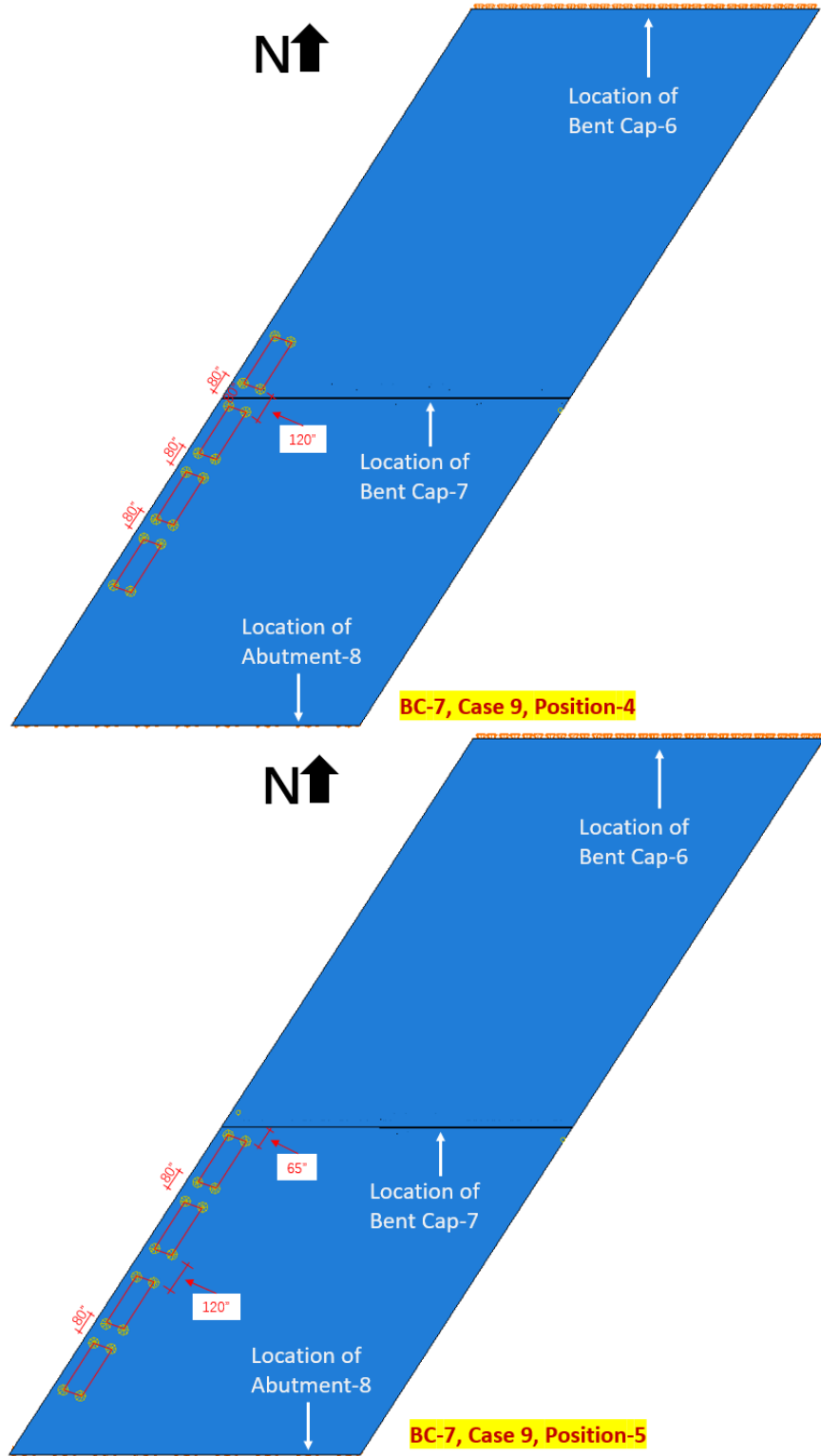
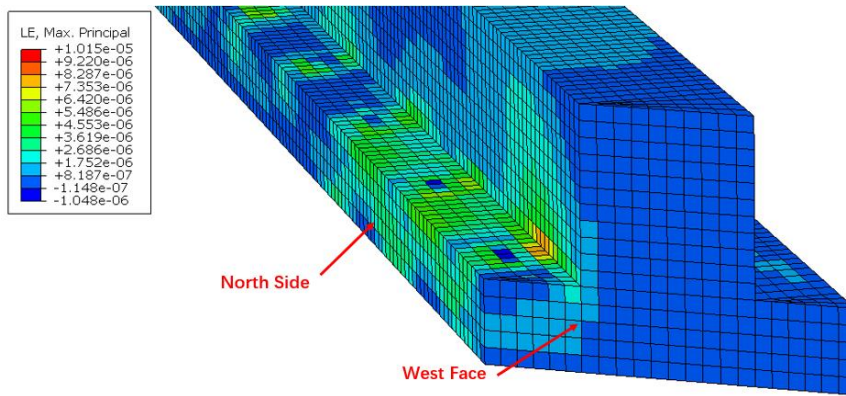
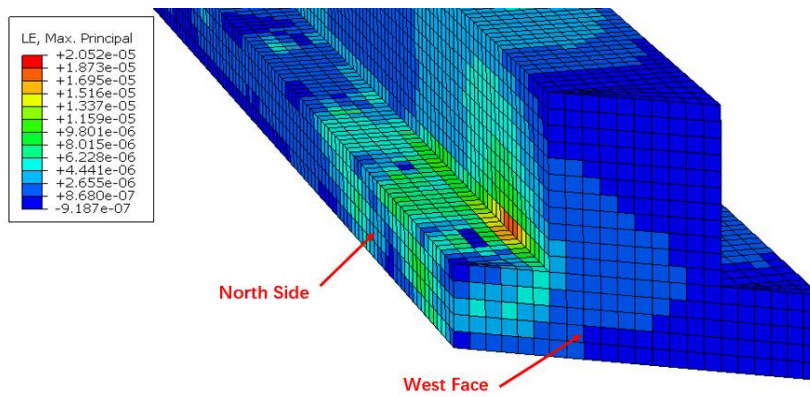


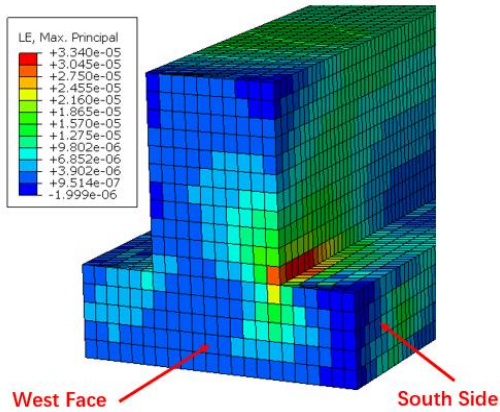
**Figure 2.25. Four-Truck Loading at Five Positions for Case 9 of Bent Cap 7**



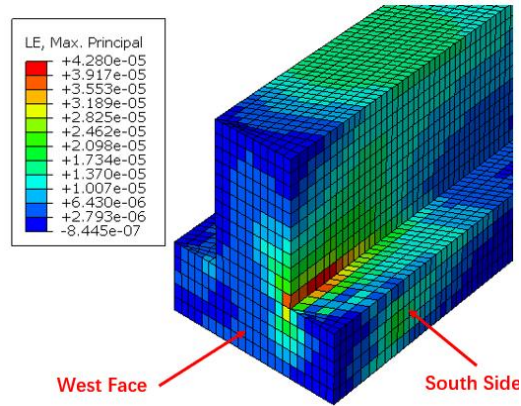
(a) Concrete Tensile Strain for Case 9 of Bent Cap 7 at Position 1



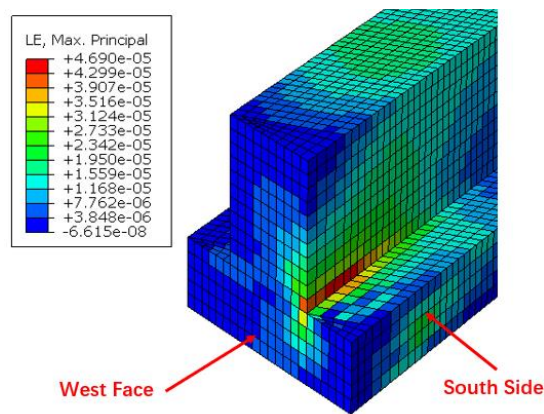
(b) Concrete Tensile Strain for Case 9 of Bent Cap 7 at Position 2



(c) Concrete Tensile Strain for Case 9 of Bent Cap 7 at Position 3

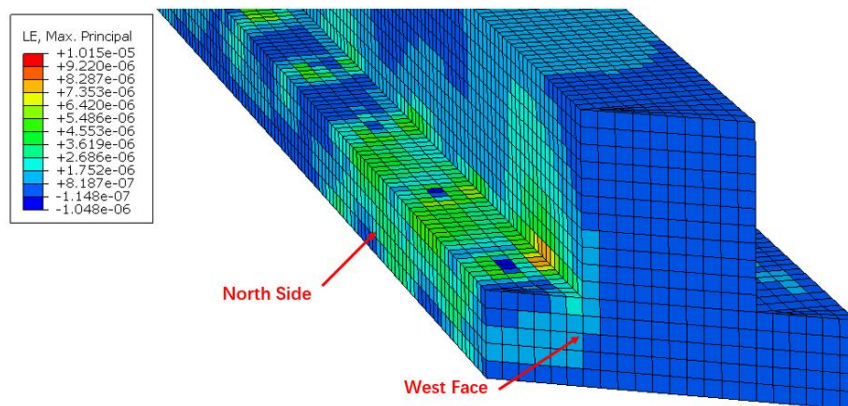


(d) Concrete Tensile Strain for Case 9 of Bent Cap 7 at Position 4

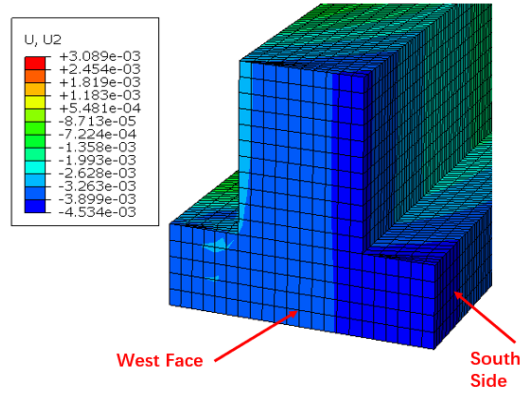


(e) Concrete Tensile Strain for Case 9 of Bent Cap 7 at Position 5

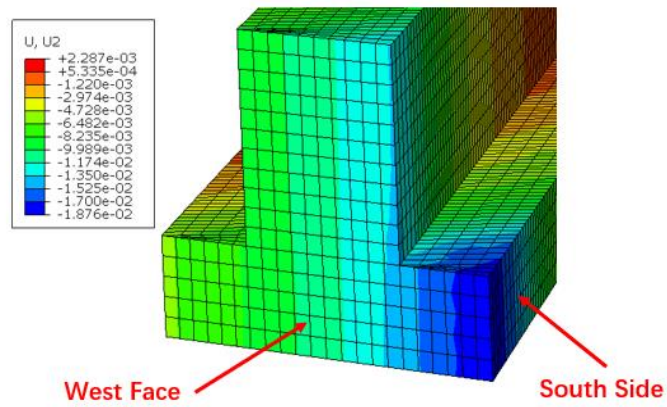
**Figure 2.26. Tensile Strain Distribution of Concrete for Case 9 of Bent Cap 7 under Four-Truck Loading at Five Positions**



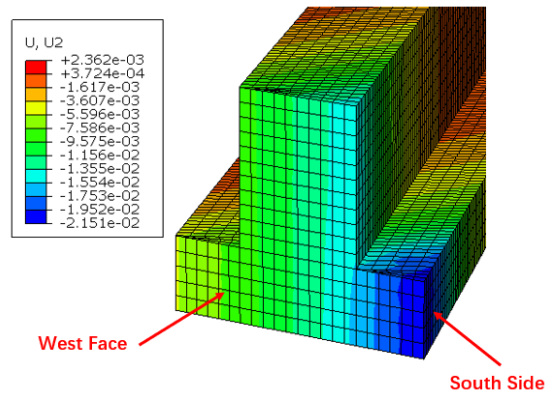
(a) West Face Displacement for Case 9 of Bent Cap 7 at Position 1 (units in inches)



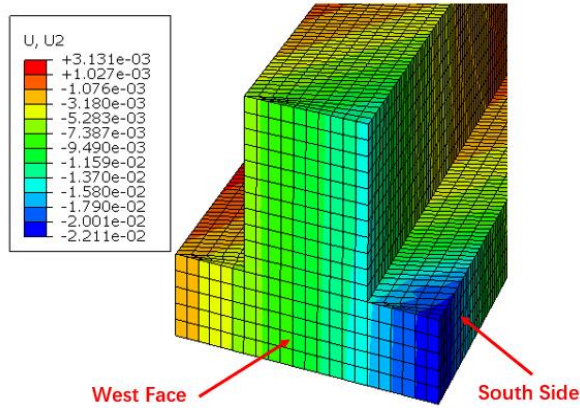
(b) West Face Displacement for Case 9 of Bent Cap 7 at Position 2 (units in inches)



(c) West Face Displacement for Case 9 of Bent Cap 7 at Position 3 (units in inches)

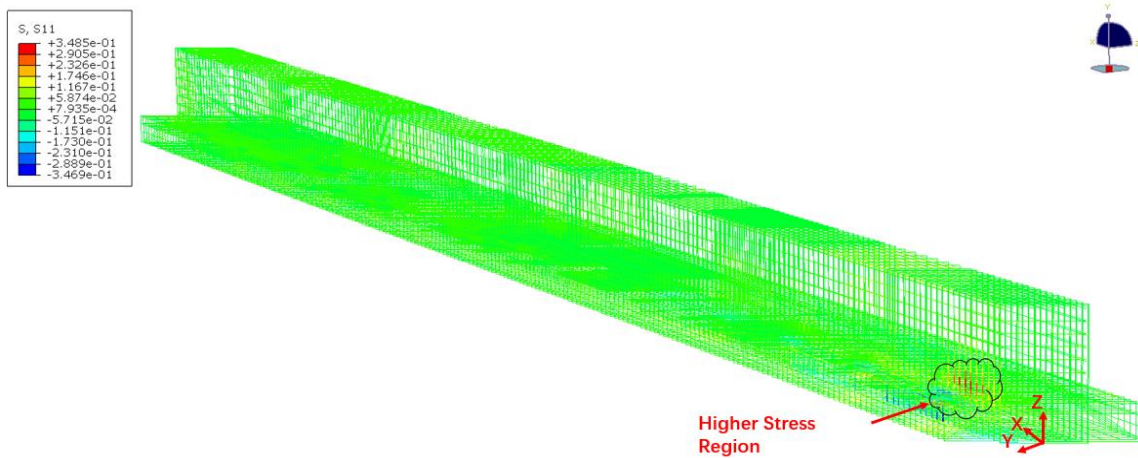


(d) West Face Displacement for Case 9 of Bent Cap 7 at Position 4 (units in inches)

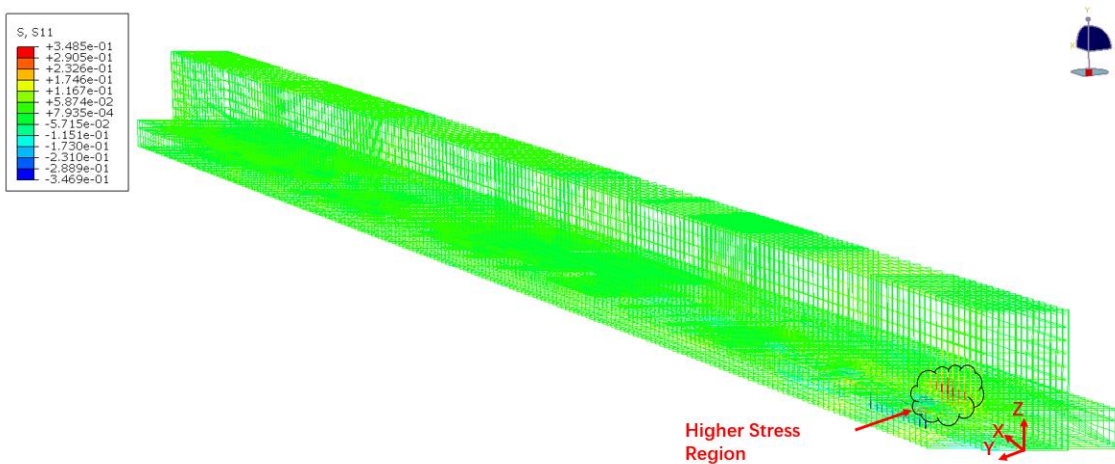


(e) West Face Displacement for Case 9 of Bent Cap 7 at Position 5 (units in inches)

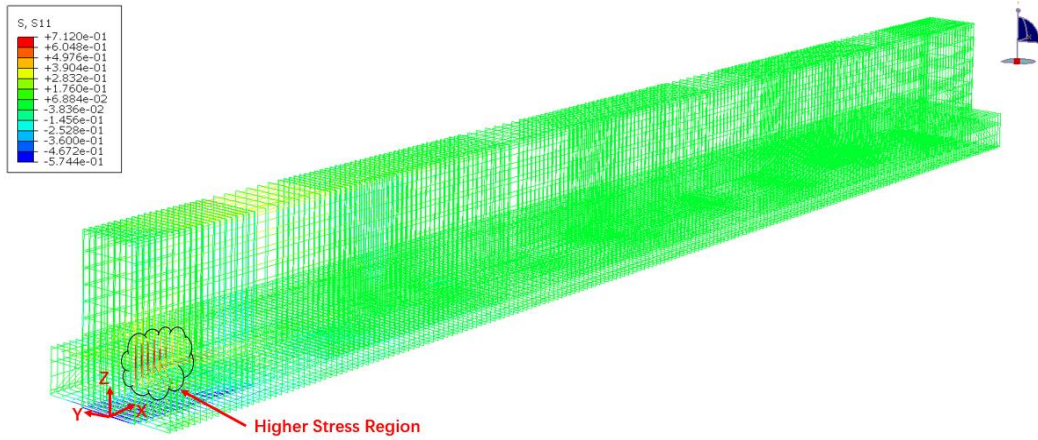
**Figure 2.27. Displacement Profile for Case 9 of Bent Cap 7 under Four-Truck Loading at Five Positions**



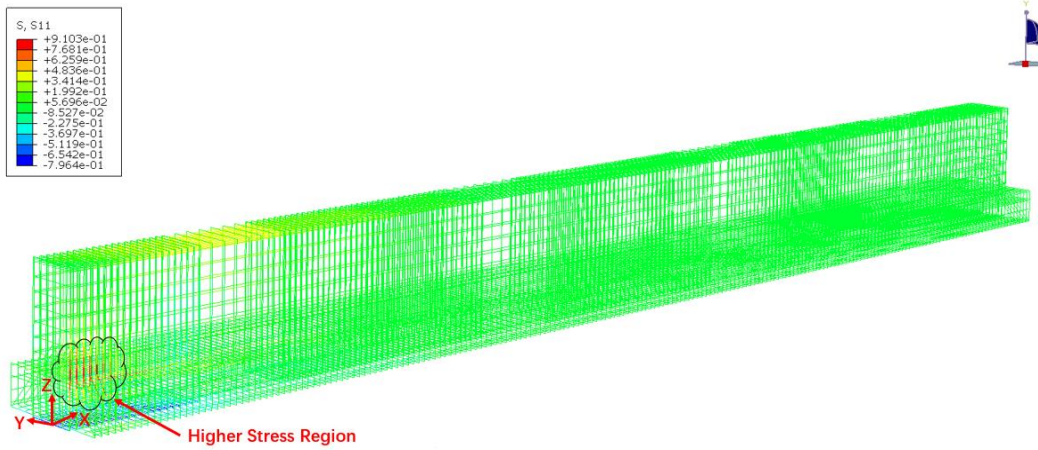
(a) Stresses in Rebar Cage for Case 9 of Bent Cap 7 at Position 1 (units in ksi)



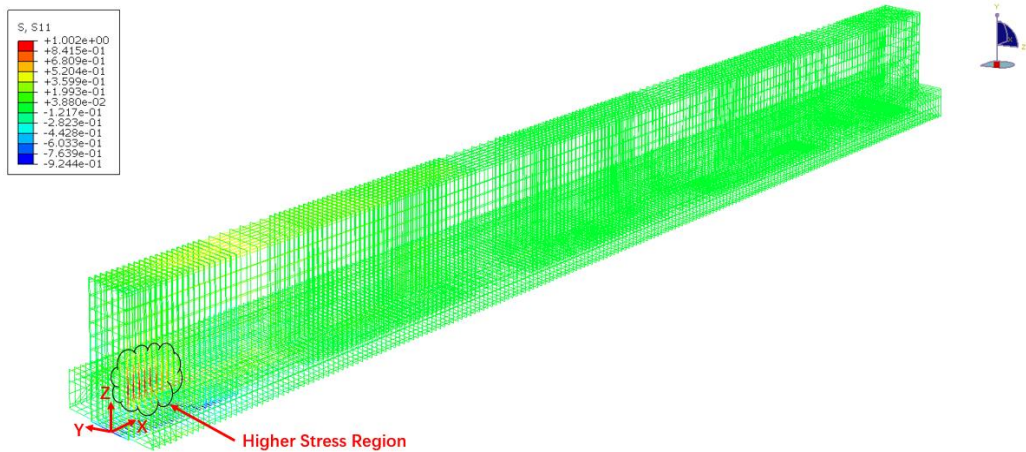
(b) Stresses in Rebar Cage for Case 9 of Bent Cap 7 at Position 2 (units in ksi)



(c) Stresses in Rebar Cage for Case 9 of Bent Cap 7 at Position 3 (units in ksi)



(d) Stresses in Rebar Cage for Case 9 of Bent Cap 7 at Position 4 (units in ksi)

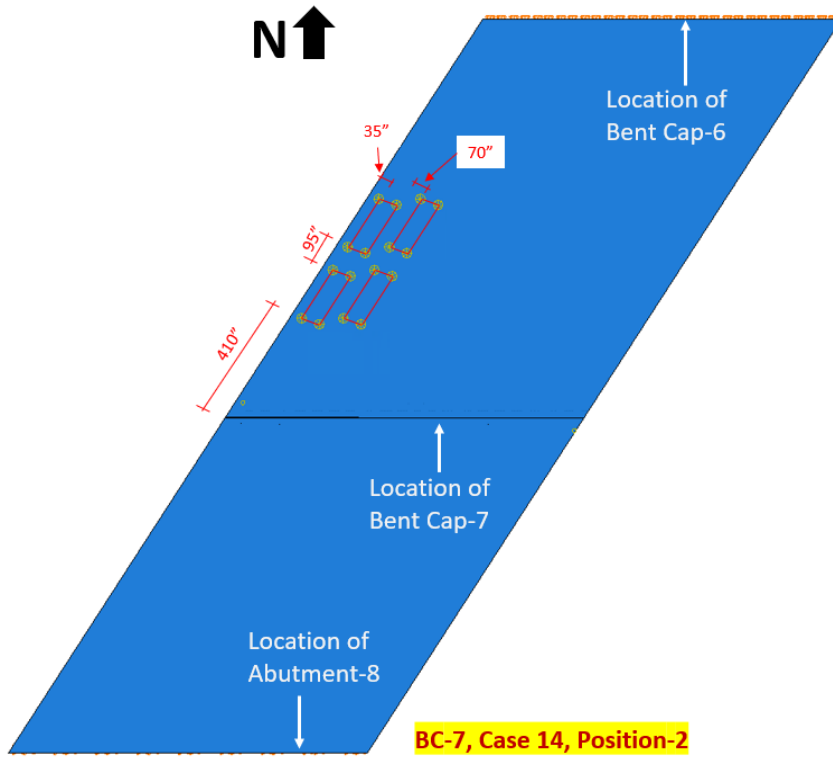
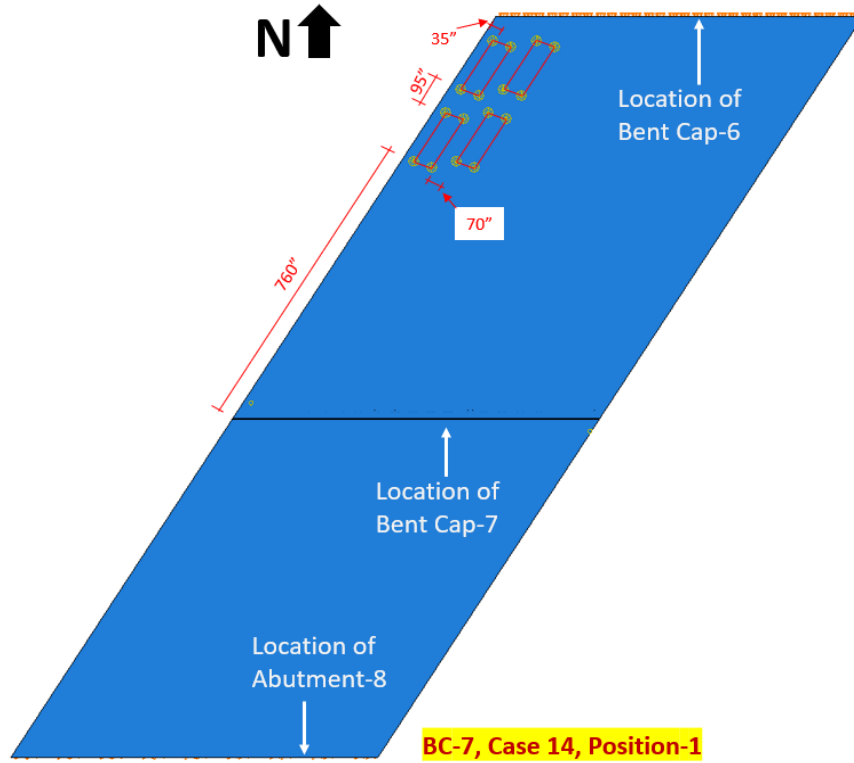


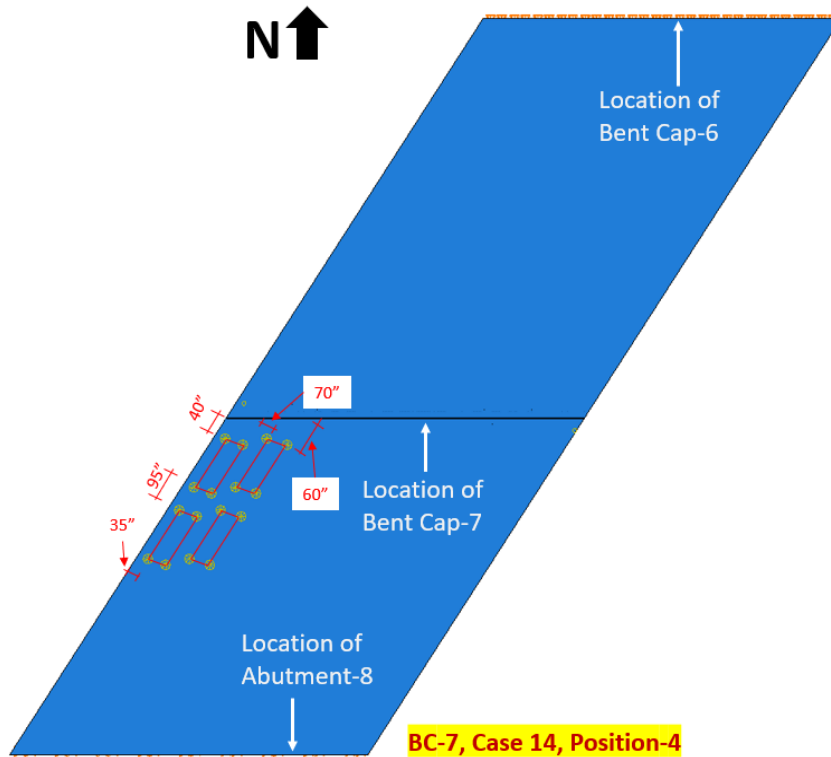
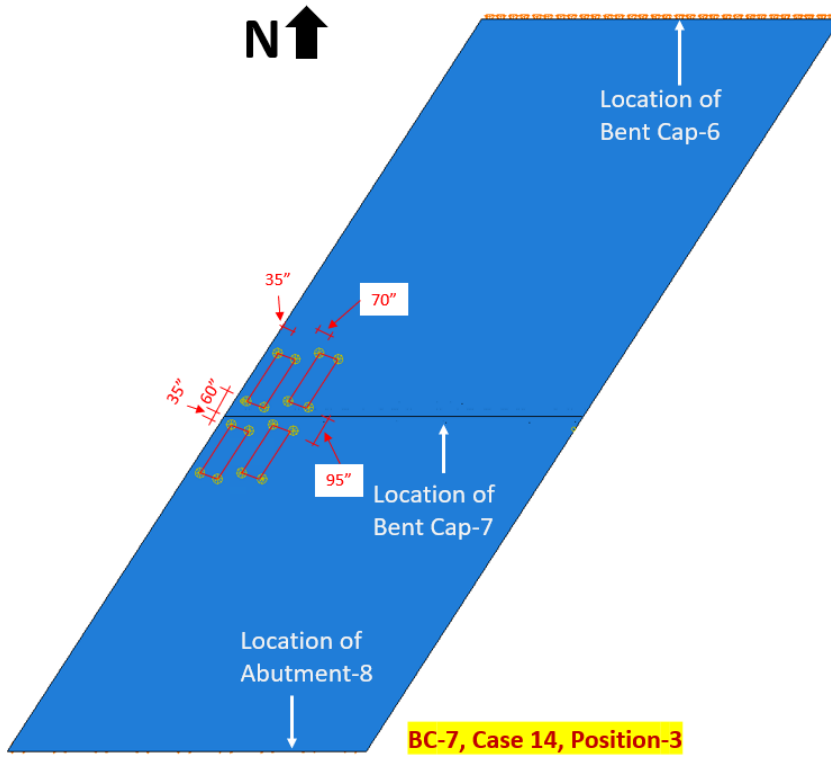
(e) Stresses in Rebar Cage for Case 9 of Bent Cap 7 at Position 5 (units in ksi)

**Figure 2.28. Stress Distribution in Rebar Cage for Case 9 of Bent Cap 7 under Four-Truck Loading at Five Positions**

At Position 1, four-truck loading is placed in the backward span of Bent Cap 7. The 3D FE simulation results show that the higher tensile strain is distributed on the North side of Bent Cap 7. The higher displacement of Bent Cap 7 is observed at the end of the South side of Bent Cap 7. The stresses on the rebar cage are concentrated on the S-bars of the North side. The concrete tensile strain and stresses in the S-bars at Position 2 are higher than those at Position 1 while the displacement at Position 1 is higher than at Position 2. Four trucks loaded at Positions 3 to 5 are concentrated on the forward span of the Bent Cap 7. Positions 3 to 5 show that the concrete tensile strain, displacement of the West face, and stresses in the S-bars are higher in the extended region of the South side. The concrete tensile strains at the intersection of the ledge and stem under four-truck loading at five positions are 10.15  $\mu\epsilon$ , 20.52  $\mu\epsilon$ , 33.40  $\mu\epsilon$ , 42.80  $\mu\epsilon$ , and 46.90  $\mu\epsilon$ , respectively. The peak displacements of the West face under four-truck loading at Positions 1 to 5 are -0.004799-inch, -0.004534-inch, -0.01876-inch, -0.02151-inch, and -0.02211-inch, respectively. The highest stresses in the S-bar under four-truck loading at Positions 1 to 5 are 0.16 ksi, 0.35 ksi, 0.71 ksi, 0.91 ksi, and 1.0 ksi, respectively. Based on these simulation results, Position 4 and Position 5 for Case 9 of Bent Cap 7 yielded higher stresses in the transverse rebars, higher concrete strain, and greater displacement.

Case 14 of Bent Cap 7 is one of the critical loading cases with four-truck load. Case 14 of Bent Cap 7 yields higher strains and stresses in the stem/ledge interface and the rebars. Case 14 of Bent Cap 7 is critically examined with four-truck load at five positions, as shown in Figure 2.29. The finite element simulated strains for Case 14 of Bent Cap 7 under four-truck loading at five positions, the maximum tensile and compressive concrete strains and the displacements for Case 14 of Bent Cap 7 under four-truck loading at five positions, Carbon Nanofiber Aggregates (CNFAs) stress values for Case 14 of Bent Cap 7 under four-truck loading at five positions are presented in APPENDIX-2. Figures 2.30(a) – 2.30(e) show the tensile strain distribution of concrete for Case 14 of Bent Cap 7, respectively. Figures 2.31(a) – 2.31(e) show the displacements of the West face for Case 14 of Bent Cap 7, respectively. Figures 2.32(a) – 2.32(e) show the stress distribution in the rebar cage for Case 14 of Bent Cap 7, respectively.





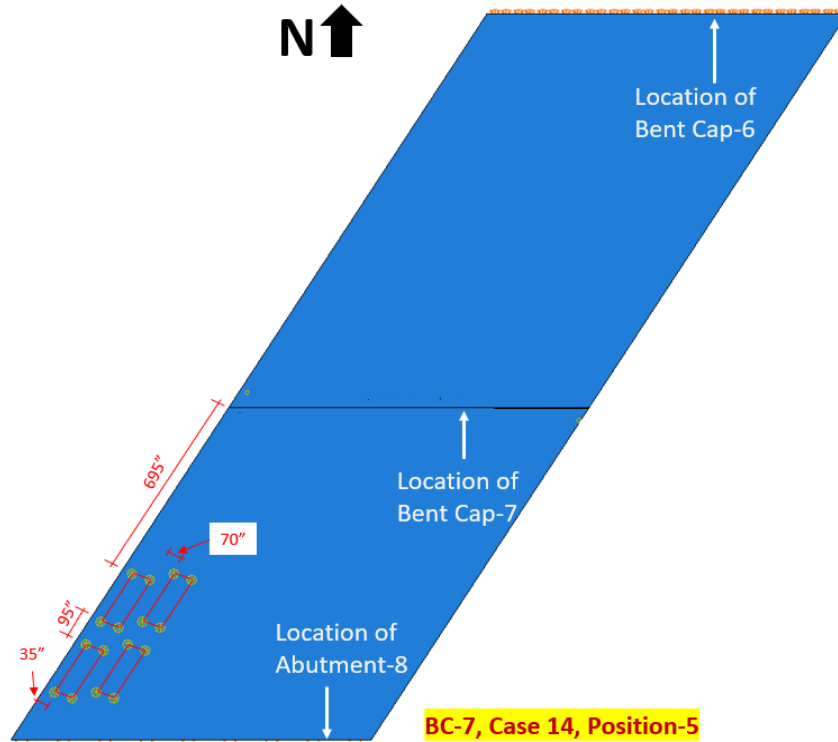
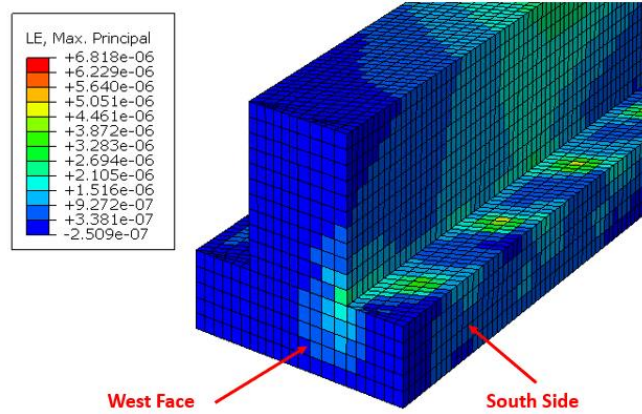
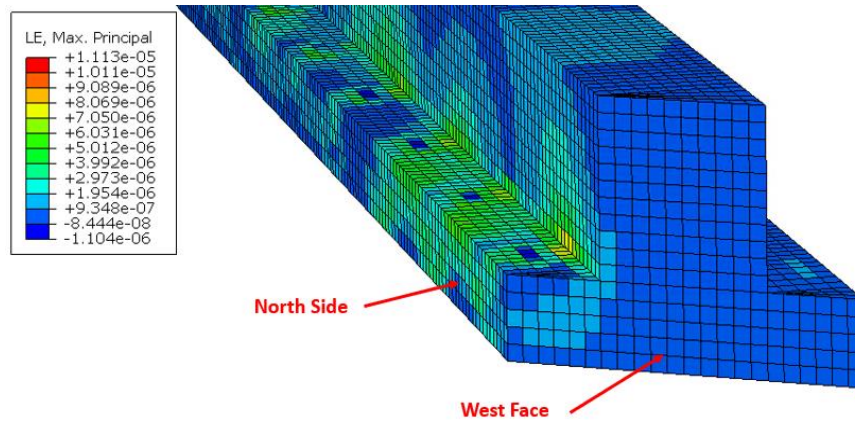


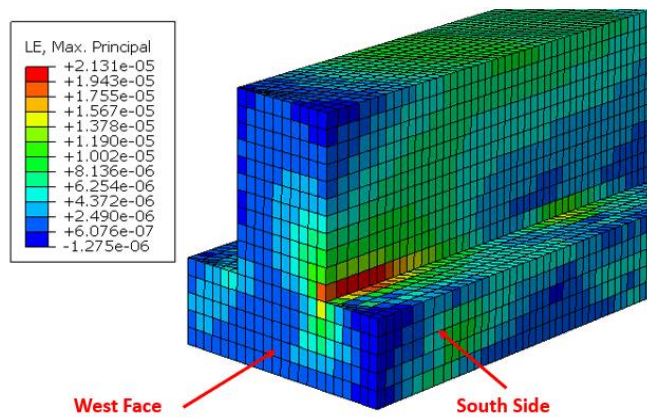
Figure 2.29. Four-Truck Loading at Five Positions for Case 14 of Bent Cap 7



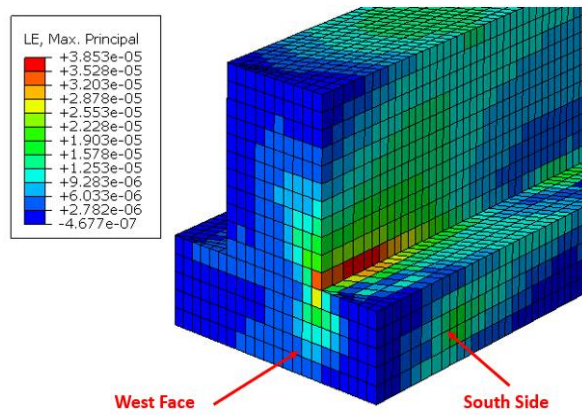
(a) Concrete Tensile Strain for Case 14 of Bent Cap 7 at Position 1



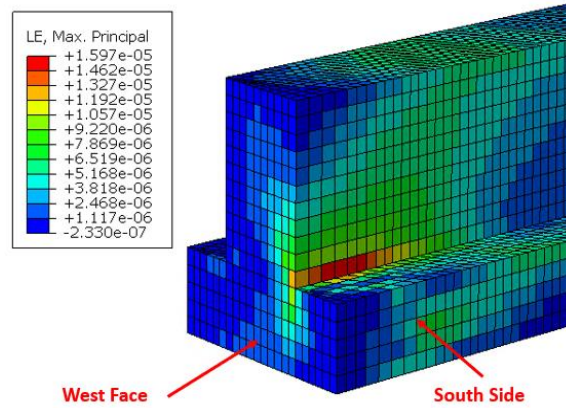
(b) Concrete Tensile Strain for Case 14 of Bent Cap 7 at Position 2



(c) Concrete Tensile Strain for Case 14 of Bent Cap 7 at Position 3

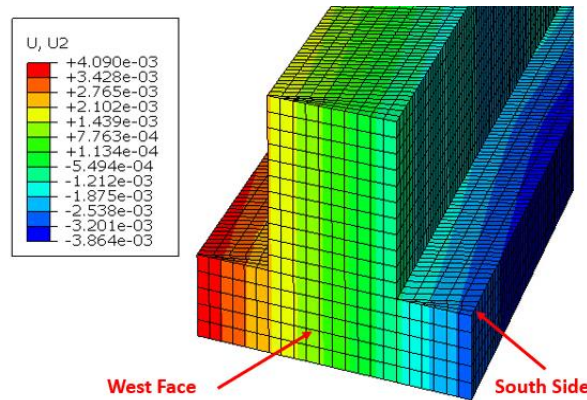


(d) Concrete Tensile Strain for Case 14 of Bent Cap 7 at Position 4

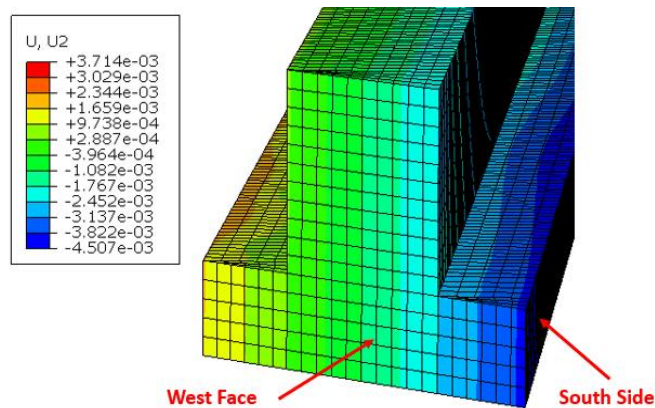


(e) Concrete Tensile Strain for Case 14 of Bent Cap 7 at Position 5

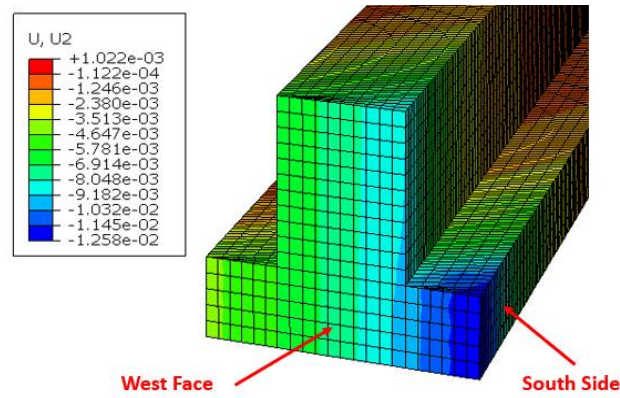
**Figure 2.30. Tensile Strain Distribution of Concrete for Case 14 of Bent Cap 7 under Four-Truck Loading at Five Positions**



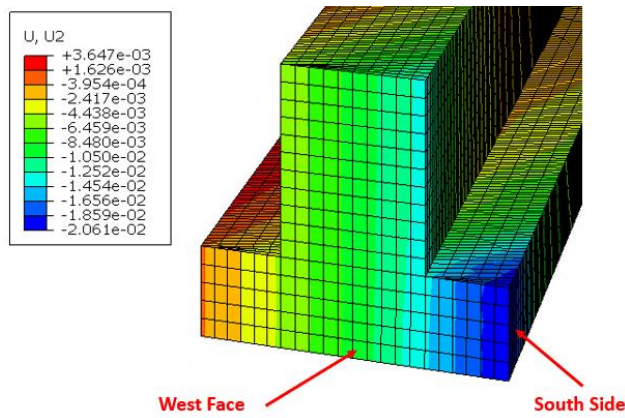
(a) West Face Displacement for Case 14 of Bent Cap 7 at Position 1 (units in inches)



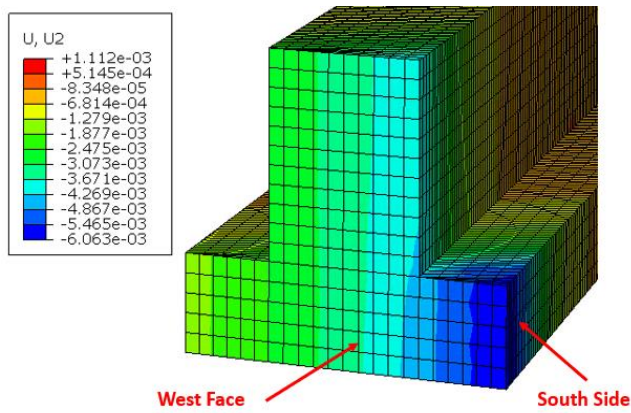
(b) West Face Displacement for Case 14 of Bent Cap 7 at Position 2 (units in inches)



(c) West Face Displacement for Case 14 of Bent Cap 7 at Position 3 (units in inches)

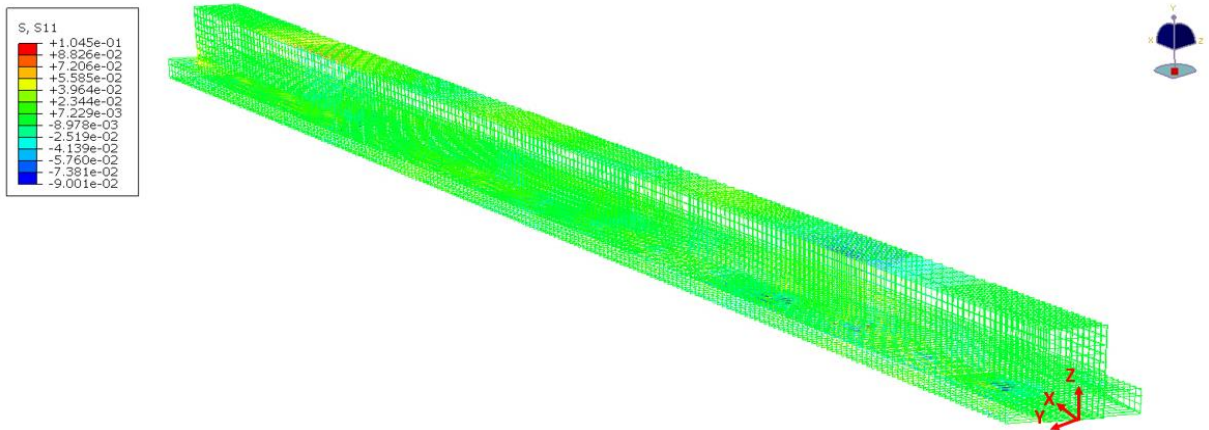


(d) West Face Displacement for Case 14 of Bent Cap 7 at Position 4 (units in inches)



(e) West Face Displacement for Case 14 of Bent Cap 7 at Position 5 (units in inches)

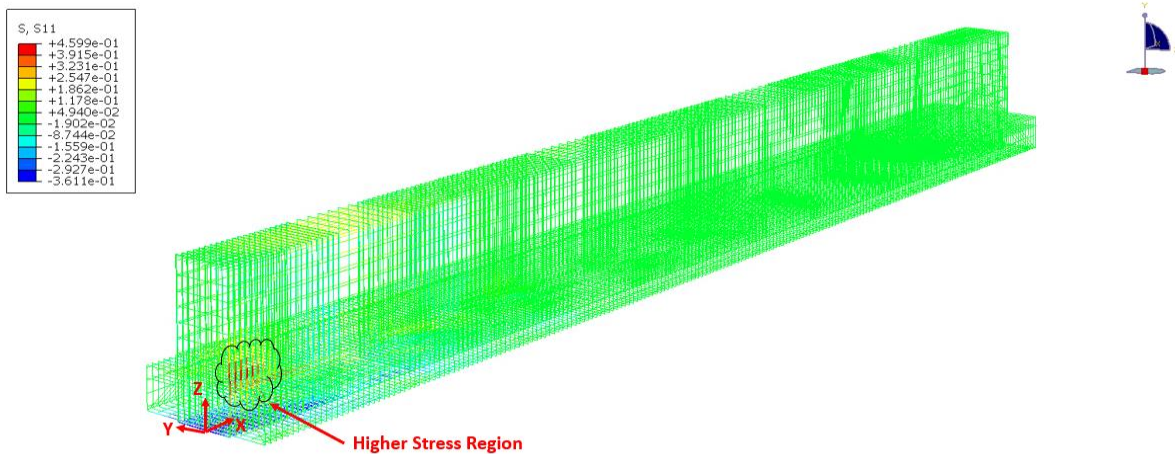
**Figure 2.31. Displacement Profile for Case 14 of Bent Cap 7 under Four-Truck Loading at Five Positions**



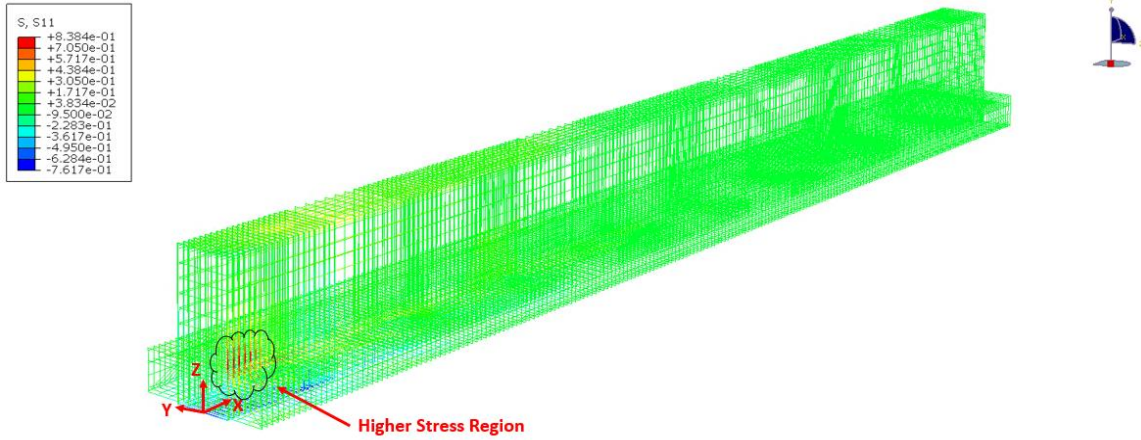
(f) Stresses in Rebar Cage for Case 14 of Bent Cap 7 at Position 1 (units in ksi)



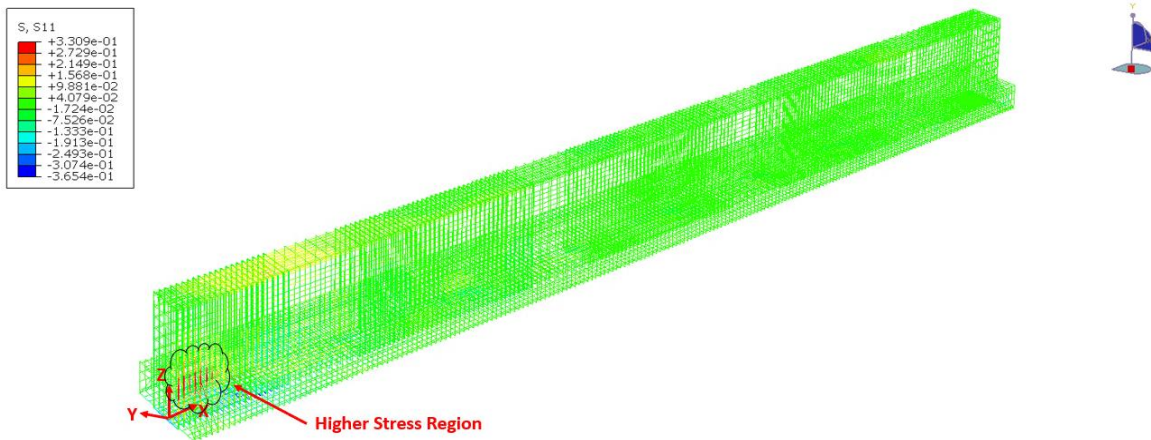
(b) Stresses in Rebar Cage for Case 14 of Bent Cap 7 at Position 2 (units in ksi)



(c) Stress in Rebar Cage for Case 14 of Bent Cap 7 at Position 3 (units in ksi)



(d) Stresses in Rebar Cage for Case 14 of Bent Cap 7 at Position 4 (units in ksi)



(e) Stresses in Rebar Cage for Case 14 of Bent Cap 7 at Position 5 (units in ksi)

**Figure 2.32. Stress Distribution in Rebar Cage for Case 14 of Bent Cap 7 under Four-Truck Loading at Five Positions**

At Position 1, four-truck loading is placed in the backward span of Bent Cap 7. The 3D FE simulation results show that the higher tensile strain is distributed on the North side of Bent Cap 7. The higher displacement of Bent Cap 7 is observed at the end of the North side of Bent Cap 7. The stresses on the rebar cage are concentrated on the S-bars of the North side. The concrete tensile strains and stresses in the S-bars at Position 2 are higher than those at Position 1. The displacement at Position 2 is greater than at Position 1 on the South side. Four trucks loaded at Positions 3 to 5 are concentrated on the forward span of Bent Cap 7. Positions 3 to 5 show that the concrete tensile strains on the ledge and stem interface, displacement of the West face, and stresses in the S-bars are higher in the extended region of the South side. The concrete tensile strains at the intersection

of the ledge and stem under four-truck loading at five positions are 6.82  $\mu\epsilon$ , 11.13  $\mu\epsilon$ , 21.31  $\mu\epsilon$ , 38.53  $\mu\epsilon$ , and 15.97  $\mu\epsilon$ , respectively. The peak displacements of the West face (on the South end) under four-truck loading at Positions 1 to 5 are -0.002911-inch, -0.003985-inch, -0.012583-inch, -0.020607-inch, and -0.006063-inch, respectively. The highest stresses in the S-bar under four-truck loading at Position 1 to 5 are 0.1 ksi, 0.18 ksi, 0.46 ksi, 0.84 ksi, and 0.33 ksi, respectively. Based on these simulation results, Position-3 and Position-4 for Case 14 of Bent Cap 7 yielded higher stresses in the transverse rebars, higher concrete strain, and greater displacement.

### 3 CALIBRATION AND INSTALLATION OF SENSORS

#### 3.1 OVERVIEW

The loading cases that produce higher tensile strains on the rebars, higher concrete strains, and greater west face displacements were selected for the load tests based on the finite element analyses of bent caps. The locations of the sensors are identified for the selected loading cases. The CNFAs and strain gauges were installed on the rebar cage of bent caps. This chapter elaborates on the calibration of CNFAs and the installation of sensors at the identified locations.

#### 3.2 CALIBRATION OF CNFAs

The carbon nanofiber aggregates (CNFAs) have 0.05% carbon nanofiber (CNFs) contents (by the weight of the cement) adhered to the steel mesh using silver conductive epoxy adhesive. It is crucial to have the compressive strength of the CNFA samples be greater than that of the compressive strength of the bent caps in the Donigan Road Bridge to maintain structural integrity. The design strength of the ITBCs 2 and 7 is 5 ksi. Hence, the CNFAs were cured for 28 days to fabricate the sample with compressive strength higher than 5 ksi.

Three 28-day cured CNFAs were tested under uniaxial compression to identify the compressive strength. Table 3.1 shows the average compressive strength of CNFAs. A typical stress-strain diagram of CNFA from the compressive test is shown in Figure 3.1.

**Table 3.1 Compressive strength of 28-day Cured CNFA Samples**

<b>Sample</b>	<b>Compressive Strength (in ksi)</b>
A	7.80
B	8.08
C	8.29
<b>Average</b>	<b>8.06</b>

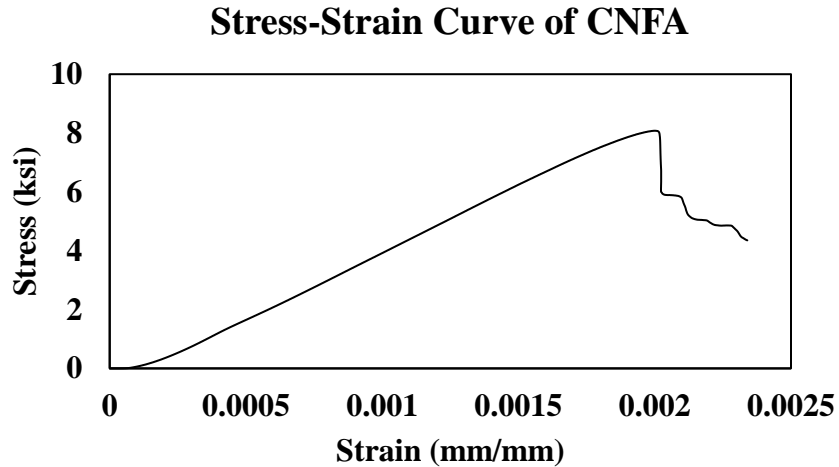


**Figure 3.1. A Typical Stress-Strain Curve of a CNFA**

A total of 16 CNFAs (Samples A to P) are calibrated at 21°C, 30°C, and 40°C to be instrumented on the rebar cages of Bent Cap 2 and Bent Cap 7. As per the TxDOT Project 0-6905-01 schedule, the load test was scheduled from May 2023 to September 2023. The 30-year temperature averages for Houston (1991 to 2020) were considered for the calibration. The maximum and minimum temperature range in the considered period is 23°C to 34°C (National Centers for Environmental Information, 2023). However, the field temperature was in the range of 9.2°C to 12.2°C during the load test at the bridge site (December 2022). Henceforth, the calibration of SSCNFAs at 5°C is extrapolated.

The CNFAs are fabricated to be embedded in the concrete of bent caps. The CNFAs are examined at 300 kHz at 0.5V. The Stress-Strain-EZV relationships of 13 CNFAs at 300 kHz instrumented on the rebar cages of two bent caps are presented in APPENDIX-3.

### **3.3 INSTRUMENTATION OF SENSOR**

Based on the preliminary finite element simulation, the critical locations for sensor installation are identified. Strain gauges (SGs) and carbon nanofiber aggregates (CNFAs) are instrumented on the rebar cage of both bent caps. CNFAs are robust and supersensitive cement-based sensors (Joshi, Li, Oz, Wang, et al., 2021b; Joshi, Shan, Wang, Oz, et al., 2021; Joshi et al., 2023). CNFAs are waterproofed before installation. SGs on the rebars were installed with the following steps.

- Rebar surface was ground to create a plane surface for SG placement,
- Ground surface was cleaned using acid and neutralizer,
- SG was glued on the surface using adhesive and scotch tape,
- M-Coat A followed by M-Coat B was applied on the SG to waterproof,
- Nitrile butyl rubber was used for additional safety,
- Aluminum tape was applied on the nitrile butyl rubber and was sealed by tape, and
- All the strain gauges are checked with an Ohmmeter to examine if they are functioning properly.

Moreover, since the CNFAs were waterproofed and robust in nature, they were anchored to the rebars using zip ties. A few locations were required to be modified because of the inaccessibility and rebar congestion.

### 3.3.1 Bent Cap 2

A detailed location of the 32 strain gauges and 10 CNFAs installed on Bent Cap 2 are presented in Table 3.2 and Table 3.3. The coordinate system for each sensor is based on the reference image, as presented in Figure 2.12. The pasting of SGs and anchoring CNFA on the rebars of Bent Cap 2 is shown in Figure 3.2 (a-b). Figure 3.3 shows the sensors installed on the West end of Bent Cap 2.

**Table 3.2. Locations of Strain Gauges Installed in Bent Cap 2**

No.	Label	Explanation	X (in)	Y (in)	Z (in)	Bar Group
			Coordinates shown in Figure 2.12			
1	B2-SS1s1	Bent Cap 2 - Southside, 1st S Bar from the east face, 1st SG located on the Side of the bar	-19.1	-20.5	35	S Bars
2	B2-SS1s2	Bent Cap 2 - Southside, 1st S Bar from the east face, 2nd SG located on the Side of the bar	-19.1	-20.5	30	
3	B2-SS2s1	Bent Cap 2 - Southside, 2nd S Bar from the east face, 1st SG located on the Side of the bar	-13.3	-20.5	35	
4	B2-SS2s2	Bent Cap 2 - Southside, 2nd S Bar from the east face, 2nd SG located on the Side of the bar	-13.3	-20.5	30	
5	B2-SS3s1	Bent Cap 2 - Southside, 3rd S Bar from the east face, 1st SG located on the Side of the bar	-7.4	-20.5	35	

<b>6</b>	<b>B2-SS3s2</b>	Bent Cap 2 - Southside, 3rd S Bar from the east face, 2nd SG located on the Side of the bar	-7.4	-20.5	30		
<b>7</b>	<b>B2-SS4s1</b>	Bent Cap 2 - Southside, 4th S Bar from the east face, 2nd SG located on the Side of the bar	-1.56	-20.5	35		
<b>8</b>	<b>B2-SS4s2</b>	Bent Cap 2 - Southside, 4th S Bar from the east face, 2nd SG located on the Side of the bar	-1.56	-20.5	30		
<b>9</b>	<b>B2-NS5s1</b>	Bent Cap 2 - North side, 5th S Bar from the east face, 1st SG located on the Side of the bar	49.21	20.5	35		
<b>10</b>	<b>B2-NS5s2</b>	Bent Cap 2 - North side, 5th S Bar from the east face, 2nd SG located on the Side of the bar	49.21	20.5	30		
<b>11</b>	<b>B2-NS6s1</b>	Bent Cap 2 - North side, 6th S Bar from the east face, 1st SG located on the Side of the bar	55.07	20.5	35		S Bars
<b>12</b>	<b>B2-NS6s2</b>	Bent Cap 2 - North side, 6th S Bar from the east face, 2nd SG located on the Side of the bar	55.07	20.5	30		
<b>13</b>	<b>B2-NS7s1</b>	Bent Cap 2 - North side, 7th S Bar from the east face, 1st SG located on the Side of the bar	60.93	20.5	35		
<b>14</b>	<b>B2-NS7s2</b>	Bent Cap 2 - North side, 7th S Bar from the east face, 2nd SG located on the Side of the bar	60.93	20.5	30		
<b>15</b>	<b>B2-NS8s1</b>	Bent Cap 2 - North side, 8th S Bar from the east face, 1st SG located on the Side of the bar	66.77	20.5	35		
<b>16</b>	<b>B2-NS8s2</b>	Bent Cap 2 - North side, 8th S Bar from the east face, 2nd SG located on the Side of the bar	66.77	20.5	30		
<b>17</b>	<b>B2-SM5t</b>	Bent Cap 2 - Southside, 5th M Bar from the east face, SG located on the top of the bar	7.8	-24	23	M Bars	
<b>18</b>	<b>B2-SM6t</b>	Bent Cap 2 - Southside, 6th M Bar from the east face, SG located on the Top of the bar	13.6	-24	23		
<b>19</b>	<b>B2-SM7t</b>	Bent Cap 2 - Southside, 7th M Bar from the east face, SG located on the Top of the bar	19.4	-24	23		
<b>20</b>	<b>B2-SM8t</b>	Bent Cap 2 - Southside, 8th M Bar from the east face, SG located on the Top of the bar	25.3	-24	23		

21	<b>B2-SM14b</b>	Bent Cap 2 - Southside, 14th M Bar from the east face, SG located on the Bottom of the bar	67.4	-16.7	0	
22	<b>B2-SM16b</b>	Bent Cap 2 - Southside, 16th M Bar from the east face, SG located on the Bottom of the bar	79	-16.7	0	
23	<b>B2-A7</b>	Bent Cap 2 – 7th A Bar from the south side	94.3	9.9	78.2	A Bars
24	<b>B2-A8</b>	Bent Cap 2 – 8th A Bar from the south side	98.9	14.8	78.2	
25	<b>B2-A9</b>	Bent Cap 2 – 9th A Bar from the south side	103.5	19.8	78.2	
26	<b>B2-U1-1</b>	Bent Cap 2 - 1st U1 Bar from the west face	-10.84	-12.07	17	U1 Bar
27	<b>B2-SG1</b>	Bent Cap 2 - Southside 1st G Bar from the west face	-19.1	-22.03	23.27	G Bar
28	<b>B2-SG4</b>	Bent Cap 2 - Southside, 4th G Bar from the east face	-1.59	-22.03	23.27	
29	<b>B2-SG5</b>	Bent Cap 2 - Southside, 5th G Bar from the east face	4.25	-22.03	23.27	
30	<b>B2-B10</b>	Bent Cap 2 - 10th B Bar from the west face	70.4	8.5	1.1	B Bar
31	<b>B2-T7-N</b>	Bent Cap 2- Northside, 7th T bar from the East face under the bearing pad	62.3	37.5	24	T Bar
32	<b>B2-T3-S</b>	Bent Cap 2- Southside 3rd T bar from the East face under the bearing pad	5.36	36.8	24	T Bar

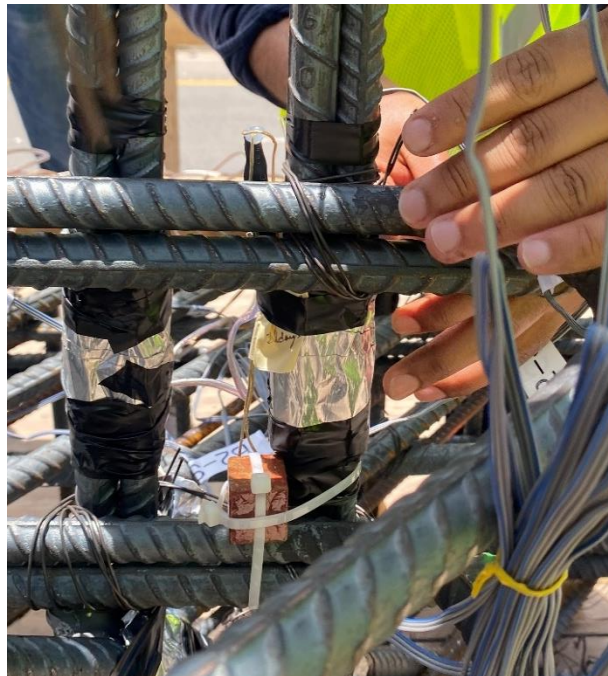
**Table 3.3. Locations of CNFAs Installed in Bent Cap 2**

No.	Label	Explanation	X (in)	Y (in)	Z (in)	Group
1	<b>B2-CNFA1zz1</b>	Bent Cap 2 - 10th B Bar from the west face, First CNFA location in Z-Z direction	77.3	8.5	1.1	Location 1
2	<b>B2-CNFA2zz1</b>	Bent Cap 2 - T Bar, First CNFA at Location 2 on Z-Z direction (Bearing Pad-North face)	57.3	37.5	24	Location 2
3	<b>B2-CNFA2zz2</b>	Bent Cap 2 - T Bar, Second CNFA at Location 2 on Z-Z direction (Bearing Pad-North face)	62.3	37.5	24	
4	<b>B2-CNFA2zz3</b>	Bent Cap 2 - T Bar, Third CNFA at Location 2 on Z-	67.3	37.5	24	

		Z direction (Bearing Pad-North face)				
<b>5</b>	<b>B2-CNFA3zz1</b>	Bent Cap 2 - 1st S Bar, First CNFA at Location 3 on Z-Z direction (First S-bar-South face)	-19.1	-20.5	30	Location 3
<b>6</b>	<b>B2-CNFA3zz2</b>	Bent Cap 2 – 2nd S Bar, Second CNFA at Location 3 on Z-Z direction (Second S-bar-South face)	-13.3	-20.5	30	
<b>7</b>	<b>B2-CNFA3zz3</b>	Bent Cap 2 – 3rd S Bar, Third CNFA at Location 3 on Z-Z direction (Third S-bar-South face)	-7.4	-20.5	30	
<b>8</b>	<b>B2-CNFA4zz1</b>	Bent Cap 2 - T Bar, First CNFA at Location 4 on Z-Z direction (Bearing Pad-South face)	5.36	-20.5	24	Location 4
<b>9</b>	<b>B2-CNFA4zz2</b>	Bent Cap 2 - T Bar, Second CNFA at Location 4 on Z-Z direction (Bearing Pad-South face)	11.36	-20.5	24	
<b>10</b>	<b>B2-CNFA4zz3</b>	Bent Cap 2 - T Bar, Third CNFA at Location 4 on Z-Z direction (Bearing Pad-South face)	17.36	-20.5	24	



**(a) Pasting Strain Gauges on Rebars**



**(b) CNFA Anchored to Rebar**

**Figure 3.2. Sensors Installation on Rebars of Bent Cap 2**



**Figure 3.3. Sensors Installed in Bent Cap 2**

### 3.3.2 Bent Cap 7

A detailed location of the 30 strain gauges and 9 CNFAs installed on Bent Cap 7 are presented in Table 3.4 and Table 3.5. The coordinate system for each sensor is based on the reference image, as presented in Figure 2.24. The pasting of SGs and anchoring CNFA on the rebars of Bent Cap 2 is shown in Figure 3.4 (a-b). Figure 3.5 shows the sensors installed on the West end of Bent Cap 2.

**Table 3.4. Location of Strain Gauges Installed in Bent Cap 7**

No	Label	Explanation	X (in)	Y (in)	Z (in)	Bar Group
			Coordinates shown in Figure 2.24			
1	<b>B7-SS1s1</b>	Bent Cap 7 - South side, 1st S Bar from the West face, 1st SG located on the Side of the bar	-13.3	-20.5	30	S Bars
2	<b>B7-SS1s2</b>	Bent Cap 7 - South side, 1st S Bar from the West face, 2nd SG located on the Side of the bar	-13.3	-20.5	35	
3	<b>B7-SS2s1</b>	Bent Cap 7 - South side, 2nd S Bar from the West face, 1st SG located on the Side of the bar	-7.5	-20.5	30	
4	<b>B7-SS2s2</b>	Bent Cap 7 - South side, 2nd S Bar from the West face, 2nd SG located on the Side of the bar	-7.5	-20.5	35	
5	<b>B7-SS3s1</b>	Bent Cap 7 - South side, 3rd S Bar from the West face, 1st SG located on the Side of the bar	-1.6	-20.5	30	
6	<b>B7-SS3s2</b>	Bent Cap 7 - South side, 3rd S Bar from the West face, 2nd SG located on the Side of the bar	-1.6	-20.5	35	
7	<b>B7-SS4s1</b>	Bent Cap 7 - South side, 4th S Bar from the West face, 1st SG located on the Side of the bar	4.72	-20.5	30	
8	<b>B7-SS4s2</b>	Bent Cap 7 - South side, 4th S Bar from the West face, 2nd SG located on the Side of the bar	4.72	-20.5	35	
9	<b>B7-NS5s1</b>	Bent Cap 7 - North side, 5th S Bar from the West face, 1st SG located on the Side of the bar	43.9	20.5	30	
10	<b>B7-NS5s2</b>	Bent Cap 7 - North side, 5th S Bar from the West face, 2nd SG located on the Side of the bar	43.9	20.5	35	

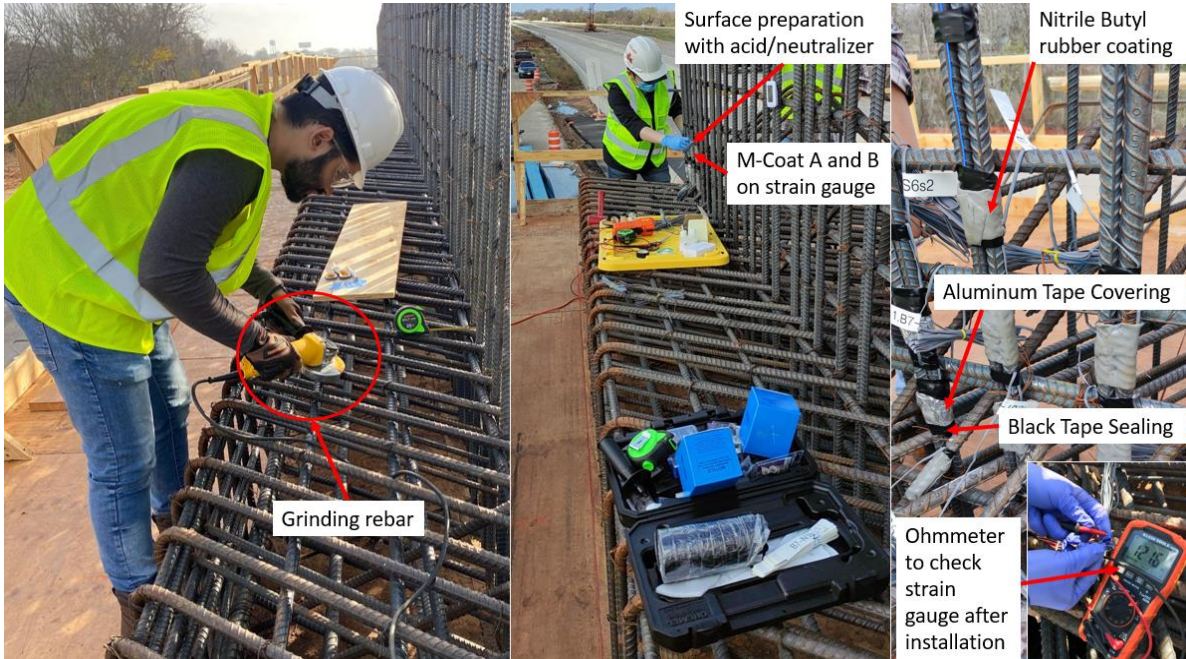
11	<b>B7-NS6s1</b>	Bent Cap 7 - North side, 6th S Bar from the West face, 1st SG located on the Side of the bar	49.9	20.5	30	
12	<b>B7-NS6s2</b>	Bent Cap 7 - North side, 6th S Bar from the West face, 2nd SG located on the Side of the bar	49.9	20.5	35	
13	<b>B7-NS7s1</b>	Bent Cap 7 - North side, 7th S Bar from the West face, 1st SG located on the Side of the bar	55.7	20.5	30	
14	<b>B7-NS7s2</b>	Bent Cap 7 - North side, 7th S Bar from the West face, 2nd SG located on the Side of the bar	55.7	20.5	35	
15	<b>B7-NS8s1</b>	Bent Cap 7 - North side, 8th S Bar from the West face, 1st SG located on the Side of the bar	61.57	20.5	30	
16	<b>B7-NS8s2</b>	Bent Cap 7 - North side, 8th S Bar from the West face, 2nd SG located on the Side of the bar	61.57	20.5	35	
17	<b>B7-SM5t</b>	Bent Cap 7 - South side, 5th M Bar from the West face, SG located on the Top of the bar	10.8	-20.8	23	
18	<b>B7-SM6t</b>	Bent Cap 7 - South side, 6th M Bar from the West face, SG located on the Top of the bar	16.6	-20.8	23	
19	<b>B7-SM7t</b>	Bent Cap 7 - South side, 7th M Bar from the West face, SG located on the Top of the bar	22.4	-20.8	23	
20	<b>B7-SM8t</b>	Bent Cap 7 - South side, 8th M Bar from the West face, SG located on the Top of the bar	28.2	-20.8	23	M Bar
21	<b>B7-SM15b</b>	Bent Cap 7 - South side, 15th M Bar from the West face, SG located on the Bottom of the bar	71.6	-17	0	
22	<b>B7-SM17b</b>	Bent Cap 7 - South side, 17th M Bar from the West face, SG located on the Bottom of the bar	83	-17	0	
23	<b>B7-A7</b>	Bent Cap 7 - 7th A Bar of 1st alignment from the West face	99	9.9	78.2	A Bars

24	<b>B7-A8</b>	Bent Cap 7 - 8th A Bar of 1st alignment from the West face	107	14.8	78.2	
25	<b>B7-A9</b>	Bent Cap 7 - 9th A Bar of 1st alignment from the West face	109	19.8	78.2	
26	<b>B7-U1-1</b>	Bent Cap 7 - 1st U1 Bar from the West face	-7.24	12.05	39.25	U1 Bar
27	<b>B7-SG4</b>	Bent Cap 7 - South side, 4th G Bar from the West face	5.39	-21	25.5	G Bar
28	<b>B7-SG5</b>	Bent Cap 7 - South side, 5th G Bar from the West face	11.25	-21	25.5	
29	<b>B7-B10</b>	Bent Cap 7 - 10th B Bar from the West face	76	18	1.1	B Bar
30	<b>B7-T7</b>	Bent Cap 7 - North side, 7th T bar from the West face under the bearing pad	51.2	39.5	24	T Bar

**Table 3.5. Location of CNFAs Installed in Bent Cap 7**

No.	Label	Explanation	X (in)	Y (in)	Z (in)	Group
1	<b>B7-CNFA1zz1</b>	Bent Cap 7 - 10th B Bar from the West face, CNFA1 located in Z-direction	68.7	8.5	1.1	Location 1
2	<b>B7-CNFA1zz2</b>	Bent Cap 7 - 13th M Bar from the West face, CNFA2 located in Z-direction	77	8.5	1.1	
3	<b>B7-CNFA2zz1</b>	Bent Cap 7 - T Bar, First CNFA at Location 2 in Z-direction (North face)	43.7	37.5	24	Location 2
4	<b>B7-CNFA2zz2</b>	Bent Cap 7 - T Bar, Second CNFA at Location 2 in Z-direction (North face)	46.2	37.5	24	
5	<b>B7-CNFA2zz3</b>	Bent Cap 7 - T Bar, Third CNFA at Location 2 in Z-direction (North face)	48.7	37.5	24	
6	<b>B7-CNFA2zz4</b>	Bent Cap 7 - T Bar, Fourth CNFA at Location 2 in Z-direction (North face)	51.2	37.5	24	
7	<b>B7-CNFA3zz1</b>	Bent Cap 7 - 1st S Bar, First CNFA at Location 3 in Z-direction	-13.3	-20.5	30	Location 3
8	<b>B7-CNFA3zz2</b>	Bent Cap 7 - 2nd S Bar, Second CNFA at Location 3 in Z-direction	-7.5	-20.5	35	

9	B7-CNFA3zz3	Bent Cap 7 - 3rd S Bar, Third CNFA at Location 3 in Z-direction	-1.6	-20.5	35	
---	-------------	---	------	-------	----	--

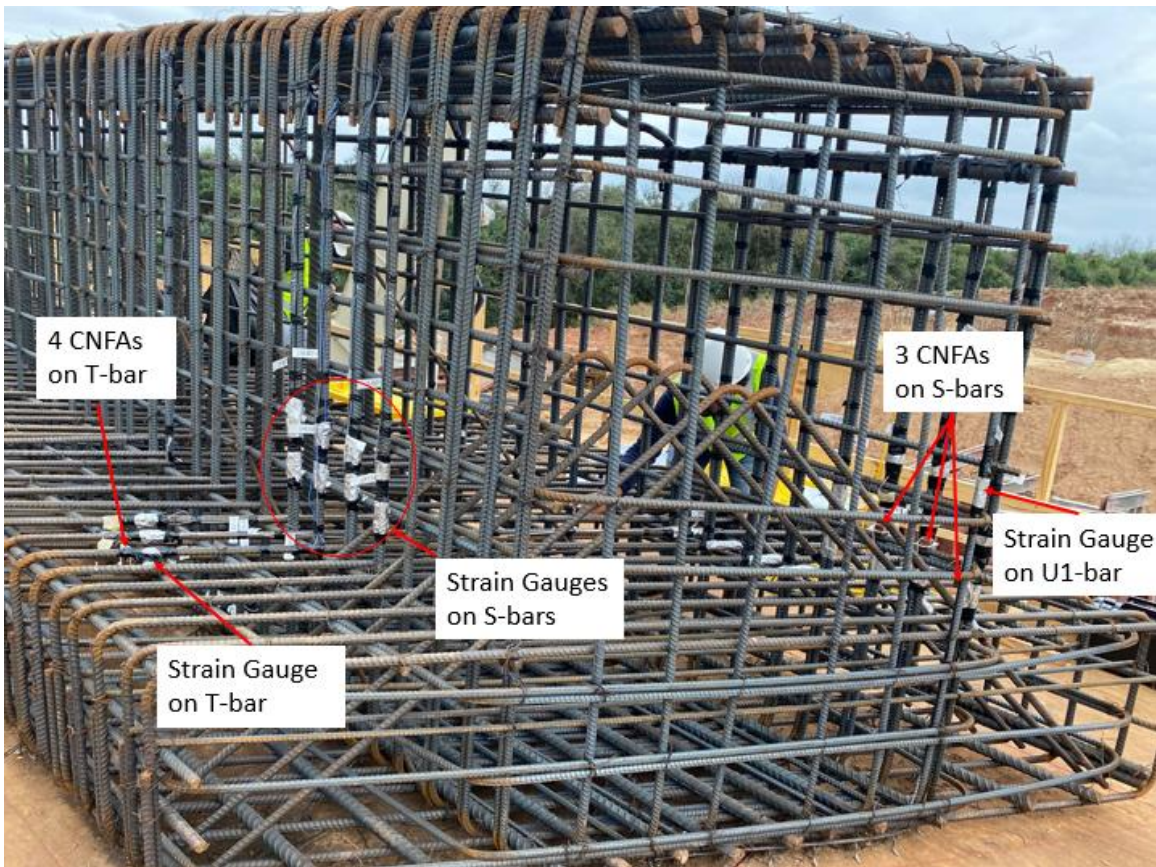
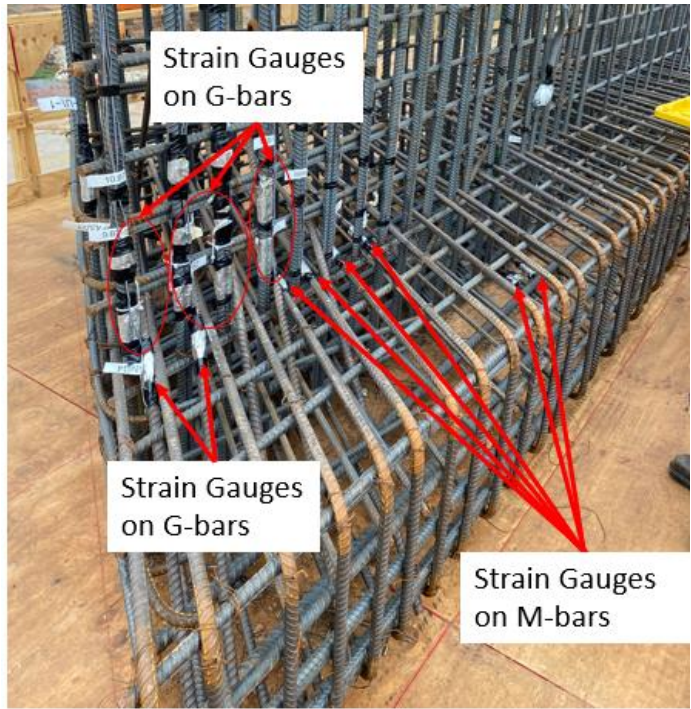


(a) Pasting Strain Gauges on Rebars



(b) CNFA Anchored to Rebar

Figure 3.4. Sensors Installation on Rebars of Bent Cap 7



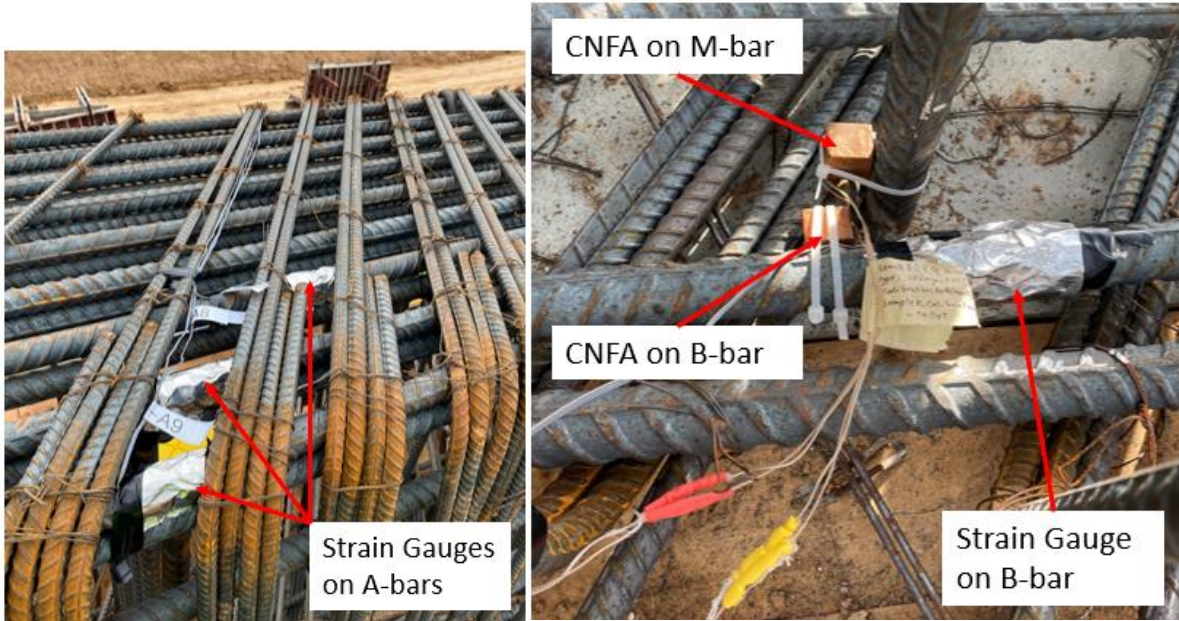
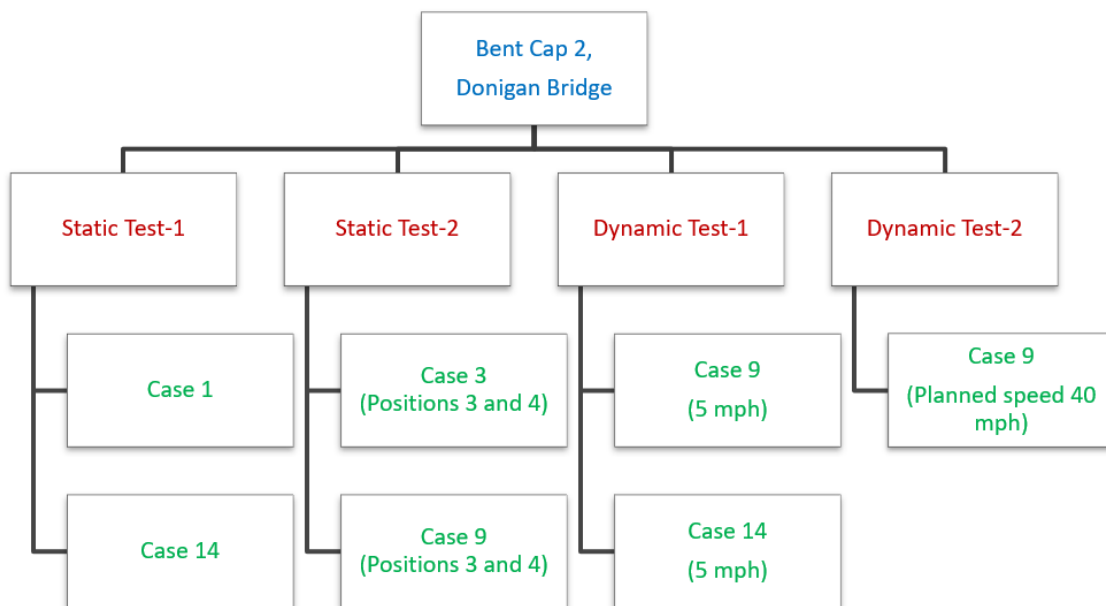


**Figure 3.5. Sensors Installed in Bent Cap 7**

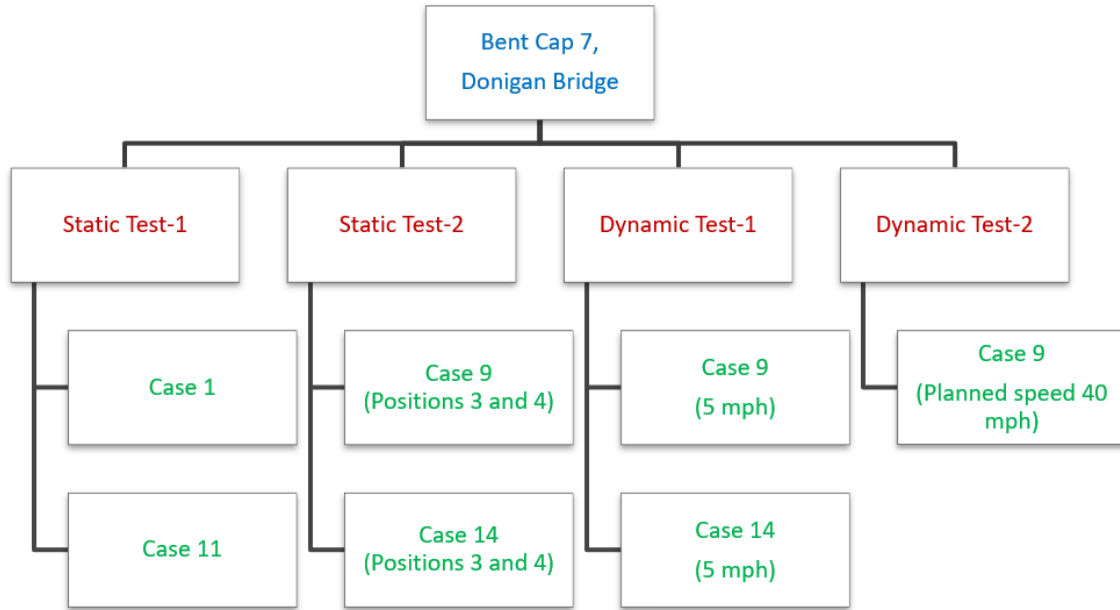
## 4 EXPERIMENTAL PROGRAMS

### 4.1 OVERVIEW

The load tests on Bent Cap 7 and Bent Cap 2 were conducted on Dec 20, 2023, and Dec 21, 2023, with co-ordination with TxDOT, CONSOR Engineers, and Williams Brothers. Each bent cap was tested in two cases of Static Test-1, Static Test-2, Dynamic Test-1 and one case of Dynamic Test-2, as presented in schematic Figures 4.1 and 4.2. The strains in rebar are acquired from strain gauges, the displacements of the west face of bent caps are obtained from laserimeters, and the compressive stresses are obtained from CNFA using the Stress-Electrical Impedance Variation-Temperature Model (S-E-T Model). The S-E-T models of embedded sensors are presented in APPENDIX-3. This chapter elaborates the load tests on Bent Cap 2 and Bent Cap 7, experimental results, and analysis of load test data. Further, the concrete cylinders from both the construction phases of each bent cap were tested per ASTM C39 to determine the compressive strength of the concrete (American Society for Testing and Materials, 2001).



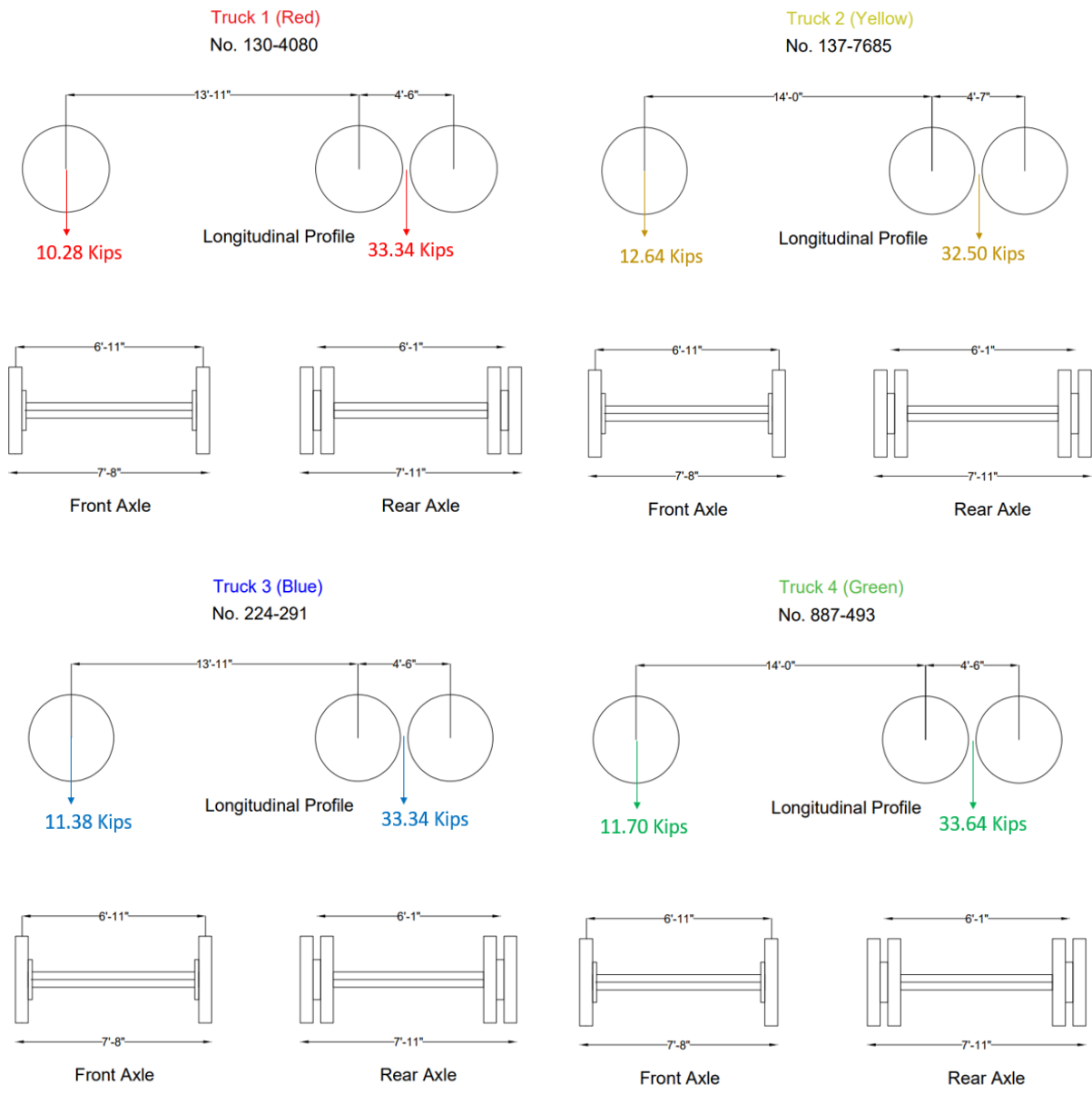
**Figure 4.1. Load Tests on Bent Cap 2**



**Figure 4.2. Load Tests on Bent Cap 7**

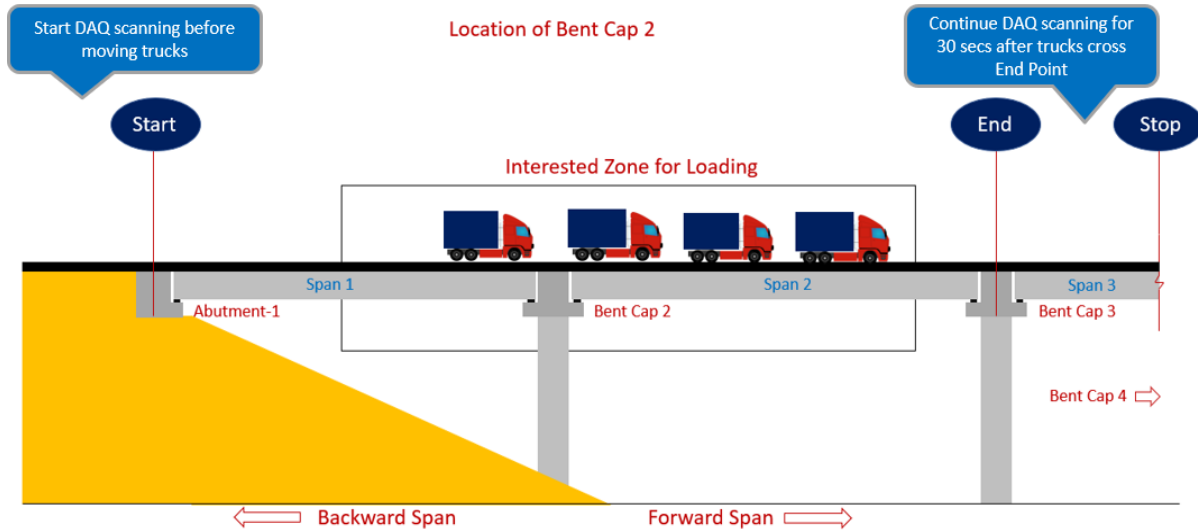
## 4.2 LOAD TEST

Figure 4.3 shows the schematic of the profile of the four trucks. The schematic includes the dimensions and the weight of the steer axle and drive axle. Four trucks were moved at a speed of 5 mph for Static Test-1 and Static Test-2 and stopped at the designated locations on the deck over bent caps. However, four trucks were continuously moved at a speed of 5 mph for Dynamic Test-1 and at a planned speed of 40 mph for Dynamic Test-2 over bent caps.



**Figure 4.3. Schematic Profile of Four Trucks**

The schematic of the load test on Bent Cap2 and Bent Cap 7 are shown in Figures 4.4 and 4.5.



**Figure 4.4. Schematic of Load Test on Bent Cap 2**

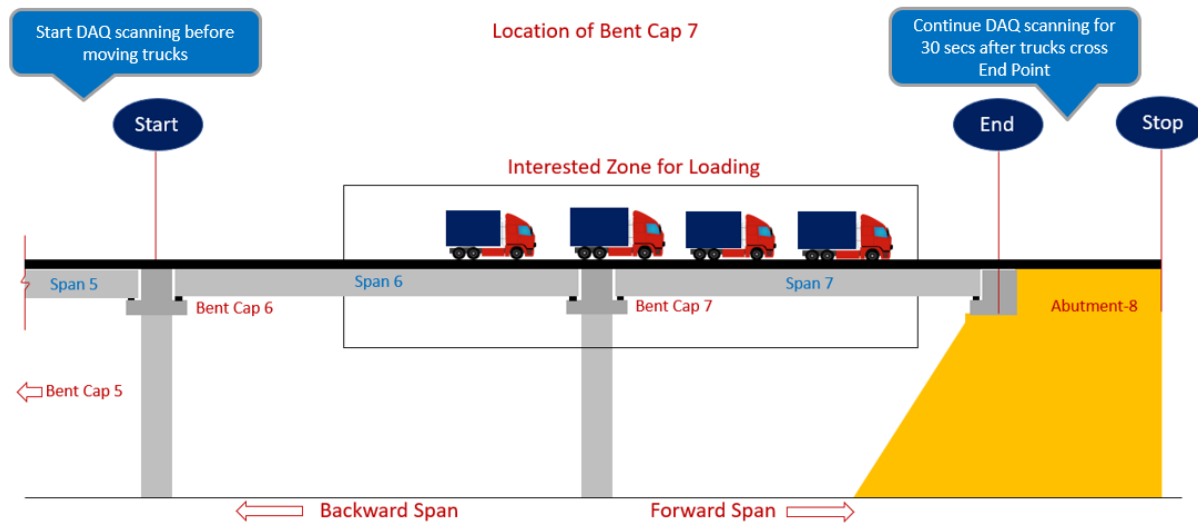


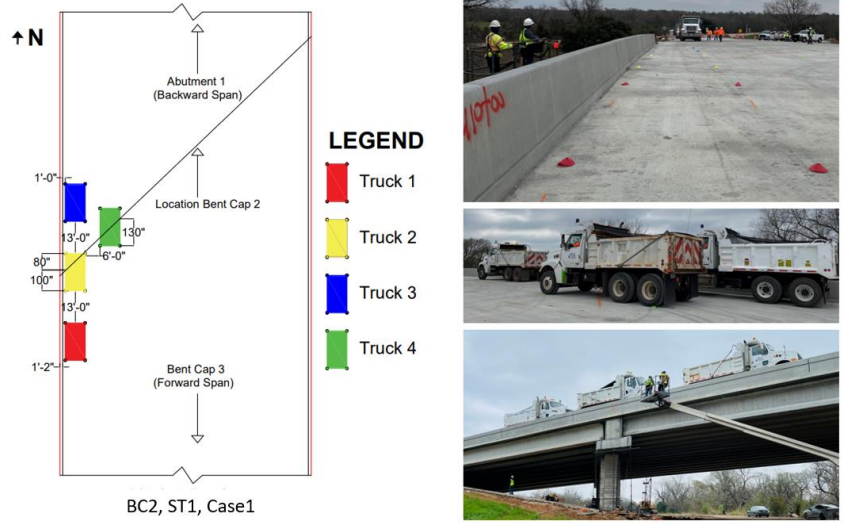
**Figure 4.5. Schematic of Load Test on Bent Cap 7**

### 4.3 EXPERIMENTAL RESULTS

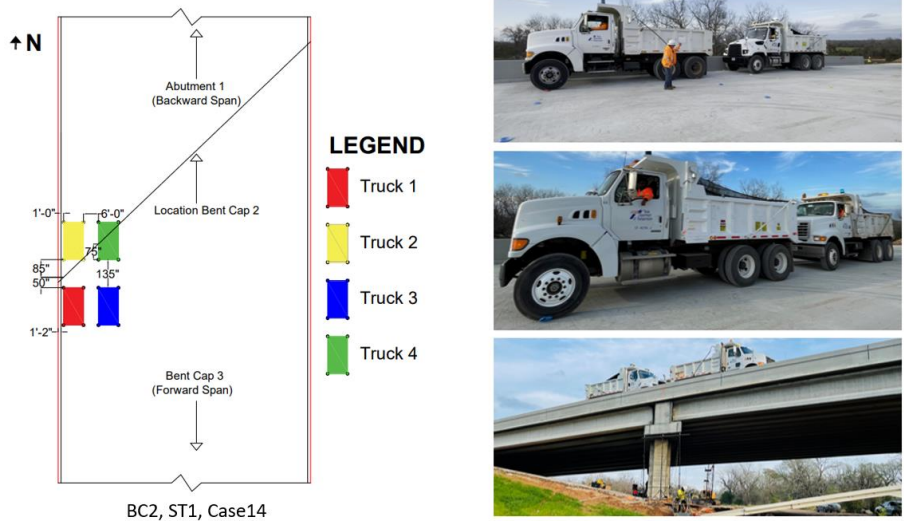
#### 4.3.1 Bent Cap 2

##### 4.3.1.1 Static Test-1

Based on the preliminary finite element analyses, Case 1 and Case 14 were selected for Static Test-1 (ST1). The layouts of four trucks on the deck over Bent Cap 2 for Static Test-1 (Case 1 and Case 14) are shown in Figures 4.6(a-b).



(a) Static Test-1 on Bent Cap 2 for Case 1



(b) Static Test-1 on Bent Cap 2 for Case 14

**Figure 4.6. Static Test-1 on Bent Cap 2**

**4.3.1.1.1 Case 1**

It is observed that the transverse rebars in the stem have higher strains on the south side than those on the north side in Case 1. The S bar near the west face on the south side reported the highest strain of  $13.18 \mu\epsilon$ . The highest strain on the north side S bar is  $5.26 \mu\epsilon$  on the 6<sup>th</sup> S bar. The bottom of the 16<sup>th</sup> M bar (stirrup in the ledge) is subjected to compression ( $-5.12 \mu\epsilon$ ), whereas the top of the 5<sup>th</sup> to 8<sup>th</sup> M bars (stirrups in the ledge) are subjected to tension ( $1.84 \mu\epsilon$ ,  $2.35 \mu\epsilon$ ,  $1.84 \mu\epsilon$ , and  $2.35 \mu\epsilon$ , respectively). Further, the A, U, and G bars are subjected to tension. The

strain on the 4<sup>th</sup> G bar reported is 12.9  $\mu\epsilon$ . The external girder on the west face of Bent Cap 2 is rested on the ledge near the 4<sup>th</sup> G bars. This causes higher strains on the 4<sup>th</sup> G bar. The tip displacement of the extended region of Bent Cap 2 (south side) is -0.0126 inches. The strains and the displacements recorded during the Static Test-1, Case 1 on Bent Cap 2 are presented in Figures 4.7 and 4.8, respectively.

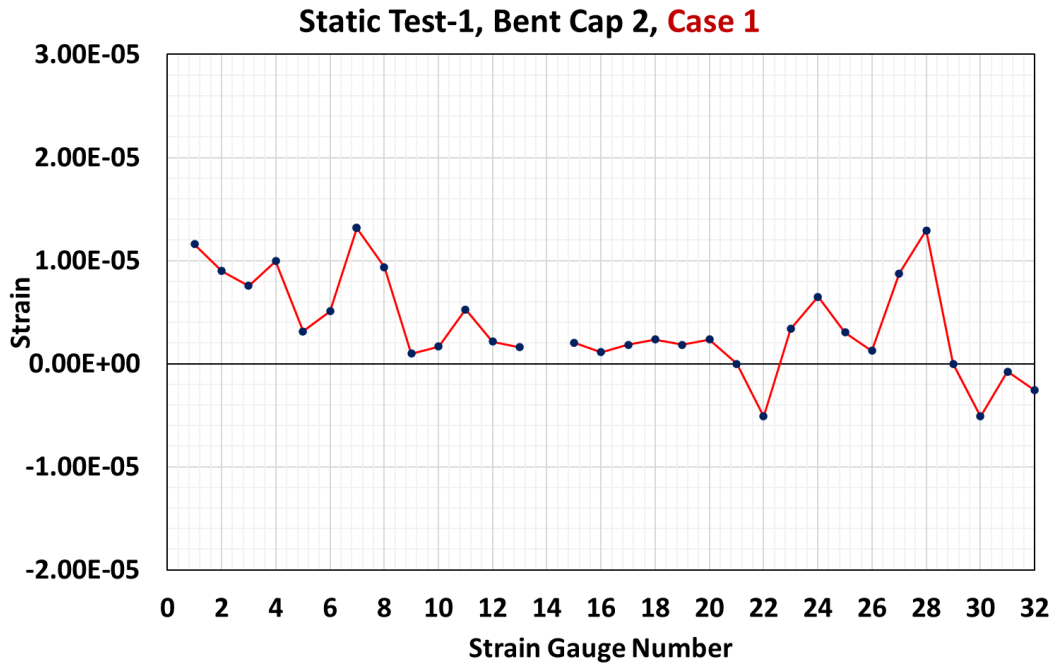


Figure 4.7. Rebar Strains in Static Test-1, Case 1 on Bent Cap 2

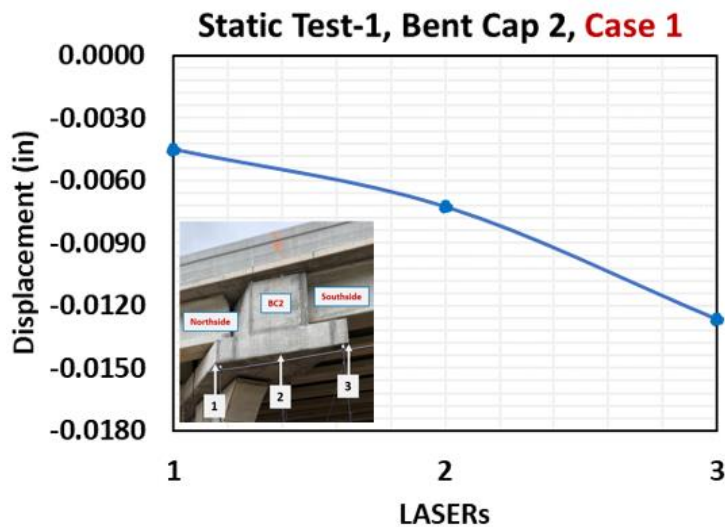
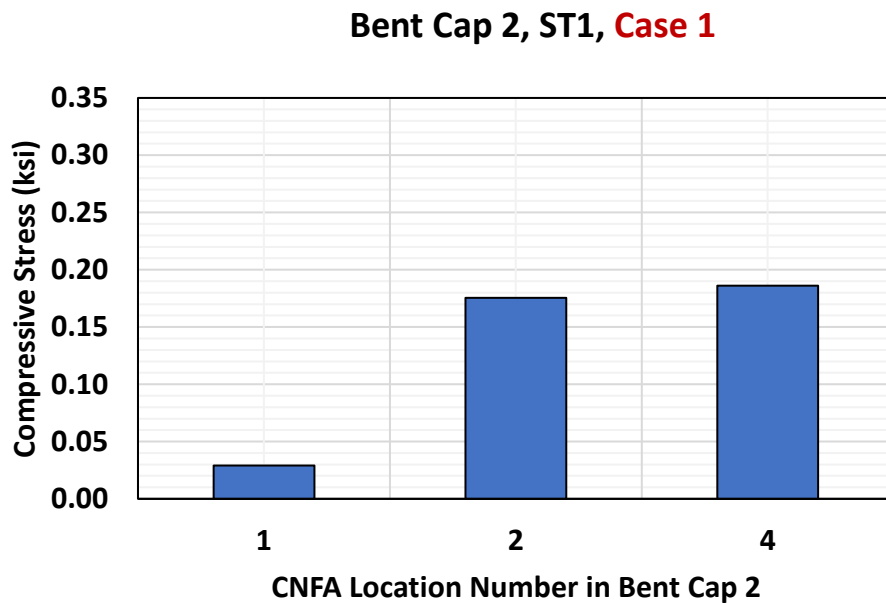


Figure 4.8. West Face Displacement of Bent Cap 2 in Static Test-1, Case 1

The average compressive stress on concrete at Location-1 (at Column-Bent Cap 2 interface) is 0.03 ksi, at Location-2 (under the exterior bearing pad at the north side of Bent Cap 2) is 0.18 ksi, and at Location-4 (under the exterior bearing pad at the south side of Bent Cap 2) is 0.19 ksi. The average compressive stress on concrete recorded by CNFA during the Static Test-1, Case 1 on Bent Cap 2 is presented in Figure 4.9. The average electrical impedance variation (EZV) reported by CNFAs at Location-3 (CNFAs anchored to S bars on the south side near the west face of Bent Cap 2) is -2.43%. The negative EZV indicates tensile stress on the concrete adjacent to the S bars.



**Figure 4.9. Average Compressive Stresses on Concrete in Static Test-1, Case 1 on Bent Cap 2**

#### 4.3.1.1.2 Case 14

It is observed that the transverse rebars in the stem have higher strains on the south side than those on the north side in Case 14. The S bar near the west face on the south side reported the highest strain of 13.26  $\mu\epsilon$ . The highest strain on the north side S bar is 5.46  $\mu\epsilon$  on the 8<sup>th</sup> S bar. The bottom of the 16<sup>th</sup> M bar is subjected to compression (-11.06  $\mu\epsilon$ ), whereas the top of the 5<sup>th</sup> to 8<sup>th</sup> M bars are subjected to tension (11.9  $\mu\epsilon$ , 3.81  $\mu\epsilon$ , 18.42  $\mu\epsilon$ , and 15.83  $\mu\epsilon$ , respectively). In this case, the highest strain is observed in M bars rather than S bars. It may have been attributed to the fact that the two trucks are aligned far from the extended region of Bent Cap 2. In addition, the A, U, and G bars are subjected to tension. The strain on the 4<sup>th</sup> G bar is 4.01  $\mu\epsilon$ . The tip displacement

of the extended region of Bent Cap 2 (south side) is -0.0101 inches. The strains and displacements recorded during the Static Test-1, Case 14 on Bent Cap 2 are presented in Figures 4.10 and 4.11.

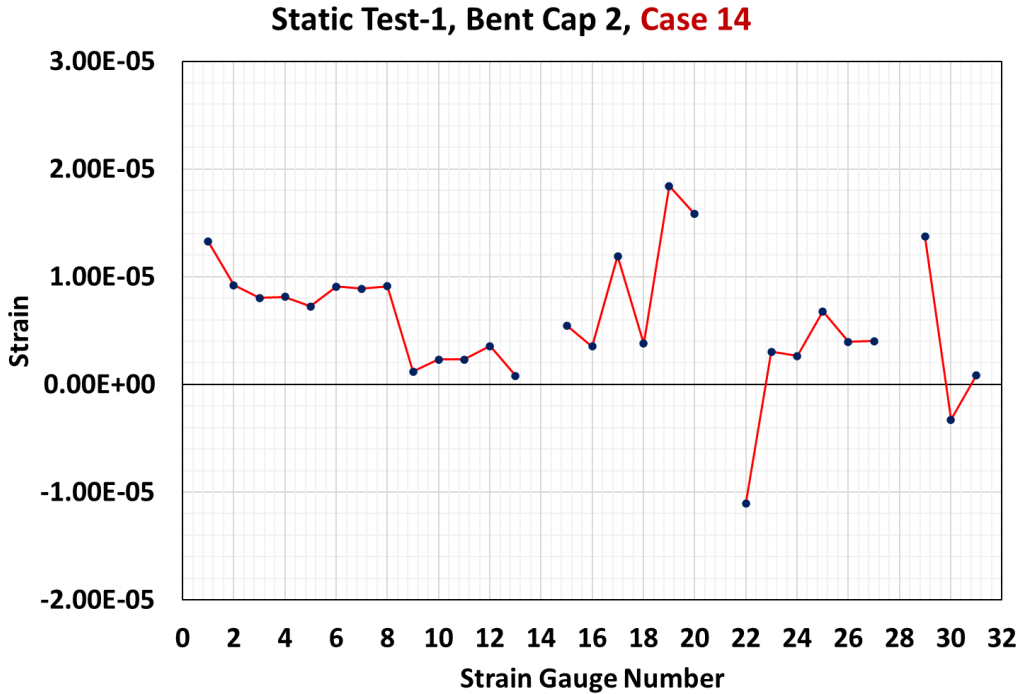


Figure 4.10. Rebar Strains in Static Test-1, Case 14 on Bent Cap 2

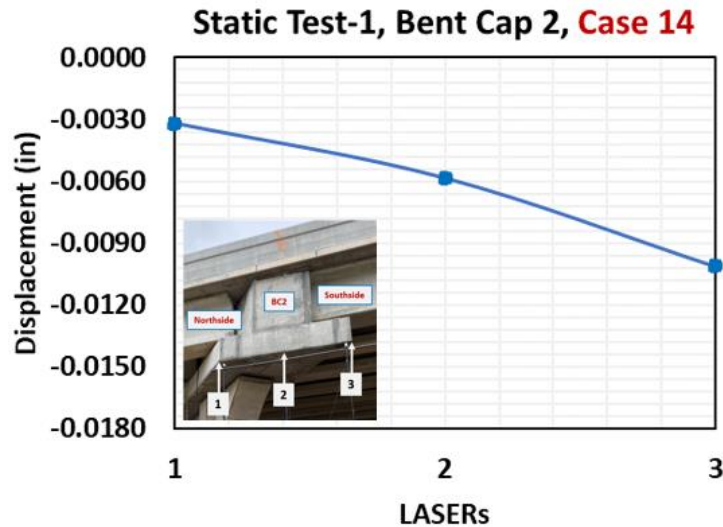
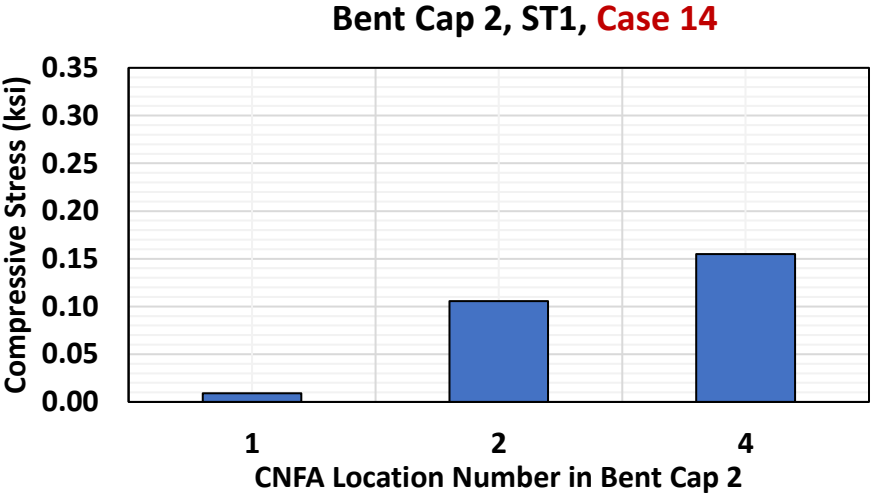


Figure 4.11. West Face Displacement of Bent Cap 2 in Static Test-1, Case 14

The average compressive stress on concrete at Location-1 (at Column-Bent Cap 2 interface) is 0.01 ksi, at Location-2 (under the exterior bearing pad at the north side of Bent Cap 2) is 0.11 ksi, and at Location-4 (under the exterior bearing pad at the south side of Bent Cap 2) is

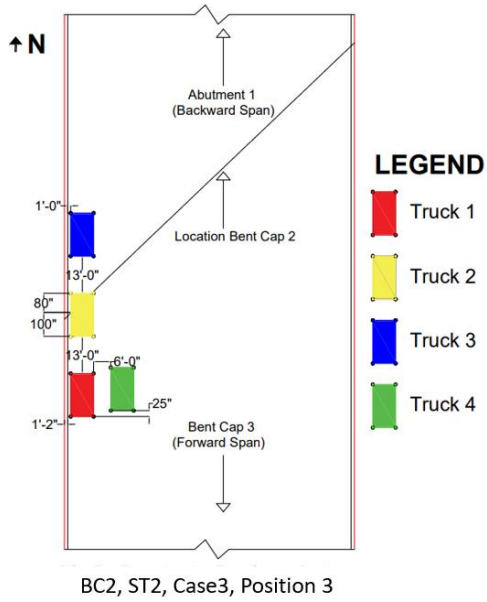
0.16 ksi. The average compressive stress on concrete recorded by CNFA during the Static Test-1 Case 1 on Bent Cap 2 is presented in Figure 4.12. The average electrical impedance variation (EZV) reported by CNFAs at Location-3 (CNFAs anchored to S bars on the south side near the west face of Bent Cap 2) is -2.54%. The negative EZV indicates tensile stress on the concrete adjacent to the S bars.



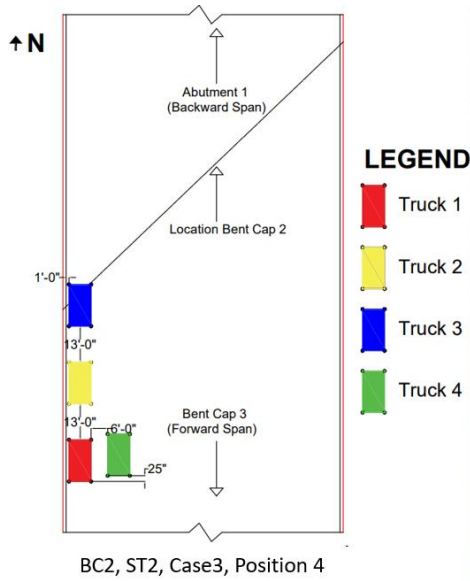
**Figure 4.12. Average Compressive Stresses on Concrete in Static Test-1, Case 14 on Bent Cap 2**

**4.3.1.2 Static Test-2**

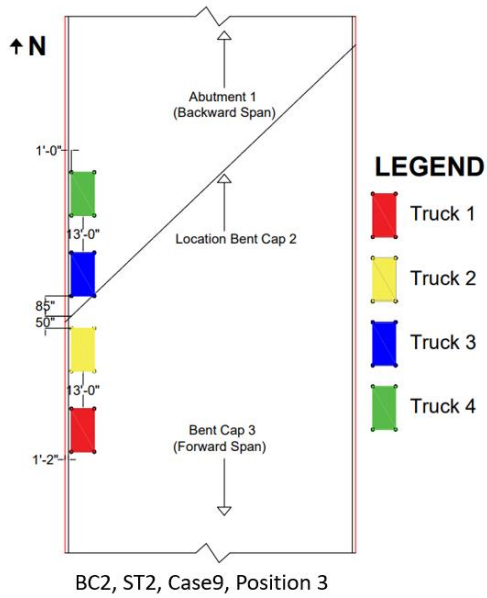
Based on the preliminary finite element analysis, both Case 3 and Case 9 at Position 3 and Position 4 were selected for Static Test-2 (ST2). The layouts of the four trucks on the deck over Bent Cap 2 for Static Test-2 (Case 3 and Case 9) are shown in Figures 4.13(a-d).



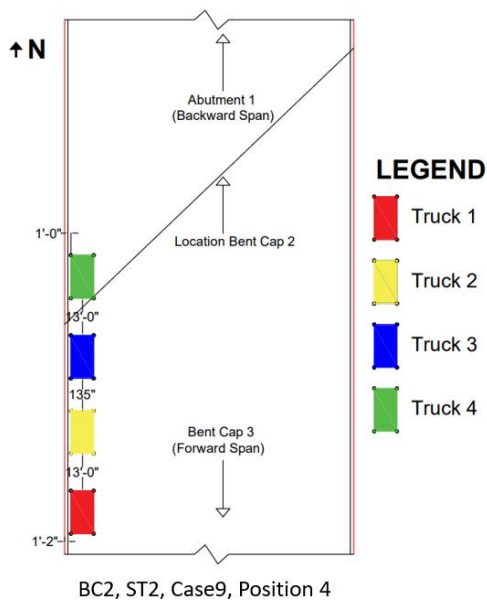
(a) Static Test-2 on Bent Cap 2 for Case 3 at Position 3



(b) Static Test-2 on Bent Cap 2 for Case 3 at Position 4



(c) Static Test-2 on Bent Cap 2 for Case 9 at Position 3



(d) Static Test-2 on Bent Cap 2 for Case 9 at Position 4

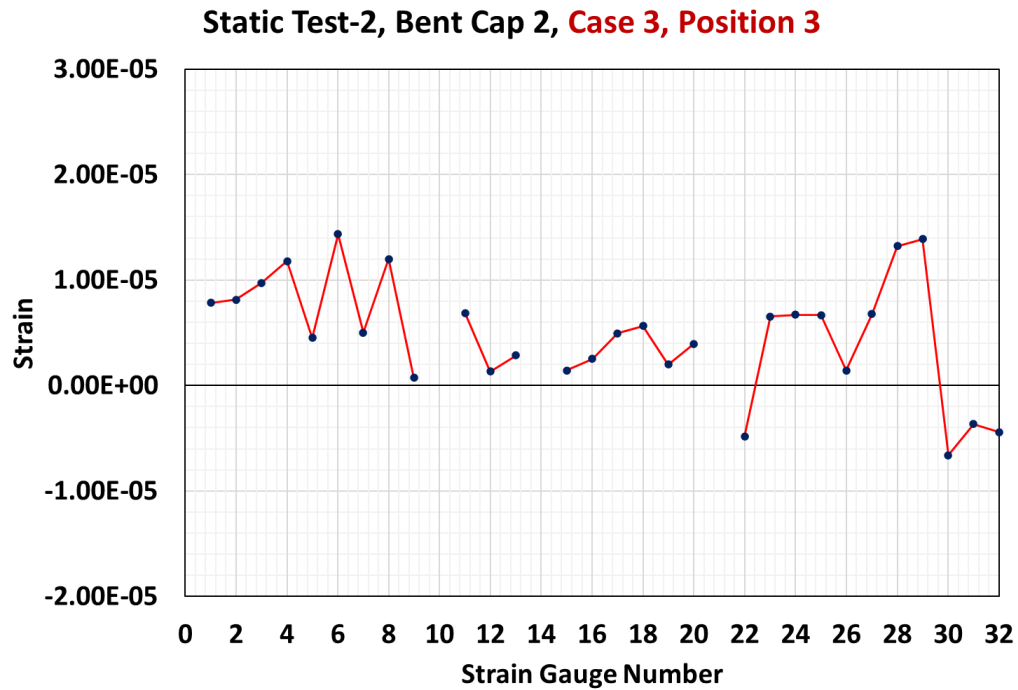
### Figure 4.13. Static Test-2 on Bent Cap 2

#### 4.3.1.2.1 Case 3

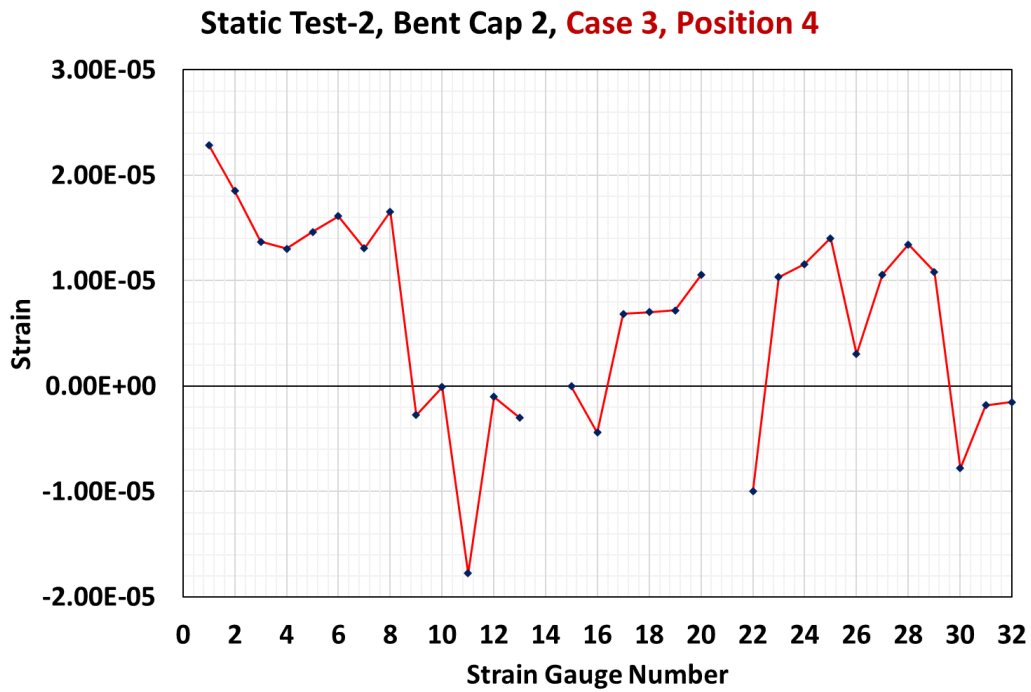
The Static Test-2 for Case 3 shows that the strains on S bars on the south side at Position 4 are higher than those at Position 3. The S bar near the west on the south side at Position 3 reported the highest strain of  $14.34 \mu\epsilon$ , whereas the highest strain in the S bar at Position 4 was  $22.87 \mu\epsilon$ .

The highest strain in the S bar on the north side at Position 3 is  $6.88 \mu\epsilon$ , whereas the highest strain in the S bar on the north side at Position 4 is  $-4.42 \mu\epsilon$ . At Position 3, the bottom of the 16<sup>th</sup> M bar is subjected to compression ( $-4.82 \mu\epsilon$ ), whereas the top of the 5<sup>th</sup> to 8<sup>th</sup> M bars are subjected to tension ( $4.94 \mu\epsilon$ ,  $5.64 \mu\epsilon$ ,  $2.00 \mu\epsilon$ , and  $3.94 \mu\epsilon$ , *respectively*). In addition, the A, U, and G bars are subjected to tension. The strains of the 4<sup>th</sup> and 5<sup>th</sup> G bars are  $13.2 \mu\epsilon$  and  $13.9 \mu\epsilon$ , respectively.

At Position 4, the bottom of the 16<sup>th</sup> M bar is subjected to compression ( $-10.0 \mu\epsilon$ ), whereas the top of the 5<sup>th</sup> to 8<sup>th</sup> M bars are subjected to tension ( $6.86 \mu\epsilon$ ,  $7.02 \mu\epsilon$ ,  $7.20 \mu\epsilon$ , and  $1.05 \mu\epsilon$ , *respectively*). Furthermore, the A, U, and G bars are subjected to tension. The strain in the 4<sup>th</sup> and 5<sup>th</sup> G bars reported  $13.4 \mu\epsilon$  and  $10.8 \mu\epsilon$ , respectively. The tip displacement of the extended region of Bent Cap 2 (south side) in Static Test-2 for Case 3 at Position 3 and Position 4 are  $-0.0133$  inches and  $-0.0161$  inches, respectively. The strains and displacements recorded during Static Test-2, Case 3 on Bent Cap 2 at Position 3 and Position 4 are presented in Figures 4.14(a-b) and Figure 4.15.



(a) Static Test-2 on Bent Cap 2 for Case 3, Position 3



(b) Static Test-2 on Bent Cap 2 for Case 3, Position 4

**Figure 4.14. Rebar Strains in Static Test-2, Case 3 on Bent Cap 2**

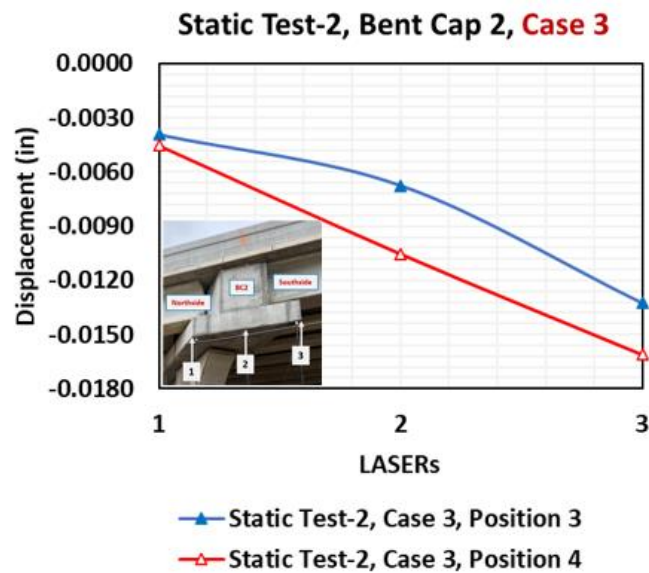


**Figure 4.15. West Face Displacements of Bent Cap 2 in Static Test-2, Case 3**

At Position 3, the average compressive stress on concrete at Location-1 (at Column-Bent Cap 2 interface) is 0.03 ksi, at Location-2 (under the exterior bearing pad at the north side of Bent Cap 2) is 0.12 ksi, and at Location-4 (under the exterior bearing pad at the south side of Bent Cap

2) is 0.17 ksi. At Position 4, the average compressive stress on concrete at Location-1 (at Column-Bent Cap 2 interface) is 0.02 ksi, at Location-2 (under the exterior bearing pad at the north side of Bent Cap 2) is 0.04 ksi, and at Location-4 (under the exterior bearing pad at the south side of Bent Cap 2) is 0.28 ksi. The average compressive stresses on concrete recorded by CNFA during Static Test-2, Case 3 at Position 3, and Position 4 on Bent Cap 2 are presented in Figures 4.16 and 4.17. The average electrical impedance variation (EZV) reported by CNFAs at Location-3 (CNFAs anchored to S bars on the south side near the west face of Bent Cap 2) in Static Test-2, Case 3 at Position 3 and Position 4 are -0.24% and -0.29%, respectively. The negative EZV indicates tensile stress on the concrete adjacent to the S bars.

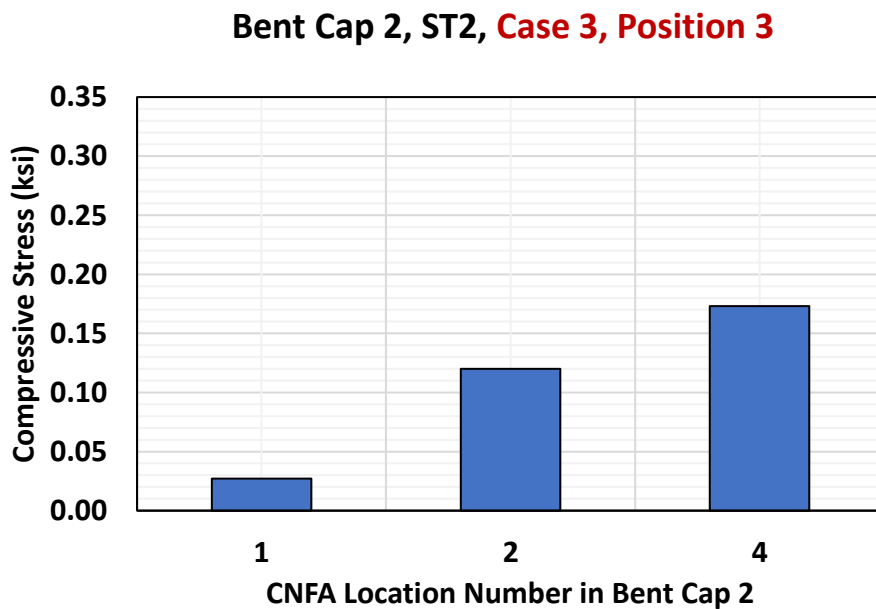


**Figure 4.16. Average Compressive Stresses on Concrete in Static Test-2, Case 3 at Position 3 on Bent Cap 2**

### Bent Cap 2, ST2, Case 3, Position 4

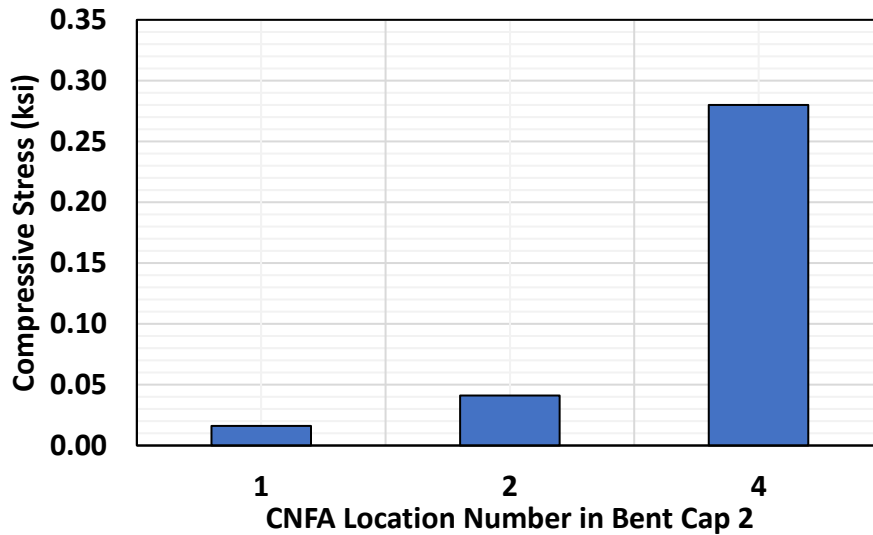


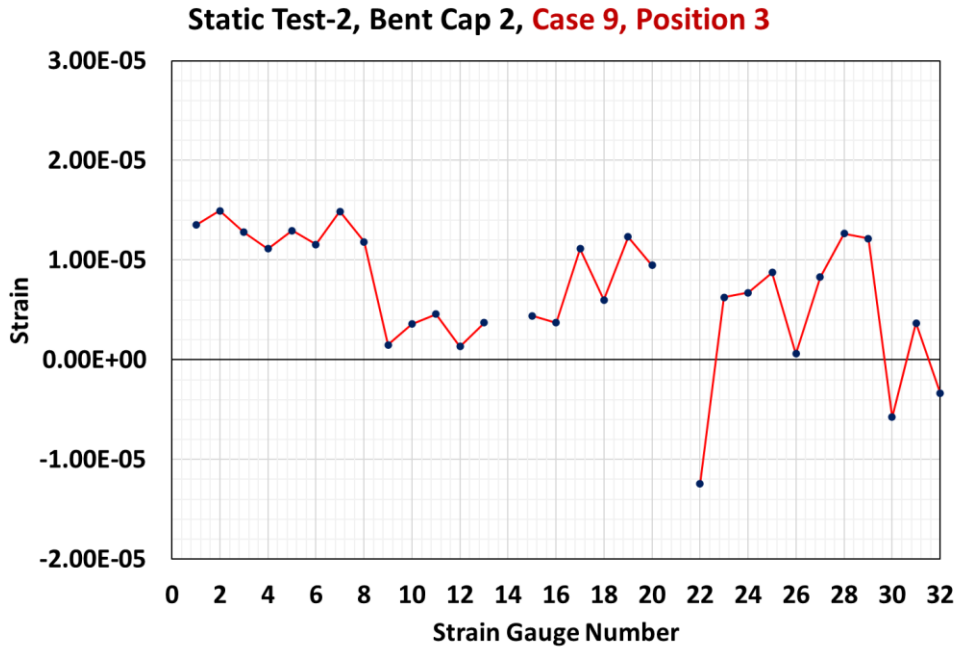
**Figure 4.17. Average Compressive Stresses on Concrete in Static Test-2, Case 3 at Position 4 on Bent Cap 2**

#### 4.3.1.2.2 Case 9

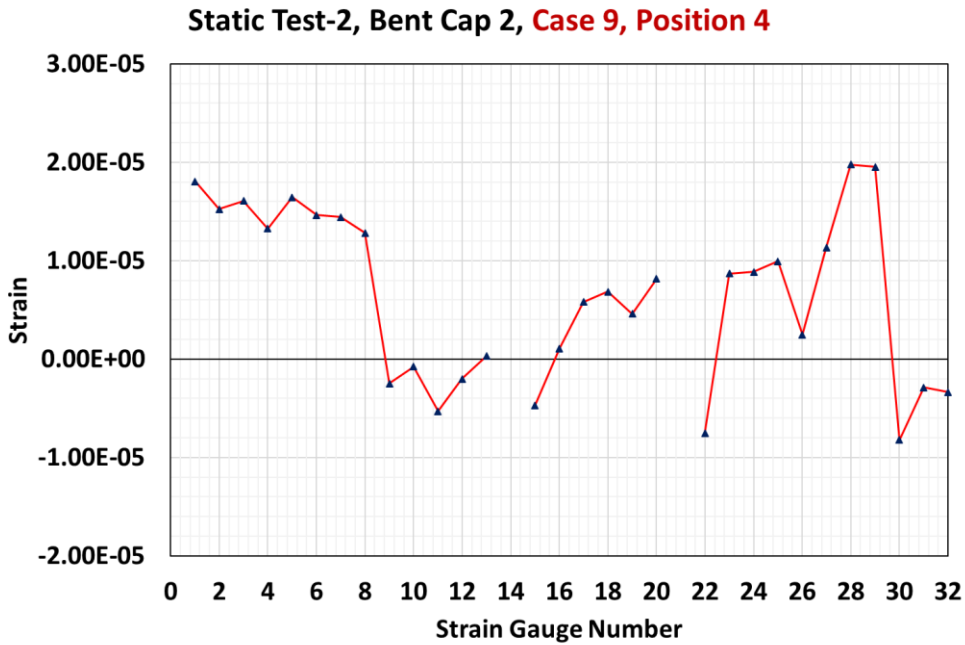
Static Test-2, Case 9 shows that the strains in S bars on the south side at Position 4 are higher than those at Position 3. The S bar near the west face on the south side at Position 3 reported the highest strain of  $14.95 \mu\epsilon$ , whereas the highest strain in the S bars at Position 4 was  $18.04 \mu\epsilon$ . The highest strain in the S bar on the north side at Position 3 is  $4.42 \mu\epsilon$ , whereas the highest strain in the S bar on the north side at Position 4 is  $-5.29 \mu\epsilon$ . At Position 3, the bottom of the 16<sup>th</sup> M bar is subjected to compression ( $-12.41 \mu\epsilon$ ), whereas the top of the 5<sup>th</sup> to 8<sup>th</sup> M bars are subjected to tension ( $11.1 \mu\epsilon$ ,  $6.00 \mu\epsilon$ ,  $12.3 \mu\epsilon$ , and  $9.47 \mu\epsilon$ , respectively). In addition, the A, U, and G bars are subjected to tension. The strains of the 4<sup>th</sup> and 5<sup>th</sup> G bars are  $12.7 \mu\epsilon$  and  $12.2 \mu\epsilon$ , respectively.

At Position 4, the bottom of the 16<sup>th</sup> M bar is subjected to compression ( $-7.51 \mu\epsilon$ ), whereas the top of the 5<sup>th</sup> to 8<sup>th</sup> M bars are subjected to tension ( $5.79 \mu\epsilon$ ,  $6.86 \mu\epsilon$ ,  $4.60 \mu\epsilon$ , and  $8.16 \mu\epsilon$ , respectively). Furthermore, the A, U, and G bars are subjected to tension. The strains in the 4<sup>th</sup> and 5<sup>th</sup> G bars reported  $19.8 \mu\epsilon$  and  $19.5 \mu\epsilon$ , respectively. The tip displacement of the extended region of Bent Cap 2 (south side) in Static Test-2 for Case 9 at Position 3 and Position 4 are  $-0.0149$  inches and  $-0.0163$  inches, respectively. The strains and displacements recorded during

Static Test-2, Case 9 on Bent Cap 2 at Position 3 and Position 4 are presented in Figures 4.18(a-b) and Figure 4.19.



(a) Static Test-2 on Bent Cap 2 for Case 9 at Position 3



(b) Static Test-2 on Bent Cap 2 for Case 9 at Position 4

**Figure 4.18. Rebar Strains in Static Test-2, Case 9 on Bent Cap 2**

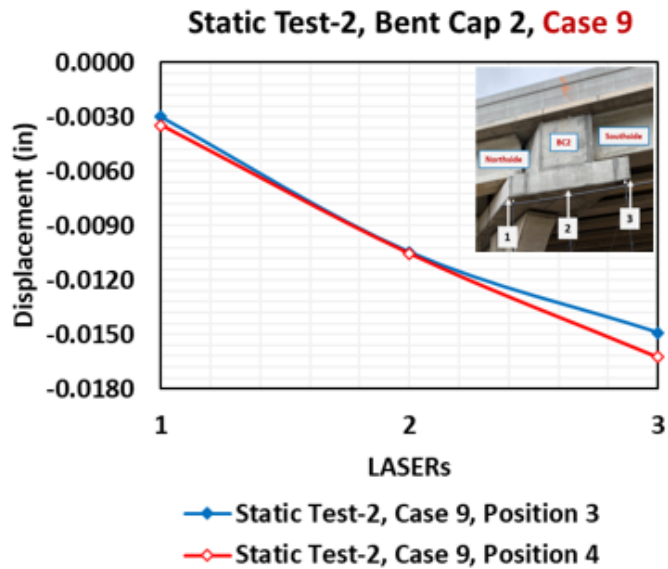


**Figure 4.19. West Face Displacements of Bent Cap 2 in Static Test-2, Case 9**

At Position 3, the average compressive stress on concrete at Location-1 (at Column-Bent Cap 2 interface) is 0.03 ksi, at Location-2 (under the exterior bearing pad at the north side of Bent Cap 2) is 0.15 ksi, and at Location-4 (under the exterior bearing pad at the south side of Bent Cap 2) is 0.22 ksi. At Position 4, the average compressive stress on concrete at Location-1 (at Column-Bent Cap 2 interface) is 0.01 ksi, at Location-2 (under the exterior bearing pad at the north side of Bent Cap 2) is 0.04 ksi, and at Location-4 (under the exterior bearing pad at the south side of Bent Cap 2) is 0.33 ksi. The average compressive stresses on concrete recorded by CNFA during Static Test-2, Case 9 at Position 3, and Position 4 on Bent Cap 2 are presented in Figures 4.20 and 4.21. The average electrical impedance variations (EZVs) reported by CNFAs at Location-3 (CNFAs anchored to S bars on the south side near the west face of Bent Cap 2) in Static Test-2, Case 9 at Position 3 and Position 4 are -0.20% and -2.89%, respectively. The negative EZV indicates tensile stress on the concrete adjacent to the S bars.

**Bent Cap 2, ST2, Case 9, Position 3**

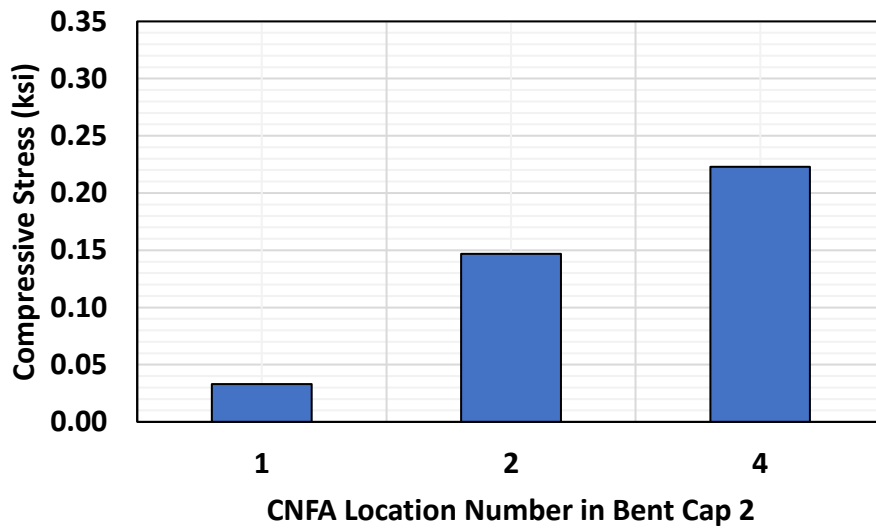


**Figure 4.20. Average Compressive Stresses on Concrete in Static Test-2, Case 9 at Position 3 on Bent Cap 2**

**Bent Cap 2, ST2, Case 9, Position 4**

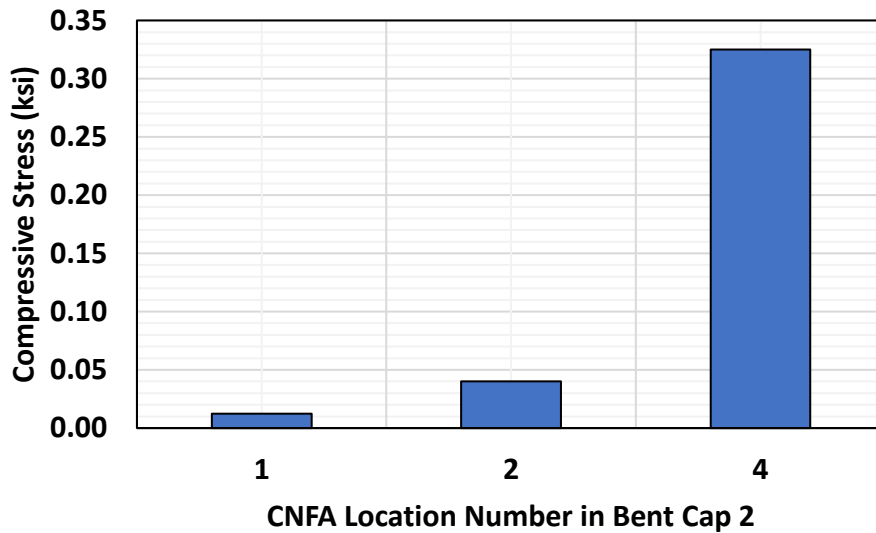


**Figure 4.21. Average Compressive Stresses on Concrete in Static Test-2, Case 9 at Position 4 on Bent Cap 2**

### 4.3.1.3 Dynamic Test-1

Case 9 and Case 14 were selected for Dynamic Test-1 (DT1) based on the layout of the trucks on the deck. Case 9 and Case 14 provide varieties in a load distribution on the deck along the forward and backward span of Bent Cap 2. Case 9 has a load distribution along one lane whereas Case 14 has a load distribution along two lanes. The layouts of the four trucks on the deck over Bent Cap 2 for Dynamic Test-1 (Case 9 and Case 14) are shown in Figures 4.22(a-b). The four trucks moved on the top of the deck over Bent Cap 2 at 5 mph.

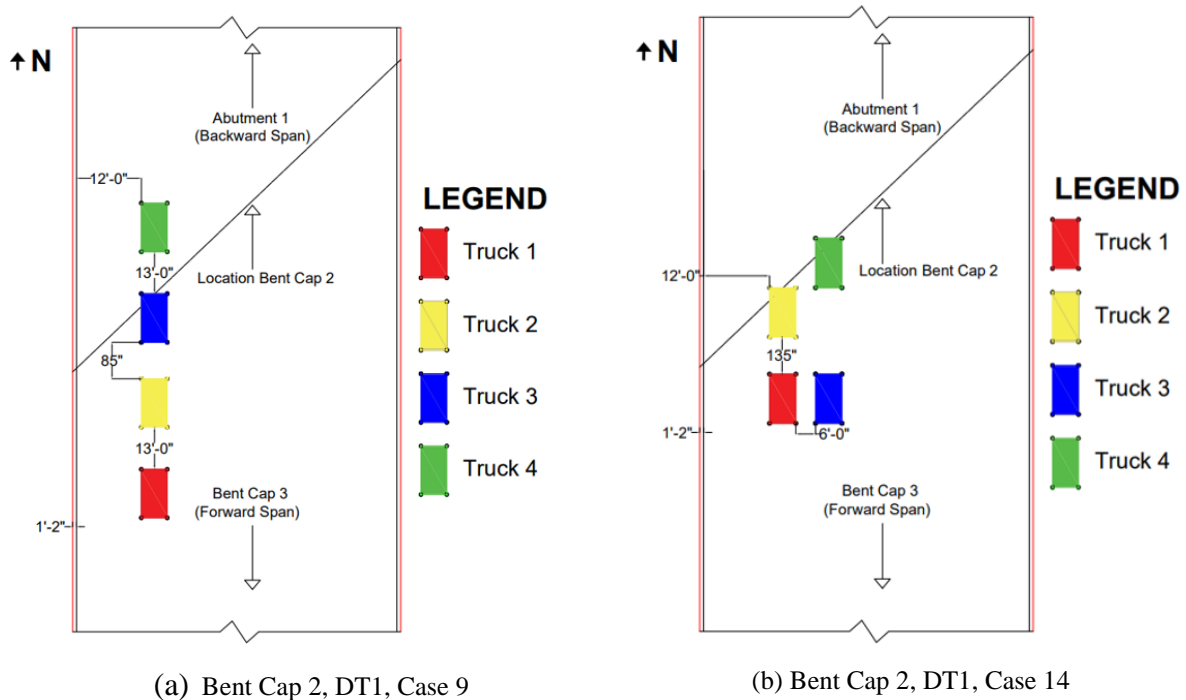


**Figure 4.22 Dynamic Test-1 on Bent Cap 2**

#### 4.3.1.3.1 Case 9

It is observed that the transverse rebars in the stem have higher strains on the south side than those on the north side in DT1, Case 9. The S bar near the west face on the south side reported the highest strain of  $3.42 \mu\epsilon$ . The 6<sup>th</sup> S bar has the highest strain of  $1.01 \mu\epsilon$ . Further, the 5<sup>th</sup> to 8<sup>th</sup> S bars on the north side at 35 inches (from the bottom of Bent Cap 2) reported compressive strain. The bottom of the 16<sup>th</sup> M bar (stirrup in the ledge) is subjected to compression ( $-1.78 \mu\epsilon$ ), whereas the top of the 5<sup>th</sup> to 8<sup>th</sup> M bars (stirrups in the ledge) are subjected to tension ( $2.96 \mu\epsilon$ ,  $1.91 \mu\epsilon$ ,  $1.41 \mu\epsilon$ , and  $2.54 \mu\epsilon$ , respectively). In addition, the A, U, and G bars are subjected to tension. The strain on the 4<sup>th</sup> and 5<sup>th</sup> G bars are  $3.00 \mu\epsilon$  and  $2.77 \mu\epsilon$ . The external girder near the west face of Bent Cap 2 rests on the ledge near the 4<sup>th</sup> and 5<sup>th</sup> G bars. This causes higher strains on these G

bars, comparable to S bars on the south side. The tip displacement of the extended region of Bent Cap 2 (south side) is -0.0051 inches. The strains and the displacements recorded during the Dynamic Test-1, Case 9 on Bent Cap 2 are presented in Figures 4.23 and 4.24.

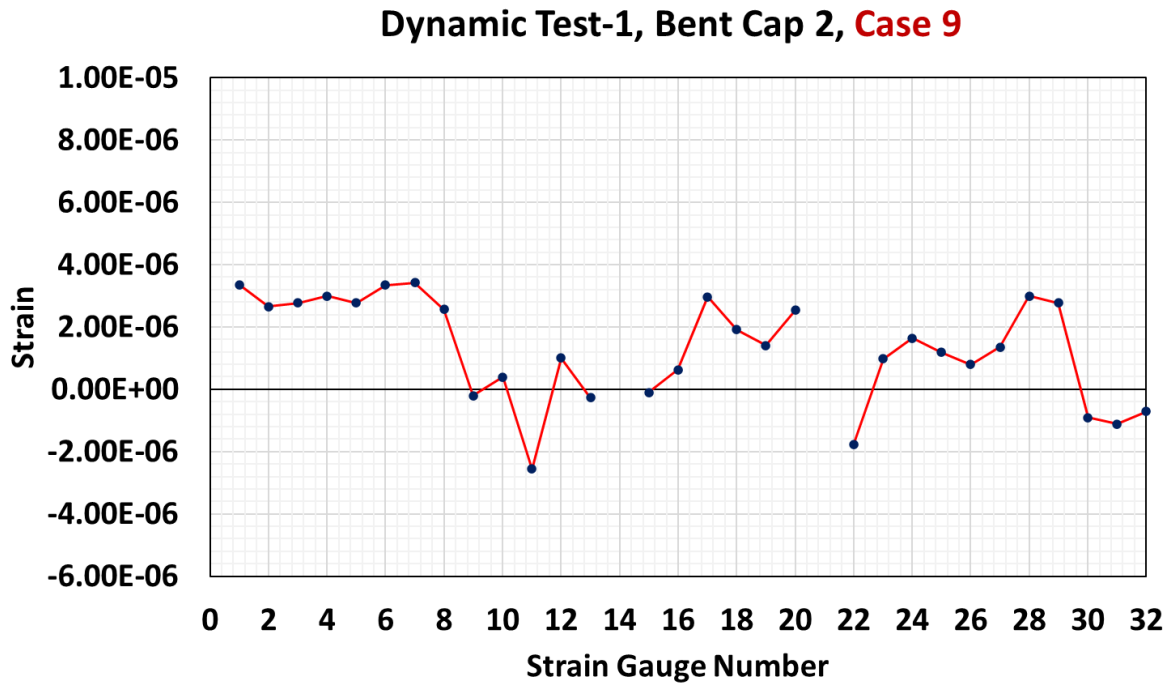


Figure 4.23. Rebar Strains in Dynamic Test-1, Case 9 on Bent Cap 2

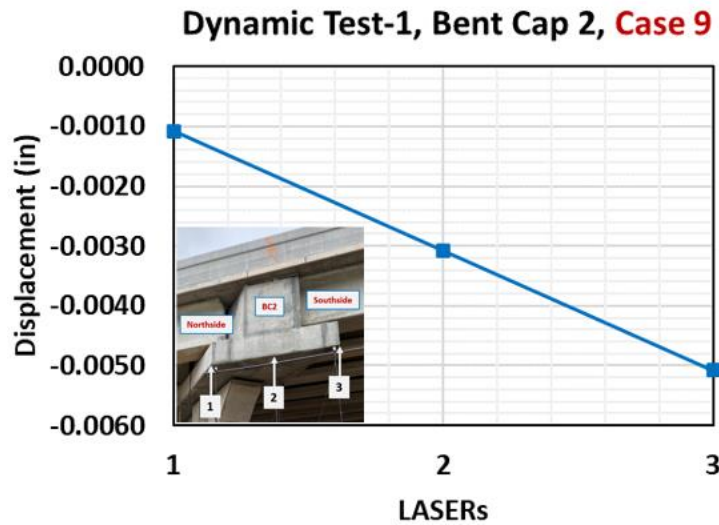


Figure 4.24. West Face Displacement of Bent Cap 2 in Dynamic Test-1, Case 9

### 4.3.1.3.2 Case 14

It is observed that the transverse rebars in the stem have higher strains on the south side than those on the north side in DT1, Case 14. The S bar near the west face on the south side reported the highest strain of  $8.06 \mu\epsilon$ . The highest strain on the north side S bar is  $-3.28 \mu\epsilon$  on the 8<sup>th</sup> S bar. The S bars (5<sup>th</sup> to 8<sup>th</sup>) on the north side reported compression. The bottom of the 16<sup>th</sup> M bar (stirrup in the ledge) is subjected to compression ( $-4.40 \mu\epsilon$ ), whereas the top of the 5<sup>th</sup> to 8<sup>th</sup> M bars (stirrups in the ledge) are subjected to tension ( $2.04 \mu\epsilon$ ,  $1.67 \mu\epsilon$ ,  $3.10 \mu\epsilon$ , and  $4.91 \mu\epsilon$ , respectively). In addition, the A, U, and G bars are subjected to tension. The strain on the 4<sup>th</sup> and 5<sup>th</sup> G bars are  $1.13 \mu\epsilon$  and  $2.93 \mu\epsilon$ . The external girder near the west face of Bent Cap 2 rests on the ledge near the 4<sup>th</sup> and 5<sup>th</sup> G bars. This causes higher strains on these G bars, comparable to S bars on the south side. The tip displacement of the extended region of Bent Cap 2 (south side) is  $-0.0036$  inches. The strains and the displacements recorded during the Dynamic Test-1, Case 14 on Bent Cap 2 are presented in Figures 4.25 and 4.26.

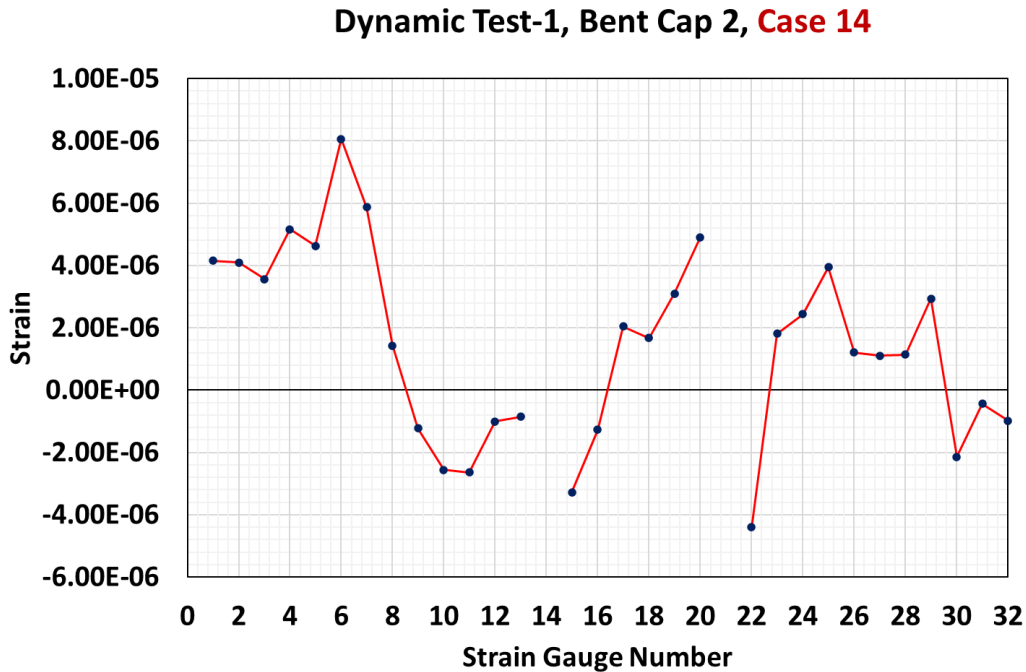
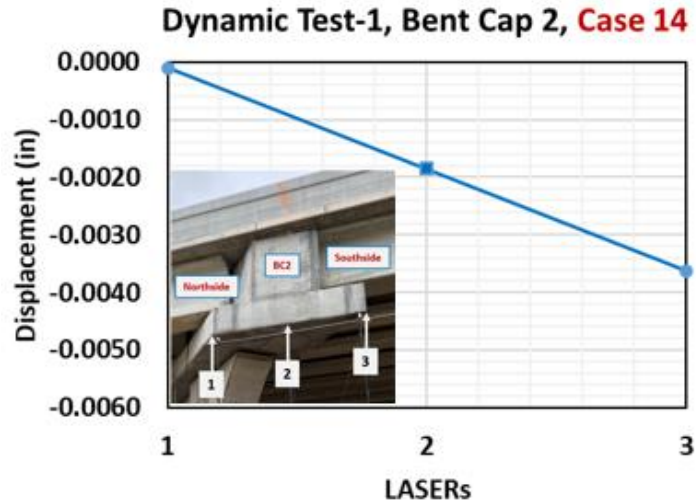


Figure 4.25. Rebar Strains in Dynamic Test-1, Case 14 on Bent Cap 2



**Figure 4.26. West Face Displacement of Bent Cap 2 in Dynamic Test-1, Case 14**

#### 4.3.1.4 Dynamic Test-2

Based on preliminary FE simulation, Case 9 is the most critical case for the load test on Bent Cap 2 as it results in higher stress/strain on the rebars and higher displacement of the west face of Bent Cap 2. Case 9 was selected for Dynamic Test-2 (DT2). The position of four trucks on the deck over Bent Cap 2 for Dynamic Test-2 (Case 9) is shown in Figure 4.27. The speed attained by the four trucks is 28 mph, 25 mph, 25 mph, and 25 mph. The four trucks were planned to move on the deck over Bent Cap 2 at a speed of 40 mph. However, the planned speed was not able to be reached due to the following reasons:

- a. Inadequate run-up length for trucks due to ongoing pavement construction outside the backward span, and
- b. Safety concerns.

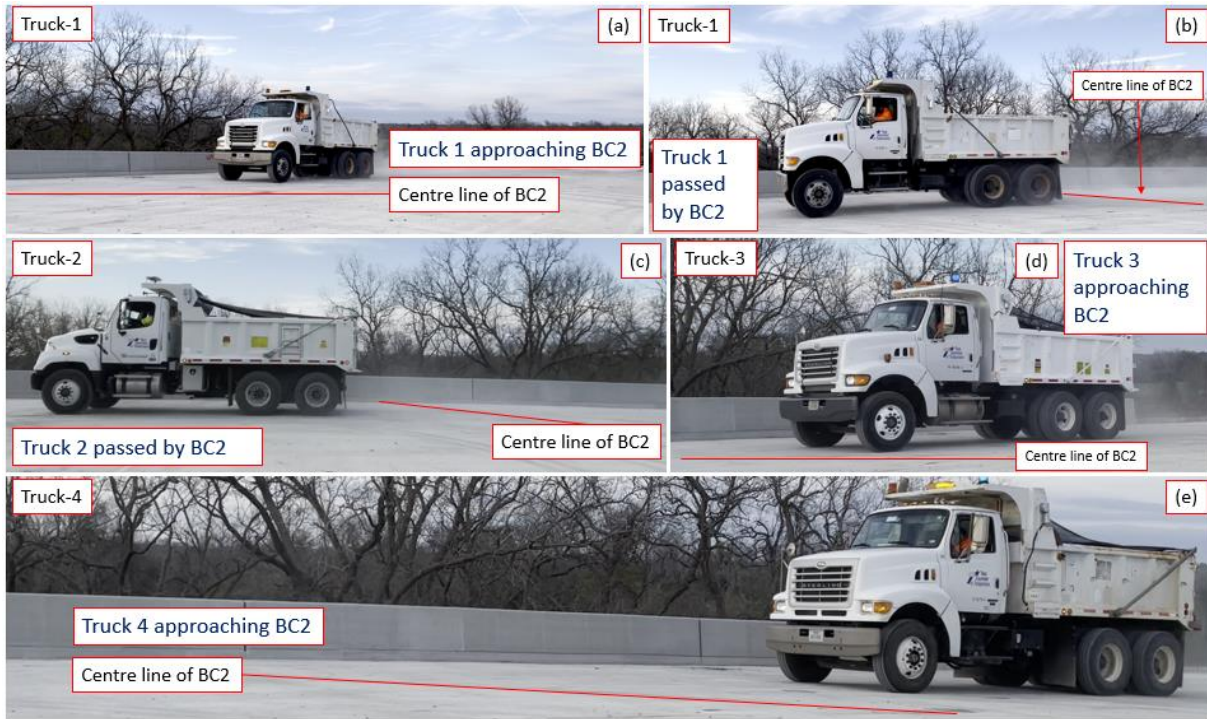


**Figure 4.27. Dynamic Test-2, Case 9 on Bent Cap 2**

Furthermore, due to safety concerns with high speed, the truck drivers could not maintain the planned distance between the trucks. Hence, the strain on the rebars and displacements of the west face of Bent Cap 2 are presented in this section when each truck reaches the center line of Bent Cap 2. The detail of the position of the trucks during the load test is described in Table 4.1.

**Table 4.1. Trucks Position in Dynamic Test-2 (Case 9) on Bent Cap 2**

Truck 'Ti' at CL of BC2	Position of Truck			
	T <sub>1</sub>	T <sub>2</sub>	T <sub>3</sub>	T <sub>4</sub>
T <sub>1</sub>	CL of BC2	CL of Abutment-1	Outside of backward span	Outside of backward span
T <sub>2</sub>	Exited BC3	CL of BC2	Entered backward span	Outside of backward span
T <sub>3</sub>	Exited BC3	Mid of forward span	CL of BC2	Entered backward span
T <sub>4</sub>	Exited BC3	Exited BC3	Mid of forward span	CL of BC2

\*Note: CL = Centerline; BC = Bent Cap

It is observed that the S bars on the south side were subjected to tensile strain throughout the movement of trucks over Bent Cap 2. The highest tensile strain on the south side S bar is 2.71  $\mu\epsilon$  on the 3<sup>rd</sup> S bar. However, S bars on the north side (5<sup>th</sup>, 6<sup>th</sup>, and 8<sup>th</sup>) reported compressive strain

throughout the movement of trucks over Bent Cap 2. The highest compressive strain on the north side S bar is  $3.64 \mu\epsilon$  on the 8<sup>th</sup> S bar. The bottom of the 16<sup>th</sup> M bar (stirrup in the ledge) is subjected to compression (highest of  $-1.64 \mu\epsilon$ ), whereas the top of the 5<sup>th</sup> to 8<sup>th</sup> M bars (stirrups in the ledge) are subjected to tension. Further, the A, U, and G bars are subjected to tension. This load test recorded the highest tensile strain on the 4<sup>th</sup> G bar, higher than the S bars. The 4<sup>th</sup> G bar recorded strains of  $6.14 \mu\epsilon$ ,  $8.04 \mu\epsilon$ ,  $7.56 \mu\epsilon$ , and  $7.99 \mu\epsilon$ , when four trucks consecutively passed through Bent Cap 2. The tip displacement of the extended region of Bent Cap 2 (South side) is  $-0.0006$  inches,  $-0.0019$  inches,  $-0.0033$  inches, and  $-0.0013$  inches, respectively, when four trucks consecutively passed through Bent Cap 2. The strains and the displacements recorded during the Dynamic Test-2, Case 9 on Bent Cap 2 are presented in Figures 4.28 and 4.29.

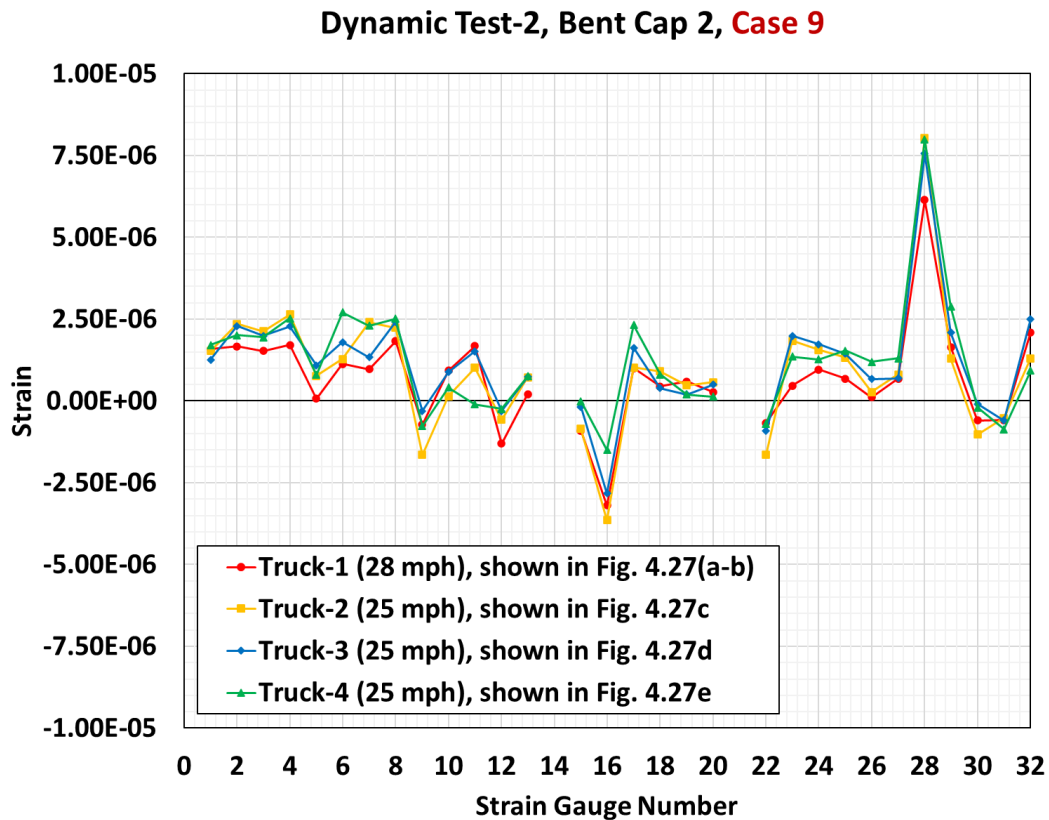


**Figure 4.28. Rebar Strains in Dynamic Test-2, Case 9 on Bent Cap 2**

### Dynamic Test-2, Bent Cap 2, Case 9

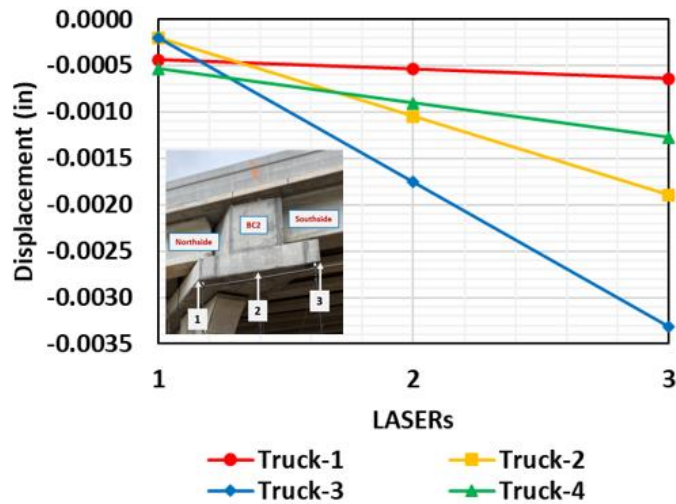
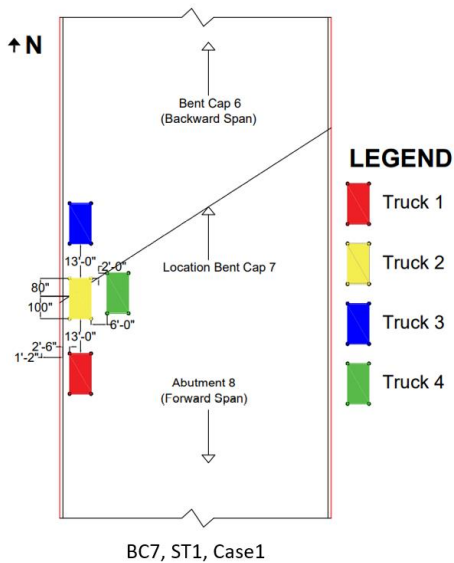


Figure 4.29. West Face Displacements of Bent Cap 2 in Dynamic Test-2, Case 9

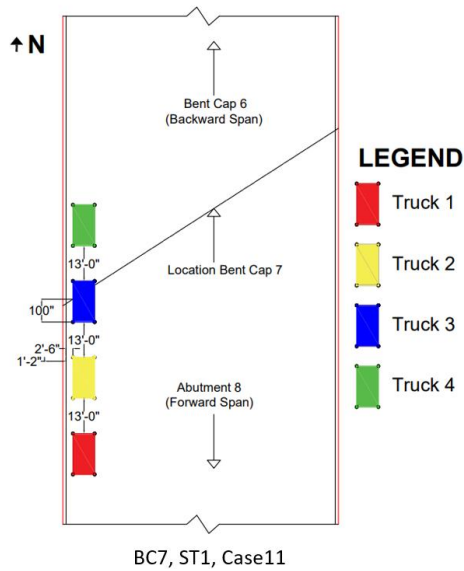
## 4.3.2 Bent Cap 7

### 4.3.2.1 Static Test-1

Based on the preliminary finite element analysis, Case 1 and Case 11 were selected for Static Test-1 (ST1). The layouts of four trucks on the deck over Bent Cap 7 for Static Test-1 (Case 1 and Case 11) are shown in Figures 4.30(a-b).



(a) Static Test-1 on Bent Cap 7 for Case 1



(b) Static Test-1 on Bent Cap 7 for Case 11

**Figure 4.30. Static Test-1 on Bent Cap 7**

#### 4.3.2.1.1 Case 1

It is observed that the transverse rebars in the stem have higher strains on the south side than those on the northside in Case 1. The 1<sup>st</sup> and 2<sup>nd</sup> S bars near the west face on the south side reported the highest strains of  $12.37 \mu\epsilon$  and  $13.74 \mu\epsilon$ , respectively. The highest strain on the north side S bar is  $10.16 \mu\epsilon$  in the 7<sup>th</sup> S bar. The bottom of the 15<sup>th</sup> M bar (stirrup in the ledge) is subjected to compression ( $-6.16 \mu\epsilon$ ), whereas the top of the 5<sup>th</sup>, 6<sup>th</sup>, and 8<sup>th</sup> M bars (stirrups in the ledge) is subjected to tension ( $3.11 \mu\epsilon$ ,  $2.96 \mu\epsilon$ , and  $6.46 \mu\epsilon$ , respectively). Further, the A, U, and G bars are subjected to tension. The strain in the 1<sup>st</sup> G bar reported is  $11.04 \mu\epsilon$ . The tensile strain on G bars is comparable to the S bars on the south side. The tip displacement of the outmost point of Bent Cap 7 (south side) is  $-0.0091$  inches. The strains and the displacements recorded during the Static Test-1 Case 1 on Bent Cap 7 are presented in Figure 4.31 and Figure 4.32.

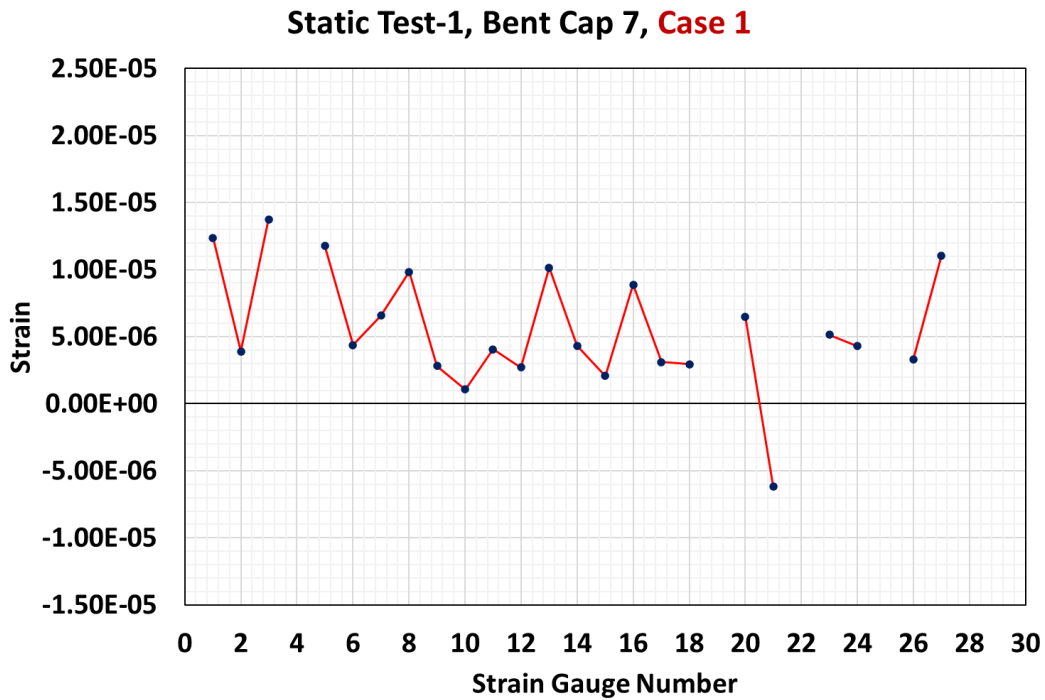


**Figure 4.31. Rebar Strains in Static Test-1, Case 1 on Bent Cap 7**

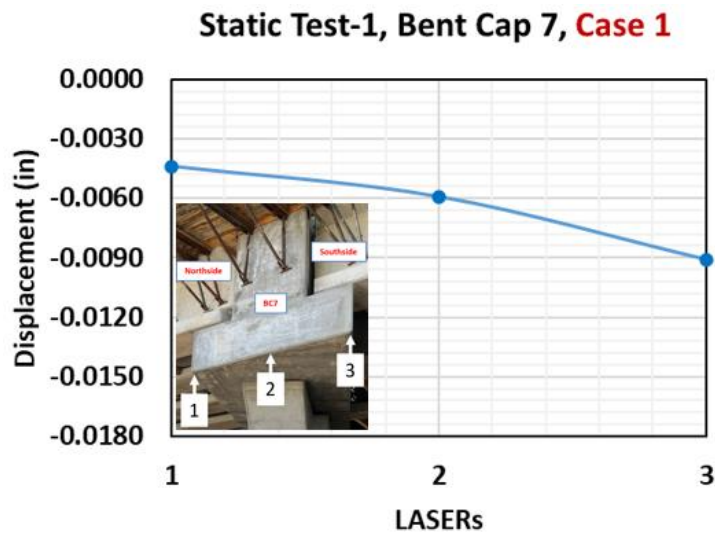


**Figure 4.32. West Face Displacement of Bent Cap 2 in Static Test-1, Case 7**

The average compressive stress on concrete at Location-1 (at Column-Bent Cap 7 interface) is 0.03 ksi, and at Location-2 (under the exterior bearing pad at the north side of Bent Cap 7), is 0.14 ksi. The average compressive stresses on concrete recorded by CNFA during the Static Test-1, Case 1 on Bent Cap 7 is presented in Figure 4.33. The average electrical impedance variation (EZV) reported by CNFAs at Location-3 (CNFAs anchored to S bars on the south side

near the west face of Bent Cap 7) is -1.43%. The negative EZV indicates tensile stress on the concrete adjacent to the S bars.

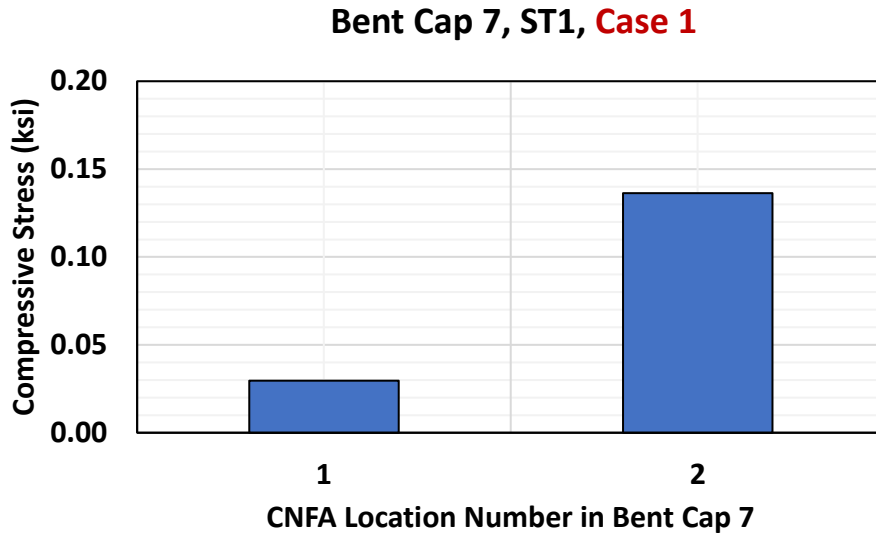


**Figure 4.33. Average Compressive Stresses on Concrete in Static Test-1, Case 1 on Bent Cap 7**

#### 4.3.2.1.2 Case 11

It is observed that the transverse rebars in the stem have higher strains on the south side than those on the northside in Case 11. The S bar near the west face on the southside reported the highest strain of  $16.74 \mu\epsilon$ . The strain on the 1<sup>st</sup>, 2<sup>nd</sup> and 3<sup>rd</sup> S bars on the south side are  $15.40 \mu\epsilon$ ,  $15.82 \mu\epsilon$ , and  $16.74 \mu\epsilon$ , respectively. The highest strain on the northside S bar is  $6.63 \mu\epsilon$  in the 7<sup>th</sup> S bar. The bottom of the 15<sup>th</sup> M bar is subjected to compression ( $-6.31 \mu\epsilon$ ), whereas the top of the 5<sup>th</sup>, 6<sup>th</sup> and 8<sup>th</sup> M bars are subjected to tension ( $10.36 \mu\epsilon$ ,  $8.49 \mu\epsilon$ , and  $8.97 \mu\epsilon$ , respectively). The strains observed in the M bars in Case 11 are higher than those in Case 1. It may have been attributed to the trucks being aligned in two lanes from the extended region of Bent Cap 7 in Case 1. Further, the A, U, and G bars are subjected to tension. The strain in the 1<sup>st</sup> G bar is  $12.46 \mu\epsilon$ . As seen in the previous ST1, Case 1, Bent Cap 7, the strains on the G bars are comparable to the S bars. The tip displacement of the outmost point of Bent Cap 7 (south side) is -0.0151 inches. The strains and the displacements recorded during the Static Test-1, Case 11 on Bent Cap 7 are presented in Figure 4.34 and Figure 4.35.

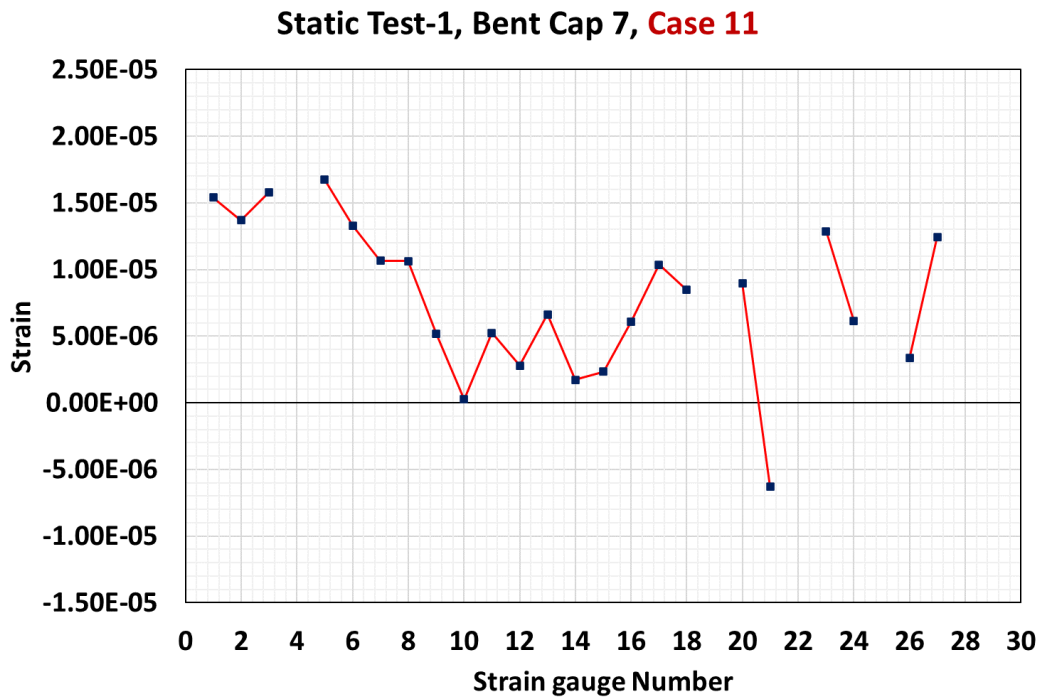


**Figure 4.34. Rebar Strain in Static Test-1, Case 11 on Bent Cap 7**

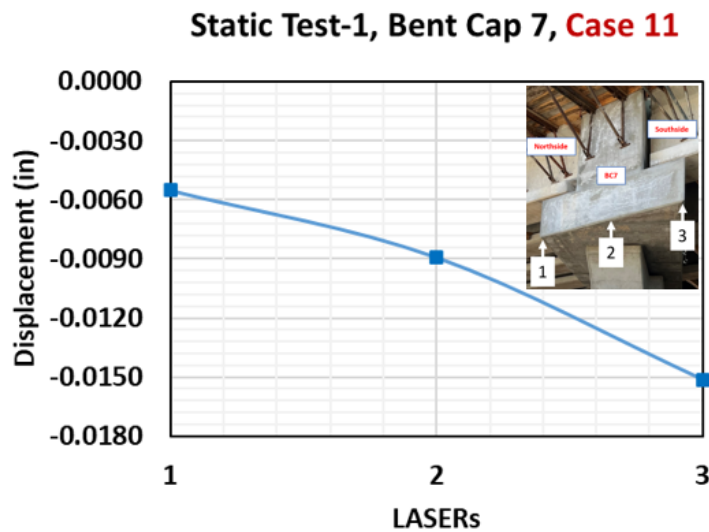


**Figure 4.35. West Face Displacement of Bent Cap 7 in Static Test-1, Case 11**

The average compressive stress on concrete at Location-1 (at Column-Bent Cap 7 interface) is 0.02 ksi, and at Location-2 (under the exterior bearing pad at the north side of Bent Cap 7), is 0.15 ksi. The average compressive stresses on concrete recorded by CNFA during the Static Test-1, Case 11 on Bent Cap 7 is presented in Figure 4.36. The average electrical impedance variation (EZV) reported by CNFAs at Location-3 (CNFAs anchored to S bars on the south side

near the west face of Bent Cap 7) is -1.21%. The negative EZV indicates tensile stress on the concrete adjacent to the S bars.

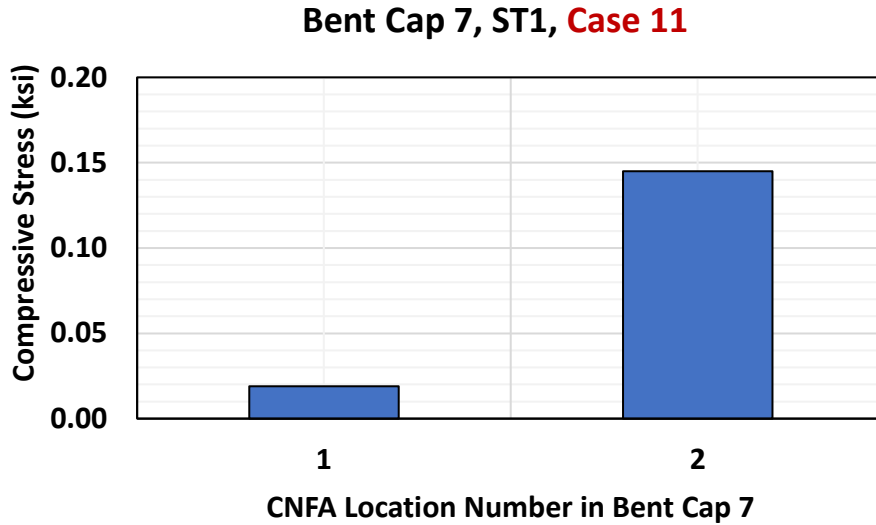
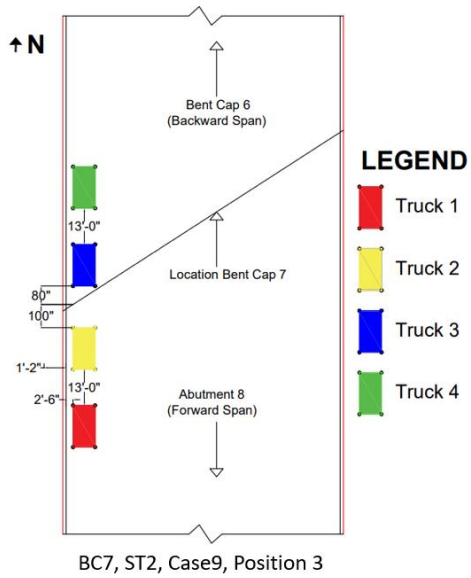


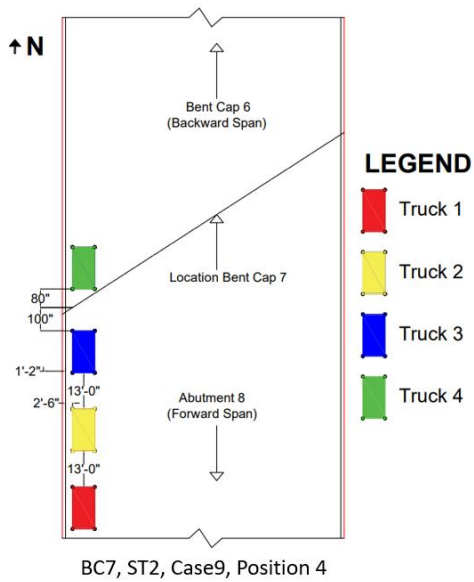
**Figure 4.36. Average Compressive Stresses on Concrete in Static Test-1, Case 11 on Bent Cap 7**

#### 4.3.2.2 Static Test-2

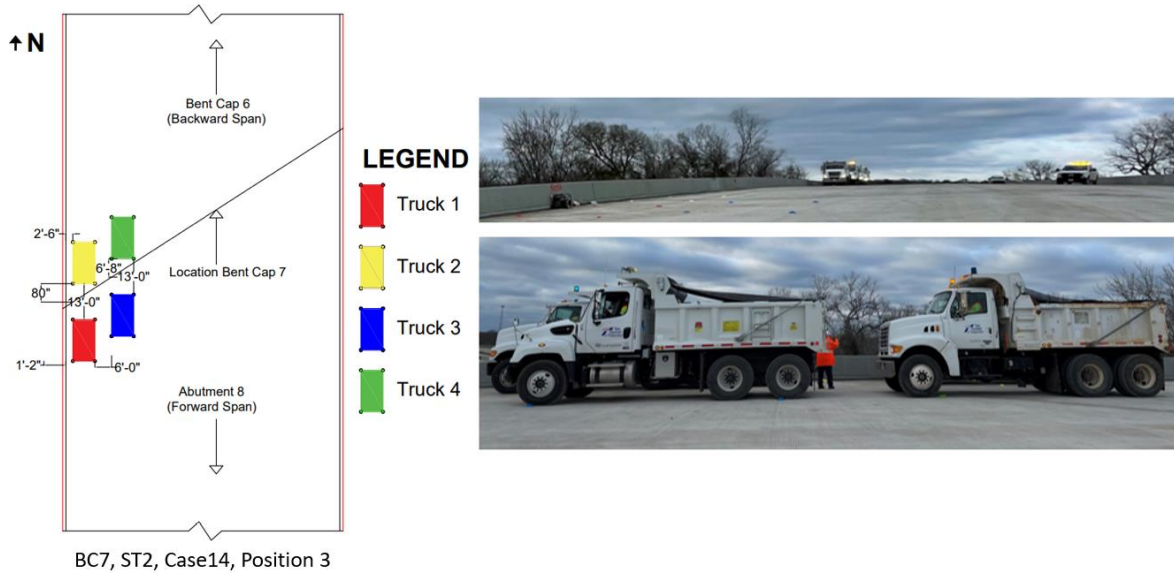
Based on the preliminary finite element analysis results, both Case 9 and Case 14 at Position 3 and Position 4 were selected for Static Test-2 (ST2). The layouts of the four trucks on the deck over Bent Cap 7 for Static Test-2 (Case 9 and Case 14) are shown in Figures 4.37(a-d).



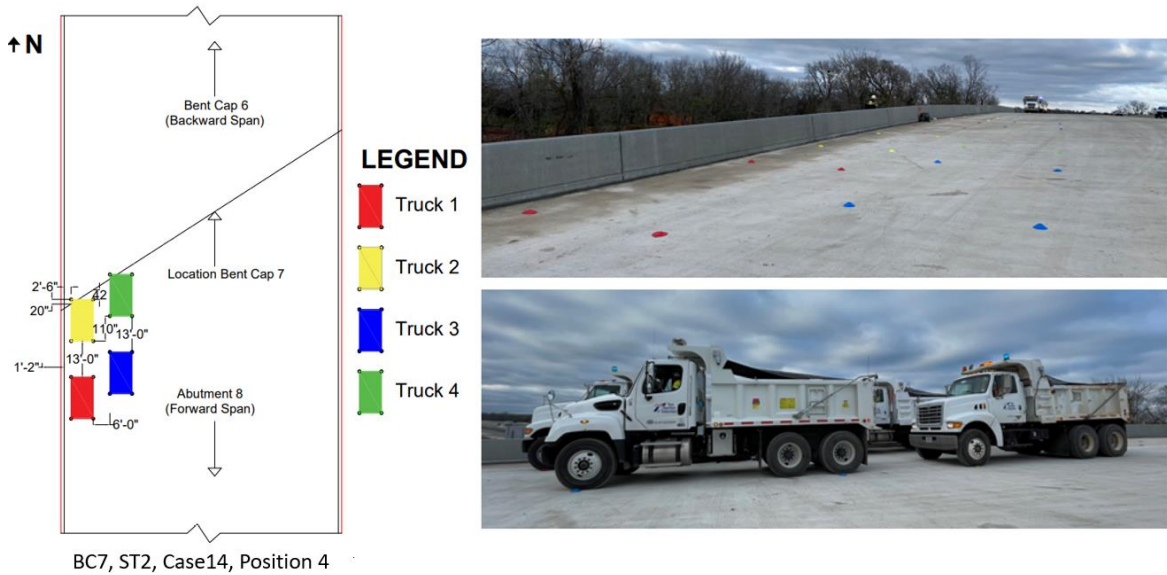
(a) Static Test-2 on Bent Cap 7 for Case 9 at Position 3



(b) Static Test-2 on Bent Cap 7 for Case 9 at Position 4



(c) Static Test-2 on Bent Cap 7 for Case 14 at Position 3



(d) Static Test-2 on Bent Cap 7 for Case 14 at Position 4

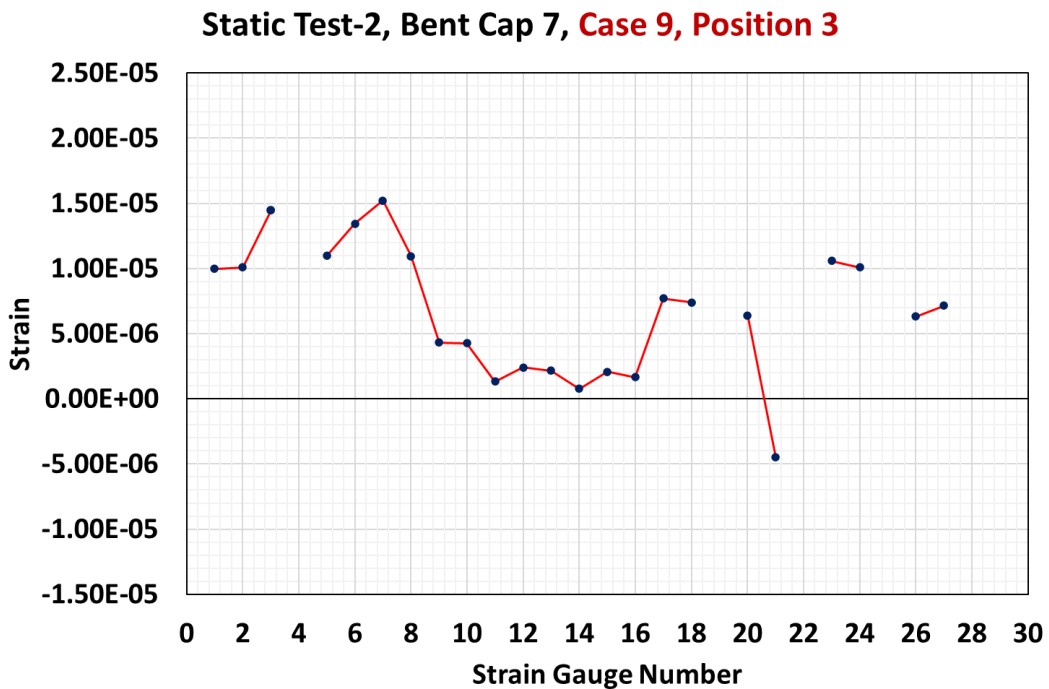
**Figure 4.37. Static Test-2 on Bent Cap 7**

#### 4.3.2.2.1 Case 9

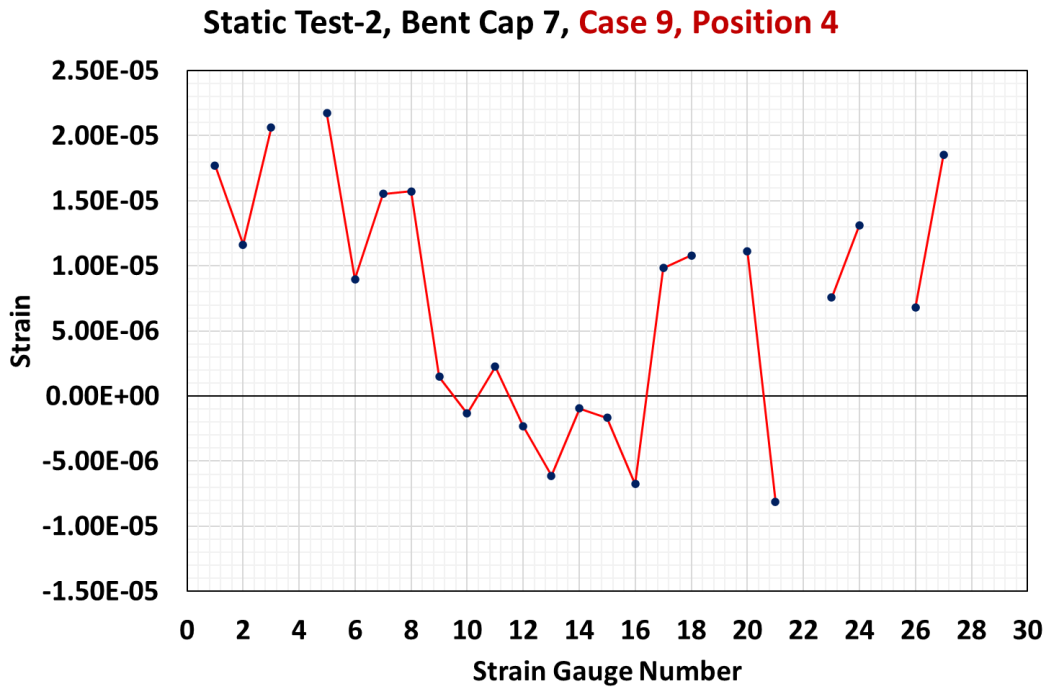
The Static Test-2 for Case 9 shows that the strains in S bars on the south side at Position 4 are higher than those at Position 3. The S bar near the west face on the south side at Position 3 reported the highest strain of  $15.20 \mu\epsilon$ , whereas the highest strain in the S bars at Position 4 was  $20.61 \mu\epsilon$ . The highest strain in the S bar on the north side at Position 3 is  $4.31 \mu\epsilon$ , whereas the

highest strain in the S bar on the north side at Position 4 is  $-6.77 \mu\epsilon$ . At Position 3, the bottom of the 15<sup>th</sup> M bar is subjected to compression ( $-4.50 \mu\epsilon$ ), whereas the top of the 5<sup>th</sup>, 6<sup>th</sup>, and 8<sup>th</sup> M bars are subjected to tension ( $7.69 \mu\epsilon$ ,  $7.39 \mu\epsilon$ , and  $6.40 \mu\epsilon$ , respectively). In addition, the A, U, and G bars are subjected to tension. The strain in the 1<sup>st</sup> G bar is  $7.15 \mu\epsilon$ .

At Position 4, the bottom of the 15<sup>th</sup> M bar is subjected to compression ( $-8.12 \mu\epsilon$ ), whereas the top of the 5<sup>th</sup>, 6<sup>th</sup>, and 8<sup>th</sup> M bars are subjected to tension ( $9.84 \mu\epsilon$ ,  $10.08 \mu\epsilon$ , and  $11.10 \mu\epsilon$ , respectively). Furthermore, the A, U, and G bars are subjected to tension. The strain in the 1<sup>st</sup> G bar is  $18.52 \mu\epsilon$ . The tip displacement of the extended region of Bent Cap 7 (south side) in Static Test-2, Case 9 at Position 3 and Position 4 are  $-0.0097$  inches and  $-0.0161$  inches, respectively. The strains and displacements recorded during the Static Test-2, Case 9 on Bent Cap 7 at Position 3 and Position 4 are presented in Figures 4.38(a-b) and Figure 4.39.



(a) Static Test-2 on Bent Cap 7 for Case 9 at Position 3



(b) Static Test-2 on Bent Cap 7 for Case 9 at Position 4

**Figure 4.38. Rebar Strains in Static Test-2, Case 9 on Bent Cap 7**

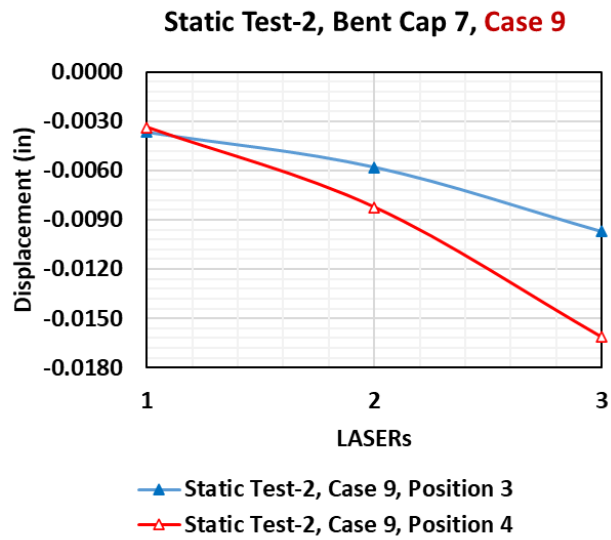


**Figure 4.49. West Face Displacements of Bent Cap 7 in Static Test-2, Case 9**

At Position 3, the average compressive stress on concrete at Location-1 (at Column-Bent Cap 7 interface) is 0.04 ksi, and at Location-2 (under the exterior bearing pad at the north side of Bent Cap 7) is 0.17 ksi. At Position 4, the average compressive stress on concrete at Location-1

(at Column-Bent Cap 7 interface) is 0.003 ksi, and at Location-2 (under the exterior bearing pad at the north side of Bent Cap 7) is 0.05 ksi. The average compressive stresses on concrete recorded by CNFA during Static Test-2, Case 9 at Position 3, and Position 4 on Bent Cap 7 are presented in Figures 4.50 and 4.51. The average electrical impedance variation (EZV) reported by CNFAs at Location-3 (CNFAs anchored to S bars on the south side near the west face of Bent Cap 7) in Static Test-2, Case 9 at Position 3 and Position 4 are -0.10% and -0.25%, respectively. The negative EZV indicates tensile stress on the concrete adjacent to the S bars.

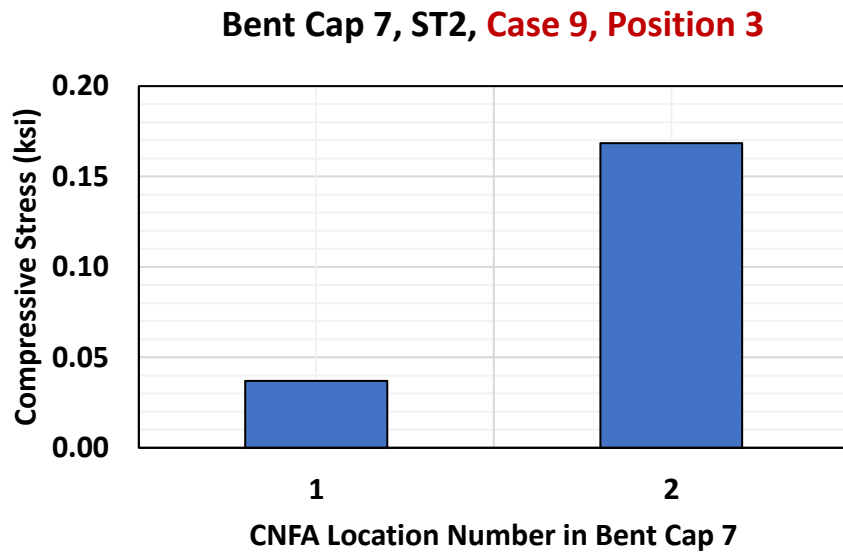


**Figure 4.50. Average Compressive Stresses on Concrete in Static Test-2, Case 9 at Position 3 on Bent Cap 7**

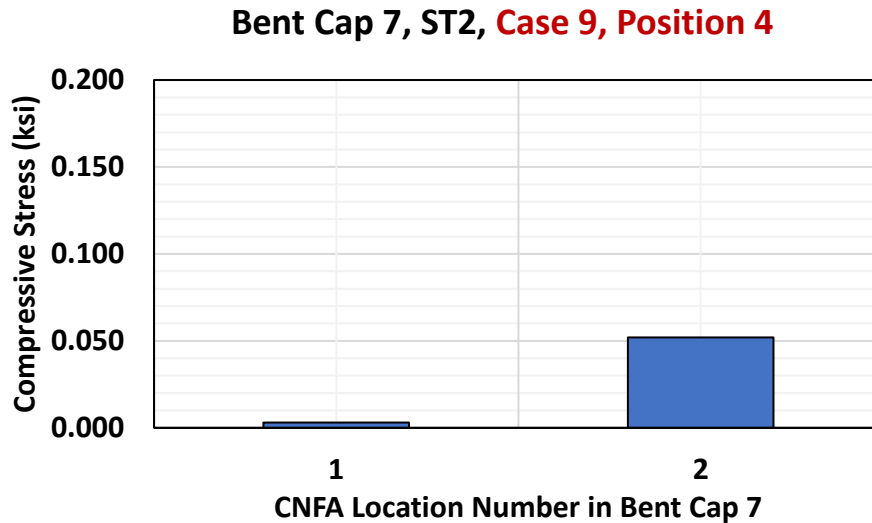


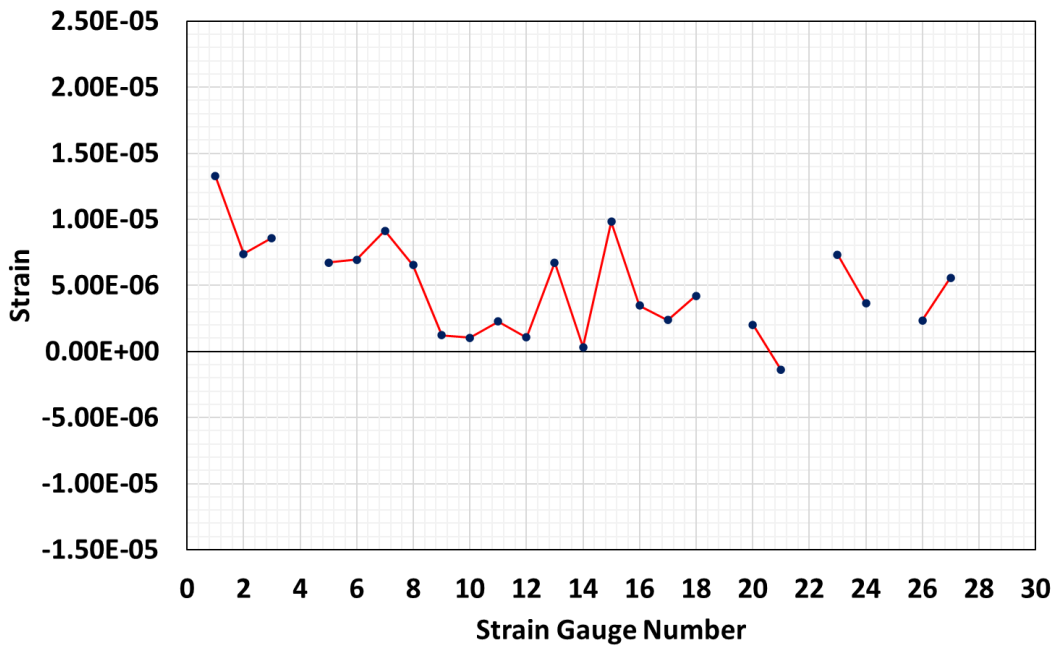
**Figure 4.51. Average Compressive Stresses on Concrete in Static Test-2, Case 9 at Position 4 on Bent Cap 7**

#### 4.3.2.2.2 Case 14

The Static Test-2, Case 14, shows that the strains in the S bars on the south side at Position 4 are higher than those at Position 3. The S bar near the west face on the south side at Position 3 reported the highest strain of  $13.25 \mu\epsilon$ , whereas the highest strain in the S bar at Position 4 was  $13.12 \mu\epsilon$ . The highest strain in the S bar on the north side at Position 3 is  $9.81 \mu\epsilon$ , whereas the highest strain in the S bar on the north side at Position 4 is  $-6.11 \mu\epsilon$ . At Position 3, the bottom of the 15<sup>th</sup> M bar is subjected to compression ( $-1.40 \mu\epsilon$ ), whereas the top of the 5<sup>th</sup>, 6<sup>th</sup>, and 8<sup>th</sup> M bars are subjected to tension ( $2.39 \mu\epsilon$ ,  $4.20 \mu\epsilon$ , and  $2.01 \mu\epsilon$ , respectively). Further, the A, U, and G bars are subjected to tension. The strain in the 1<sup>st</sup> G bar is  $5.58 \mu\epsilon$ .

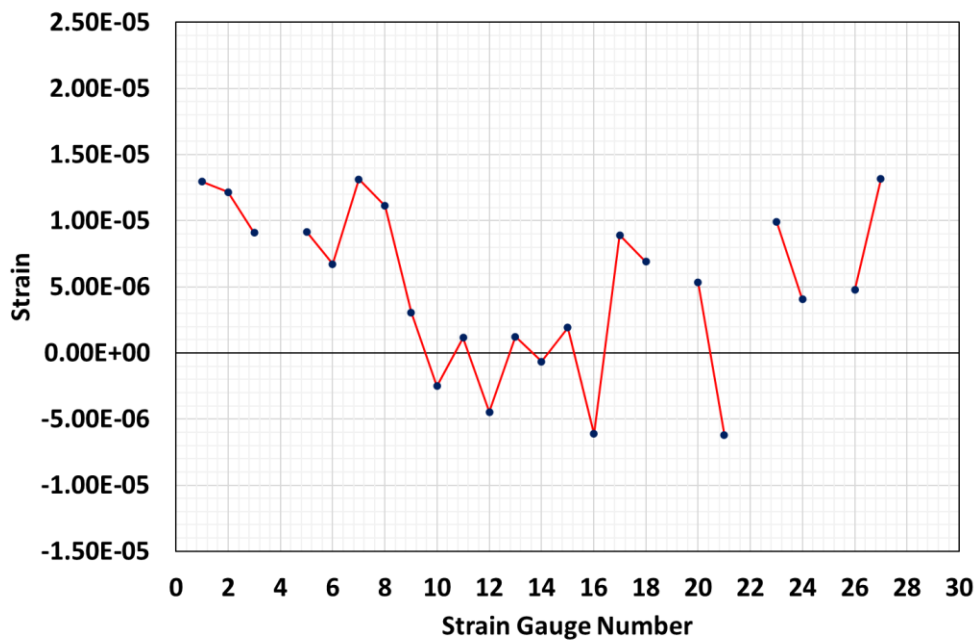
At Position 4, the bottom of the 15<sup>th</sup> M bar is subjected to compression ( $-6.20 \mu\epsilon$ ), whereas the top of the 5<sup>th</sup>, 6<sup>th</sup>, and 8<sup>th</sup> M bars are subjected to tension ( $8.89 \mu\epsilon$ ,  $6.91 \mu\epsilon$ , and  $5.32 \mu\epsilon$ , respectively). Furthermore, the A, U, and G bars are subjected to tension. The strain in the 1<sup>st</sup> G bar is  $13.14 \mu\epsilon$ . The tip displacement of the extended region of Bent Cap 7 (south side) in Static Test-2, Case 14 at Position 3 and Position 4 are  $-0.0094$  inches and  $-0.0133$  inches, respectively. The strains and displacements recorded during the Static Test-2, Case 14 on Bent Cap 7 at Position 3 and Position 4 are presented in Figures 4.52(a-b) and Figure 4.53.

**Static Test-2, Bent Cap 7, Case 14, Position 3**



(a) Static Test-2 on Bent Cap 7 for Case 14 at Position 3

**Static Test-2, Bent Cap 7, Case 14, Position 4**



(b) Static Test-2 on Bent Cap 7 for Case 14 at Position 4

**Figure 4.52. Rebar Strains in Static Test-2, Case 14 on Bent Cap 7**

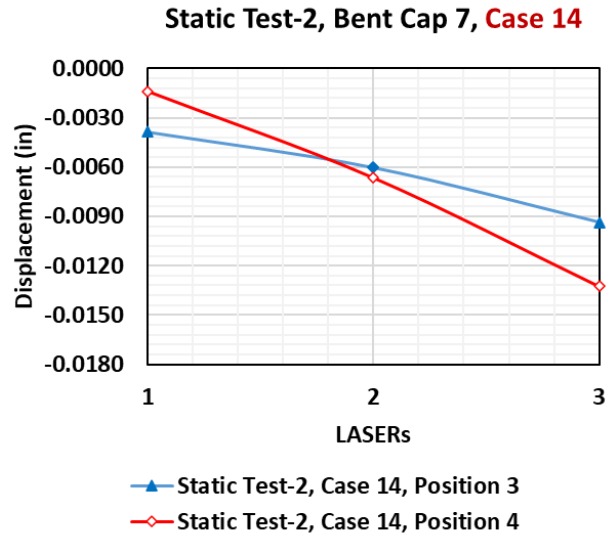


**Figure 4.53. West Face Displacements of Bent Cap 7 in Static Test-2, Case 14**

At Position 3, the average compressive stress on concrete at Location-1 (at Column-Bent Cap 7 interface) is 0.03 ksi, and at Location-2 (under the exterior bearing pad at the north side of Bent Cap 7) is 0.13 ksi. At Position 4, the average compressive stress on concrete at Location-1 (at Column-Bent Cap 7 interface) is 0.02 ksi, and at Location-2 (under the exterior bearing pad at the north side of Bent Cap 7) is 0.05 ksi. The average compressive stresses on concrete recorded by CNFA during the Static Test-2, Case 14 at Position 3, and Position 4 on Bent Cap 7 are presented in Figures 4.54 and 4.55. The average electrical impedance variation (EZV) reported by CNFAs at Location-3 (CNFAs anchored to S bars on the south side near the west face of Bent Cap 7) in Static Test-2, Case 14 at Position 3 and Position 4 are -0.17% and -0.44%, respectively. The negative EZV indicates tensile stress on the concrete adjacent to the S bars.

**Bent Cap 7, ST2, Case 14, Position 3**

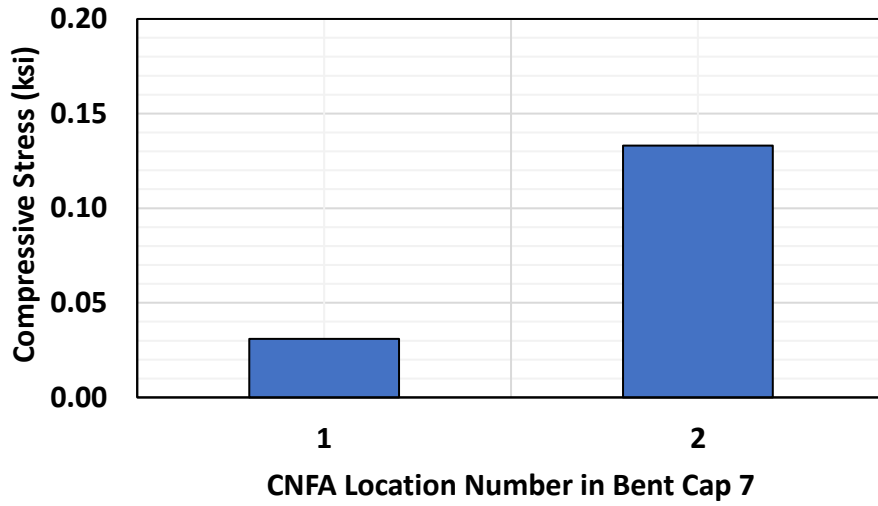


**Figure 4.54. Average Compressive Stresses on Concrete in Static Test-2, Case 14 at Position 3 on Bent Cap 7**

**Bent Cap 7, ST2, Case 14, Position 4**

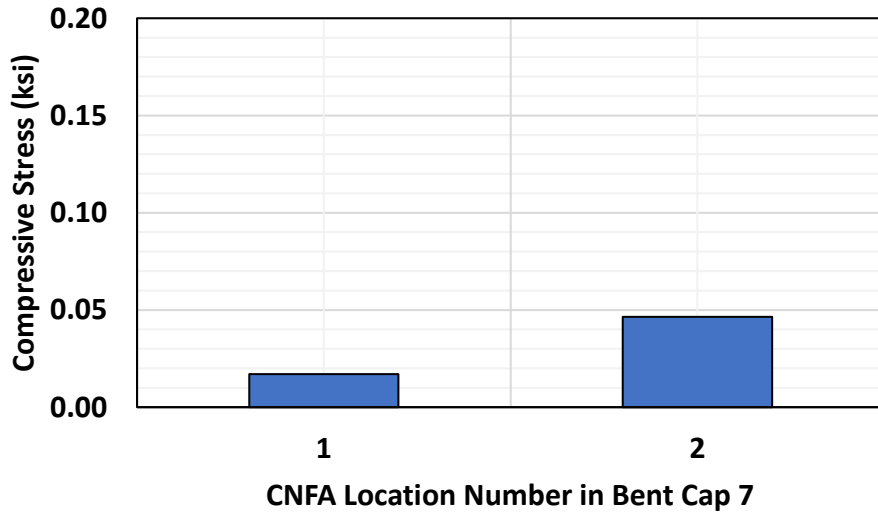


**Figure 4.55. Average Compressive Stresses on Concrete in Static Test-2, Case 14 at Position 4 on Bent Cap 7**

### 4.3.2.3 Dynamic Test-1

Case 9 and Case 14 were selected for Dynamic Test-1 (DT1) based on the layout of the trucks on the deck. Case 9 and Case 14 provide varieties in the load distribution on the deck along the forward and backward span of Bent Cap 7. Case 9 has a load distribution along one lane, whereas Case 14 has a load distribution along two lanes. The layouts of the four trucks on the deck over Bent Cap 7 for Dynamic Test-1 (Case 9 and Case 14) are shown in Figures 4.56(a-b). The four trucks moved on the top of the deck over Bent Cap 7 at 5 mph.

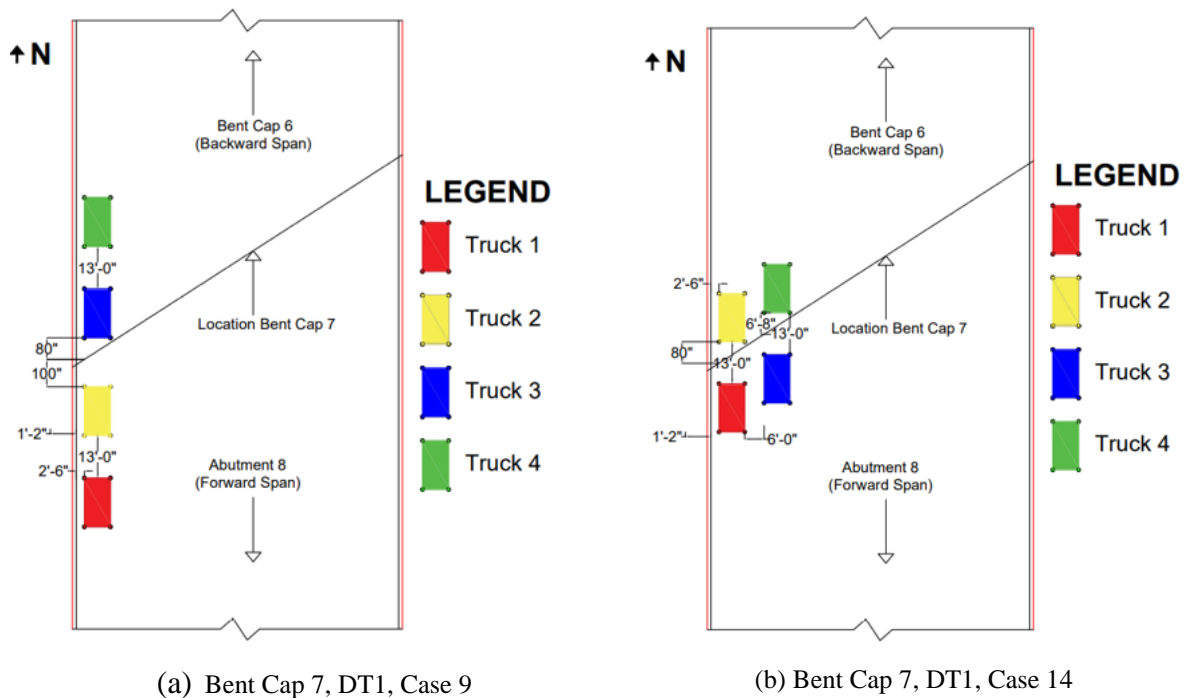


Figure 4.56. Dynamic Test-1 on Bent Cap 7

#### 4.3.2.3.1 Case 9

It is observed that the transverse rebars in the stem have higher strains on the south side than those on the north side in DT1, Case 9. The S bar near the west face on the south side reported the highest strain of  $11.04 \mu\epsilon$ . The highest strain on the north side S bar is  $2.08 \mu\epsilon$  on the 5<sup>th</sup> S bar. The bottom of the 15<sup>th</sup> M bar (stirrup in the ledge) is subjected to compression ( $-1.60 \mu\epsilon$ ), whereas the top of the 5<sup>th</sup>, 6<sup>th</sup> and 8<sup>th</sup> M bars (stirrups in the ledge) are subjected to tension ( $1.33 \mu\epsilon$ ,  $2.66 \mu\epsilon$ , and  $5.21 \mu\epsilon$ , respectively). Further, the A, U, and G bars are subjected to tension. The strain on the 1<sup>st</sup> G bar is  $6.11 \mu\epsilon$ . The external girder near the west face of Bent Cap 7 is rested on the ledge near the G bars. This causes higher strains on the G bars, comparable to strains on the S bars on the south side. The tip displacement of the extended region of Bent Cap 7 (south side) is  $-0.0092$

inches. The strains and the displacements recorded during the Dynamic Test-1, Case 9 on Bent Cap 7 are presented in Figures 4.57 and 4.58.

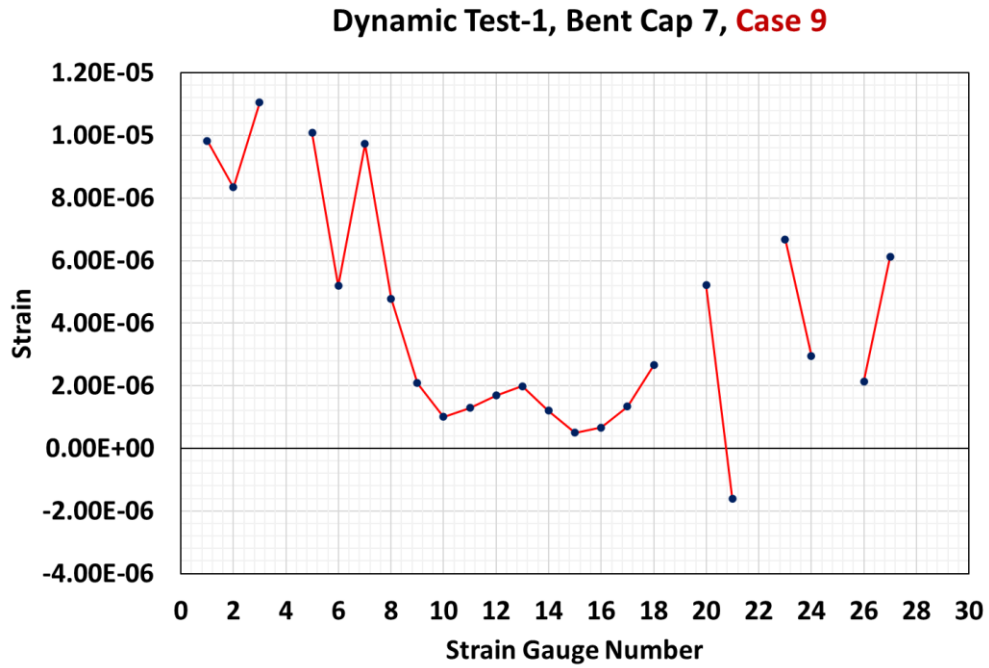


Figure 4.57. Rebar Strains in Dynamic Test-1, Case 9 on Bent Cap 7

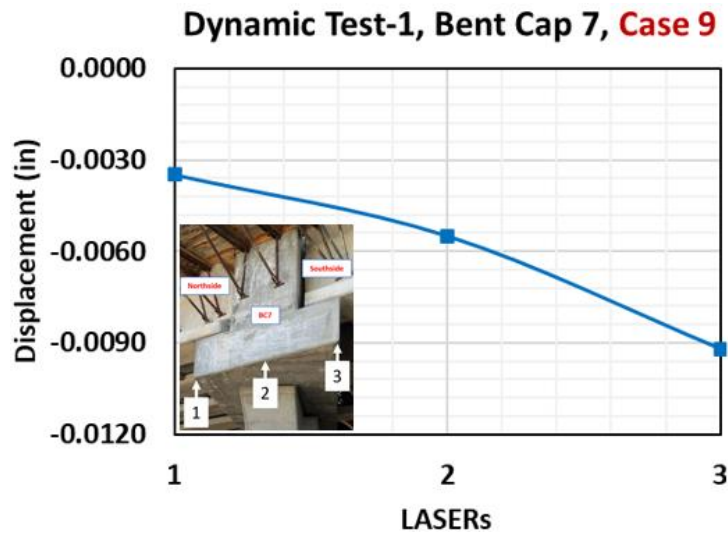
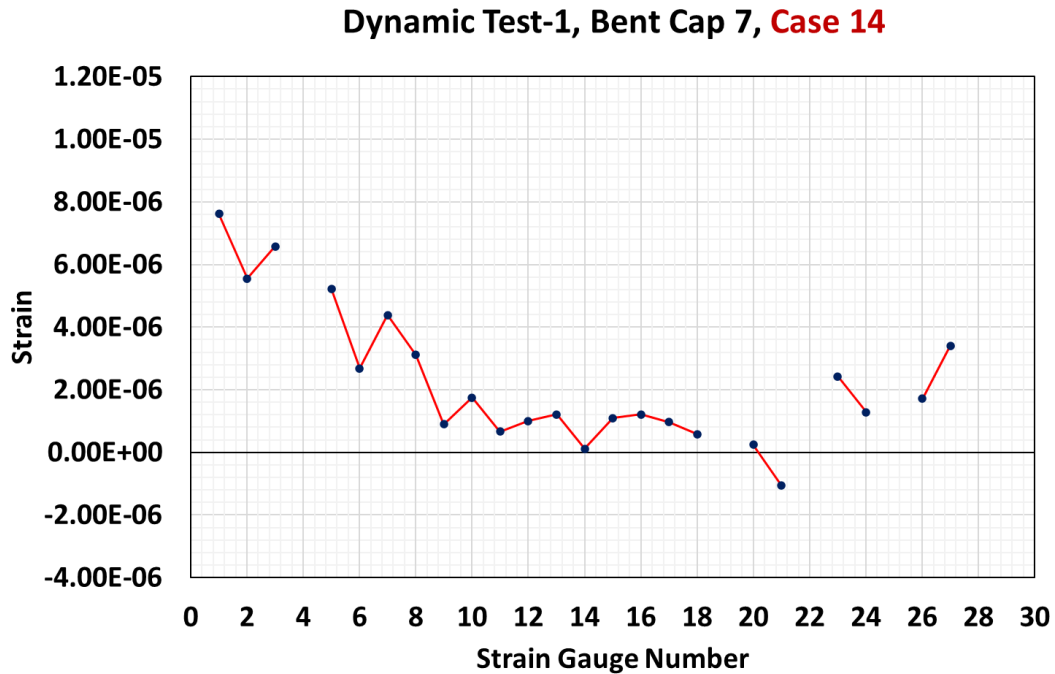


Figure 4.58. West Face Displacement of Bent Cap 7 in Dynamic Test-1, Case 9

#### 4.3.2.3.2 Case 14

It is observed that the transverse rebars in the stem have higher strains on the south side than those on the north side in DT1, Case 14. The S bar near the west face on the south side

reported the highest strain of  $7.62 \mu\epsilon$ . The highest strain on the north side S bar is  $1.74 \mu\epsilon$  on the 5<sup>th</sup> S bar. The bottom of the 15<sup>th</sup> M bar (stirrup in the ledge) is subjected to compression ( $-1.06 \mu\epsilon$ ), whereas the top of the 5<sup>th</sup>, 6<sup>th</sup>, and 8<sup>th</sup> M bars (stirrups in the ledge) are subjected to tension ( $0.97 \mu\epsilon$ ,  $0.58 \mu\epsilon$ , and  $0.25 \mu\epsilon$ , respectively). Further, the A, U, and G bars are subjected to tension. The strain on the 1<sup>st</sup> G bar is  $3.40 \mu\epsilon$ . The external girder near the west face of Bent Cap is rested on the ledge near G bars. This causes higher strains on the G bars, comparable to strains on the S bars on the south side. The tip displacement of the extended region of Bent Cap 7 (south side) is  $-0.0105$  inches. The strains and the displacements recorded during the Dynamic Test-1, Case 14 on Bent Cap 7 are presented in Figures 4.59 and 4.60.



**Figure 4.59. Rebar Strains in Dynamic Test-1, Case 14 on Bent Cap 7**

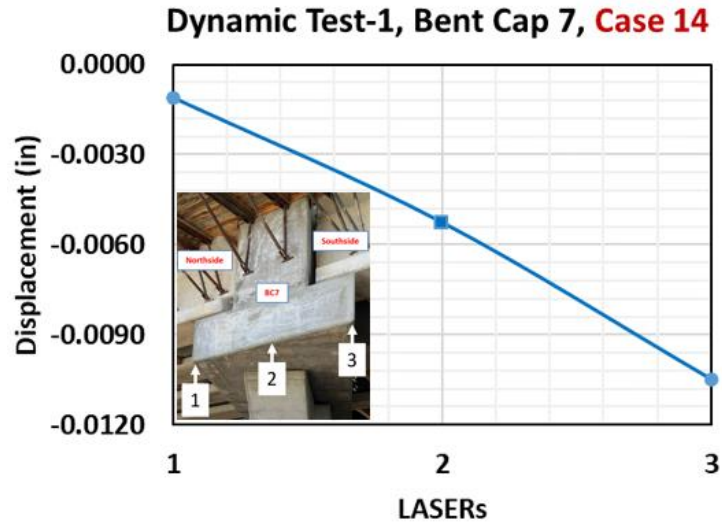


**Figure 4.60. West Face Displacement of Bent Cap 7 in Dynamic Test-1, Case 14**

#### 4.3.2.4 Dynamic Test-2

Based on preliminary FE simulation, Case 9 is the most critical case for load test on Bent Cap 7 as it results in higher stress/strain on the rebars and higher displacement of the west face of Bent Cap 7. Case 9 was selected for Dynamic Test-2 (DT2). The position of four trucks on the deck over Bent Cap 2 for Dynamic Test-2 (Case 9) is shown in Figure 4.61. The four trucks were planned to move on the deck over Bent Cap 7 at a speed of 40 mph. The speed attained by the four trucks is 35 mph, 35 mph, 37 mph, and 36 mph.





**Figure 4.61. Dynamic Test-2, Case 9 on Bent Cap 7**

Furthermore, due to safety concerns with high speed, the truck drivers could not maintain the planned distance between the trucks. Hence, the strain on the rebars and displacements of the west face of Bent Cap 7 are presented in this section when each truck reaches the center line of Bent Cap 7. The details of the position of the truck during the load test are described in Table 4.2.

**Table 4.2. Trucks Position in Dynamic Test-2 (Case 9) on Bent Cap 7**

Truck 'T <sub>i</sub> ' at CL of BC7	Position of Truck			
	T <sub>1</sub>	T <sub>2</sub>	T <sub>3</sub>	T <sub>4</sub>
T <sub>1</sub>	CL of BC7	CL of BC6	Outside of the backward span	Outside of the backward span
T <sub>2</sub>	Exited Abutment-8	CL of BC7	Mid of the backward span	Outside of backward span
T <sub>3</sub>	Exited Abutment-8	Mid of the forward span	CL of BC7	Entered the backward span
T <sub>4</sub>	Exited Abutment-8	Exited Abutment-8	Exited Abutment-8	CL of BC7

\*Note: CL = Centerline; BC = Bent Cap

It is observed that the S bars on the south side were subjected to tensile strain throughout the movement of trucks over Bent Cap 7. The highest tensile strain on the south side S bar is  $6.02 \mu\epsilon$  on the 1<sup>st</sup> S bar. However, S bars on the north side (5<sup>th</sup> to 8<sup>th</sup>) reported compressive strain throughout the movement of trucks over Bent Cap 7. The highest compressive strain on the north side S bar is  $2.58 \mu\epsilon$  on the 6<sup>th</sup> S bar. The bottom of the 15<sup>th</sup> M bar (stirrup in the ledge) is subjected to compression (highest of  $-2.61 \mu\epsilon$ ), whereas the top of the 5<sup>th</sup> to 8<sup>th</sup> M bars (stirrups in the ledge) are subjected to tension when Trucks T<sub>2</sub>, T<sub>3</sub>, and T<sub>4</sub> passed by Bent Cap 7. However, the top of the 5<sup>th</sup> to 8<sup>th</sup> M bars (stirrups in the ledge) were subjected to compression when Truck T<sub>1</sub> passed through Bent Cap 7. Further, the A, U, and G bars are subjected to tension when Trucks T<sub>2</sub>, T<sub>3</sub>, and T<sub>4</sub> pass by Bent Cap 7. However, the A and U bars were subjected to tension when Truck T<sub>1</sub> passed through Bent Cap 7. The 1<sup>st</sup> G bar recorded strains of  $0.82 \mu\epsilon$ ,  $3.99 \mu\epsilon$ ,  $4.55 \mu\epsilon$ , and  $4.18 \mu\epsilon$ , when four trucks consecutively passed by Bent Cap 2. The middle displacements of Bent Cap 2 were -0.0067 inches, -0.0117 inches, -0.0073 inches, and -0.0049 inches, respectively, when four trucks consecutively passed through Bent Cap 7. During this load test, the laser on the south and north sides had technical issues, which could have been due to the windy condition at the test site. The strains and displacements recorded during the Dynamic Test-2, Case 9 on Bent Cap 2 are presented in Figure 4.62 and Table 4.3.

### Dynamic Test-2, Bent Cap 7, Case 9

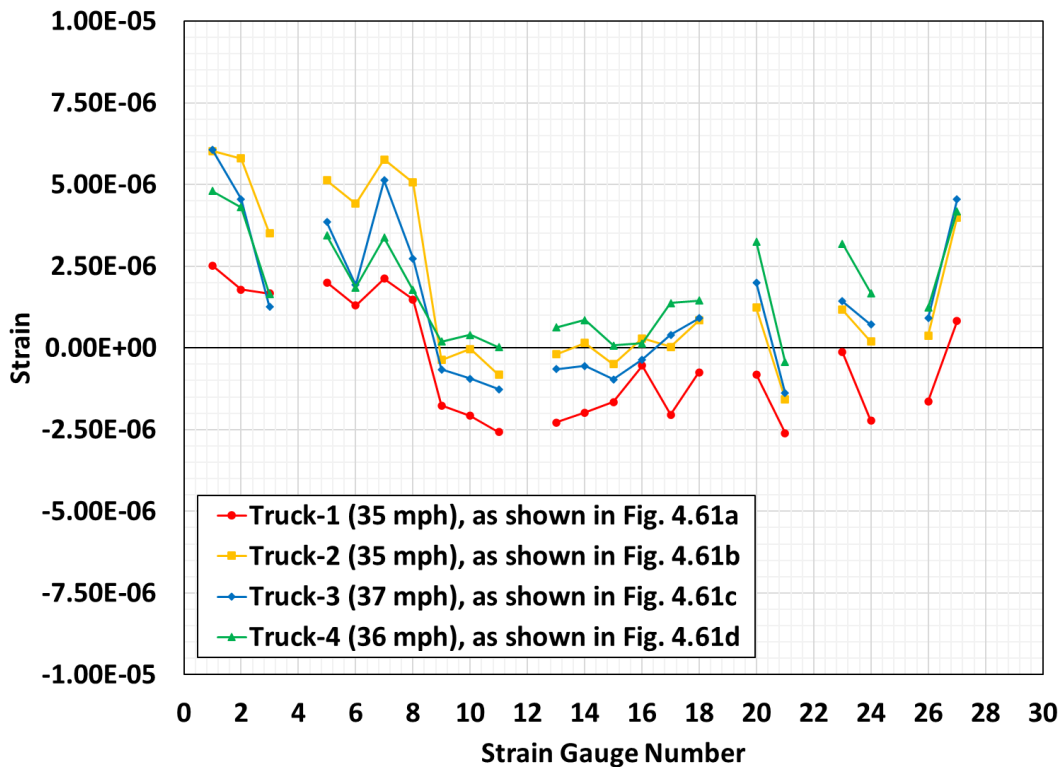


Figure 4.62. Rebar Strains in Dynamic Test-2, Case 9 on Bent Cap 7

Table 4.3. West Face Displacement of Bent Cap 7 for Case 9 from Dynamic Test-2

LASER	Truck-1	Truck-2	Truck-3	Truck-4
Middle (in.)	-0.0067	-0.0117	-0.0073	-0.0049

#### 4.4 DISCUSSION OF TEST RESULTS

TxDOT Project 0-6905 investigated three critical parameters in the experimental program for inverted-T bent caps (ITBC) (Sapath et al., 2019). Those three critical parameters are (a) skew angle, (b) detailing of transverse reinforcement, and (c) amount of transverse reinforcement. It was observed that the influence of shear and torsion is highly dominant with the higher skew angles. Further, Technical Report 0-6905-R1 (TxDOT Project 0-6905) elaborated that the interface between the ledge and stem of the ITBC is highly concentrated with tensile stress/strain on both concrete and transverse rebars (Wang et al., 2020). Moreover, the preliminary finite element simulations of ITBC-2 and ITBC-7 exhibit higher stress/strain concentration on the interface of the ledge and stem, with a higher displacement of the west face of bent caps. TxDOT Project 0-

6905-01 primarily focuses on the performance of the transverse rebars and the influence of the skew angle (Wang et al., 2020).

This section discusses the load test analysis of Bent Cap 2 and Bent Cap 7. Based on the data analysis of the load test, stress/strain concentration on transverse rebars, displacement of the west face of bent caps (overhanging cantilever part), the influence of the skew angle, stress under exterior bearing pads, critical load cases for both bent caps and the performance in the static and dynamic test are discussed.

#### **4.4.1 Performance of Transverse Rebars**

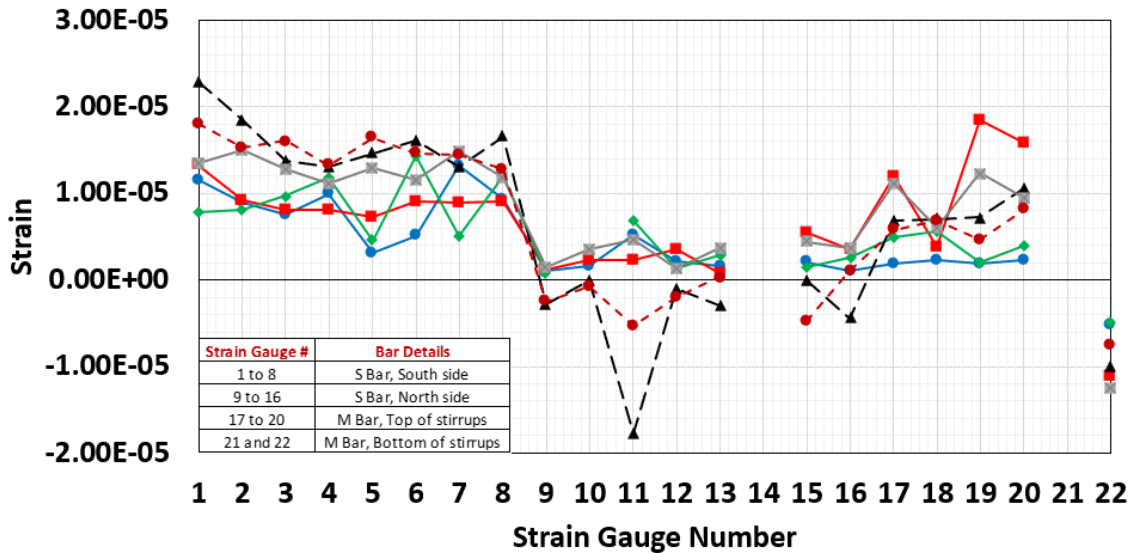
##### **4.4.1.1 Bent Cap 2**

A total of six load tests were conducted in static tests (Static Test-1 and Static Test-2) on Bent Cap 2. Figure 4.63 (a-b) shows the strain on transverse rebars in static tests on Bent Cap 2. In Figure 4.63a, Strain Gauge Number 1-8 and Strain Gauge Number 9-16 represent S bars on the south side and the north side of Bent Cap 2. The strain on the S bars at the interface between the ledge and stem on the projected side (south side) of Bent Cap 2 is higher than on the north side. Static Test-2, both Case 3, and Case 9, at Position 4 exhibit higher strain concentration on S bars on south side than other cases. It is primarily due to the higher truckload placement on the forward span of Bent Cap 2. Even though all S bars on the south side have a tensile strain, S bars on the north side reported compressive strain in Static Test 2, both Case 3, and Case 9, at Position 4, due to larger torsion. Further, the tensile strain on the 5<sup>th</sup> to 8<sup>th</sup> M bars (top of stirrups) in Case 9, Position 3, and Case 14 is higher, comparable to the strain on S bars on the south side.

Figure 4.63b shows the strain distribution on the G bars of Bent Cap 2 in static tests. The 4<sup>th</sup> and 5<sup>th</sup> G bars strains in static tests show higher strains comparable to the strain on S bars on the south side. The external girder near the west face of Bent Cap 2 rests on the ledge near the 4<sup>th</sup> and 5<sup>th</sup> G bars. This causes higher strains on the 4<sup>th</sup> and 5<sup>th</sup> G bars. Generally, the tensile strain on the 7<sup>th</sup> and 8<sup>th</sup> M bars is lower than on the 5<sup>th</sup> and 6<sup>th</sup> M bars. It may have been due to the influence of the 4<sup>th</sup> and 5<sup>th</sup> G bars located adjacent to the 5<sup>th</sup> and 6<sup>th</sup> M bars. The transverse rebars located around the location of external girders have higher tensile strains. TxDOT Project 0-6905 reports the exterior girder and the end face of the ITBC should be at least 24 inches to prevent punching shear failure and delaying the occurrence of diagonal cracks at the re-entrant corner between the cantilever ledge and stem (Sapath et al., 2019). In Bent Cap 2, there are five G bars (#7) at a

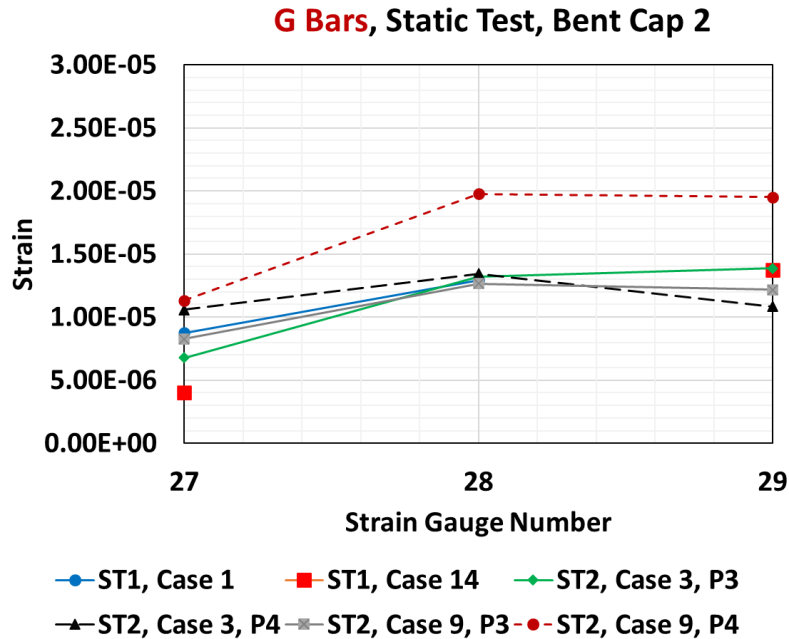
spacing of 6” maximum (a coverage of 24 inches with five G bars) and an exterior girder at 3.079’ (at least 24 inches) from the end face. Even though the prescribed recommendation is adopted for the distance between end face and the location of the exterior loading pads, the tensile strain on G bars are higher, which are comparable to S bars on the south side.

### S and M Bars, Static Test, Bent Cap 2



- ST1, Case 1      —■— ST1, Case 14      —●— ST2, Case 3, P3
- ▲— ST2, Case 3, P4    —■— ST2, Case 9, P3    —●— ST2, Case 9, P4

(a) Strain on S Bars and M Bars of Bent Cap 2 in Static Tests



(b) Strain on G Bars of Bent Cap 2 in Static Tests

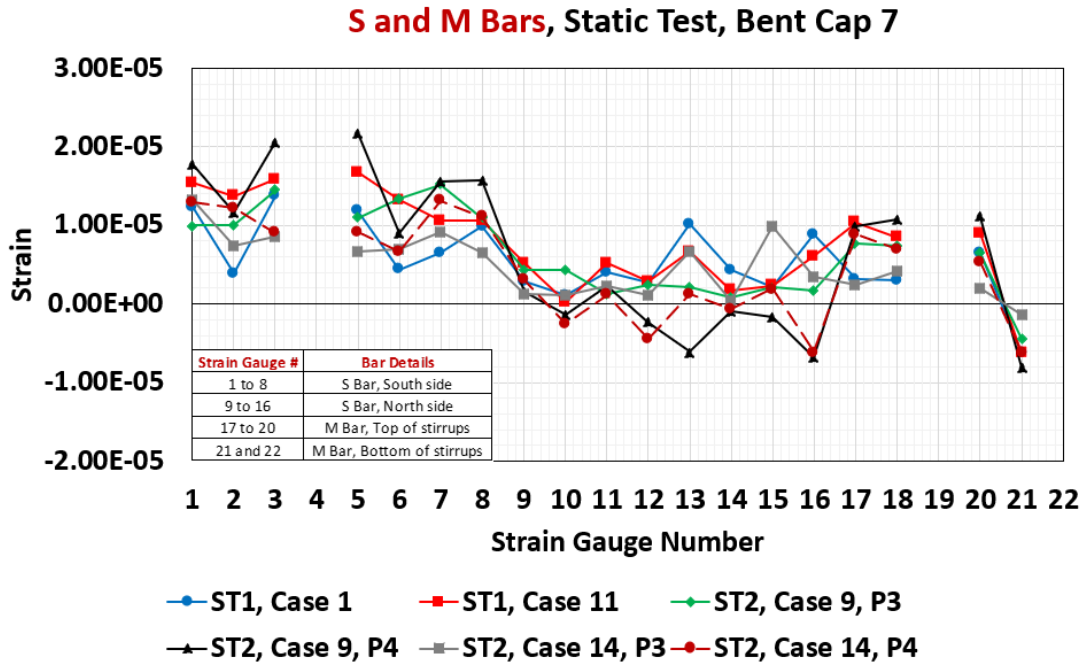
**Figure 4.63. Transverse Rebar Strains in Static Test on Bent Cap 2**

#### 4.4.1.2 Bent Cap 7

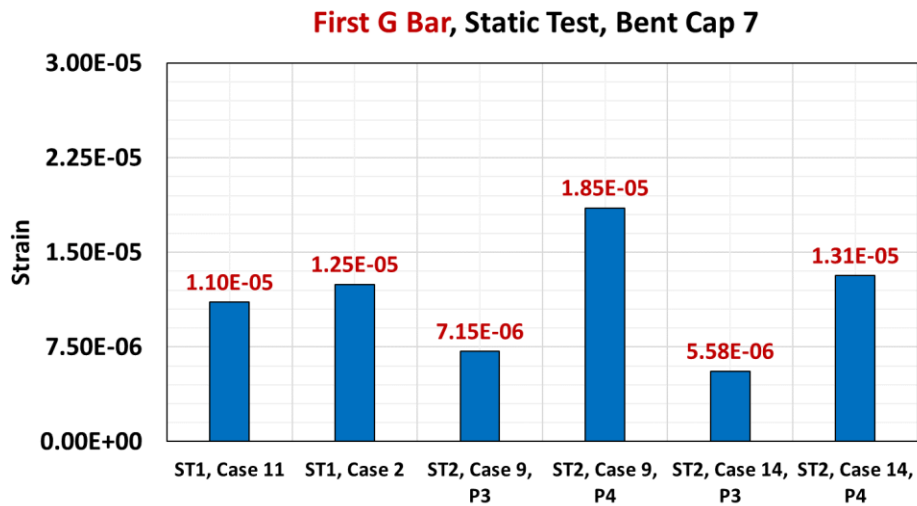
A total of six load tests were conducted in static tests (Static Test-1 and Static Test-2) on Bent Cap 7. Figure 4.64 (a-b) shows the strain on transverse rebars in static tests on Bent Cap 7. In Figure 4.64a, Strain Gauge Number 1-8 and Strain Gauge Number 9-16 represent S bars on the south side and the north side of Bent Cap 7. The strain on the S bars at the interface between the ledge and stem on the projected side (south side) of Bent Cap 7 is higher than on the north side. The static test in Case 11 and Case 9 at Position 4 exhibit higher strain concentration on the S bar (south side of Bent Cap 7). It is primarily due to the higher truckload placement on the forward span of Bent Cap 7. Even though all the S bars on the south side have tensile strains, most of the S bars on the north side reported compressive strain in Static Test-2, both Case 9, and Case 14, at Position 4 due to larger torsion. Further, the tensile strain on the 5<sup>th</sup> to 8<sup>th</sup> M bars (top of stirrups) in Case 1, and Case 14, Position 3 is higher, comparable to the strain on S bars on the south side.

Figure 4.64b shows the strain distribution on G bars of Bent Cap 7 in static tests. The strain of the 1<sup>st</sup> G bar (close to the end face) in static tests shows higher strain, comparable to strain on the S bars on the south side. Generally, the tensile strains on the 5<sup>th</sup>, 6<sup>th</sup>, and 8<sup>th</sup> M bars are comparable in all cases. It may have been due to the influence of the 4<sup>th</sup> and 5<sup>th</sup> G bars located

adjacent to the 5<sup>th</sup> and 6<sup>th</sup> M bars. The transverse rebars located around the location of external girders have to undergo tensile strains. In Bent Cap 7, there are five G bars (#7) at a spacing of 6” maximum (coverage of 24 inches with five G bars) and an exterior girder at 2.684’ (at least 24 inches) from the end face.



(a) Strain on S Bars and M Bars of Bent Cap 7 in Static Tests



(b) Strain on 1<sup>st</sup> G Bar of Bent Cap 7 in Static Tests

**Figure 4.64. Transverse Rebar Strains in Static Test on Bent Cap 7**

#### 4.4.2 Displacement of West Face of Bent Cap 2 and Bent Cap 7

Figure 4.65 shows the west face displacement of Bent Cap 2 in static tests (Static Test-1 and Static Test-2). The displacement of the north side of the west face of Bent Cap 2 is extrapolated from the displacement of the middle-Laser and south side-Laser. The south side of the west face of Bent Cap 2 in Case 3 and Case 9 at Position 4 in Static Test-2 recorded the highest displacements of -0.0161 inches and -0.0163 inches, respectively. Case 14 in Static Test-1 has the least displacement of -0.0101 inches.

The south side of the west face is the most projected end of the overhanging cantilever part of Bent Cap 2. The exterior girder on the south side of the Bent Cap 2 rests on the exterior bearing pad at 3.079' from the west face. Both Case 3 and Case 9 at Position 4 in Static Test-2 are designed with truckloads arranged close to the parapet on the deck over Bent Cap 2. Further, the truckloads are positioned more on the forward span (away from the centerline of Bent Cap 2). Hence, the truckloads in these two cases are concentrated on the forward span with the higher load transferred to the ledge of the bent cap through the exterior girder (near the west face). However, in Case 14, the truckloads are positioned closer to the centerline of the Bent Cap 2, which resulted in the least west face displacement of Bent Cap 2 on the south side.

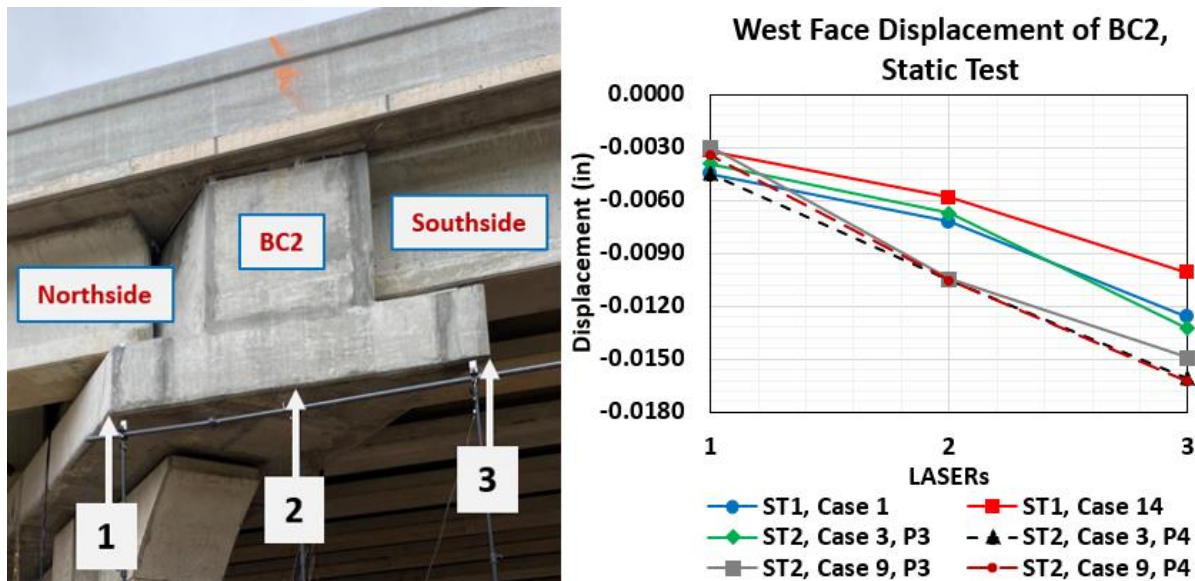
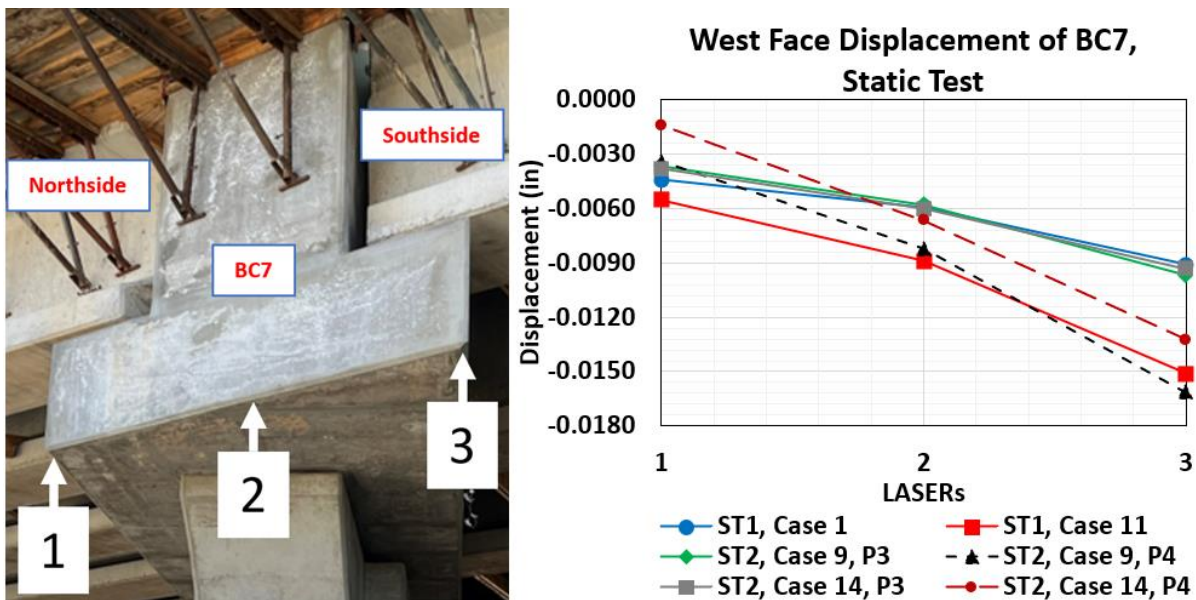


Figure 4.65. West Face Displacement of Bent Cap 2 in Static Test

Figure 4.66 shows the west face displacement of Bent Cap 7 in static tests (Static Test-1 and Static Test-2). The displacement of the north side of the west face of Bent Cap 7 is extrapolated from a displacement of the middle-Laser and south side-Laser. The south side of the west face of

Bent Cap 7 in Case 9 at Position 4 in Static Test-2 and Case 11 in Static Test-1 recorded the highest displacements of -0.0161 inches and -0.0151 inches, respectively. Case 1 in Static Test-1 and Case 14 at Position 3 in Static Test-2 have the least displacements of -0.0091 inches and -0.0094 inches, respectively.

The south side of the west face is the most projected end of the overhanging cantilever part of Bent Cap 7. The exterior girder on the south side of the Bent Cap 7 rests on the exterior bearing pad at 2.684' from the west face. Case 9 at Position 4 in Static Test-2 and Case 11 in Static Test-1 are designed with truckloads arranged close to the parapet on the deck over Bent Cap 7. Further, the truckloads are positioned more on the forward span (away from the centerline of Bent Cap 7). Hence, the truckloads in these two cases are concentrated on the forward span with higher load transferred to the ledge of the bent cap through the exterior girder (near to the west face). However, in Case 1 and Case 14 at Position 3, the truckloads are positioned closer to the centerline of the Bent Cap 7, which resulted in the least west face displacement of Bent Cap 7 on the south side.



**Figure 4.66. West Face Displacement of Bent Cap 7 in Static Test**

Based on the static load test, the displacement of the west face of both Bent Cap 2 and Bent Cap 7 for Case 9 at Position 4 in Static Test-2 has recorded the highest displacement of the west face in the south side. Additionally, the tensile strain on the transverse rebar is higher in Case 9 at Position 4 among all load test cases for both Bent Cap 2 and Bent Cap 7. Hence, Case 9 at Position 4 in Static Test-2 is critical for both bent caps.

In general, the load cases (both Case 3 and Case 9 at Position 4 in Static Test-2 on Bent Cap 2, Case 11 in Static Test-1, and Case 9 at Position 4 in Static Test-2 on Bent Cap 7) with truckloads concentrated on the forward span have the higher strains on the transverse rebars and yield higher displacements of the west face in the south side. The load cases (Case 1 and Case 14 in Static Test-1 of Bent Cap 2, and Case 1 in Static Test-1, and Case 14 at Position 3 in Static Test-2 of Bent Cap 7) with truckloads distributed and concentrated on the centerline of the bent cap have a comparatively lower strains on the transverse rebars and yielded lower displacements of the west face in the south side.

#### 4.4.3 Compressive Stress on Exterior Loading Pad

The CNFA-obtained average compressive stress on the exterior loading pads on Bent Cap 2 in static tests is shown in Table 4.4. Irrespective of the loading case, the compressive stress on the south side exterior loading pad is higher than the north side exterior loading pad. Both Case 3 and Case 9, at Position 4, yielded higher compressive strength among the static load test cases on the south side. The compressive stresses on the south side exterior loading pad are 0.28 ksi and 0.33 ksi in Case 3 and Case 9, respectively, at Position 4, respectively.

**Table 4.4. Compressive Stress on Exterior Loading Pad of Bent Cap 2 in Static Tests**

CNFA Location	Stress Detected by CNFA (ksi) in Exterior Loading Pad					
	Case 1	Case 14	Case 3, P3	Case 3, P4	Case 9, P3	Case 9, P4
North side	0.18	0.11	0.12	0.04	0.15	0.04
South side	0.19	0.16	0.17	0.28	0.22	0.33

However, in Bent Cap 7, CNFAs were installed in the north side exterior loading pad. Table 4.5 shows the CNFA-obtained average compressive stress from the static load test on Bent Cap 7.

**Table 4.5. Compressive Stress on Exterior Loading Pad of Bent Cap 7 in Static Tests**

CNFA Location	Stress Detected by CNFA (ksi) in Exterior Loading Pad					
	Case 1	Case 11	Case 9, P3	Case 9, P4	Case 14, P3	Case 14, P4
North side	0.14	0.15	0.17	0.05	0.13	0.05

Based on the loading positions, Case 1, Case 9 at Position 3 and Position 4, and Case 14 are comparable cases between Bent Cap 2 and Bent Cap 7. The comparison is summarized in Table 4.6. The compressive stress on the north side exterior bearing pads in both bent caps are comparable. Hence, the compressive stress on the south side exterior loading pad of Bent Cap 7 could be higher than on the north side.

It must be noted that the exterior loading pads on Bent Cap 7 are 2.684' from the end face, whereas the exterior loading pads on Bent Cap 2 are 3.079' from the end face. TxDOT Project 0-6905 reported the profound influence of the location of the exterior loading pad on ITBC on its structural performance (Sapath et al., 2019). The location of the exterior loading pads of Bent Cap 7 is closer to the end face than the location of the exterior loading pads of Bent Cap 2 to its end face. The strain on the transverse reinforcement increases when the exterior loading pads are closer to the end face of the ITBC. Based on these facts, it can be inferred that the compressive stress on the exterior loading pads of Bent Cap 7 should be higher than on Bent Cap 2. However, the compressive stresses in the exterior loading pads reported in Table 4.6 are comparable for Bent Cap 2 and Bent Cap 7. The skew angle of the inverted-T bent caps is the most influential parameter. The skew angle of Bent Cap 2 (43°) is larger than Bent Cap 7 (33°). Thus, it can be observed experimentally that the skew angle of an ITBC is the governing parameter that influences the compressive stress transferred to the ledge through the exterior loading pads.

**Table 4.6. Compressive Stress on North side Exterior Loading Pad of Bent Cap 2 and Bent Cap 7 in Static Tests**

Case	Compressive Stress (in ksi) in North side Exterior Loading Pad	
	Bent Cap 2 (Skew angle 43°)	Bent Cap 7 (Skew angle 33°)
Case 1	0.18	0.14
Case 9, P3	0.15	0.17
Case 9, P4	0.04	0.05
Case 14	0.11	0.13

\*Note: Case 14 at Position 3 reported for Bent Cap 7

#### 4.4.4 Comparison of Static and Dynamic Tests

##### 4.4.4.1 Bent Cap 2

Case 9 at Position 3 in Static Test-2 and Case 9 (at 5mph) in Dynamic Test-1 and Case 14 in Static Test-1 and Case 14 in Dynamic Test-1 are compared in this section. Due to safety concerns, as elaborated in Section 4.1.4, the drivers choose to move trucks away from the parapet in Dynamic Test-1.

Figure 4.67 shows the rebar strains comparison of Case 9, Bent Cap 2 in static and dynamic tests, respectively. The strain on the transverse rebars (S bar-south side, M bars, and G bars) in the static test is higher than in the dynamic test. Further, the S bar on the north side exhibits the

compressive strain due to torsion. Figure 4.68 shows a significant difference in the displacements of the west face of Bent Cap 2 in Case 9 (static versus dynamic tests).

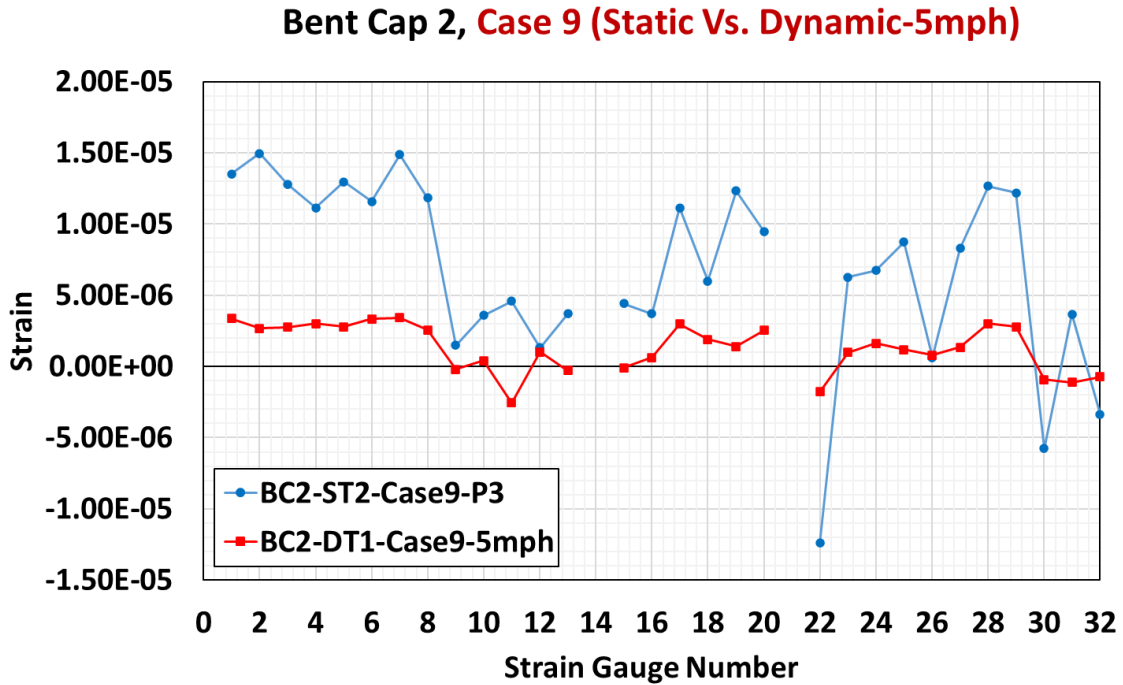


Figure 4.67. Rebar Strain Comparison in Case 9 (Static Test Vs. Dynamic Test)

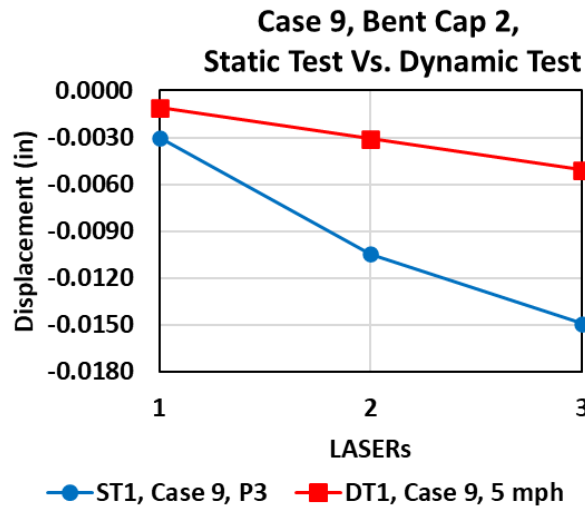
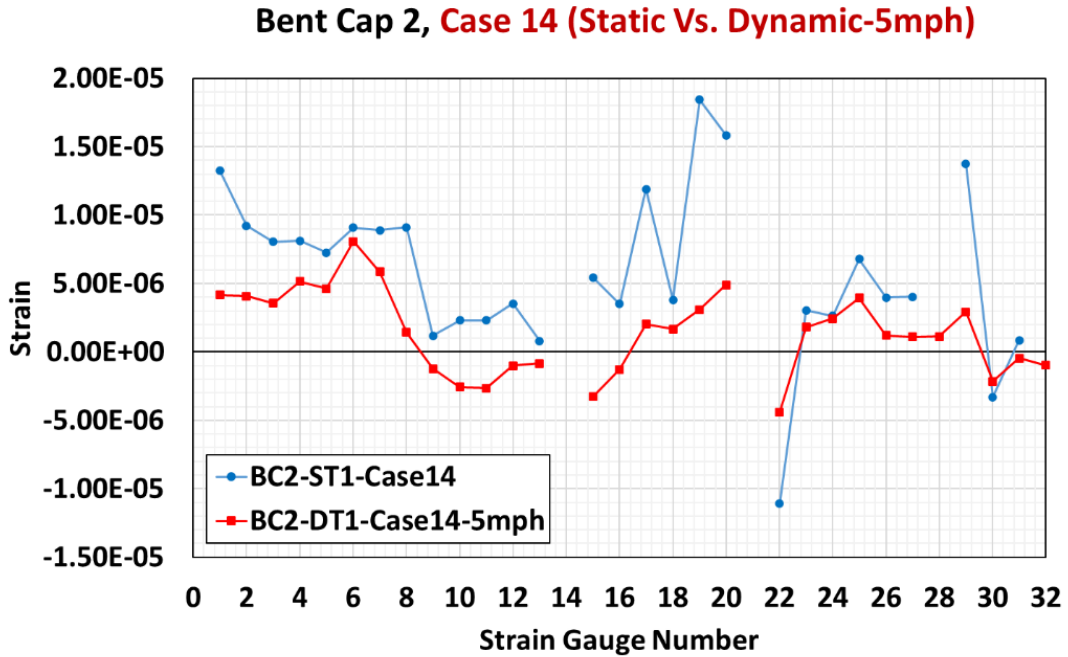
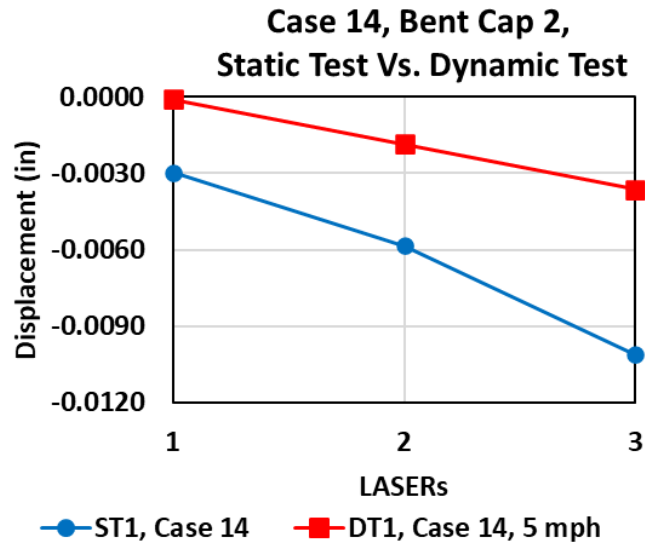


Figure 4.68. West Face Displacements Comparison of Bent Cap 2 in Case 9 (Static Test Vs. Dynamic Test)

Figure 4.69 shows the rebar strains comparison of Case 14, Bent Cap 2 in static and dynamic tests, respectively. Similar to Case 9, the strains on the transverse rebars (S bar-south side, M bars, and G bars) in the static test are higher than in the dynamic test in Case 14. Further, the S bar on the north side exhibits the compressive strain due to torsion. Figure 4.70 shows a significant difference in the displacements of the west face of Bent Cap 2 in Case 14 (static versus dynamic tests).



**Figure 4.69. Rebar Strains Comparison in Case 14, Bent Cap 2  
(Static Test Vs. Dynamic Test)**



**Figure 4.70. West Face Displacements Comparison of Bent Cap 2 in Case 14 (Static Test Vs. Dynamic Test)**

The comparison of the static test and dynamic test in Case 9 and Case 14 shows that strain on transverse rebars and displacement of the west face of Bent Cap 2 is higher in the static test. The position of trucks in the dynamic test is located far from the parapet, which has a lower load transfer to the cantilever portion of the bent cap. The comparison of static and dynamic tests on Bent Cap 7 has similar truck position on the deck, which is discussed in the following section.

#### 4.4.4.2 Bent Cap 7

Case 9 at Position 3 in Static Test-2 and Case 9 (at 5mph) in Dynamic Test-1, and Case 14 in Static Test-1 and Case 14 in Dynamic Test-1 are compared in this section. The trucks positions on deck for both static and dynamic tests are similar.

Figure 4.71 shows the rebar strains comparison of Case 9, Bent Cap 7 in static and dynamic tests, respectively. The strains on the rebar in the static test is higher than in the dynamic test. Figure 4.72 show displacements comparison of the west face of Bent Cap 7 in Case 9 (static versus dynamic tests). The displacement of the west face in the static test is 38.36% higher than the dynamic test in Case 9.

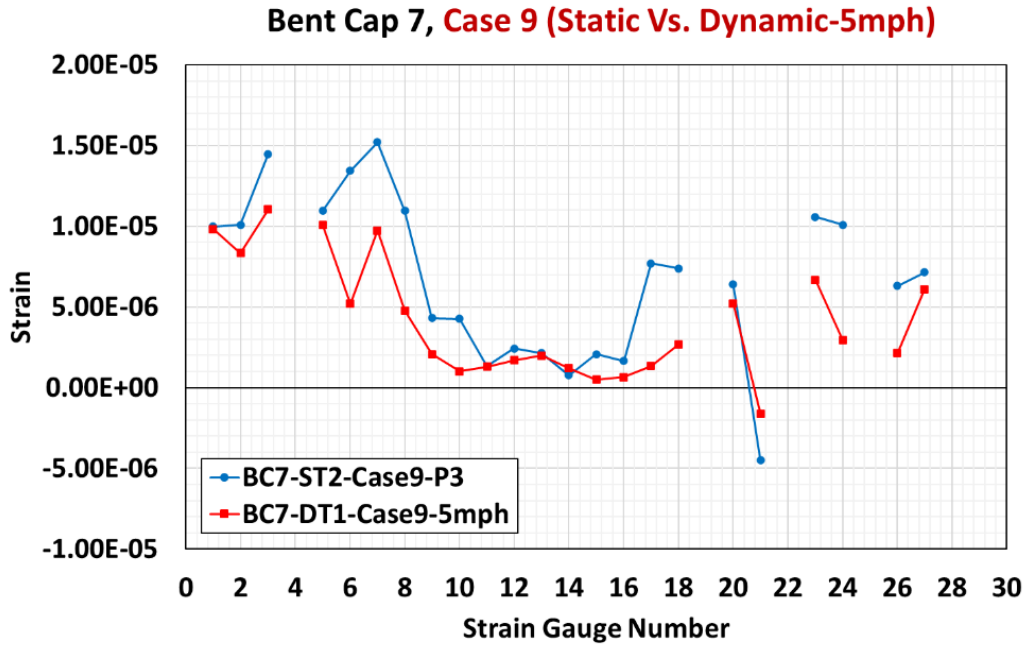


**Figure 4.71. Rebar Strains Comparison in Case 9, Bent Cap 7  
(Static Test Vs. Dynamic Test)**

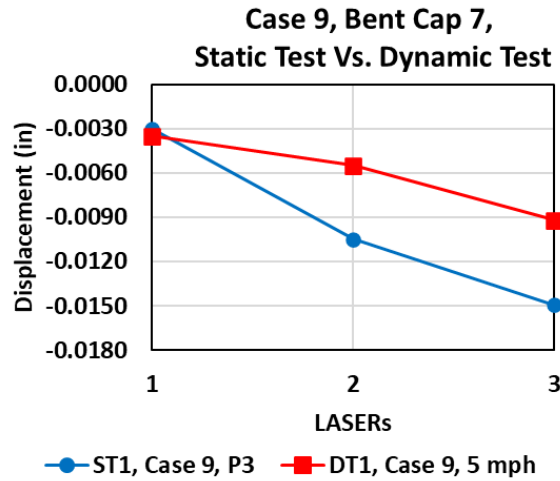


**Figure 4.72. West Face Displacements Comparison of Bent Cap 2 in Case 9  
(Static Test Vs. Dynamic Test)**

Figure 4.73 shows the strain comparison of Case 14, Bent Cap 7 in static and dynamic tests, respectively. Similar to Case 9, the strain on the rebar in the static test is higher than in the dynamic test in Case 14. Figure 4.74 show displacement comparison of the west face of Bent Cap

7 in Case 14 (static versus dynamic tests). The displacement of the west face in the static test is 20.93% higher than in the dynamic test in Case 14.

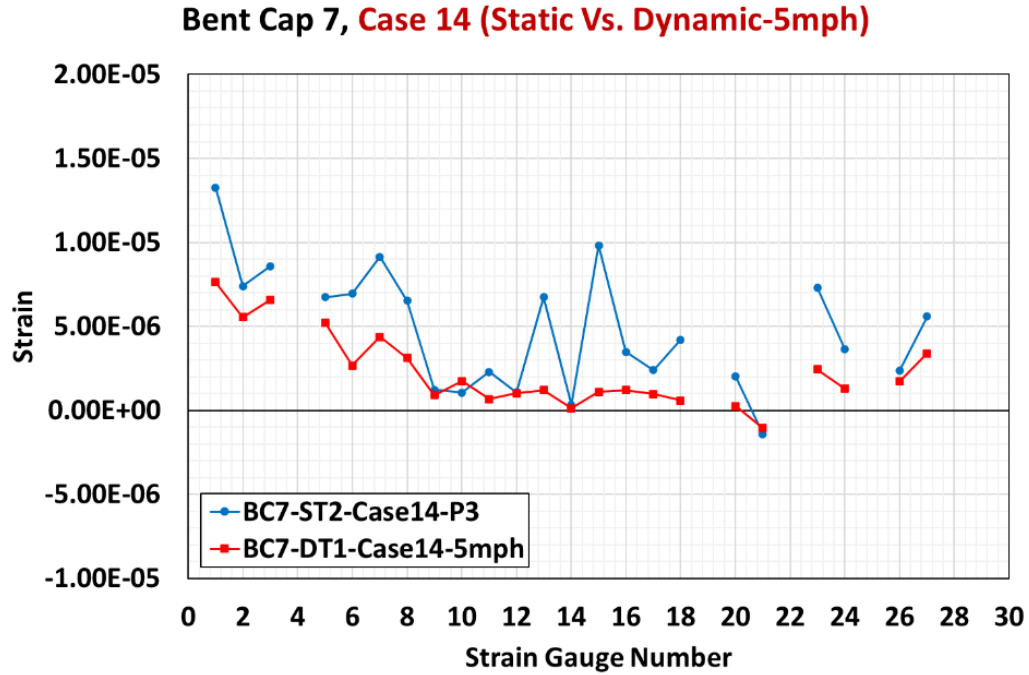


Figure 4.73. Rebar Strains Comparison in Case 14, Bent Cap 7 (Static Test Vs. Dynamic Test)

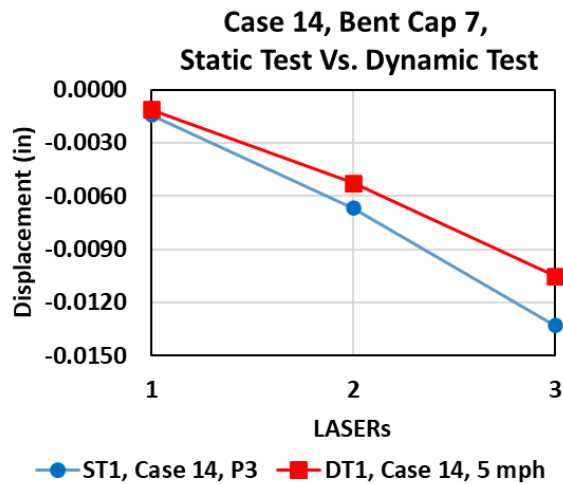


Figure 4.74. West Face Displacements Comparison of Bent Cap 7 in Case 14 (Static Test Vs. Dynamic Test)

With the truckloads and the similar position of trucks taken into the consideration, the comparison of the static test and dynamic test in Case 9 and Case 14 shows that the strain on transverse rebars and displacement of the west face of Bent Cap 7 is higher in the static test than in the dynamic test at 5 mph. In addition, it is experimentally observed that Case 9 in Dynamic Test-1 is critical when compared to Case 14 in Dynamic Test-1. Case 9 at 5 mph results in higher stress on transverse rebar with higher west face displacement than in Case 14 at 5 mph.

#### **4.4.5 Influence of Skew Angle**

Based on the experimental investigation of the scaled ITBC specimen in TxDOT Project 0-6905 (Sapath et al., 2019):

- A higher skew angle increases the influence of shear and torsion in the bent cap,
- A larger skew angle creates higher asymmetry in the bearing pad location, which weakens the bent cap,
- Torsional deformation increases when the skew angle increases,
- The ultimate shear capacity of the ITBC decreases with increases in the skew angle.

The skew angle of an inverted-T bent cap is an influential parameter that governs the structural performance of the bent cap. The skew angle of Bent Cap 2 is  $43^{\circ}$ , and Bent Cap 7 is  $33^{\circ}$ . This section compares the performance of Bent Cap 2 and Bent Cap 7 against the load test as shown in Table 4.7.

**Table 4.7. Performance Comparison of Bent Cap 2 and Bent Cap 7 in Static Tests**

Details	Bent Cap 2 (BC2)	Bent Cap 7 (BC7)	Commentary
Skew angle	43 <sup>o</sup>	33 <sup>o</sup>	
<b>Highest Strain (µε) in Transverse Rebars</b>			
S bar (south side)	22.87	21.73	<i>BC2: Case 3, Position 4 BC7: Case 9, Position 4</i>
<b>S bar (north side)</b>			
Tensile Strain	6.88	7.42	<i>BC2: Case 3, Position 3 BC7: Case 9, Position 3</i>
Compressive Strain	-17.76	-6.77	<i>BC2: Case 3, Position 4 BC7: Case 9, Position 4</i>
M bar (top of stirrups)	18.43	11.11	<i>BC2: Case 14 BC7: Case 9, Position 4</i>
M bar (bottom of stirrups)	-12.41	-8.12	<i>BC2: Case 9, Position 3 BC7: Case 9, Position 4</i>
G Bar (1 <sup>st</sup> )	11.33	18.52	<i>BC2: Case 9, Position 4 BC7: Case 9, Position 4</i>
G Bar (4 <sup>th</sup> )	19.76	-	<i>BC2: Case 9, Position 4</i>
<b>West Face Displacement on south side (in)</b>			
Highest	-0.0163	-0.0161	<i>BC2: Case 9, Position 4 BC7: Case 9, Position 4</i>
Lowest	-0.0101	-0.0091	<i>BC2: Case 14 BC2: Case 1</i>
<b>End Face to Exterior Loading Pad Distance (ft)</b>	3.079	2.684	
<b>Compressive Stress in North side Exterior Loading Pad (ksi)</b>			
Case 1	0.18	0.14	
Case 9, P3	0.15	0.17	
Case 9, P4	0.04	0.05	
Case 14	0.11	0.13	<i>BC2: Case 14 BC7: Case 14, Position 3</i>
<b>Critical Cases</b>	Case 3, Position 4	Case 11	
	Case 9, Position 4	Case 9, Position 4	

The influence of the skew angle in the field implementation of skew reinforcement in ITBCs is observed in the following four aspects:

- (a) **Strain in transverse reinforcements:** Table 4.7 shows that the strain in transverse reinforcements is higher in Bent Cap 2 than in Bent Cap 7. The increase in skew angle can result in higher strain on transverse reinforcement.

- (b) **Torsional effect:** The S bar on the north side exhibited the compressive strain while the S bar on the south side had the tensile strain during the Static Test-2 at Position 4. Both ITBCs exhibited torsion. However, Bent Cap 2 (skew angle  $43^\circ$ ) has significantly higher compressive strain on the S bar (north side) than Bent Cap 7 (skew angle  $33^\circ$ ), as shown in Table 4.7. This shows that the influence of torsion is higher in the ITBC with a higher skew angle.
- (c) **Higher west face displacement:** Geometrically, the projection of Bent Cap 2 (18.13' from the center of the exterior column to the west face of the bent cap) is higher than the Bent Cap 7 (13.00' from the center of the exterior column to the west face of the bent cap). The location of the exterior loading pad of Bent Cap 7 is closer to the west face (2.684') than the location of exterior loading pads from west face Bent Cap 2 (3.079'). The closer location of the exterior loading pads from the end face influences the structural performance of ITBC. However, the west face tip displacement in the south side (i.e., longer side) of Bent Cap 2 is higher. The lowest west face tip displacement among six static load tests of Bent Cap 2 is -0.0101 inches, whereas the lowest west face tip displacement is -0.0091 inches for Bent Cap 7. It can be observed that the higher skew angle increases the end face displacement of an ITBC.
- (d) **Compressive stress on exterior loading pads:** The location of the exterior loading pad significantly affects the structural performance of ITBC. The exterior loading pad is located on the overhanging cantilever portion of both bent caps. The loads from exterior girders are transferred to the ledge through the exterior loading pads. This load causes tensile strain on the adjacent transverse rebars. The CNFA-obtained average compressive stresses on the north side exterior loading pads are comparable in both bent caps. Three possible parameters can influence the compressive stress on the exterior loading pads: Bent Cap 2 has a longer cantilever projection than Bent Cap 7, the location of the exterior loading pads, and the skew angle.

## 4.5 SUMMARY

Based on the load tests conducted on Bent Cap 2 and Bent Cap 7, the following summarizes are presented.

1. The concrete compression tests on the concrete cylinders of both phases of Bent Cap 2 and Bent Cap 7 are conducted.

- a. The compressive strength of Phase-1 and Phase-2 of Bent Cap 2 are 7000 psi and 7691 psi, respectively.
- b. The compressive strength of Phase-1 and Phase-2 of Bent Cap 7 are 6608 psi and 7398 psi, respectively.
2. The tensile strain on the S bars on the south side closest to the end face of both ITBCs are higher in all loading cases. Due to larger torsion, the S bars on the north side exhibited compressive strain in Static Test-2 at Position 4 in both ITBCs.
3. The tensile strain on the M bars (at the top of stirrups, and the interface of ledge and stem) is larger in the loading cases with truckloads positioned in two lanes (Case 3 of Bent Cap 2, and Case 14 of both Bent Cap 2 and Bent Cap 7).
4. Bent Cap 2 exhibited higher tensile strain on the 4<sup>th</sup> and 5<sup>th</sup> G bars. This is due to location of exterior loading pads close to the 4<sup>th</sup> and 5<sup>th</sup> G bars. The tensile strains on G bars are comparable to S bars on the south side.
5. The inclusion of diagonal G bars at the end faces will reduce the strains in the transverse bars (i.e. S and M bars) near the exterior loading pads.
6. The loading cases with truckloads (all trucks positioned in one lane, and closer to the parapet) concentrated on the forward span result higher strains on the transverse rebar and higher displacements of the west face of both ITBCs, which make these cases critical. Case 14 (trucks positioned in two lanes) with truckloads concentrated around centerline of ITBCs has comparatively lower strains on transverse rebar and lower displacements of west face of both ITBCs.
7. The longer side of the overhanging cantilever portion of ITBCs has a higher compressive stress on the exterior loading pads. Bent Cap 2 exhibited higher average compressive stress on the south side than on the north side in all static load tests.
8. Bent Cap 7 exhibited that the static test yields higher strains on rebar and higher end face displacements than the dynamic test. It may be because the static test provides adequate time for stress to be transferred to the ledge of the ITBC, while dynamic tests are swift in action.
9. The skew angle of an ITBC is the most influential parameter. Experimentally, it is observed that:

- a. An ITBC with a higher skew angle has higher tensile strain on transverse reinforcement,
- b. An ITBC with a higher skew angle influences the torsional effect on the bent cap,
- c. Higher end face displacement of the longer side of an ITBC with a higher skew angle,
- d. The skew angle magnifies the compressive stress on the exterior loading pad.

## 5 FINITE ELEMENT ANALYSES

### 5.1 OVERVIEW

In this chapter, the 3D finite element (FE) analysis models of Bent Cap 2 and Bent Cap 7 using ABAQUS are calibrated with the load test results. Furthermore, a comprehensive parametric study has been presented to understand the overall structural behavior of skew reinforcement in inverted-T bridge caps.

### 5.2 FINITE ELEMENT ANALYSIS OF BENT CAP 2 AND BENT CAP 7

#### 5.2.1 Finite Element Modeling

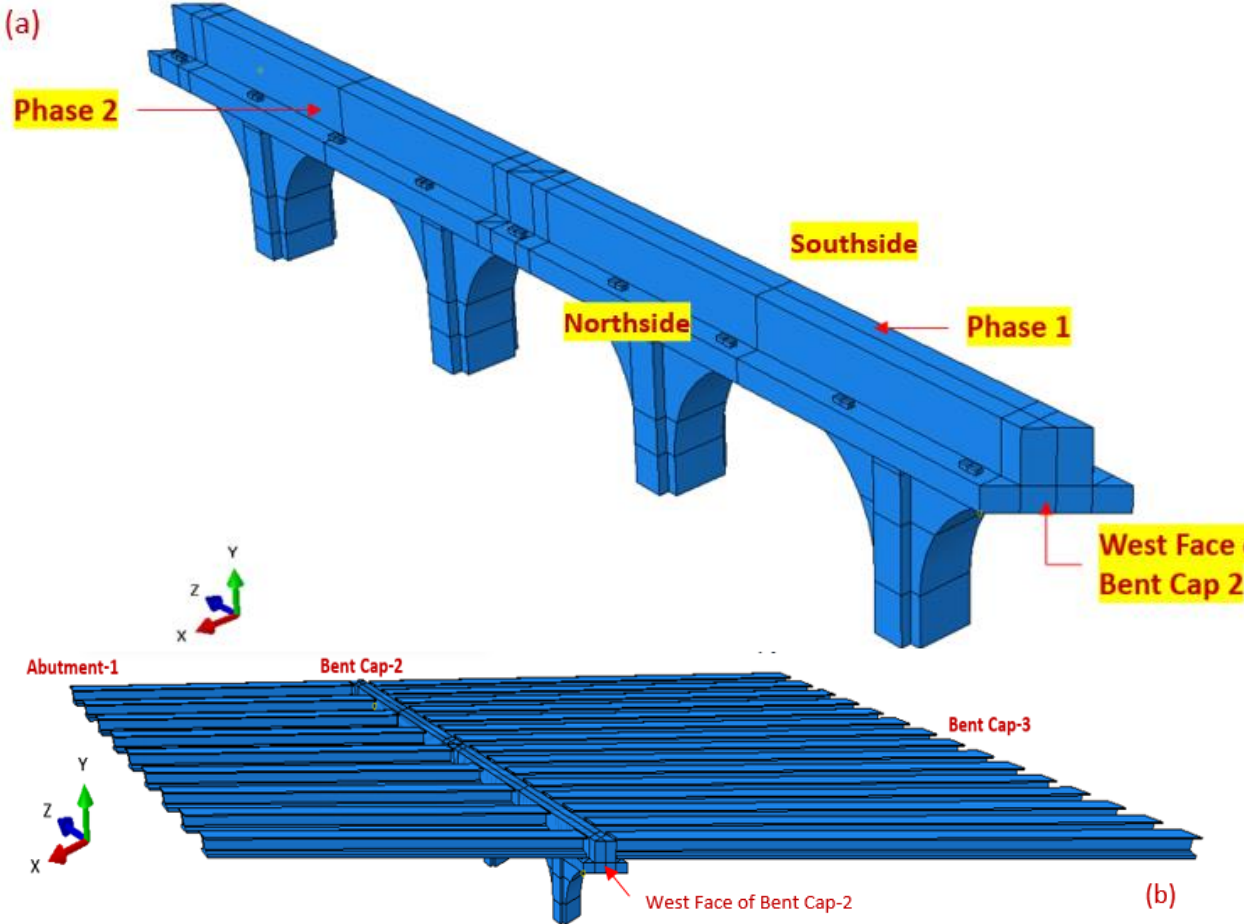
The preliminary three-dimensional (3D) finite element (FE) models of Inverted-T Bent Cap 2 (ITBC 2) and Inverted-T Bent Cap 7 (ITBC 7) were updated using material property of concrete based on concrete compression test. The compression tests on concrete cylinders of Bent Cap 2 and Bent Cap 7 are summarized in Table 5.1.

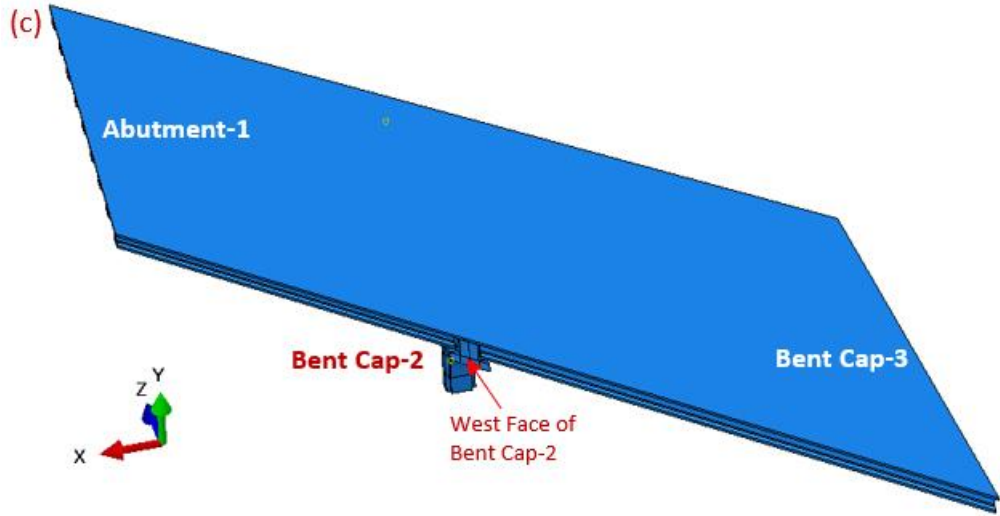
**Table 5.1. Compressive Strength of Bent Cap 2 and Bent Cap 7**

<b>Bent Cap</b>	<b>Phase</b>	<b>Specimen</b>	<b>Compressive Strength (psi)</b>
<b>2</b>	<b>1</b>	A	7264
		B	6905
		C	6832
	<b>Average</b>		<b>7000</b>
	<b>2</b>	A	7711
		B	7413
		C	7948
<b>Average</b>		<b>7691</b>	
<b>7</b>	<b>1</b>	A	6583
		B	6395
		C	6845
	<b>Average</b>		<b>6608</b>
	<b>2</b>	A	7176
		B	7675
		C	7342
<b>Average</b>		<b>7398</b>	

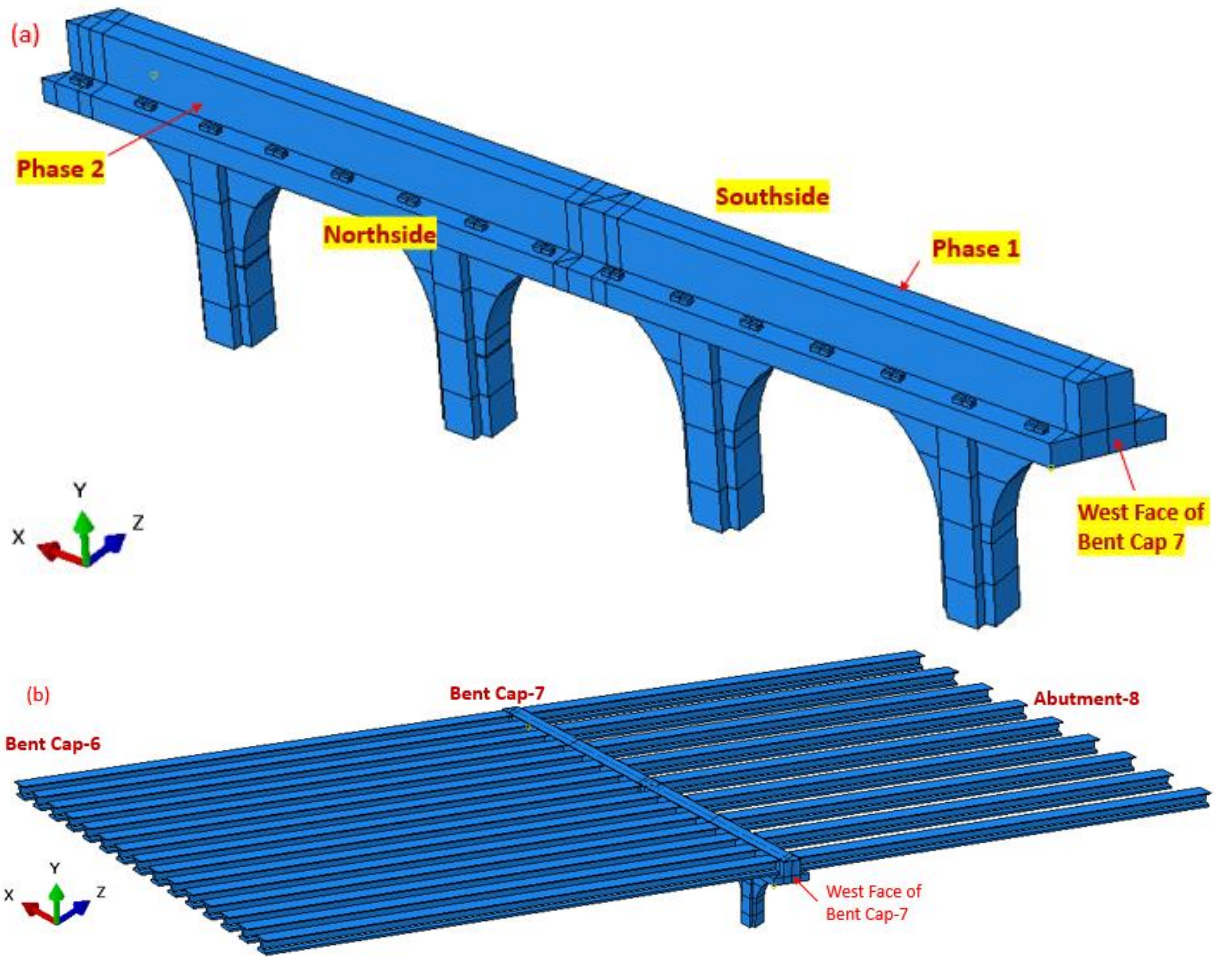
The global FE models with the deck, girders, ITBC, and four supporting columns were developed. The global FE models for ITBC 2 and ITBC 7 are shown in Figures 5.1(a-c) and 5.2(a-c), respectively. The geometry of the FE models is based on the design drawing of the Donigan Road Bridge provided by TxDOT. The boundary conditions of columns for both models are

provided with fixed supports, and girders on ITBCS are assumed to be simply supported. The concrete structures for both bent caps were meshed using the eight-node, reduced integration, hourglass control solid elements (C3D8R), as shown in Figures 5 and 6. The two-node linear three-dimensional (3D) truss elements (T3D2) were used to model the reinforcement since it is only subjected to axial force.





**Figure 5.1. 3D Finite Element Model of Bent Cap 2, including Columns, Girders, and Deck**



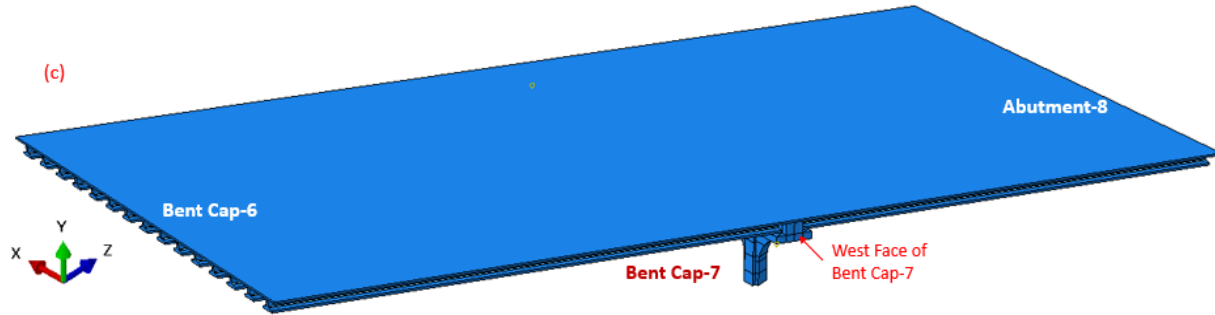


**Figure 5.2. 3D Finite Element Model of Bent Cap 7, including Columns, Girders, and Deck**

### **5.2.2 Concrete Material Property**

Bent Cap 2 and Bent Cap 7 were cast in two phases during construction. Based on the concrete compression test, two phases of the concrete cast have different concrete properties. Hence, the FE model is updated to match the real structural properties of Bent Cap 2 and Bent Cap 7.

The concrete deck, girders, and columns were assigned the elastic material behavior. The Concrete Damaged Plasticity (CDP) model was used as the constitutive model of bent cap concrete in the FE model (Lee & Fenves, 1998). The CDP model requires the definition of uniaxial behavior in compression and tension. The compressive and tensile stress-strain curves of concrete considered in the constitutive model were adopted from the book “Unified Theory of Concrete Structures” (Hsu & Mo, 2010).

The details of the material parameters of the concrete damaged plasticity model for Bent Caps 2 and 7 are listed in Table 5.2.

**Table 5.2. Material Parameters of the Concrete Damaged Plasticity Model of Bent Cap 2 and Bent Cap 7**

Bent Cap	Test (Case)	Compressive Strength (ksi)		Young's Modulus (ksi)		Tensile Strength (ksi)		Poisson's Ratio	Density ( <i>lb/ft</i> <sup>3</sup> )	Dilation angle (°)	Flow Potential Eccentricity	K	Viscosity Coefficient (Relaxation Time)
		P1	P2	P1	P2	P1	P2						
2	ST-1 (1 and 14)	7.0	7.7	4769	5002	0.38	0.40	0.2	150	31	0.1	0.667	1.0E-05
	ST-2 (3 and 9)												
	DT-1 (9 and 14)												
7	ST-1 (1 and 11)	6.6	7.4	4634	4903	0.37	0.39	0.2	150	31	0.1	0.667	1.0E-05
	ST-2 (9 and 14)												
	DT-1 (9 and 14)												

\*Note: ST-1 is Static Test-1, ST-2 is Static Test-2 at Position 3 and Position 4, DT-1 is Dynamic Test-1, P1 is Phase 1, and P2 is Phase 2.

### 5.3 CALIBRATION OF FE MODELS OF BENT CAP 2 WITH LOAD TEST DATA

The FE model of Bent Cap 2 is revised into two phases (Phase 1 and Phase 2) as it was cast during construction (see Figure 5.1). The revised FE model of Bent Cap 2 is updated with the concrete properties as presented in Table 5.2. The updated model of Bent Cap 2 is simulated in ABAQUS with the four trucks positioned on the deck.

#### 5.3.1 Static Test-1

The 3D FE analyses of Static Test-1 for Case 1 and Case 14 were performed on an updated model of Bent Cap 2 with four trucks on the Donigan Road Bridge. Figures 5.3 and 5.4 show the position of four trucks on the deck over Bent Cap 2 in Static Test-1 for Case 1 and Case 14, respectively.

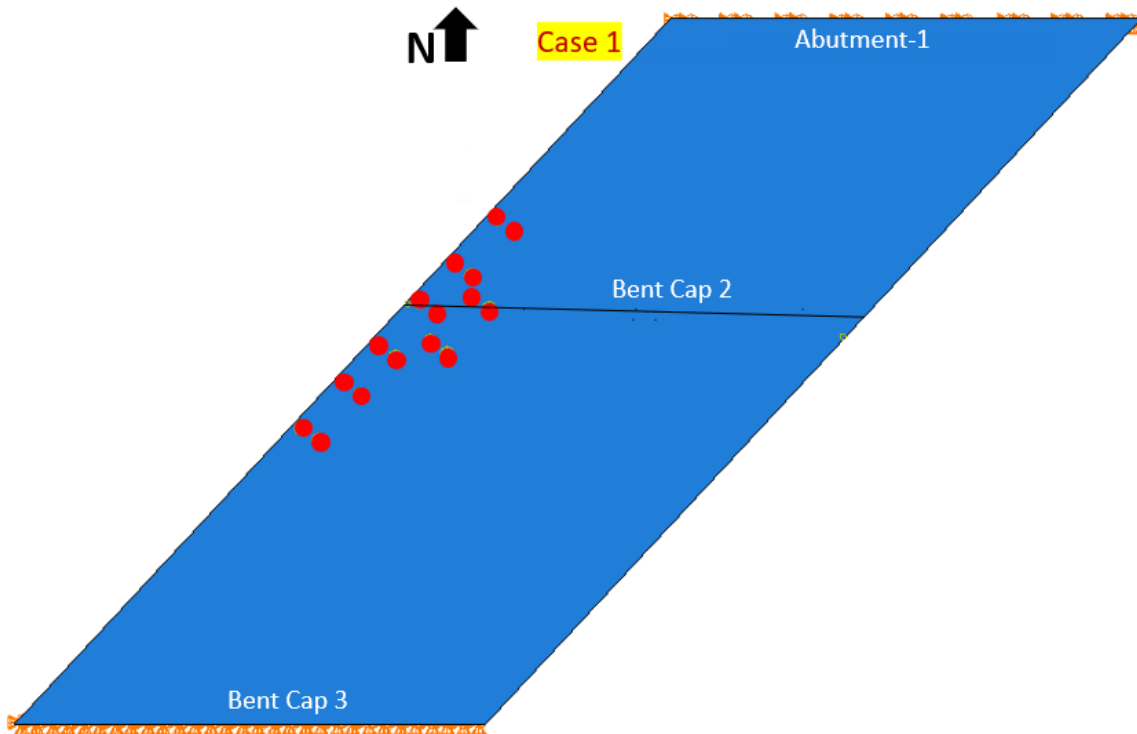


**Figure 5.3. Locations of Trucks in Static Test-1, Case 1 on Bent Cap 2**

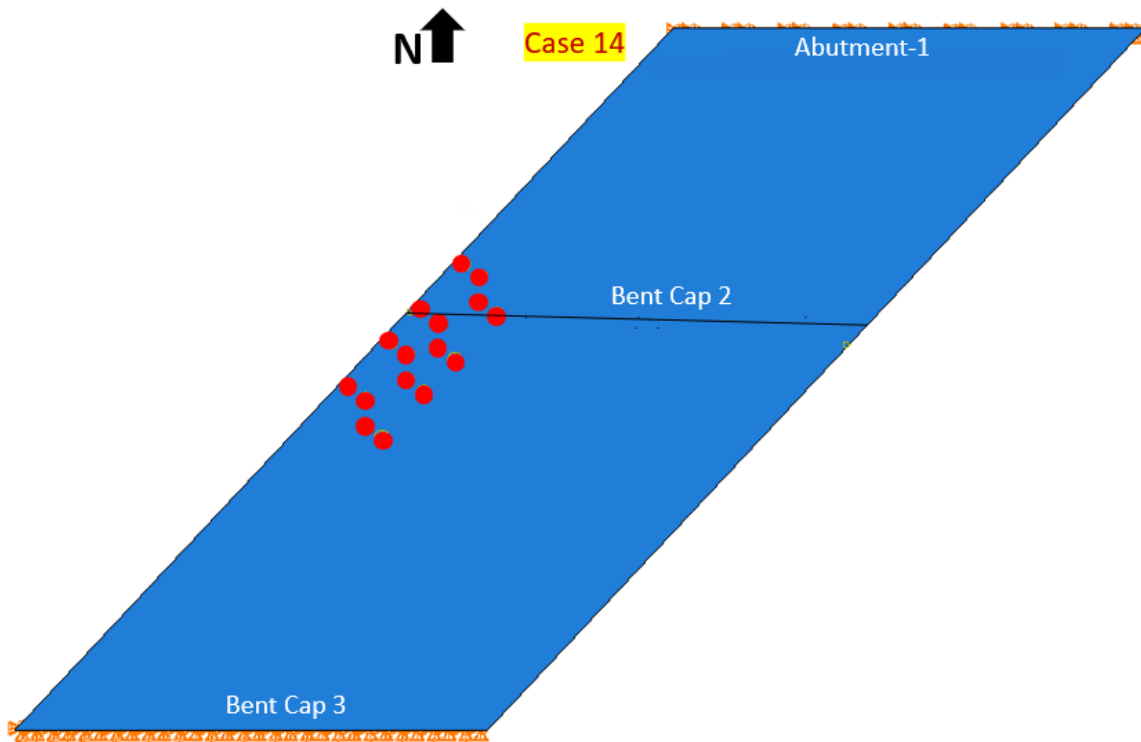


**Figure 5.4. Locations of Trucks in Static Test-1, Case 14 on Bent Cap 2**

### 5.3.1.1 Case 1

Figure 5.5 shows the comparative analysis of the load test and updated FE model of Case 1. Figure 5.6 shows the comparative plot of west face displacements from the load test and updated model of Bent Cap 2 in Static Test-1 for Case 1. The tip displacements of the extended region of Bent Cap 2 (south side) in Static Test-1 for Case 1 from the load test and FE simulation are -0.0126 inches and -0.0103 inches, respectively.

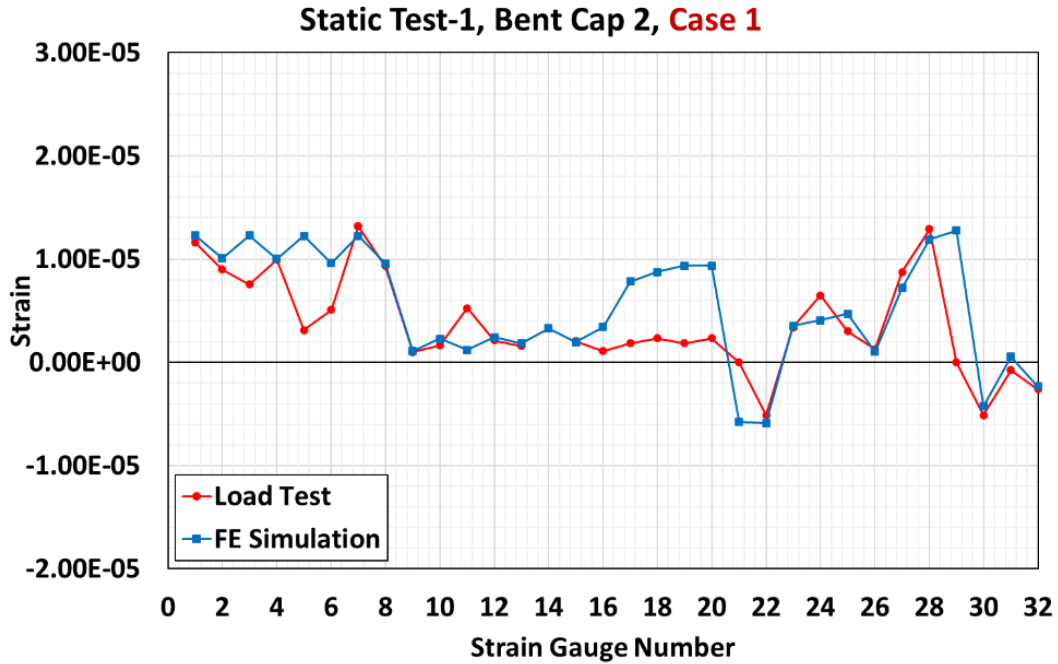


Figure 5.5. Rebar Strains Comparison of Static Test-1, Bent Cap 2 for Case 1

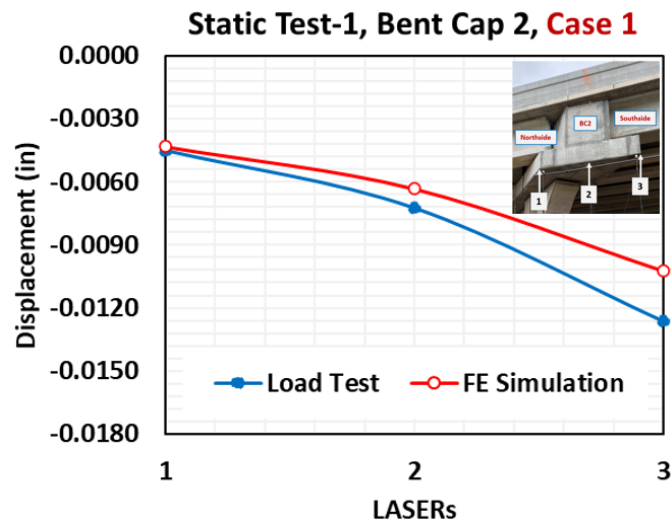
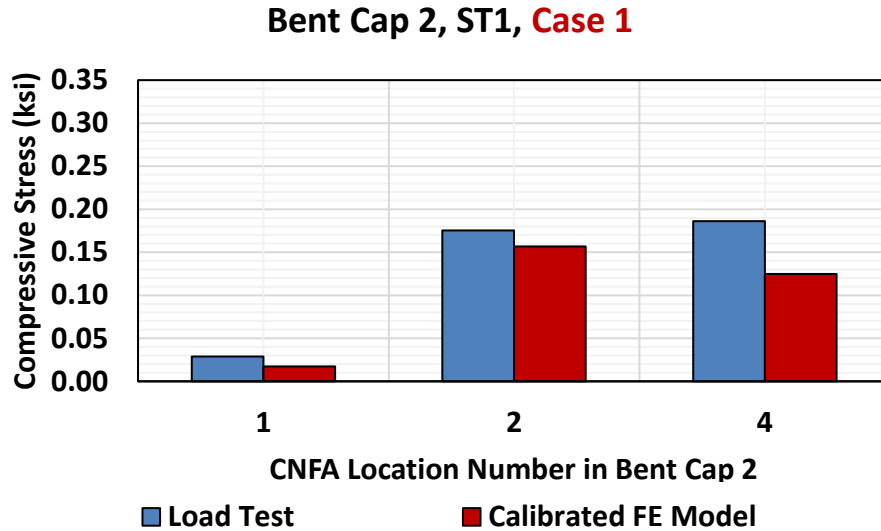


Figure 5.6. West Face Displacements Comparison of Static Test-1, Bent Cap 2 for Case 1

Figure 5.7 shows the comparative analysis of CNFA-obtained average compressive stresses from the load test and average compressive stresses from the updated FE model of Case 1. In Figure 5.7, Location 1 is at Column-Bent Cap 2 interface, Location 2 is under the exterior loading pad at the north side, and Location 4 is under the exterior loading pad at the south side.

The comparison of strains in rebars, west face displacements, and CNFA-obtained compressive stresses are presented in APPENDIX-4.



**Figure 5.7. Comparison of Average Compressive Stresses on Concrete of Static Test-1, Bent Cap 2 for Case 1**

### 5.3.1.2 Case 14

Figure 5.8 illustrates the comparative analysis of the load test and the updated FE model of Case 14. Figure 5.9 shows the comparative plot of the west face displacements from the load test and the updated model of Bent Cap 2 in Static Test-1 for Case 14. The tip displacements of the extended region of Bent Cap 2 (south side) in Static Test-1 for Case 14 from the load test and FE simulation are -0.0101 inches and -0.0097 inches, respectively.

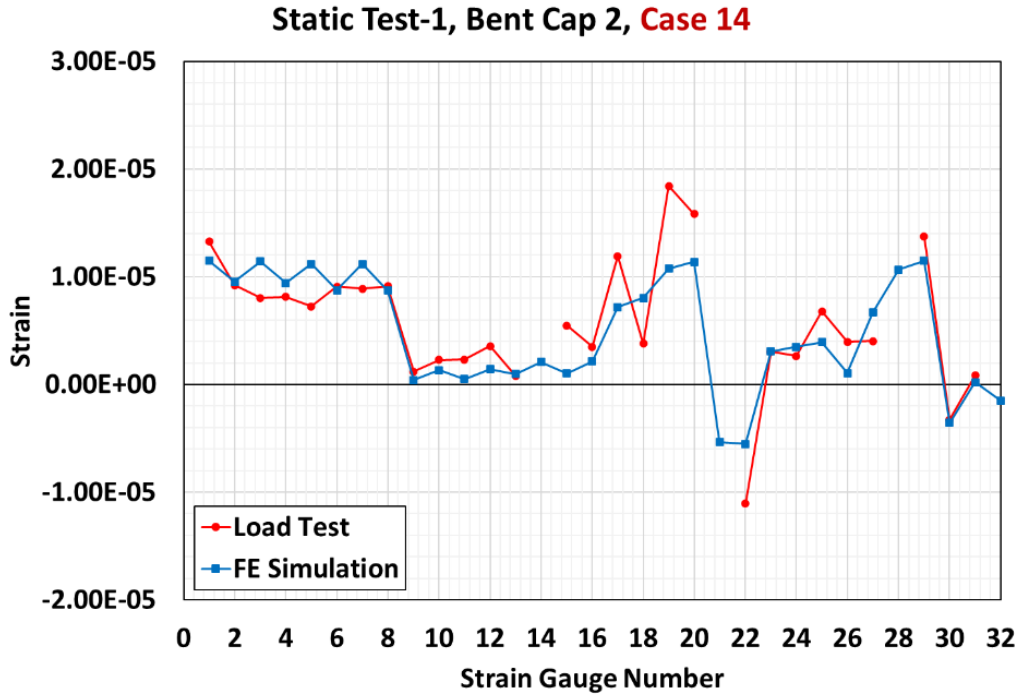


Figure 5.8. Rebar Strains Comparison of Static Test-1, Bent Cap 2 for Case 14

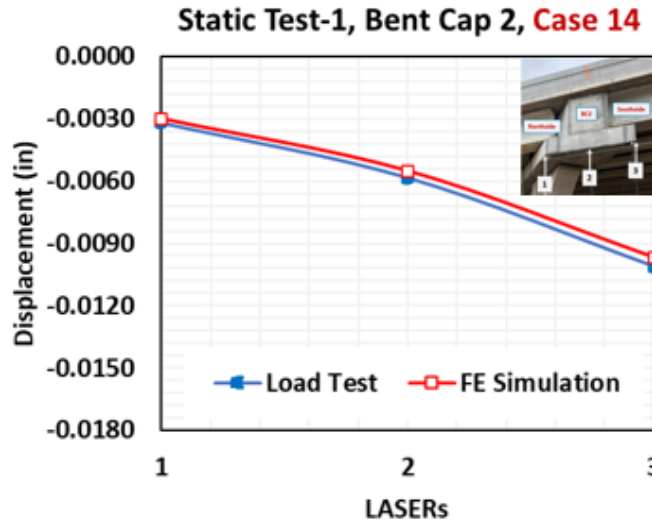
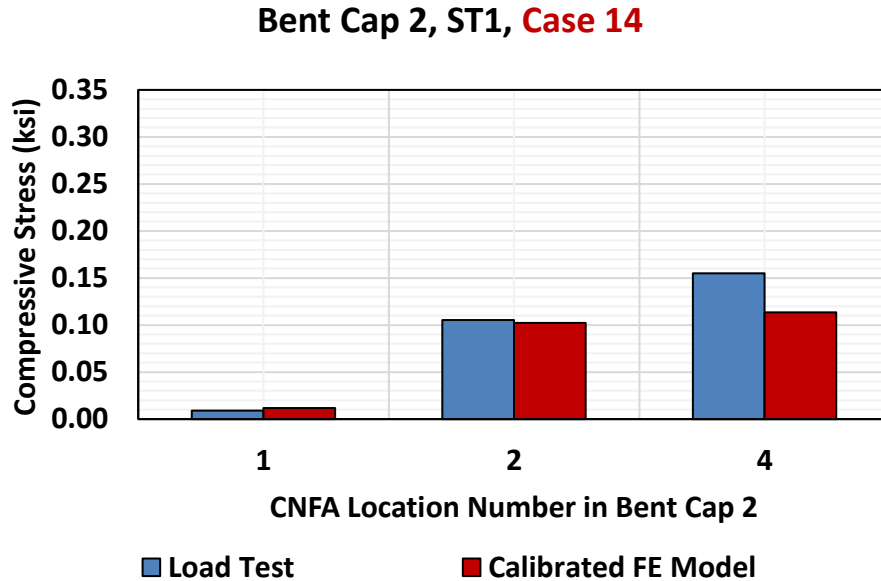


Figure 5.9. West Face Displacements Comparison of Static Test-1, Bent Cap 2 for Case 14

Figure 5.10 shows the comparative analysis of CNFA-obtained average compressive stresses in the load test and average compressive stresses from the updated FE model for Case 14. In Figure 5.10, Location 1 is at Column-Bent Cap 2 interface, Location 2 is under the exterior loading pad at the north side, and Location 4 is under the exterior loading pad at the south side.

The comparison of strains in rebars, west face displacements, and CNFA-obtained compressive stresses are presented in APPENDIX-4.

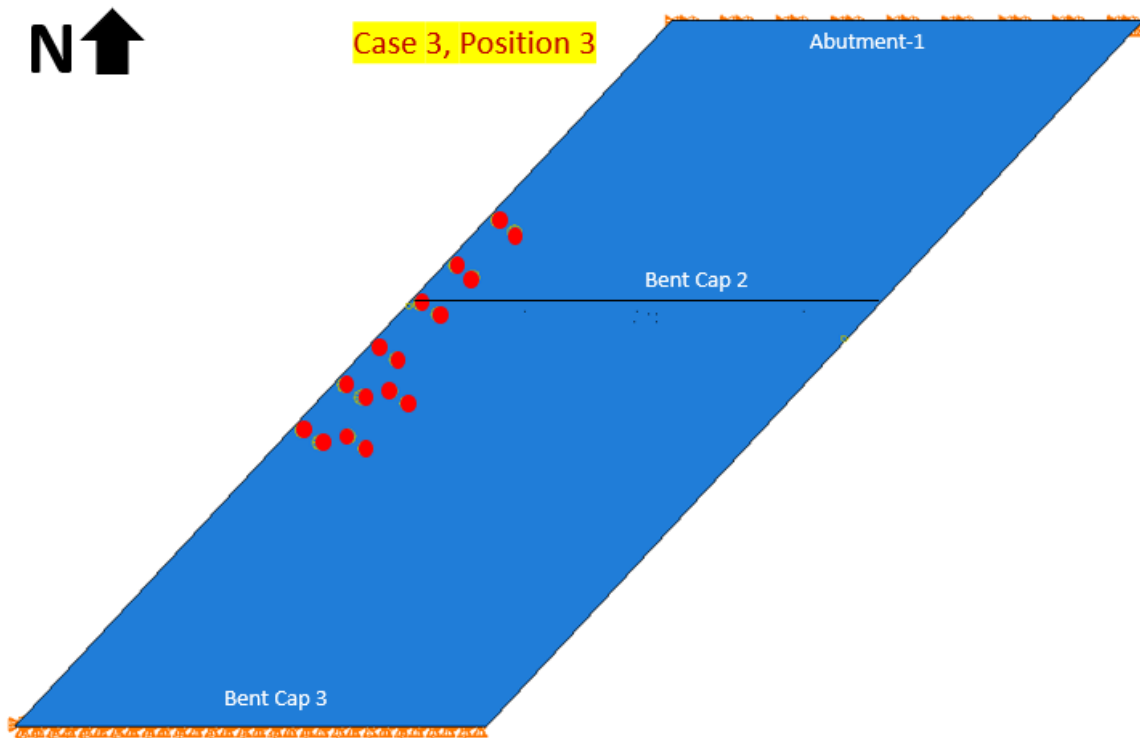


**Figure 5.10. Comparison of Average Compressive Stresses on Concrete of Static Test-1, Bent Cap 2 for Case 14**

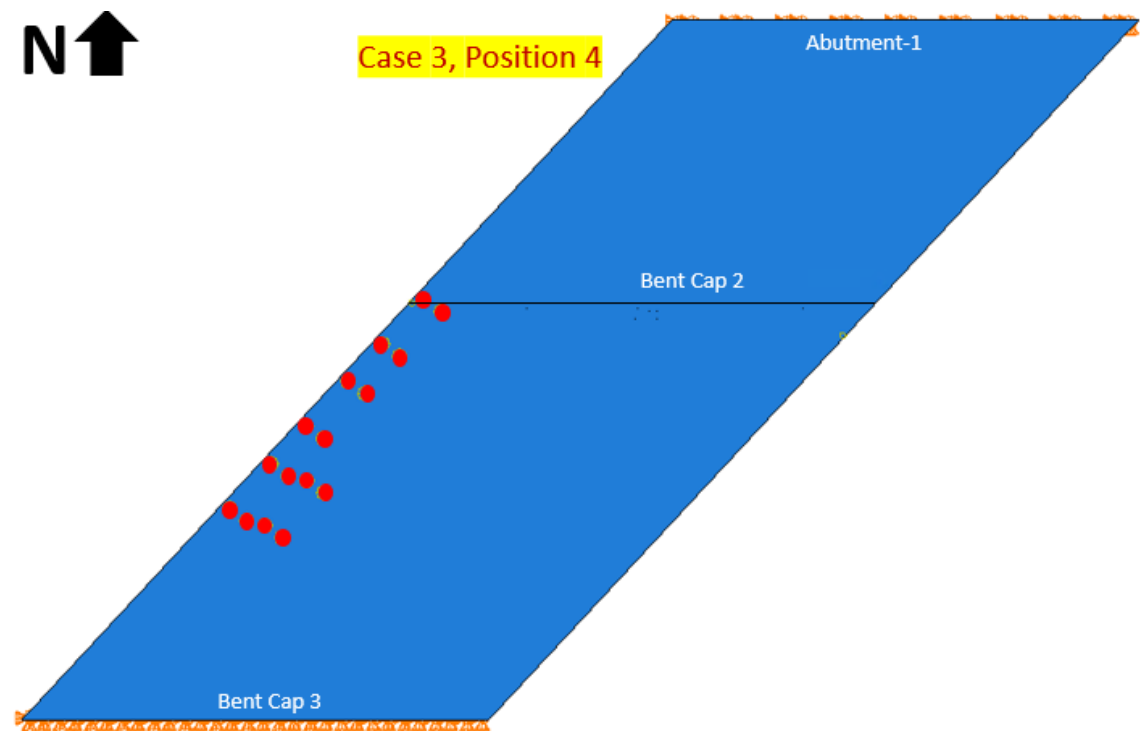
The strains in rebars, west face displacements, and average compressive stresses on concrete from the load test and updated model of Bent Cap 2 are comparable, as presented in Figures 5.5-5.10. The model calibration of Bent Cap 2 based on Static Load Test-1 (Case 1 and Case 14) is achieved from the updated material parameters (compressive strength, Young’s modulus) and concrete damaged plasticity model (CDP).

### 5.3.2 Static Test-2

The 3D FE analyses of Static Test-2 for both Case 3 and Case 9 at Position 3 and Position 4 were performed on an updated model of Bent Cap 2 with four trucks on the Donigan Road Bridge. Figures 5.11(a-b) and 5.12(a-b) show the position of four trucks on the deck over Bent Cap 2 in Static Test-2 for both Case 3 and Case 9 at Position 3 and Position 4.

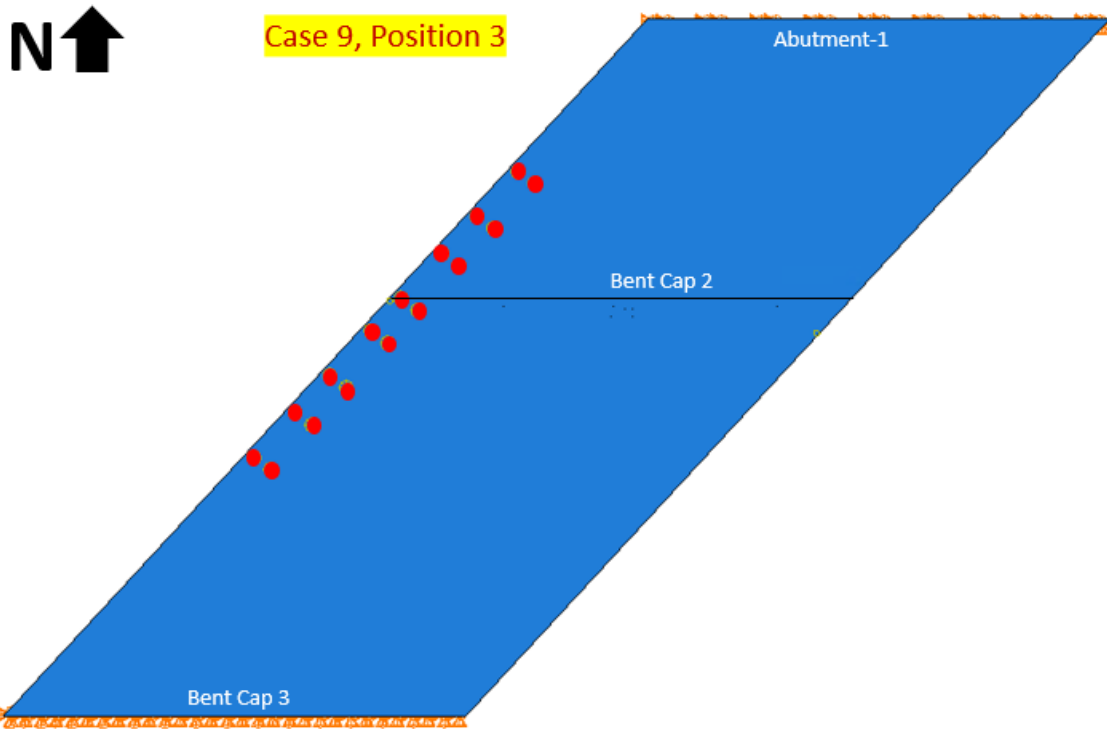


(a) Static Test-2 on Bent Cap 2 for Case 3 at Position 3

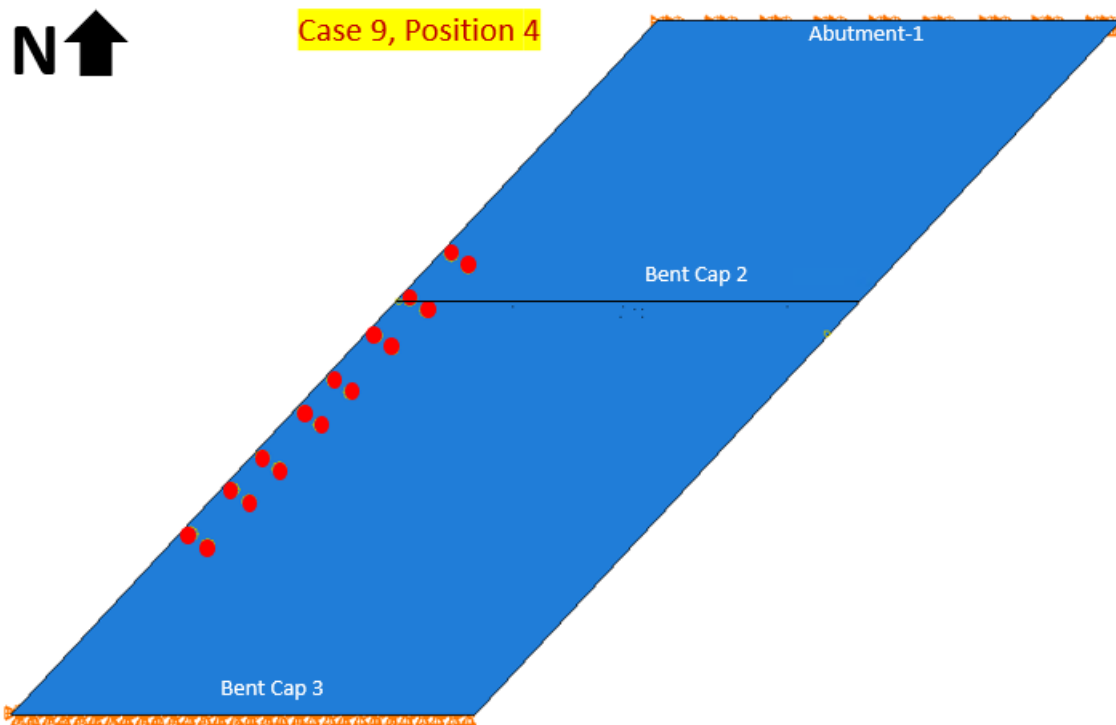


(b) Static Test-2 on Bent Cap 2 for Case 3 at Position 4

**Figure 5.11. Locations of Trucks in Static Test-2, Case 3 on Bent Cap 2**



(a) Static Test-2 on Bent Cap 2 for Case 9 at Position 3



(b) Static Test-2 on Bent Cap 2 for Case 9 at Position 4

**Figure 5.12. Locations of Trucks in Static Test-2, Case 9 on Bent Cap 2**

### 5.3.2.1 Case 3

Figures 5.13 and 5.14 illustrate the comparative analysis of the load test and updated FE model of Case 3 at Position 3 and Position 4. Figures 5.15 and 5.16 show the comparative plots of the west face displacements from the load test and updated model of Bent Cap 2 in Static Test-2 for Case 3 at Position 3 and Position 4. The tip displacements of the extended region of Bent Cap 2 (south side) in Static Test-2 for Case 3 at Position 3 from the load test and FE simulation are -0.0133 inches and -0.0121 inches, respectively. The tip displacements of the extended region of Bent Cap 2 (south side) in Static Test-2 for Case 3 at Position 4 from the load test and FE simulation are -0.0161 inches and -0.0156 inches, respectively.

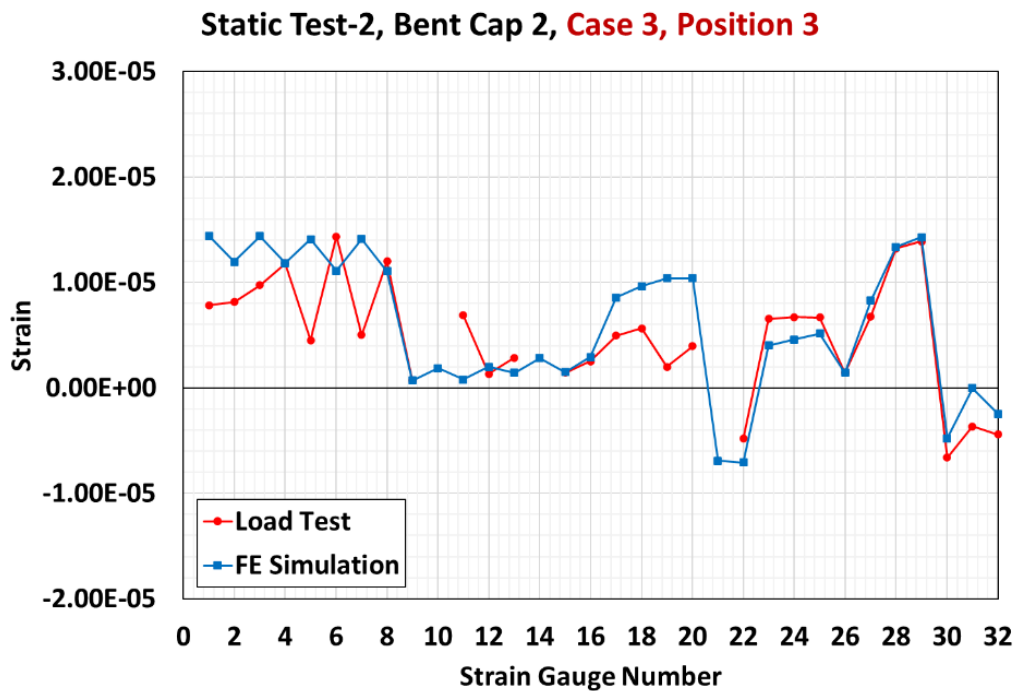


**Figure 5.13. Rebar Strains Comparison of Static Test-2, Case 3 at Position 3 on Bent Cap 2**

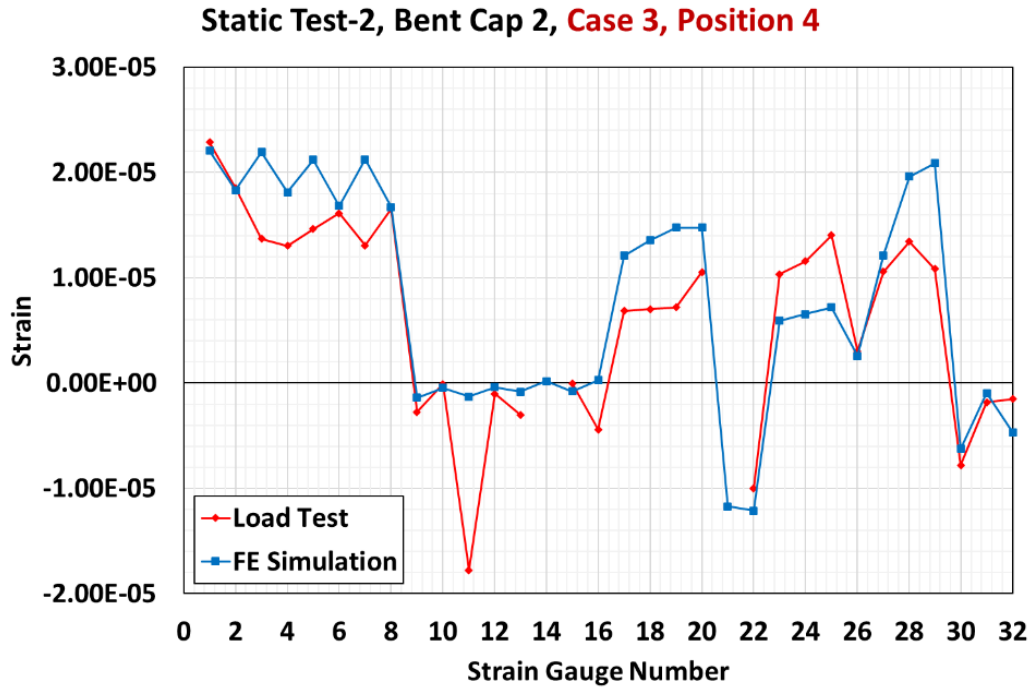


**Figure 5.14. Rebar Strains Comparison of Static Test-2, Case 3 at Position 4 on Bent Cap 2**

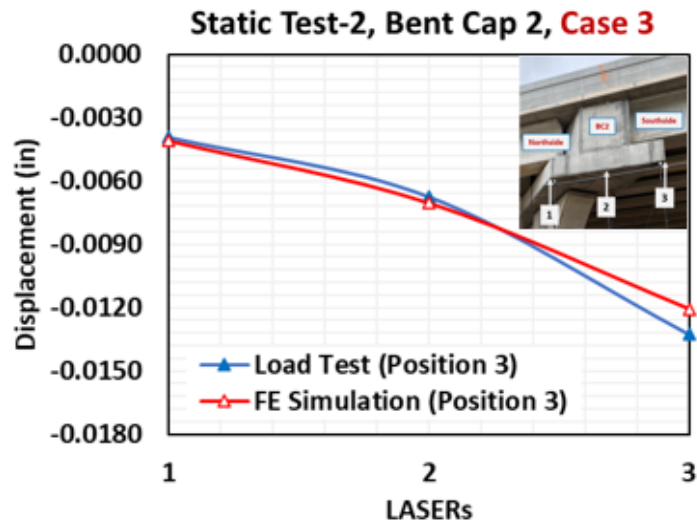


**Figure 5.15. West Face Displacements Comparison of Static Test-2, Case 3 at Position 3 on Bent Cap 2**

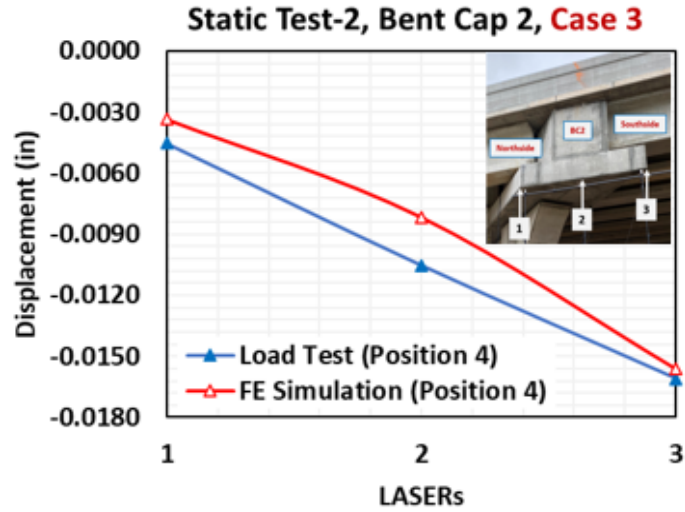


**Figure 5.16. West Face Displacements Comparison of Static Test-2, Case 3 at Position 4 on Bent Cap 2**

Figures 5.17-5.18 show the comparative analysis of CNFA-obtained average compressive stresses in the load test and average compressive stresses from the updated FE model of Case 3. In Figures 5.17-5.18, Location 1 is at Column-Bent Cap 2 interface, Location 2 is under the exterior loading pad at the north side, and Location 4 is under the exterior loading pad at the south side. The comparison of strains in rebars, west face displacements, and CNFA-obtained compressive stresses are presented in APPENDIX-4.

**Bent Cap 2, ST2, Case 3, Position 3**

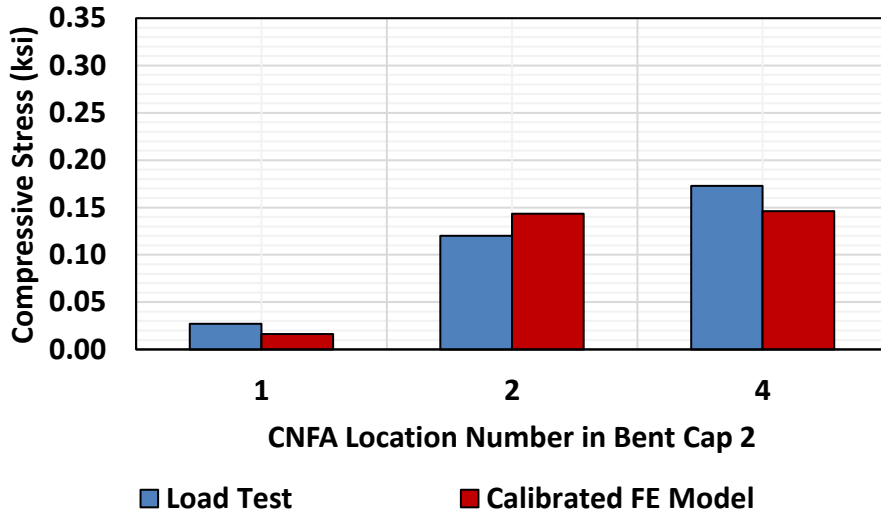


**Figure 5.17. Comparison of Average Compressive Stresses on Concrete of Static Test-2, Bent Cap 2 for Case 3 at Position 3**

**Bent Cap 2, ST2, Case 3, Position 4**

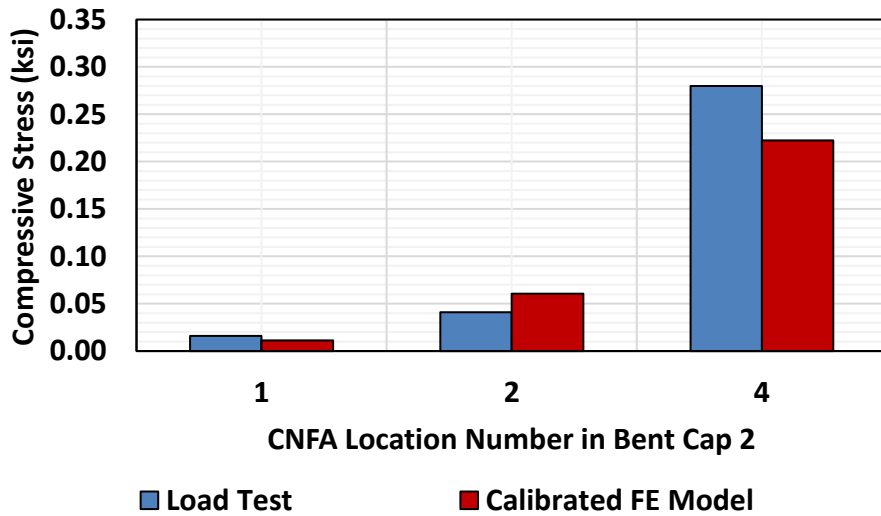


**Figure 5.18. Comparison of Average Compressive Stresses on Concrete of Static Test-2, Bent Cap 2 for Case 3 at Position 4**

### 5.3.2.2 Case 9

Figures 5.19 and 5.20 illustrate the comparative analysis of the load test and updated FE model of Case 9 at Position 3 and Position 4. Figures 5.21 and 5.22 show the comparative plots of west face displacements from the load test and updated model of Bent Cap 2 in Static Test-2 for Case 9 at Position 3 and Position 4. The tip displacements of the extended region of Bent Cap 2 (south side) in Static Test-2 for Case 9 at Position 3 from the load test and FE simulation are -0.0149 inches and -0.0137 inches, respectively. The tip displacements of the extended region of Bent Cap 2 (south side) in Static Test-2 for Case 9 at Position 4 from the load test and FE simulation are -0.0163 inches and -0.0169 inches, respectively.

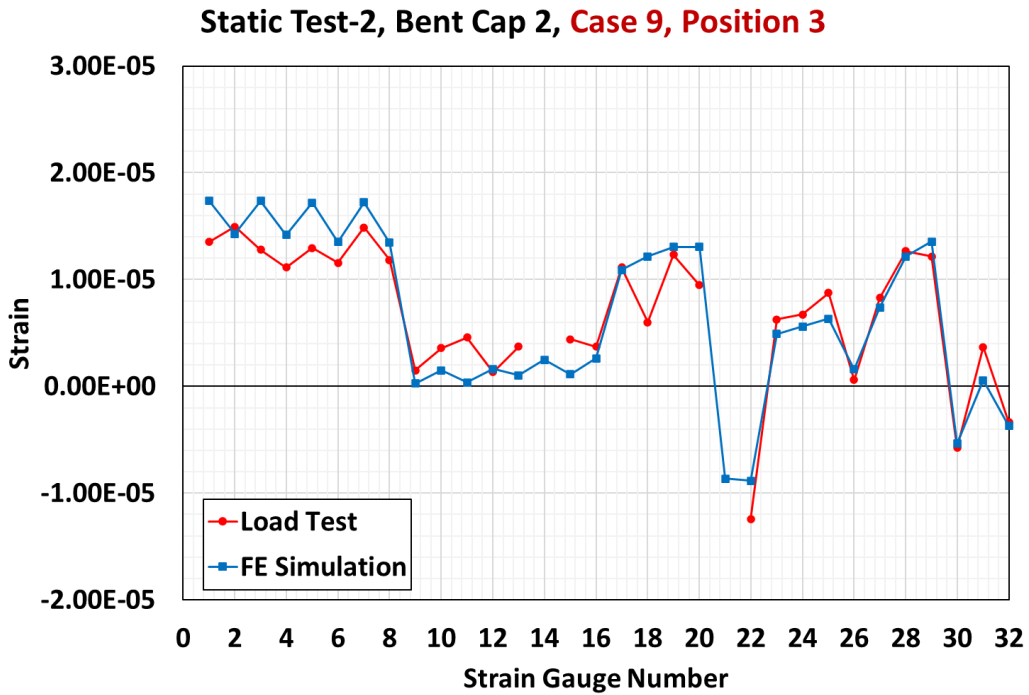


**Figure 5.19. Rebar Strains Comparison of Static Test-2, Case 9  
at Position 3 on Bent Cap 2**

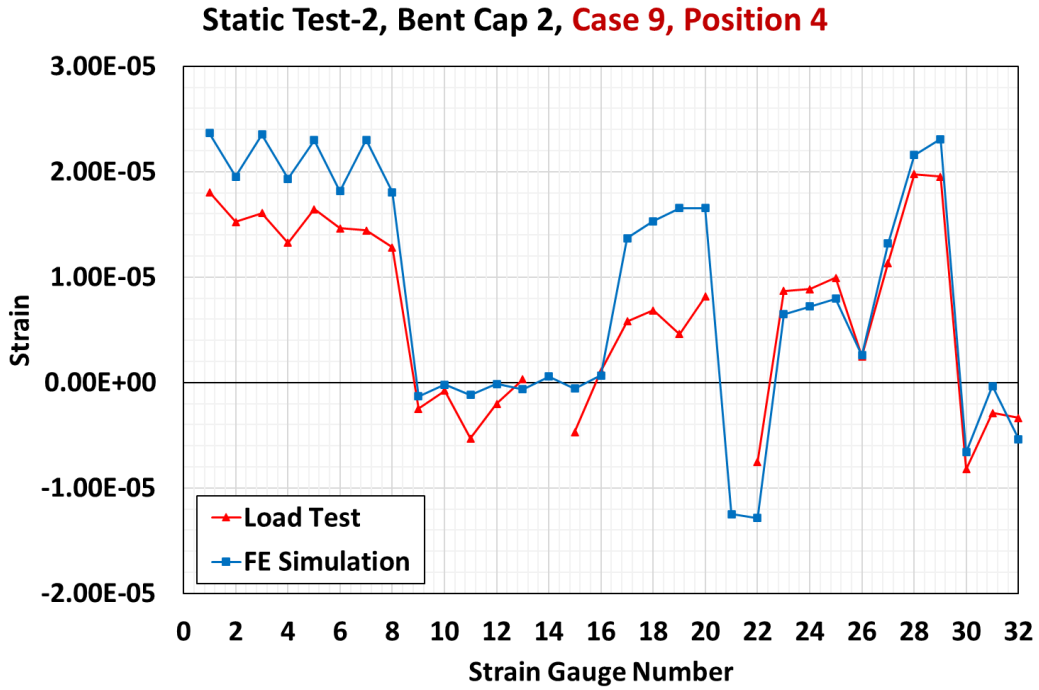


**Figure 5.20. Rebar Strains Comparison of Static Test-2, Case 9 at Position 4 on Bent Cap 2**

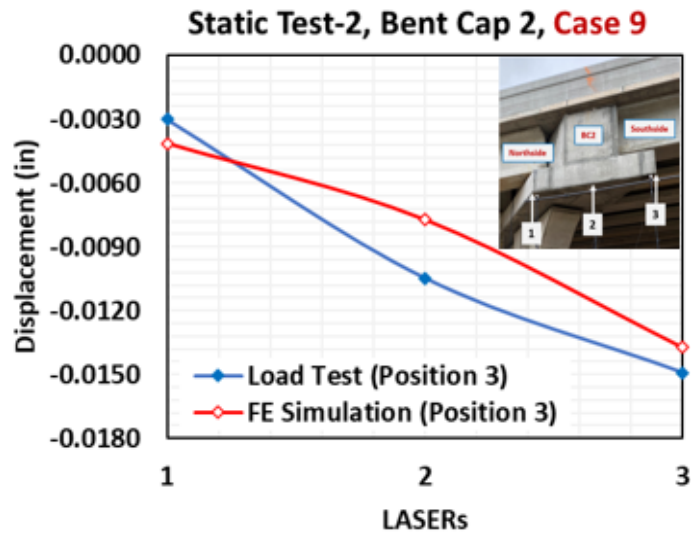


**Figure 5.21. West Face Displacements Comparison of Static Test-2, Case 3 at Position 3 on Bent Cap 2**

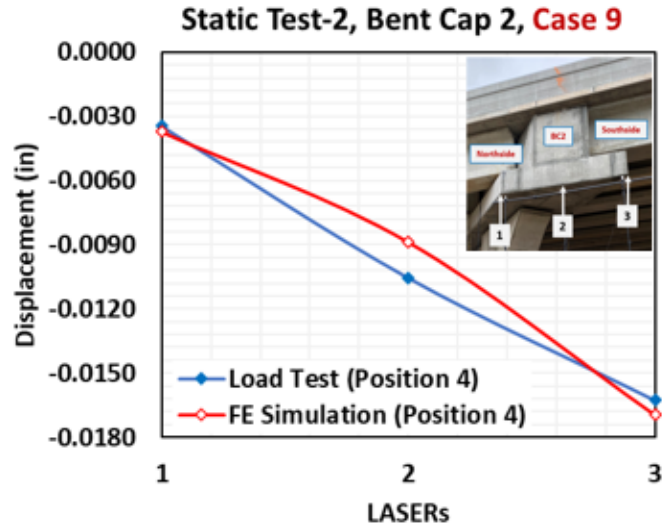


**Figure 5.22. West Face Displacements Comparison of Static Test-2, Case 3 at Position 4 on Bent Cap 2**

Figures 5.23-5.24 show the comparative analysis of CNFA-obtained average compressive stresses in the load test and average compressive stresses from the updated FE model of Case 9. In Figures 5.23-5.24, Location 1 is at Column-Bent Cap 2 interface, Location 2 is under the exterior loading pad at the north side, and Location 4 is under the exterior loading pad at the south side. The comparison of strains in rebars, west face displacements, and CNFA-obtained compressive stresses are presented in APPENDIX-4.

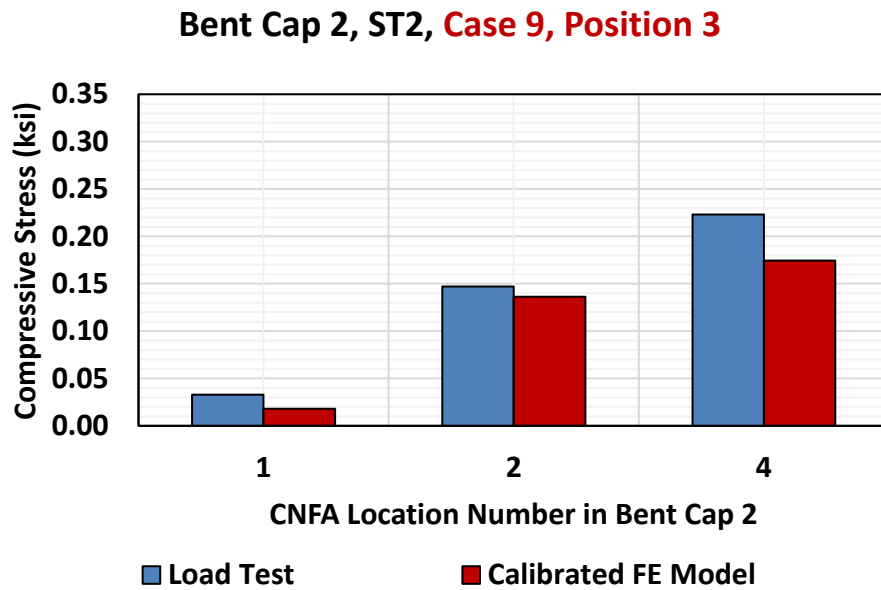


**Figure 5.23. Comparison of Average Compressive Stresses on Concrete of Static Test-2, Bent Cap 2 for Case 9 at Position 3**

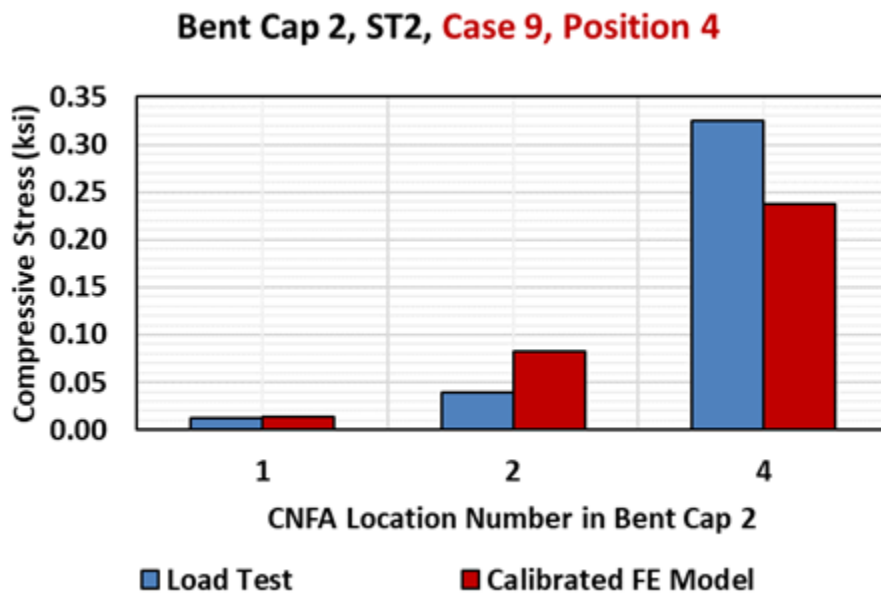


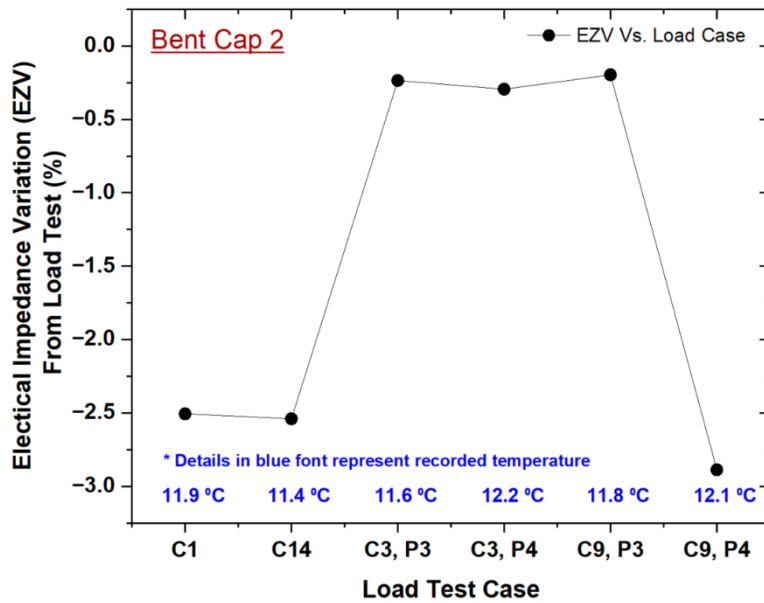
**Figure 5.24. Comparison of Average Compressive Stresses on Concrete of Static Test-2, Bent Cap 2 for Case 9 at Position 4**

The performance of CNFAs embedded in the tension zone of Bent Cap 2 (Location-3, anchored to S bars) in the static tests are summarized in Table 5.3. Figure 5.25 (a) shows the EZV

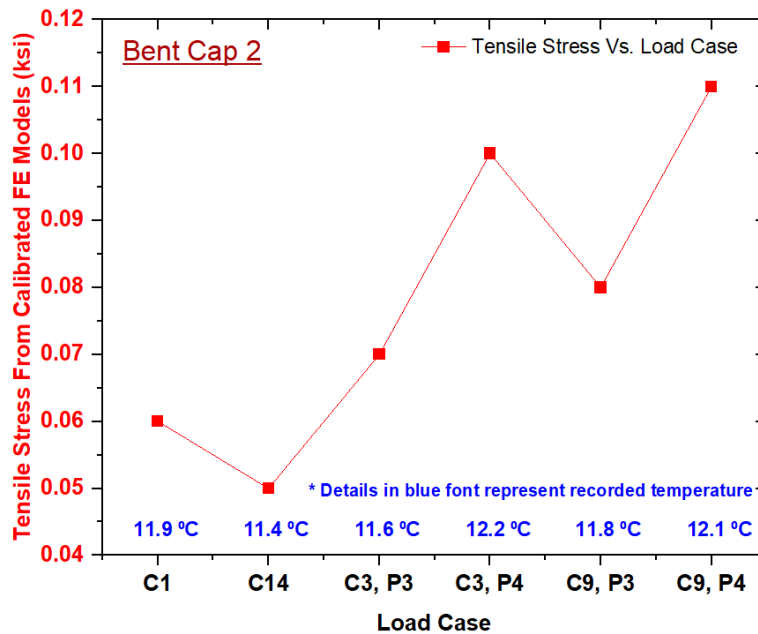
and temperature recorded during the load tests. Figure 5.25 (b) presents the equivalent tensile stresses from the calibrated model of Bent Cap 2 at Location-3.

**Table 5.3. Performance of CNFAs in Tension Zone (Location-3) of Bent Cap 2**

Case	EZV (%) from Load Test	Tensile Stress from Calibrated FE Model (ksi)	Temperature (°C)
1	-2.51	0.06	11.9
14	-2.54	0.05	11.4
3, Position 3	-0.24	0.07	11.6
3, Position 4	-0.29	0.10	12.2
9, Position 3	-0.20	0.08	11.8
9, Position 4	-2.89	0.11	12.1



(a) EZV of CNFA at Location-3 of Bent Cap 2



(b) Tensile Stresses from Calibrated FE Models of Bent Cap 2

**Figure 5.26. Performance of CNFAs in Tension Zone of Bent Cap 2**

The strains in rebars, west face displacement, and average compressive stresses on concrete from the load test and updated model of Bent Cap 2 are comparable, as presented in Figures 5.13-5.24. The model calibration of Bent Cap 2 based on Static Load Test-2 (Case 3 and Case 9) is achieved from the updated material parameters (compressive strength, Young's modulus) and the concrete damaged plasticity model (CDP).

### 5.3.3 Dynamic Test-1

The 3D FE analyses of Dynamic Test-1 for Case 9 and Case 14 were performed on an updated model of Bent Cap 2 with four trucks on the Donigan Road Bridge. Figures 5.27 and 5.28 show the position of four trucks on the deck over Bent Cap 2 in Dynamic Test-1 for Case 9 and Case 14.

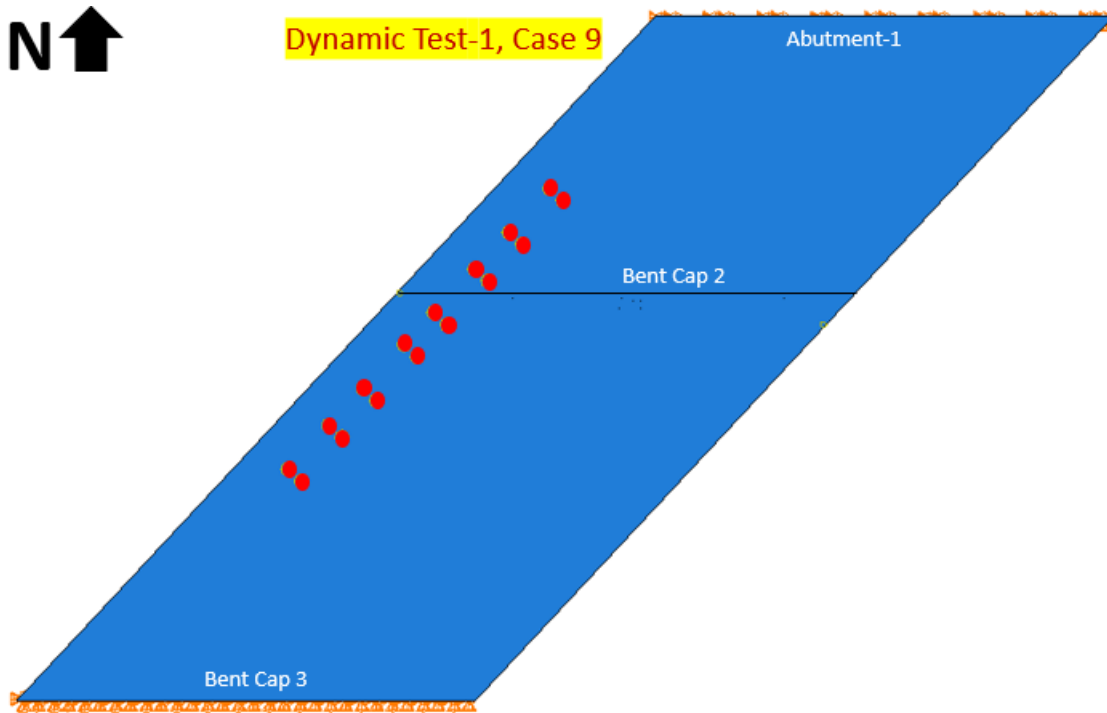


Figure 5.27 Locations of Trucks in Dynamic Test-1, Case 9 on Bent Cap 2

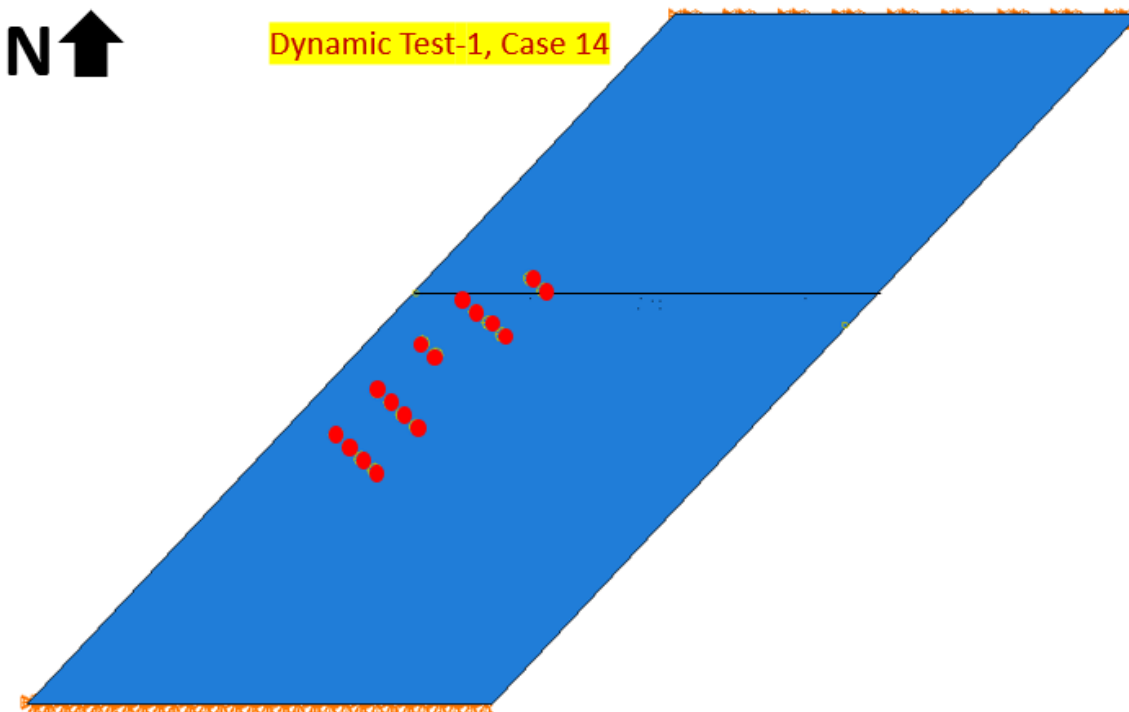


Figure 5.28. Locations of Trucks in Dynamic Test-1, Case 14 on Bent Cap 2

### 5.3.3.1 Case 9

Figure 5.29 illustrates the comparative analysis of the load test and updated FE model of Case 9. Figure 5.30 shows the comparative plot of west face displacements from the load test and updated model of Bent Cap 2 in Dynamic Test-1 for Case 9. The tip displacements of the extended region of Bent Cap 2 (south side) in Dynamic Test-1 for Case 9 from the load test and FE simulation are -0.0051 inches and -0.0047 inches, respectively. The comparison of strains in rebars, and west face displacements, are presented in APPENDIX-4.

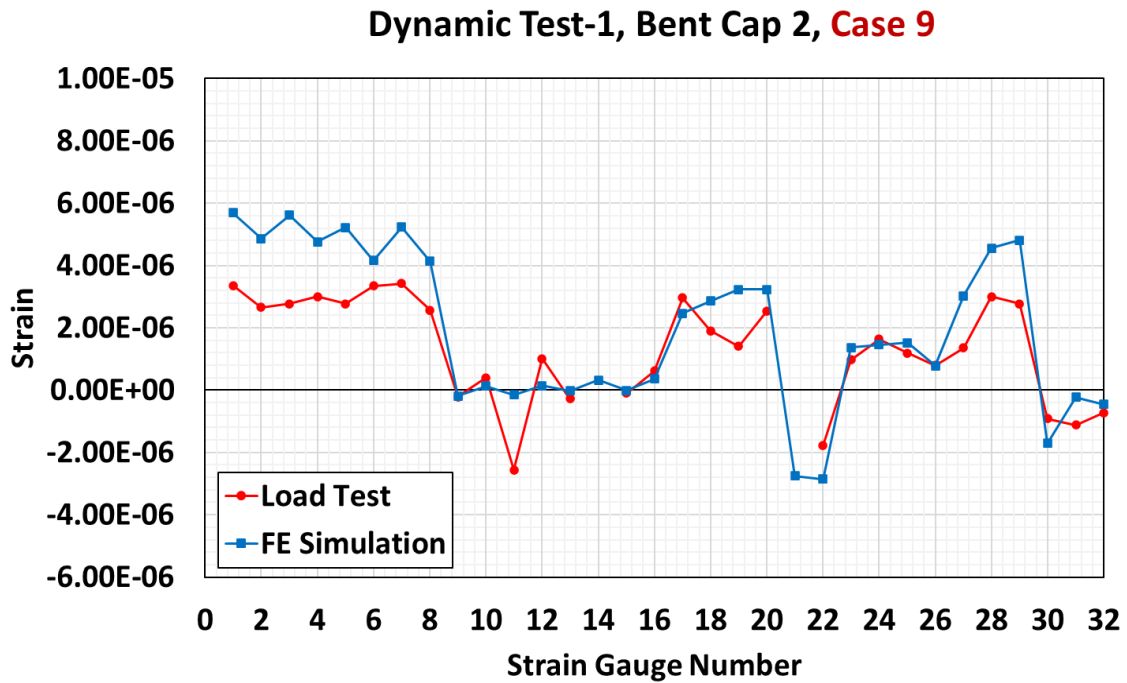
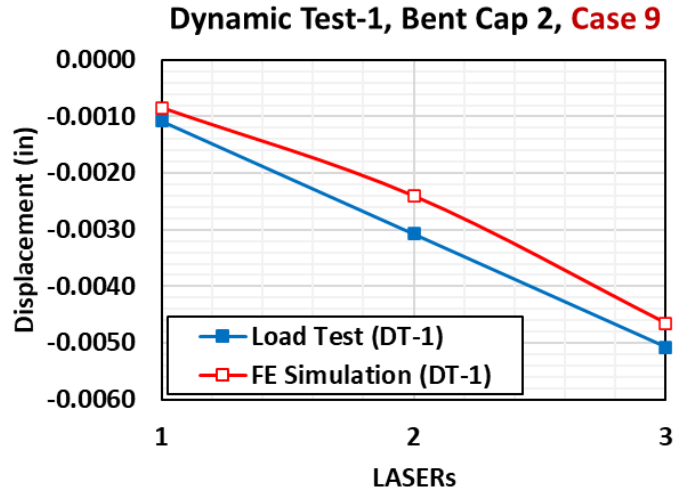


Figure 5.29. Rebar Strains Comparison of Dynamic Test-1, Bent Cap 2 for Case 9



**Figure 5.30. West Face Displacements Comparison of Dynamic Test-1, Bent Cap 2 for Case 9**

### 5.3.3.2 Case 14

Figure 5.31 illustrates the comparative analysis of the load test and updated FE model of Case 14. Figure 5.32 shows the comparative plot of west face displacements from the load test and updated model of Bent Cap 2 in Dynamic Test-1 for Case 14. The tip displacements of the extended region of Bent Cap 2 (south side) in Dynamic Test-1 for Case 9 from the load test and FE simulation are -0.0036 inches and -0.0033 inches, respectively. The comparison of strains in rebars, and west face displacements, are presented in APPENDIX-4.

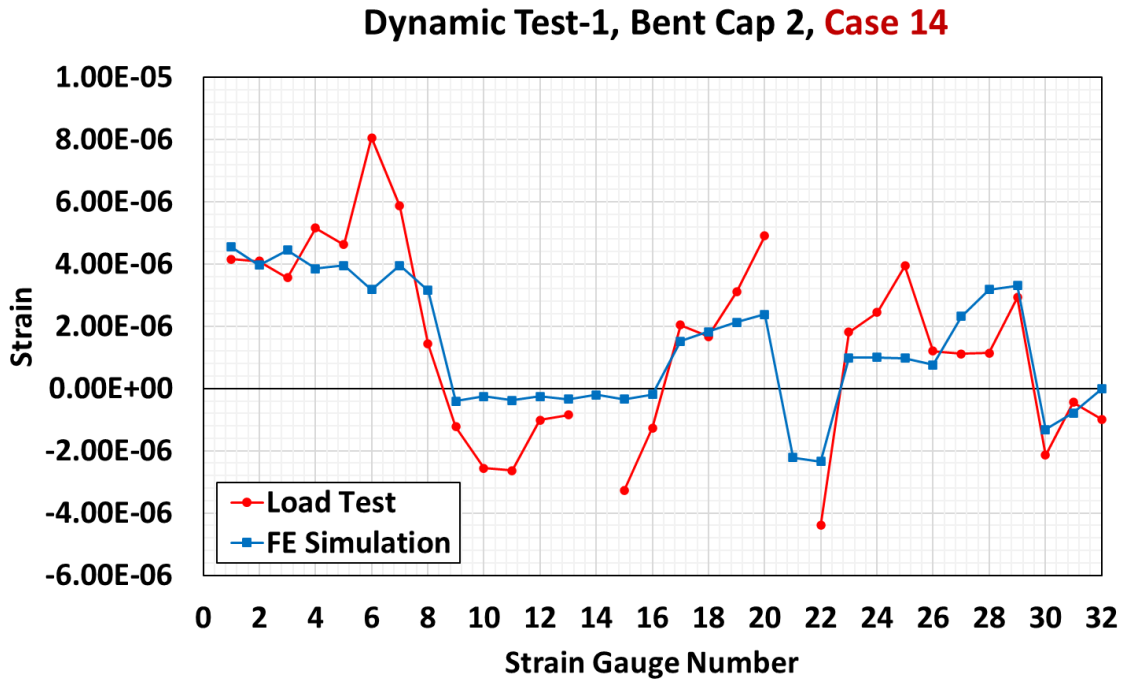


Figure 5.31. Rebar Strains Comparison of Dynamic Test-1, Bent Cap 2 for Case 14

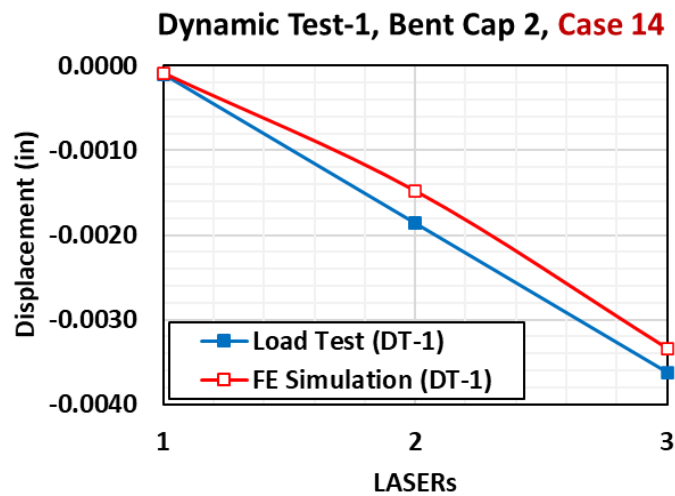


Figure 5.32. West Face Displacements Comparison of Dynamic Test-1, Bent Cap 2 for Case 14

The strains in rebars, west face displacements, and average compressive stresses on concrete from the load test and updated model of Bent Cap 2 are comparable, as presented in Figures 5-29-5.32. The model calibration of Bent Cap 2 based on Dynamic Load Test-1 (Case 9

and Case 14) is achieved from the updated material parameters (compressive strength, Young's modulus) and the concrete damaged plasticity model (CDP).

#### 5.4 CALIBRATION OF FE MODELS OF BENT CAP 7 WITH LOAD TEST DATA

The FE model of Bent Cap 7 is revised into two phases (Phase 1 and Phase 2) as it was cast during construction (see Figure 5.2). The revised FE model of Bent Cap 7 is updated with the concrete properties as presented in Table 5.2. The updated model of Bent Cap 7 is simulated in ABAQUS with the four trucks positioned on the deck during the load tests.

##### 5.4.1 Static Test-1

The 3D FE analyses of Static Test-1 for Case 1 and Case 11 were performed on an updated model of Bent Cap 7 with four trucks on the Donigan Road Bridge. Figures 5.33 and 5.34 show the position of four trucks on the deck over Bent Cap 7 in Static Test-1 for Case 1 and Case 11.

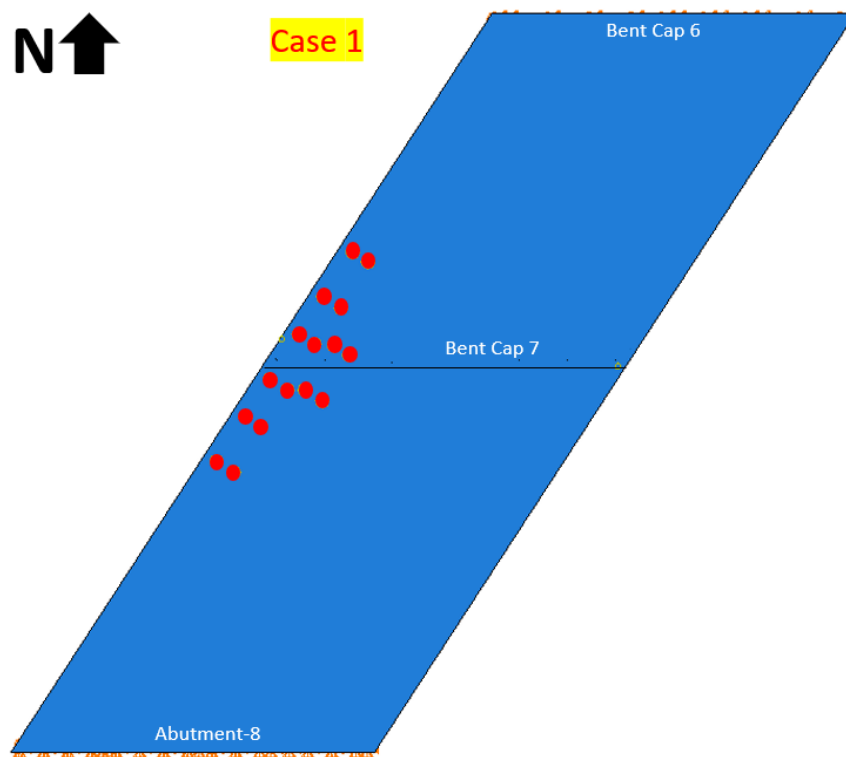
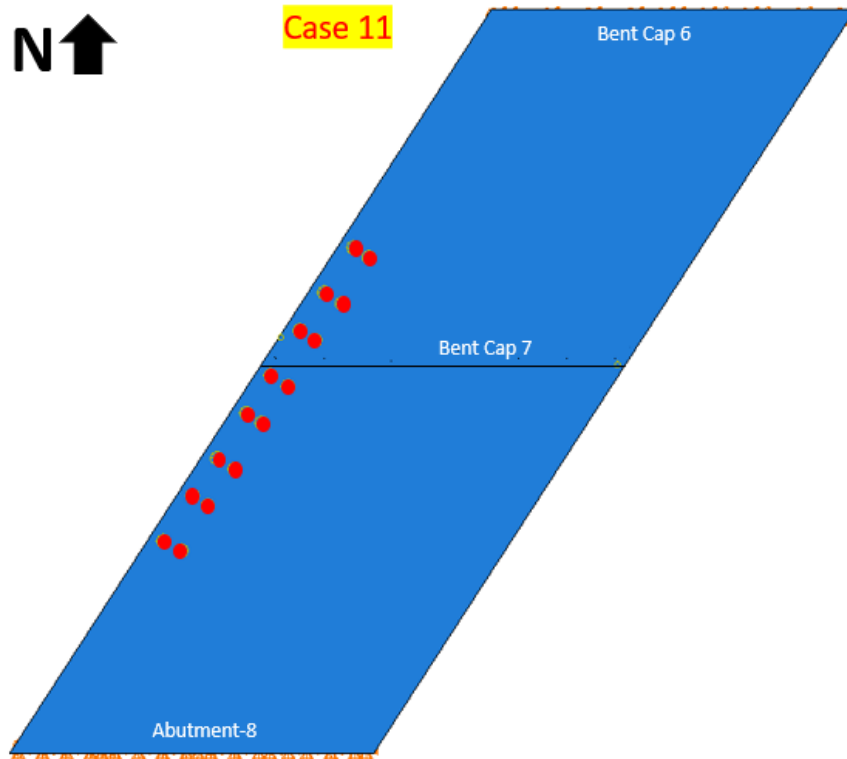


Figure 5.33. Locations of Trucks in Static Test-1, Case 1 on Bent Cap 7



**Figure 5.34. Locations of Trucks in Static Test-1, Case 11 on Bent Cap 7**

#### **5.4.1.1 Case 1**

Figure 5.35 shows the comparative analysis of the load test and updated FE model of Case 1. Figure 5.36 shows the comparative plot of west face displacements from the load test and updated model of Bent Cap 7 in Static Test-1 for Case 1. The tip displacements of the extended region of Bent Cap 7 (south side) in Static Test-1 for Case 1 from the load test and FE simulation are -0.0091 inches and -0.0098 inches, respectively.

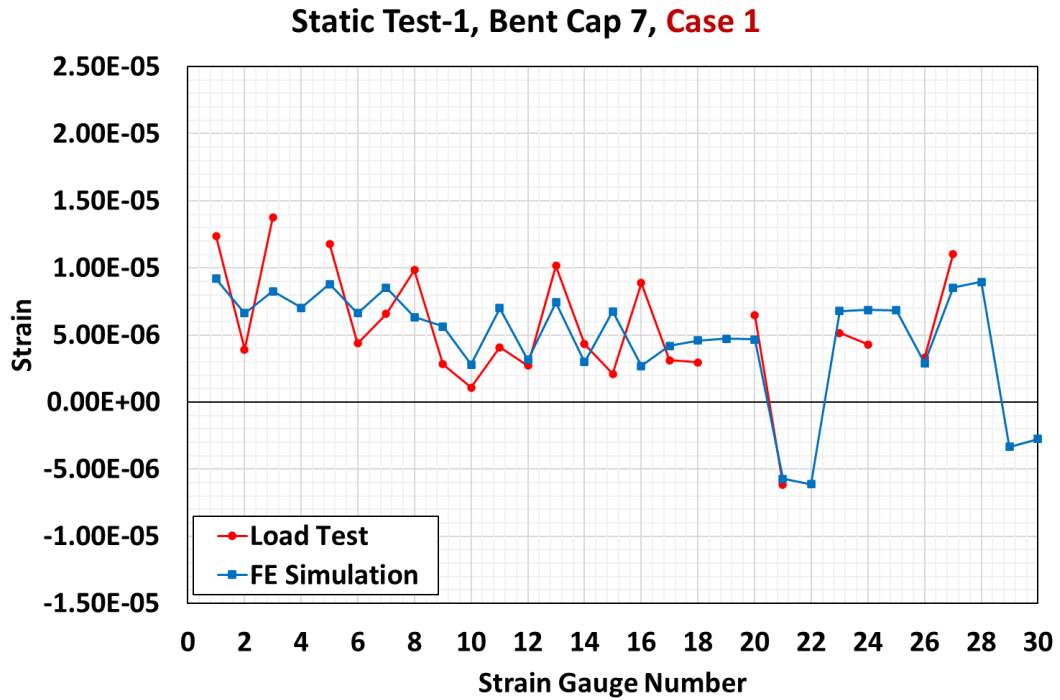


Figure 5.35. Rebar Strains Comparison of Static Test-1, Bent Cap 7 for Case 1

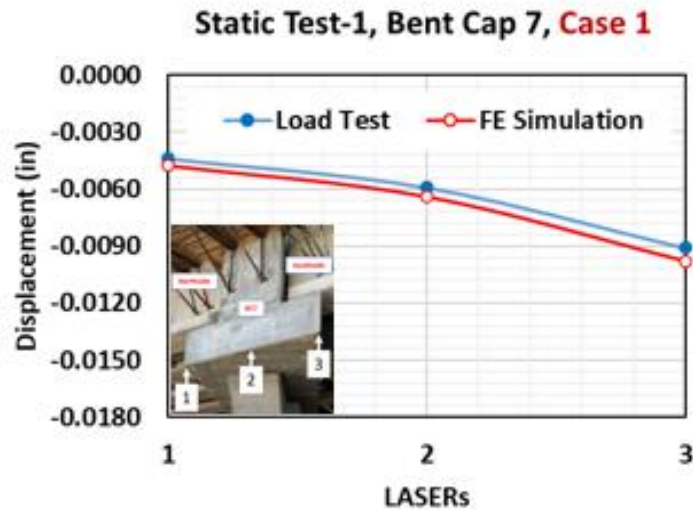
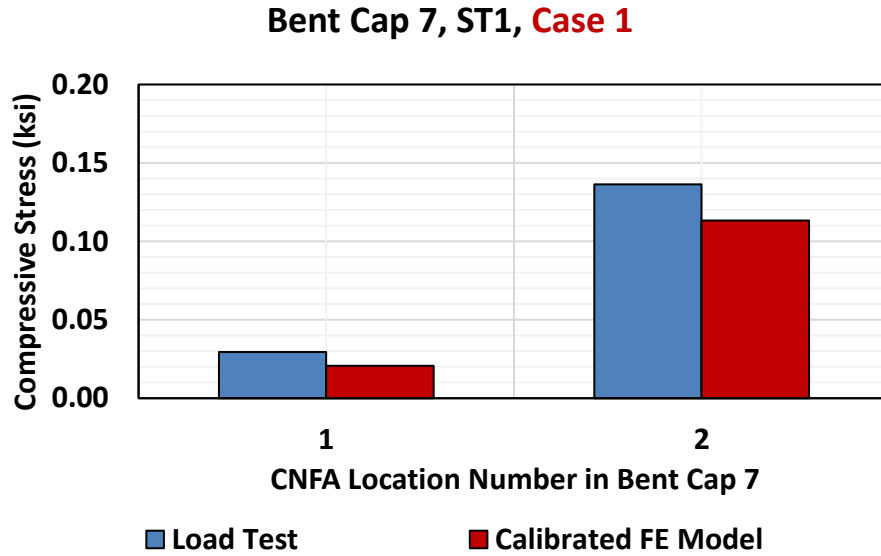


Figure 5.36. West Face Displacements Comparison of Static Test-1, Bent Cap 7 for Case 1

Figure 5.37 shows the comparative analysis of CNFA-obtained compressive stresses in the load test and compressive stresses from the updated FE model of Case 1. In Figure 5.37, Location 1 is at Column-Bent Cap 7 interface, and Location 2 is under the exterior loading pad at the north

side. The comparison of strains in rebars, west face displacements, and CNFA-obtained compressive stresses are presented in APPENDIX-5.



**Figure 5.37. Comparison of Average Compressive Stresses on Concrete of Static Test-1, Bent Cap 7 for Case 1**

#### 5.4.1.2 Case 11

Figure 5.38 shows the comparative analysis of the load test and updated FE model of Case 11. Figure 5.39 shows the comparative plot of west face displacements from the load test and updated model of Bent Cap 7 in Static Test-1 for Case 11. The tip displacements of the extended region of Bent Cap 7 (south side) in Static Test-1 for Case 11 from the load test and FE simulation are -0.0151 inches and -0.0136 inches, respectively.

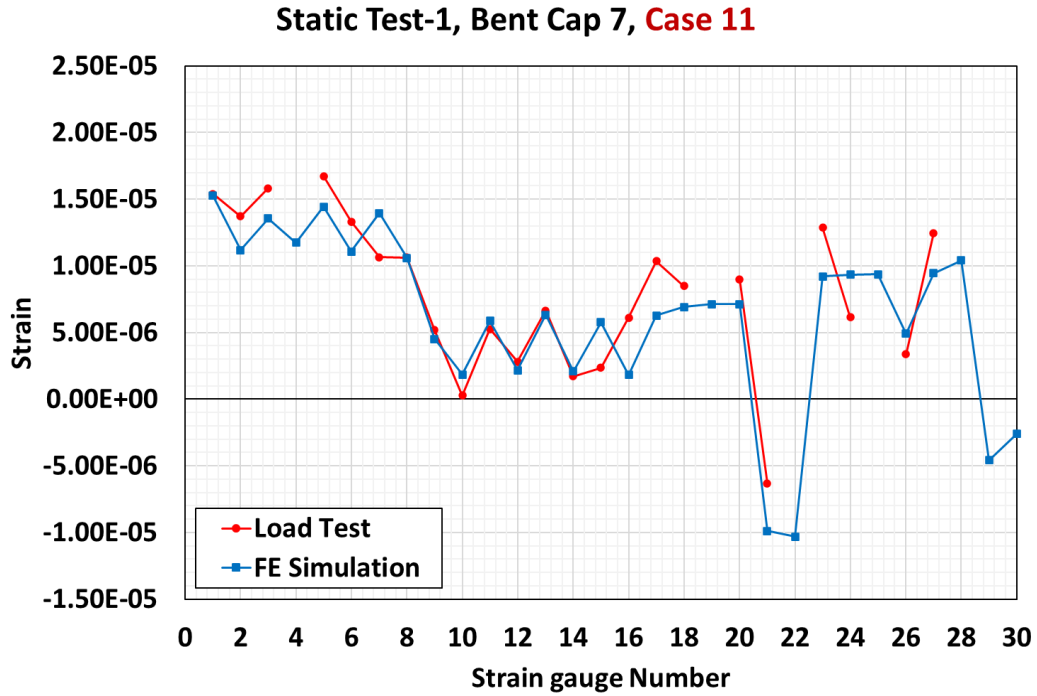


Figure 5.38. Rebar Strains Comparison of Static Test-1, Bent Cap 7 for Case 11

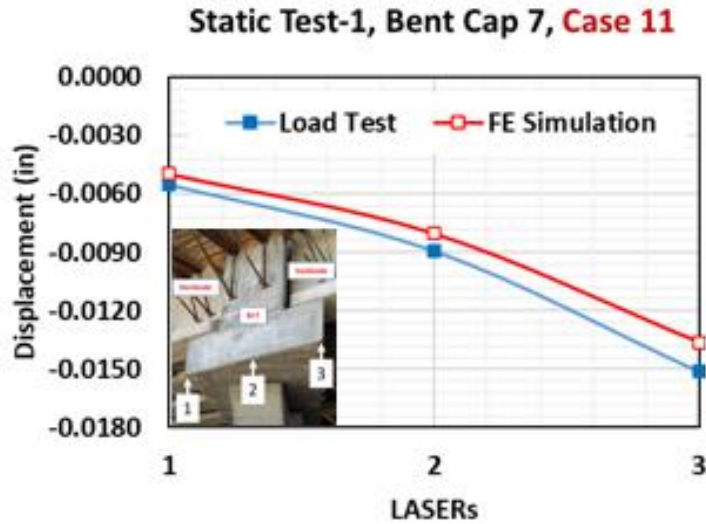
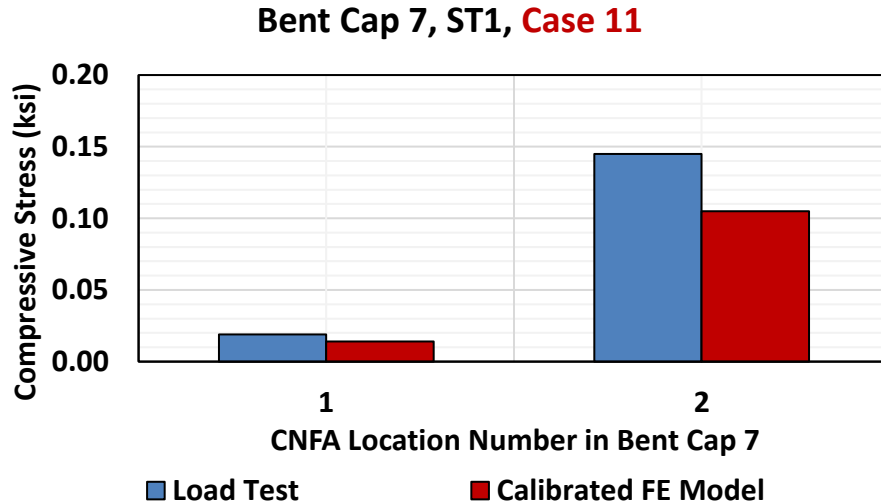


Figure 5.39. West Face Displacements Comparison of Static Test-1, Bent Cap 7 for Case 11

Figure 5.40 shows the comparative analysis of CNFA-obtained compressive stresses in the load test and the compressive stresses from the updated FE model of Case 11. In Figure 5.40, Location 1 is at Column-Bent Cap 7 interface, and Location 2 is under the exterior loading pad at

the north side. The comparison of strains in rebars, west face displacements, and CNFA-obtained compressive stresses are presented in APPENDIX-5.

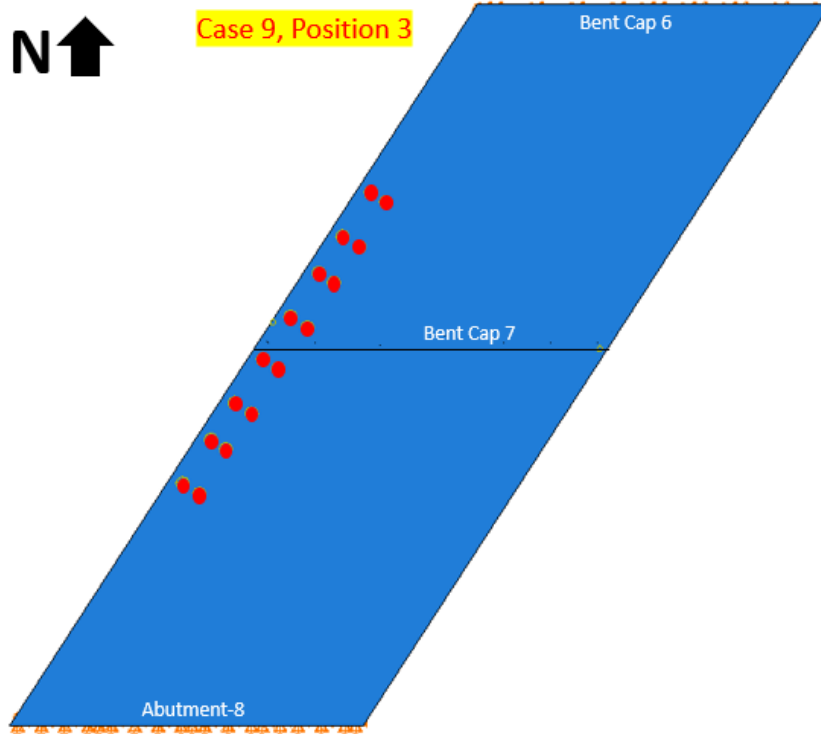


**Figure 5.40. Comparison of Average Compressive Stresses on Concrete of Static Test-1, Bent Cap 7 for Case 11**

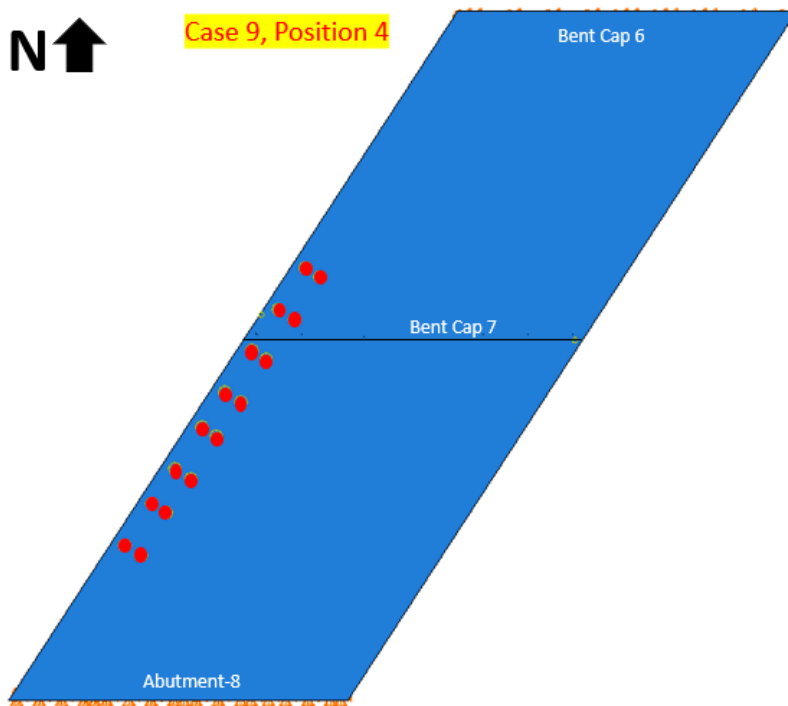
The strains in rebars, west face displacements, and average compressive stresses on concrete from the load test and updated model of Bent Cap 7 are comparable, as presented in Figures 5.35-5.40. The model calibration of Bent Cap 7 based on Static Load Test-1 (Case 1 and Case 11) is achieved from the updated material parameters (compressive strength, Young’s modulus) and concrete damaged plasticity model (CDP).

#### **5.4.2 Static Test-2**

The 3D FE analyses of Static Test-2 for both Case 9 and Case 14 at Position 3 and Position 4 were performed on an updated model of Bent Cap 7 with four trucks on the Donigan Road Bridge. Figures 5.41(a-b) and 5.42(a-b) show the position of four trucks on the deck over Bent Cap 7 in Static Test-2 for both Case 9 and Case 14 at Position 3 and Position 4.

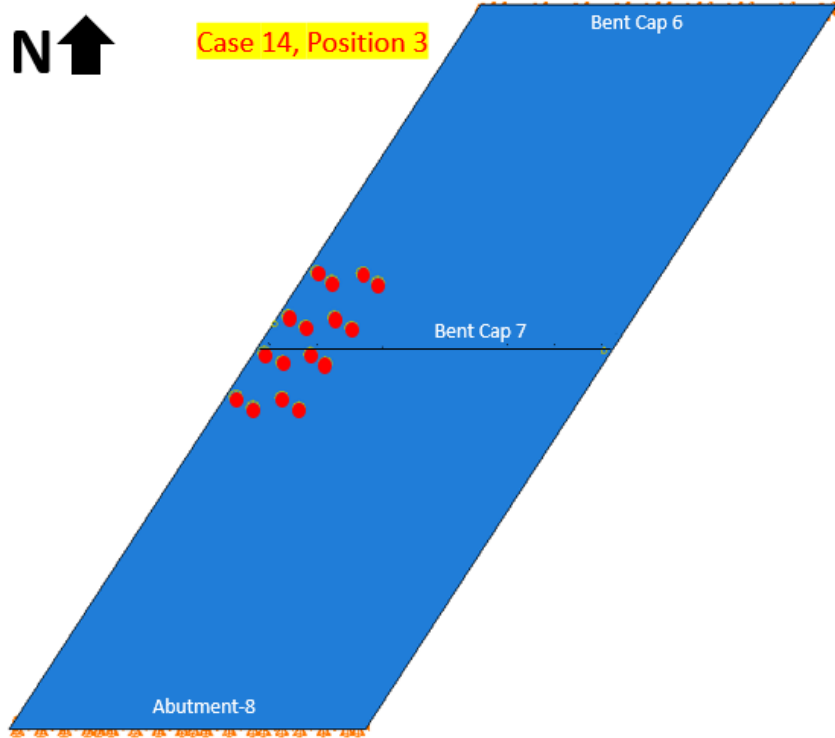


(a) Static Test-2 on Bent Cap 7 for Case 9 at Position 3

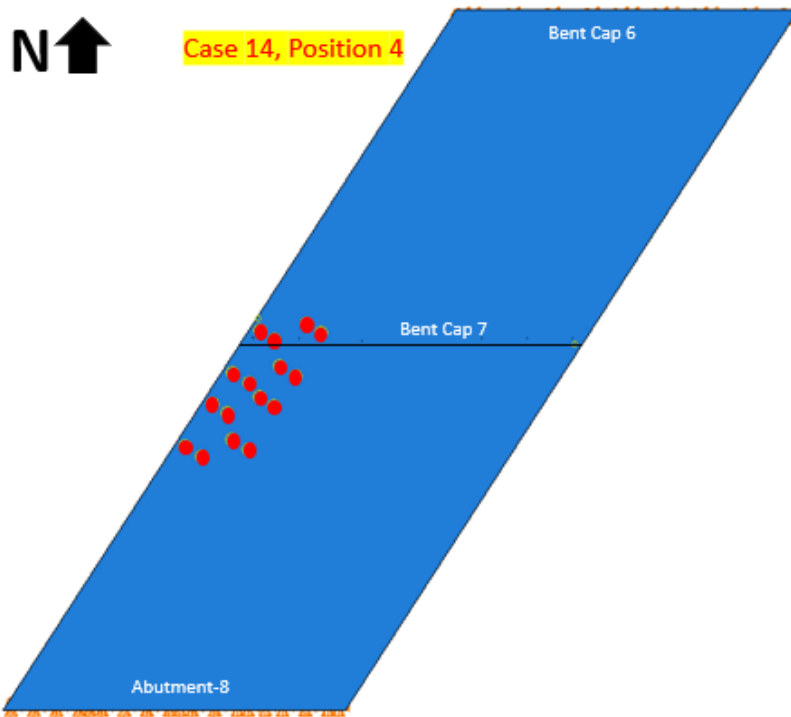


(b) Static Test-2 on Bent Cap 7 for Case 9 at Position 4

**Figure 5.41. Locations of Trucks in Static Test-2, Case 9 on Bent Cap 7**



(a) Static Test-2 on Bent Cap 7 for Case 14 at Position 3



(b) Static Test-2 on Bent Cap 7 for Case 14 at Position 4

**Figure 5.42. Locations of Trucks in Static Test-2, Case 14 on Bent Cap 7**

### 5.4.2.1 Case 9

Figures 5.43 and 5.44 illustrate the comparative analysis of the load test and updated FE model of Case 9 at Position 3 and Position 4. Figures 5.45 and 5.46 show the comparative plots of west face displacements from the load test and updated model of Bent Cap 7 in Static Test-2 for Case 9 at Position 3 and Position 4. The tip displacements of the extended region of Bent Cap 7 (south side) in Static Test-2 for Case 9 at Position 3 from the load test and FE simulation are -0.0097 inches and -0.0125 inches, respectively. The tip displacements of the extended region of Bent Cap 7 (south side) in Static Test-2 for Case 9 at Position 4 from the load test and FE simulation are -0.0161 inches and -0.0158 inches, respectively.

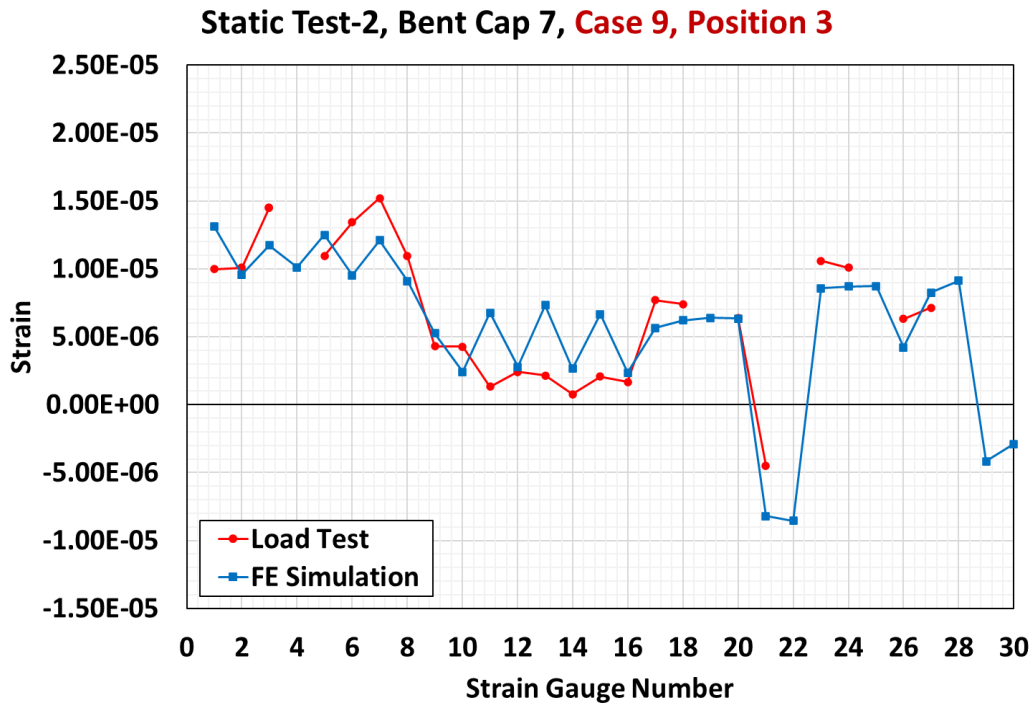
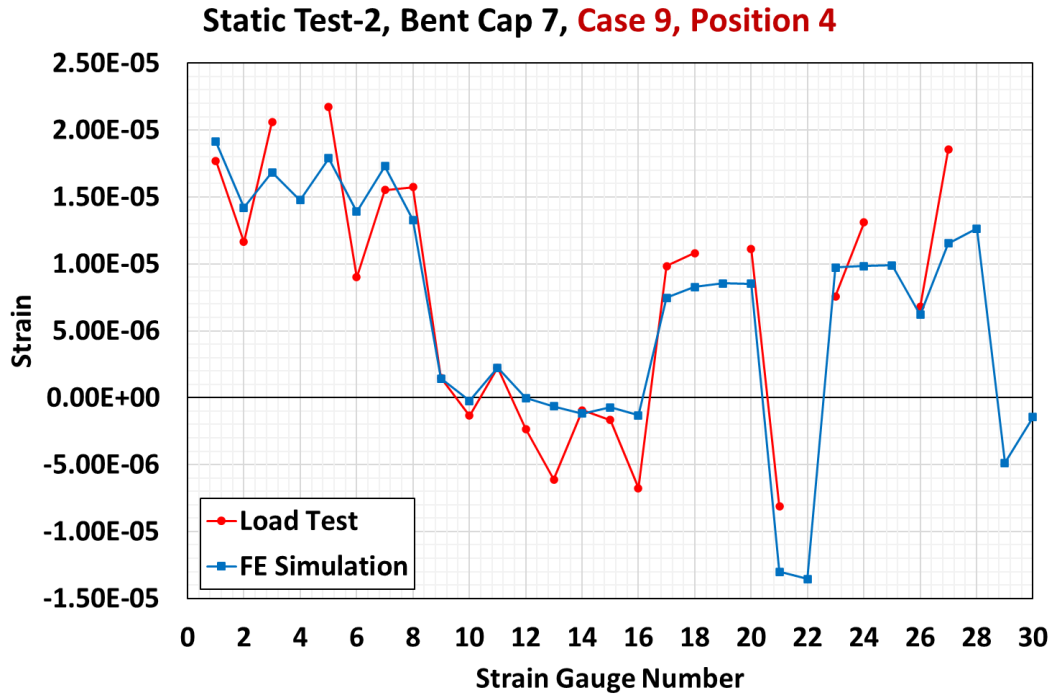
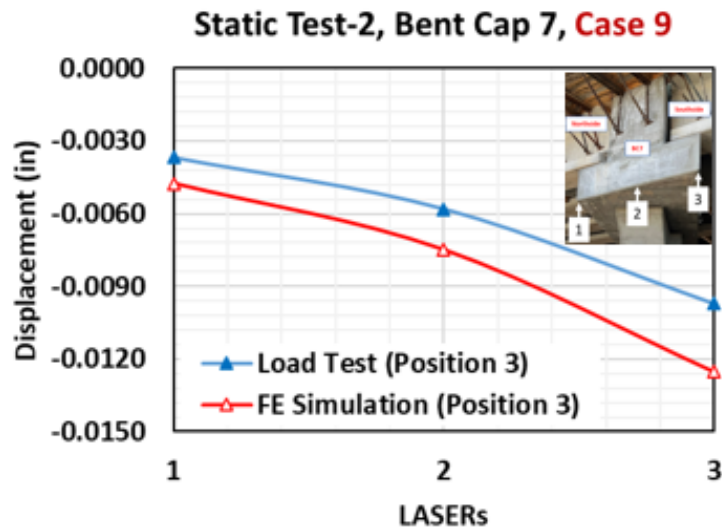


Figure 5.43. Rebar Strains Comparison of Static Test-2, Case 9 at Position 3 on Bent Cap 7



**Figure 5.44. Rebar Strains Comparison of Static Test-2, Case 9 at Position 4 on Bent Cap 7**



**Figure 5.45. West Face Displacements Comparison of Static Test-2, Case 3 at Position 3 on Bent Cap 7**

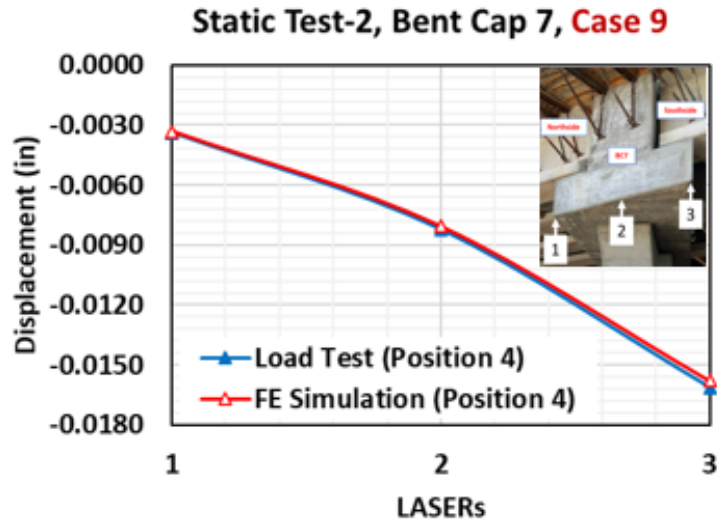


**Figure 5.46. West Face Displacements Comparison of Static Test-2, Case 3 at Position 4 on Bent Cap 7**

Figures 5.47-5.48 show the comparative analysis of CNFA-obtained average compressive stresses in the load test and average compressive stresses from the updated FE model of Case 9. In Figures 5.47-5.48, Location 1 is at Column-Bent Cap 7 interface, and Location 2 is under the exterior loading pad at the north side. The comparison of strains in rebars, west face displacements, and CNFA-obtained compressive stresses are presented in APPENDIX-5.

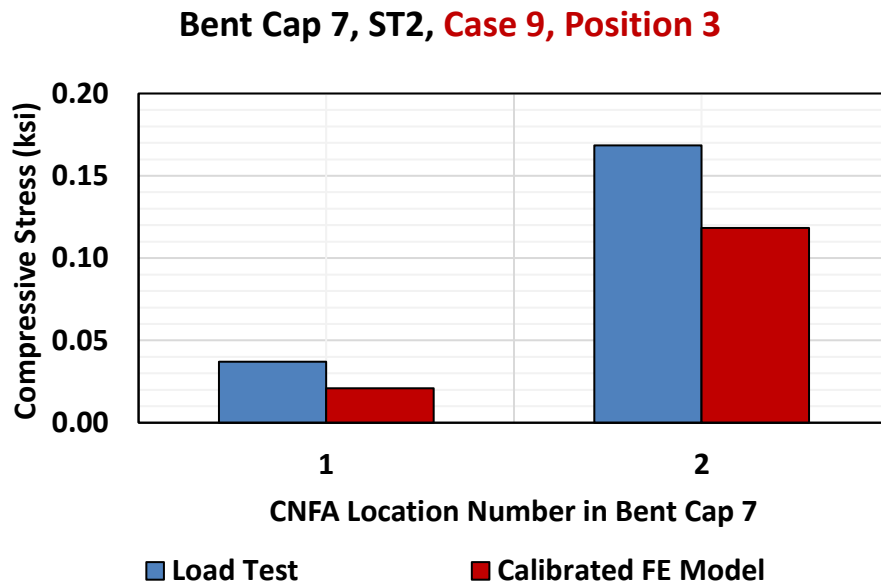


Figure 5.47. Comparison of Average Compressive Stresses on Concrete of Static Test-2, Bent Cap 7 for Case 9 at Position 3

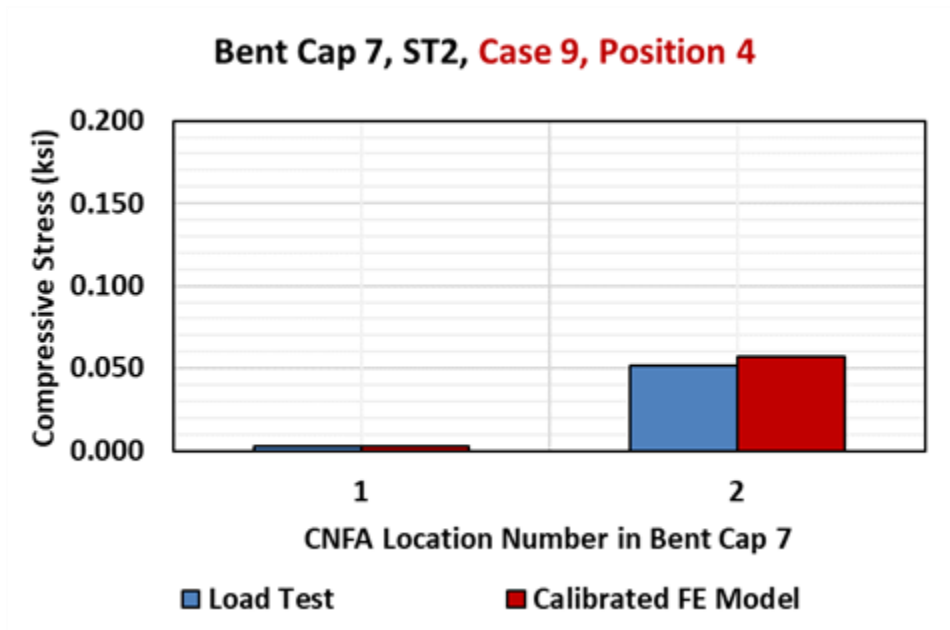
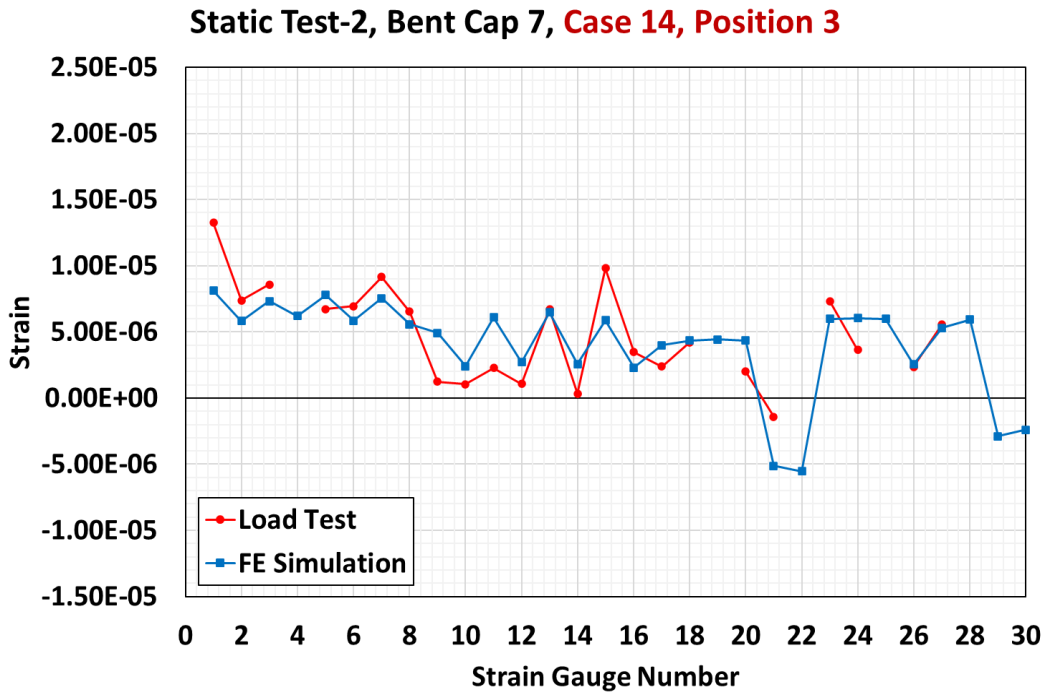


Figure 5.48. Comparison of Average Compressive Stresses on Concrete of Static Test-2, Bent Cap 7 for Case 9 at Position 4

### 5.4.2.2 Case 14

Figures 5.49 and 5.50 illustrate the comparative analysis of the load test and updated FE model of Case 14 at Position 3 and Position 4. Figures 5.51 and 5.52 show the comparative plots of west face displacements from the load test and updated model of Bent Cap 7 in Static Test-2 for Case 14 at Position 3 and Position 4. The tip displacements of the extended region of Bent Cap 7 (south side) in Static Test-2 for Case 14 at Position 3 from the load test and FE simulation are -0.0094 inches and -0.0092 inches, respectively. The tip displacements of the extended region of Bent Cap 7 (south side) in Static Test-2 for Case 14 at Position 4 from the load test and FE simulation are -0.0133 inches and -0.0140 inches, respectively.



**Figure 5.49. Rebar Strains Comparison of Static Test-2, Case 14  
at Position 3 on Bent Cap 7**

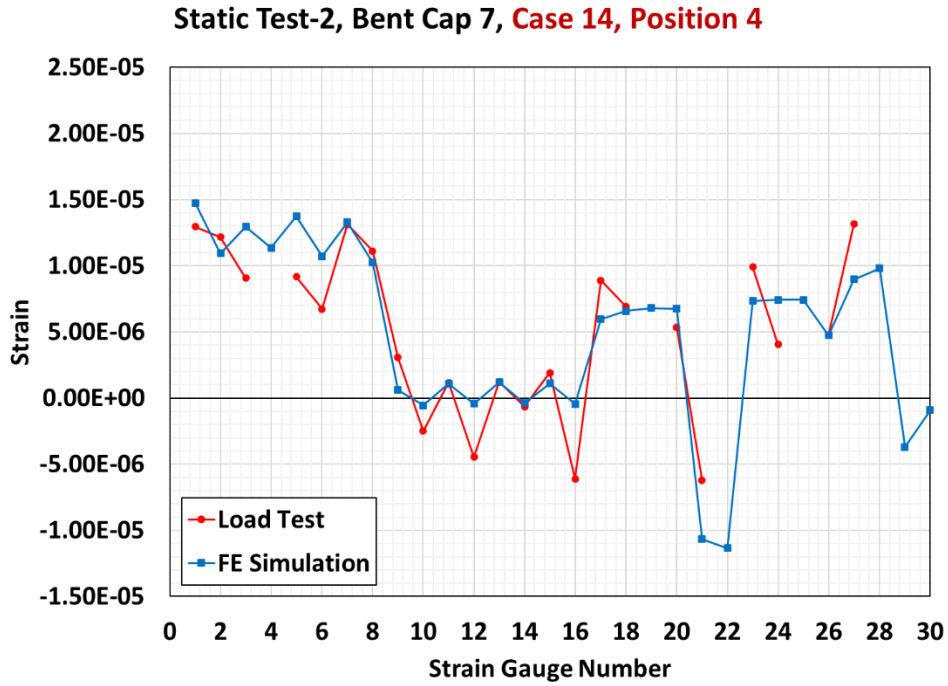


**Figure 5.50. Rebar Strains Comparison of Static Test-2, Case 14 at Position 4 on Bent Cap 7**

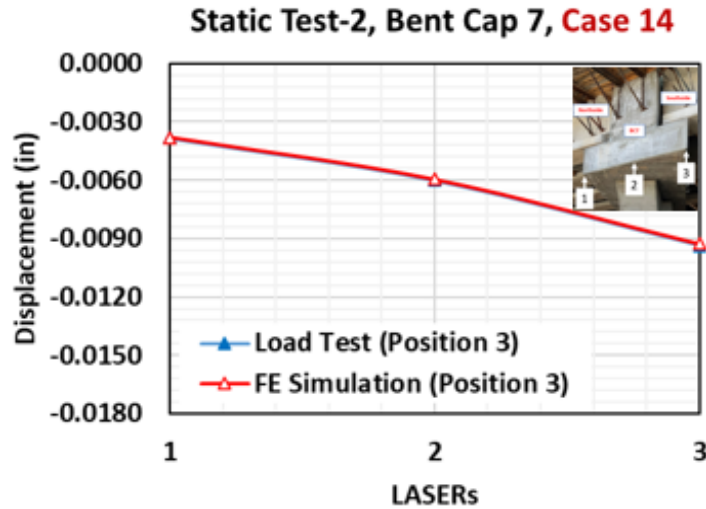


**Figure 5.51. West Face Displacements Comparison of Static Test-2, Case 14 at Position 3 on Bent Cap 7**

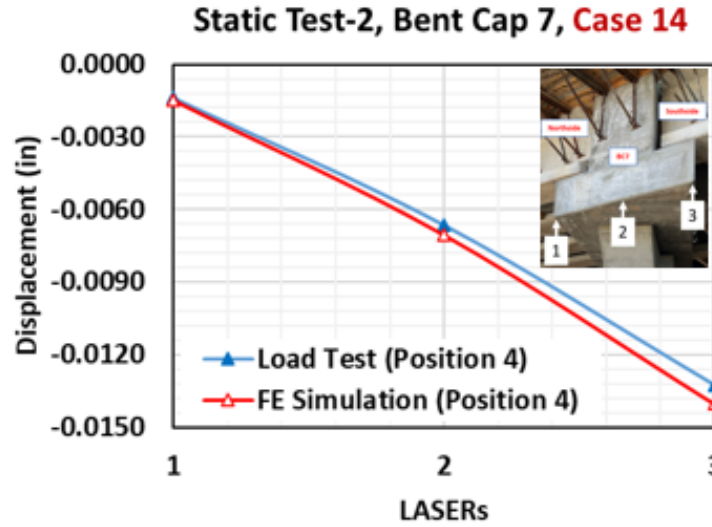


**Figure 5.52. West Face Displacements Comparison of Static Test-2, Case 14 at Position 4 on Bent Cap 7**

Figures 5.53-5.54 show the comparative analysis of CNFA-obtained average compressive stresses in the load test and average compressive stresses from the updated FE model of Case 14. In Figures 5.53-5.54, Location 1 is at Column-Bent Cap 7 interface, and Location 2 is under the exterior loading pad at the north side. The comparison of strains in rebars, west face displacements, and CNFA-obtained compressive stresses are presented in APPENDIX-5.

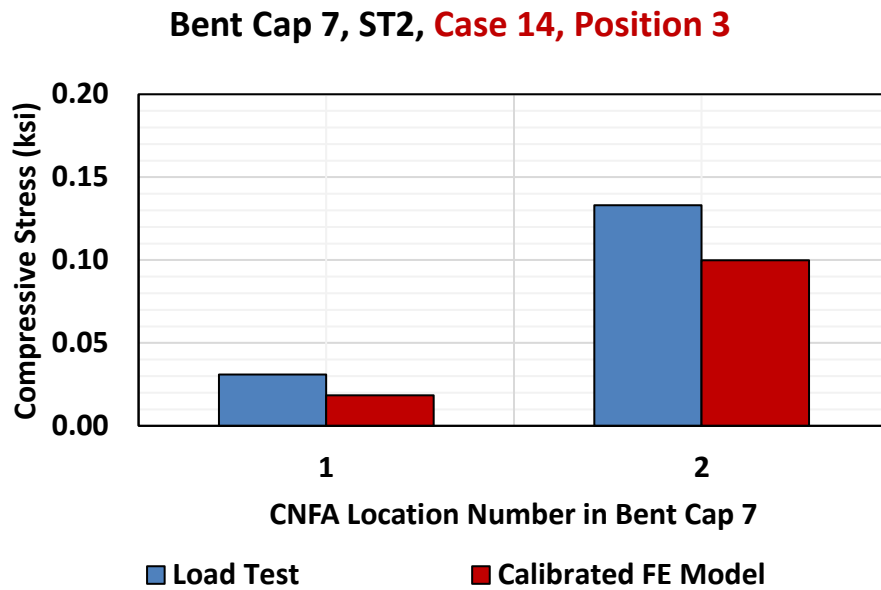


**Figure 5.53. Comparison of Average Compressive Stresses on Concrete of Static Test-2, Bent Cap 7 for Case 14 at Position 3**

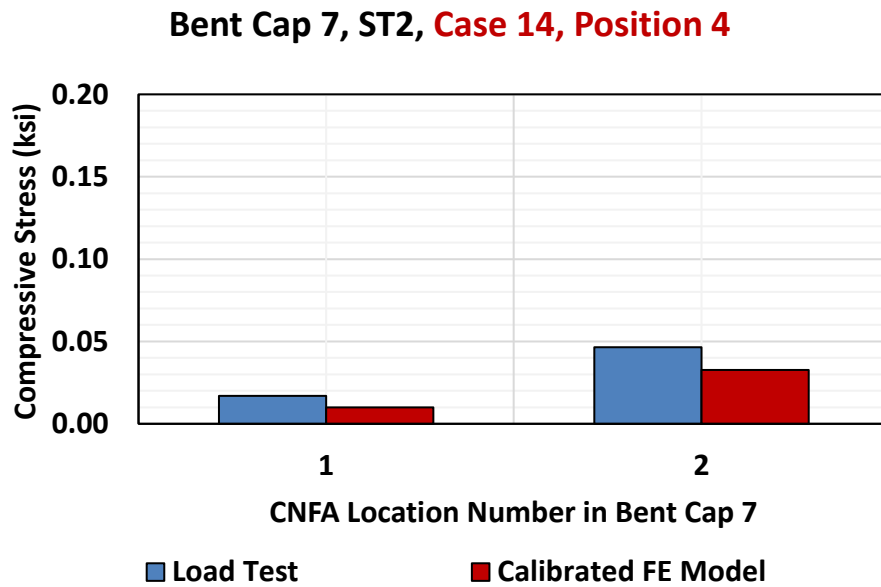


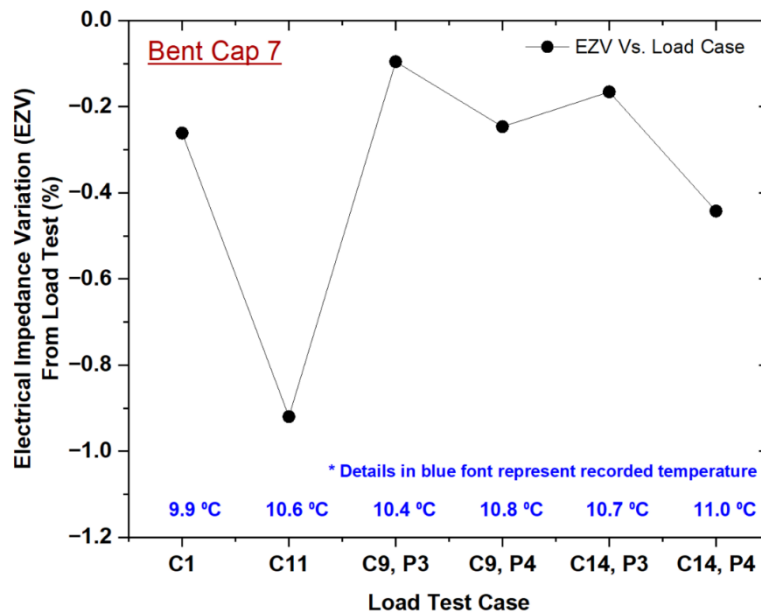
**Figure 5.54. Comparison of Average Compressive Stresses on Concrete of Static Test-2, Bent Cap 7 for Case 14 at Position 4**

The performance of CNFAs embedded in the tension zone of Bent Cap 2 (Location-3, anchored to S bars) in the static tests are summarized in Table 5.4. Figure 5.55 (a) shows the EZV

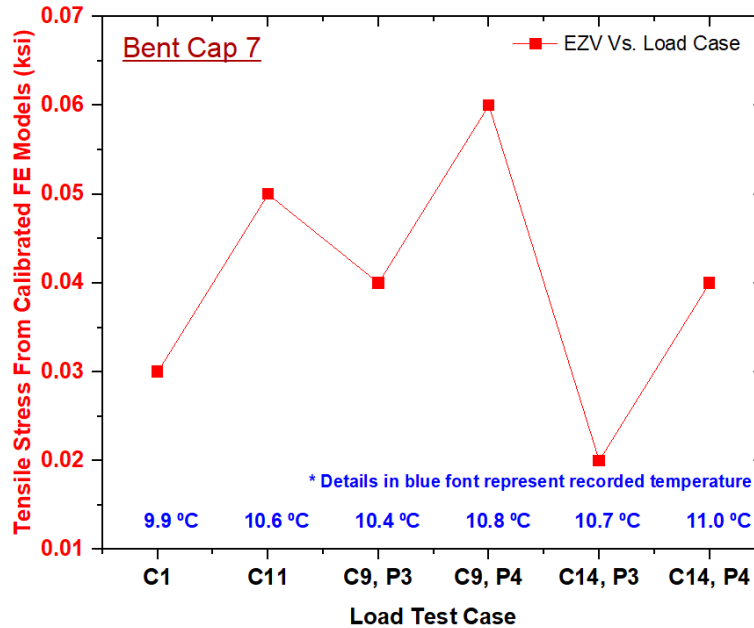
and temperature recorded during the load tests. Figure 5.55 (b) presents the equivalent tensile stresses from the calibrated model of Bent Cap 2 at Location-3.

**Table 5.4. Performance of SSCNFAs in Tension Zone (Location-3) of Bent Cap 7**

Case	EZV (%) from Load Test	Tensile Stress from Calibrated FE Model (ksi)	Temperature (°C)
1	-0.26	0.03	9.9
14	-0.92	0.05	10.6
9, Position 3	-0.10	0.04	10.4
9, Position 4	-0.25	0.06	10.8
14, Position 3	-0.17	0.02	10.7
14, Position 4	-0.44	0.04	11.0



(a) EZV of CNFA at Location-3 of Bent Cap 7



(b) Tensile Stress From Calibrated FE Models at Location-3 of Bent Cap 7

**Figure 5.55. Performance of CNFAs in Tension Zone of Bent Cap 7**

The strains in rebars, west face displacements, and average compressive stresses on concrete from the load test and updated model of Bent Cap 7 are comparable, as presented in Figures 5.43-5.54. The model calibration of Bent Cap 7 based on Static Load Test-2 (Case 9 and Case 14) is achieved from the updated material parameters (compressive strength, Young’s modulus) and the concrete damaged plasticity model (CDP).

### 5.4.3 Dynamic Test-1

The 3D FE analyses of Dynamic Test-1 for Case 9 and Case 14 were performed on an updated model of Bent Cap 7 with four trucks on the Donigan Road Bridge. Figures 5.56 and 5.57 show the position of four trucks on the deck over Bent Cap 7 in Dynamic Test-1 for Case 9 and Case 14.

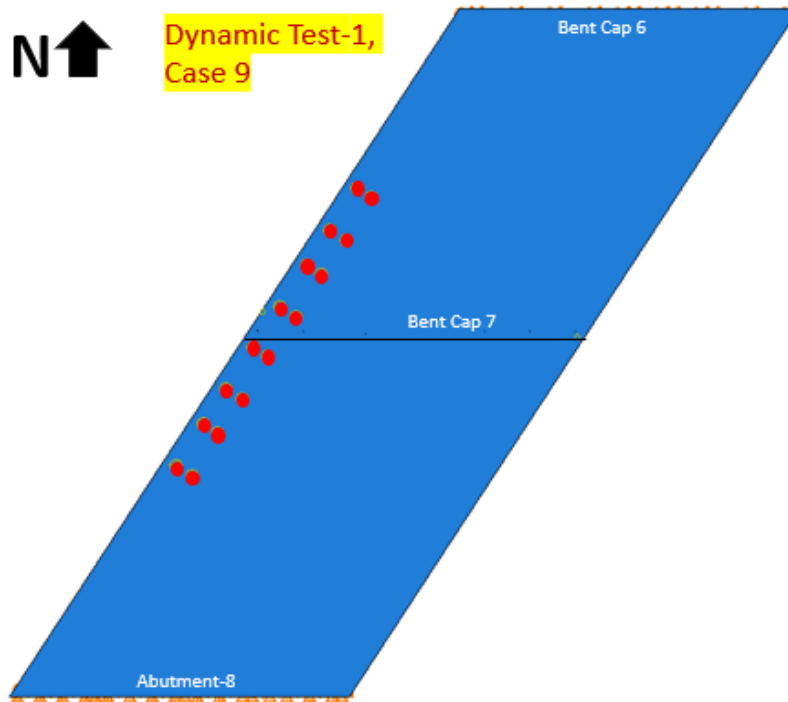


Figure 5.56. Locations of Trucks in Dynamic Test-1, Case 9 on Bent Cap 7

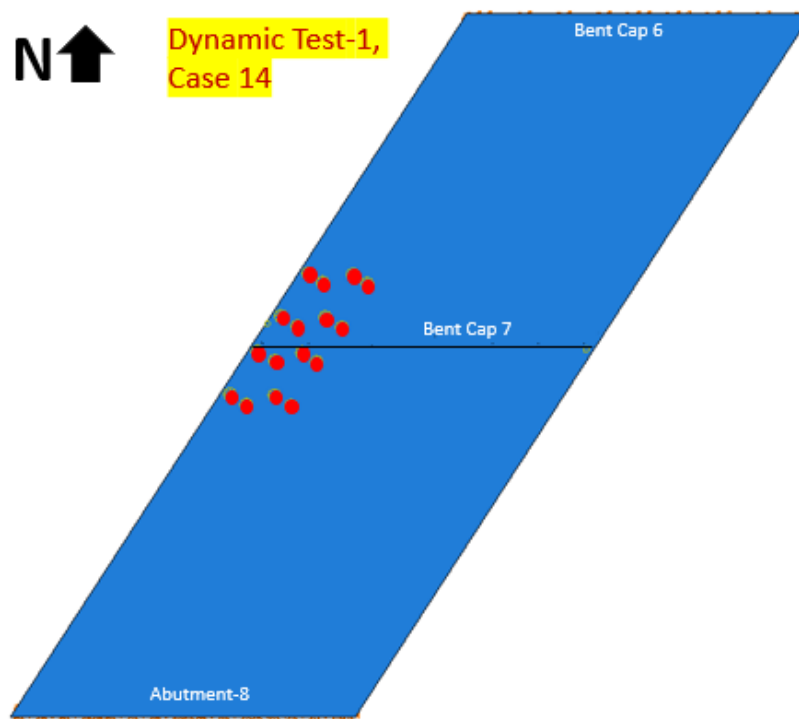


Figure 5.57. Locations of Trucks in Dynamic Test-1, Case 14 on Bent Cap 7

### 5.4.3.1 Case 9

Figure 5.58 illustrates the comparative analysis of the load test and updated FE model of Case 9. Figure 5.59 shows the comparative plot of west face displacements from the load test and updated model of Bent Cap 7 in Dynamic Test-1 for Case 9. The tip displacements of the extended region of Bent Cap 7 (south side) in Dynamic Test-1 for Case 9 from the load test and FE simulation are -0.0092 inches and -0.0125 inches, respectively.

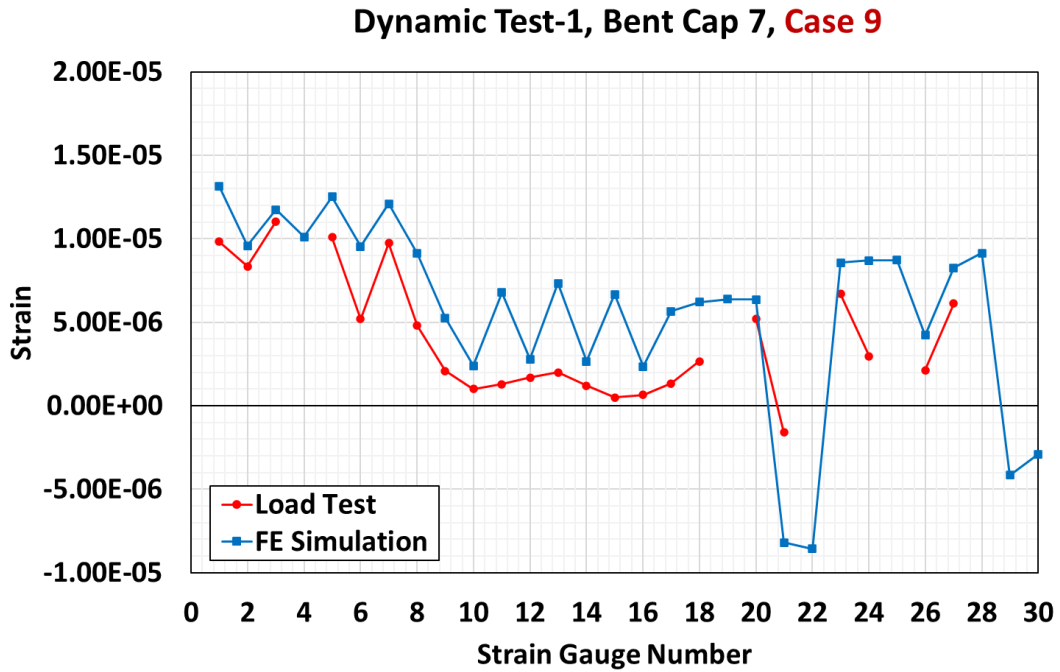
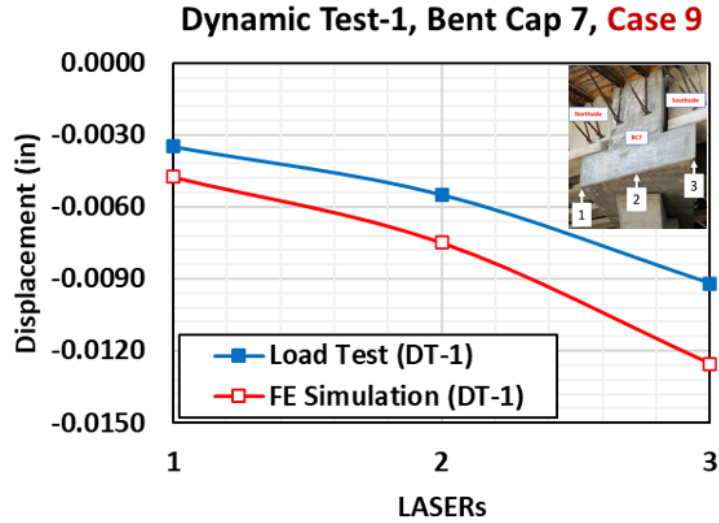


Figure 5.58. Rebar Strain Comparison of Dynamic Test-1, Bent Cap 7 for Case 9



**Figure 5.59. West Face Displacements Comparison of Dynamic Test-1, Bent Cap 7 for Case 9**

#### 5.4.3.2 Case 14

Figure 5.60 illustrates the comparative analysis of the load test and updated FE model of Case 14. Figure 5.61 shows the comparative plot of west face displacements from the load test and updated model of Bent Cap 7 in Dynamic Test-1 for Case 14. The tip displacements of the extended region of Bent Cap 7 (south side) in Dynamic Test-1 for Case 14 from the load test and FE simulation are -0.0105 inches and -0.0140 inches, respectively.

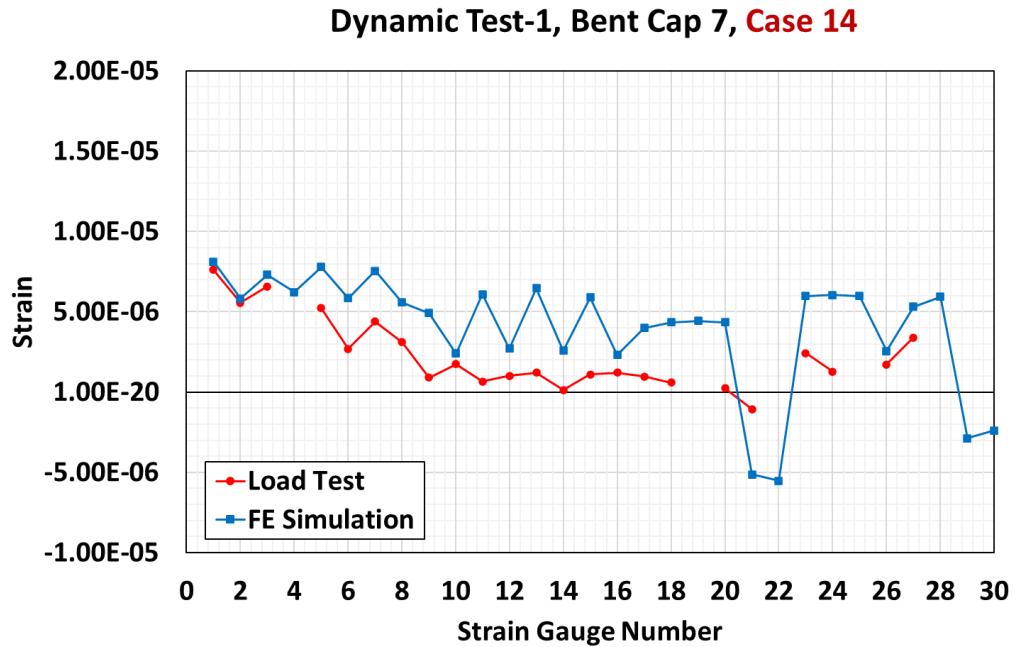


Figure 5.60. Rebar Strains Comparison of Dynamic Test-1, Bent Cap 7 for Case 14

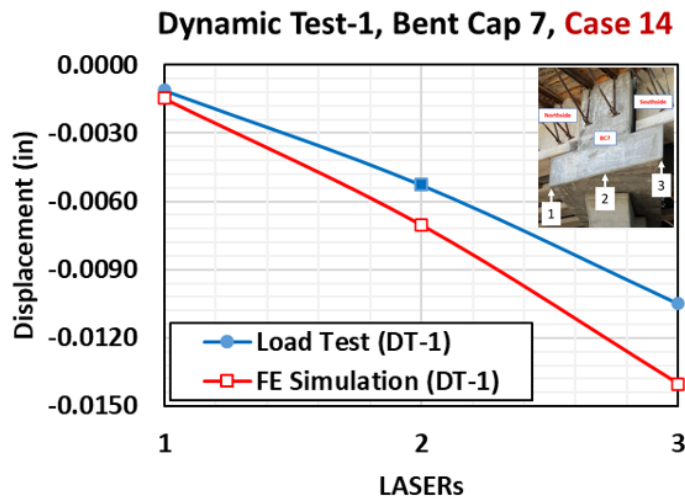


Figure 5.61. West Face Displacements Comparison of Dynamic Test-1, Bent Cap 7 for Case 14

The strains in rebars and west face displacements from the load test and updated model of Bent Cap 7 are comparable, as presented in Figures 5.58-5.61. The model calibration of Bent Cap 7 based on Dynamic Load Test-1 (Case 9 and Case 14) is achieved from the updated material parameters (compressive strength, Young's modulus) and the concrete damaged plasticity model (CDP).

## 5.5 PARAMETRIC STUDY

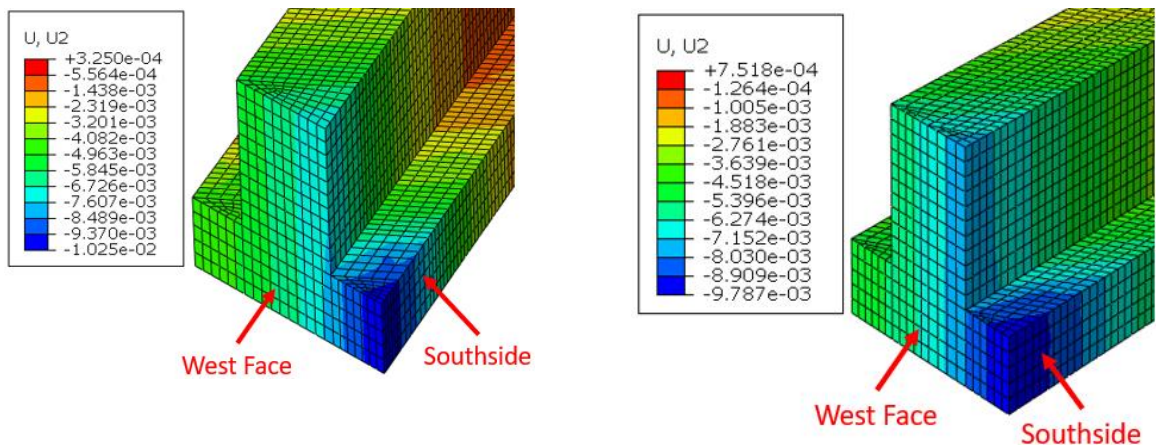
The FE model of Bent Cap 2 and Bent Cap 7 are calibrated with the measured load test data from Static Test-1, Static Test-2, and Dynamic Test-1. The parametric analysis of the calibrated models presented in this section examines the following:

- Structural performance of both bent caps from the comparable load cases,
- Deformation of the end face, transverse rebar strains, concrete tensile strains, compressive stresses on exterior loading pads, and
- Influence of skew angle on the performance of ITBC.

### 5.5.1 West Face Deformation of Bent Cap 2 and Bent Cap 7

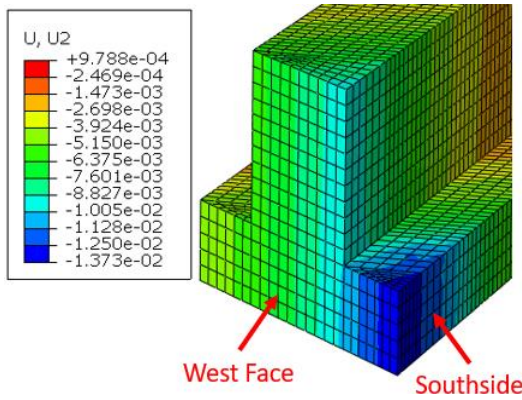
Due to the technical issues with the Lasermeters during the load test, the displacements of the west face of both bent caps on the north side were not recorded. The south side and middle displacements of both bent caps were extrapolated to interpret the north side displacements. The FE models of both bent caps are calibrated, which are examined to have better insight into the west face displacements.

Case 1, Case 9 (at Position 3 and Position 4), and Case 14 (at Position 3 for Bent Cap 7) are comparable cases for Bent Cap 2 and Bent Cap 7. Figure 5.62 (a-h) shows the west face displacements of Bent Cap 2 and Bent Cap 7 in these comparable cases.

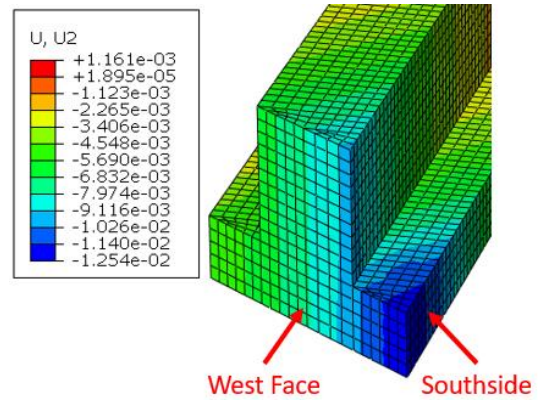


(a) West Face Displacement, Bent Cap 2, Case 1 (unit in inches)

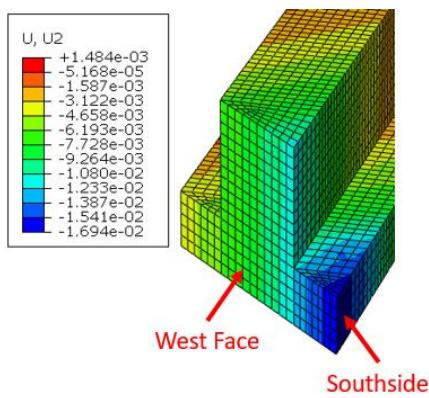
(b) West Face Displacement, Bent Cap 7, Case 1 (unit in inches)



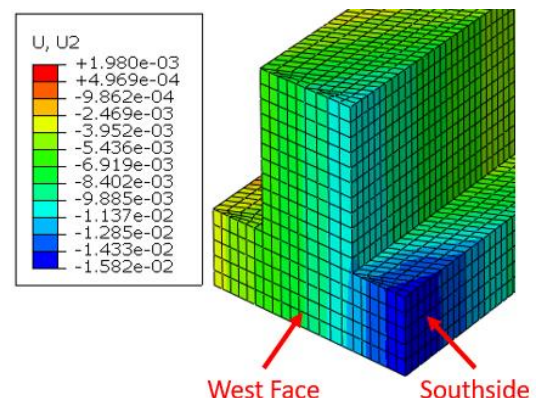
(c) West Face Displacement, Bent Cap 2, Case 9 at Position 3 (unit in inches)



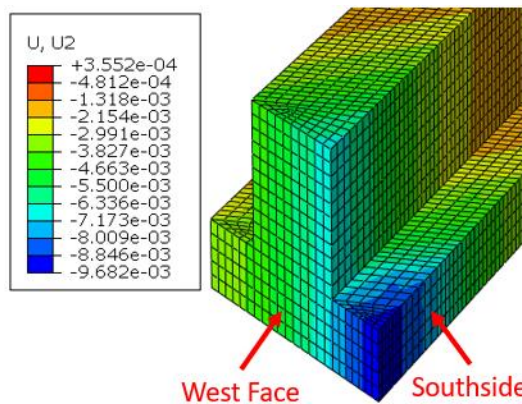
(d) West Face Displacement, Bent Cap 7, Case 9 at Position 3 (unit in inches)



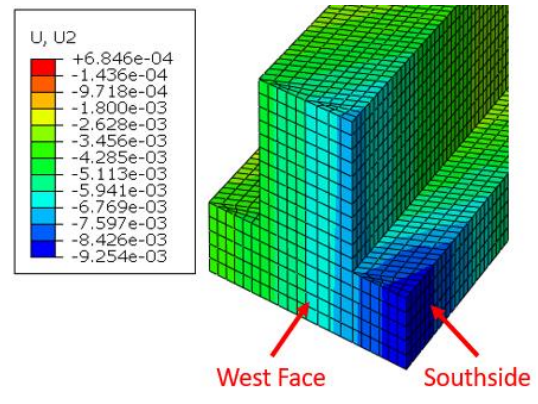
(e) West Face Displacement, Bent Cap 2, Case 9 at Position 4 (unit in inches)



(f) West Face Displacement, Bent Cap 7, Case 9 at Position 4 (unit in inches)



(g) West Face Displacement, Bent Cap 2, Case 14 (unit in inches)



(h) West Face Displacement, Bent Cap 7, Case 14 at Position 3 (unit in inches)

**Figure 5.62. West Face Displacements of Bent Cap 2 and Bent Cap 7**

The deformations of Bent Cap 2 and Bent Cap 7 (shown in Figure 5.62) are unsymmetrical. The unsymmetrical deformation of the skewed ITBC is caused by the torsional moments generated by the unsymmetrical location of loading pads on the ledges of the bridge cap. The tip displacements of Bent Cap 2 and Bent Cap 7 at the most projected end (south side) are the highest. Both bent caps for Case 9 at Position 4 exhibited the highest displacements among the static test cases. Furthermore, the unsymmetrical deformation of Bent Cap 2 (43°) for Case 9 at Position 4 is highest due to the higher skew angle than Bent Cap 7 (33°). The higher skew angle increases the torsional deformation of ITBC.

### 5.5.2 Tensile Strains of Transverse Rebars

The load test on Bent Cap 2 and Bent Cap 7 exhibited higher tensile strain on the transverse rebar on the extended overhanging portion. The tensile strain on the transverse rebars at the ledge and stem interface near the exterior loading pad on the south side are higher than on the north side. The tensile strains of the fourth and fifth G bars of Bent Cap 2 are comparable to the tensile strains on the S bars at the south side. During sensor instrumentation on the Bent Cap 7, the strain gauges were only installed on the first and second G bars. Hence, the tensile strains of the fourth and fifth G bars of calibrated models of both bent caps are examined to investigate the influence of the skew angle and the effect of exterior loading pads on the ledge of the cantilever portion of an ITBC. Table 5.5 compares strains on the first (closest to the west face), fourth, and fifth (closest to the exterior loading pad) G bars of Bent Cap 2 and Bent Cap 7 in the comparable cases (based on the position of trucks on the deck over bent caps).

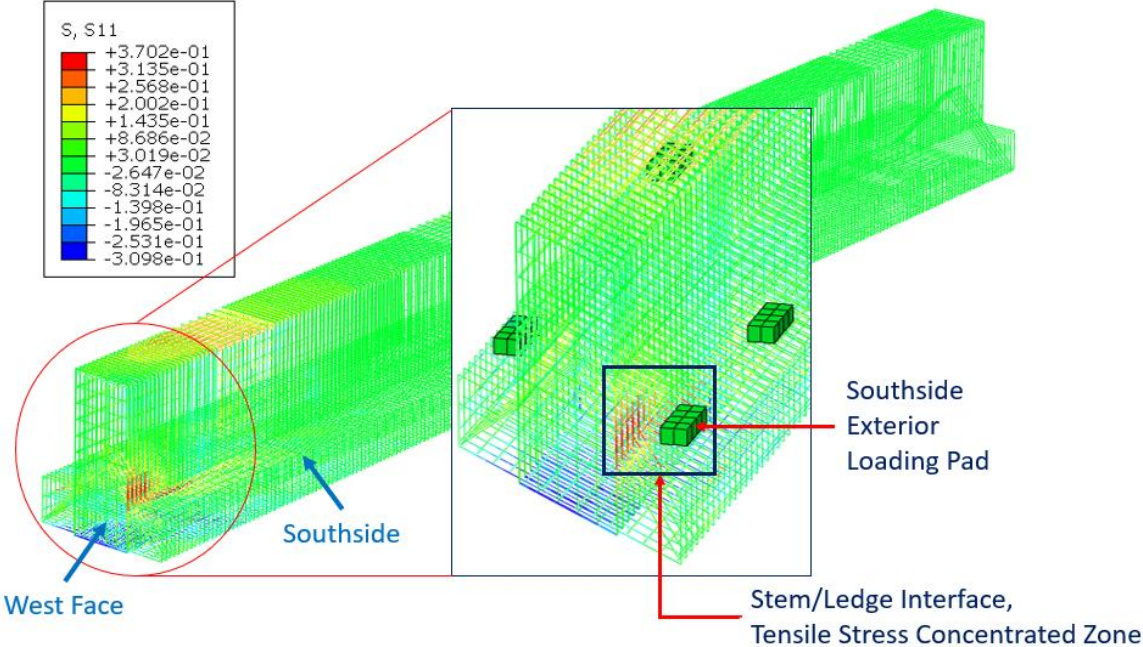
**Table 5.5. Tensile Strains on G bars of Bent Cap 2 and Bent Cap 7**

Comparable Cases	Bent Cap 2 (Skew Angle 43°)			Bent Cap 7 (Skew Angle 33°)		
	1st G bar	4th G bar	5th G bar	1st G bar	4th G bar	5th G bar
Case 1	7.20E-06	1.19E-05	1.28E-05	8.52E-06	6.79E-06	6.99E-06
Case 9, P3	7.38E-06	1.22E-05	1.36E-05	8.25E-06	9.42E-06	9.70E-06
Case 9, P4	1.32E-05	2.16E-05	2.31E-05	1.15E-05	1.31E-05	1.35E-05
Case 14	6.67E-06	1.07E-05	1.15E-05	5.32E-06	6.13E-06	6.35E-06

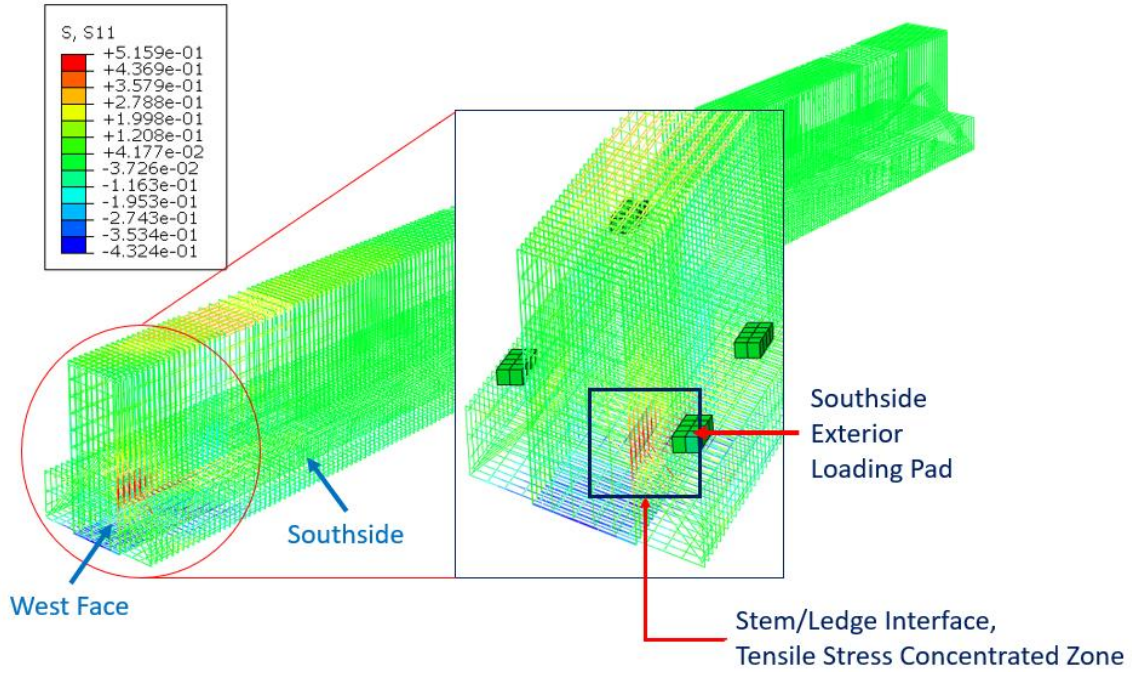
From the calibrated FE models of both bent caps, it is observed that the strains on the fifth G bar are higher than the strains on the first and fourth G bars (at the ledge and stem interface). It is because the exterior loading pad on the south side of both the bent caps rests on the ledge near the fifth G bar. The strains on the first G bar (of both bent caps) are the least in the comparison.

Moreover, in all the comparable cases, the strains on the G bars of Bent Cap 2 (skew angle 43°) are higher than those of Bent Cap 7 (skew angle 33°).

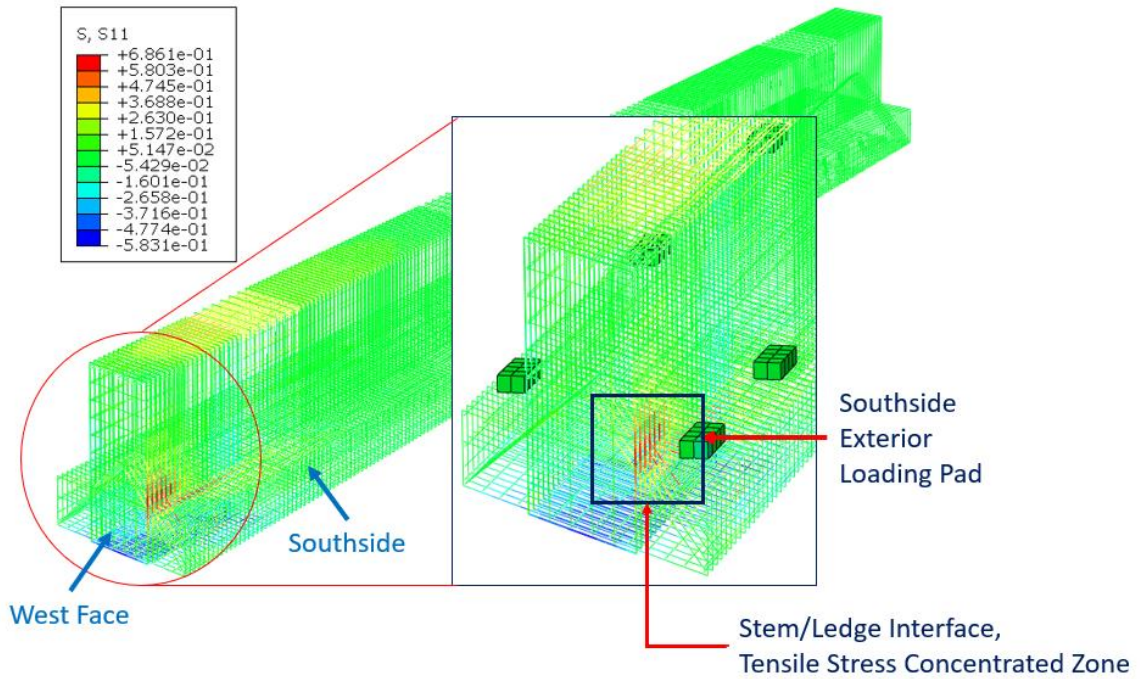
Figures 5.63 (a-d) and 5.64 (a-d) show the FE simulated stresses on the rebar cage of Bent Cap 2 and Bent Cap 7 from the calibrated models for the comparable cases. In each case, the transverse rebars at the steel and ledge interface of both bent caps have higher tensile stress contours (red color in the contours).



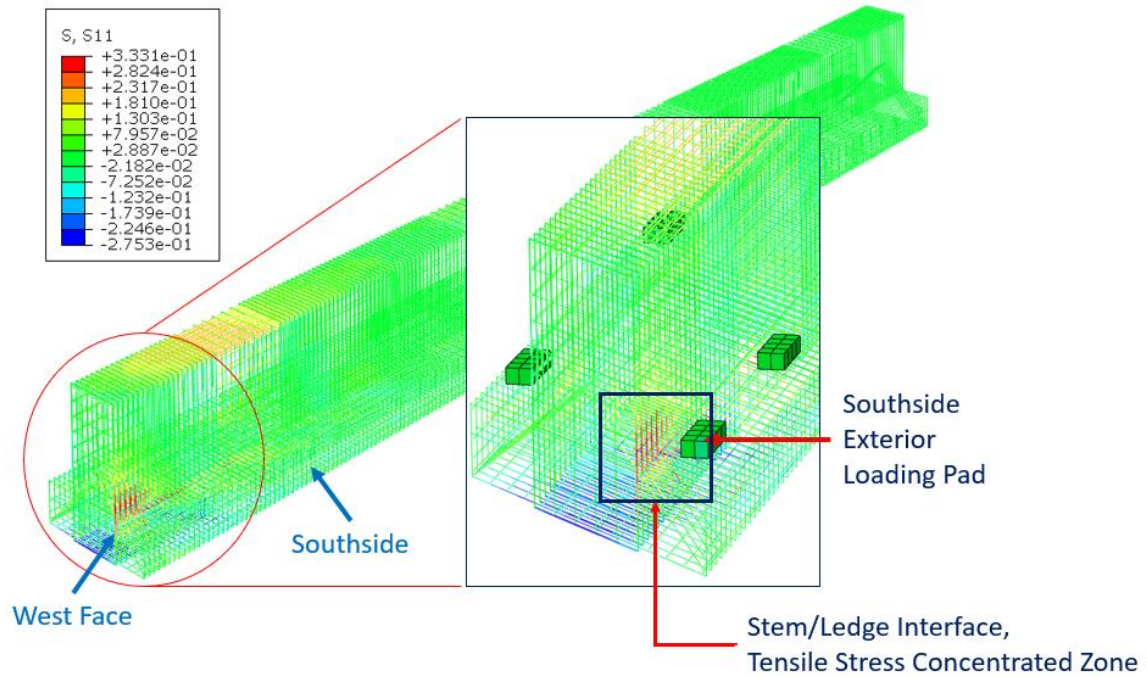
(a) Stresses on Rebars of Bent Cap 2 for Case 1 (unit in ksi)



(b) Stresses on Rebars of Bent Cap 2 for Case 9 at Position 3 (unit in ksi)

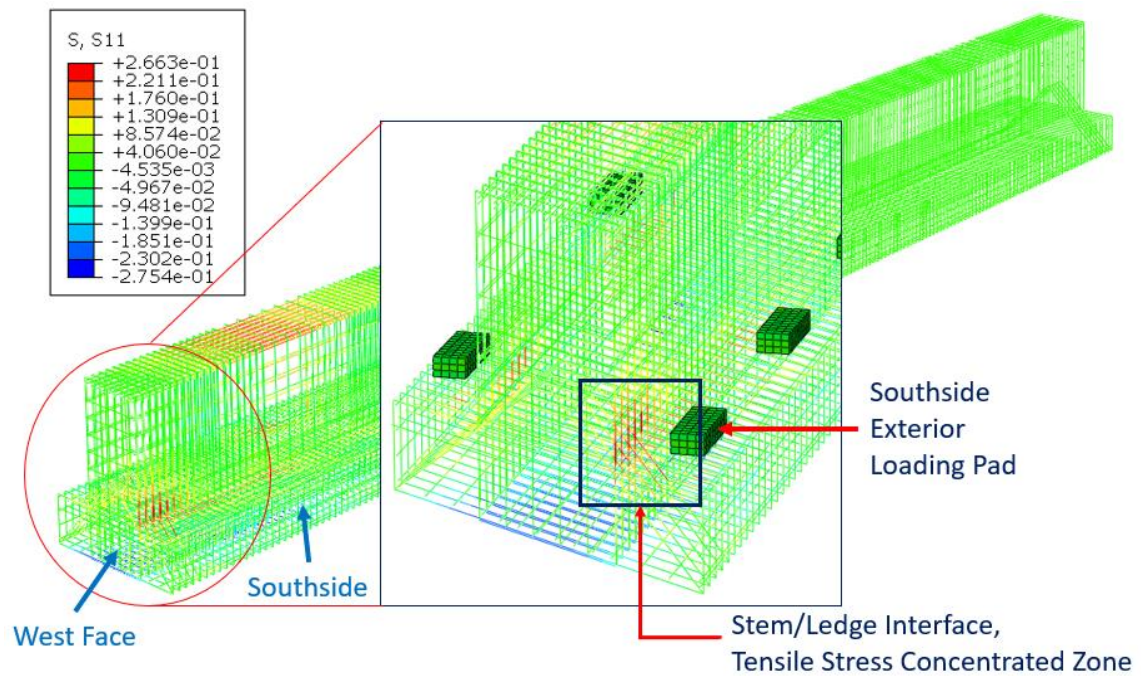


(c) Stresses on Rebars of Bent Cap 2 for Case 9 at Position 4 (unit in ksi)

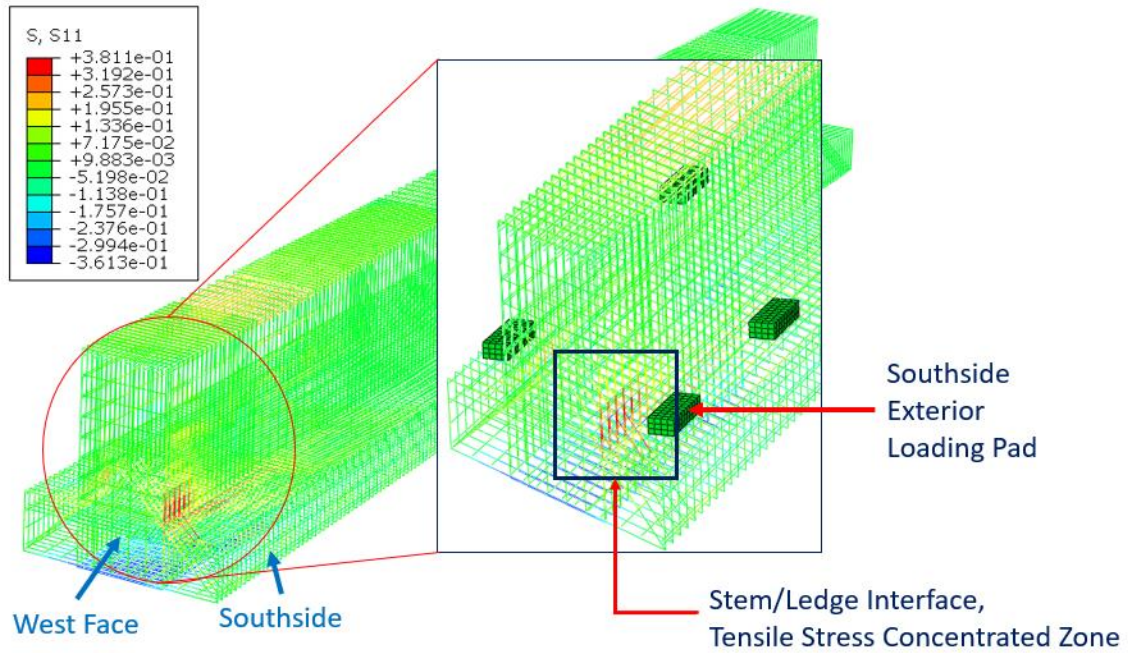


(d) Stresses on Rebars of Bent Cap 2 for Case 14 (unit in ksi)

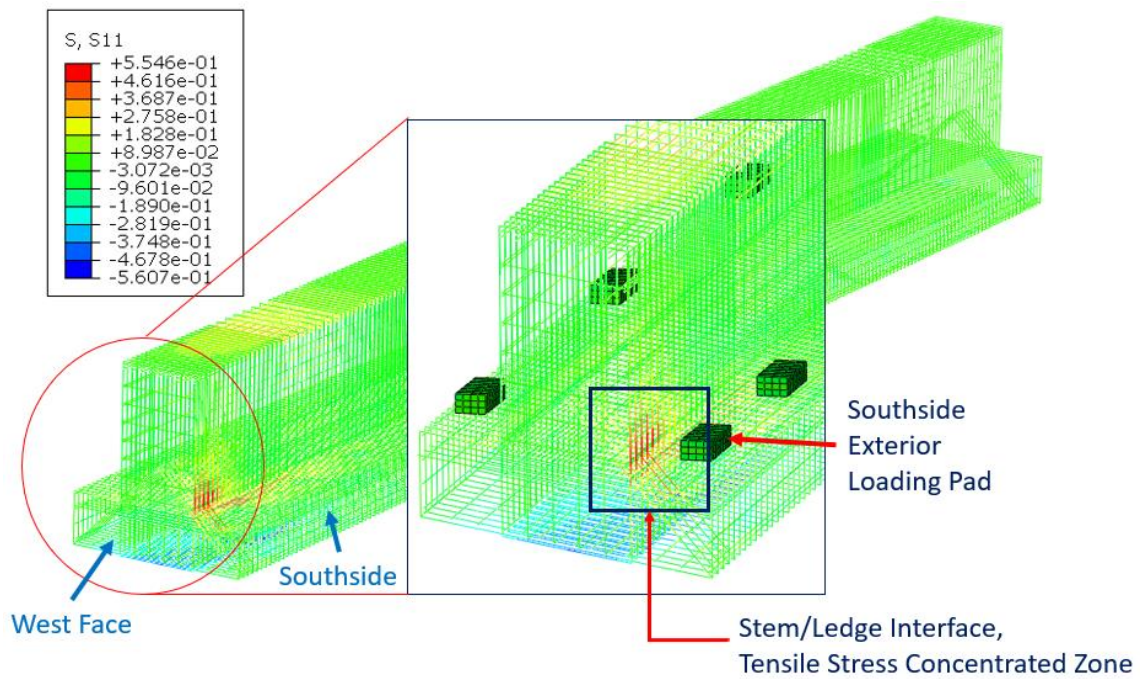
**Figure 5.63. Stresses on Rebars of Bent Cap 2 Calibrated Model for Static Tests**



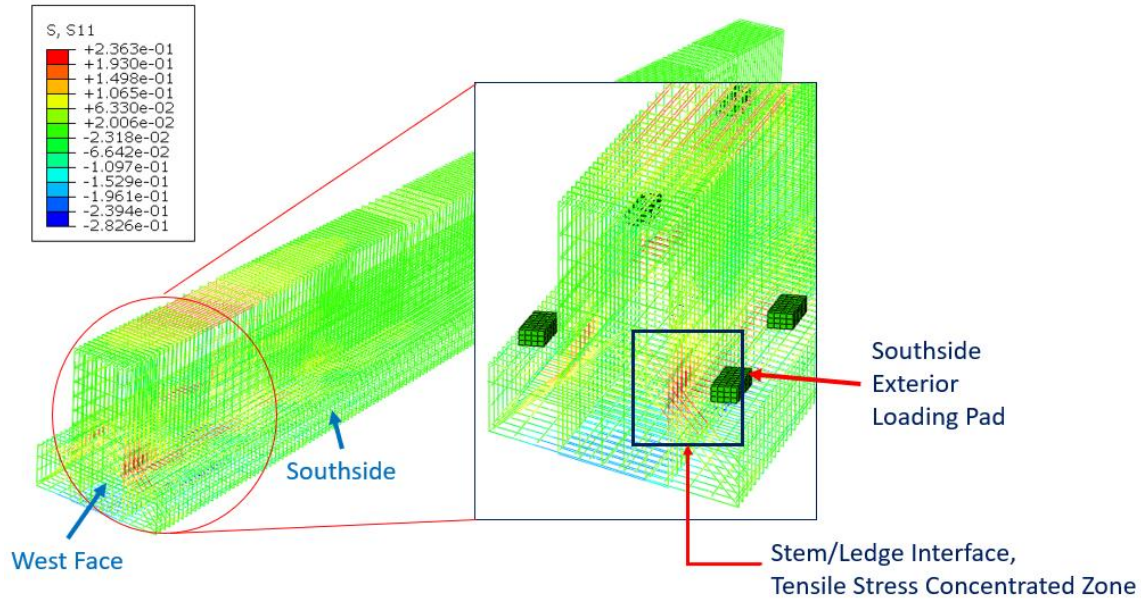
(a) Stresses on Rebars of Bent Cap 7 for Case 1 (unit in ksi)



(b) Stresses on Rebars of Bent Cap 7 for Case 9 at Position 3 (unit in ksi)



(c) Stresses on Rebars of Bent Cap 7 for Case 9 at Position 4 (unit in ksi)

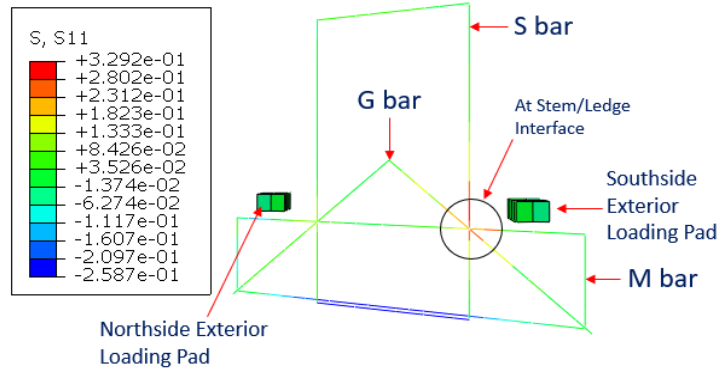


(d) Stresses on Rebars of Bent Cap 7 for Case 14 at Position 3 (unit in ksi)

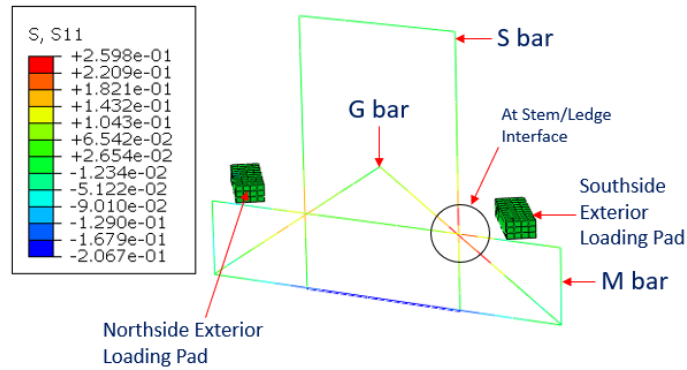
**Figure 5.64. Stresses on Rebars of Bent Cap 7 Calibrated Model for Static Tests**

From Figures 5.63-5.64, it can be observed that the tensile stress contours (red color in the contour) of the transverse rebars are higher from the location of the exterior loading pad (south side) to the west face of both the bent caps. In addition, the tensile stresses on the M bars (top of stirrups) are higher at the location closer to the exterior loading pads. The transverse rebars closer to the exterior loading pads (on the south side) are subjected to higher tensile stresses. The fifth transverse rebars (i.e., S bar, M bar, and G bar) are the closest transverse rebars to the exterior loading pads on the south side of both bent caps. Figure 5.65 shows the tensile stresses on the fifth transverse rebar from the west face. The tensile stresses at the ledge and stem interface of Bent Cap 2 (skew angle 43°) are higher than those at Bent Cap 7 (skew angle 33°). The inclusion of diagonal G bars at the end faces reduces the strains in the transverse bars (i.e., S and M bars) near the exterior loading pads.

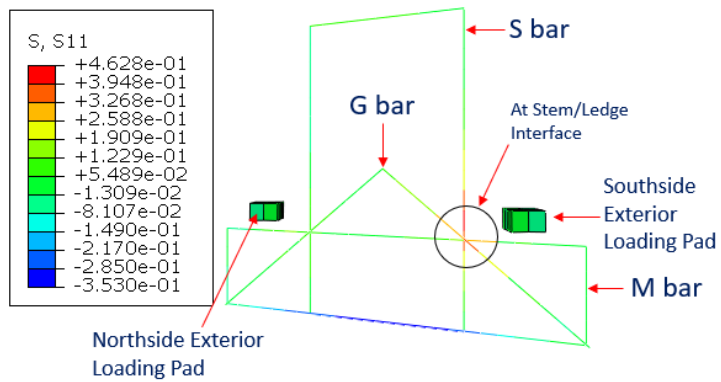
The higher tensile stresses on the longitudinal rebars (A bars) for Case 14 of both bent caps may have been attributed to the arrangement of the truckloads in two lanes on the deck. Further, the higher stresses (for all cases) on A bars are observed at the region where the transverse rebars are highly spaced (see Figures 5.63-5.64).



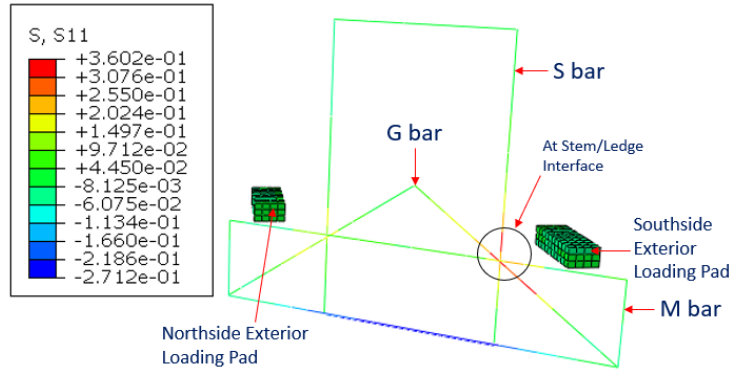
(a) Tensile Stresses on Transverse Rebars, Bent Cap 2, Case 1 (unit in ksi)



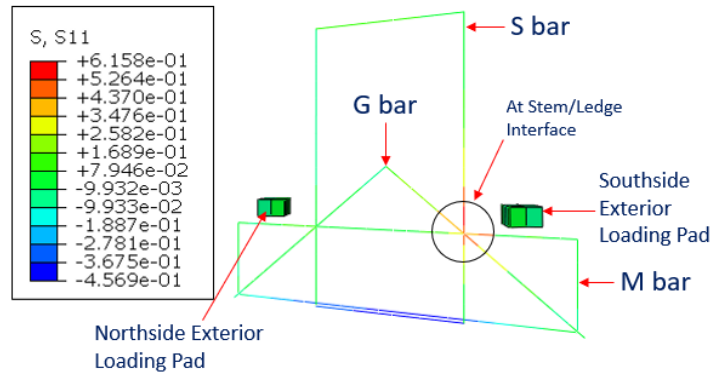
(b) Tensile Stresses on Transverse Rebars, Bent Cap 7, Case 1 (unit in ksi)



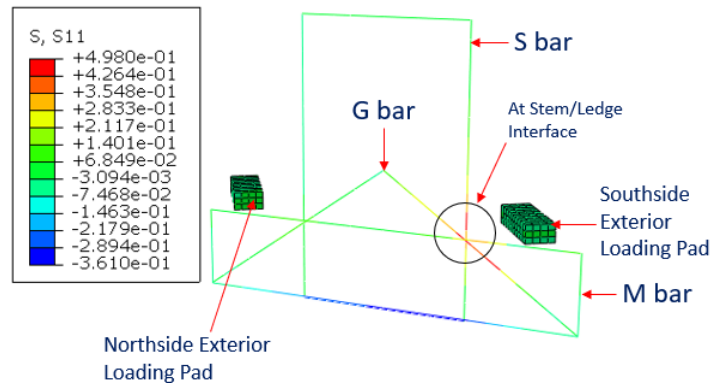
(c) Tensile Stresses on Transverse Rebars, Bent Cap 2, Case 9 at Position 3 (unit in ksi)



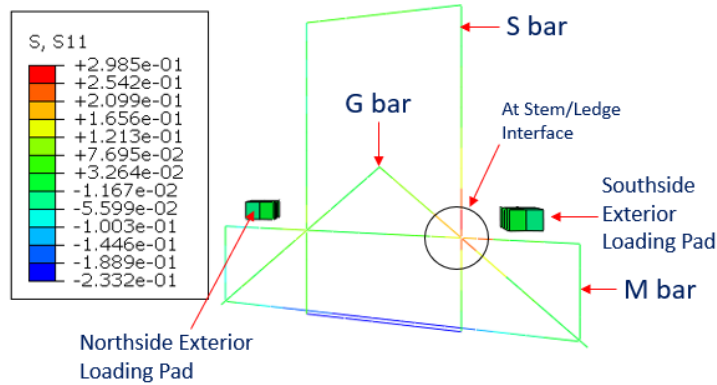
(d) Tensile Stresses on Transverse Rebars, Bent Cap 7, Case 9 at Position 3 (unit in ksi)



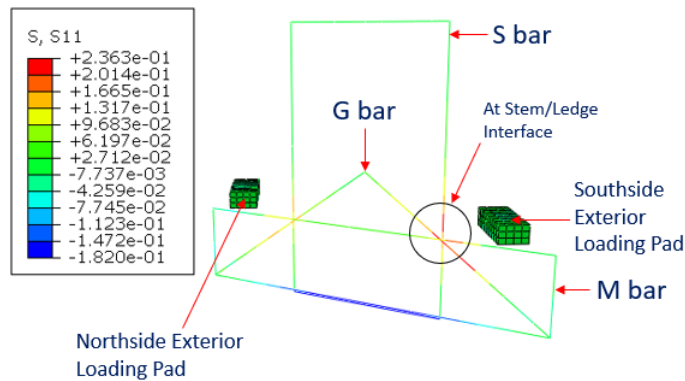
(e) Tensile Stresses on Transverse Rebars, Bent Cap 2, Case 9 at Position 4 (unit in ksi)



(f) Tensile Stresses on Transverse Rebars, Bent Cap 7, Case 9 at Position 4 (unit in ksi)



(g) Tensile Stresses on Transverse Rebars, Bent Cap 2, Case 14 (unit in ksi)

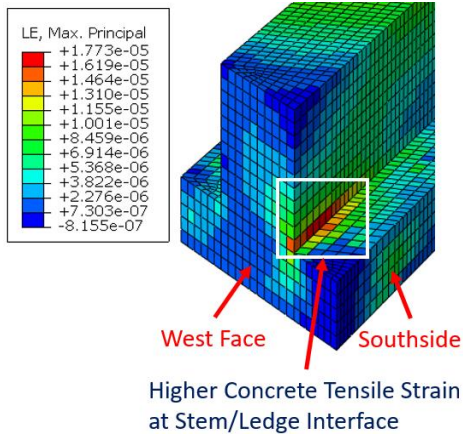


(h) Tensile Stresses on Transverse Rebars, Bent Cap 7, Case 14 at Position 3 (unit in ksi)

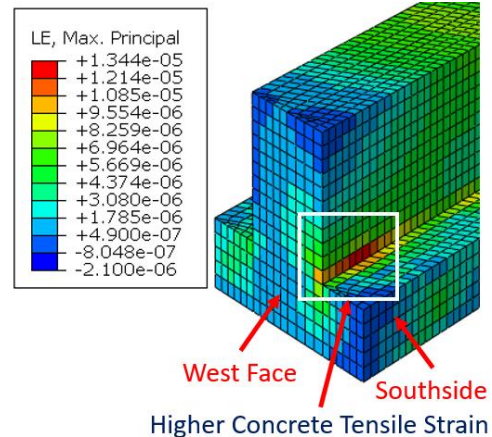
**Figure 5.65. Tensile Stresses on 5th Transverse Rebars of Bent Cap 2 and Bent Cap 7**

### 5.5.3 Maximum Tensile Concrete Strain

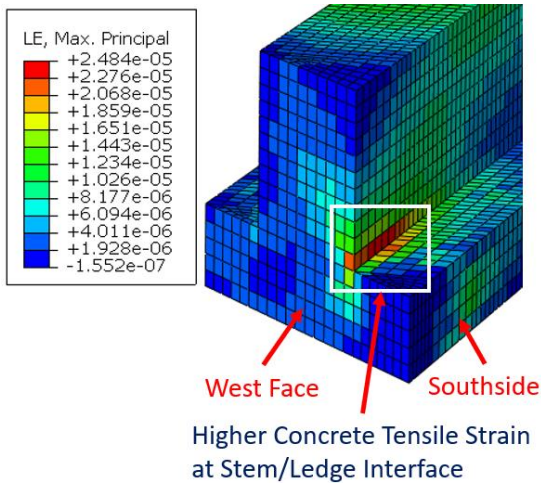
The calibrated FE models of Bent Cap 2 and Bent Cap 7 are investigated to examine the concrete tensile stresses. The stem and ledge interface at the overhanging cantilever portion of an ITBC at the projected end are a critical region (Zhou et al., 2020). Both bent caps exhibited higher compressive stresses under the exterior loading pads on the south side than on the north side. In addition, the tensile stresses/strains on the transverse rebar at the stem and ledge interface are higher. The concrete tensile strain could be higher at the interface near the exterior loading pads and the west face on the bent caps. Figure 5.66 shows the concrete tensile strain on Bent Cap 2 and Bent Cap 7 for the comparable cases (see Table 5.5 for comparable cases).



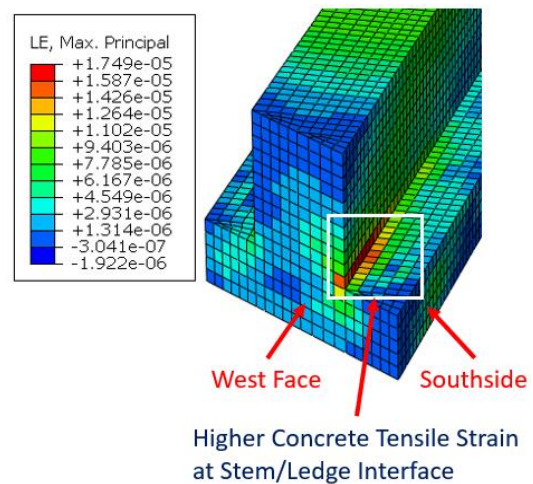
(a) Concrete Tensile Strain, Bent Cap 2, Case 1



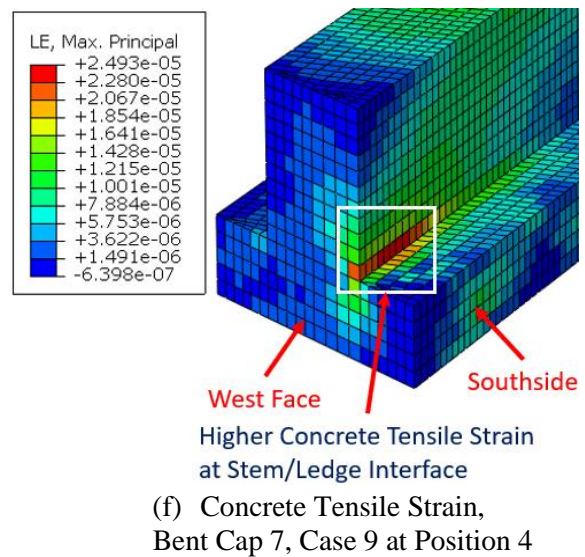
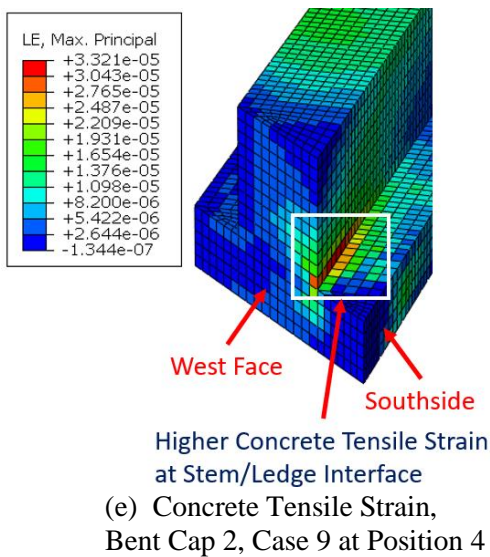
(b) Concrete Tensile Strain, Bent Cap 7, Case 1



(c) Concrete Tensile Strain, Bent Cap 2, Case 9 at Position 3



(d) Concrete Tensile Strain, Bent Cap 7, Case 9 at Position 3



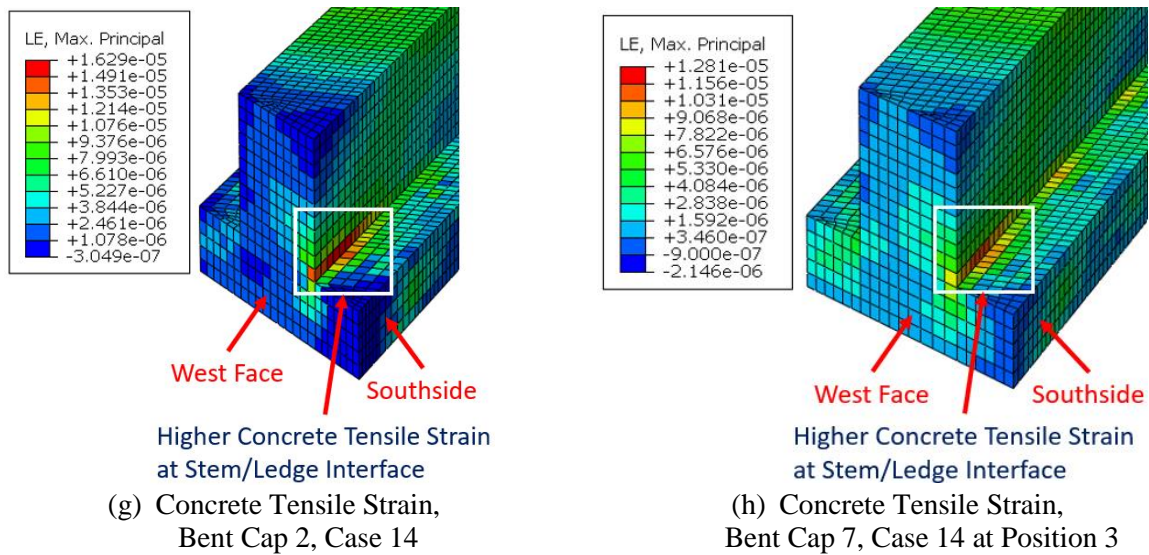


**Figure 5.66. Concrete Tensile Strain of Bent Cap 2 and Bent Cap 7**

The concrete tensile strains on both bent caps are higher at the stem and ledge interface near the west face. Case 9 at Position 4 exhibited higher concrete tensile strains for both bent caps. It is because the truckloads are concentrated on the forward span of the bent caps for Case 9 at Position 4. In addition, Bent Cap 2 exhibited higher concrete tensile strains than Bent Cap 7 in each comparable case due to a higher skew angle.

The cracking strain of the concrete is  $8.0E-05$  (Hsu & Mo, 2010). The concrete tensile strains of the calibrated models for all cases are smaller than the cracking strain. Hence, the implementation of skew reinforcing ensures the resilience of ITBCs.

#### 5.5.4 Compressive Stresses Under Exterior Loading Pads

From the load test on Bent Cap 2, the CNFA-obtained compressive stresses on the south side of the exterior loading pad are higher than on the north side of the exterior loading pad. CNFAs were installed on the north side exterior loading pads of Bent Cap 7 but not on the south side. The calibrated FE models of both bent caps are examined to find the compressive stresses on both the north side and the south side of the exterior loading pads.

Figures 5.67-5.68 show the compressive stresses on the exterior loading pads of Bent Cap 2 and Bent Cap 7 for the comparable cases. In the comparative bar graphs, it is observed that the compressive stresses on the south side exterior loading pads are higher than that on the north side, while the compressive stresses for Case 1 and Case 14 (at Position 3 for Bent Cap 7) on both bent caps are comparable.

Static load tests with the truckloads concentrated on the forward span of the bent caps resulted in a significant difference in the average compressive stresses on the exterior loading pads. On Bent Cap 2, the average compressive stresses on the south side are 266% and 189% higher than on the north side for both Case 3 and Case 9 at Position 4. Similarly, on Bent Cap 7, the average compressive stresses on the south side are 242% and 417% higher than on the north side for both Case 9 and Case 14 at Position 4.

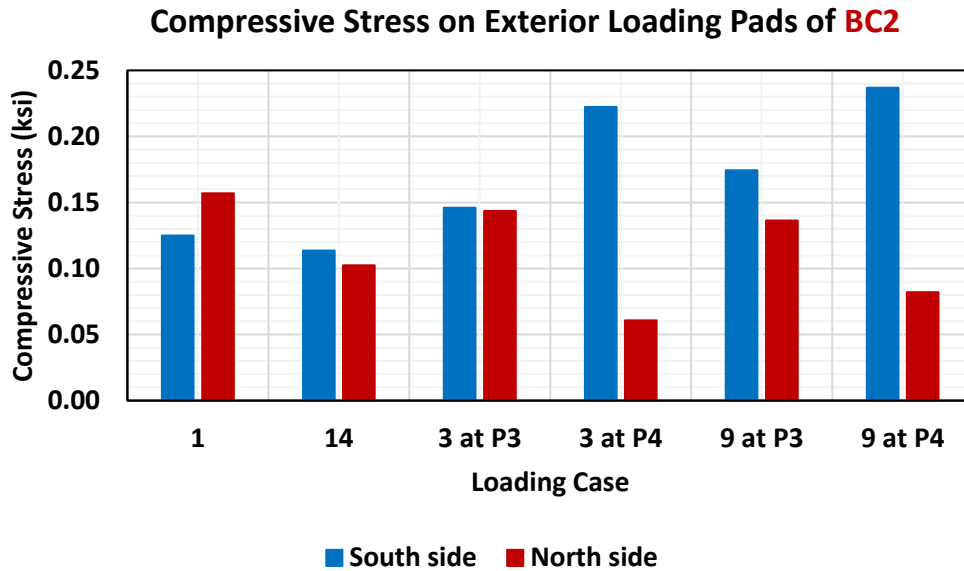


**Figure 5.67. Average Compressive Stresses on the Exterior Loading Pads of Bent Cap 2**

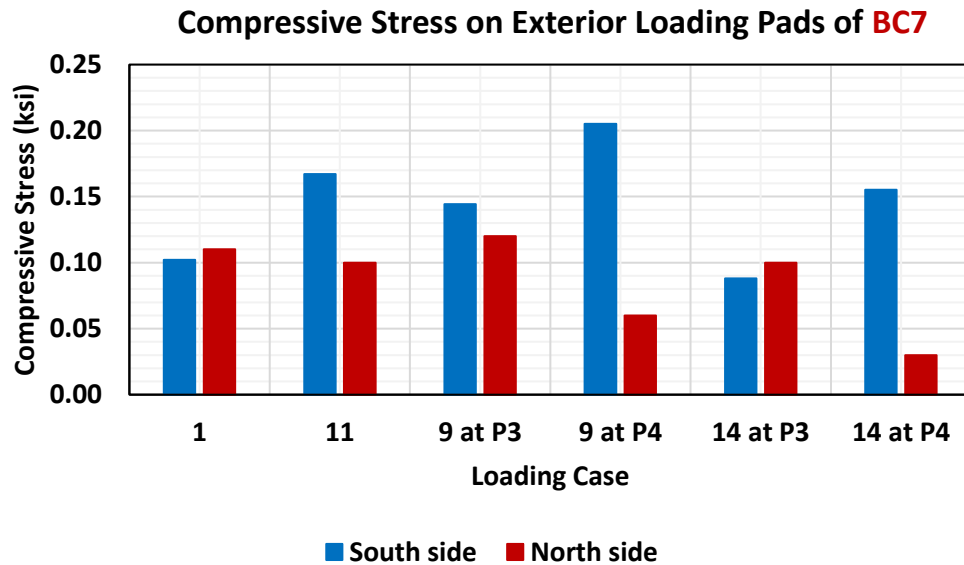


**Figure 5.68. Average Compressive Stresses on the Exterior Loading Pads of Bent Cap 7**

Figure 5.69 compares the compressive stresses on the south side of both bent caps for the comparable cases. Similarly, Figure 5.70 compares the compressive stresses on the north side of both bent caps for the comparable cases. These figures show that the compressive stresses on the exterior loading pads of Bent Cap 2 (skew angle 43°) are higher than those of Bent Cap 7 (skew angle 33°).

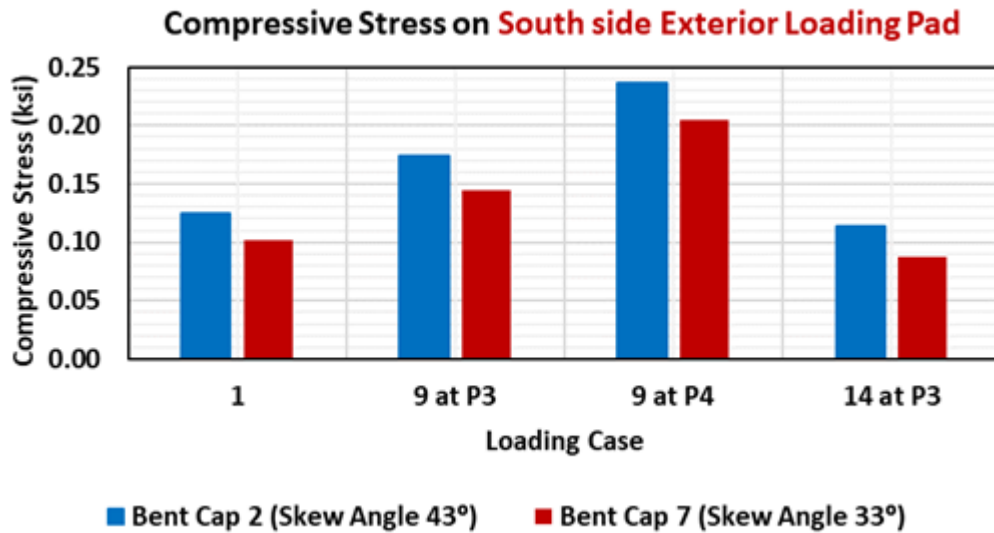


Figure 5.69. Average Compressive Stresses on the South Side Exterior Loading Pads

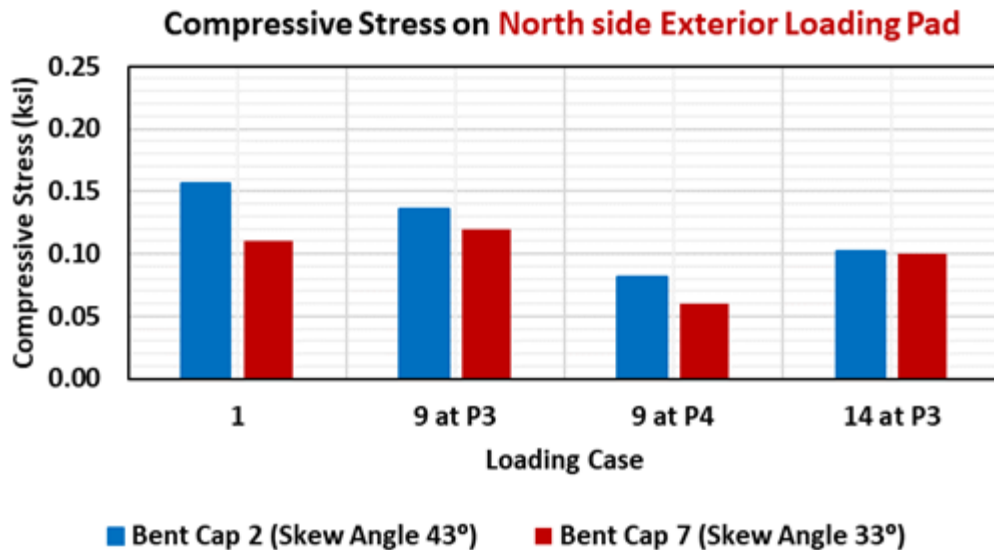


Figure 5.70. Average Compressive Stresses on the North Side Loading Pads

### **5.5.5 Influence of Skew Angle**

The skew angle is the critical parameter that influences the structural performance of an ITBC. Based on the calibrated FE models of Bent Cap 2 and Bent Cap 7, the following observations are presented:

1. An ITBC with a higher skew angle has higher tensile strain on transverse reinforcement,
2. An ITBC with a higher skew angle influences the torsional effect on the bent cap,
3. Higher end face displacement of the longer side of an ITBC with a higher skew angle,
4. The skew angle magnifies the compressive stress on the exterior loading pad.
5. A higher skew angle increases the higher tensile strain on the concrete.

### **5.6 SUMMARY**

The following summarizes are made from finite element analysis of calibrated models:

1. The deformation of the west face of bent caps is unsymmetrical. The tip displacements of both bent caps at the projected end (south side) are the highest. The tip displacement of Bent Cap 2 is higher than that of Bent Cap 7 in all loading cases.
2. The tensile strains on the S bars on the south side closest to the end face of both ITBCs are higher in all loading cases. Due to larger torsion, the S bars on the north side exhibited compressive strains in Static Test-2 at Position 4 in both ITBCs.
3. The tensile stresses on the transverse rebars are higher from the location of the exterior loading pads at the south side to the end face of the ITBC.
4. The inclusion of diagonal G bars at the end faces reduces the strains in the transverse bars (i.e., S and M bars) near the exterior loading pads. The tensile strain on the fifth G bar (closest to the exterior loading pads on the south side) is the highest among G bars.
5. The tensile strains are concentrated on the transverse rebars at the ledge and stem interface on the south side.
6. The concrete tensile strains at the stem and ledge interface are higher in all loading cases. The concrete tensile strains of the calibrated models for all cases are smaller than the cracking strain. Hence, the implementation of skew reinforcing ensures the resilience of ITBCs.
7. The compressive stresses on the south side exterior loading pads are higher than on the north side.

8. The loading cases with the truckloads closer to the parapet and concentrated on the forward span of the bent caps are critical. These critical cases result in higher tip displacements at the south side, higher concrete tensile strains, higher tensile strains on transverse bars at the south side, compressive strains on the S bars at the north side due to torsion, and higher compressive stresses on the exterior loading pads.
9. The stem and ledge interface at the projected side of the cantilever portion of an ITBC are a critical region.
10. The skew angle of an ITBC is the most influential parameter. From the calibrated FE models, it is observed that:
  - a. An ITBC with a higher skew angle has higher tensile strain on the transverse reinforcements.
  - b. An ITBC with a higher skew angle influences the torsional effect on the bent cap.
  - c. Higher unsymmetrical end face displacement with a higher skew angle.
  - d. The skew angle magnifies the compressive stresses on the exterior loading pads.
  - e. A higher skew angle increases the higher tensile strain on the concrete.

## **6 DESIGN RECOMMENDATIONS**

### **6.1 OVERVIEW**

TxDOT Research Project 0-6905 investigated the performance of skewed reinforcing in Inverted-T Bridge Caps (ITBC). The structural performance of skewed ITBCs with skew reinforcing was compared with that of ITBCs with traditional transverse reinforcing. TxDOT Project 0-6905 investigated three critical parameters in the experimental program for inverted-T bent caps (ITBC) (Sapath et al., 2019). Those three critical parameters are: (1) skew angle, (2) detailing of transverse reinforcement, and (3) amount of transverse reinforcement. To examine three critical parameters, 13 skew ITBC specimens were fabricated and tested. Further, the finite element models of 13 skew ITBCs were calibrated with the test results to conduct parametric analyses. Based on the lab test and the parametric study on the calibrated FE models, the following design recommendations were proposed:

1. All S bars (shear and hanger stirrups), M bars (primary ledge bars), and N bars (secondary ledge bars) will be skewed to match the skew angle of the inverted-T bridge caps. The spacing of skew transverse reinforcement will be measured from center to center of the hanger and ledge stirrups along the central line of the skew bent cap (not the perpendicular distance between hanger or ledge stirrups).
2. Avoid using a shorter ledge. The distance between the central line of the exterior girder and the end face of the inverted-T bridge caps should be maintained at least 24 inches to provide adequate punching shear capacity. It positively delays the appearance of the diagonal crack at the re-entrant corner between the cantilever ledge and the web at the end faces of the ITBC.
3. Vertical rebars should be provided across both end faces of the skew web. The spacing of these rebars should be equivalent to the spacing of shear and hanger stirrups (at least 6") and will be provided along the end face. The vertical rebars at the end face reduce the stress concentration on the hanger and shear stirrups and restrict the formation of cracks.
4. The addition of diagonal bars (G bars) does not prevent the formation of diagonal cracks at the re-entrant corner between the cantilever ledge and the web. The distance from the end face to the exterior loading pad is the effective variable to control the crack. The diagonal crack occurs at a lower load as the skew angle increases (from 0 degrees to 60 degrees).
5. A minimum area of transverse reinforcement is required to restrain the growth of diagonal (inclined) cracking, increase ductility, and prevent the sudden shear failure of the bent cap. All

the test results show that there were no sudden shear failures. Transverse rebars are considerably yielded before the failure of the specimens. Therefore, the equations in AASHTO LRFD 2014 can be used to design the minimum transverse reinforcing in skew inverted-T bent caps.

Due to the advantage of skew reinforcing, the skewed transverse reinforcement has been applied to the design of ITBC in TxDOT bridges. The finite element analysis of three inverted-T bridge caps (Bent Cap 2, Bent Cap 6, and Bent Cap 7) of Donigan Road Bridge over I-10 were performed using ABAQUS. The parametric study of 96 full-scale specimens and the cost-benefit analysis was performed to examine the performance of skewed reinforcing and traditional reinforcing in ITBCs, the effect of increment in the S bar area, the effect of increment in the G bar area, and the influence of increased concrete strength. The following design recommendations were provided for skew reinforcing bars (Wang et al., 2020):

1. It is recommended to use the skew transverse reinforcement to design skewed ITBCs. The skew transverse reinforcement achieves better structural performance than the traditional transverse reinforcement with notably reduced construction cost.
2. It is recommended to design double S bars throughout the bent cap. The spacing of S bars can be increased at the location of the column support, no greater than 12 inches.
3. For the skewed ITBCs design, M bars and N bars are paired with equal spacing, which needs to be equal to or an integer multiple of the spacing of S bars.
4. The stem width of an ITBC is at least 3 inches wider than the column diameter.
5. In general, the depth of the ledge is greater than or equal to 2 feet 3 inches, which is the depth at which a bent cap from a typical bridge will pass the punching shear check.
6. The distance from the longitudinal face of the stem to the center of the bearing pad is 12 inches for TxGirders.
7. The end bars (U1 bars, U2 bars, U3 bars, and G bars) notably reduce the maximum crack width. It is recommended to place #6 U1 bars, U2 bars, and U3 bars at the end faces and #7 G bars at approximately a 6-inch spacing at the first 30 to 35 inches of the end of the bent cap. U1 bars are vertical end reinforcements, and U2 bars and U3 bars are horizontal end reinforcements at the stem and the ledge. G bars are the diagonal end reinforcement.

8. TxDOT Bridge Design Manual – LRFD Ch. 4, Sect. 5 limits the minimum concrete compressive strength as  $f'_c = 3.6$  ksi. However, finite element models show that concrete strength notably increases the ultimate strength and the stiffness of ITBCs and reduces crack width. Therefore, it is recommended to have a concrete compressive strength of at least  $f'_c = 5$  ksi.

## 6.2 DESIGN RECOMMENDATIONS

The static and dynamic load tests were performed on Bent Cap 2 and Bent Cap 7 of Donigan Road Bridge over I-10 near Brookshire in Waller County of Texas. The finite element models of both bent caps were calibrated by the results of the load tests. The following design recommendations are provided based on the load tests and the parametric study performed on the calibrated FE models of Bent Cap 2 and Bent Cap 7.

1. The tensile strains in the S bars on the extended side (south side) of the cantilever portion of ITBC are higher among all the transverse rebars. Due to larger torsion, the S bars exhibited compressive strain on the north side. The load test on the full-scale ITBC validates the findings of TxDOT Project 0-6905 about the higher strains in S bars. It is recommended to continue designing double S bars throughout the bent cap, as suggested in TxDOT Project 0-6905.
2. As per the TxDOT Project 0-6905 design recommendation, the spacing of S bars can be increased at the location of the column support, no greater than 12 inches. The parametric study shows a higher strain on longitudinal rebars (A bars, top of stem) where S bars are highly spaced. Hence, it is recommended not to exceed a spacing of 12 inches, as previously suggested.
3. The provision of end bars notably reduced the maximum crack width (Wang et al., 2020). The concrete tensile strains at the stem and ledge interface are higher in all the cases of load tests. The concrete tensile strains from the calibrated models for all the cases are smaller than the cracking strain. Hence, the implementation of skew reinforcing with end bars ensures the resilience of ITBCs. It is recommended to place #6 U1 bars, U2 bars, and U3 bars at the end faces.
4. The finite element models show that the increase in concrete strength increases the ultimate strength and the stiffness of ITBCs and reduces crack width (Wang et al., 2020). The compressive strength of both bent caps is at least 6.5 ksi. As the calibrated FE models of Bent

Cap 2 and Bent Cap 7 show that concrete tensile strains are lower than the cracking strain of concrete, it is recommended to have a compressive design strength of at least  $f'_c = 5$  ksi.

5. The G bars (diagonal bars at the end face) were provided to delay the appearance of cracks at the stem and ledge interface. However, the load tests show that including diagonal G bars at the end faces reduced the strains in the transverse bars (i.e., S bars and M bars) near the exterior loading pads. There are five G bars (#7) at a spacing of 6 inches maximum (a coverage of 24 inches with five G bars) and exterior girder at 3.079 feet and 2.684 feet (at least 24 inches) from the end face of Bent Cap 2 and Bent Cap 7, respectively. It is recommended to provide G bars (#7) up to the location of exterior loading pads. The reason for this is the G bars have the dual purpose of delaying the crack appearance at the stem and ledge interface and reducing the strain in the transverse bars (S bars and M bars) near the exterior loading pads.
6. Even though the skew angle of Bent Cap 7 is smaller than that of Bent Cap 2, the compressive stresses on the exterior loading pad in both cases are comparable. The reason is that the distance between the center line of the exterior loading pad to the end face of Bent Cap 7 is smaller than that of Bent Cap 2. The distance between the center line of the exterior girder and the end face of the inverted-T bridge caps should be maintained at least 24 inches, as recommended by TxDOT Project 0-6905.

### **6.3 DISCUSSION ON DESIGN EXAMPLES**

The technical report 0-6905-R1 (TxDOT Project 0-6905) presented the design examples of ITBCs (for skew angles  $0^\circ$ ,  $30^\circ$ ,  $45^\circ$ , and  $60^\circ$ ) (Wang et al., 2020). The following two comments are provided in this report.

1. The lab test found that the skewed ITBC with a skew angle of more than  $45^\circ$  is prone to torsional failure. Bent Cap 2 (skew angle  $43^\circ$ ) and Bent Cap 7 (skew angle  $33^\circ$ ) exhibited torsional effects during the load tests. Further, the torsional effect is higher on the ITBC with a higher skew angle. The value of alpha ' $\alpha$ ' ( $\alpha = 90^\circ - \text{skew angle}$ ) is a crucial parameter in torsional longitudinal reinforcement design in the design example from Report 0-6905-R1. It is recommended to consider the torsional effect in the skewed ITBC with a skew angle equal to or greater than  $30^\circ$ .

- 
2. The design examples in the report are based on AASHTO LRFD Bridge Design Specifications, 8<sup>th</sup> Edition (2017). The RT recommends updating the design example with the latest AASHTO LRFD Bridge Design Specifications, 9<sup>th</sup> Edition (2020).

## 7 CONCLUSIONS

This chapter presents the summary of the research work, conclusions based on load tests on the Donigan Road Bridge and finite element analysis of calibrated finite element models, and future studies on inverted-T bridge caps.

### 7.1 SUMMARY OF THE RESEARCH WORKS

The summary of the research conducted on the implementation of skew reinforcing on Bent Cap 2 and Bent Cap 7 of Donigan Road Bridge can be expressed as follows:

1. The preliminary finite element analysis (FEA) of Bent Cap 2 and Bent Cap 7 was performed per the structural drawing the project team (PT) provided. Each bent cap was analyzed in 15 cases of four truckloads to identify critical cases.
2. Cases 1 and 14 (Static Test 1), Cases 3 and 9 (Static Test 2), Cases 9 and 14 (Dynamic Test-1, and Case 9 (Dynamic Test 2) were selected for the load test on Bent Cap 2.
3. Cases 1 and 11 (Static Test 1), Cases 9 and 14 (Static Test 2 and Dynamic Test 1), and Case 9 (Dynamic Test 2) were selected for the load test on Bent Cap 7.
4. The research team (RT) assembled a well-functioning data acquisition system and performed rehearsal tests for sensor installations.
5. The rebar cage of both bent caps was instrumented with strain gauges, carbon nanofiber aggregates, and thermocouples.
6. Both bent caps were cast in two phases (Phase 1 and Phase 2). The concrete samples were collected to identify the concrete material properties. The concrete cylinders were tested on the 7<sup>th</sup> day, the 28<sup>th</sup> day, and the day of the load test.
7. The load tests on inverted-T bent caps focused on the influence of the skew angles, which further investigated the strain on transverse rebars, torsional effect, end face displacement, and compressive stresses on the exterior loading pads. In addition, the influence of the location of exterior loading pads from the end face was examined.
8. The preliminary FE models of both bent caps were calibrated with load test results, and the parametric study was conducted. The parametric study identified concrete tensile strains at the critical zone, discovered the dual function of diagonal G bars [delay crack appearance at the ledge and stem interface and reduce strain on transverse rebars (S bars and M bars)], examined the stress concentration on the transverse rebars at the location of the exterior

loading pads on the projected side, and critically examined the influence of a higher skew angle on the structural performance of the ITBC.

9. The sensor boxes on both bent caps are installed to secure the wires/cables and utilization for structural health monitoring of resilient ITBCs, as presented in APPENDIX-6

## 7.2 CONCLUSIONS

Based on the load tests and finite element analysis (FEA) on Bent Cap 2 and Bent Cap 7 of Donigan Road Bridge over I-10, the following main conclusions are presented:

1. The tensile strains on the S bars on the south side closest to the end face of both ITBCs are higher in all loading cases. Due to larger torsion, the S bars on the north side exhibited compressive strain in Static Test 2 at Position 4 in both ITBCs.
2. The tensile strain on the M bars (at the top of the stirrups, and the interface of ledge and stem) is larger in the loading cases with truckloads positioned in two lanes (Case 3 of Bent Cap 2, and Case 14 of both Bent Cap 2 and Bent Cap 7).
3. Bent Cap 2 exhibited higher tensile strain on the fourth and fifth G bars. It is due to the location of exterior loading pads close to the fourth and fifth G bars. The tensile strains on the G bars are comparable to the S bars on the south side.
4. The inclusion of diagonal G bars at the end faces reduces the strains in the transverse bars (i.e., S and M bars) near the exterior loading pads.
5. The tensile stresses on the transverse rebars are higher from the location of the exterior loading pads at the south side to the end face of the ITBC (concentrated at the ledge and stem interface).
6. The loading cases with truckloads (all trucks positioned in one lane and closer to the parapet) concentrated on the forward span result in higher strains on the transverse rebar and higher displacements of the west face of both ITBCs, which make these cases critical. Case 14 (trucks positioned in two lanes) with truckloads concentrated around the centerline of the ITBCs has comparatively lower strains on the transverse rebar and lower displacements of the west face of both ITBCs.
7. The concrete tensile strains at the stem and ledge interface are higher in all loading cases. The concrete tensile strains of the calibrated models for all cases are smaller than the cracking strain. Hence, the implementation of skew reinforcing ensures the resilience of ITBCs.

8. The longer side of the overhanging cantilever portion of the ITBCs has a higher compressive stress on the exterior loading pads. Bent Cap 2 exhibited higher average compressive stress on the south side than on the north side in all static load tests.
9. The deformations of the west face of bent caps are unsymmetrical. The tip displacements of both bent caps at the projected end (south side) are the highest. The tip displacement of Bent Cap 2 is higher than that of Bent Cap 7 in all loading cases.
10. Bent Cap 7 exhibited that the static test yields higher strains on rebar and higher-end face displacements than the dynamic test. It may be because the static test provides adequate time for stress to be transferred to the ledge of the ITBC, while dynamic tests are swift in action.
11. The stem and ledge interface at the projected side of the cantilever portion of an ITBC is a critical region.

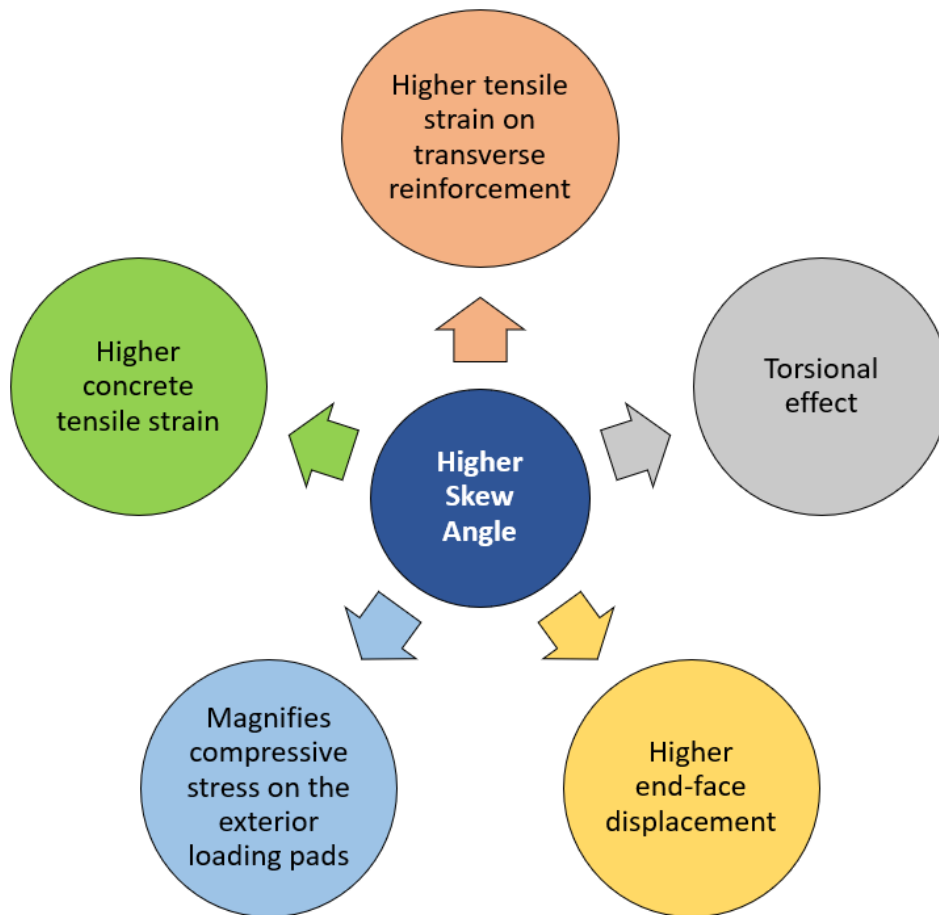


**Figure 7.1. Influence of Higher Skew Angle on Structural Performance of an Inverted-T Bridge Cap**

12. The skew angle of an ITBC is the most influential parameter (as presented in Figure 7.1).

From the load tests and FEA, it is observed that:

- a. An ITBC with a higher skew angle has a higher tensile strain on transverse reinforcement.
- b. An ITBC with a higher skew angle influences the torsional effect on the bent cap.
- c. Higher end face displacement of the longer side of an ITBC with a higher skew angle.
- d. The skew angle magnifies the compressive stress on the exterior loading pad.
- e. A higher skew angle increases the higher tensile strain on the concrete.

### **7.3 FUTURE STUDY**

Based on the load tests and parametric study on the well-calibrated models of Bent Cap 2 and Bent Cap 7, the following future studies are proposed:

1. The well-calibrated FE models can be utilized to examine the performance of the ITBCs for serviceability with HL 93 loading (structural health monitoring of resilient bent caps).
2. The assembled sensor box can be utilized to monitor the effect of traffic on the bent caps. Furthermore, this system can help examine the potential deterioration of bent caps due to environmental factors, aging of the bridge, and natural disaster.
3. The rebar congestion in the bent cap needs to be addressed. Figure 7.2 shows rebar congestion on Bent Cap 2. Assembly/preparation of rebar cages and casting concrete consumes time due to rebar congestion. The time consumption in the rebar cage assembly and concrete casting increases the cost of the project (Wang et al., 2020). Bent Cap 2 and Bent Cap 7 used 60 ksi #6 rebars for S bars (transverse bar). Using a high-strength steel ( $f_y = 80$  ksi and 100 ksi) rebar for S bars can reduce rebar dimension requirements and increase rebar spacing requirements without compromising the structural performance. The well-calibrated FE models of the ITBC can be used to investigate 80 ksi- and 100 ksi- strength rebars.



**Figure 7.2. Rebar Congestion (S-bars), Bent Cap 2**

4. The diagonal G bars (five No.7s) are currently provided to prevent the early appearance of cracks at the stem and ledge interface. The load tests and parametric study show that the G bars contribute to reducing the strain on the S bars and M bars. The increments in the numbers and size of the G bars can be further explored to enhance the dual benefits of the diagonal G bars.

## REFERENCES

- AASHTO LRFD bridge design specifications*. (8th edition). (2014). American Association of State Highway and Transportation Officials.
- AASHTO Standard Specifications for Highway Bridges* (17th Edition). (2002). AASHTO Standard Specifications for Highway Bridges,.
- Ambare, S., & Peterman, R. J. (2006). *Evaluation of the Inverted Tee Shallow Bridge System for use in Kansas*. Kansas Department of Transportation Report No. K-TRAN: KSU-00-1.
- American Society for Testing and Materials. (2001). *Standard Test Method for Compressive Strength of Cylindrical Concrete Specimens*. [https://doi.org/10.1520/C0039\\_C0039M-18](https://doi.org/10.1520/C0039_C0039M-18)
- Gautam, A., Mo, Y. L., Chen, Y., Chen, J., & Joshi, B. (2019). Carbon Nanofiber Aggregate Sensors for Sustaining Resilience of Civil Infrastructures to Multi-Hazards. *Advancements in Civil Engineering & Technology*, 3(1), 263–269. <https://doi.org/10.31031/acet.2019.03.000551>
- Gomez, E. F. (2012). *Design Criteria for Strength and Serviceability of Inverted-T Straddle Bent Caps Committee*. <http://hdl.handle.net/2152/ETD-UT-2012-08-6340>
- Hsu, T. T. C., & Zhu, R. R. H. (2005). Crack Width Prediction for Ledges in Inverted ‘T’ Bent Caps. *ACI Symposium Publication*, 179–196. <https://doi.org/10.14359/14384>
- Joshi, B., Li, X., Oz, Y., Wang, J., Shan, X., & Mo, Y. L. (2021). Effects of fiber dosage, loading orientation and stress on frequency response of enhanced Carbon Nano-Fiber Aggregates. *Composites Part B: Engineering*, 225. <https://doi.org/10.1016/j.compositesb.2021.109257>
- Joshi, B., Shan, X., Wang, J., Oz, Y., & Mo, Y. L. (2021). Cast Method Effect of Carbon Nanofiber Aggregates on Structural Health Monitoring. In P. Rizzo & A. Milazzo (Eds.), *European Workshop on Structural Health Monitoring* (pp. 517–526). Springer International Publishing.
- Joshi, B., Shan, X., Wang, J., Yang, X., Öz, Y., Mo, Y. L., & Moores Professor, R. (2021). Correlation of Impedance and Compressive Stress of Carbon Nanofiber Aggregates for Structural Health Monitoring. *17th Biennial International Conference on Engineering*,

- Science, Construction, and Operations in Challenging Environments*, 321–330.  
<https://doi.org/10.1061/9780784483381.029>
- Joshi, B., Wang, J., Li, X., Ramaswamy, N. H., Shrestha, P., Shan, X., Mo, Y. L., & Hsu, T. T. C. (2023). Development of robust ultra-high-performance carbon nanofiber aggregates (UHPCNFAs) for structural health monitoring. *Engineering Structures*, 279, 115559.  
<https://doi.org/10.1016/J.ENGSTRUCT.2022.115559>
- Mirza, S. A., & Furlong, R. W. (1983). Serviceability Behavior and Failure Mechanisms of Concrete Inverted T-Beam Bridge Bentcaps. *ACI Journal Proceedings*, 80(4), 294–304.  
<https://doi.org/10.14359/10850>
- Mirza, S. A., & Furlong, R. W. (1985). Design of Reinforced and Prestressed Concrete Inverted T Beams for Bridge Structures. *PCI Journal*, 30(4), 112–136.  
<https://doi.org/10.15554/pcij.07011985.112.136>
- Mo, Y. L., Gautam, A., Chen, Y., Chen, J., & Joshi, B. (2020). Electrical impedance of carbon nanofiber aggregates. *Smart Nanoconcretes and Cement-Based Materials*, 333–349.  
<https://doi.org/10.1016/b978-0-12-817854-6.00014-3>
- National Centers for Environmental Information. (2023). *U.S. Climate Normals 2020: U.S. Monthly Climate Normals (1991-2020)*.
- Oz, Y. (2020). *STRUCTURAL PERFORMANCE AND ECONOMIC IMPACT OF SKEWED REINFORCING IN INVERTED-T BRIDGE CAPS*. Master's Thesis, University of Houston, USA.
- Oz, Y., Wang, J., Roy, S. S., Zhang, S., Joshi, B., Guo, Z., Mo, Y. L., & Hsu, T. T. C. (2022). Finite-Element Simulation and Cost–Benefit Analysis of Full-Scale Skewed Inverted-T Bridge Caps with Traditional and Skew Reinforcements. *Journal of Bridge Engineering*, 27(7). [https://doi.org/10.1061/\(asce\)be.1943-5592.0001864](https://doi.org/10.1061/(asce)be.1943-5592.0001864)
- Roy, S. S. (2019). *Structural Performance of Skew Reinforcing in Inverted-T Bridge Caps*. Ph.D. Dissertation, University of Houston, Texas, USA.
- Sapath Roy, S., Sawab, J., Zhou, T., Wang, J., Mo, Y. L., & Hsu, T. T. C. (2021). Experimental study on skew inverted-T bent caps with minimum traditional and skew transverse

reinforcing. *Engineering Structures*, 230, 111653.  
<https://doi.org/10.1016/J.ENGSTRUCT.2020.111653>

Sapath, S., Sawab, R. J., Zhou, T., Mo, Y. L., & Hsu, T. T. C. (2019). *Initial Investigation of Performance of Skewed Reinforcing in Inverted-T Bridge Caps*. [www.ntis.gov](http://www.ntis.gov).

Snyder, R. M. (2010). *Seismic performance of an I-girder to inverted-T bent cap bridge connection* [Iowa State University, Digital Repository]. <https://doi.org/10.31274/etd-180810-2981>

Texas Department of Transportation. (2020). *Bridge Design Manual-LRFD*.

Texas Department of Transportation. (2022a). *Bridge Detailing Guide (Bridge Division)*.

Texas Department of Transportation. (2022b). *Bridge Design Guide (Bridge Division)*.

Wang, J., Oz, Y., Joshi, B., Sapath, S. R., Mo, Y. L., & Hsu, T. T. C. (2020). *Investigation of Performance of Skewed Reinforcing in Inverted-T Bridge Caps*.

Zhou, T., Roy, S. S., Wang, J., Nie, X., Chen, H., & Mo, Y. L. (2020). Parametric Study on the Structural Behavior and Failure Mechanism of Skewed Inverted-T Bent Caps. *Journal of Bridge Engineering*, 25(11), 04020092. [https://doi.org/10.1061/\(asce\)be.1943-5592.0001629](https://doi.org/10.1061/(asce)be.1943-5592.0001629)

**APPENDIX-1**

**Table A1.1. Strain Values in Cases 1 to 15 of Bent Cap 2 for 31 Locations**

# SG	Label	Loading Case				
		1	2	3	4	5
1	B2-SS1s1	1.33E-05	1.29E-05	1.48E-05	3.57E-06	1.47E-05
2	B2-SS1s2	1.14E-05	1.10E-05	1.27E-05	2.98E-06	1.27E-05
3	B2-SS2s1	1.36E-05	1.32E-05	1.50E-05	3.70E-06	1.49E-05
4	B2-SS2s2	1.11E-05	1.07E-05	1.23E-05	2.95E-06	1.22E-05
5	B2-SS3s1	1.40E-05	1.37E-05	1.52E-05	4.10E-06	1.49E-05
6	B2-SS3s2	1.05E-05	1.03E-05	1.15E-05	3.07E-06	1.13E-05
7	B2-SS4s1	1.37E-05	1.34E-05	1.49E-05	4.05E-06	1.46E-05
8	B2-SS4s2	1.08E-05	1.06E-05	1.18E-05	3.16E-06	1.16E-05
9	B2-NS5s1	1.57E-06	1.65E-06	1.22E-06	2.67E-06	9.22E-09
10	B2-NS5s2	2.99E-06	3.08E-06	2.60E-06	3.85E-06	9.73E-07
11	B2-NS6s1	1.71E-06	1.79E-06	1.35E-06	2.79E-06	1.01E-07
12	B2-NS6s2	3.13E-06	3.22E-06	2.73E-06	3.98E-06	1.06E-06
13	B2-NS7s1	2.43E-06	2.53E-06	2.06E-06	3.40E-06	5.72E-07
14	B2-NS7s2	4.27E-06	4.38E-06	3.83E-06	4.98E-06	1.78E-06
15	B2-NS8s1	2.52E-06	2.61E-06	2.14E-06	3.47E-06	6.25E-07
16	B2-NS8s2	4.46E-06	4.57E-06	4.01E-06	5.14E-06	1.89E-06
17	B2-SM5t	9.06E-06	8.91E-06	9.51E-06	3.00E-06	9.10E-06
18	B2-SM6t	1.03E-05	1.01E-05	1.08E-05	3.41E-06	1.03E-05
19	B2-SM7t	1.08E-05	1.06E-05	1.14E-05	3.55E-06	1.10E-05
20	B2-SM8t	1.08E-05	1.06E-05	1.14E-05	3.55E-06	1.10E-05
21	B2-SM15b	-6.56E-06	-6.38E-06	-7.36E-06	-1.00E-06	-7.68E-06
22	B2-SM16b	-6.18E-06	-6.00E-06	-6.98E-06	-7.45E-07	-7.38E-06
23	B2-A7	4.01E-06	3.96E-06	4.29E-06	1.38E-06	4.05E-06
24	B2-A8	4.60E-06	4.57E-06	4.87E-06	1.73E-06	4.49E-06
25	B2-A9	5.35E-06	5.34E-06	5.59E-06	2.23E-06	5.00E-06
26	B2-U1-1	1.10E-06	1.03E-06	1.41E-06	-2.41E-08	1.54E-06
27	B2-SG1	8.01E-06	7.80E-06	8.75E-06	2.48E-06	8.50E-06
28	B2-SG2	9.96E-06	9.77E-06	1.06E-05	3.23E-06	1.03E-05
29	B2-B10	-4.92E-06	-4.87E-06	-5.22E-06	-2.61E-06	-4.46E-06
30	B2-T7-N	9.43E-07	1.08E-06	3.78E-07	1.21E-06	-3.56E-08
31	B2-T3-S	-1.46E-06	-1.59E-06	-1.40E-06	-1.73E-07	-1.32E-06
# SG	Label	Loading Case				
		6	7	8	9	10
1	B2-SS1s1	3.49E-06	2.01E-07	1.11E-05	2.02E-05	1.36E-05
2	B2-SS1s2	2.97E-06	1.07E-07	9.57E-06	1.72E-05	1.15E-05

3	B2-SS2s1	3.57E-06	2.64E-07	1.12E-05	2.05E-05	1.39E-05
4	B2-SS2s2	2.90E-06	1.52E-07	9.23E-06	1.67E-05	1.12E-05
5	B2-SS3s1	3.71E-06	5.40E-07	1.11E-05	2.09E-05	1.44E-05
6	B2-SS3s2	2.80E-06	3.87E-07	8.43E-06	1.58E-05	1.08E-05
7	B2-SS4s1	3.65E-06	5.49E-07	1.09E-05	2.06E-05	1.42E-05
8	B2-SS4s2	2.87E-06	4.07E-07	8.63E-06	1.62E-05	1.11E-05
9	B2-NS5s1	1.15E-06	1.61E-06	-1.00E-06	3.63E-07	2.05E-06
10	B2-NS5s2	1.79E-06	2.21E-06	-6.26E-07	1.81E-06	3.64E-06
11	B2-NS6s1	1.21E-06	1.67E-06	-9.68E-07	5.11E-07	2.21E-06
12	B2-NS6s2	1.85E-06	2.27E-06	-5.94E-07	1.94E-06	3.80E-06
13	B2-NS7s1	1.54E-06	1.99E-06	-7.83E-07	1.26E-06	3.04E-06
14	B2-NS7s2	2.38E-06	2.79E-06	-3.50E-07	3.08E-06	5.11E-06
15	B2-NS8s1	1.58E-06	2.02E-06	-7.61E-07	1.34E-06	3.14E-06
16	B2-NS8s2	2.46E-06	2.87E-06	-3.11E-07	3.27E-06	5.33E-06
17	B2-SM5t	2.56E-06	5.76E-07	6.96E-06	1.33E-05	9.45E-06
18	B2-SM6t	2.90E-06	6.58E-07	7.91E-06	1.51E-05	1.07E-05
19	B2-SM7t	3.04E-06	6.79E-07	8.35E-06	1.58E-05	1.12E-05
20	B2-SM8t	3.04E-06	6.79E-07	8.35E-06	1.58E-05	1.12E-05
21	B2-SM15b	-1.43E-06	3.75E-07	-6.06E-06	-1.06E-05	-6.58E-06
22	B2-SM16b	-1.30E-06	5.02E-07	-5.90E-06	-1.02E-05	-6.14E-06
23	B2-A7	1.09E-06	3.10E-07	2.93E-06	5.89E-06	4.24E-06
24	B2-A8	1.30E-06	4.64E-07	3.21E-06	6.66E-06	4.92E-06
25	B2-A9	1.57E-06	7.00E-07	3.49E-06	7.57E-06	5.80E-06
26	B2-U1-1	1.85E-07	-2.27E-07	1.23E-06	1.93E-06	1.03E-06
27	B2-SG1	2.22E-06	3.44E-07	6.35E-06	1.18E-05	8.22E-06
28	B2-SG2	2.78E-06	5.89E-07	7.67E-06	1.46E-05	1.03E-05
29	B2-B10	-1.74E-06	-1.02E-06	-2.74E-06	-6.32E-06	-5.30E-06
30	B2-T7-N	2.63E-07	7.80E-07	-3.99E-07	9.34E-07	1.30E-06
31	B2-T3-S	-1.32E-07	-6.70E-08	-1.01E-06	-2.82E-06	-1.75E-06
# SG	Label	Loading Case				
		11	12	13	14	15
1	B2-SS1s1	2.24E-05	1.46E-05	1.93E-05	1.20E-05	1.50E-05
2	B2-SS1s2	1.93E-05	1.26E-05	1.66E-05	1.03E-05	1.28E-05
3	B2-SS2s1	2.29E-05	1.49E-05	1.97E-05	1.22E-05	1.52E-05
4	B2-SS2s2	1.87E-05	1.22E-05	1.60E-05	9.97E-06	1.24E-05
5	B2-SS3s1	2.32E-05	1.50E-05	1.98E-05	1.24E-05	1.55E-05
6	B2-SS3s2	1.75E-05	1.14E-05	1.50E-05	9.35E-06	1.17E-05
7	B2-SS4s1	2.28E-05	1.47E-05	1.95E-05	1.22E-05	1.52E-05
8	B2-SS4s2	1.80E-05	1.16E-05	1.54E-05	9.59E-06	1.20E-05
9	B2-NS5s1	2.37E-07	2.41E-07	-1.57E-06	7.40E-07	1.28E-06

<b>10</b>	<b>B2-NS5s2</b>	1.76E-06	1.30E-06	-8.30E-07	1.81E-06	2.70E-06
<b>11</b>	<b>B2-NS6s1</b>	3.92E-07	3.42E-07	-1.50E-06	8.43E-07	1.42E-06
<b>12</b>	<b>B2-NS6s2</b>	1.90E-06	1.40E-06	-7.72E-07	1.92E-06	2.84E-06
<b>13</b>	<b>B2-NS7s1</b>	1.17E-06	8.64E-07	-1.14E-06	1.38E-06	2.14E-06
<b>14</b>	<b>B2-NS7s2</b>	3.08E-06	2.20E-06	-2.71E-07	2.75E-06	3.98E-06
<b>15</b>	<b>B2-NS8s1</b>	1.25E-06	9.24E-07	-1.10E-06	1.44E-06	2.23E-06
<b>16</b>	<b>B2-NS8s2</b>	3.28E-06	2.33E-06	-1.86E-07	2.88E-06	4.16E-06
<b>17</b>	<b>B2-SM5t</b>	1.42E-05	9.48E-06	1.24E-05	8.19E-06	9.90E-06
<b>18</b>	<b>B2-SM6t</b>	1.61E-05	1.08E-05	1.40E-05	9.30E-06	1.12E-05
<b>19</b>	<b>B2-SM7t</b>	1.70E-05	1.13E-05	1.48E-05	9.75E-06	1.18E-05
<b>20</b>	<b>B2-SM8t</b>	1.70E-05	1.13E-05	1.48E-05	9.75E-06	1.18E-05
<b>21</b>	<b>B2-SM15b</b>	-1.21E-05	-7.63E-06	-1.09E-05	-5.94E-06	-7.46E-06
<b>22</b>	<b>B2-SM16b</b>	-1.16E-05	-7.31E-06	-1.06E-05	-5.64E-06	-7.06E-06
<b>23</b>	<b>B2-A7</b>	6.54E-06	4.13E-06	5.38E-06	3.43E-06	4.39E-06
<b>24</b>	<b>B2-A8</b>	7.36E-06	4.62E-06	5.93E-06	3.88E-06	4.99E-06
<b>25</b>	<b>B2-A9</b>	8.32E-06	5.19E-06	6.53E-06	4.42E-06	5.74E-06
<b>26</b>	<b>B2-U1-1</b>	2.28E-06	1.43E-06	2.05E-06	1.03E-06	1.34E-06
<b>27</b>	<b>B2-SG1</b>	1.30E-05	8.57E-06	1.10E-05	7.17E-06	8.91E-06
<b>28</b>	<b>B2-SG2</b>	1.60E-05	1.05E-05	1.36E-05	8.86E-06	1.10E-05
<b>29</b>	<b>B2-B10</b>	-7.10E-06	-4.52E-06	-4.88E-06	-3.92E-06	-5.27E-06
<b>30</b>	<b>B2-T7-N</b>	4.21E-07	4.25E-07	5.85E-07	7.95E-07	6.27E-07
<b>31</b>	<b>B2-T3-S</b>	-3.19E-06	-1.49E-06	-2.90E-06	-1.02E-06	-1.48E-06

**Table A1.2. Maximum Concrete Strain in Tension and Compression and Displacement at West Face of ITBC 2 in Cases 1 to 15**

Case	Maximum Concrete Strain		Displacement at West Face (in)		
	Tension	Compression	Left	Middle	Right
<b>1</b>	2.03E-05	-6.33E-05	-0.00486	-0.00659	-0.01099
<b>2</b>	2.06E-05	-6.51E-05	-0.00486	-0.00648	-0.01072
<b>3</b>	2.22E-05	-5.85E-05	-0.00451	-0.00735	-0.01250
<b>4</b>	1.98E-05	-6.84E-05	-0.00414	-0.00359	-0.00413
<b>5</b>	2.17E-05	-5.63E-05	-0.00295	-0.00583	-0.01140
<b>6</b>	1.11E-05	-4.13E-05	-0.00204	-0.00203	-0.00282
<b>7</b>	1.35E-05	-5.05E-05	-0.00207	-0.00117	-0.00054
<b>8</b>	1.62E-05	-4.06E-05	0.00001	-0.00312	-0.00823
<b>9</b>	3.04E-05	-8.13E-05	-0.00464	-0.00858	-0.01546
<b>10</b>	2.38E-05	-7.49E-05	-0.00535	-0.00713	-0.01175
<b>11</b>	3.36E-05	-9.20E-05	-5.17E-03	-0.00897	-0.01683
<b>12</b>	2.19E-05	-5.70E-05	-0.00321	-0.00601	-0.01157
<b>13</b>	2.88E-05	-7.66E-05	-0.00202	-0.00590	-0.01300
<b>14</b>	1.82E-05	-4.80E-05	-0.00321	-0.00543	-0.01005
<b>15</b>	2.26E-05	-6.08E-05	-0.00454	-0.00720	-0.01288

**Table A1.3. CNFA Stress Values of Loading Cases 1 to 15 of Bent Cap 2**

# CNFA	Label	Stress Values of Loading Case (ksi)							
		1	2	3	4	5	6	7	
1	B2-CNFA1z1	-0.04	-0.04	-0.04	-0.03	-0.03	-0.02	-0.02	
2	B2-CNFA2z1	-0.27	-0.30	-0.26	-0.29	-0.15	-0.14	-0.16	
3	B2-CNFA2z2	-0.29	-0.28	-0.27	-0.27	-0.15	-0.13	-0.15	
4	B2-CNFA2z3	-0.28	-0.28	-0.25	-0.24	-0.13	-0.12	-0.13	
5	B2-CNFA3z1	0.39	0.38	0.43	0.10	0.43	0.10	0.01	
6	B2-CNFA3z2	0.39	0.38	0.43	0.11	0.43	0.10	0.01	
7	B2-CNFA3z3	0.40	0.40	0.44	0.12	0.43	0.11	0.02	
8	B2-CNFA4z1	-0.24	-0.24	-0.26	-0.07	-0.21	-0.06	-0.01	
9	B2-CNFA4z2	-0.20	-0.19	-0.22	-0.07	-0.26	-0.06	-0.01	
# CNFA	Label	Stress Values of Loading Case (ksi)							
		8	9	10	11	12	13	14	15
1	B2-CNFA1z1	-0.01	-0.05	-0.05	-0.05	-0.03	-0.03	-0.03	-0.04
2	B2-CNFA2z1	-0.02	-0.22	-0.34	-0.25	-0.18	-0.08	-0.20	-0.28
3	B2-CNFA2z2	-0.02	-0.25	-0.33	-0.26	-0.17	-0.06	-0.19	-0.27
4	B2-CNFA2z3	-0.02	-0.26	-0.29	-0.26	-0.15	-0.05	-0.17	-0.24
5	B2-CNFA3z1	0.32	0.58	0.39	0.65	0.42	0.56	0.35	0.43
6	B2-CNFA3z2	0.33	0.60	0.40	0.66	0.43	0.57	0.35	0.44
7	B2-CNFA3z3	0.32	0.61	0.42	0.67	0.44	0.58	0.36	0.45
8	B2-CNFA4z1	-0.16	-0.37	-0.21	-0.32	-0.21	-0.27	-0.18	-0.22
9	B2-CNFA4z2	-0.18	-0.29	-0.25	-0.41	-0.26	-0.35	-0.21	-0.27

**Table A1.4. Strain Values at Five Positions for Case 3 of Bent Cap 2 under Static Test-2**

# SG	Label	Strain in Case 3, Bent Cap 2				
		Position 1	Position 2	Position 3	Position 4	Position 5
1	B2-SS1s1	-1.11E-06	-5.82E-07	1.48E-05	2.87E-05	1.35E-05
2	B2-SS1s2	-1.05E-06	-6.17E-07	1.27E-05	2.49E-05	1.18E-05
3	B2-SS2s1	-1.05E-06	-4.76E-07	1.50E-05	2.91E-05	1.37E-05
4	B2-SS2s2	-9.52E-07	-5.11E-07	1.23E-05	2.40E-05	1.13E-05
5	B2-SS3s1	-6.93E-07	3.39E-08	1.52E-05	2.89E-05	1.36E-05
6	B2-SS3s2	-5.60E-07	-1.65E-08	1.15E-05	2.20E-05	1.04E-05
7	B2-SS4s1	-6.57E-07	6.36E-08	1.49E-05	2.83E-05	1.32E-05
8	B2-SS4s2	-5.54E-07	7.16E-09	1.18E-05	2.26E-05	1.07E-05
9	B2-NS5s1	1.38E-06	2.77E-06	1.22E-06	-3.56E-06	-2.06E-06
10	B2-NS5s2	1.80E-06	3.71E-06	2.60E-06	-3.00E-06	-1.98E-06
11	B2-NS6s1	1.42E-06	2.87E-06	1.35E-06	-3.50E-06	-2.05E-06
12	B2-NS6s2	1.84E-06	3.81E-06	2.73E-06	-2.99E-06	-2.00E-06
13	B2-NS7s1	1.67E-06	3.38E-06	2.06E-06	-3.25E-06	-2.03E-06
14	B2-NS7s2	2.25E-06	4.66E-06	3.83E-06	-2.70E-06	-2.00E-06
15	B2-NS8s1	1.69E-06	3.44E-06	2.14E-06	-3.24E-06	-2.03E-06
16	B2-NS8s2	2.32E-06	4.80E-06	4.01E-06	-2.64E-06	-1.99E-06
17	B2-SM5t	-3.02E-07	3.12E-07	9.51E-06	1.58E-05	5.91E-06
18	B2-SM6t	-3.36E-07	3.57E-07	1.08E-05	1.78E-05	6.65E-06
19	B2-SM7t	-3.47E-07	3.66E-07	1.14E-05	1.92E-05	7.50E-06
20	B2-SM8t	-3.47E-07	3.66E-07	1.14E-05	1.92E-05	7.50E-06
21	B2-SM15b	9.64E-07	1.16E-06	-7.36E-06	-1.69E-05	-8.61E-06
22	B2-SM16b	1.10E-06	1.39E-06	-6.98E-06	-1.66E-05	-8.48E-06
23	B2-A7	7.12E-09	3.42E-07	4.29E-06	7.81E-06	3.75E-06
24	B2-A8	1.31E-07	6.03E-07	4.87E-06	8.45E-06	4.00E-06
25	B2-A9	3.30E-07	1.01E-06	5.59E-06	9.08E-06	4.23E-06
26	B2-U1-1	-3.56E-07	-4.66E-07	1.41E-06	3.81E-06	2.13E-06
27	B2-SG1	-4.93E-07	2.52E-08	8.75E-06	1.58E-05	6.98E-06
28	B2-SG4	-2.30E-07	6.24E-07	1.39E-05	2.49E-05	1.11E-05
29	B2-SG5	-2.72E-07	6.50E-07	1.54E-05	2.77E-05	1.24E-05
30	B2-B10	-4.70E-07	-1.45E-06	-5.22E-06	-7.15E-06	-3.60E-06
31	B2-T7-N	1.23E-06	1.72E-06	3.78E-07	-1.49E-06	-1.61E-06
32	B2-T3-S	-2.89E-07	-1.76E-07	-1.40E-06	-4.61E-06	-2.97E-06

**Table A1.5. Maximum Concrete Strains in Tension and Compression and Displacement of Five Positions of Four-Trucks Load in Case 3 at West Face of ITBC**

Case 3, Bent Cap 2	Maximum Strain on Concrete in		Displacement (in) from West Face		
	Tension	Compression	Left	Middle	Right
Position 1	9.32E-06	-1.97E-05	-0.00096	-0.00066	-0.00049
Position 2	1.82E-05	-5.93E-05	-0.00301	-0.00208	-0.00152
Position 3	2.22E-05	-5.85E-05	-0.00451	-0.00735	-0.01250
Position 4	4.17E-05	-1.17E-05	-0.00183	-0.00850	-0.01838
Position 5	1.95E-05	-6.04E-05	-0.00065	-0.00329	-0.00778

**Table A1.6. CNFA Stress Values of Five Positions of Four-Trucks Load in Case 3**

# CNFA	Label	Stress (ksi) in Case 3, Bent Cap 2				
		Position 1	Position 2	Position 3	Position 4	Position 5
1	B2-CNFA1zz1	-0.01	-0.03	-0.04	-0.03	-0.01
2	B2-CNFA2zz1	-0.12	-0.25	-0.26	0.04	0.01
3	B2-CNFA2zz2	-0.14	-0.27	-0.27	0.03	0.01
4	B2-CNFA2zz3	-0.13	-0.25	-0.25	0.04	0.01
5	B2-CNFA3zz1	-0.03	-0.02	0.43	0.83	0.39
6	B2-CNFA3zz2	-0.03	-0.01	0.43	0.84	0.40
7	B2-CNFA3zz3	-0.02	0.00	0.44	0.84	0.39
8	B2-CNFA4zz1	0.00	-0.01	-0.26	-0.52	-0.26
9	B2-CNFA4zz2	0.01	-0.01	-0.22	-0.38	-0.17
10	B2-CNFA4zz3	0.01	-0.01	-0.19	-0.34	-0.16

**Table A1.7. Strain Values at Five Positions for Case 9 of Bent Cap 2 under Four-Truck Loading**

# SG	Label	Strain in Case 9				
		Position-1	Position-2	Position-3	Position-4	Position-5
1	B2-SS1s1	-1.79E-07	7.21E-06	2.02E-05	2.54E-05	2.04E-05
2	B2-SS1s2	-2.65E-07	6.06E-06	1.72E-05	2.19E-05	1.78E-05
3	B2-SS2s1	-7.33E-08	7.41E-06	2.05E-05	2.58E-05	2.08E-05
4	B2-SS2s2	-1.74E-07	5.95E-06	1.67E-05	2.11E-05	1.71E-05
5	B2-SS3s1	4.10E-07	7.92E-06	2.09E-05	2.61E-05	2.07E-05
6	B2-SS3s2	2.71E-07	5.94E-06	1.58E-05	1.97E-05	1.58E-05
7	B2-SS4s1	4.31E-07	7.81E-06	2.06E-05	2.55E-05	2.02E-05
8	B2-SS4s2	2.99E-07	6.11E-06	1.62E-05	2.03E-05	1.62E-05
9	B2-NS5s1	2.78E-06	2.60E-06	3.63E-07	-8.52E-07	-2.84E-06
10	B2-NS5s2	3.74E-06	3.98E-06	1.81E-06	4.87E-07	-2.58E-06
11	B2-NS6s1	2.88E-06	2.74E-06	5.11E-07	-7.14E-07	-2.81E-06
12	B2-NS6s2	3.84E-06	4.13E-06	1.94E-06	5.99E-07	-2.58E-06
13	B2-NS7s1	3.41E-06	3.48E-06	1.26E-06	-4.21E-08	-2.70E-06
14	B2-NS7s2	4.71E-06	5.32E-06	3.08E-06	1.60E-06	-2.47E-06
15	B2-NS8s1	3.47E-06	3.56E-06	1.34E-06	2.92E-08	-2.70E-06
16	B2-NS8s2	4.86E-06	5.51E-06	3.27E-06	1.77E-06	-2.44E-06
17	B2-SM5t	5.72E-07	5.64E-06	1.33E-05	1.56E-05	1.03E-05
18	B2-SM6t	6.48E-07	6.39E-06	1.51E-05	1.77E-05	1.15E-05
19	B2-SM7t	6.62E-07	6.63E-06	1.58E-05	1.87E-05	1.26E-05
20	B2-SM8t	6.62E-07	6.63E-06	1.58E-05	1.87E-05	1.26E-05
21	B2-SM14b	9.58E-07	-2.89E-06	-1.06E-05	-1.40E-05	-1.26E-05
22	B2-SM16b	1.19E-06	-2.53E-06	-1.02E-05	-1.36E-05	-1.24E-05
23	B2-A7	4.42E-07	2.46E-06	5.89E-06	7.21E-06	5.67E-06
24	B2-A8	7.18E-07	2.96E-06	6.66E-06	8.02E-06	6.11E-06
25	B2-A9	1.14E-06	3.64E-06	7.57E-06	8.93E-06	6.53E-06
26	B2-U1-1	1.19E-06	2.90E-07	1.93E-06	2.81E-06	2.93E-06
27	B2-SG1	2.75E-07	4.65E-06	1.18E-05	1.46E-05	1.09E-05
28	B2-SG4	7.05E-07	7.93E-06	1.93E-05	2.33E-05	1.75E-05
29	B2-SG5	7.85E-07	8.69E-06	2.13E-05	2.58E-05	1.95E-05
30	B2-B10	-1.60E-06	-3.66E-06	-6.32E-06	-7.44E-06	-5.26E-06
31	B2-T7-N	1.44E-06	1.40E-06	9.34E-07	-1.71E-07	-1.58E-06
32	B2-T3-S	-1.25E-07	-7.48E-07	-2.82E-06	-3.67E-06	-4.14E-06

**Table A1.8. Maximum Concrete Strains in Tension and Compression and Displacement of Five Positions of Four-Trucks Load in Case 9 at West Face of ITBC**

Case 9	Maximum Strain on Concrete In		Displacement (in) from West Face		
	Tension	Compression	Left	Middle	Right
Position-1	1.84E-05	-5.91E-05	-0.00314	-0.00236	-0.00212
Position-2	2.29E-05	-7.25E-05	-0.00454	-0.00537	-0.00764
Position-3	3.04E-05	-8.13E-05	-0.00464	-0.00858	-0.01546
Position-4	3.77E-05	-1.04E-05	-0.00447	-0.00954	-0.01835
Position-5	2.98E-05	-8.90E-05	-0.00109	-0.00570	-0.01248

**Table A1.9. CNFA Stress Values of Five Positions of Four-Trucks Load in Case 9**

# CNFA	Label	Stress (ksi) in Case 9				
		Position-1	Position-2	Position-3	Position-4	Position-5
1	B2-CNFA1zz1	-0.03	-0.04	-0.05	-0.05	-0.02
2	B2-CNFA2zz1	-0.25	-0.32	-0.22	-0.19	0.05
3	B2-CNFA2zz2	-0.27	-0.33	-0.25	-0.19	0.05
4	B2-CNFA2zz3	-0.25	-0.31	-0.26	-0.18	0.04
5	B2-CNFA3zz1	-0.01	0.21	0.58	0.74	0.59
6	B2-CNFA3zz2	0.00	0.21	0.60	0.75	0.60
7	B2-CNFA3zz3	0.01	0.23	0.61	0.76	0.60
8	B2-CNFA4zz1	-0.01	-0.14	-0.37	-0.47	-0.39
9	B2-CNFA4zz2	-0.01	-0.12	-0.29	-0.35	-0.27
10	B2-CNFA4zz3	-0.02	-0.11	-0.26	-0.31	-0.24

**APPENDIX-2**

**Table A2.1. Strain Values in Cases 1 to 15 of Bent Cap 7 for 30 Locations**

# SG	Label	Loading Case				
		1	2	3	4	5
1	B7-SS1s1	1.17E-05	1.26E-05	1.07E-05	2.25E-06	1.60E-05
2	B7-SS1s2	8.38E-06	8.93E-06	1.07E-05	1.34E-06	1.16E-05
3	B7-SS2s1	1.17E-05	1.26E-05	1.50E-05	2.25E-06	1.60E-05
4	B7-SS2s2	8.34E-06	8.88E-06	1.07E-05	1.31E-06	1.16E-05
5	B7-SS3s1	1.19E-05	1.26E-05	1.50E-05	2.30E-06	1.61E-05
6	B7-SS3s2	8.06E-06	8.55E-06	1.03E-05	1.18E-06	1.13E-05
7	B7-SS4s1	1.19E-05	1.26E-05	1.50E-05	2.31E-06	1.60E-05
8	B7-SS4s2	8.04E-06	8.52E-06	1.03E-05	1.18E-06	1.12E-05
9	B7-NS5s1	8.49E-06	9.06E-06	8.56E-06	1.03E-05	3.90E-06
10	B7-NS5s2	5.31E-06	5.75E-06	5.27E-06	7.23E-06	1.84E-06
11	B7-NS6s1	8.61E-06	9.17E-06	8.67E-06	1.04E-05	3.97E-06
12	B7-NS6s2	5.42E-06	5.89E-06	5.41E-06	7.35E-06	1.93E-06
13	B7-NS7s1	9.87E-06	1.06E-05	1.01E-05	1.18E-05	4.76E-06
14	B7-NS7s2	6.28E-06	6.72E-06	6.21E-06	8.13E-06	2.40E-06
15	B7-NS8s1	1.01E-05	1.09E-05	1.04E-05	1.21E-05	4.91E-06
16	B7-NS8s2	6.42E-06	6.84E-06	6.32E-06	8.24E-06	2.46E-06
17	B7-SM5t	7.54E-07	1.43E-06	1.87E-06	2.82E-07	1.99E-06
18	B7-SM6t	-3.03E-06	2.00E-07	1.76E-08	2.61E-08	1.93E-07
19	B7-SM7t	-3.56E-06	5.40E-07	1.67E-07	8.38E-08	4.08E-07
20	B7-SM8t	-2.65E-06	1.64E-06	1.12E-06	4.39E-07	1.46E-06
21	B7-SM15b	-9.11E-06	-8.97E-06	-1.13E-05	5.65E-08	-1.29E-05
22	B7-SM17b	-7.54E-06	-7.38E-06	-9.58E-06	7.13E-07	-1.13E-05
23	B7-A7	4.09E-06	4.25E-06	4.84E-06	1.48E-06	4.70E-06
24	B7-A8	4.68E-06	4.87E-06	5.45E-06	1.92E-06	5.14E-06
25	B7-A9	5.33E-06	5.53E-06	6.11E-06	2.44E-06	5.58E-06
26	B7-U1-1	5.57E-06	5.98E-06	7.08E-06	1.17E-06	1.31E-05
27	B7-SG1	9.95E-06	1.09E-05	1.27E-05	2.94E-06	1.31E-05
28	B7-SG2	1.22E-05	1.30E-05	1.50E-05	3.54E-06	1.53E-05
29	B7-B10	-4.40E-06	-4.60E-06	-5.28E-06	-2.14E-06	-4.67E-06
30	B7-T7	-4.83E-06	-4.67E-06	-5.09E-06	-4.51E-06	-2.39E-06
# SG	Label	Loading Case				
		6	7	8	9	10
1	B7-SS1s1	2.83E-06	-7.83E-07	1.42E-05	2.08E-05	1.09E-05
2	B7-SS1s2	1.91E-06	-7.53E-07	1.04E-05	1.50E-05	7.72E-06

3	B7-SS2s1	2.84E-06	-7.81E-07	1.42E-05	2.08E-05	1.09E-05
4	B7-SS2s2	1.89E-06	-7.61E-07	1.04E-05	1.50E-05	7.68E-06
5	B7-SS3s1	2.85E-06	-7.53E-07	1.42E-05	2.09E-05	1.11E-05
6	B7-SS3s2	1.79E-06	-7.97E-07	1.01E-05	1.45E-05	7.41E-06
7	B7-SS4s1	2.84E-06	-7.36E-07	1.41E-05	2.08E-05	1.11E-05
8	B7-SS4s2	1.78E-06	-7.87E-07	1.01E-05	1.44E-05	7.39E-06
9	B7-NS5s1	5.04E-06	5.98E-06	-1.27E-06	6.96E-06	1.05E-05
10	B7-NS5s2	3.42E-06	4.33E-06	-1.75E-06	3.77E-06	6.86E-06
11	B7-NS6s1	5.09E-06	6.03E-06	-1.25E-06	7.07E-06	1.07E-05
12	B7-NS6s2	3.48E-06	4.39E-06	-1.71E-06	3.91E-06	7.00E-06
13	B7-NS7s1	5.81E-06	6.84E-06	-1.16E-06	8.44E-06	1.22E-05
14	B7-NS7s2	3.87E-06	4.83E-06	-1.61E-06	4.72E-06	8.07E-06
15	B7-NS8s1	5.95E-06	7.01E-06	-1.15E-06	8.70E-06	1.25E-05
16	B7-NS8s2	3.93E-06	4.90E-06	-1.61E-06	4.83E-06	8.24E-06
17	B7-SM5t	3.32E-07	-8.89E-08	1.66E-06	2.32E-06	6.72E-07
18	B7-SM6t	1.77E-07	-5.09E-09	4.62E-07	3.88E-07	-3.03E-06
19	B7-SM7t	2.97E-07	1.02E-08	7.67E-07	9.52E-07	-3.64E-06
20	B7-SM8t	7.06E-07	8.37E-08	1.98E-06	2.69E-06	-2.85E-06
21	B7-SM15b	-1.41E-06	1.94E-06	-1.22E-05	-1.63E-05	-7.98E-06
22	B7-SM17b	-9.18E-07	2.16E-06	-1.11E-05	-1.40E-05	-6.45E-06
23	B7-A7	1.17E-06	2.60E-07	3.77E-06	6.37E-06	4.05E-06
24	B7-A8	1.40E-06	4.59E-07	4.01E-06	7.09E-06	4.71E-06
25	B7-A9	1.67E-06	7.05E-07	4.22E-06	7.80E-06	5.45E-06
26	B7-U1-1	1.38E-06	-2.97E-07	6.60E-06	9.81E-06	-4.60E-06
27	B7-SG1	2.87E-06	5.07E-08	1.13E-05	1.72E-05	9.45E-06
28	B7-SG2	3.42E-06	1.33E-07	1.31E-05	2.04E-05	1.17E-05
29	B7-B10	-1.53E-06	-7.17E-07	-3.45E-06	-6.28E-06	-4.60E-06
30	B7-T7	-2.27E-06	-2.45E-06	-1.82E-07	-4.15E-06	-6.72E-06
# SG	Label	Loading Case				
		11	12	13	14	15
1	B7-SS1s1	1.75E-05	1.40E-05	1.37E-05	1.35E-05	2.19E-05
2	B7-SS1s2	1.27E-05	1.01E-05	9.82E-06	9.68E-06	1.61E-05
3	B7-SS2s1	1.75E-05	1.40E-05	1.37E-05	1.35E-05	2.19E-05
4	B7-SS2s2	1.27E-05	1.01E-05	9.77E-06	9.64E-06	1.60E-05
5	B7-SS3s1	1.78E-05	1.41E-05	1.37E-05	1.36E-05	2.20E-05
6	B7-SS3s2	1.23E-05	9.84E-06	9.46E-06	9.35E-06	1.56E-05
7	B7-SS4s1	1.78E-05	1.41E-05	1.36E-05	1.36E-05	2.19E-05
8	B7-SS4s2	1.23E-05	9.81E-06	9.42E-06	9.33E-06	1.55E-05
9	B7-NS5s1	7.35E-06	4.12E-06	4.84E-06	7.95E-06	-1.69E-06

<b>10</b>	<b>B7-NS5s2</b>	4.13E-06	2.05E-06	2.64E-06	4.84E-06	-2.53E-06
<b>11</b>	<b>B7-NS6s1</b>	7.46E-06	4.19E-06	4.92E-06	8.06E-06	-1.65E-06
<b>12</b>	<b>B7-NS6s2</b>	4.25E-06	2.12E-06	2.73E-06	4.96E-06	-2.48E-06
<b>13</b>	<b>B7-NS7s1</b>	8.73E-06	4.94E-06	5.81E-06	9.31E-06	-1.43E-06
<b>14</b>	<b>B7-NS7s2</b>	5.13E-06	2.66E-06	3.26E-06	5.82E-06	-2.26E-06
<b>15</b>	<b>B7-NS8s1</b>	8.96E-06	5.08E-06	5.98E-06	9.55E-06	-1.40E-06
<b>16</b>	<b>B7-NS8s2</b>	5.27E-06	2.73E-06	3.32E-06	5.95E-06	-2.23E-06
<b>17</b>	<b>B7-SM5t</b>	1.19E-06	1.11E-06	1.55E-06	1.09E-06	2.41E-06
<b>18</b>	<b>B7-SM6t</b>	-5.05E-06	-3.33E-06	6.14E-07	-3.46E-06	6.34E-07
<b>19</b>	<b>B7-SM7t</b>	-6.15E-06	-3.99E-06	1.03E-06	-4.20E-06	1.31E-06
<b>20</b>	<b>B7-SM8t</b>	-5.51E-06	-3.14E-06	2.49E-06	-3.44E-06	3.16E-06
<b>21</b>	<b>B7-SM15b</b>	-1.51E-05	-1.17E-05	-1.04E-05	-1.07E-05	-1.85E-05
<b>22</b>	<b>B7-SM17b</b>	-1.29E-05	-1.02E-05	-9.01E-06	-9.15E-06	-1.64E-05
<b>23</b>	<b>B7-A7</b>	5.76E-06	4.28E-06	4.11E-06	4.47E-06	5.92E-06
<b>24</b>	<b>B7-A8</b>	6.45E-06	4.73E-06	4.55E-06	5.06E-06	5.92E-06
<b>25</b>	<b>B7-A9</b>	7.17E-06	5.17E-06	5.00E-06	5.68E-06	6.60E-06
<b>26</b>	<b>B7-U1-1</b>	8.28E-06	6.55E-06	6.43E-06	6.36E-06	1.02E-05
<b>27</b>	<b>B7-SG1</b>	1.39E-05	1.13E-05	1.16E-05	1.13E-05	1.72E-05
<b>28</b>	<b>B7-SG2</b>	1.73E-05	1.36E-05	1.36E-05	1.36E-05	2.04E-05
<b>29</b>	<b>B7-B10</b>	-5.96E-06	-4.23E-06	-4.01E-06	-4.88E-06	-4.96E-06
<b>30</b>	<b>B7-T7</b>	-5.08E-06	-2.49E-06	-2.46E-06	-5.47E-06	8.51E-07

**Table A2.2. Maximum Concrete Strain in Tension and Compression and Displacement at West Face of ITBC 7 in Cases 1 to 15**

Case	Maximum Concrete Strain		Displacement (in) from West Face		
	Tension	Compression	Left	Middle	Right
<b>1</b>	2.26E-05	-7.03E-05	-0.00854	-0.00930	-0.01224
<b>2</b>	2.25E-05	-6.29E-05	-0.00862	-0.00948	-0.01265
<b>3</b>	2.64E-05	-6.04E-05	-0.00755	-0.01055	-0.01055
<b>4</b>	2.17E-05	-6.38E-05	-0.00928	-0.00576	-0.00337
<b>5</b>	2.76E-05	-6.02E-05	-0.00571	-0.00899	-0.01456
<b>6</b>	1.10E-05	-3.19E-05	-0.00596	-0.00319	-0.00120
<b>7</b>	1.24E-05	-3.70E-05	-0.00618	-0.00203	0.00171
<b>8</b>	2.42E-05	-5.48E-05	0.00285	-0.00528	-0.01507
<b>9</b>	3.64E-05	-8.20E-05	-0.00694	-0.01213	-0.02046
<b>10</b>	2.73E-05	-8.60E-05	-0.00780	-0.00974	-0.01389
<b>11</b>	3.32E-05	-9.62E-05	-0.00752	-0.01133	-0.01792
<b>12</b>	2.59E-05	-7.25E-05	-0.00472	-0.00837	-0.01410
<b>13</b>	2.39E-05	-5.18E-05	-0.00498	-0.00844	-0.01401
<b>14</b>	2.54E-05	-7.26E-05	-0.00612	-0.00997	-0.01615
<b>15</b>	3.75E-05	-8.21E-05	-0.00231	-0.00856	-0.01739

**Table A2.3. CNFA Stress Values of Loading Cases 1 to 15 of Bent Cap 7**

# CNFA	Label	Stress values of Loading Case (ksi)							
		1	2	3	4	5	6	7	
1	B7-CNFA1z1	-0.10	-0.10	-0.12	-0.07	-0.07	-0.03	-0.04	
2	B7-CNFA1z2	-0.10	-0.10	-0.09	-0.14	-0.06	-0.07	-0.09	
3	B7-CNFA2z1	-0.29	-0.28	-0.27	-0.28	-0.15	-0.14	-0.16	
4	B7-CNFA2z2	-0.31	-0.25	-0.24	-0.25	-0.13	-0.13	-0.14	
5	B7-CNFA2z3	-0.32	-0.29	-0.27	-0.29	-0.15	-0.15	-0.17	
6	B7-CNFA2z4	-0.23	-0.21	-0.20	-0.22	-0.11	-0.11	-0.13	
7	B7-CNFA3z1	0.34	0.36	0.43	0.07	0.46	0.08	-0.02	
8	B7-CNFA3z2	0.24	0.26	0.31	0.04	0.34	0.05	-0.02	
9	B7-CNFA3z3	0.23	0.25	0.43	0.03	0.46	0.08	-0.02	
# CNFA	Label	Stress values of Loading Case (ksi)							
		8	9	10	11	12	13	14	15
1	B7-CNFA1z1	0.00	-0.05	-0.03	-0.05	-0.03	-0.03	-0.10	-0.01
2	B7-CNFA1z2	0.00	-0.13	-0.16	-0.13	-0.07	-0.08	-0.12	-0.04
3	B7-CNFA2z1	0.00	-0.25	-0.36	-0.28	-0.16	-0.17	-0.28	-0.02
4	B7-CNFA2z2	0.00	-0.23	-0.38	-0.30	-0.18	-0.15	-0.30	-0.02
5	B7-CNFA2z3	0.00	-0.25	-0.39	-0.31	-0.18	-0.17	-0.31	-0.03
6	B7-CNFA2z4	0.00	-0.19	-0.28	-0.21	-0.13	-0.13	-0.21	-0.03
7	B7-CNFA3z1	0.41	0.60	0.32	0.51	0.40	0.40	0.39	0.64
8	B7-CNFA3z2	0.30	0.43	0.22	0.37	0.29	0.28	0.28	0.46
9	B7-CNFA3z3	0.41	0.60	0.32	0.52	0.41	0.39	0.27	0.63

**Table A2.4. Strain Values for Case 9 of Bent Cap 7 under Four-Truck Loading at Five Positions**

# SG	Label	Strain in Case 9, ITBC-7				
		Position 1	Position 2	Position 3	Position 4	Position 5
1	B7-SS1s1	-3.98E-07	-1.17E-06	1.91E-05	2.48E-05	2.75E-05
2	B7-SS1s2	-3.46E-07	-1.08E-06	1.39E-05	1.82E-05	2.04E-05
3	B7-SS2s1	-3.88E-07	-1.16E-06	1.92E-05	2.49E-05	2.75E-05
4	B7-SS2s2	-3.42E-07	-1.09E-06	1.38E-05	1.81E-05	2.03E-05
5	B7-SS3s1	-3.11E-07	-1.07E-06	1.92E-05	2.49E-05	2.76E-05
6	B7-SS3s2	-3.21E-07	-1.11E-06	1.34E-05	1.77E-05	1.98E-05
7	B7-SS4s1	-2.96E-07	-1.04E-06	1.91E-05	2.48E-05	2.75E-05
8	B7-SS4s2	-3.17E-07	-1.10E-06	1.33E-05	1.76E-05	1.98E-05
9	B7-NS5s1	3.85E-06	9.50E-06	5.86E-06	2.46E-06	-2.88E-06
10	B7-NS5s2	2.96E-06	7.03E-06	3.09E-06	2.78E-07	-3.70E-06
11	B7-NS6s1	3.88E-06	9.58E-06	5.95E-06	2.52E-06	-2.86E-06
12	B7-NS6s2	3.04E-06	7.15E-06	3.21E-06	3.77E-07	-3.65E-06
13	B7-NS7s1	3.04E-06	1.10E-05	7.13E-06	3.30E-06	-2.74E-06
14	B7-NS7s2	3.53E-06	7.98E-06	3.91E-06	8.79E-07	-3.48E-06
15	B7-NS8s1	4.84E-06	1.13E-05	7.35E-06	3.45E-06	-2.72E-06
16	B7-NS8s2	3.60E-06	8.10E-06	4.01E-06	9.37E-07	-3.48E-06
17	B7-SM5t	5.73E-08	5.64E-06	2.23E-06	2.97E-06	3.38E-06
18	B7-SM6t	-5.55E-07	-5.47E-07	3.14E-07	-2.65E-08	-4.27E-07
19	B7-SM7t	-8.34E-07	-8.10E-07	7.21E-07	3.06E-07	-2.95E-07
20	B7-SM8t	-1.27E-06	-1.17E-06	2.21E-06	1.61E-06	5.55E-07
21	B7-SM15b	1.60E-06	3.08E-06	-1.50E-05	-2.10E-05	-2.45E-05
22	B7-SM17b	1.66E-06	3.30E-06	-1.29E-05	-1.84E-05	-2.19E-05
23	B7-A7	2.24E-07	5.06E-07	5.78E-06	7.13E-06	7.48E-06
24	B7-A8	3.62E-07	8.55E-07	5.78E-06	7.74E-06	7.93E-06
25	B7-A9	5.16E-07	1.29E-06	7.01E-06	8.29E-06	8.26E-06
26	B7-U1-1	1.19E-06	-4.57E-07	9.01E-06	1.16E-05	1.28E-05
27	B7-SG1	-8.55E-08	-5.36E-08	1.58E-05	1.96E-05	2.08E-05
28	B7-SG2	-1.50E-07	-4.14E-08	1.87E-05	2.32E-05	2.47E-05
29	B7-B10	-4.58E-07	-1.20E-06	-5.66E-06	-6.76E-06	-6.72E-06
30	B7-T7	-2.78E-06	-4.98E-06	-3.33E-06	-1.96E-06	2.73E-07

**Table A2.5. Maximum Tensile and Compressive Concrete Strains and Displacements for Case 9 of Bent Cap 7 under Four-Truck Loading at Five Positions**

Case 9, Bent Cap 7	Maximum Strain on Concrete in		Displacement (in) from West Face		
	Tension	Compression	Left	Middle	Right
Position 1	1.02E-05	-3.43E-05	0.00212	-0.00121	-0.00471
Position 2	2.05E-05	-6.10E-05	-0.00335	-0.00358	-0.00453
Position 3	3.34E-05	-7.37E-05	-0.00618	-0.01105	-0.01876
Position 4	4.28E-05	-9.59E-05	-0.00545	-0.01187	-0.02151
Position 5	4.69E-05	-1.05E-04	-0.00177	-0.01040	-0.02211

**Table A2.6. CNFA Stress Values for Case 9 of Bent Cap 7 under Four-Truck Loading at Five Positions**

# CNFA	Label	Stress (ksi) in Case 9, ITBC-7				
		Position 1	Position 2	Position 3	Position 4	Position 5
1	B7-CNFA1z1	-0.07	-0.14	-0.11	-0.07	-0.01
2	B7-CNFA1z2	-0.04	-0.06	-0.09	-0.08	-0.06
3	B7-CNFA2z1	-0.11	-0.26	-0.22	-0.13	-0.02
4	B7-CNFA2z2	-0.11	-0.24	-0.19	-0.14	-0.03
5	B7-CNFA2z3	-0.13	-0.28	-0.22	-0.14	-0.01
6	B7-CNFA2z4	-0.11	-0.21	-0.16	-0.10	-0.01
7	B7-CNFA3z1	-0.01	-0.03	0.56	0.72	0.80
8	B7-CNFA3z2	-0.01	-0.03	0.56	0.72	0.80
9	B7-CNFA3z3	-0.01	-0.03	0.56	0.72	0.80

**Table A2.7. Strain Values for Case 14 of Bent Cap 7 under Four-Truck Loading at Five Positions**

# SG	Label	Strain in Case 14				
		Position-1	Position-2	Position-3	Position-4	Position-5
1	B7-SS1s1	1.10E-07	-3.98E-07	1.22E-05	2.28E-05	9.22E-06
2	B7-SS1s2	1.26E-07	-3.47E-07	8.80E-06	1.68E-05	7.08E-06
3	B7-SS2s1	1.16E-07	-3.88E-07	1.23E-05	2.28E-05	9.26E-06
4	B7-SS2s2	1.31E-07	-3.44E-07	8.76E-06	1.68E-05	7.07E-06
5	B7-SS3s1	1.51E-07	-3.11E-07	1.23E-05	2.29E-05	9.48E-06
6	B7-SS3s2	1.62E-07	-3.21E-07	8.50E-06	1.64E-05	7.02E-06
7	B7-SS4s1	1.53E-07	-2.97E-07	1.22E-05	2.27E-05	9.48E-06
8	B7-SS4s2	1.60E-07	-3.17E-07	8.45E-06	1.63E-05	7.01E-06
9	B7-NS5s1	-2.79E-07	3.75E-06	4.11E-06	-2.17E-06	-8.15E-07
10	B7-NS5s2	-9.10E-08	2.87E-06	2.21E-06	-2.88E-06	-1.09E-06
11	B7-NS6s1	-2.83E-07	3.80E-06	4.17E-06	-2.16E-06	-8.20E-07
12	B7-NS6s2	-6.71E-08	2.94E-06	2.29E-06	-2.83E-06	-1.07E-06
13	B7-NS7s1	-1.14E-07	4.53E-06	4.94E-06	-2.03E-06	-7.47E-07
14	B7-NS7s2	8.75E-08	3.41E-06	2.74E-06	-2.69E-06	-9.94E-07
15	B7-NS8s1	-7.00E-08	4.68E-06	5.08E-06	-2.01E-06	-7.26E-07
16	B7-NS8s2	-7.00E-08	3.48E-06	2.79E-06	-2.68E-06	-9.94E-07
17	B7-SM5t	7.43E-08	5.17E-08	1.44E-06	3.00E-06	1.71E-06
18	B7-SM6t	-3.28E-07	-5.18E-07	5.18E-07	-2.08E-07	-1.77E-06
19	B7-SM7t	-5.00E-07	-7.78E-07	8.26E-07	-2.53E-07	-2.73E-06
20	B7-SM8t	-7.92E-07	-1.18E-06	2.06E-06	5.31E-07	-4.34E-06
21	B7-SM15b	1.75E-07	1.61E-06	-9.30E-06	-1.99E-05	-9.56E-06
22	B7-SM17b	1.50E-07	1.69E-06	-8.05E-06	-1.79E-05	-8.47E-06
23	B7-A7	3.95E-09	2.05E-07	3.63E-06	6.04E-06	2.72E-06
24	B7-A8	-9.09E-09	3.35E-07	4.01E-06	6.36E-06	2.87E-06
25	B7-A9	-9.09E-09	4.76E-07	4.39E-06	6.59E-06	2.97E-06
26	B7-U1-1	2.76E-08	-1.72E-07	5.74E-06	1.06E-05	4.29E-06
27	B7-SG1	-6.38E-08	-8.30E-08	1.03E-05	1.75E-05	6.08E-06
28	B7-SG2	-1.36E-07	-1.38E-07	1.21E-05	2.04E-05	7.27E-06
29	B7-B10	1.27E-08	-4.14E-07	-3.54E-06	-5.58E-06	-2.92E-06
30	B7-T7	-8.61E-07	-2.27E-06	-1.95E-06	-2.38E-07	-3.73E-07

**Table A2.8. Maximum Tensile and Compressive Concrete Strains and Displacements for Case 14 of Bent Cap 7 under Four-Truck Loading at Five Positions**

Case 14, Bent Cap 7	Maximum Strain on Concrete In		Displacement (in) from West Face		
	Tension	Compression	Left	Middle	Right
Position-1	6.82E-06	-1.22E-05	0.00409	0.00055	-0.002912
Position-2	1.11E-05	-3.84E-05	0.00169	-0.00107	-0.003985
Position-3	2.13E-05	-5.37E-05	-0.00433	-0.00716	-0.012583
Position-4	3.85E-05	-8.24E-05	-0.00015	-0.00910	-0.020607
Position-5	1.60E-05	-3.94E-05	-0.00164	-0.00339	-0.006063

**Table A2.9. CNFA Stress Values for Case 14 of Bent Cap 7 under Four-Truck Loading at Five Positions**

# CNFA	Label	Stress (ksi) in Case 14				
		Position-1	Position-2	Position-3	Position-4	Position-5
1	B7-CNFA1z1	-0.01	-0.07	-0.07	-0.04	-0.01
2	B7-CNFA1z2	-0.01	-0.04	-0.05	-0.05	-0.01
3	B7-CNFA2z1	-0.02	-0.11	-0.14	0.00	0.00
4	B7-CNFA2z2	-0.01	-0.11	-0.13	0.00	0.00
5	B7-CNFA2z3	-0.01	-0.13	-0.15	0.00	0.00
6	B7-CNFA2z4	0.01	-0.11	-0.11	0.00	0.00
7	B7-CNFA3z1	0.00	-0.01	0.35	0.66	0.27
8	B7-CNFA3z2	0.00	-0.01	0.36	0.66	0.27
9	B7-CNFA3z3	0.00	-0.01	0.36	0.66	0.27

### APPENDIX-3

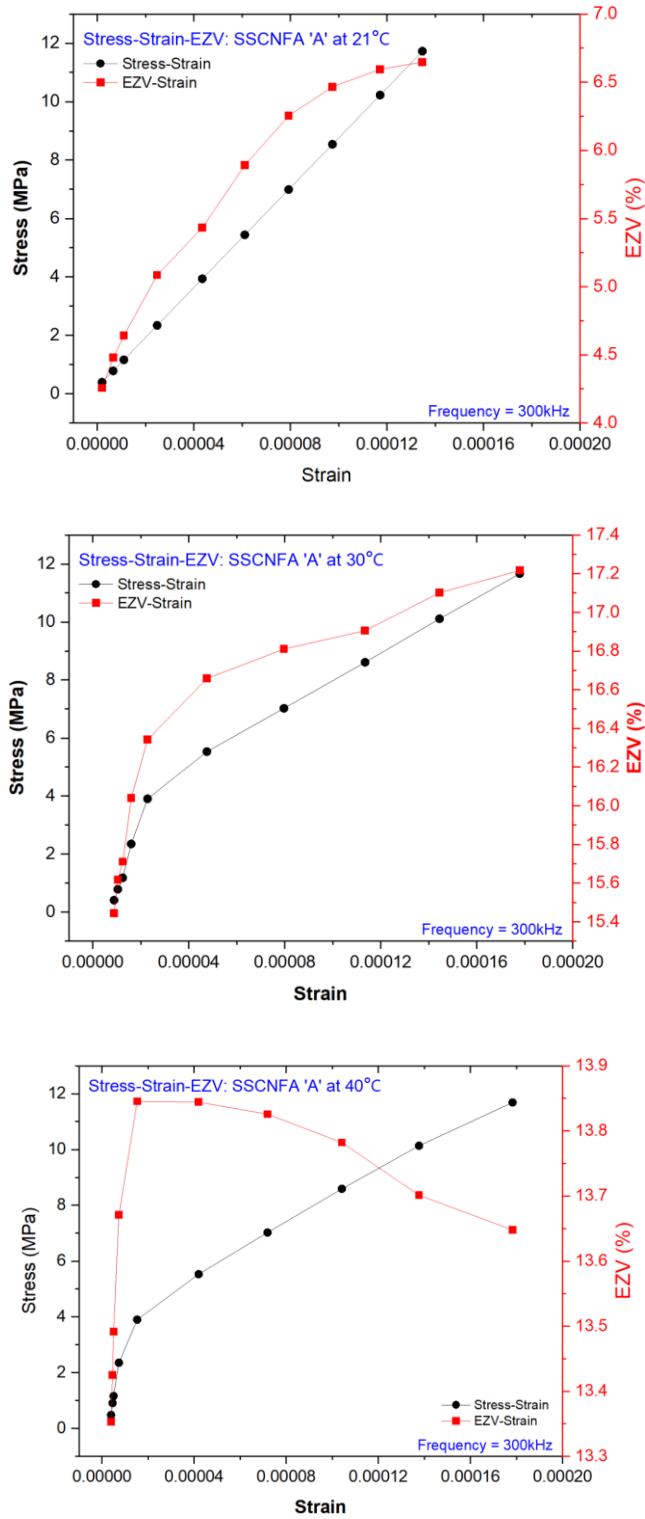


Figure A3.1. Stress-Strain-EZV Curves of CNFA 'A' at 21°C, 30°C, and 40°C

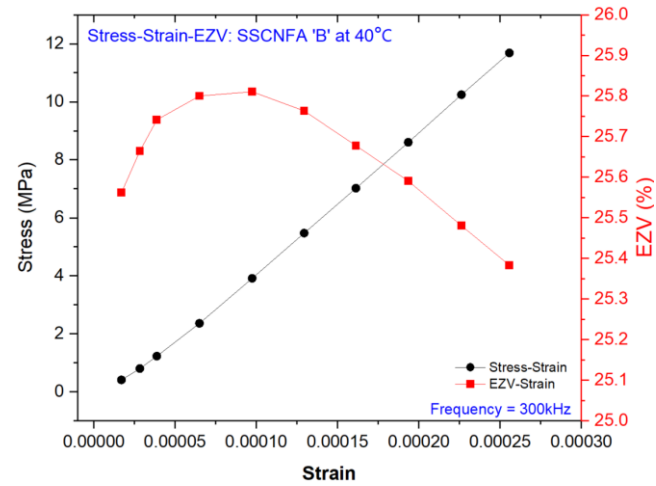
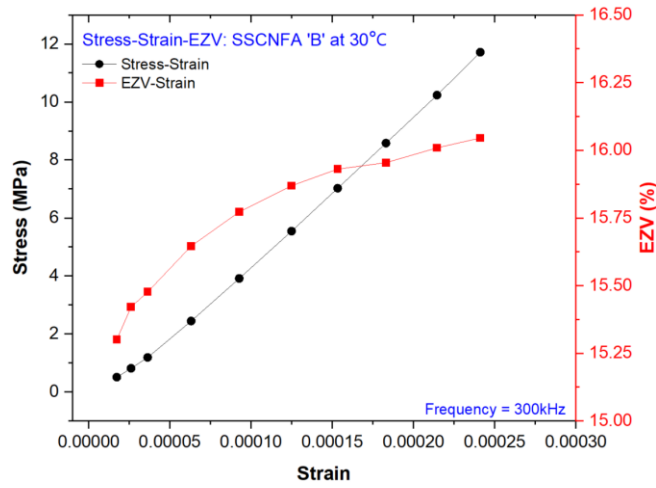
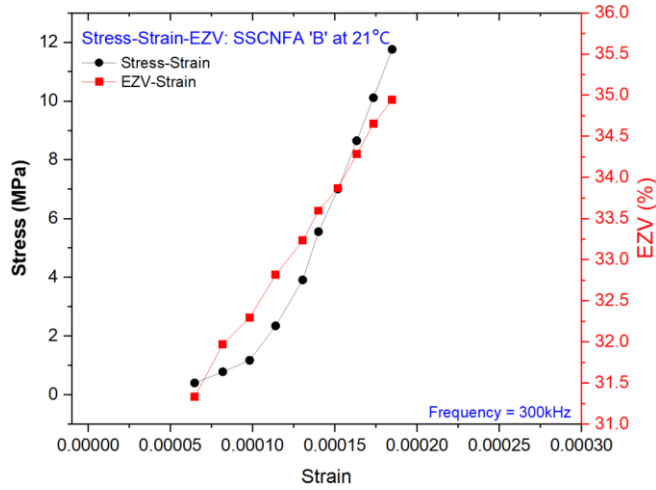


Figure A3.2. Stress-Strain-EZV Curves of CNFA 'B' at 21°C, 30°C, and 40°C

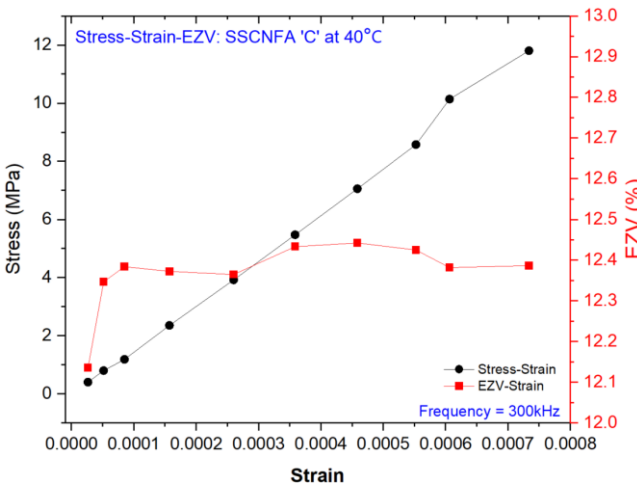
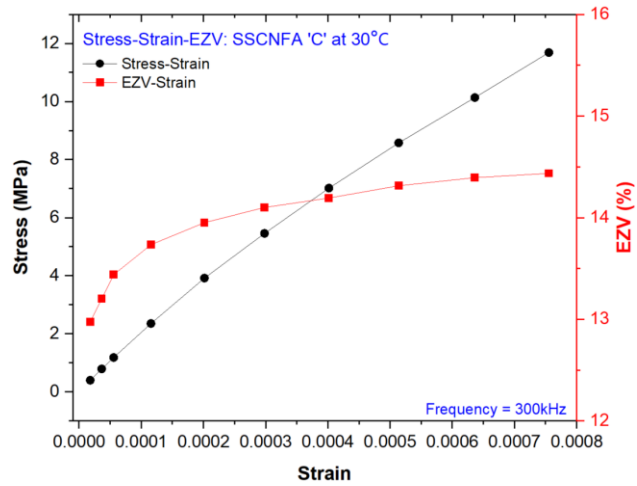
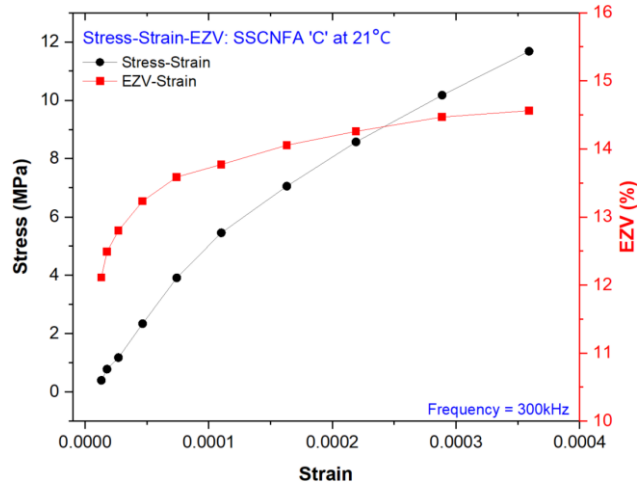


Figure A3.3. Stress-Strain-EZV Curves of CNFA 'C' at 21°C, 30°C, and 40°C

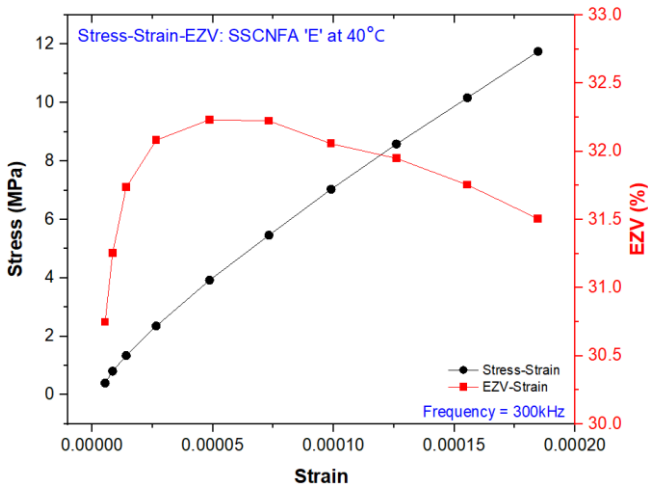
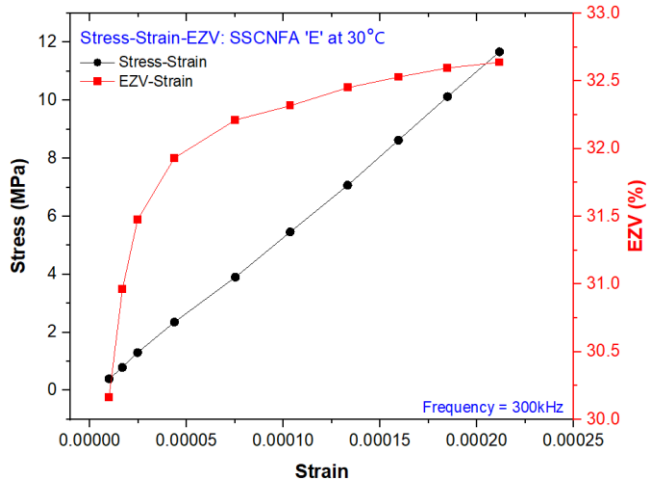
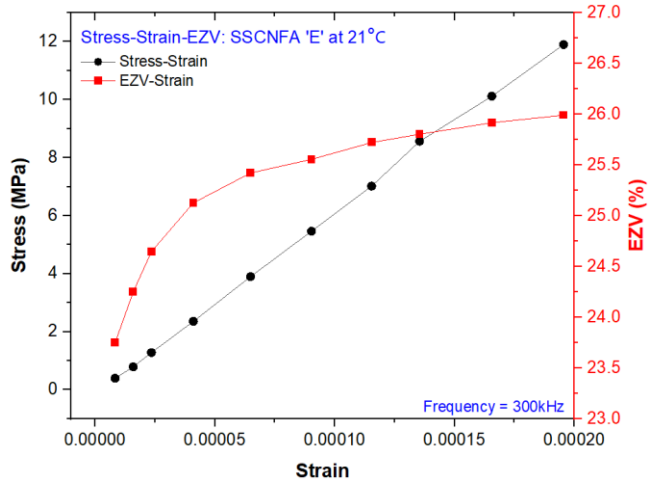


Figure A3.4. Stress-Strain-EZV Curves of CNFA 'E' at 21°C, 30°C, and 40°C

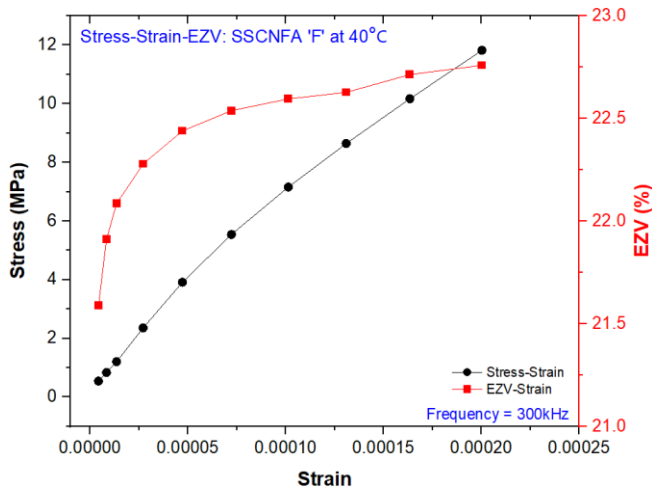
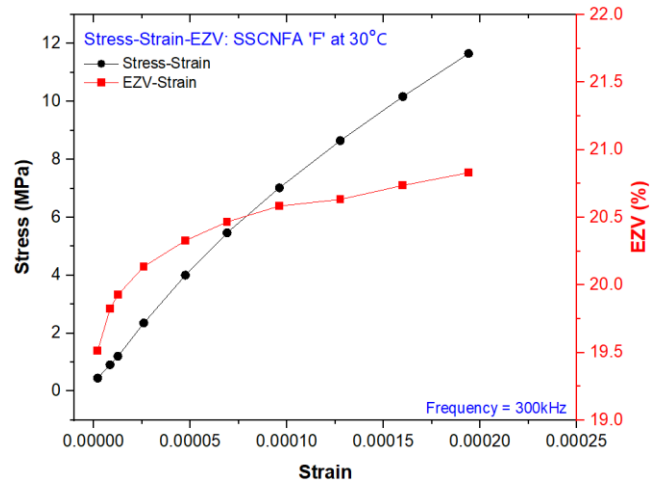
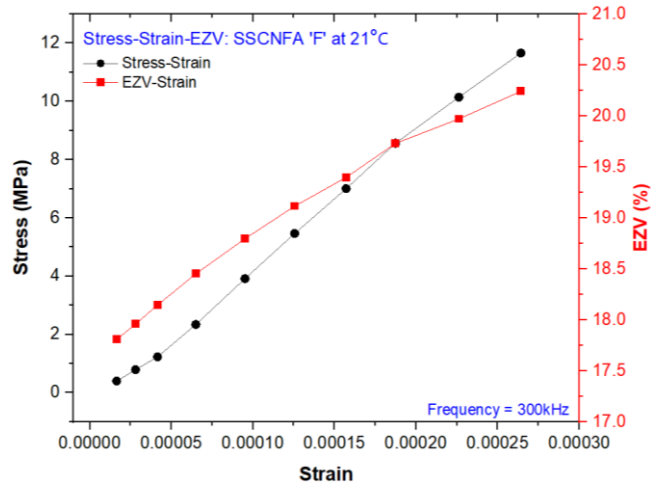


Figure A3.5. Stress-Strain-EZV Curves of CNFA 'F' at 21°C, 30°C, and 40°C

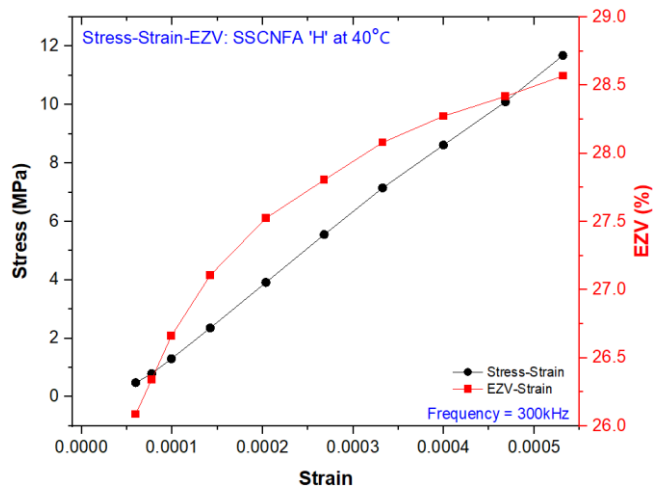
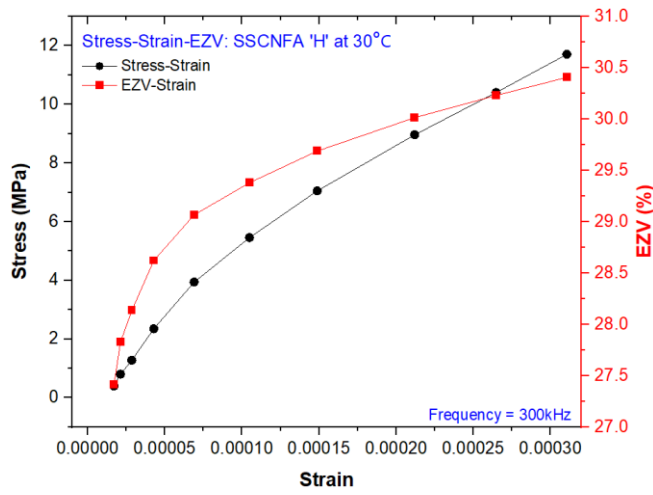
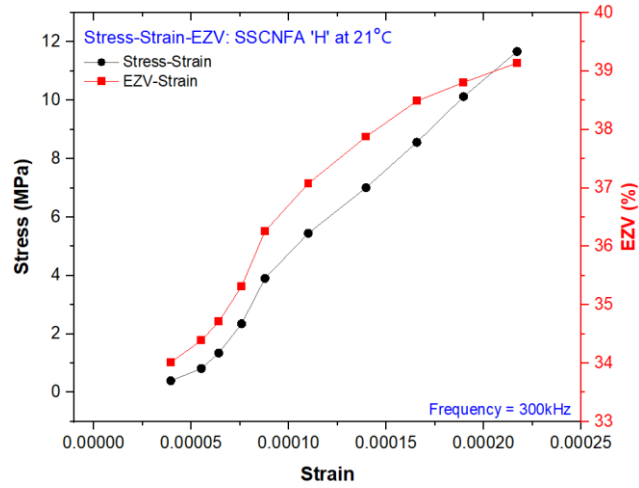


Figure A3.6. Stress-Strain-EZV Curves of CNFA 'H' at 21°C, 30°C, and 40°C

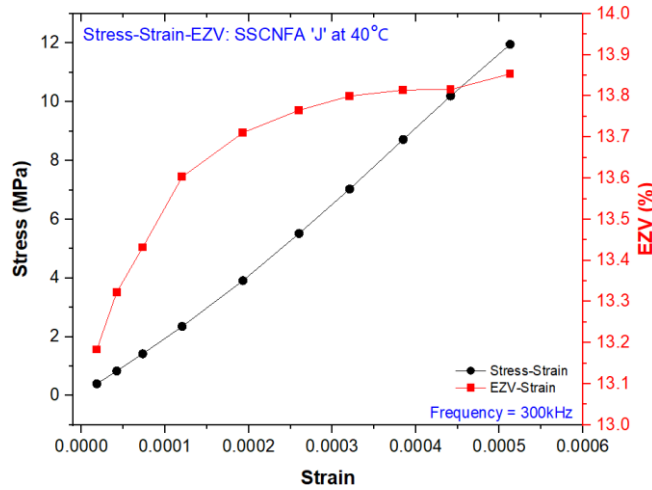
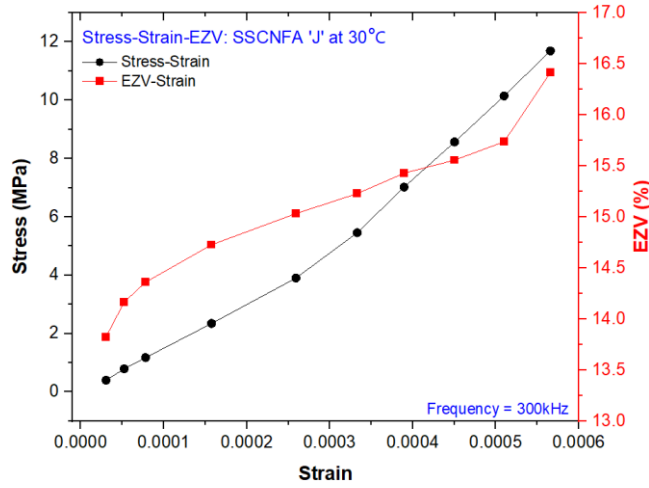
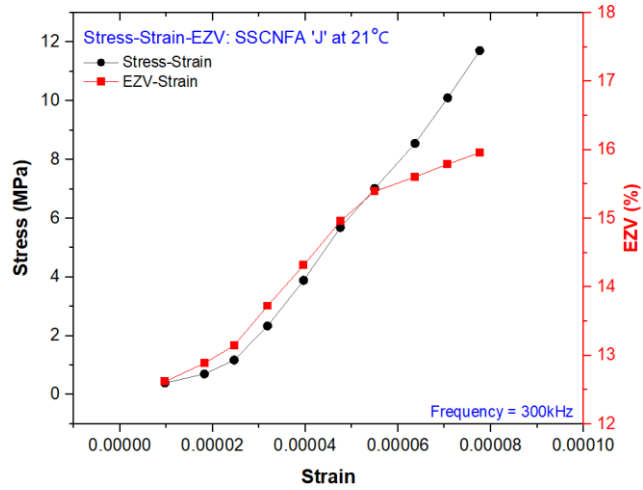


Figure A3.7. Stress-Strain-EZV Curves of CNFA 'J' at 21°C, 30°C, and 40°C

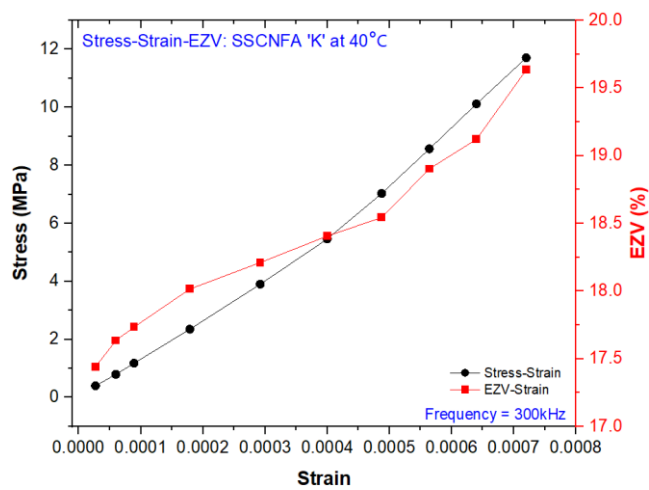
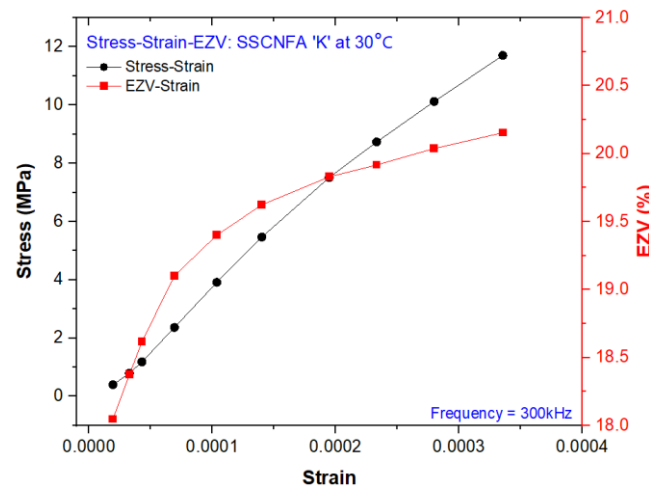
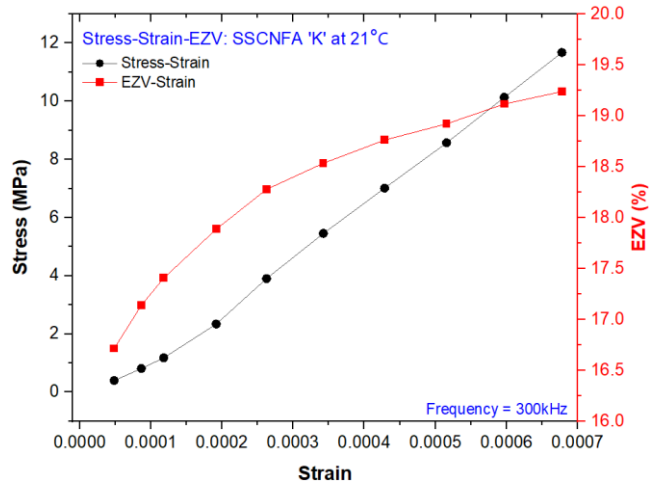


Figure A3.8. Stress-Strain-EZV Curves of CNFA 'K' at 21°C, 30°C, and 40°C

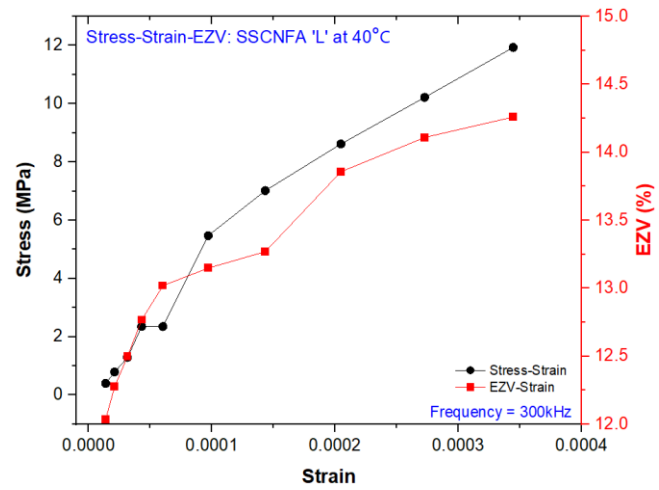
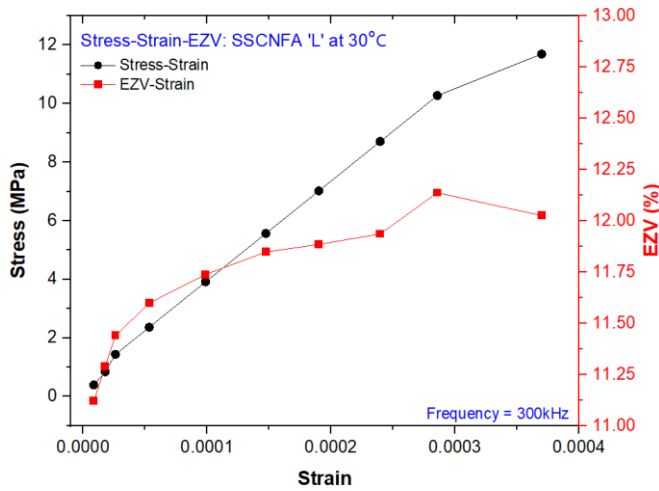
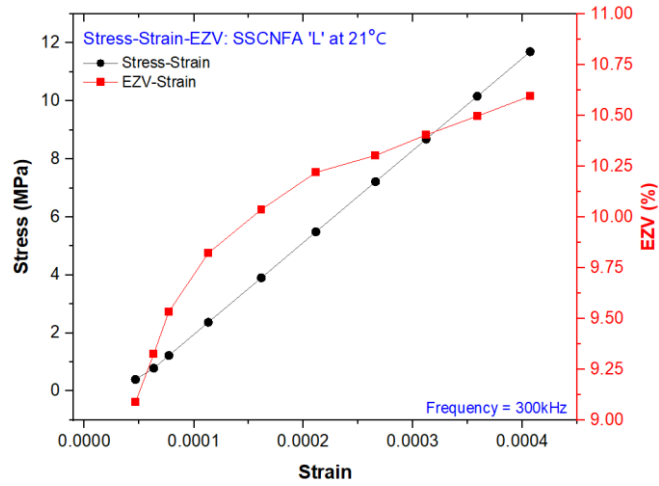


Figure A3.9. Stress-Strain-EZV Curves of CNFA 'L' at 21°C, 30°C, and 40°C

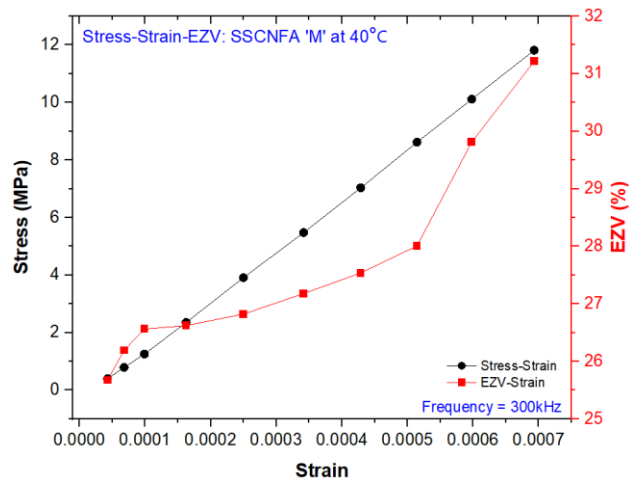
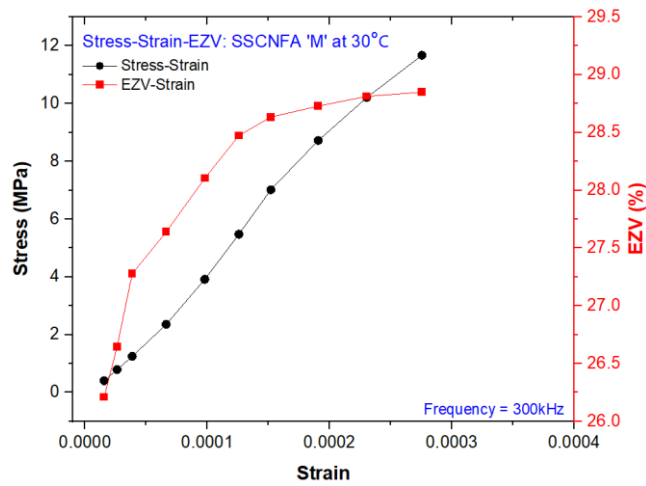
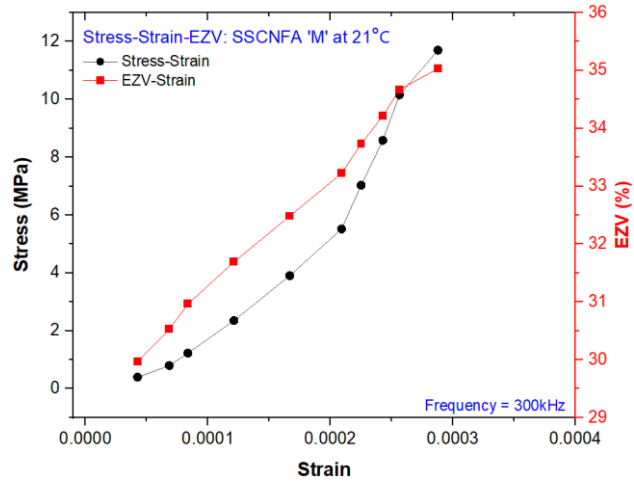


Figure A3.10. Stress-Strain-EZV Curves of CNFA 'M' at 21°C, 30°C, and 40°C

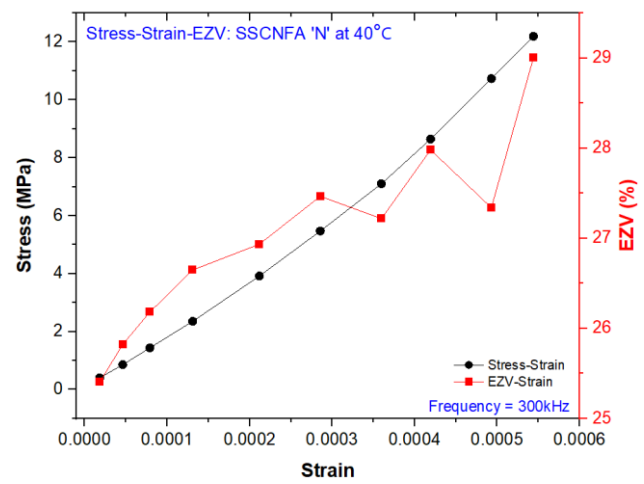
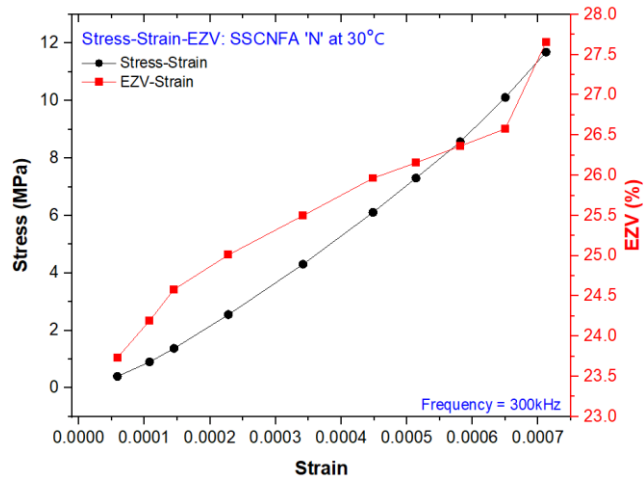
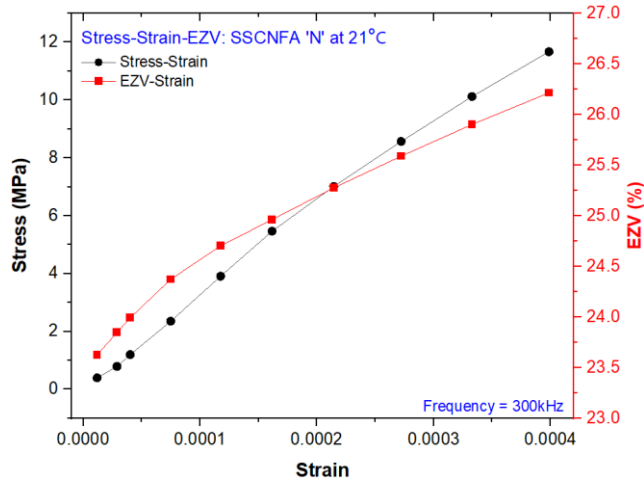


Figure A3.11. Stress-Strain-EZV Curves of CNFA 'N' at 21°C, 30°C, and 40°C

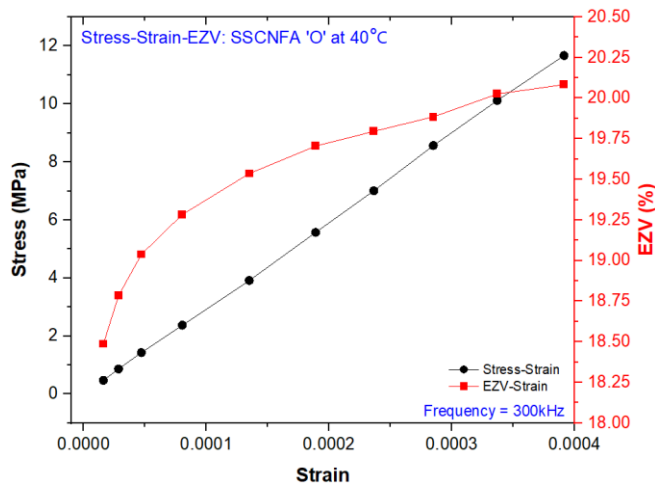
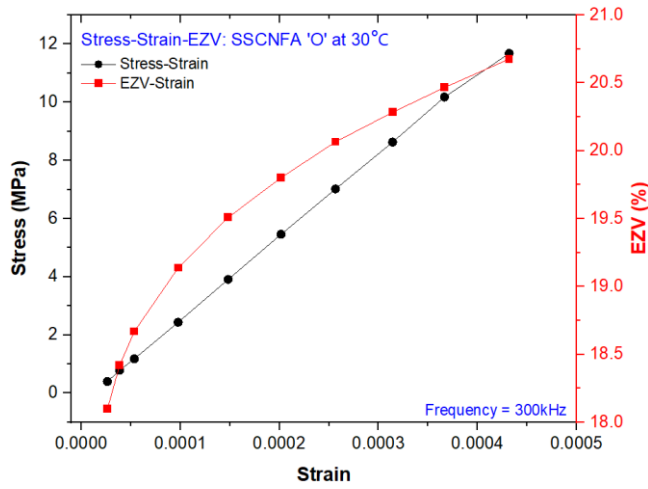
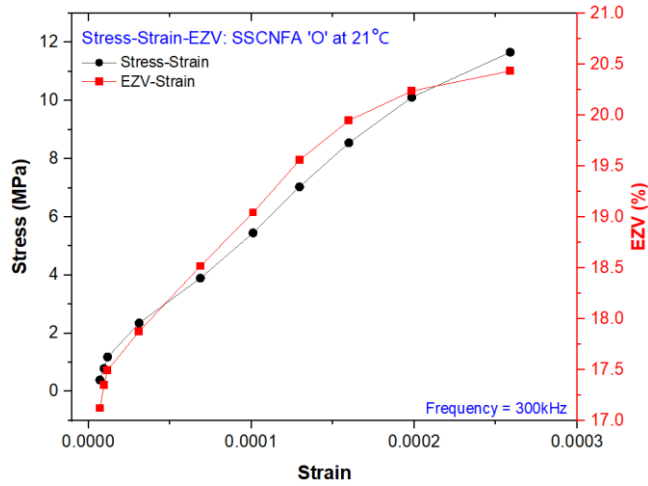


Figure A3.12. Stress-Strain-EZV Curves of CNFA 'O' at 21°C, 30°C, and 40°C

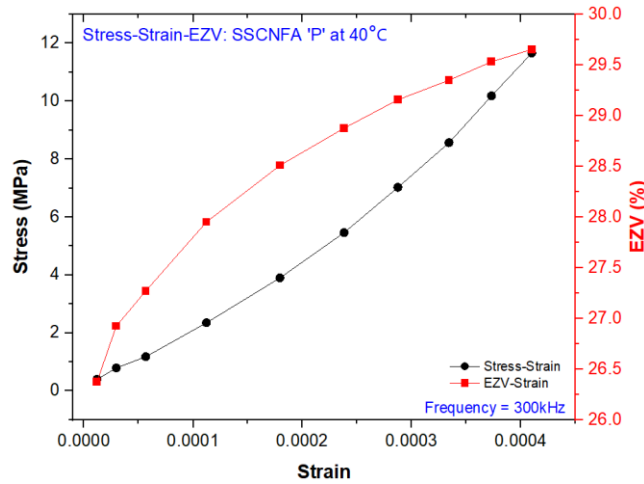
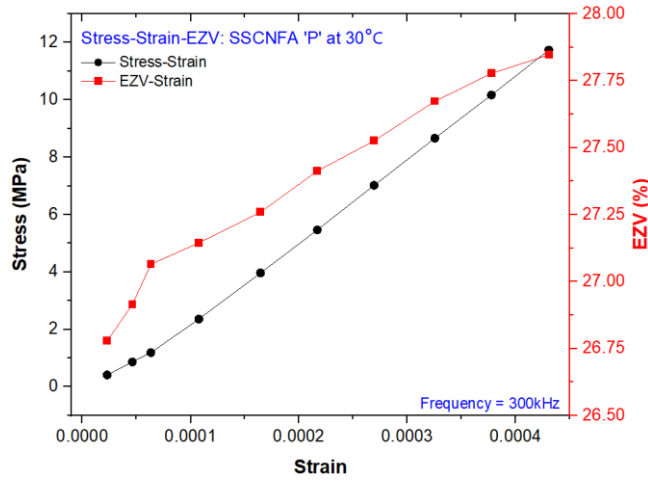
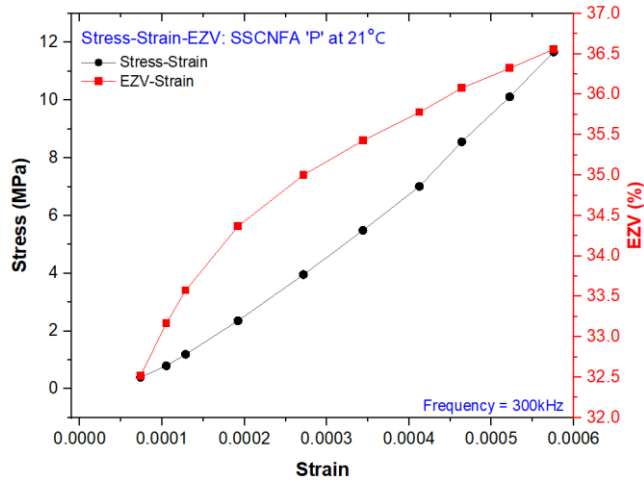
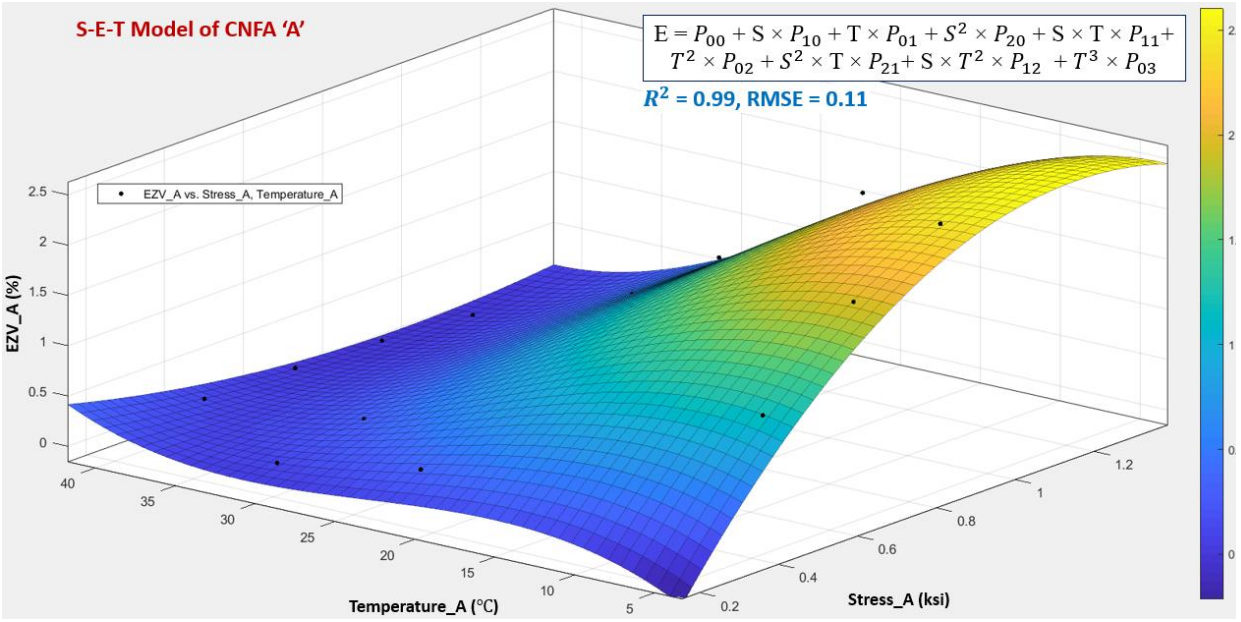
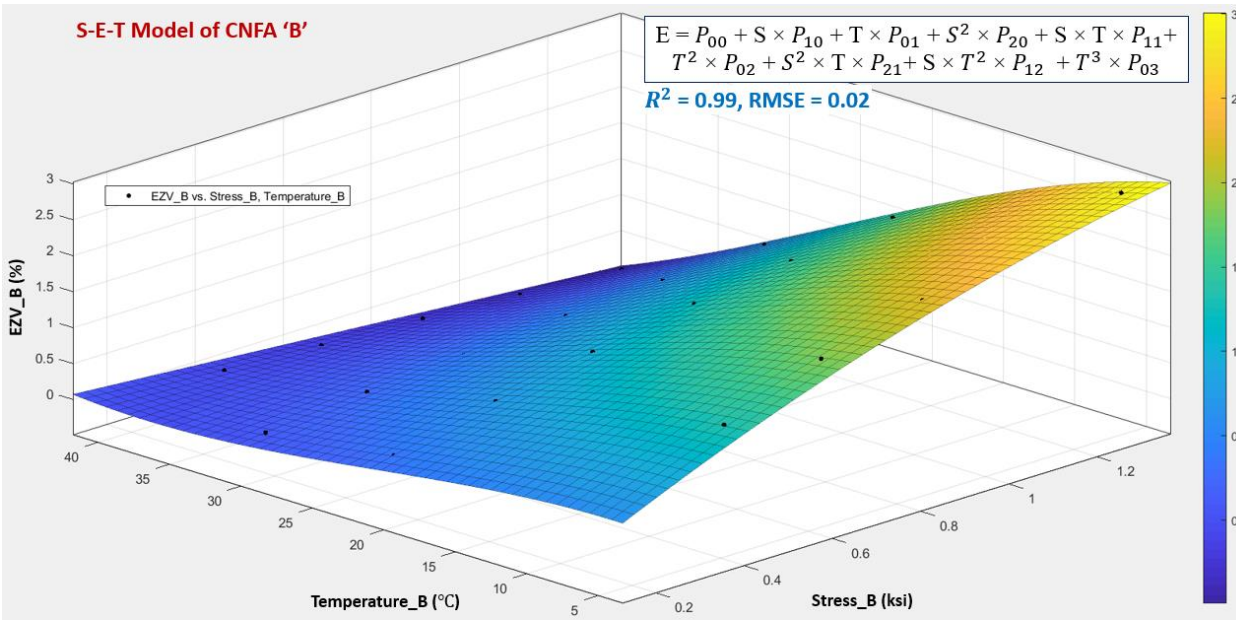


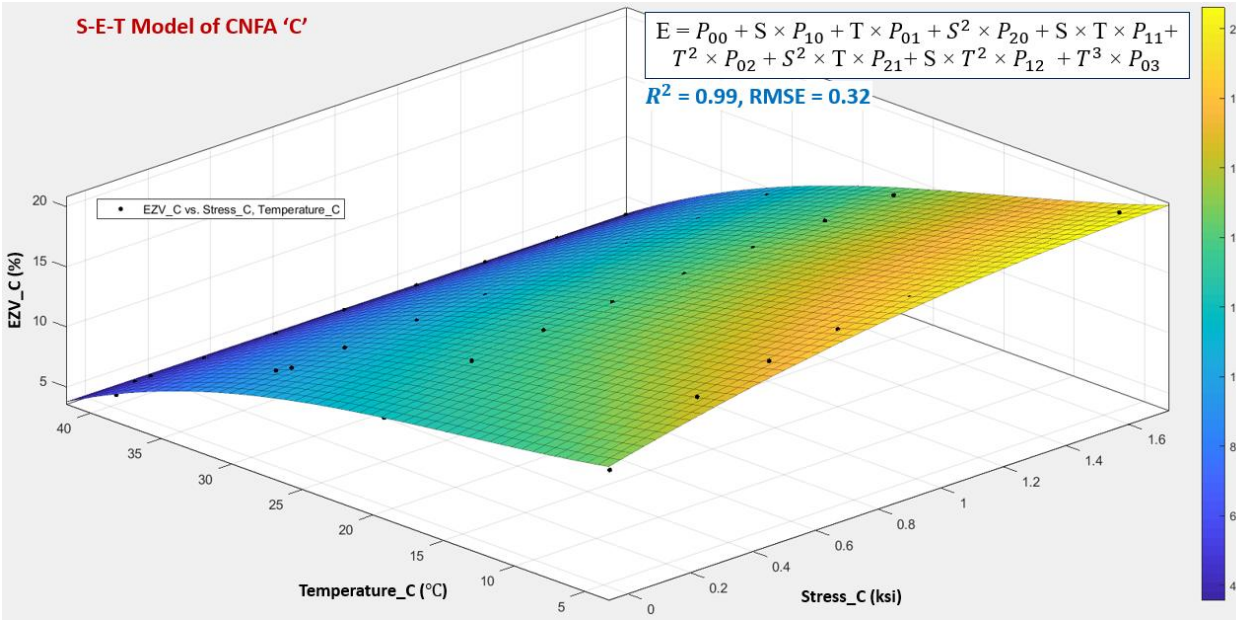
Figure A3.13. Stress-Strain-EZV Curves of CNFA 'P' at 21°C, 30°C, and 40°C



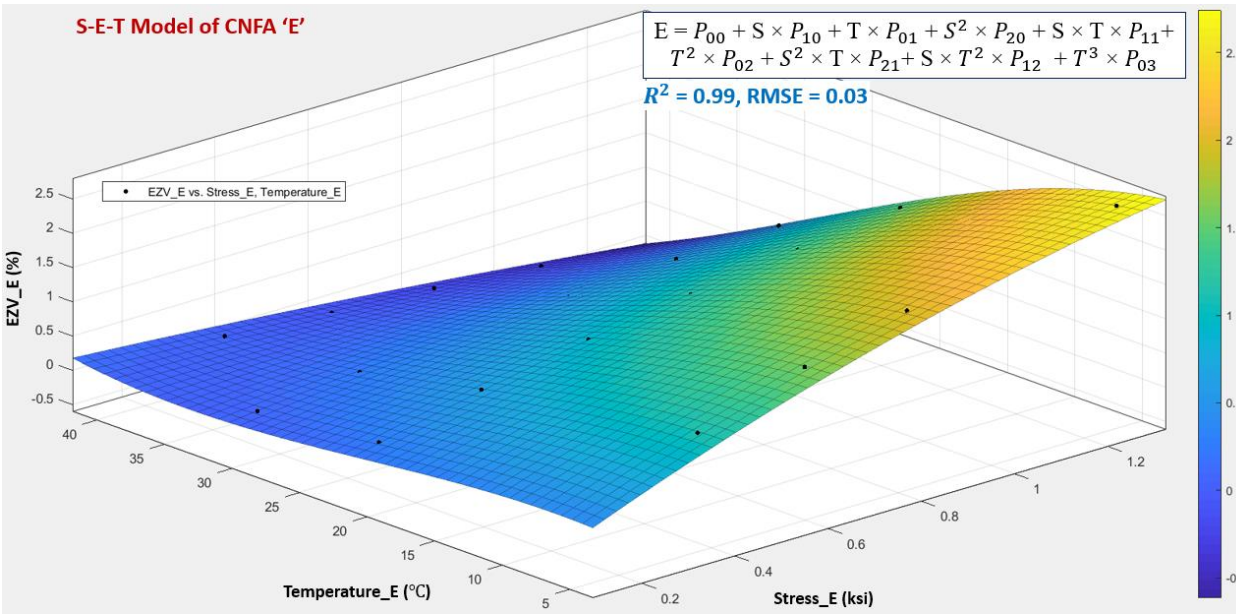
(a) S-E-T Model of CNFA 'A'



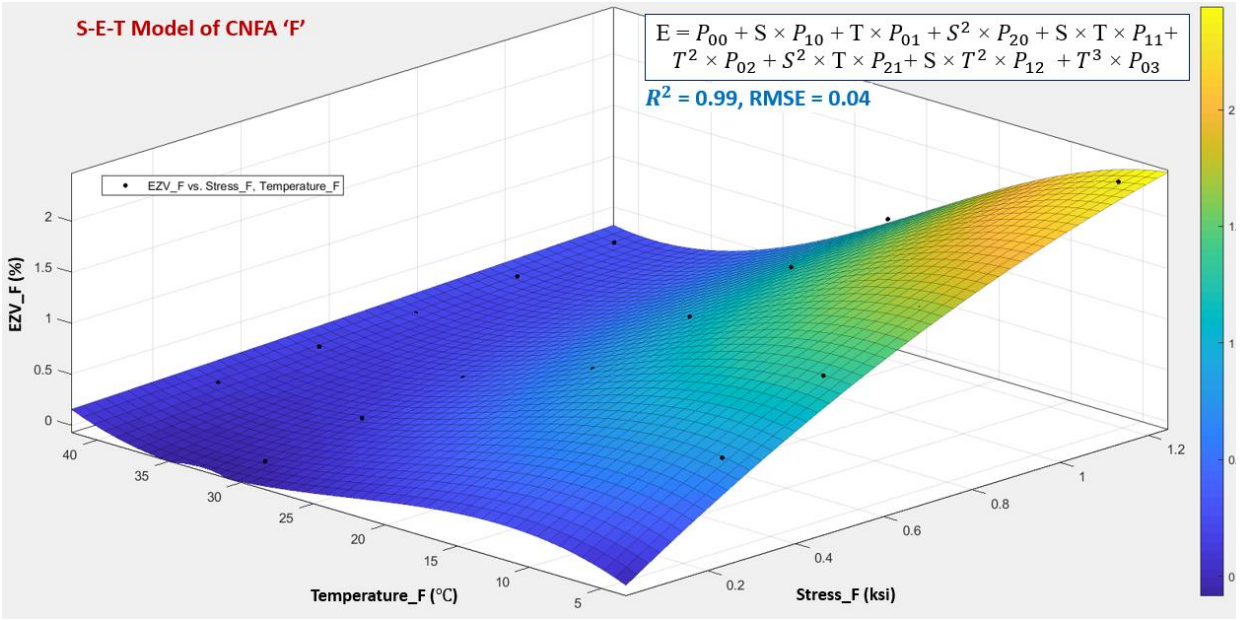
(b) S-E-T Model of CNFA 'B'



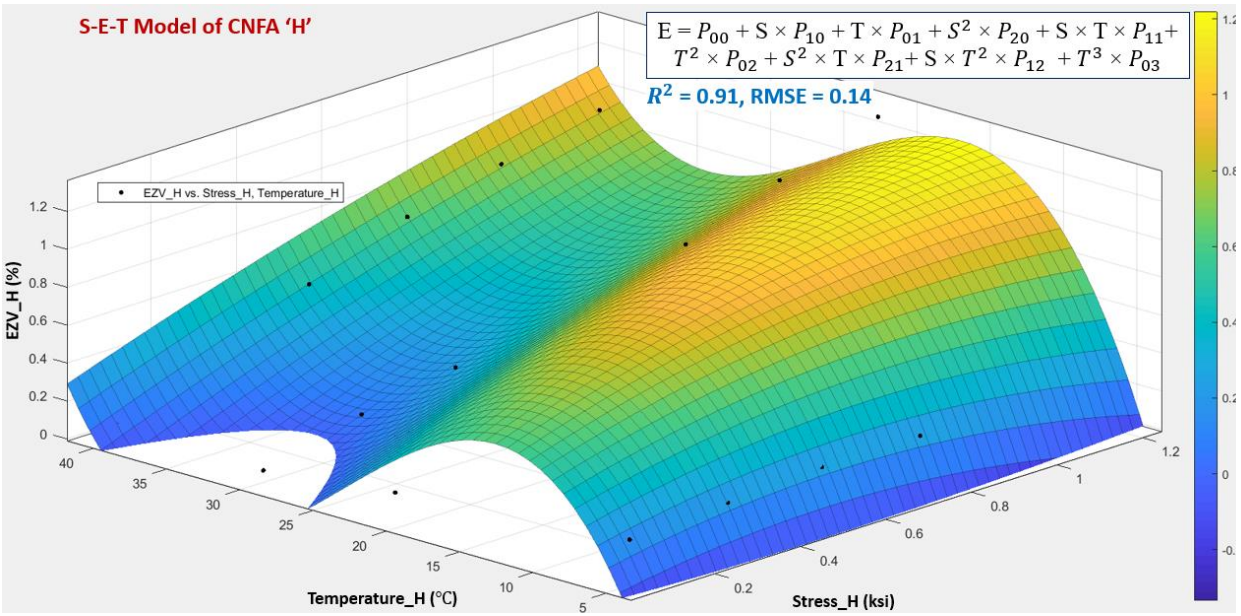
(c) S-E-T Model of CNFA 'C'



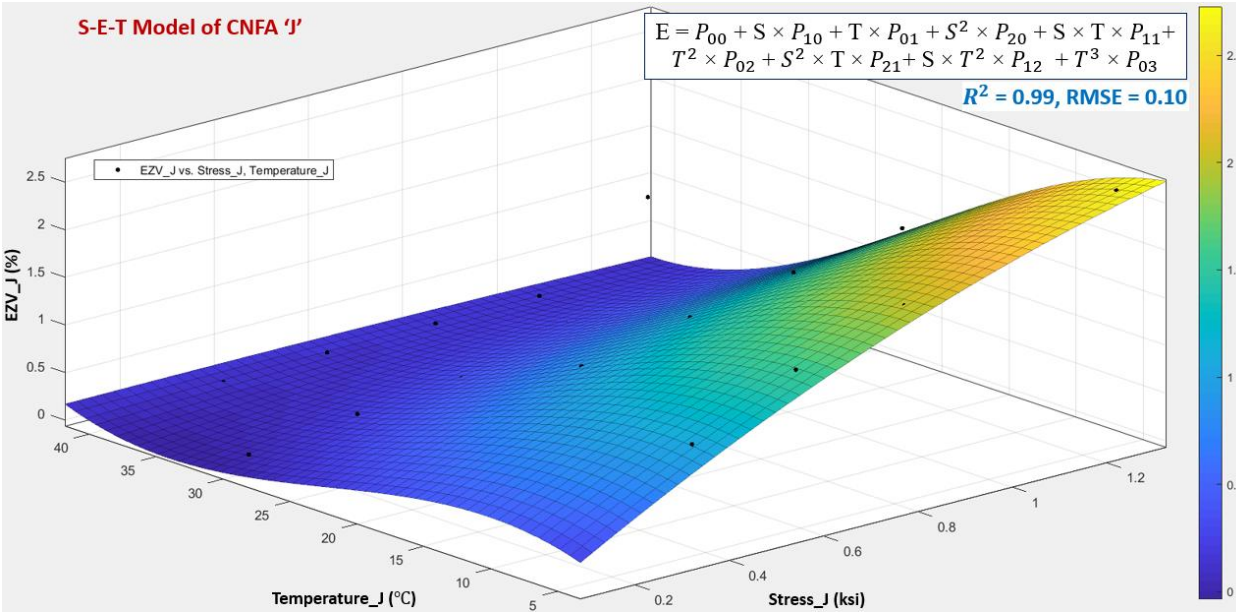
(d) S-E-T Model of CNFA 'E'



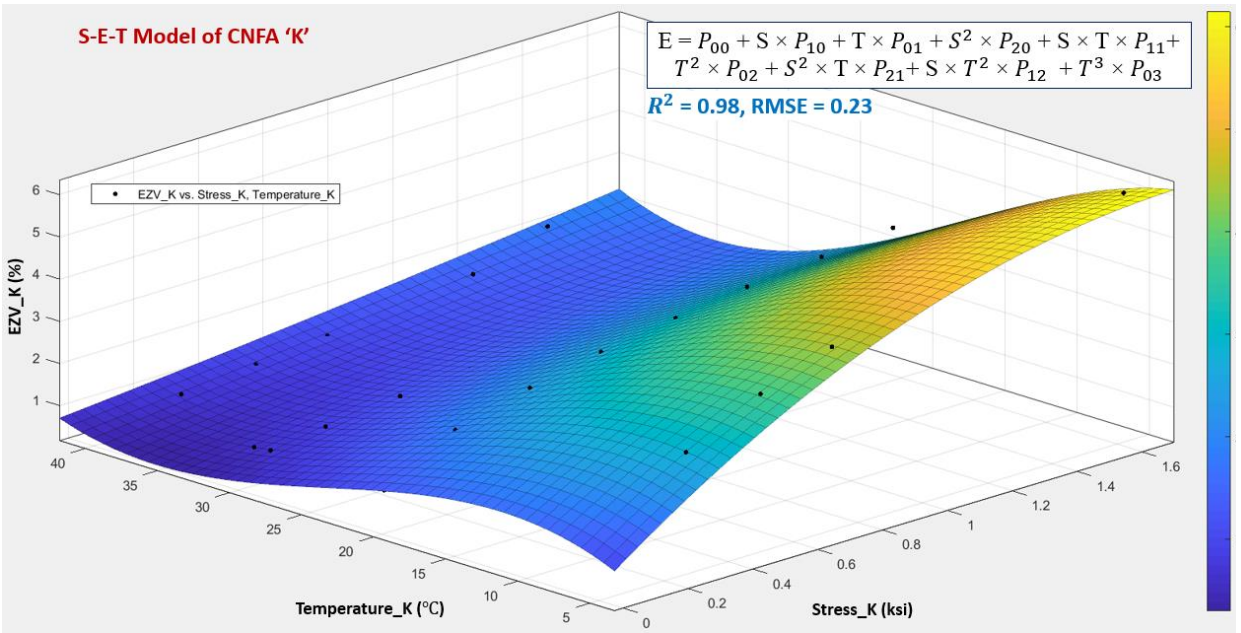
(e) S-E-T Model of CNFA 'F'



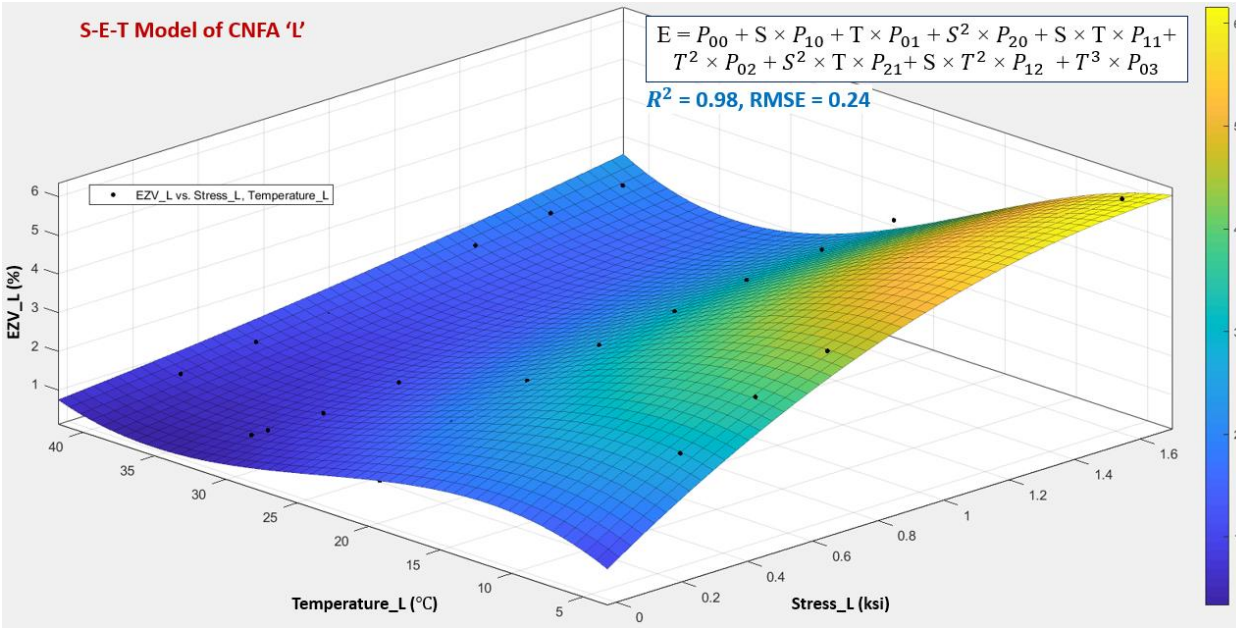
(f) S-E-T Model of CNFA 'H'



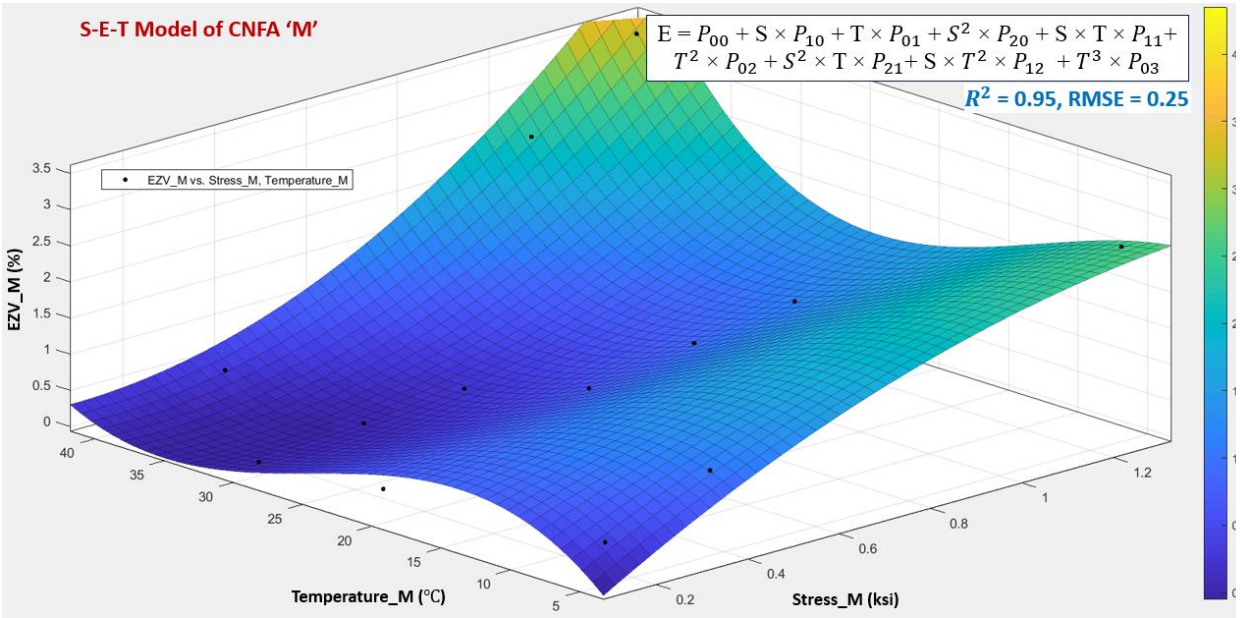
(g) S-E-T Model of CNFA 'J'



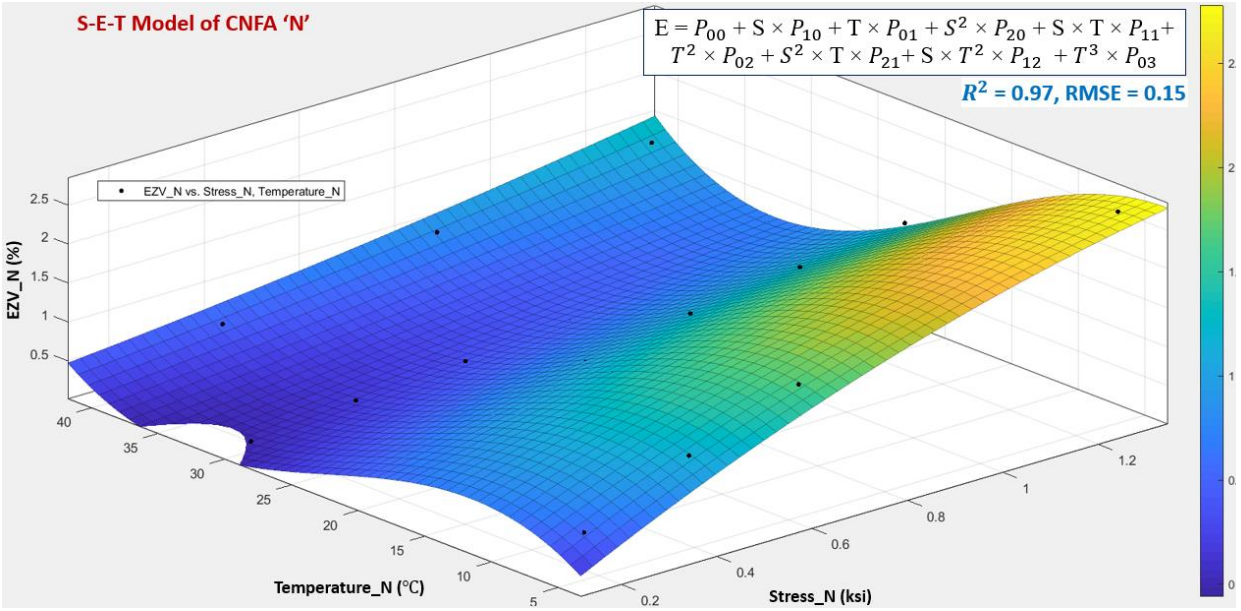
(h) S-E-T Model of CNFA 'K'



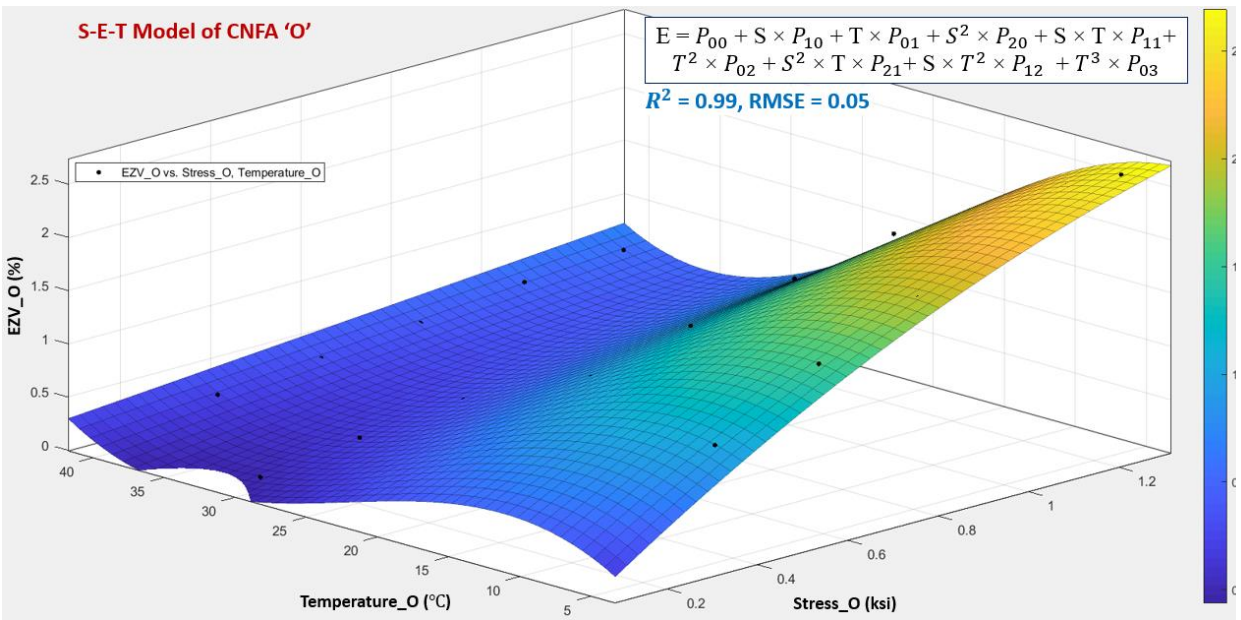
(i) S-E-T Model of CNFA 'L'



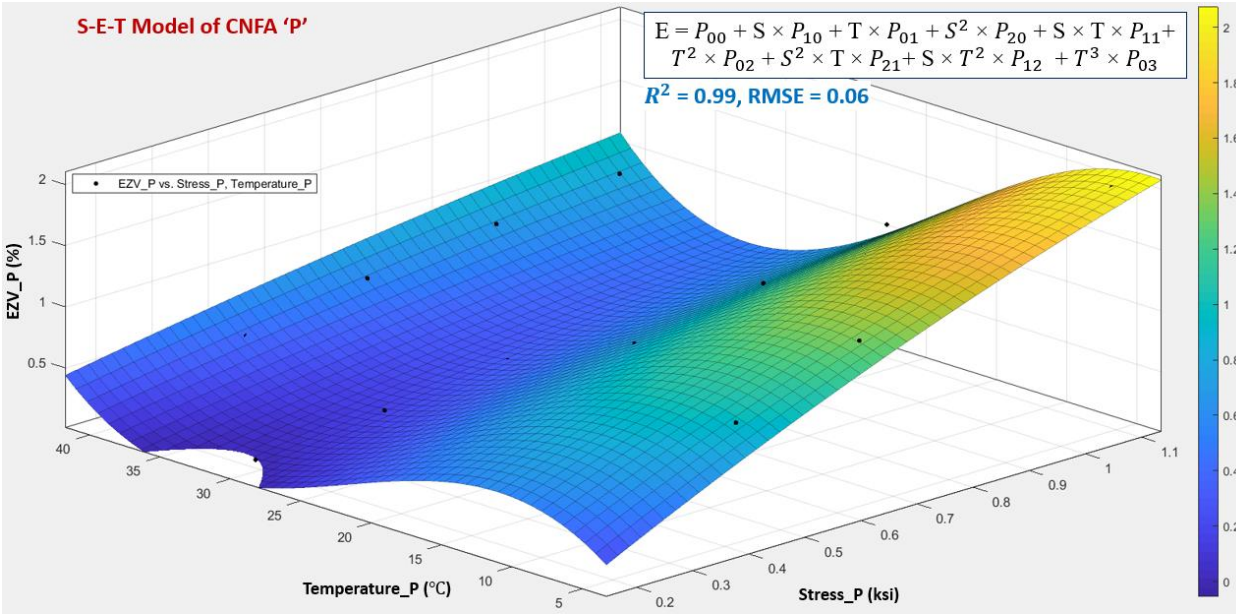
(j) S-E-T Model of CNFA 'M'



(k) S-E-T Model of CNFA 'N'



(l) S-E-T Model of CNFA 'O'



(m) S-E-T Model of CNFA 'P'

**Figure A3.14. S-E-T Models of CNFAs Embedded in Bent Cap 2 and Bent Cap 7**

**Table A3.1. Constants of S-E-T Models of CNFAs Embedded in Bent Cap 2**

#CNFA in BC2	ID	Location	P00	P10	P01	P20	P11	P02	P21	P12	P03
1	C	1	-0.019	4.098	0.104	-1.072	-0.107	-0.006	0.026	1.5E-04	9.6E-05
2	H	2	0.819	0.160	0.261	-0.473	0.073	-0.014	0.008	-1.4E-03	2.1E-04
3	E		0.087	3.021	0.028	0.734	-0.045	-0.002	0.014	-8.9E-04	3.9E-05
4	J		-0.156	3.209	0.087	-0.764	-0.084	-0.005	0.017	1.9E-04	7.7E-05
8	A	4	-1.583	7.207	0.150	-3.136	-0.205	-0.006	0.090	8.2E-05	8.6E-05
9	B		0.214	3.203	0.023	-0.777	-0.065	-0.002	0.019	-5.3E-04	3.5E-05
10	F		-0.261	3.193	0.093	-0.804	-0.094	-0.005	0.020	5.0E-04	7.7E-05

**Table A3.2. Constants of S-E-T Models of CNFAs Embedded in Bent Cap 7**

#CNFA in BC7	ID	Location	P00	P10	P01	P20	P11	P02	P21	P12	P03
1	K	1	-0.571	4.249	0.193	-1.112	-0.152	-0.011	0.028	1.6E-03	1.6E-04
2	L		-0.440	2.271	0.123	-0.547	-0.156	-0.006	0.033	2.7E-03	7.8E-05
3	P	2	-0.492	2.761	0.157	-0.518	-0.102	-0.009	0.008	1.3E-03	1.3E-04
4	O		-0.376	3.370	0.138	-0.802	-0.109	-0.008	0.019	8.8E-04	1.2E-04
5	N		-0.625	3.685	0.202	-0.907	-0.145	-0.011	0.026	1.6E-03	1.6E-04
6	M		-1.132	5.007	0.288	-1.617	-0.342	-0.014	0.102	5.1E-03	1.8E-04

**Table A3.3. Temperature Recorded During Static Load Tests on Bent Cap 2**

CNFA # on BC2	ID	Location Details	Temperature at the time of Load Test (in °C)					
			Case 1	Case 14	Case 3, P3	Case 3, P4	Case 9, P3	Case 9, P4
1	C	Interface of Column-Bent Cap 2 <b>(Location 1)</b>	10.0	10.0	10.2	9.9	10.0	10.0
2	H	Under the exterior girder on the ledge of North side <b>(Location 2)</b>	9.3	9.4	9.5	9.3	9.4	9.3
3	E							
4	J							
5		Outmost three S bars <b>(Location 3)</b>	11.9	11.4	11.6	12.2	11.8	12.1
6								
7								
8	A	Under the exterior girder on the ledge of South side <b>(Location 4)</b>	9.4	9.3	9.5	9.3	9.3	9.3
9	B							
10	F							

**Table A3.4. Temperature Recorded During Static Load Tests on Bent Cap 7**

CNFA # on BC7	ID	Location Details	Temperature at the time of Load Test (in °C)					
			Case 1	Case 11	Case 9, P3	Case 9, P4	Case 14, P3	Case 14, P4
1	L	Interface of Column-Bent Cap 7 <b>(Location 1)</b>	10.3	10.6	10.6	10.5	10.6	10.7
2	K							
3	P	Under the exterior girder on the ledge of North side <b>(Location 2)</b>	9.7	9.9	9.2	10.2	10.1	10.3
4	O							
5	N							
6	M							
7		Outmost three S bars <b>(Location 3)</b>	9.9	10.6	10.4	10.8	10.7	11.0
8								
9								

**APPENDIX-4**

**Table A4.1. Rebar Strains from Load Test and FE Simulation from Static Test-1, Case 1 on Bent Cap 2**

<b># SG</b>	<b>Label</b>	<b>Strain From Load Test</b>	<b>Strain From FE Simulation</b>
<b>1</b>	<b>B2-SS1s1</b>	1.16E-05	1.23E-05
<b>2</b>	<b>B2-SS1s2</b>	8.99E-06	1.01E-05
<b>3</b>	<b>B2-SS2s1</b>	7.55E-06	1.23E-05
<b>4</b>	<b>B2-SS2s2</b>	9.96E-06	1.00E-05
<b>5</b>	<b>B2-SS3s1</b>	3.12E-06	1.23E-05
<b>6</b>	<b>B2-SS3s2</b>	5.09E-06	9.62E-06
<b>7</b>	<b>B2-SS4s1</b>	1.32E-05	1.23E-05
<b>8</b>	<b>B2-SS4s2</b>	9.35E-06	9.59E-06
<b>9</b>	<b>B2-NS5s1</b>	9.92E-07	1.10E-06
<b>10</b>	<b>B2-NS5s2</b>	1.65E-06	2.30E-06
<b>11</b>	<b>B2-NS6s1</b>	5.26E-06	1.21E-06
<b>12</b>	<b>B2-NS6s2</b>	2.13E-06	2.43E-06
<b>13</b>	<b>B2-NS7s1</b>	1.59E-06	1.86E-06
<b>14</b>	<b>B2-NS7s2</b>	-	3.31E-06
<b>15</b>	<b>B2-NS8s1</b>	2.06E-06	1.94E-06
<b>16</b>	<b>B2-NS8s2</b>	1.12E-06	3.43E-06
<b>17</b>	<b>B2-SM5t</b>	1.84E-06	7.83E-06
<b>18</b>	<b>B2-SM6t</b>	2.35E-06	8.75E-06
<b>19</b>	<b>B2-SM7t</b>	1.84E-06	9.39E-06
<b>20</b>	<b>B2-SM8t</b>	2.35E-06	9.39E-06
<b>21</b>	<b>B2-SM15b</b>	-	-5.78E-06
<b>22</b>	<b>B2-SM16b</b>	-5.12E-06	-5.88E-06
<b>23</b>	<b>B2-A7</b>	3.39E-06	3.54E-06
<b>24</b>	<b>B2-A8</b>	6.48E-06	4.10E-06
<b>25</b>	<b>B2-A9</b>	3.03E-06	4.71E-06
<b>26</b>	<b>B2-U1-1</b>	1.27E-06	1.04E-06
<b>27</b>	<b>B2-SG1</b>	8.74E-06	7.20E-06
<b>28</b>	<b>B2-SG4</b>	1.29E-05	1.19E-05
<b>29</b>	<b>B2-SG5</b>	-	1.28E-05
<b>30</b>	<b>B2-B10</b>	-5.13E-06	-4.27E-06
<b>31</b>	<b>B2-T7-N</b>	-7.61E-07	5.48E-07
<b>32</b>	<b>B2-T3-S</b>	-2.59E-06	-2.33E-06

**Table A4.2. West Face Displacements of Bent Cap 2 from Static Test-1 for Case 1**

Case	West Face Displacements (in) of Bent Cap 2 from Static Test-1, Case 1 in					
	Load Test			FE Simulation		
	Southside	Middle	Northside	Southside	Middle	Northside
<b>1</b>	-0.0126	-0.0072	-0.0045	-0.0103	-0.0063	-0.0043

**Table A4.3. Average Compressive Stresses on Concrete from Load Tests and FE Simulation of Static Test-1, Case 1 of Bent Cap 2**

CNFA Location	Average Compressive Stresses (ksi) for Case 1	
	Measured by CNFAs	From Updated FE Models
1	0.03	0.02
2	0.18	0.16
4	0.19	0.12

**Table A4.4. Rebar Strains from Load Test and FE Simulation from Static Test-1, Case 14 on Bent Cap 2**

<b># SG</b>	<b>Label</b>	<b>Strain From Load Test</b>	<b>Strain From FE Simulation</b>
1	B2-SS1s1	1.33E-05	1.15E-05
2	B2-SS1s2	9.22E-06	9.53E-06
3	B2-SS2s1	8.05E-06	1.14E-05
4	B2-SS2s2	8.12E-06	9.41E-06
5	B2-SS3s1	7.25E-06	1.12E-05
6	B2-SS3s2	9.08E-06	8.75E-06
7	B2-SS4s1	8.88E-06	1.12E-05
8	B2-SS4s2	9.12E-06	8.72E-06
9	B2-NS5s1	1.20E-06	4.16E-07
10	B2-NS5s2	2.30E-06	1.34E-06
11	B2-NS6s1	2.30E-06	5.00E-07
12	B2-NS6s2	3.55E-06	1.43E-06
13	B2-NS7s1	8.07E-07	9.76E-07
14	B2-NS7s2	-	2.07E-06
15	B2-NS8s1	5.46E-06	1.04E-06
16	B2-NS8s2	3.51E-06	2.16E-06
17	B2-SM5t	1.19E-05	7.17E-06
18	B2-SM6t	3.81E-06	8.04E-06
19	B2-SM7t	1.84E-05	1.08E-05
20	B2-SM8t	1.58E-05	1.14E-05
21	B2-SM15b	-	-5.36E-06
22	B2-SM16b	-1.11E-05	-5.50E-06
23	B2-A7	3.04E-06	3.09E-06
24	B2-A8	2.64E-06	3.50E-06
25	B2-A9	6.79E-06	3.93E-06
26	B2-U1-1	3.97E-06	1.06E-06
27	B2-SG1	4.01E-06	6.67E-06
28	B2-SG4	-	1.07E-05
29	B2-SG5	1.37E-05	1.15E-05
30	B2-B10	-3.29E-06	-3.59E-06
31	B2-T7-N	8.49E-07	2.08E-07
32	B2-T3-S	-	-1.49E-06

**Table A4.5. West Face Displacements of Bent Cap 2 from Static Test-1 for Case 14**

Case	West Face Displacements of Bent Cap 2 from Static Test-1, Case 14 (in)					
	Load Test			FE Simulation		
	Southside	Middle	Northside	Southside	Middle	Northside
<b>14</b>	-0.0101	-0.0058	-0.0030	-0.0097	-0.0055	-0.0030

**Table A4.6. Average Compressive Stresses on Concrete from Load Tests and FE Simulation of Static Test-1, Case 14 of Bent Cap 2**

CNFA Location	Average Compressive Stresses (ksi) for Case 14	
	Measured by CNFAs	From Updated FE Models
1	0.01	0.01
2	0.11	0.10
4	0.16	0.11

**Table A4.7. Rebar Strains from Load Test and FE Simulation from Static Test-2, Case 3 at Position 3 and Position 4 on Bent Cap 2**

# SG	Label	Rebar Strains From Static Test-2, Case 3 on Bent Cap 2			
		at Position 3		at Position 4	
		Load Test	FE Simulation	Load Test	FE Simulation
1	B2-SS1s1	7.84E-06	1.44E-05	2.29E-05	2.21E-05
2	B2-SS1s2	8.14E-06	1.19E-05	1.85E-05	1.83E-05
3	B2-SS2s1	9.72E-06	1.44E-05	1.37E-05	2.19E-05
4	B2-SS2s2	1.18E-05	1.18E-05	1.30E-05	1.81E-05
5	B2-SS3s1	4.53E-06	1.41E-05	1.46E-05	2.12E-05
6	B2-SS3s2	1.43E-05	1.11E-05	1.61E-05	1.68E-05
7	B2-SS4s1	5.02E-06	1.41E-05	1.31E-05	2.12E-05
8	B2-SS4s2	1.20E-05	1.10E-05	1.65E-05	1.67E-05
9	B2-NS5s1	7.18E-07	6.85E-07	-2.76E-06	-1.39E-06
10	B2-NS5s2	-	1.86E-06	-1.00E-07	-4.55E-07
11	B2-NS6s1	6.88E-06	7.96E-07	-1.78E-05	-1.28E-06
12	B2-NS6s2	1.33E-06	1.98E-06	-1.01E-06	-3.98E-07
13	B2-NS7s1	2.86E-06	1.42E-06	-3.00E-06	-8.29E-07
14	B2-NS7s2	-	2.81E-06	-	1.69E-07
15	B2-NS8s1	1.42E-06	1.50E-06	-2.00E-08	-7.88E-07
16	B2-NS8s2	2.51E-06	2.94E-06	-4.42E-06	2.71E-07
17	B2-SM5t	4.94E-06	8.58E-06	6.86E-06	1.21E-05
18	B2-SM6t	5.64E-06	9.62E-06	7.02E-06	1.36E-05
19	B2-SM7t	2.00E-06	1.04E-05	7.20E-06	1.48E-05
20	B2-SM8t	3.94E-06	1.04E-05	1.05E-05	1.48E-05
21	B2-SM15b	-	-6.91E-06	-	-1.17E-05
22	B2-SM16b	-4.82E-06	-7.08E-06	-1.00E-05	-1.21E-05
23	B2-A7	6.55E-06	4.01E-06	1.04E-05	5.93E-06
24	B2-A8	6.72E-06	4.57E-06	1.16E-05	6.57E-06
25	B2-A9	6.67E-06	5.16E-06	1.40E-05	7.18E-06
26	B2-U1-1	1.43E-06	1.41E-06	3.05E-06	2.58E-06
27	B2-SG1	6.77E-06	8.27E-06	1.06E-05	1.21E-05
28	B2-SG4	1.32E-05	1.34E-05	1.34E-05	1.96E-05
29	B2-SG5	1.39E-05	1.43E-05	1.08E-05	2.09E-05
30	B2-B10	-6.63E-06	-4.78E-06	-7.79E-06	-6.23E-06
31	B2-T7-N	-3.66E-06	-2.06E-08	-1.83E-06	-9.61E-07
32	B2-T3-S	-4.41E-06	-2.45E-06	-1.51E-06	-4.67E-06

**Table A4.8. West Face Displacements of Bent Cap 2 from Static Test-2 for Case 3**

Case	Position	West Face Displacements (in) of Bent Cap 2 From Static Test-2 in					
		Load Test			FE Simulation		
		Southside	Middle	Northside	Southside	Middle	Northside
3	3	-0.0133	-0.0067	-0.0039	-0.0121	-0.0070	-0.0041
	4	-0.0161	-0.0105	-0.0045	-0.0156	-0.0082	-0.0033

**Table A4.9. Average Compressive Stresses on Concrete from Load Tests and FE Simulation of Static Test-2, Case 3 of Bent Cap 2**

CNFA Location	Average Compressive Stresses (ksi) for Case 3			
	at Position 3		at Position 4	
	Measured by CNFAs	From Updated FE Models	Measured by CNFAs	From Updated FE Models
1	0.03	0.02	0.02	0.01
2	0.12	0.14	0.04	0.06
4	0.17	0.15	0.28	0.22

**Table A4.10. Rebar Strains from Load Test and FE Simulation from Static Test-2, Case 9 at Position 3 and Position 4 on Bent Cap 2**

# SG	Label	Rebar Strains From Static Test-2, Case 9 on Bent Cap 2			
		at Position 3		at Position 4	
		Load Test	FE Simulation	Load Test	FE Simulation
1	B2-SS1s1	1.35E-05	1.74E-05	1.80E-05	2.37E-05
2	B2-SS1s2	1.50E-05	1.43E-05	1.52E-05	1.95E-05
3	B2-SS2s1	1.28E-05	1.74E-05	1.61E-05	2.35E-05
4	B2-SS2s2	1.11E-05	1.42E-05	1.33E-05	1.93E-05
5	B2-SS3s1	1.30E-05	1.72E-05	1.64E-05	2.30E-05
6	B2-SS3s2	1.16E-05	1.35E-05	1.46E-05	1.82E-05
7	B2-SS4s1	1.49E-05	1.72E-05	1.44E-05	2.30E-05
8	B2-SS4s2	1.18E-05	1.35E-05	1.28E-05	1.81E-05
9	B2-NS5s1	1.50E-06	2.57E-07	-2.48E-06	-1.30E-06
10	B2-NS5s2	3.60E-06	1.49E-06	-7.85E-07	-2.08E-07
11	B2-NS6s1	4.59E-06	3.77E-07	-5.30E-06	-1.18E-06
12	B2-NS6s2	1.32E-06	1.62E-06	-2.00E-06	-1.29E-07
13	B2-NS7s1	3.71E-06	1.04E-06	2.97E-07	-6.30E-07
14	B2-NS7s2	-	2.49E-06	-	5.61E-07
15	B2-NS8s1	4.42E-06	1.12E-06	-4.70E-06	-5.74E-07
16	B2-NS8s2	3.71E-06	2.62E-06	1.06E-06	6.78E-07
17	B2-SM5t	1.11E-05	1.09E-05	5.79E-06	1.37E-05
18	B2-SM6t	6.00E-06	1.21E-05	6.86E-06	1.53E-05
19	B2-SM7t	1.23E-05	1.31E-05	4.60E-06	1.66E-05
20	B2-SM8t	9.47E-06	1.30E-05	8.16E-06	1.66E-05
21	B2-SM15b	-	-8.64E-06	-	-1.25E-05
22	B2-SM16b	-1.24E-05	-8.83E-06	-7.51E-06	-1.29E-05
23	B2-A7	6.28E-06	4.91E-06	8.70E-06	6.46E-06
24	B2-A8	6.75E-06	5.61E-06	8.87E-06	7.22E-06
25	B2-A9	8.74E-06	6.34E-06	9.94E-06	7.96E-06
26	B2-U1-1	6.20E-07	1.61E-06	2.48E-06	2.57E-06
27	B2-SG1	8.28E-06	7.38E-06	1.13E-05	1.32E-05
28	B2-SG4	1.27E-05	1.22E-05	1.98E-05	2.16E-05
29	B2-SG5	1.22E-05	1.36E-05	1.95E-05	2.31E-05
30	B2-B10	-5.76E-06	-5.35E-06	-8.24E-06	-6.63E-06
31	B2-T7-N	3.67E-06	5.56E-07	-2.87E-06	-3.41E-07
32	B2-T3-S	-3.36E-06	-3.71E-06	-3.34E-06	-5.36E-06

**Table A4.11. West Face Displacements of Bent Cap 2 from Static Test-2 for Case 9**

Case	Position	West Face Displacements (in) of Bent Cap 2 From Static Test-2 in					
		Load Test			FE Simulation		
		Southside	Middle	Northside	Southside	Middle	Northside
9	3	-0.0149	-0.0105	-0.0030	-0.0137	-0.0077	-0.0042
	4	-0.0163	-0.0105	-0.0035	-0.0169	-0.0089	-0.0037

**Table A4.12. Average Compressive Stresses on Concrete from Load Tests and FE Simulation of Static Test-2, Case 9 of Bent Cap 2**

CNFA Location	Average Compressive Stresses (ksi) for Case 9			
	at Position 3		at Position 4	
	Measured by CNFAs	From Updated FE Models	Measured by CNFAs	From Updated FE Models
1	0.03	0.02	0.01	0.01
2	0.15	0.14	0.04	0.08
4	0.22	0.17	0.33	0.24

**Table A4.13. Rebar Strains from Load Test and FE Simulation of Dynamic Test-1, Case 9 of Bent Cap 2**

# SG	Label	Strain From Load Test	Strain From FE Simulation
1	<b>B2-SS1s1</b>	3.36E-06	5.70E-06
2	<b>B2-SS1s2</b>	2.66E-06	4.87E-06
3	<b>B2-SS2s1</b>	2.77E-06	5.62E-06
4	<b>B2-SS2s2</b>	3.00E-06	4.76E-06
5	<b>B2-SS3s1</b>	2.78E-06	5.22E-06
6	<b>B2-SS3s2</b>	3.35E-06	4.17E-06
7	<b>B2-SS4s1</b>	3.42E-06	5.23E-06
8	<b>B2-SS4s2</b>	2.56E-06	4.14E-06
9	<b>B2-NS5s1</b>	-2.11E-07	-1.85E-07
10	<b>B2-NS5s2</b>	3.94E-07	1.31E-07
11	<b>B2-NS6s1</b>	-2.56E-06	-1.54E-07
12	<b>B2-NS6s2</b>	1.01E-06	1.48E-07
13	<b>B2-NS7s1</b>	-2.73E-07	-2.21E-08
14	<b>B2-NS7s2</b>	-	3.24E-07
15	<b>B2-NS8s1</b>	-9.70E-08	-1.11E-08
16	<b>B2-NS8s2</b>	6.21E-07	3.57E-07
17	<b>B2-SM5t</b>	2.96E-06	2.46E-06
18	<b>B2-SM6t</b>	1.91E-06	2.87E-06
19	<b>B2-SM7t</b>	1.41E-06	3.23E-06
20	<b>B2-SM8t</b>	2.54E-06	3.23E-06
21	<b>B2-SM15b</b>	-	-2.75E-06
22	<b>B2-SM16b</b>	-1.78E-06	-2.86E-06
23	<b>B2-A7</b>	9.78E-07	1.37E-06
24	<b>B2-A8</b>	1.64E-06	1.46E-06
25	<b>B2-A9</b>	1.19E-06	1.52E-06
26	<b>B2-U1-1</b>	7.98E-07	7.85E-07
27	<b>B2-SG1</b>	1.36E-06	3.02E-06
28	<b>B2-SG4</b>	3.00E-06	4.55E-06
29	<b>B2-SG5</b>	2.77E-06	4.81E-06
30	<b>B2-B10</b>	-9.09E-07	-1.71E-06
31	<b>B2-T7-N</b>	-1.12E-06	-2.29E-07
32	<b>B2-T3-S</b>	-7.19E-07	-4.54E-07

**Table A4.14. West Face Displacements of Bent Cap 2 from Dynamic Test-1, Case 9**

<b>Dynamic Test Case</b>	<b>West Face Displacements (in) of Bent Cap 2 From Dynamic Test-1 in</b>					
	<b>Load Test</b>			<b>FE Simulation</b>		
	<b>Southside</b>	<b>Middle</b>	<b>Northside</b>	<b>Southside</b>	<b>Middle</b>	<b>Northside</b>
<b>9 at 5 mph</b>	-0.0051	-0.0031	-0.0011	-0.0047	-0.0024	-0.0008

**Table A4.15. Rebar Strains from Load Test and FE Simulation of Dynamic Test-1, Case 14 of Bent Cap 2**

# SG	Label	Strain From Load Test	Strain from FE Simulation
1	<b>B2-SS1s1</b>	4.15E-06	4.54E-06
2	<b>B2-SS1s2</b>	4.09E-06	3.96E-06
3	<b>B2-SS2s1</b>	3.56E-06	4.45E-06
4	<b>B2-SS2s2</b>	5.16E-06	3.85E-06
5	<b>B2-SS3s1</b>	4.63E-06	3.95E-06
6	<b>B2-SS3s2</b>	8.06E-06	3.18E-06
7	<b>B2-SS4s1</b>	5.87E-06	3.95E-06
8	<b>B2-SS4s2</b>	1.43E-06	3.15E-06
9	<b>B2-NS5s1</b>	-1.23E-06	-4.01E-07
10	<b>B2-NS5s2</b>	-2.56E-06	-2.55E-07
11	<b>B2-NS6s1</b>	-2.64E-06	-3.83E-07
12	<b>B2-NS6s2</b>	-1.01E-06	-2.59E-07
13	<b>B2-NS7s1</b>	-8.51E-07	-3.44E-07
14	<b>B2-NS7s2</b>	-	-2.08E-07
15	<b>B2-NS8s1</b>	-3.28E-06	-3.46E-07
16	<b>B2-NS8s2</b>	-1.27E-06	-1.92E-07
17	<b>B2-SM5t</b>	2.04E-06	1.52E-06
18	<b>B2-SM6t</b>	1.67E-06	1.83E-06
19	<b>B2-SM7t</b>	3.10E-06	2.13E-06
20	<b>B2-SM8t</b>	4.91E-06	2.38E-06
21	<b>B2-SM15b</b>	-	-2.22E-06
22	<b>B2-SM16b</b>	-4.40E-06	-2.34E-06
23	<b>B2-A7</b>	1.81E-06	9.84E-07
24	<b>B2-A8</b>	2.44E-06	1.00E-06
25	<b>B2-A9</b>	3.94E-06	9.80E-07
26	<b>B2-U1-1</b>	1.21E-06	7.55E-07
27	<b>B2-SG1</b>	1.11E-06	2.31E-06
28	<b>B2-SG4</b>	1.13E-06	3.18E-06
29	<b>B2-SG5</b>	2.93E-06	3.31E-06
30	<b>B2-B10</b>	-2.14E-06	-1.32E-06
31	<b>B2-T7-N</b>	-4.44E-07	-7.83E-07
32	<b>B2-T3-S</b>	-9.87E-07	-1.67E-08

**Table A4.16. West Face Displacements of Bent Cap 2 from Dynamic Test-1, Case 14**

<b>Dynamic Test Case</b>	<b>West Face Displacements (in) of Bent Cap 2 From Dynamic Test-1 in</b>					
	<b>Load Test</b>			<b>FE Simulation</b>		
	<b>Southside</b>	<b>Middle</b>	<b>Northside</b>	<b>Southside</b>	<b>Middle</b>	<b>Northside</b>
<b>14 at 5 mph</b>	-0.0036	-0.0019	-0.0001	-0.0033	-0.0015	-0.0001

**APPENDIX-5**

**Table A5.1. Rebar Strains from Load Test and FE Simulation from Static Test-1, Case 1 on Bent Cap 7**

<b># SG</b>	<b>Label</b>	<b>Strain From Load Test</b>	<b>Strain From FE Simulation</b>
<b>1</b>	<b>B7-SS1s1</b>	1.24E-05	9.18E-06
<b>2</b>	<b>B7-SS1s2</b>	3.91E-06	6.61E-06
<b>3</b>	<b>B7-SS2s1</b>	1.37E-05	8.25E-06
<b>4</b>	<b>B7-SS2s2</b>	-	7.04E-06
<b>5</b>	<b>B7-SS3s1</b>	1.18E-05	8.80E-06
<b>6</b>	<b>B7-SS3s2</b>	4.38E-06	6.63E-06
<b>7</b>	<b>B7-SS4s1</b>	6.58E-06	8.52E-06
<b>8</b>	<b>B7-SS4s2</b>	9.83E-06	6.33E-06
<b>9</b>	<b>B7-NS5s1</b>	2.83E-06	5.63E-06
<b>10</b>	<b>B7-NS5s2</b>	1.08E-06	2.80E-06
<b>11</b>	<b>B7-NS6s1</b>	4.07E-06	6.99E-06
<b>12</b>	<b>B7-NS6s2</b>	2.70E-06	3.14E-06
<b>13</b>	<b>B7-NS7s1</b>	1.02E-05	7.42E-06
<b>14</b>	<b>B7-NS7s2</b>	4.33E-06	2.99E-06
<b>15</b>	<b>B7-NS8s1</b>	2.08E-06	6.76E-06
<b>16</b>	<b>B7-NS8s2</b>	8.87E-06	2.69E-06
<b>17</b>	<b>B7-SM5t</b>	3.11E-06	4.18E-06
<b>18</b>	<b>B7-SM6t</b>	2.96E-06	4.59E-06
<b>19</b>	<b>B7-SM7t</b>	-	4.71E-06
<b>20</b>	<b>B7-SM8t</b>	6.46E-06	4.68E-06
<b>21</b>	<b>B7-SM15b</b>	-6.16E-06	-5.74E-06
<b>22</b>	<b>B7-SM17b</b>	-	-6.12E-06
<b>23</b>	<b>B7-A7</b>	5.14E-06	6.77E-06
<b>24</b>	<b>B7-A8</b>	4.30E-06	6.86E-06
<b>25</b>	<b>B7-A9</b>	-	6.84E-06
<b>26</b>	<b>B7-U1-1</b>	3.30E-06	2.91E-06
<b>27</b>	<b>B7-SG1</b>	1.10E-05	8.52E-06
<b>28</b>	<b>B7-SG2</b>	-	8.96E-06
<b>29</b>	<b>B7-B10</b>	-	-3.34E-06
<b>30</b>	<b>B7-T7</b>	-	-2.74E-06

**Table A5.2. West Face Displacements of Bent Cap 7 from Load Test and FE Simulation of Static Test-1 for Case 1**

Case	West Face Displacements (in) of Bent Cap 7 From Static Test-1, Case 1 in					
	Load Test			FE Simulation		
	Southside	Middle	Northside	Southside	Middle	Northside
<b>1</b>	-0.0091	-0.0059	-0.0044	-0.0097	-0.0064	-0.0047

**Table A5.3. Average Compressive Stresses on Concrete from Load Tests and FE Simulation of Static Test-1, Case 1 of Bent Cap 7**

CNFA Location	Average Compressive Stresses (ksi) for Case 1	
	Measured by CNFAs	From Updated FE Models
1	0.03	0.02
2	0.14	0.11

**Table A5.4. Rebar Strains from Load Test and FE Simulation from Static Test-1, Case 11 on Bent Cap 7**

# SG	Label	Strain During Load Test	Strain From FE Simulation
1	B7-SS1s1	1.54E-05	1.52E-05
2	B7-SS1s2	1.37E-05	1.12E-05
3	B7-SS2s1	1.58E-05	1.35E-05
4	B7-SS2s2	-	1.17E-05
5	B7-SS3s1	1.67E-05	1.44E-05
6	B7-SS3s2	1.33E-05	1.11E-05
7	B7-SS4s1	1.07E-05	1.40E-05
8	B7-SS4s2	1.06E-05	1.06E-05
9	B7-NS5s1	5.17E-06	4.52E-06
10	B7-NS5s2	2.70E-07	1.83E-06
11	B7-NS6s1	5.26E-06	5.88E-06
12	B7-NS6s2	2.80E-06	2.18E-06
13	B7-NS7s1	6.63E-06	6.34E-06
14	B7-NS7s2	1.72E-06	2.08E-06
15	B7-NS8s1	2.35E-06	5.78E-06
16	B7-NS8s2	6.10E-06	1.82E-06
17	B7-SM5t	1.04E-05	6.27E-06
18	B7-SM6t	8.49E-06	6.92E-06
19	B7-SM7t	-	7.13E-06
20	B7-SM8t	8.97E-06	7.12E-06
21	B7-SM15b	-6.31E-06	-9.89E-06
22	B7-SM17b	-	-1.03E-05
23	B7-A7	1.29E-05	9.20E-06
24	B7-A8	6.13E-06	9.33E-06
25	B7-A9	-	9.35E-06
26	B7-U1-1	3.37E-06	4.91E-06
27	B7-SG1	1.25E-05	9.44E-06
28	B7-SG2	-	1.04E-05
29	B7-B10	-	-4.57E-06
30	B7-T7	-	-2.62E-06

**Table A5.5. West Face Displacements of Bent Cap 7 from Load Test and FE Simulation of Static Test-1 for Case 11**

Case	West Face Displacements (in) of Bent Cap 7 From Static Test-1, Case 11 in					
	Load Test			FE Simulation		
	Southside	Middle	Northside	Southside	Middle	Northside
<b>11</b>	-0.0151	-0.0089	-0.0055	-0.0136	-0.0080	-0.0050

**Table A5.6. Average Compressive Stresses on Concrete from Load Tests and FE Simulation of Static Test-1, Case 1 of Bent Cap 7**

CNFA Location	Average Compressive Stresses (ksi) for Case 1	
	Measured by CNFAs	From Updated FE Models
1	0.02	0.01
2	0.15	0.10

**Table A5.7. Rebar Strains from Load Test and FE Simulation from Static Test-2, Case 9 at Position 3, and Position 4 on Bent Cap 7**

# SG	Label	Rebar Strains From Static Test-2, Case 9 on Bent Cap 7			
		at Position 3		at Position 4	
		Load Test	FE Simulation	Load Test	FE Simulation
1	B7-SS1s1	9.98E-06	1.31E-05	1.77E-05	1.91E-05
2	B7-SS1s2	1.01E-05	9.58E-06	1.16E-05	1.42E-05
3	B7-SS2s1	1.45E-05	1.17E-05	2.06E-05	1.68E-05
4	B7-SS2s2	-	1.01E-05	-	1.48E-05
5	B7-SS3s1	1.10E-05	1.25E-05	2.17E-05	1.79E-05
6	B7-SS3s2	1.34E-05	9.53E-06	8.99E-06	1.39E-05
7	B7-SS4s1	1.52E-05	1.21E-05	1.55E-05	1.73E-05
8	B7-SS4s2	1.09E-05	9.11E-06	1.57E-05	1.33E-05
9	B7-NS5s1	4.31E-06	5.25E-06	1.49E-06	1.42E-06
10	B7-NS5s2	4.27E-06	2.40E-06	-1.33E-06	-2.38E-07
11	B7-NS6s1	1.33E-06	6.78E-06	2.25E-06	2.25E-06
12	B7-NS6s2	2.42E-06	2.79E-06	-2.34E-06	-2.53E-08
13	B7-NS7s1	2.15E-06	7.32E-06	-6.11E-06	-6.31E-07
14	B7-NS7s2	7.65E-07	2.65E-06	-9.38E-07	-1.18E-06
15	B7-NS8s1	2.07E-06	6.66E-06	-1.67E-06	-7.33E-07
16	B7-NS8s2	1.66E-06	2.35E-06	-6.77E-06	-1.32E-06
17	B7-SM5t	7.69E-06	5.65E-06	9.84E-06	7.47E-06
18	B7-SM6t	7.39E-06	6.21E-06	1.08E-05	8.26E-06
19	B7-SM7t	-	6.39E-06	-	8.53E-06
20	B7-SM8t	6.40E-06	6.35E-06	1.11E-05	8.52E-06
21	B7-SM15b	-4.50E-06	-8.19E-06	-8.12E-06	-1.30E-05
22	B7-SM17b	-	-8.56E-06	-	-1.36E-05
23	B7-A7	1.06E-05	8.56E-06	7.56E-06	9.73E-06
24	B7-A8	1.01E-05	8.70E-06	1.31E-05	9.83E-06
25	B7-A9	-	8.72E-06	-	9.88E-06
26	B7-U1-1	6.30E-06	4.21E-06	6.80E-06	6.19E-06
27	B7-SG1	7.15E-06	8.25E-06	1.85E-05	1.15E-05
28	B7-SG2	-	9.14E-06	-	1.26E-05
29	B7-B10	-	-4.16E-06	-	-4.89E-06
30	B7-T7	-	-2.90E-06	-	-1.45E-06

**Table A5.8. West Face Displacements of Bent Cap 7 in Static Test-2 for Case 9**

Case	Position	West Face Displacements of Bent Cap 7 From Static Test-2 in (in)					
		Load Test			FE Simulation		
		Southside	Middle	Northside	Southside	Middle	Northside
9	3	-0.0097	-0.0058	-0.0037	-0.0125	-0.0075	-0.0047
	4	-0.0161	-0.0082	-0.0034	-0.0158	-0.0081	-0.0033

**Table A5.9. Average Compressive Stresses on Concrete from Load Tests and FE Simulation of Static Test-2, Case 9 of Bent Cap 7**

CNFA Location	Average Compressive Stresses (ksi) for Case 9			
	at Position 3		at Position 4	
	Measured by CNFAs	From Updated FE Models	Measured by CNFAs	From Updated FE Models
1	0.04	0.02	0.003	0.003
2	0.17	0.12	0.05	0.06

**Table A5.10. Rebar Strains from Load Test and FE Simulation from Static Test-2, Case 14 at Position 3, and Position 4 on Bent Cap 7**

# SG	Label	Rebar Strains From Static Test-2, Case 14 on Bent Cap 7			
		at Position 3		at Position 4	
		Load Test	FE Simulation	Load Test	FE Simulation
1	B7-SS1s1	1.33E-05	8.13E-06	1.30E-05	1.48E-05
2	B7-SS1s2	7.39E-06	5.83E-06	1.22E-05	1.09E-05
3	B7-SS2s1	8.59E-06	7.31E-06	9.07E-06	1.29E-05
4	B7-SS2s2	-	6.21E-06	-	1.14E-05
5	B7-SS3s1	6.73E-06	7.79E-06	9.16E-06	1.37E-05
6	B7-SS3s2	6.95E-06	5.85E-06	6.72E-06	1.07E-05
7	B7-SS4s1	9.14E-06	7.54E-06	1.31E-05	1.33E-05
8	B7-SS4s2	6.53E-06	5.59E-06	1.11E-05	1.02E-05
9	B7-NS5s1	1.23E-06	4.93E-06	3.06E-06	6.04E-07
10	B7-NS5s2	1.05E-06	2.41E-06	-2.50E-06	-5.56E-07
11	B7-NS6s1	2.28E-06	6.10E-06	1.16E-06	1.07E-06
12	B7-NS6s2	1.07E-06	2.71E-06	-4.47E-06	-4.34E-07
13	B7-NS7s1	6.73E-06	6.47E-06	1.22E-06	1.19E-06
14	B7-NS7s2	3.28E-07	2.58E-06	-6.54E-07	-3.77E-07
15	B7-NS8s1	9.81E-06	5.88E-06	1.92E-06	1.10E-06
16	B7-NS8s2	3.48E-06	2.30E-06	-6.11E-06	-4.43E-07
17	B7-SM5t	2.39E-06	3.99E-06	8.89E-06	5.96E-06
18	B7-SM6t	4.20E-06	4.36E-06	6.91E-06	6.59E-06
19	B7-SM7t	-	4.43E-06	-	6.79E-06
20	B7-SM8t	2.01E-06	4.35E-06	5.32E-06	6.76E-06
21	B7-SM15b	-1.40E-06	-5.12E-06	-6.20E-06	-1.07E-05
22	B7-SM17b	-	-5.52E-06	-	-1.14E-05
23	B7-A7	7.32E-06	5.98E-06	9.89E-06	7.35E-06
24	B7-A8	3.63E-06	6.04E-06	4.04E-06	7.41E-06
25	B7-A9	-	5.98E-06	-	7.41E-06
26	B7-U1-1	2.35E-06	2.55E-06	4.76E-06	4.73E-06
27	B7-SG1	5.58E-06	5.32E-06	1.31E-05	8.96E-06
28	B7-SG2	-	5.94E-06	-	9.80E-06
29	B7-B10	-	-2.88E-06	-	-3.70E-06
30	B7-T7	-	-2.39E-06	-	-9.17E-07

**Table A5.11. West Face Displacements of Bent Cap 7 in Static Test-2 for Case 14**

Case	Position	West Face Displacements (in) of Bent Cap 7 From Static Test-2 in					
		Load Test			FE Simulation		
		Southside	Middle	Northside	Southside	Middle	Northside
14	3	-0.0094	-0.0060	-0.0038	-0.0092	-0.0059	-0.0038
	4	-0.0133	-0.0067	-0.0014	-0.0140	-0.0070	-0.0015

**Table A5.12. Average Compressive Stresses on Concrete from Load Tests and FE Simulation of Static Test-2, Case 14 of Bent Cap 7**

CNFA Location	Average Compressive Stresses (ksi) for Case 14			
	at Position 3		at Position 4	
	Measured by CNFAs	From Updated FE Models	Measured by CNFAs	From Updated FE Models
1	0.03	0.02	0.02	0.01
2	0.13	0.10	0.05	0.03

**Table A5.13. Rebar Strains from Load Test and FE Simulation of Dynamic Test-1, Case 9 of Bent Cap 7**

# SG	Label	Strain From Load Test	Strain From FE Simulation
1	<b>B7-SS1s1</b>	9.82E-06	1.31E-05
2	<b>B7-SS1s2</b>	8.34E-06	9.58E-06
3	<b>B7-SS2s1</b>	1.10E-05	1.17E-05
4	<b>B7-SS2s2</b>	-	1.01E-05
5	<b>B7-SS3s1</b>	1.01E-05	1.25E-05
6	<b>B7-SS3s2</b>	5.19E-06	9.53E-06
7	<b>B7-SS4s1</b>	9.73E-06	1.21E-05
8	<b>B7-SS4s2</b>	4.79E-06	9.11E-06
9	<b>B7-NS5s1</b>	2.08E-06	5.25E-06
10	<b>B7-NS5s2</b>	1.00E-06	2.40E-06
11	<b>B7-NS6s1</b>	1.29E-06	6.78E-06
12	<b>B7-NS6s2</b>	1.69E-06	2.79E-06
13	<b>B7-NS7s1</b>	1.99E-06	7.32E-06
14	<b>B7-NS7s2</b>	1.21E-06	2.65E-06
15	<b>B7-NS8s1</b>	5.01E-07	6.66E-06
16	<b>B7-NS8s2</b>	6.61E-07	2.35E-06
17	<b>B7-SM5t</b>	1.33E-06	5.65E-06
18	<b>B7-SM6t</b>	2.66E-06	6.21E-06
19	<b>B7-SM7t</b>	-	6.39E-06
20	<b>B7-SM8t</b>	5.21E-06	6.35E-06
21	<b>B7-SM15b</b>	-1.60E-06	-8.19E-06
22	<b>B7-SM17b</b>	-	-8.56E-06
23	<b>B7-A7</b>	6.68E-06	8.56E-06
24	<b>B7-A8</b>	2.96E-06	8.70E-06
25	<b>B7-A9</b>	-	8.72E-06
26	<b>B7-U1-1</b>	2.14E-06	4.21E-06
27	<b>B7-SG1</b>	6.11E-06	8.25E-06
28	<b>B7-SG2</b>	-	9.14E-06
29	<b>B7-B10</b>	-	-4.16E-06
30	<b>B7-T7</b>	-	-2.90E-06

**Table A5.14. West Face Displacements of Bent Cap 7 from Dynamic Test-1, Case 9**

<b>Dynamic Test Case</b>	<b>West Face Displacements (in) of Bent Cap 7 From Dynamic Test-1 in</b>					
	<b>Load Test</b>			<b>FE Simulation</b>		
	<b>Southside</b>	<b>Middle</b>	<b>Northside</b>	<b>Southside</b>	<b>Middle</b>	<b>Northside</b>
<b>9 at 5 mph</b>	-0.0092	-0.0055	-0.0035	-0.0125	-0.0075	-0.0047

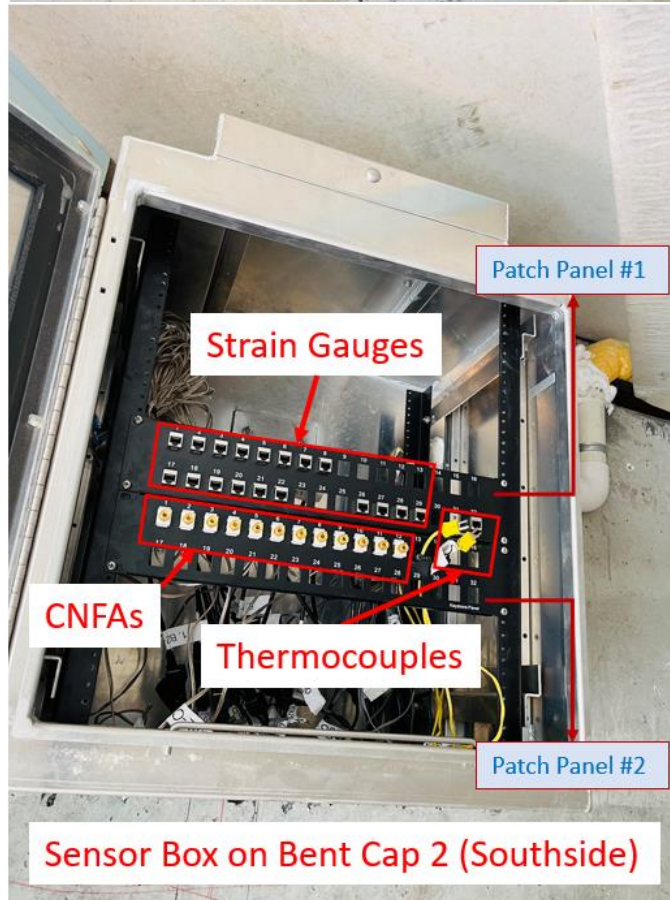
**Table A5.15. Rebar Strains from Load Test and FE Simulation of Dynamic Test-1, Case 14 of Bent Cap 7**

# SG	Label	Strain From Load Test	Strain From FE Simulation
1	<b>B7-SS1s1</b>	7.62E-06	8.13E-06
2	<b>B7-SS1s2</b>	5.55E-06	5.83E-06
3	<b>B7-SS2s1</b>	6.58E-06	7.31E-06
4	<b>B7-SS2s2</b>	-	6.21E-06
5	<b>B7-SS3s1</b>	5.22E-06	7.79E-06
6	<b>B7-SS3s2</b>	2.68E-06	5.85E-06
7	<b>B7-SS4s1</b>	4.38E-06	7.54E-06
8	<b>B7-SS4s2</b>	3.11E-06	5.59E-06
9	<b>B7-NS5s1</b>	8.97E-07	4.93E-06
10	<b>B7-NS5s2</b>	1.74E-06	2.41E-06
11	<b>B7-NS6s1</b>	6.64E-07	6.10E-06
12	<b>B7-NS6s2</b>	1.01E-06	2.71E-06
13	<b>B7-NS7s1</b>	1.21E-06	6.47E-06
14	<b>B7-NS7s2</b>	1.17E-07	2.58E-06
15	<b>B7-NS8s1</b>	1.10E-06	5.88E-06
16	<b>B7-NS8s2</b>	1.21E-06	2.30E-06
17	<b>B7-SM5t</b>	9.66E-07	3.99E-06
18	<b>B7-SM6t</b>	5.82E-07	4.36E-06
19	<b>B7-SM7t</b>	-	4.43E-06
20	<b>B7-SM8t</b>	2.47E-07	4.35E-06
21	<b>B7-SM15b</b>	-1.06E-06	-5.12E-06
22	<b>B7-SM17b</b>	-	-5.52E-06
23	<b>B7-A7</b>	2.43E-06	5.98E-06
24	<b>B7-A8</b>	1.28E-06	6.04E-06
25	<b>B7-A9</b>	-	5.98E-06
26	<b>B7-U1-1</b>	1.72E-06	2.55E-06
27	<b>B7-SG1</b>	3.40E-06	5.32E-06
28	<b>B7-SG2</b>	-	5.94E-06
29	<b>B7-B10</b>	-	-2.88E-06
30	<b>B7-T7</b>	-	-2.39E-06

**Table A5.16. West Face Displacements of Bent Cap 7 from Dynamic Test-1, Case 14**

Dynamic Test Case	West Face Displacements (in) of Bent Cap 7 From Dynamic Test-1 in					
	Load Test			FE Simulation		
	Southside	Middle	Northside	Southside	Middle	Northside
<b>14 at 5 mph</b>	-0.0105	-0.0053	-0.0011	-0.0140	-0.0070	-0.0015

APPENDIX-6



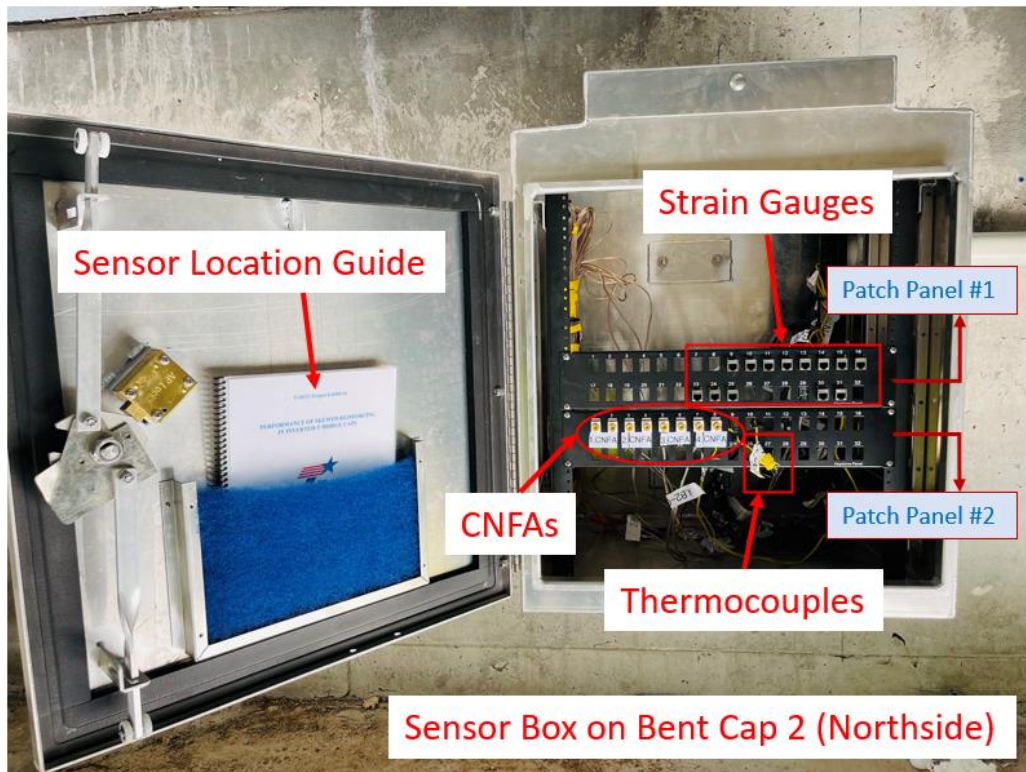


**Figure A6.1 Sensor Box Installed on Bent Cap 2**

**Table A6.1. Locations of Strain Gauges Installed in Bent Cap 2 - South Side**

<b>No.</b>	<b>Label</b>	<b>Explanation</b>	<b>Sensor Box</b>	<b>Port No. on Patch Panel 1</b>	<b>Bar Group</b>
<b>1</b>	<b>B2-SS1s1</b>	Bent Cap 2 – South side, 1st S Bar from the west face, 1st SG located on the Side of the bar	South Side	1	<b>S Bars</b>
<b>2</b>	<b>B2-SS1s2</b>	Bent Cap 2 – South side, 1st S Bar from the west face, 2nd SG located on the Side of the bar	South Side	2	
<b>3</b>	<b>B2-SS2s1</b>	Bent Cap 2 – South side, 2nd S Bar from the west face, 1st SG located on the Side of the bar	South Side	3	
<b>4</b>	<b>B2-SS2s2</b>	Bent Cap 2 – South side, 2nd S Bar from the west face, 2nd SG located on the Side of the bar	South Side	4	
<b>5</b>	<b>B2-SS3s1</b>	Bent Cap 2 – South side, 3rd S Bar from the west face, 1st SG located on the Side of the bar	South Side	5	
<b>6</b>	<b>B2-SS3s2</b>	Bent Cap 2 – South side, 3rd S Bar from the west face, 2nd SG located on the Side of the bar	South Side	6	
<b>7</b>	<b>B2-SS4s1</b>	Bent Cap 2 – South side, 4th S Bar from the west face, 2nd SG located on the Side of the bar	South Side	7	
<b>8</b>	<b>B2-SS4s2</b>	Bent Cap 2 – South side, 4th S Bar from the west face, 2nd SG located on the Side of the bar	South Side	8	
<b>17</b>	<b>B2-SM5t</b>	Bent Cap 2 – South side, 5th M Bar from the west face, SG located on the top of the bar	South Side	17	<b>M Bars</b>
<b>18</b>	<b>B2-SM6t</b>	Bent Cap 2 – South side, 6th M Bar from the west face, SG located on the Top of the bar	South Side	18	
<b>19</b>	<b>B2-SM7t</b>	Bent Cap 2 – South side, 7th M Bar from the west face, SG located on the Top of the bar	South Side	19	
<b>20</b>	<b>B2-SM8t</b>	Bent Cap 2 – South side, 8th M Bar from the west face, SG located on the Top of the bar	South Side	20	

<b>21</b>	<b>B2-SM14b</b>	Bent Cap 2 – South side, 14th M Bar from the west face, SG located on the Bottom of the bar	South Side	21	M Bars
<b>22</b>	<b>B2-SM16b</b>	Bent Cap 2 – South side, 16th M Bar from the west face, SG located on the Bottom of the bar	South Side	22	
<b>26</b>	<b>B2-U1-1</b>	Bent Cap 2 – 1st U1 Bar from the west face	South Side	26	U1 Bar
<b>27</b>	<b>B2-SG1</b>	Bent Cap 2 – South side 1st G Bar from the west face	South Side	27	G Bar
<b>28</b>	<b>B2-SG4</b>	Bent Cap 2 – South side, 4th G Bar from the west face	South Side	28	
<b>29</b>	<b>B2-SG5</b>	Bent Cap 2 – South side, 5th G Bar from the west face	South Side	29	
<b>32</b>	<b>B2-T3-S</b>	Bent Cap 2 – South side 3rd T bar from the west face under the bearing pad	South Side	32	T Bar

**Table A6.2. Locations of CNFAs Installed in Bent Cap 2- South Side**

<b>No.</b>	<b>Label</b>	<b>Explanation</b>	<b>Sensor Box</b>	<b>CNFA Terminal</b>	<b>Port No. on Patch Panel 2</b>	<b>Location</b>
<b>1</b>	<b>B2-CNFA1zz1</b>	Bent Cap 2 – 10th B Bar from the west face, First CNFA location in Z-Z direction	South Side	Left	1	1
				Right	2	
<b>2</b>	<b>B2-CNFA2zz1</b>	Bent Cap 2 – T Bar, First CNFA at Location 2 on Z-Z direction (Bearing Pad-North face)	South Side	Left	3	2
				Right	4	
<b>3</b>	<b>B2-CNFA2zz2</b>	Bent Cap 2 – T Bar, Second CNFA at Location 2 on Z-Z direction (Bearing Pad-North face)	South Side	Left	5	
				Right	6	
<b>4</b>	<b>B2-CNFA2zz3</b>	Bent Cap 2 – T Bar, Third CNFA at Location 2 on Z-Z direction (Bearing Pad-North face)	South Side	Left	7	
				Right	8	
<b>5</b>	<b>B2-CNFA3zz1</b>	Bent Cap 2 – 1st S Bar, First CNFA at Location 3 on Z-Z direction (First S-bar-South face)	South Side	Left	9	3
				Right	10	
<b>6</b>	<b>B2-CNFA3zz2</b>	Bent Cap 2 – 2nd S Bar, Second CNFA at Location 3 on Z-Z direction (Second S-bar-South face)	South Side	Left	11	
				Right	12	

**Table A6.3. Locations of Strain Gauges Installed in Bent Cap 2 - North Side**

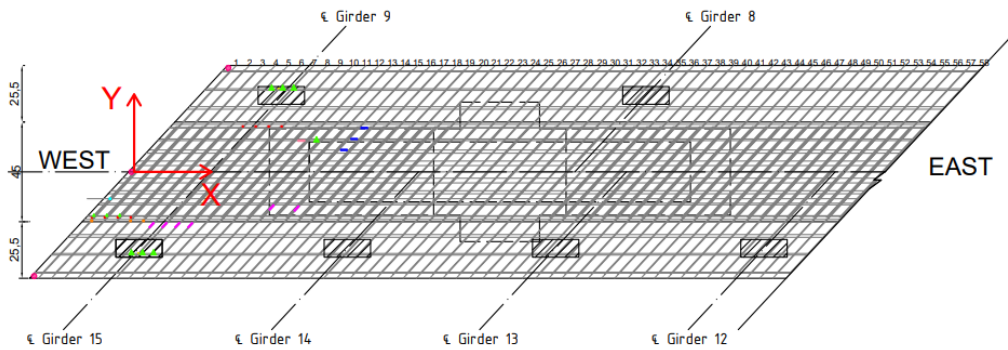
<b>No.</b>	<b>Label</b>	<b>Explanation</b>	<b>Sensor Box</b>	<b>Port No. on Patch Panel 1</b>	<b>Bar Group</b>
9	<b>B2-NS5s1</b>	Bent Cap 2 – North side, 5th S Bar from the west face, 1st SG located on the Side of the bar	North Side	9	S Bars
10	<b>B2-NS5s2</b>	Bent Cap 2 – North side, 5th S Bar from the west face, 2nd SG located on the Side of the bar	North Side	10	
11	<b>B2-NS6s1</b>	Bent Cap 2 – North side, 6th S Bar from the west face, 1st SG located on the Side of the bar	North Side	11	
12	<b>B2-NS6s2</b>	Bent Cap 2 – North side, 6th S Bar from the west face, 2nd SG located on the Side of the bar	North Side	12	
13	<b>B2-NS7s1</b>	Bent Cap 2 – North side, 7th S Bar from the west face, 1st SG located on the Side of the bar	North Side	13	
14	<b>B2-NS7s2</b>	Bent Cap 2 – North side, 7th S Bar from the west face, 2nd SG located on the Side of the bar	North Side	14	
15	<b>B2-NS8s1</b>	Bent Cap 2 – North side, 8th S Bar from the west face, 1st SG located on the Side of the bar	North Side	15	
16	<b>B2-NS8s2</b>	Bent Cap 2 – North side, 8th S Bar from the west face, 2nd SG located on the Side of the bar	North Side	16	
23	<b>B2-A7</b>	Bent Cap 2 – 7th A Bar from the south side	North Side	23	A Bars
24	<b>B2-A8</b>	Bent Cap 2 – 8th A Bar from the south side	North Side	24	
25	<b>B2-A9</b>	Bent Cap 2 – 9th A Bar from the south side	North Side	25	
30	<b>B2-B10</b>	Bent Cap 2 – 10th B Bar from the west face	North Side	30	B Bar
31	<b>B2-T7-N</b>	Bent Cap 2 – North side, 7th T bar from the west face under the bearing pad	North Side	31	T Bar

**Table A6.4. Locations of CNFAs Installed in Bent Cap 2 - North Side**

<b>No.</b>	<b>Label</b>	<b>Explanation</b>	<b>Sensor Box</b>	<b>CNFA Terminal</b>	<b>Port No. on Patch Panel 2</b>	<b>Location</b>
<b>7</b>	<b>B2-CNFA3zz3</b>	Bent Cap 2 – 3rd S Bar, Third CNFA at Location 3 on Z-Z direction (Third S-bar-South face)	North Side	Left	1	3
				Right	2	
<b>8</b>	<b>B2-CNFA4zz1</b>	Bent Cap 2 – T Bar, First CNFA at Location 4 on Z-Z direction (Bearing Pad-South face)	North Side	Left	3	4
				Right	4	
<b>9</b>	<b>B2-CNFA4zz2</b>	Bent Cap 2 – T Bar, Second CNFA at Location 4 on Z-Z direction (Bearing Pad-South face)	North Side	Left	5	4
				Right	6	
<b>10</b>	<b>B2-CNFA4zz3</b>	Bent Cap 2 – T Bar, Third CNFA at Location 4 on Z-Z direction (Bearing Pad-South face)	North Side	Left	7	4
				Right	8	

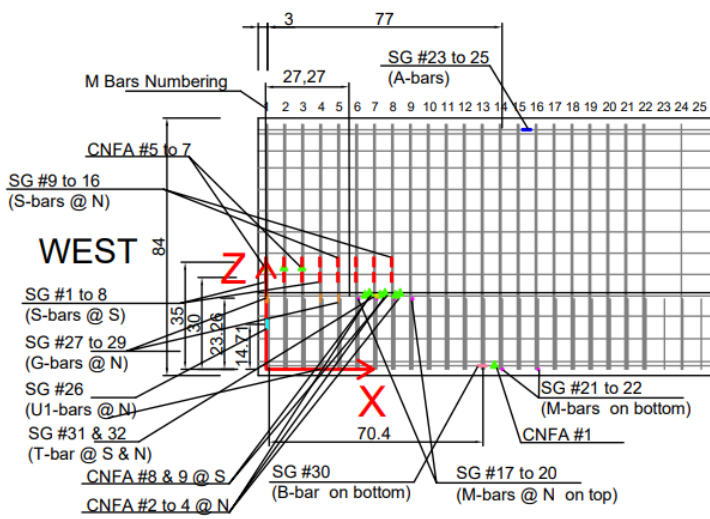


**Figure A6.2. Strain Gauges and CNFA Instrumented on Bent Cap 2**

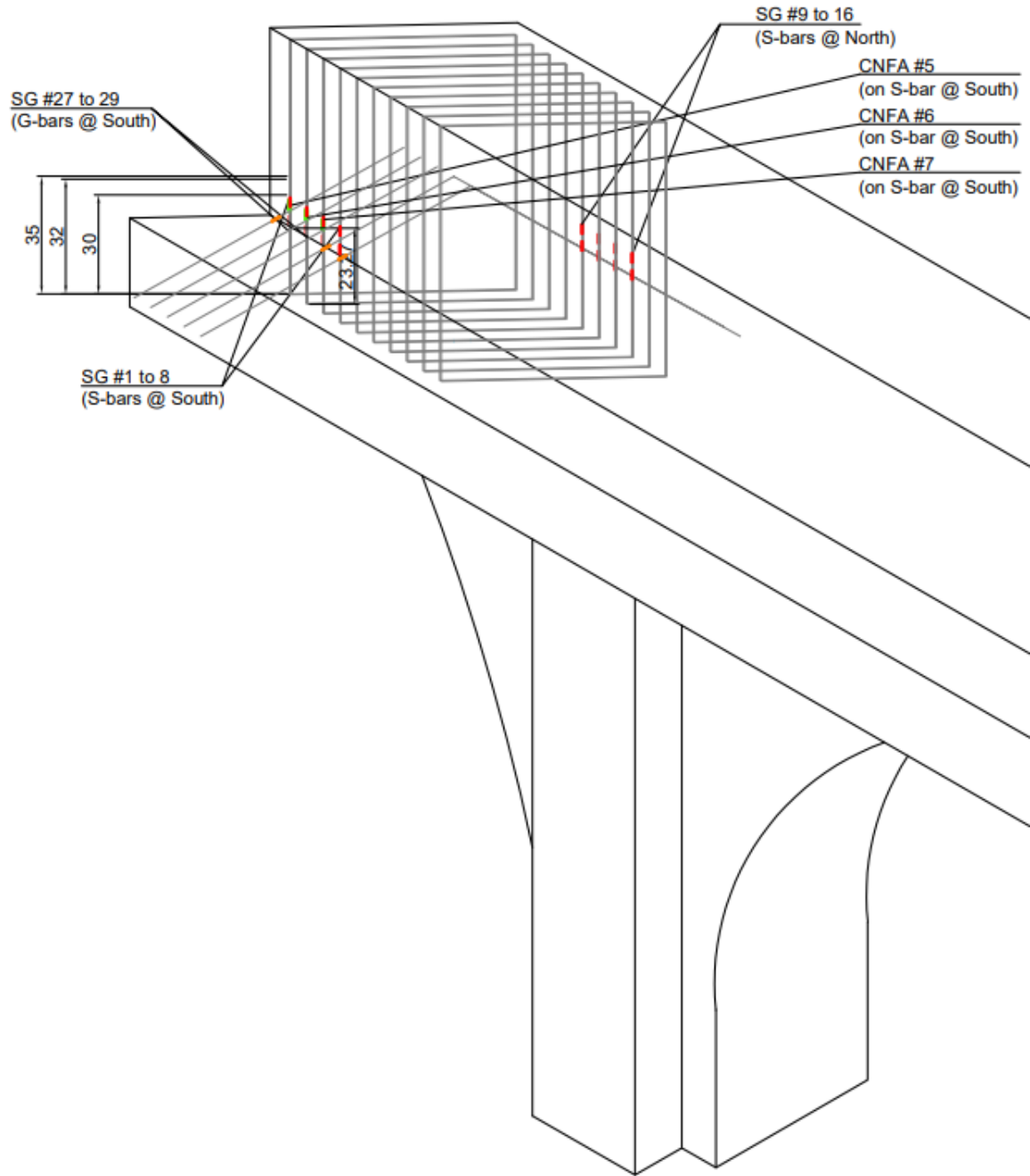


PLAN VIEW

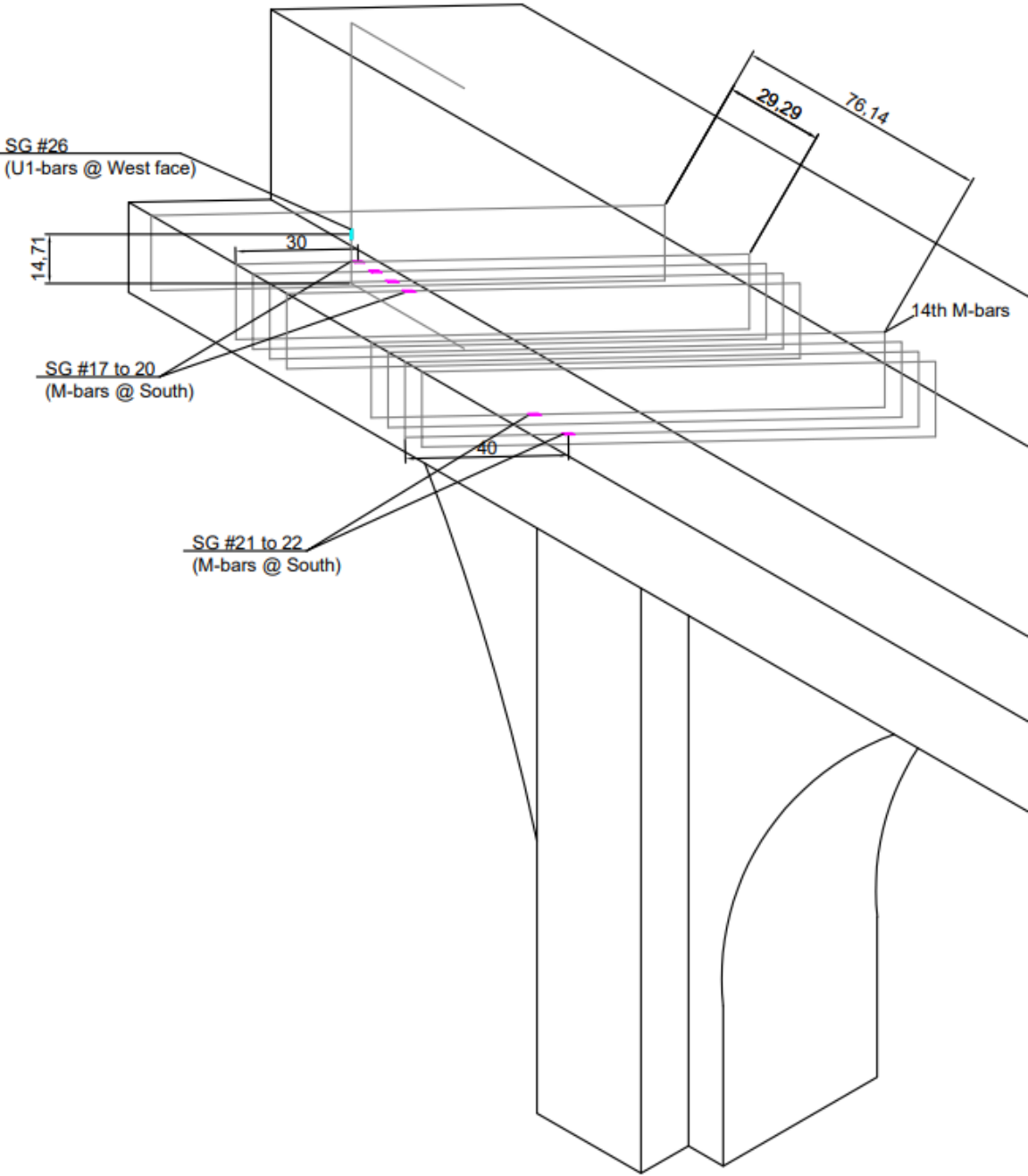
Measurement labels	
Strain Gauges at S Bars:	■
Strain Gauges at A Bars:	■
Strain Gauges at M Bars:	■
Strain Gauges at G Bars:	■
Strain Gauges at U1 Bars:	■
Strain Gauges at B Bars:	■
Strain Gauges at T Bars:	■
Laser-optical point:	●
CNFA:	▲



# WEST



# WEST



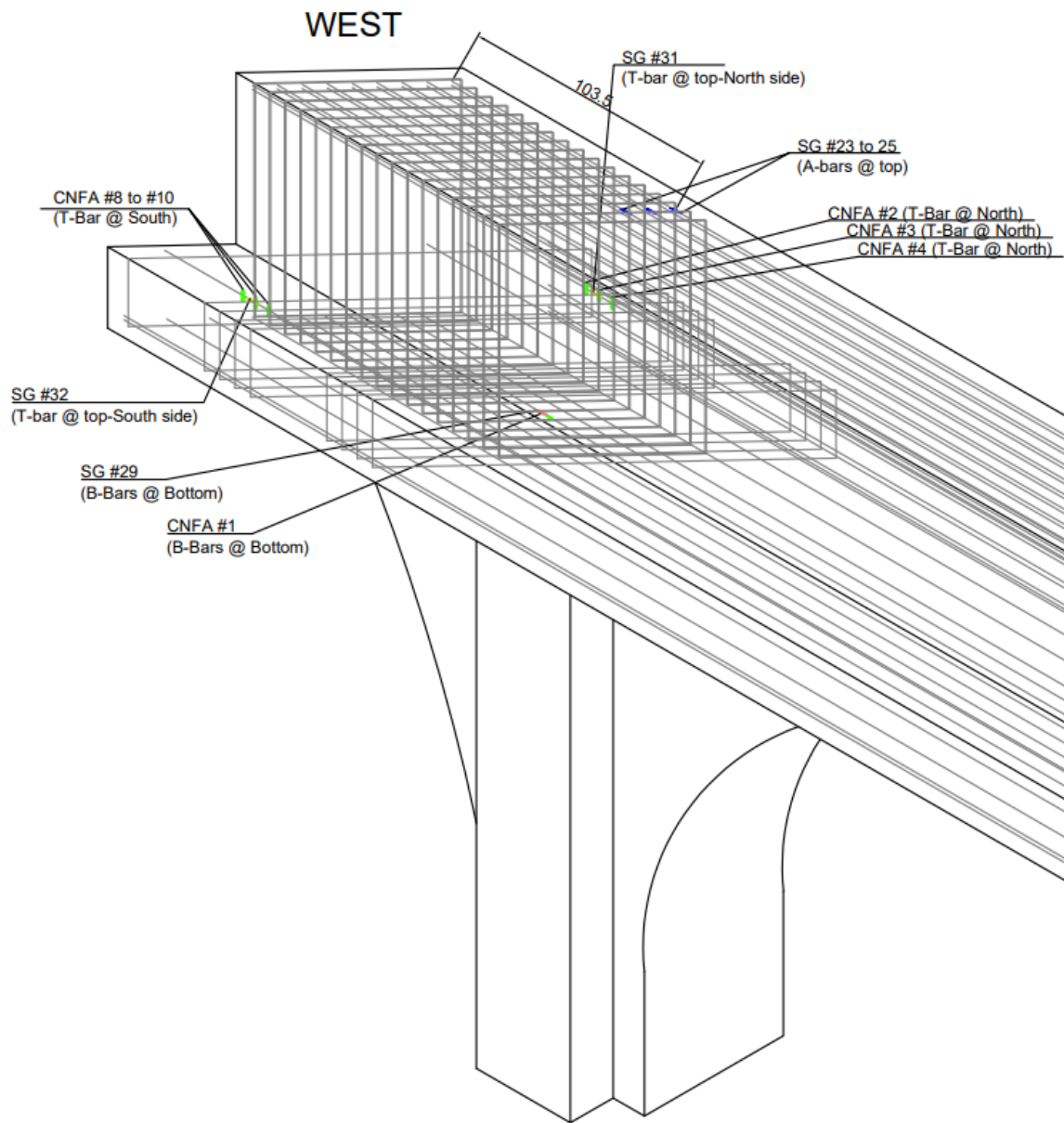


**Figure A6.3. 3D Visualization of Instrumented Sensors on Rebar Cage of Bent Cap 2**

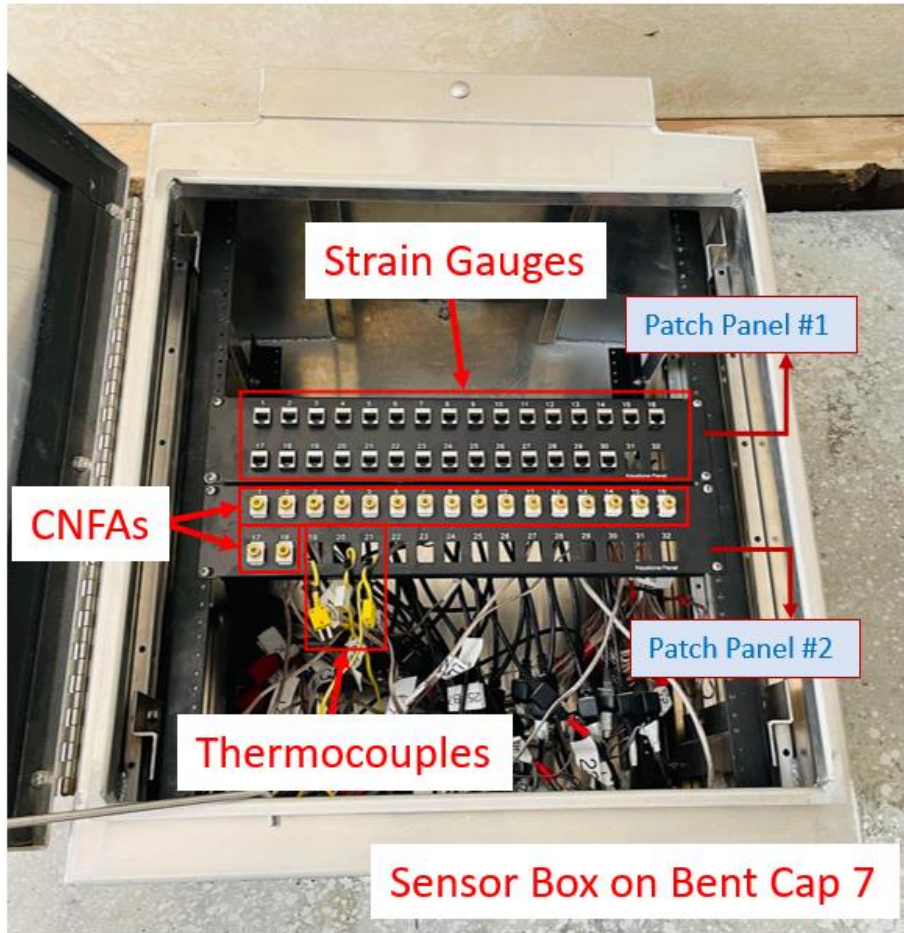


**Figure A6.4. Sensor Box Installed on Bent Cap 7**

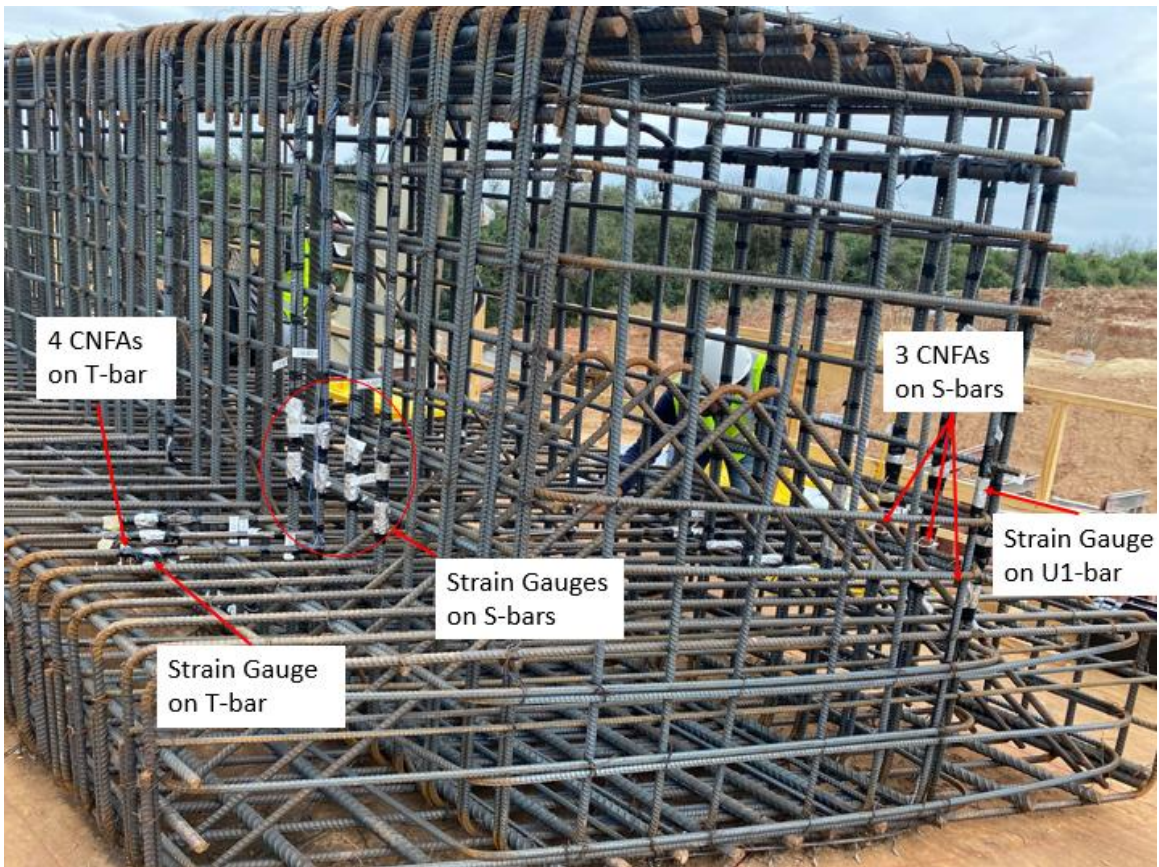
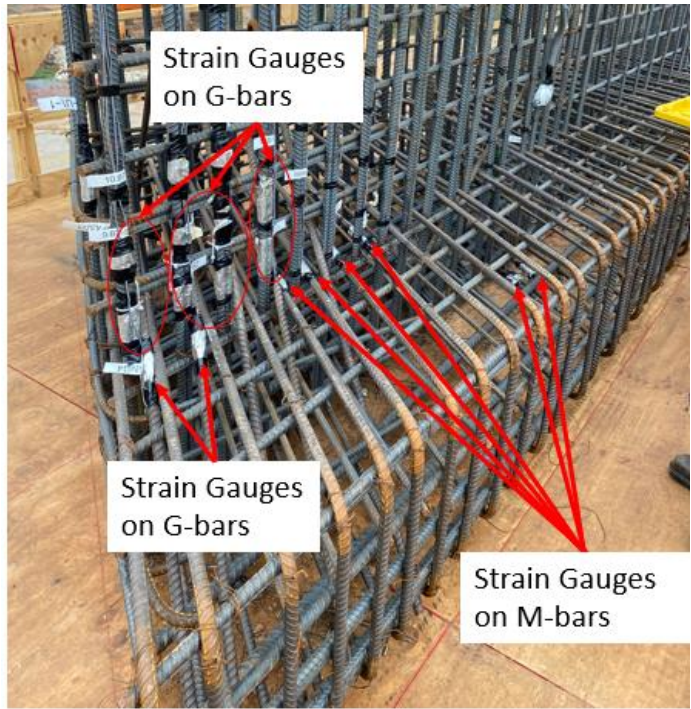
**Table A6.5. Locations of Strain Gauges Installed in Bent Cap 7**

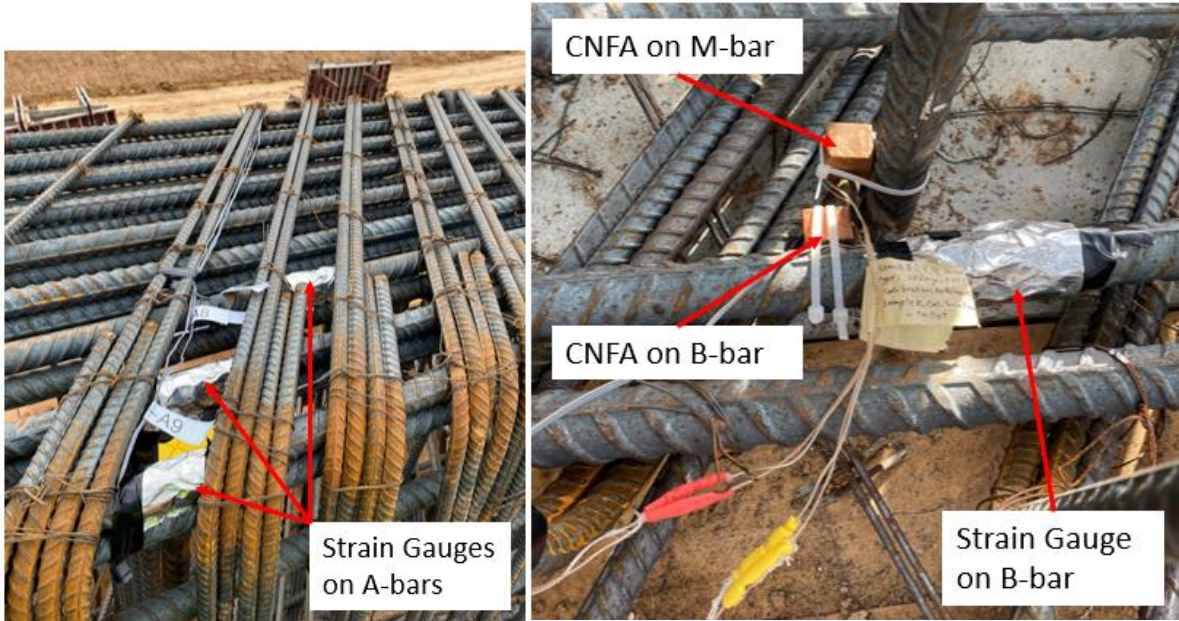
<b>No.</b>	<b>Label</b>	<b>Explanation</b>	<b>Sensor Box</b>	<b>Port No. on Patch Panel 1</b>	<b>Bar Group</b>
<b>1</b>	<b>B7-SS1s1</b>	Bent Cap 7 – South side, 1st S Bar from the west face, 1st SG located on the Side of the bar	South Side	1	S Bars
<b>2</b>	<b>B7-SS1s2</b>	Bent Cap 7 – South side, 1st S Bar from the west face, 2nd SG located on the Side of the bar	South Side	2	
<b>3</b>	<b>B7-SS2s1</b>	Bent Cap 7 – South side, 2nd S Bar from the west face, 1st SG located on the Side of the bar	South Side	3	
<b>4</b>	<b>B7-SS2s2</b>	Bent Cap 7 – South side, 2nd S Bar from the west face, 2nd SG located on the Side of the bar	South Side	4	
<b>5</b>	<b>B7-SS3s1</b>	Bent Cap 7 – South side, 3rd S Bar from the west face, 1st SG located on the Side of the bar	South Side	5	
<b>6</b>	<b>B7-SS3s2</b>	Bent Cap 7 – South side, 3rd S Bar from the west face, 2nd SG located on the Side of the bar	South Side	6	
<b>7</b>	<b>B7-SS4s1</b>	Bent Cap 7 – South side, 4th S Bar from the west face, 1st SG located on the Side of the bar	South Side	7	
<b>8</b>	<b>B7-SS4s2</b>	Bent Cap 7 – South side, 4th S Bar from the west face, 2nd SG located on the Side of the bar	South Side	8	
<b>9</b>	<b>B7-NS5s1</b>	Bent Cap 7 – North side, 5th S Bar from the west face, 1st SG located on the Side of the bar	South Side	9	
<b>10</b>	<b>B7-NS5s2</b>	Bent Cap 7 – North side, 5th S Bar from the west face, 2nd SG located on the Side of the bar	South Side	10	
<b>11</b>	<b>B7-NS6s1</b>	Bent Cap 7 – North side, 6th S Bar from the west face, 1st SG located on the Side of the bar	South Side	11	
<b>12</b>	<b>B7-NS6s2</b>	Bent Cap 7 – North side, 6th S Bar from the west face, 2nd SG located on the Side of the bar	South Side	12	
<b>13</b>	<b>B7-NS7s1</b>	Bent Cap 7 – North side, 7th S Bar from the west face, 1st SG located on the Side of the bar	South Side	13	

14	<b>B7-NS7s2</b>	Bent Cap 7 – North side, 7th S Bar from the west face, 2nd SG located on the Side of the bar	South Side	14	
15	<b>B7-NS8s1</b>	Bent Cap 7 – North side, 8th S Bar from the west face, 1st SG located on the Side of the bar	South Side	15	
16	<b>B7-NS8s2</b>	Bent Cap 7 – North side, 8th S Bar from the west face, 2nd SG located on the Side of the bar	South Side	16	
17	<b>B7-SM5t</b>	Bent Cap 7 – South side, 5th M Bar from the west face, SG located on the Top of the bar	South Side	17	M Bars
18	<b>B7-SM6t</b>	Bent Cap 7 – South side, 6th M Bar from the west face, SG located on the Top of the bar	South Side	18	
19	<b>B7-SM7t</b>	Bent Cap 7 – South side, 7th M Bar from the west face, SG located on the Top of the bar	South Side	19	
20	<b>B7-SM8t</b>	Bent Cap 7 – South side, 8th M Bar from the west face, SG located on the Top of the bar	South Side	20	
21	<b>B7-SM15b</b>	Bent Cap 7 – South side, 15th M Bar from the west face, SG located on the Bottom of the bar	South Side	21	
22	<b>B7-SM17b</b>	Bent Cap 7 – South side, 17th M Bar from the west face, SG located on the Bottom of the bar	South Side	22	
23	<b>B7-A7</b>	Bent Cap 7 – 7th A Bar of 1st alignment from the west face	South Side	23	A Bars
24	<b>B7-A8</b>	Bent Cap 7 – 8th A Bar of 1st alignment from the west face	South Side	24	
25	<b>B7-A9</b>	Bent Cap 7 – 9th A Bar of 1st alignment from the west face	South Side	25	
26	<b>B7-U1-1</b>	Bent Cap 7 – 1st U1 Bar from the west face	South Side	26	U1 Bar
27	<b>B7-SG4</b>	Bent Cap 7 – South side, 4th G Bar from the west face	South Side	27	G Bar
28	<b>B7-SG5</b>	Bent Cap 7 – South side, 5th G Bar from the west face	South Side	28	
29	<b>B7-B10</b>	Bent Cap 7 – 10th B Bar from the west face	South Side	29	B Bar
30	<b>B7-T7</b>	Bent Cap 7 – North side, 7th T bar from the west face under the bearing pad	South Side	30	T Bar

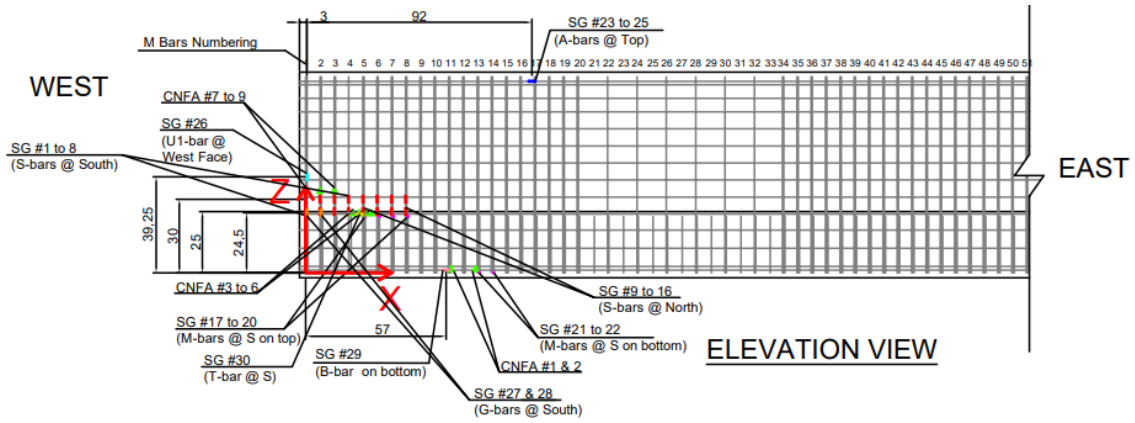
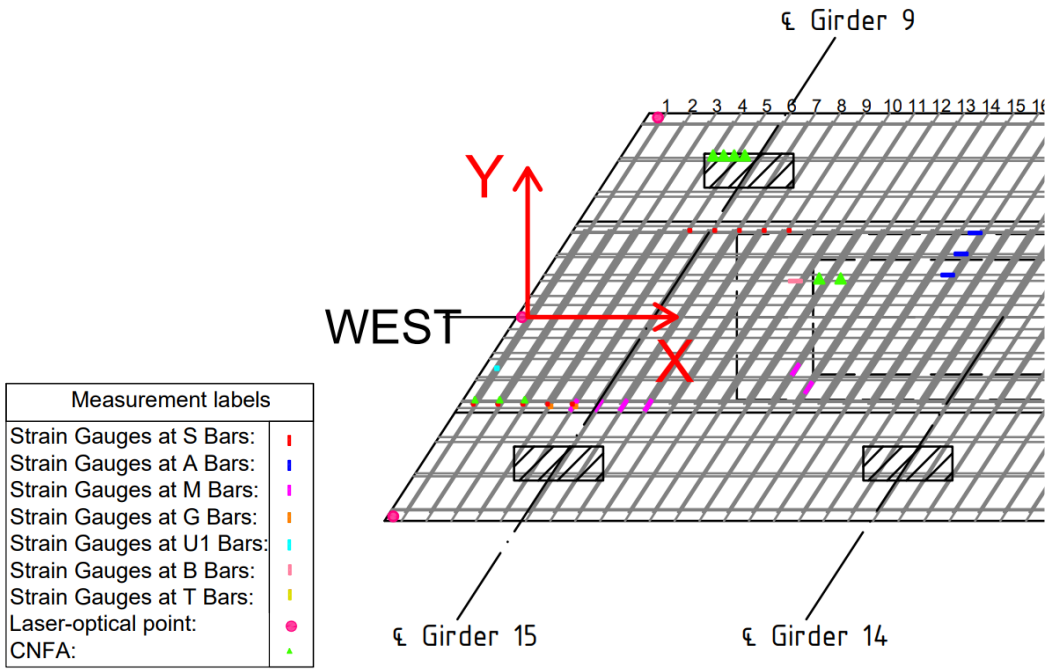
**Table A6.6. Locations of CNFAs Installed in Bent Cap 7**

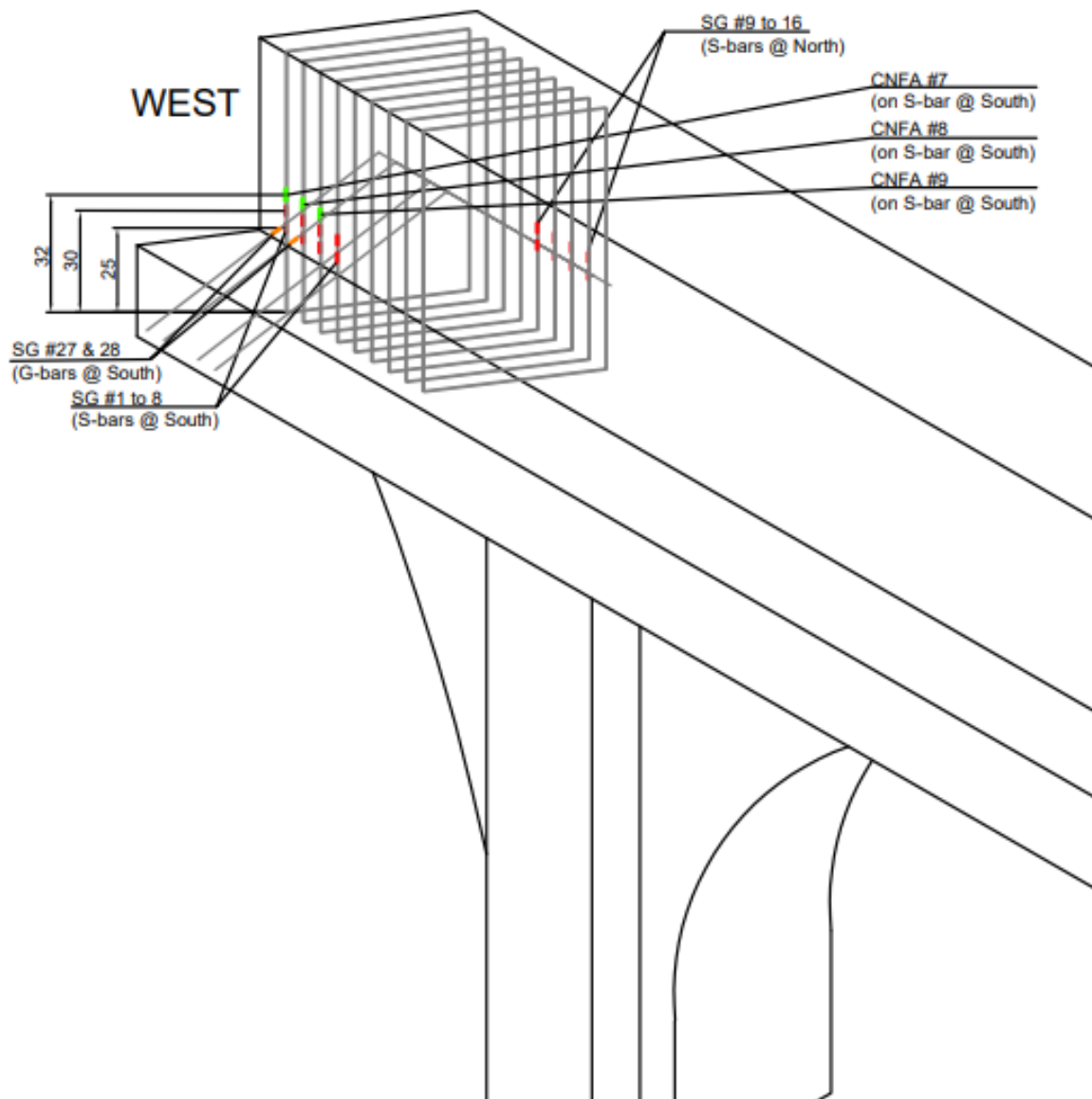
No.	Label	Explanation	Sensor Box	CNFA Terminal	Port No. on Patch Panel 2	Location
1	<b>B7-CNFA1zz1</b>	Bent Cap 7 – 10th B Bar from the west face, CNFA1 located in Z-direction	South Side	Left	1	1
				Right	2	
2	<b>B7-CNFA1zz2</b>	Bent Cap 7 – 13th M Bar from the west face, CNFA2 located in Z-direction	South Side	Left	3	
				Right	4	
3	<b>B7-CNFA2zz1</b>	Bent Cap 7 – T Bar, First CNFA at Location 2 in Z-direction (North face)	South Side	Left	5	2
				Right	6	
4	<b>B7-CNFA2zz2</b>	Bent Cap 7 – T Bar, Second CNFA at Location 2 in Z-direction (North face)	South Side	Left	7	
				Right	8	
5	<b>B7-CNFA2zz3</b>	Bent Cap 7 – T Bar, Third CNFA at Location 2 in Z-direction (North face)	South Side	Left	9	
				Right	10	
6	<b>B7-CNFA2zz4</b>	Bent Cap 7 – T Bar, Fourth CNFA at Location 2 in Z-direction (North face)	South Side	Left	11	
				Right	12	
7	<b>B2-CNFA3zz3</b>	Bent Cap 7 – 1st S Bar, First CNFA at Location 3 in Z-direction	South Side	Left	13	3
				Right	14	
8	<b>B7-CNFA3zz2</b>	Bent Cap 7 – 2nd S Bar, Second CNFA at Location 3 in Z-direction	South Side	Left	15	
				Right	16	
9	<b>B7-CNFA3zz3</b>	Bent Cap 7 – 3rd S Bar, Third CNFA at Location 3 in Z-direction	South Side	Left	17	
				Right	18	

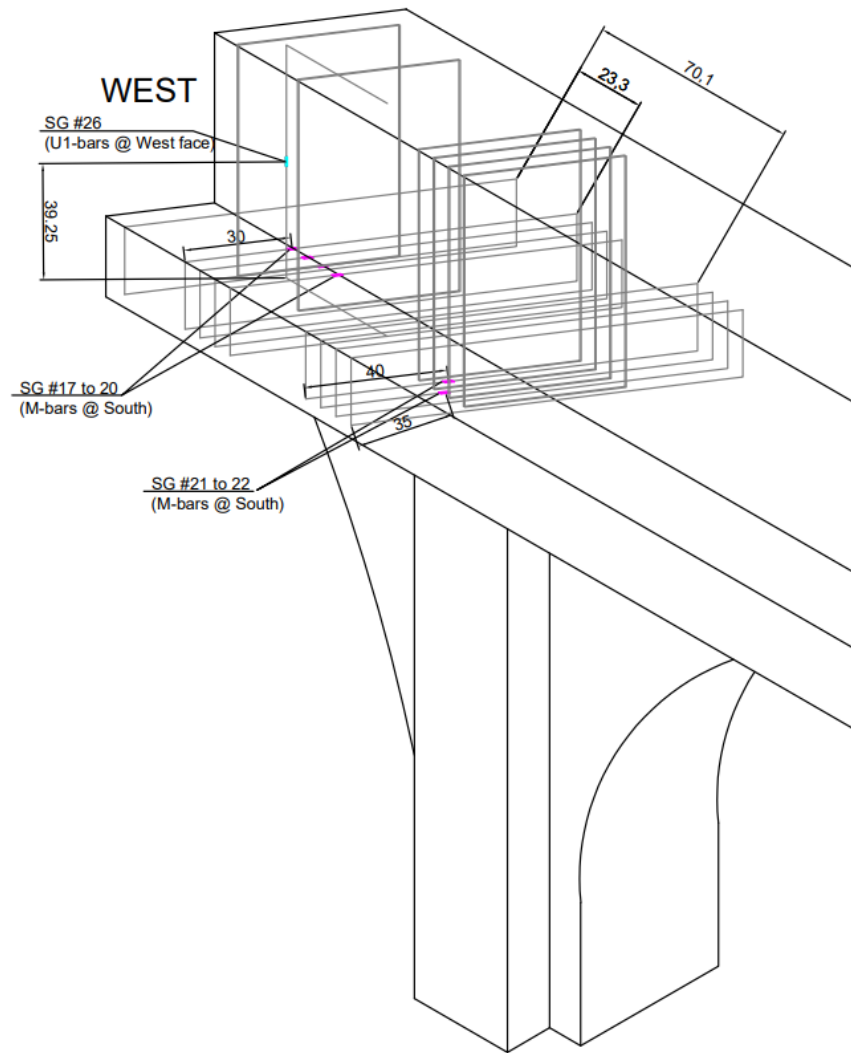




**Figure A6.5. Strain Gauges and CNFA instrumented on Bent Cap 7**







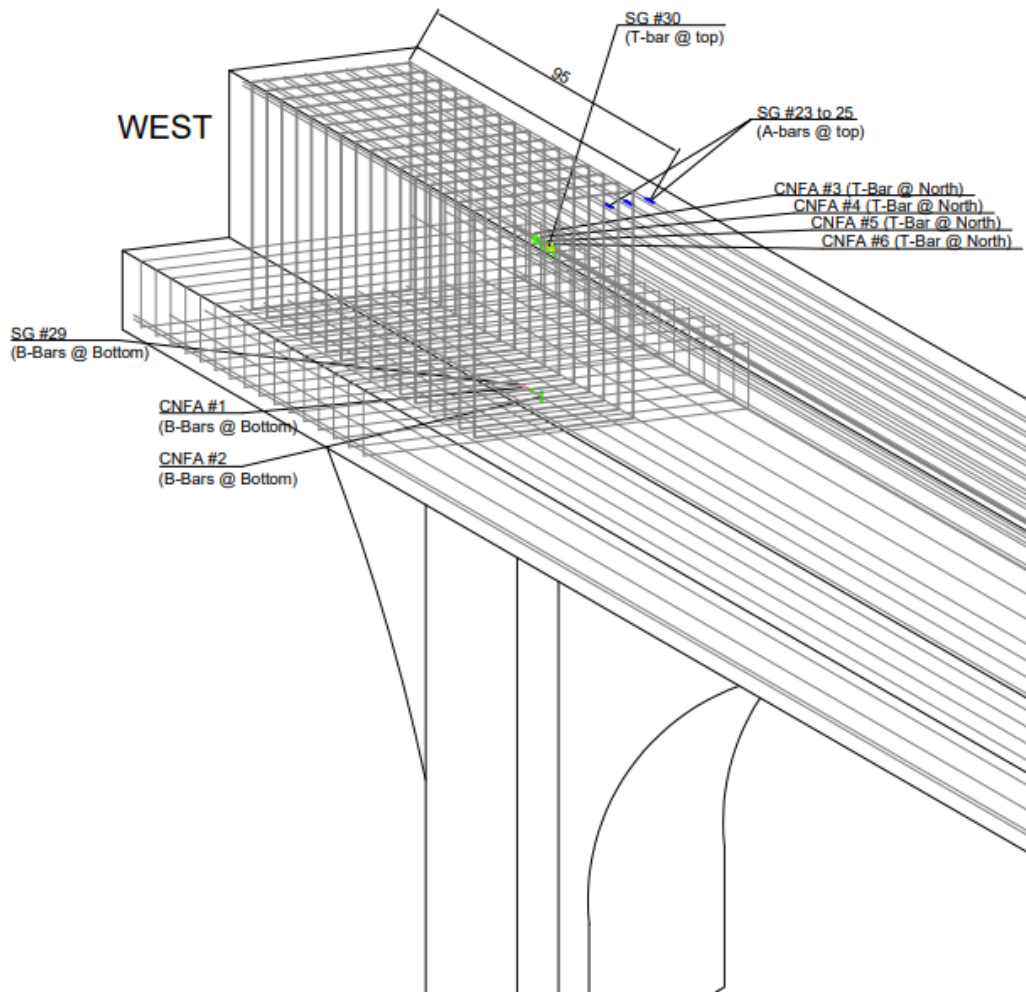
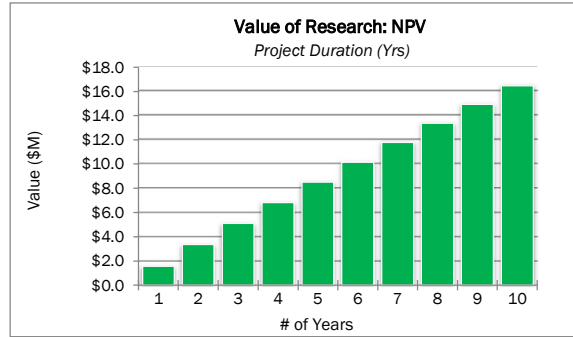


**Figure A6.6. 3D Visualization of Instrumented Sensors on Rebar Cage of Bent Cap 7**

**APPENDIX-7**

	<b>Project #</b>	0-6905-01		
	<b>Project Name:</b>	Performance of Skewed Reinforcing in Inverted-T Bridge Caps		
	<b>Agency:</b>	TxDOT	<b>Project Budget (Avg Per Yr)</b>	\$ 134,880
	<b>Project Duration (Yrs)</b>	2	<b>Exp. Value (per Yr)</b>	\$ 1,920,000
<b>Expected Value Duration (Yrs)</b>	10	<b>Discount Rate</b>	1%	
<b>Total Savings:</b>	18,930,240.00	<b>Net Present Value (NPV):</b>	\$ 17,556,830	
<b>Payback Period (Yrs):</b>	0.142804	<b>Cost Benefit Ratio (CBR, \$1 : \$15):</b>	\$ 66	

Years	Expected Value
0	-\$269,760
1	\$1,863,533
2	\$1,845,082
3	\$1,826,814
4	\$1,808,727
5	\$1,790,819
6	\$1,773,088
7	\$1,755,532
8	\$1,738,151
9	\$1,720,942
10	\$1,703,903



**Variable Justification**

Skew angle, detailing and amount of transverse reinforcement have been identified as critical parameters, which would influence the structural performance of skewed inverted-T bridge caps. The variation in skew angle would influence the concrete cracking, yielding of steel and shear capacity of the bridge cap. Furthermore, detailing of transverse steel affects the crack pattern and the shear and torsion capacities of the skewed inverted-T bent cap. In addition, the amount of transverse steel for skewed reinforcement may have a profound effect on the ductility and shear and torsion capacities of the structure. The results obtained from this research would help us establish in-depth guidelines for the design of skewed inverted-T bent caps, which has not yet been included in AASHTO and TxDOT bridge design manuals.

**Qualitative Value**

Functional Area	Value
Level of Knowledge	This functional area includes intangible benefits, influencing decisions and intangible assets. Skew angle, detailing and amount of transverse reinforcement are the three variables, which would be investigated to understand their effect on the ledge capacity, torsional capacity, cracking of concrete and shear capacity of the bent cap. Since there hasn't been any research related to skewed reinforcement, this research would enhance the level of knowledge in regards to skewed reinforcing in inverted-T bridge caps. This research would enable the TxDOT engineers to have a profound understanding of the structural performance of skewed inverted-T bent caps.
Management and Policy	By developing design guidelines for skewed reinforcement, skewed bridge inverted-T caps could be more reliably designed. The complexity and time of construction would be reduced allowing the TxDOT management to sanction skewed inverted-T bridge cap projects with increased assurance. This would provide an opportunity for the management to explore alternatives while selecting the alignments for the roadways and the bridges.
Engineering Design Development / Improvement	By studying the effect of skew angle, detailing and amount of transverse reinforcement, the structural performance and behaviour of skewed inverted-T bridge caps would be profoundly understood. This would help in establishing thorough design guidelines to be used for future skewed inverted-T bent caps in the state of Texas. The developed engineering design guidelines for skewed reinforcement would make the design process less cumbersome for the TxDOT design engineers.

**Economic Value**

Functional Area	Value
Increased Service Life	Understanding the structural performance and developing an optimized design for skewed reinforcement would lead to more reliable systems. This would, in return, increase the service life of the structures. Skew angles and the inclusion of G bars (transverse reinforcement) are the variables that may affect the service life of the structure. The skew angle of an inverted T bridge cap is the most influential parameter that causes higher tensile strains on transverse rebars and higher concrete strain on the ledge/stem interface. The inclusion of G-bars at the end face reduced the maximum crack width by more than 15%. Further, increasing the size of G-bars is a better design option in terms of controlling crack width than increasing the size of the transverse reinforcement. In addition, the experimental investigation shows the G bars reduced the tensile strain on the transverse reinforcement, quantitatively more on the rebars close to the exterior loading pads. As per TxDOT, skewed inverted-T bridges have a service life of 75 years. Implementing the design guidelines from this research would enable TxDOT engineers to design structures with an increased service life of up to 10%. The increased service life would save TxDOT around \$550,000 per year for about 20 newly constructed skewed inverted-T bridges.

Improved Productivity and Work Efficiency	Skewed reinforcement would reduce the congestion of reinforcement in the skewed region of the bridge. As a result, proper concrete placement could be achieved. It would reduce the complexity of having multiple sizes of reinforcing bars and detailing in the skewed region of the bent cap by providing uniform spacing and the same size of reinforcing bars. Therefore, lesser working hours and laborers would be required for the fabrication/construction of skewed reinforcement. Fabrication of reinforcement for the skewed region of a typical inverted-T bridge bent cap would require around 5 man-hours more than the regular reinforcement as per TxDOT. Thus, skewed reinforcement could save around \$13,000 per year in man-hours for about 20 newly constructed skewed inverted-T bridges.
Reduced Construction, Operations and Maintenance Cost	By replacing conventional reinforcement with skewed reinforcement, proper placement of concrete and less complex fabrication of reinforcement could be ensured. As a result, the construction costs involved would be reduced. As per TxDOT, average construction cost for a cap is around \$34,000 excluding any mobilization cost or column and foundation costs. This cost could be reduced by about 5% through this research. At the same time, increased reliability and service life would mean lesser cracks in concrete. So, the operations and maintenance cost of the bent caps would also be reduced. Each year TxDOT spends around \$500 million for the maintenance of all bridges in the state of Texas, of which approximate \$34.2 million is spent on the maintenance of all skewed inverted-T bridges. Skewed reinforcing could reduce this expenditure by about 10% per year. The construction, operations and maintenance cost could be reduced by around \$500,000 per year for the 20 newly constructed skewed bridges.
Engineering Design Development/Improvement	Proper design guidelines developed by addressing issues regarding skew angles, detailing and amount of transverse reinforcement would reduce the engineering man-hours necessary for designing a skewed inverted-T bridge bent cap. Therefore, less number of engineers would be needed for the projects. At the same time, precise guidelines could also reduce the necessity of hiring highly experienced engineers for the design process. Currently 120 engineering man-hours would be needed for designing a skewed inverted-T bridge bent cap. This investigation could reduce the hours by about 10%. An amount of \$320,000 per year would be saved for the design of skewed inverted-T bent caps. All in all, less working hours and less engineers would reduce the costs involved, which would benefit both TxDOT and the state of Texas.